Studies into the Effects of Hexa-hapto Spectator Ligands on the Chemistry of Ruthenium

A thesis presented to the University of London in partial fulfilment of the requirements for the degree of Doctor of Philosophy.

Jonathan W. Steed.

UNIVERSITY COLLEGE LONDON, 1993.

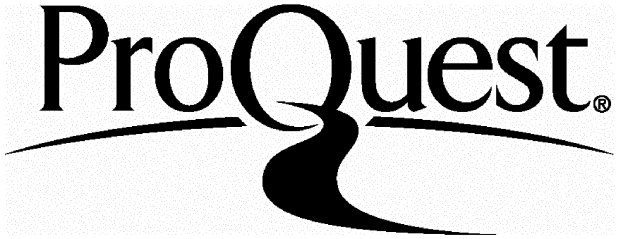

To my mother, who brought me unscathed through the first eighteen years of my life and little damaged thereafter, and to Coreena, of course.

ABSTRACT

This thesis describes the results of investigations into the chemistry of ruthenium complexes of *hexa-hapto* spectator ligands. Two specific systems have been examined. Chapters 2 - 5 describe aspects of the chemistry of the ruthenium(IV) chloride bridged compound $[\{Ru(\eta^3:\eta^3\text{-}C_{10}H_{16})Cl(\mu\text{-}Cl)\}_2]$ which contains the $\eta^3:\eta^3$-*bis*(allyl) ligand 2,7-dimethylocta-2,6-diene-1,8-diyl, derived from the ruthenium trichloride mediated dimerisation of isoprene. In Chapters 6 and 7 the reactivity of arenes and cyclohexadienes is examined in ruthenium complexes of the polyaromatic η^6-spectator [2.2]paracyclophane.

Chapter 1 offers a general introduction to arene and allyl transition metal chemistry and attempts to place the results reported herein into a wider context.

In Chapter 2 the reactions of the *bis*(allyl)ruthenium(IV) chloride bridged dimer $[\{Ru(\eta^3:\eta^3\text{-}C_{10}H_{16})Cl(\mu\text{-}Cl)\}_2]$ with amines and polypyridines are examined. Bridge cleaved amine adducts of formulae $[Ru(\eta^3:\eta^3\text{-}C_{10}H_{16})Cl_2L]$ or $[\{Ru(\eta^3:\eta^3\text{-}C_{10}H_{16})Cl_2\}_2(\mu\text{-}L)]$ (L = $PhNH_2$, *o*-pda, *p*-pda) are reported and the diastereoisomerism of the binuclear compounds examined. The mononuclear chelate compounds $[Ru(\eta^3:\eta^3\text{-}C_{10}H_{16})Cl(L\text{-}L)][BF_4]$ (L-L = 2,2'-diaminodiphenyl, 2,2'-bipyridyl, 1,10-phenanthroline) and $[Ru(\eta^3:\eta^3\text{-}C_{10}H_{16})(terpy)][BF_4]_2$ are formed from treatment of the starting material with $Ag[BF_4]$ and the appropriate ligand.

Chapter 3 reports a number of carboxylato compounds of ruthenium(IV). These products occur as either 1 : 1 bidentate chelates $[Ru(\eta^3:\eta^3\text{-}C_{10}H_{16})Cl(O_2CR)]$ (R = Me, CH_2F, CH_2Cl) or 1 : 2, monodentate carboxylato / aqua complexes $[Ru(\eta^3:\eta^3\text{-}C_{10}H_{16})(O_2CR)_2(OH_2)]$ (R = CH_2Cl, CH_2F, $CHCl_2$, CHF_2, CCl_3, CF_3). The electronic properties of the carboxylato ligand are found to be crucial to the product stoichiometry. The analogous thiocarboxylato compounds $[Ru(\eta^3:\eta^3\text{-}C_{10}H_{16})Cl(OSCR)]$ (R = Me, Ph, ^{t}Bu) exhibit bidentate coordination and exist as two alternative geometric isomers with the sulphur located either axially or equatorially. In the case where R = Me coordination is found to proceed *via* a two step process involving the monodentate thioacetic acid adduct $[Ru(\eta^3:\eta^3\text{-}C_{10}H_{16})Cl_2\{S(OH)CMe\}]$. The related nitrato compounds $[Ru(\eta^3:\eta^3\text{-}C_{10}H_{16})Cl(NO_3)]$ and $[Ru(\eta^3:\eta^3\text{-}C_{10}H_{16})(NO_3)_2]$ are also reported. In the latter case the "semi-chelating" nitrato ligands readily become monodentate in the presence of two electron ligands to give adducts $[Ru(\eta^3:\eta^3\text{-}C_{10}H_{16})(NO_3)_2L]$ (L = CO, py).

Chapter 4 reports a range of 2-pyridinol and pyridine-2-thiol compounds of

ruthenium(IV) of form $[Ru(\eta^3:\eta^3\text{-}C_{10}H_{16})Cl(pyrX)]$ (X = O, S) and related species. These compounds all exhibit *axial* and *equatorial* geometrical isomerism and a method based on ^1H NMR spectroscopy is described for distinguishing between the two forms.

In Chapter 5 a range of bi- and trinuclear compounds of ruthenium(IV) are described and their inherent diastereoisomerism studied. The bridge-cleaved adducts $[\{Ru(\eta^3:\eta^3\text{-}C_{10}H_{16})Cl_2\}_2(\mu\text{-pyz})]$ and $[\{Ru(\eta^3:\eta^3\text{-}C_{10}H_{16})Cl_2\}_n(\mu\text{-tra})]$ (n = 1, 2, 3) are reported along with the thiocyanato, carboxylato and nicotinato bridged compounds $[\{Ru(\eta^3:\eta^3\text{-}C_{10}H_{16})Cl(\mu\text{-SCN})\}_2]$, $[\{Ru(\eta^3:\eta^3\text{-}C_{10}H_{16})Cl\}_2(\mu\text{-}O_4R)]$ (R = C_2, C_3H_2) and $[Ru_2(\eta^3:\eta^3\text{-}C_{10}H_{16})_2Cl_3(\mu\text{-}NC_5H_4CO_2)]$.

In Chapter 6 the single nucleophilic addition reactions of simple anions N^- (N = H, CN, OMe, Me) to unsymmetrical *bis*(arene)ruthenium(II) compounds $[Ru(\eta^6\text{-arene})(\eta^6\text{-}$[2.2]paracyclophane$)]^{2+}$ (arene = C_6H_6, *p*-$MeC_6H_4CHMe_2$, 1,4-$(CHMe_2)_2C_6H_4$, C_6Me_6, $C_{16}H_{16}$) are examined. It is found that the cyclophane acts as a non-innocent spectator ligand, directing nucleophiles onto other arenes coordinated to the same metal centre to give the cyclohexadienyl compounds $[Ru(\eta^6\text{-}$[2.2]paracyclophane$)(\eta^5\text{-}C_6R_6N)]^+$.

Chapter 7 describes the extension of the work reported in Chapter 6 to double nucleophilic addition reactions to give ruthenium(0) compounds of general form $[Ru(\eta^6\text{-}$[2.2]paracyclophane$)(\eta^4\text{-diene})]$. The reactivity of these Ru(0) species towards $H[BF_4]$ is examined resulting in a range of novel agostic compounds. Mechanistic aspects are investigated by a range of deuteriation studies.

Finally, Chapter 8 offers some conclusions on what has been learned about the effects the two spectator ligands studied have on the chemistry of ruthenium.

CONTENTS

ACKNOWLEDGEMENTS

Spending three years pottering around a lab, having a lot of fun and playing with some interesting chemistry leaves a lot of scope for saying thank you. There are lots of people whom I shall never forget and, perhaps, one or two that I would rather I did. In the interests of brevity the list of thankyous is short but between the lines lie the names of everyone I have known and smiled with since coming to London, almost six years ago now.

First, my most sincere gratitude goes to my supervisor and, I hope, friend Dr. Derek Tocher who managed to put some order into my mad schemes and thought of even more of his own, as well as giving me that constant, all important, support and encouragement. Thanks also to Mark Elsegood who taught me most of the bench chemistry I know and is the only man in Christendom who can grow crystals of cyclophane complexes! Nilgün Mehmet is quite one of the most cheerful people I know and it has been a pleasure to work with her, and of course, Marcus Daniels, whom my mother describes accurately as a real gentleman. I would also like to thank Ken and Glyn, without whose pleasant visits I would doubtless have got much more work done.

Grateful acknowledgement is due to Brian Kavanagh with whom I collaborated on much of the work described in Chapter 3, and to Gary Belchem, Matt Rowley and Dietrich Schreiber who have also worked on aspects of ruthenium(IV) chemistry.

I have also been privileged to be able to call upon the expertise of Chris Cooksey and Edgar Anderson without whom much of the NMR spectroscopy reported herein would still only be a twinkle in my supervisor's eye, and the X-ray crystal structures which neither Derek nor I could solve didn't stand a chance against Professor Mary Truter.

ABBREVIATIONS

X-ray Crystallography

esd - Estimated Standard Deviation (in parenthesis after the quantity to which it refers)

Nuclear Magnetic Resonance Spectroscopy (NMR)

s = singlet d = doublet t = triplet

q = quartet qu = quintet se = septet

m = multiplet br = broad dd = doublet of doublets

dt = doublet of triplets AB = AB pattern

Infrared Spectroscopy (IR)

s = strong m = medium w = weak

br = broad sh = shoulder v = very

Nomenclature

bipy - 2,2'-Bipyridyl

cdt - 1,5,9--Cyclododecatriene

cht - 1,3,5-Cycloheptatriene

cod - 1,5-Cyclooctadiene

cot - 1,3,5,7-Cyclooctatetraene

cy - [2.2]Paracyclophane

dapsc - 2,6-Diacetylpyridine *bis*(semicarbazone)

ddt - Dodeca-2,6,10-triene-1,12-diyl

dmso - Dimethylsulphoxide

dmf - Dimethylformamide

Et - Ethyl

mcbt - Benzothiazole-2-thiolate

Me - Methyl

o-pda - 1,2-Diaminobenzene

p-pda - 1,4-Diaminobenzene

Ph - Phenyl

phen - 1,10-Phenanthroline

pyrO - 2-Hydroxypyridinate

pyrS - Pyridine-2-thiolate

pyz - Pyrazene

terpy - 2,2':6',2''-Terpyridine

thf - Tetrahydrofuran

tra - 1,3,5-Triazine

o-dib - 1,2-Diiminobenzene

^{t}Bu - Tertiary butyl

py - Pyridine

Chapter 1

Introduction

1.1 Motivations for the Present Work

Underpinning a great deal of modern chemistry is the concept of influencing or "tuning" reactivity by control of often subtle steric and electronic factors. One method of achieving such control is by variation of substitution patterns at sites remote from the reaction centre, which do not necessarily play a direct part in the chemical reaction itself. General examples of this type of approach include stabilisation by inclusion of reactive complexes within macrocyclic hosts such as crown ethers, cryptands[1] and hemicarcerands[2] or steric crowding of a reaction centre as in the picket fence porphorins first synthesised by Collman *et al.*, which provide protection against irreversible μ-oxo dimer formation in iron dioxygen complexes, which are of interest as models of the active site in haemoglobin.[3]

In transition metal chemistry the steric and electronic properties, and hence reactivity, of the metal centre are highly dependent upon the nature of the ligands in the primary coordination sphere. Frequently however, not all the coordination sites are directly involved in reactions taking place at the metal centre and are occupied by inert "spectator" ligands. Alteration of the steric or electronic nature of these inactive groups can have a large effect upon the rate and selectivity of a reaction at the remaining coordination sites and can contribute to the stability of the reactive transition metal species. Ubiquitous examples of such spectator groups are the cyclopentadienyl ligand ($[C_5H_5]^-$, Cp) and its bulky permethylated analogue $[C_5Me_5]^-$ (Cp^*),[4] which commonly coordinate to three *fac* sites of an octahedral transition metal centre, balancing the charge of cationic species and providing stabilisation (especially in the case of Cp^*) by virtue of steric bulk and the strong M-Cp^* bond.[5] Modification of such simple spectators to form chiral Ziegler-Natta catalysts for example, has recently been shown to give a high degree of stereoregularity in propylene polymerisation.[6]

In this study the influence of two particular 6 electron, *hexa-hapto* spectator ligands, namely [2.2]paracyclophane ($C_{16}H_{16}$, **1**) and 2,7-dimethylocta-2,6-diene-1,8-diyl (η^3:η^3-$C_{10}H_{16}$, **2**), on reactivity in organometallic ruthenium complexes has been examined.

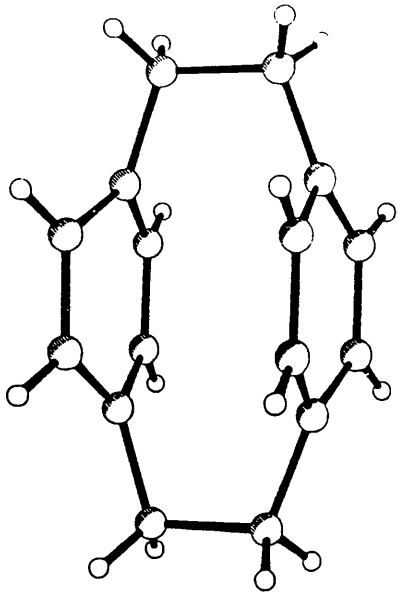

1

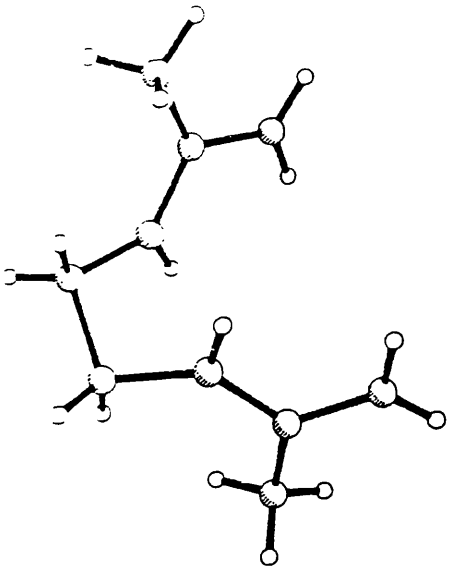

2

[2.2]Paracyclophane, **1**, is a stacked, twin decked, aromatic molecule which may be regarded as being derived from benzene. Work by Boekelheide *et al.*[7] has shown that action of the hydride source $Na[AlH_2(OC_2H_4OMe)_2]$ (Red-Al) upon unsymmetrical *bis*(arene) ruthenium complexes of the form $[Ru(\eta^6\text{-}C_{16}H_{16})(\eta^6\text{-arene})]^{2+}$ (arene = C_6H_6 **3a**, C_6Me_6 **3b**), gives exclusively the cyclohexadiene ruthenium(0) compounds $[Ru(\eta^6\text{-}C_{16}H_{16})(\eta^4\text{-diene})]$ (diene = C_6H_8 **4**, 3,6-$C_6Me_6H_2$ **5**). In contrast, reaction of nucleophiles with related, non-cyclophane, *bis*(arene)ruthenium(II) complexes results in the formation of *bis*(cyclohexadienyl) complexes of ruthenium(II) in **almost** all cases except for a few reactions with hydride.[8-11] In this study the reactivity of a range of ([2.2]paracyclophane)(arene)ruthenium(II) complexes towards nucleophiles has been examined. The hypothesis that [2.2]paracyclophane is inert towards nucleophilic addition and acts as a non-innocent spectator ligand, directing nucleophilic attack onto other arenes coordinated to the same metal centre, is explored.

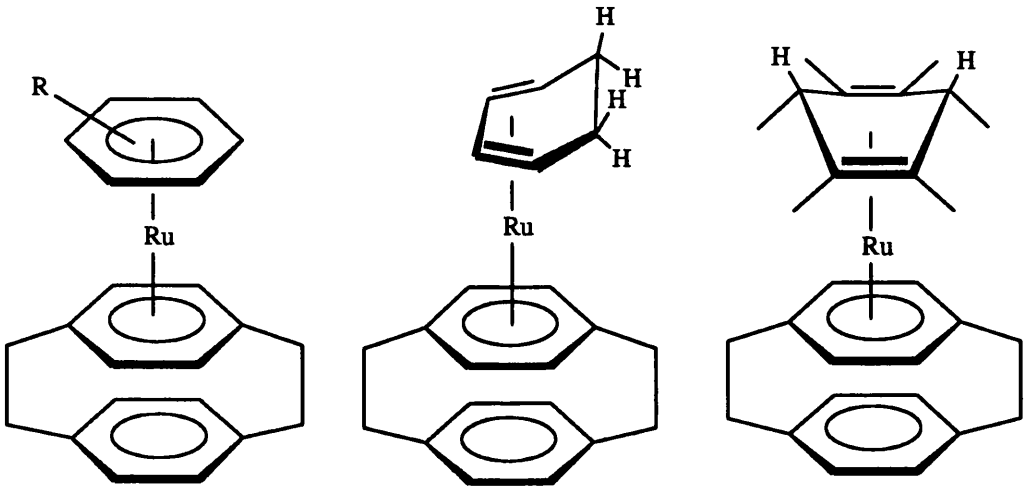

3 **4** **5**

2,7-Dimethylocta-2,6-diene-1,8-diyl, **2**, is only known as a ligand coordinated to a metal centre, where it binds through two independent η^3-allylic functionalities separated by an ethylenic backbone. The ligand is the tail-to-tail dimer of isoprene (2-methylbutadiene) and is formed in the reaction of isoprene with ruthenium trichloride[12,13] which gives a pink precipitate of the ruthenium(IV) chloride bridged dimer $[\{Ru(\eta^3:\eta^3\text{-}C_{10}H_{16})Cl(\mu\text{-}Cl)\}_2]$ **6**, Scheme 1.1.

The structural similarities between **6** and its arene ruthenium(II) analogues $[\{Ru(\eta^6\text{-arene})Cl(\mu\text{-}Cl)\}_2]$ (arene = C_6H_6 **7a**, C_6Me_6 **7b**) are apparent, yet in contrast to complexes **7**,[14] the chemistry of **6** has remained almost totally neglected[15-17] until the present work. In spite of this, **6** and species derived from it possess a number of features which make them a particularly attractive prospect for study:

i) The high formal oxidation state (+4) of the metal centre, which offers the prospect of a facile entry into high oxidation state organometallic compounds; an area of considerable current interest.[18-20]

ii) The chirality of the metal coordinated *bis*(allyl) ligand, which might be of interest[21,22] in areas such as asymmetric synthesis.

iii) The unusual geometry about the metal centre, loosely described as trigonal

bipyramidal, giving three "free" *mer*- coordination sites available on the "(η^3:η^3-$C_{10}H_{16}$)Ru^{2+}" fragment, in contrast to the *fac*- geometry usually observed in related (arene)ruthenium(II) chemistry.

iv) The high reactivity offered by the chloride-bridged structure of **6**. Bridge cleavage reactions form the starting point for a wide range of chemistry in related systems.[14]

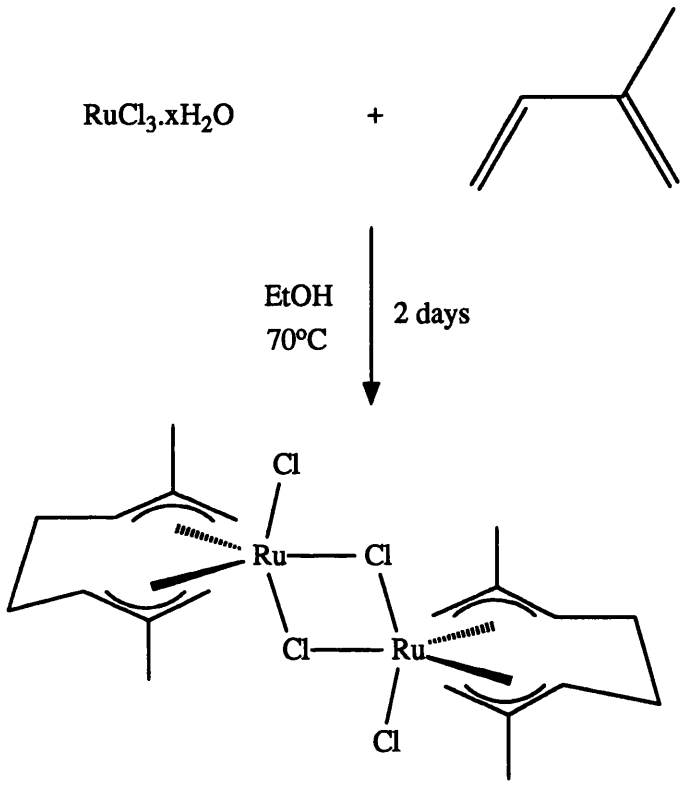

6

Scheme 1.1: Synthesis of the *bis*(allyl)ruthenium(IV) complex [{Ru(η^3:η^3-$C_{10}H_{16}$)Cl(μ-Cl)}$_2$] **6**.

We have carried out an extensive study of the chemistry of **6** and, where appropriate, highlighted the differences between η^6-arene spectator ligands and the more sterically crowded η^3:η^3-*bis*(allyl) species.

The following sections serve to introduce more fully the chemistry of *hexa-hapto* organic ligands. Examples have been chosen, where appropriate, with regard to their relevance to the chemistry of ruthenium, although effort is made to place these results in context within the wider theme of π-organo-transition metal chemistry.

1.2 η^6-Arene Ligands

1.2.1 Properties and Bonding in Arene Transition Metal Complexes

A wide range of η^6-arene complexes is known for both early and late transition metals in a variety of oxidation states and, unlike the analogous main group compounds, often possess a high degree of stability, although many are air sensitive. Some properties of representative *bis*(arene) metal complexes are summarised in Table 1.1.

Table 1.1: Scope and properties of *bis*(arene) transition metal complexes.[a]

Complex	Colour	Stability	N°. of Valence Electrons	Magnetic Moment / B.M.
$[Ti(C_6H_6)_2]$	red	air sensitive	16	0
$[V(C_6H_6)_2]$	deep red	mp 227°C, very air sensitive	17	1.7
$[Nb(C_6H_6)_2]$	purple	decomposes above 90°C, very air sensitive	17	b
$[Cr(C_6H_6)_2]$	brown	mp 284°C, air sensitive	18	0
$[Mo(C_6H_6)_2]$	green	mp 115°C, very air sensitive, pyrophoric	18	0
$[W(C_6H_6)_2]$	yellow-green	mp 160°C, air sensitive	18	b
$[Mn(C_6Me_6)_2]^+$	pale pink	air stable	18	b
$[Fe(C_6H_6)_2]^{2+}$	orange	hydrolytically sensitive	18	0
$[Fe(C_6Me_6)_2]^{2+}$	orange	air stable	18	0
$[Fe(C_6Me_6)_2]^+$	violet	air sensitive	19	1.89

$[Fe(C_6Me_6)_2]$	black	very air sensitive	20	3.08
$[Ru(C_6Me_6)_2]^{2+}$	colourless	air stable	18	0
$[Co(C_6Me_6)_2]^{+}$	yellow	very air sensitive	20	2.95

a) Adapted from refs. 23 and 24; b) not measured

A qualitative molecular orbital description of the bonding in the representative compound $[Cr(C_6H_6)_2]$ is shown in Fig. 1.1. X-ray photoelectron spectroscopy suggests that the chromium atom possesses a partial positive charge of *ca.* +0.7 electron units whereas the arene rings each have a charge of around -0.35 and hence, the arrangement of the metal *d* orbitals is described satisfactorily, to first approximation, by a simple electrostatic model incorporating repulsions between the metal *d* electrons and the arene "charge loops".[23] A more sophisticated MO approach however, based on the overlap of metal orbitals with symmetry adapted linear combinations (SALC) of ligand π-orbitals, does more justice to the covalent nature of the bonding in complexes of this type.

The metal *d* orbitals are effectively split into three levels as shown in Fig. 1.2. In the case of $[Cr(\eta^6\text{-}C_6H_6)_2]$ the six *d* electrons occupy the e_2 and a_1 levels giving a diamagnetic, low spin d^6 ground state. In the a_1 level, derived from the dz^2 orbital, the overlap is σ in nature and is effectively non-bonding. The e_2 orbitals represent a δ interaction in which back-bonding from the metal into ligand antibonding orbitals occurs. In the case of Cr(0) the metal and ligand e_2 basis orbitals are closely matched in energy and extensive back-bonding interaction takes place. In cases where the bonding is more ionic in nature (*e.g.* $[Fe(\eta^6\text{-}C_6Me_6)_2]^{2+}$) the energy matching is less precise and the L-M interaction is of a more σ-donor type.

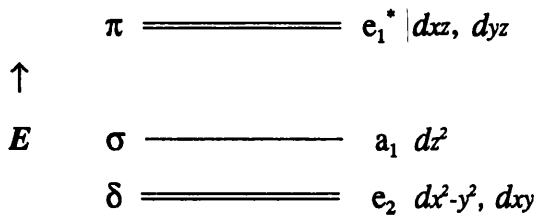

Fig. 1.2: Splitting of the metal *d* orbitals in *bis*(benzene)chromium(0)

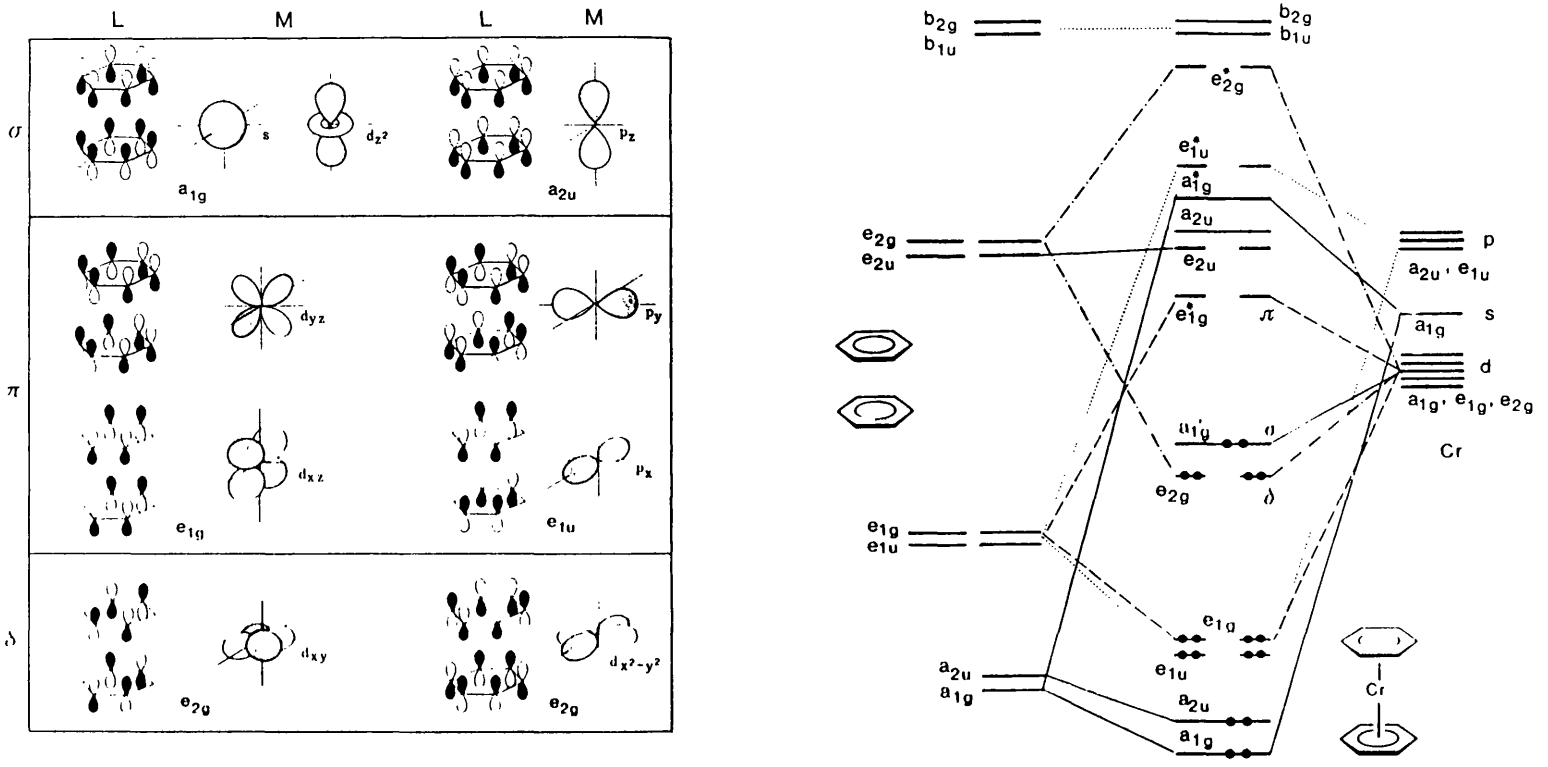

Fig. 1.1: Interactions of symmetry adapted linear combinations of the π-molecular orbitals of two benzene ligands with appropriate metal orbitals in *bis*(benzene)chromium, D_{6h}, and the resulting qualitative MO scheme.[23]

1.2.2 Synthesis of Arene Transition Metal Complexes

Bis(arene) complexes of the transition metals are commonly synthesised by three important methods. The earliest and simplest is the Fischer-Hafner synthesis[9,23,25-27] (Equations 1.1 and 1.2) in which the appropriate metal halide is heated with selected arenes (ArH) in the presence of $AlCl_3$ and aluminium metal if a reduced species is desired as the final product.

$$3\,CrCl_3 + 2\,Al + 6\,ArH \xrightarrow[2.\,H_2O]{1.\,AlCl_3} 3\,[Cr(ArH)_2]^+ + 2\,Al^{III} \qquad (1.1)$$

$$3\,[Cr(ArH)_2]^+ \xrightarrow[KOH]{Na_2S_2O_4} [Cr(\eta^6\text{-}ArH)_2]$$

$$3\,FeBr_2 + 2\,ArH \xrightarrow{AlBr_3} [Fe(\eta^6\text{-}ArH)_2][AlBr_4]_2 \qquad (1.2)$$

The method is general for metals of the Cr, Fe and Co triads as well as a number of other early and late transition metals. The arene must, however, be inert to $AlCl_3$ and severe problems are often encountered with isomerisation of alkylated arenes, although addition of alkyl aluminium reagents can alleviate this drawback to some extent. More importantly the synthesis is restricted solely to symmetrical *bis*(arene) compounds.

More exotic $M(arene)_2$ species may be synthesised *via* metal-atom ligand-vapour co-condensation (CC)[28,29] in which the metal and ligand are mixed in the gas phase and condensed at low temperature onto a cooled surface. On warming, metal complexation occurs in competition with metal atom aggregation. This method may be used to synthesise a wide range of materials such as $[M(\eta^6\text{-}C_6H_6)_2]$ (M = Ti, Nb)[29] and even the unusual air sensitive inclusion complex [Cr(η^{12}-[3.3]paracyclophane)]. The crystal structures of the more stable, oxidised Cr(I) salts [Cr(η^{12}-[3.3]paracyclophane)]X (X = I_3, PF_6) have been reported (Fig. 1.3).[30-32] The complexes [Cr(η^{12}-[2.2]paracyclophane)] and [Cr(η^{12}-octamethyltetrasilyl[2.2]paracyclophane)] are also known.[33,34] Unfortunately yields in CC reactions are often low and large amounts of coolant and ligand are required. The method

is also limited by the volatility of the co-condensates and the need for an efficient vacuum.

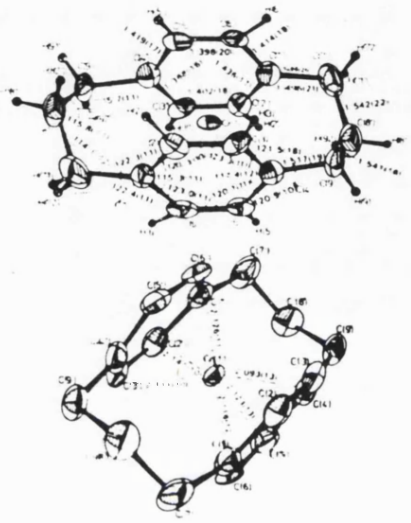

Fig. 1.3: X-ray crystal structure of the Cr(I) inclusion complex cation $[Cr(\eta^{12}\text{-}[3.3]paracyclophane)]^{+}$

By far the most versatile synthesis of *bis*(arene) complexes of ruthenium(II) and osmium(II), especially unsymmetrical examples, $[M(arene)(arene')]^{2+}$, such as **3**, is the technique developed by Bennett and Smith, Scheme 1.2.[35] Halide abstraction, using AgX (X = BF_4, PF_6, ClO_4 *etc.*) from dichloride dimer species of type **7** gives the *tris*(solvato) complexes $[M(\eta^6\text{-arene})(S)_3]X_2$ (S = H_2O, acetone, MeCN) which react with the second arene under reflux in the presence of acid to give products in good to excellent yields. In the absence of arenes, at room temperature, the acetone solvates (X = BF_4) undergo an intramolecular aldol condensation to give complexes $[Ru(\eta^6\text{-arene})(OCMe_2)\{Me_2C(OH)CH_2C(O)Me\}][BF_4]_2$ containing the chelating 4-hydroxy-4-methylpentan-2-one ligand. When X = PF_6 the "non-coordinating" anion is partially hydrolysed over several hours to give the tri-μ-difluorophosphate species $[Ru_2(\eta^6\text{-arene})_2(\mu\text{-}PO_2F_2)_3][PF_6]$.[35] Similar reactions are observed in the rhodium(III) and iridium(III) Cp^* analogues.[36,37] Use of long lived solvato intermediates and expensive silver salts may be dispensed with altogether

however, by a modification of the Bennett synthesis developed by Rybinskaya *et al.*[38] involving reaction of **7** directly with the arene in neat CF_3CO_2H. These workers have also extended their synthesis to $[M(\eta^5\text{-}Cp^*)(\eta^6\text{-arene})]^{2+}$ (M = Rh, Ir) complexes by modification of the procedure described by Maitlis *et al.*[39,40]

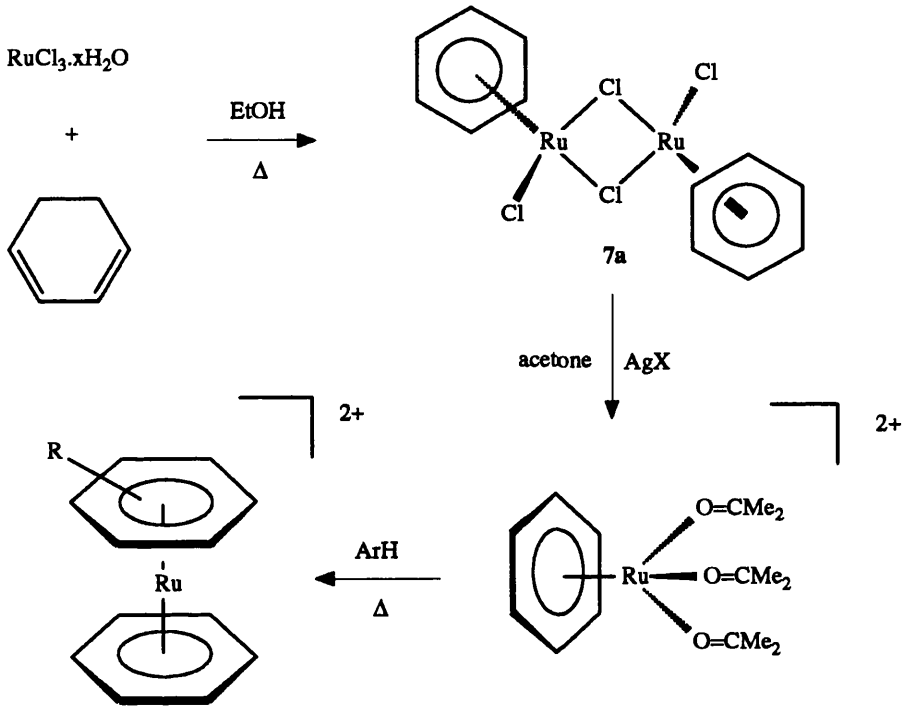

Scheme 1.2: The Bennett synthesis of unsymmetrical *bis*(arene)ruthenium compounds.

1.2.3 Piano Stool Complexes of Ruthenium Incorporating η^6-Arene Ligands

In addition to their synthetic utility in the formation of *bis*(arene) complexes, the compounds $[\{Ru(\eta^6\text{-arene})Cl(\mu\text{-}Cl)\}_2]$ **7** are also important gateways into a wide range of (arene)ruthenium(II) chemistry based on the half-sandwich, piano stool structure.[41-44] The complexes themselves are formed from the dehydrogenation of the appropriate 1,3- or 1,4-cyclohexadiene by "$RuCl_3.xH_2O$" ($x \approx 2$) in refluxing ethanol.[14,45-47] Arenes such as hexamethylbenzene which are not susceptible to Birch reduction and for which the appropriate cyclohexadiene is not available *via* convenient alternative routes may be

complexed in thermally or photochemically induced arene exchange reactions.[14,47-49] Interestingly, in the synthesis of the benzene complex **7a**, a small quantity of a coordinated cyclohexadiene by-product $[Ru(\eta^6\text{-}C_6H_6)(\eta^4\text{-}C_6H_8)Cl]X$ (X = BPh_4 **8a** or ½Hg_3Cl_4 **8b**) may be isolated, by addition of $Na[BPh_4]$ or $HgCl_2$ respectively.[50]

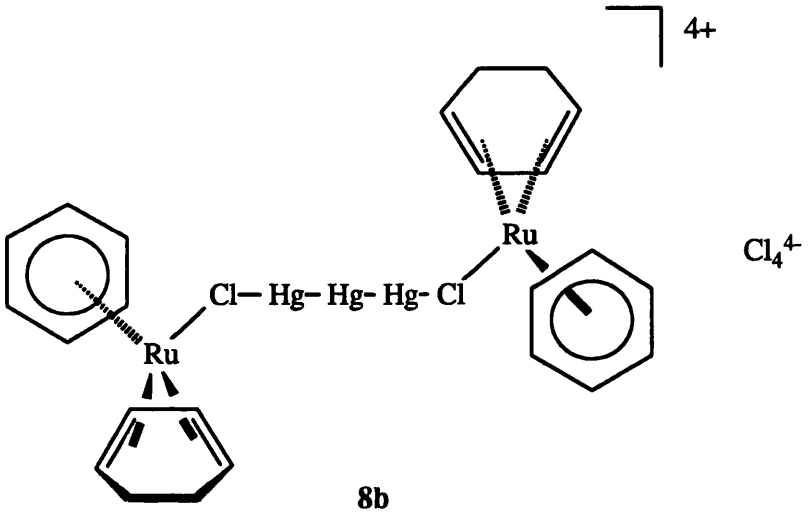

8b

Addition of HCl to the ruthenium(0) compounds $[Ru(\eta^6\text{-arene})(\eta^4\text{-diene})]$ results[51] in oxidation of the metal centre and displacement of the diene ligand to give further examples of complexes of type **7**.[52] To date this is the only available method for the synthesis of the [2.2]paracyclophane chloride bridged dimer $[\{Ru(\eta^6\text{-}C_{16}H_{16})Cl(\mu\text{-}Cl)\}_2]$ **7c**[7] although the method is not of very general synthetic utility.

The chloride bridges in complexes **7** are readily cleaved by Lewis bases in non-polar solvents to give neutral 1 : 1 adducts of general formula $[Ru(\eta^6\text{-arene})Cl_2L]$ **9** (L = pyridine, PR_3, POR_3, AsR_3, SbR_3, CNR, CO *etc.*).[14,50,53,54] Bridged compounds with bidentate ligands such as pyrazene (pyz) are also known.[55] In methanol, one of the chloride ligands is displaced to give the cationic 1 : 2 complexes $[Ru(\eta^6\text{-arene})ClL_2]^+$ **10** (L = PR_3, py, pyz; L_2 = bipy *etc.*)[56-58] which react further with PR_3 to generate dicationic species $[Ru(\eta^6\text{-arene})(PR_3)L_2]^{2+}$ **11**.[57,58] In some cases both chloride ligands may also be replaced directly to give similar 1 : 3 complexes $[Ru(\eta^6\text{-arene})L_3]^{2+}$ (L = N_2H_4, py)[59] Bidentate, anionic ligands give neutral 1 : 1 chelates $[Ru(\eta^6\text{-arene})Cl(L\text{-}L)]$ **11** (L-L = O_2CR, S_2PR_2, acac, pyrO) and 1 : 2 mixed mono- / bidentate compounds $[Ru(\eta^6\text{-arene})(L\text{-}L)_2]$ **13** (L-L

= O_2CR, S_2PR_2).[55,60-62] It is also noteworthy that a very recent report describes the synthesis of a π-toluene complex of type **10**, namely $[Ru(\eta^6\text{-}C_6H_5Me)Cl(PPh_3)_2][BF_4]$, by refluxing the sixteen electron *tris*(triphenylphosphine) compound $[RuCl_2(PPh_3)_3]$ in toluene after pre-treatment with a one mole equivalence of $Ag[BF_4]$.[63]

The benzene complex **7a** also reacts with alkylating reagents such as HgR_2 or SnR_4 in the presence of PPh_3 to give σ-alkyl compounds $[Ru(\eta^6\text{-}C_6H_6)Cl(R)(PPh_3)]$ (R = Me, Ph) and $[Ru(\eta^6\text{-}C_6H_6)Cl(\eta^3\text{-}C_3H_5)]$ (R = C_3H_5),[64] while reaction of **7a** with $Tl[C_5H_5]$ gives the monocationic sandwich compound $[Ru(\eta^6\text{-}C_6H_6)(\eta^5\text{-}C_5H_5)]Cl$.[64] The hydrido complex $[Ru(\eta^6\text{-}C_6H_6)(H)Cl(PPh_3)]$ is formed from the action of $Na[BH_4]$ upon **9** (L = PPh_3)[44] while action of Red-Al upon complexes of the type $[Ru(\eta^6\text{-}C_6Me_6)(PR_3)(O_2CCF_3)]^+$ (derived from **12**) results in the formation of the dihydrido compounds $[Ru(\eta^6\text{-}C_6Me_6)(H)_2(PR_3)]$ by displacement of the labile trifluoroacetate ligand. Protonation of the dihydrido complexes with $H[BF_4]$ leads to trihydrido compounds $[Ru(\eta^6\text{-}C_6Me_6)(H)_3(PR_3)][BF_4]$. Hydrido ruthenium(II) materials have also been synthesised from (arene)ruthenium(0) precursors such as $[Ru(\eta^6\text{-arene})(PR_3)_2]$; even weak acids such as $[NH_4][PF_6]$ will protonate and oxidise the metal centre to give (hydrido)ruthenium(II) compounds $[Ru(\eta^6\text{-}C_6Me_6)H(PR_3)_2][PF_6]$.[54,65,66]

Reaction of $[\{Ru(\eta^6\text{-arene})Cl(\mu\text{-}Cl)\}_2]$ **7** with $[NH_4][PF_6]$ in methanol gives an excellent yield of the triply chloride bridged cations $[(\eta^6\text{-arene})Ru(\mu\text{-}Cl)_3Ru(\eta^6\text{-arene})][PF_6]$ **13**, whereas shaking the benzene complex **7a** in ethanol with HCl in the presence of excess CsCl gives the mononuclear anionic complex $Cs[Ru(\eta^6\text{-}C_6H_6)Cl_3]$.[67] Hydroxide and alkoxide bridged analogues of **13** $[(\eta^6\text{-arene})Ru(\mu\text{-}OH)_3Ru(\eta^6\text{-arene})]^+$ **14a** (arene ≠ benzene) and $[(\eta^6\text{-arene})Ru(\mu\text{-}OR)_3Ru(\eta^6\text{-arene})]^+$ **14b** (R = Me, Et, Ph) have also been prepared by reaction of the appropriate chloro-bridged dimer with NaOR / ROH.[68] In the case of **14a** where arene = benzene a mixture of two products is formed: the unusual di-μ-hydroxo species $[(\eta^6\text{-arene})Ru(OH)(\mu\text{-}OH)_2Ru(H_2O)(\eta^6\text{-arene})]^+$ and a smaller quantity of the μ^4-oxo tetranuclear cation $[(\eta^6\text{-arene})_2Ru_2(\mu^2\text{-}OH)_2(\mu^4\text{-}O)Ru_2(\mu^2\text{-}OH)_2(\eta^6\text{-arene})]^{2+}$ **15**.[69] Reaction of **7a** in water with a two molar equivalence of $Na_2[CO_3]$ in the presence of excess $Na_2[SO_4]$ gives the tetrameric, cubane-like complex $[\{Ru(\eta^6\text{-arene})(\mu^3\text{-}OH)\}_4][SO_4]_2.12H_2O$ **16** in 25% yield.[70]

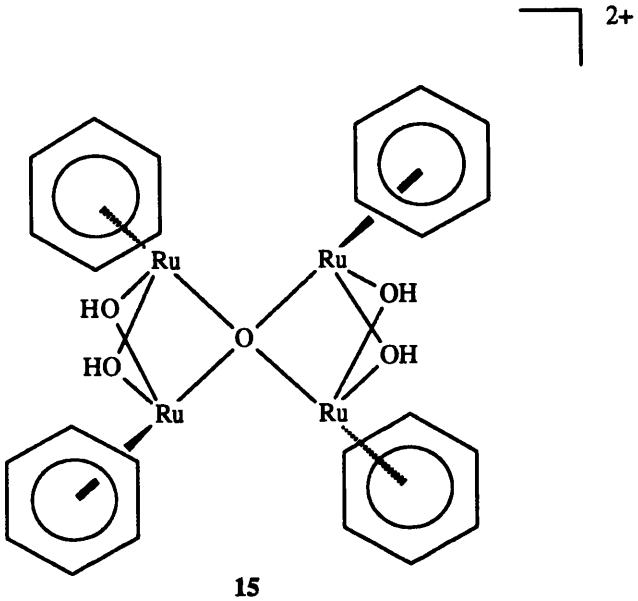

15

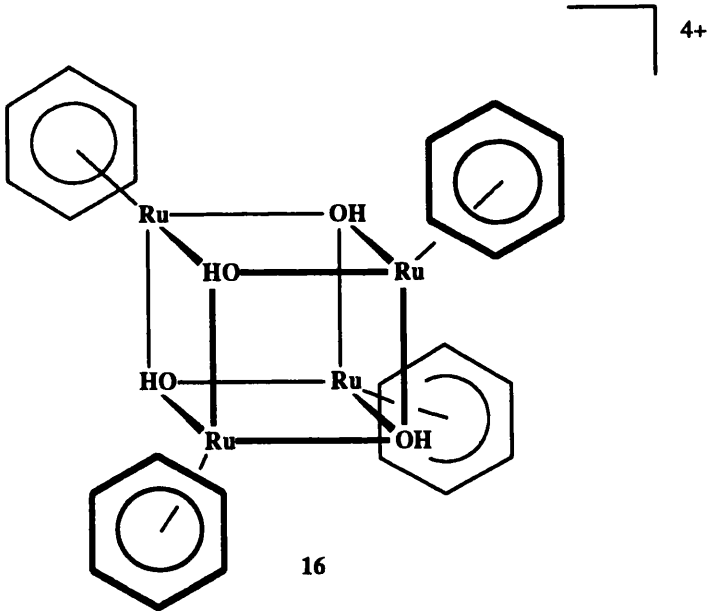

16

1.3 η^5-Dienyl and η^4-Diene Complexes

1.3.1 Reactivity of Bis*(Arene)Iron Complexes*

The relationship between η^6-arene, η^5-cyclohexadienyl and η^4-cyclohexadiene ligands has been extremely well summarised by Astruc using *bis*(hexamethylbenzene)iron(II) as a representative example, Scheme 1.3.[71]

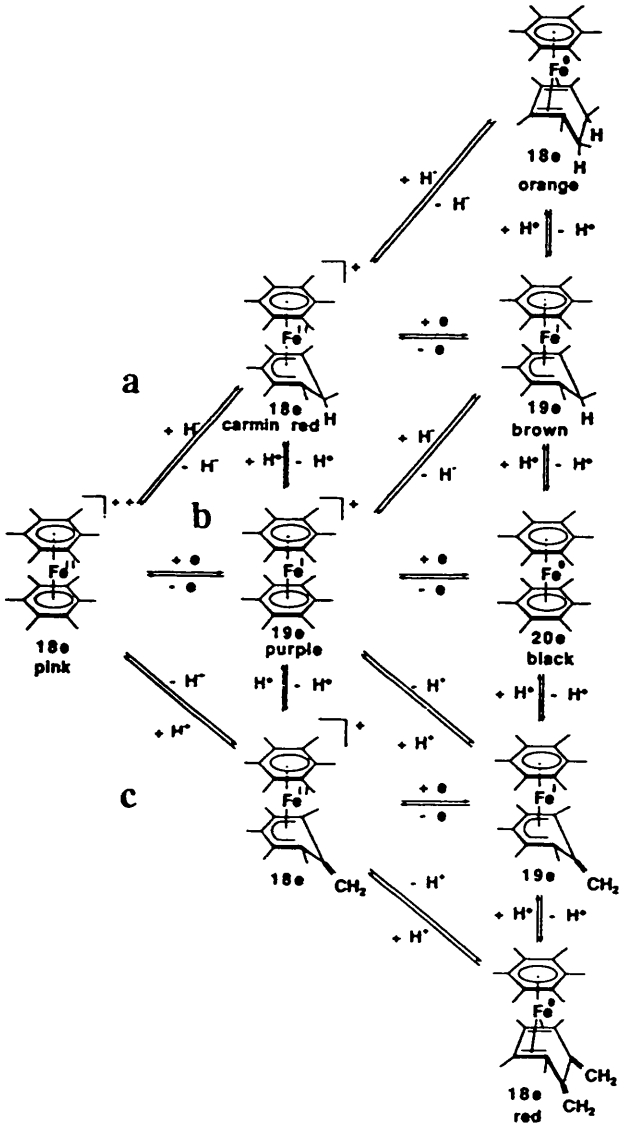

Scheme 1.3: The relationship between η^6-arene, η^5-cyclohexadienyl and η^4-cyclohexadiene ligands derived from *bis*(hexamethylbenzene)iron(II) (taken from ref. 71).

The arene rings in $[Fe(\eta^6\text{-}C_6Me_6)_2]^{2+}$ **17** and related complexes are strongly activated towards nucleophilic addition as a consequence of the electron withdrawing effect of the divalent metal centre. Donation of electron density from the arene π-system to the metal ion results in the formation of partial positive charges upon the ring carbon atoms and the complexes readily undergo addition by hydride[72] and a range of other nucleophiles, N (N = CN^-, $CH_2NO_2^-$, $CHCH_3NO_2^-$ and $CH_2COO^tBu^-$)[73] to generate η^5-cyclohexadienyl products of type $[Fe(\eta^6\text{-}C_6R_6)(\eta^5\text{-}C_6R_6N)]^+$ **18** with the nucleophile in the *exo* position, as shown in Scheme 1.3a. Unsubstituted cyclohexadienyl complexes such as **18** (N = H) and a wide range of related compounds, display an interesting ν(CH) absorption in their infrared spectra at exceptionally low wavenumber (*ca.* 2830 - 2700 cm^{-1}) which is absent in the case of free cyclopentadiene (which has a similar half-boat conformation).[74,75] X-ray crystallographic measurements along with deuteriation studies[74,76,77] have established that this band is associated with the C-H_{exo} bond of the cyclohexadienyl CH_2 group whilst the analogous C-H_{endo} vibration occurs at *ca.* 2950 cm^{-1}. The anomalously low wavenumber of the absorption is thought to be intimately connected with the metal atom in some way, although the precise nature of the interaction is unknown. Maitlis *et al.* have also noted that the observation of the band in solution spectra is somewhat solvent dependent.[39]

Addition of a second nucleophile to complexes of type **18** results in further addition to the cyclohexadienyl ring to give η^4-1,3-diene species of Fe(0), $[Fe(\eta^6\text{-}C_6R_6)(\eta^4\text{-}C_6R_6NN')]$ **19**. This reactivity has been used as the basis for a versatile synthetic route to a range of 5,6-disubstituted cyclohexa-1,3-diene complexes such as $[Fe(\eta^6\text{-}C_6H_6)\{\eta^4\text{-}$*exo,exo*-5-$(PhCH_2)$-6-$(CN)C_6H_6\}]$ which has been characterised by X-ray crystallography, Fig. 1.4.[78]

Synthesis of diene compounds of the type shown in Fig. 1.4 is complicated by the occurrence of competing electron transfer reactions in complexes of type **17** on the addition of almost all* carbon donor nucleophiles.[78] Electron transfer to the pink complex $[Fe(\eta^6\text{-}C_6Me_6)_2]^{2+}$ **17** results in the formation of the purple, 19 electron species $[Fe(\eta^6\text{-}C_6Me_6)_2]^+$ and ultimately the black, 20 electron compound $[Fe(\eta^6\text{-}C_6Me_6)_2]$, Scheme 1.3 -

* Recent work has demonstrated, however, that *bis*(arene)iron dications may be ethylated in high yield through the use of $AlEt_3$. The reaction proceeds through transfer of an ethyl radical to 19 electron electron transfer species formed in the early stages of the reaction. [78]

path *b*. The reduced products are isolable, crystalline solids (although highly air sensitive). An extensive amount of work has been carried out on the prototypical 19 electron [Fe(η^5-C_5H_5)(η^6-C_6Me_6)] **20** which is stable up to 100°C. The presence of an additional electron in the antibonding e_1^* SOMO (Fig. 1.2) in **20** results in an overall lengthening of the M-C_5H_5 ring centroid bond by *ca.* 0.1 Å. Also, the degenerate nature of the e_1^* orbital coupled with the large size differences between the two rings give rise to an alternating structure exhibiting dynamic Jahn-Teller distortions along the lattice in the solid state. Supersaturated species of this type often find application as "electron reservoirs" in redox catalysis and stoichiometric reduction.[78]

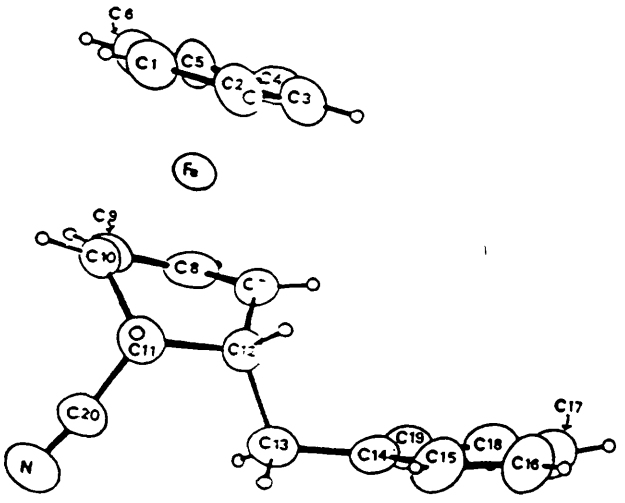

Fig. 1.4: Crystal structure of [Fe(η^6-C_6H_6){η^4-*exo,exo*-5-($PhCH_2$)-6-(CN)C_6H_6}]

Complexes such as **17** containing α-hydrogen atoms with respect to the arene ring (*e.g.* the methyl protons of the hexamethylbenzene rings in **17**) undergo deprotonation in the presence of strong bases such as NaOH or KO^{t}Bu to give, ultimately, 18 electron *o*-xylyene compounds such as [Fe(η^6-C_6Me_6){η^4-$C_6Me_4(CH_2)_2$}] **21** in which the metal atom is bound to two of the endocyclic double bonds (Scheme 1.3 - path *c*). The reaction is assumed to pass through the cyclohexadienyl complex [Fe(η^6-C_6Me_6){η^5-$C_6Me_5(CH_2)$}]$^+$

although this material, along with its 19 electron reduced analogue, has yet to be isolated.[78] In contrast, the ruthenium complexes $[Ru(\eta^6\text{-}C_6Me_6)\{\eta^4\text{-}C_6Me_4(CH_2)_2\}]$ **22** and $[Ru(\eta^6\text{-}C_6Me_6)\{\eta^5\text{-}C_6Me_5(CH_2)\}]^+$ **23** are both well known[80,81] as are their respectively neutral and anionic manganese tricarbonyl analogues.[82] Bennett has also prepared a range of Ru(0) *o*-xylylene compounds $[Ru\{\eta^4\text{-}C_6Me_4(CH_2)_2\}(PR_3)_3]$ **24** in which the metal atom is bound to the exocyclic double bonds. The migration of the metal from the endo- to exocyclic olefinic functionalities is a result of the temporary creation of a vacant coordination site of the metal during the synthesis.[83] Attempted deprotonation of xylene derivatives and other less methylated arenes has resulted in the formation of complex mixtures of products in low yields.[80]

Compound **22** reacts with $H[BF_4]$ to give **23** and with a second mole of acid to re-generate $[Ru(\eta^6\text{-}C_6Me_6)_2]^{2+}$. Treatment of **22** with methyl triflate gives an excellent yield of the 1,2-diethyltetramethylbenzene complex $[Ru(\eta^6\text{-}C_6Me_6)(\eta^6\text{-}C_6Me_4Et_2)]^{2+}$.[80] In contrast, single protonation of the exocyclic compounds **24** results in the fluxional agostic species $[Ru\{\eta^3\text{-}(HCH_2)(CH_2)C_6Me_4\}(PR_3)_3]^+$ **25**.

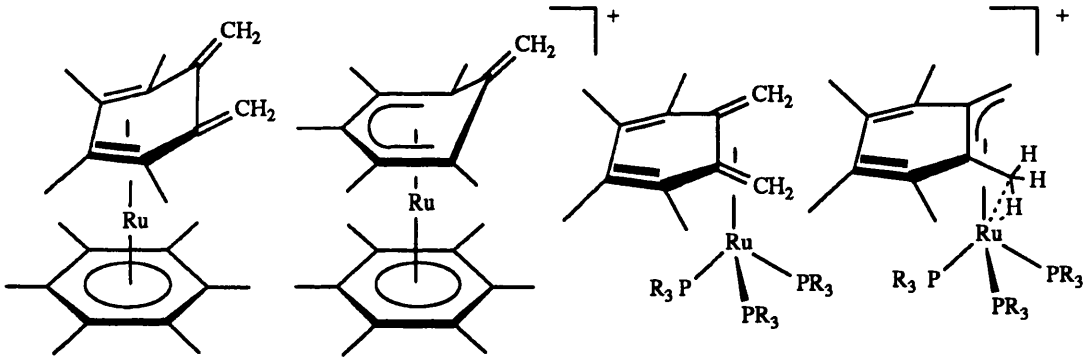

22 **23** **24** **25**

1.3.2 Nucleophilic Addition to Bis*(Arene)Ruthenium Complexes*

Like their iron analogues, *bis*(arene) ruthenium complexes and related half sandwich $[Ru(\eta^6\text{-arene})L_3]^{2+}$ species undergo single nucleophilic additions with a wide range of nucleophiles to generate *exo* cyclohexadienyl products of the form $[Ru(\eta^6\text{-}C_6R_6)(\eta^5\text{-}C_6R_6N)]^+$ **26** and $[Ru(\eta^5\text{-}C_6R_6N)L_3]^+$ **27** (N = H, Me, Ph, CN, OH, OMe, PR_3, POR_3 *etc.*).[11,58,84-86] Nucleophilic additions to (arene)ruthenium complexes are charge controlled[11] and attack occurs at the less alkylated of the two arene rings, *i.e.* the one which bears the greatest partial positive charge. Unlike the iron complexes, no electron transfer products are observed in reactions with carbon donor nucleophiles and in this respect nucleophilic additions to (arene)ruthenium compounds represents a more robust method for the functionalisation of arenes,[8] although they are *ca.* thirty times less electrophilic than their iron analogues.[84]

Ruthenium analogues of supersaturated iron compounds such as the 20 electron $[Fe(\eta^6\text{-}C_6Me_6)_2]$ may be synthesised by aluminium metal reduction of the corresponding Ru(II) dications[7] but in the ruthenium case the metal maintains an eighteen electron configuration by bonding to only two double bonds of one of the arenes to give an η^4-,η^6-coordinated metal with zero magnetic moment.[7,27]

Addition of two nucleophiles to *bis*(arene)ruthenium dications results in a single attack at each η^6-ring to give *bis*(cyclohexadienyl)ruthenium(II) compounds $[Ru(\eta^5\text{-}C_6R_6N)_2]$ **27** (N = Me, Ph) even in the hindered, unsymmetrical complex $[Ru(\eta^6\text{-benzene})(\eta^6\text{-1,3,5-tri}$*iso*$\text{propylbenzene})]^{2+}$,[8] although in some cases when N = H, (1,3-diene)ruthenium(0) compounds [analogous to the (1,3-diene)iron species] have been reported.[9-11]

1.3.3 Charge and Orbital Control in Nucleophilic Addition Reactions

The differing regioselectivities observed for *bis*(arene)iron complexes and their ruthenium analogues towards the addition of two nucleophiles [*i.e.* formation of (arene)-(diene) versus *bis*(cyclohexadienyl) species] has been partially explained in terms of two principal governing factors. The nucleophilic additions to the ruthenium complexes are thought to be "charge controlled", *i.e.* nucleophiles add at the site of greatest partial positive charge.[11] Extended Hückel calculations on the representative cyclohexadienyl iron

complex $[Fe(\eta^6\text{-}C_6H_6)(\eta^5\text{-}C_6H_7)]^+$ have demonstrated that the greatest partial positive charges lie upon the η^6-ring (+0.04 to +0.08, Fig. 1.5).

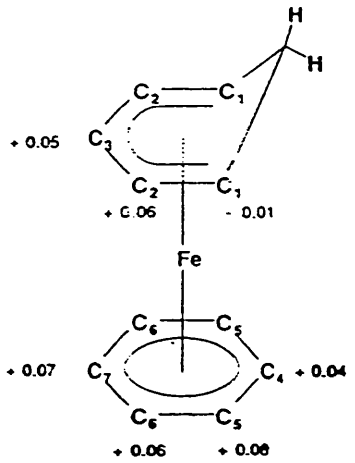

Fig. 1.5: Nett charges on carbon atoms in $[Fe(\eta^6\text{-}C_6H_6)(\eta^5\text{-}C_6H_7)]^+$.

The product of a charge controlled nucleophilic addition to this species would thus be expected to be a *bis*(cyclohexadienyl) compound and this is consistent with the observed products in the ruthenium series. In the iron analogues however, addition occurs at C_1 (Fig. 1.5 - confirmed by deuteriation studies), the site of *least* partial positive charge, indicating that the reaction is not charge controlled.[87] This has been rationalised by a frontier molecular orbital model devised by Astruc.[87] In a nucleophilic addition to a cyclohexadienyl ligand in complexes such as $[Fe(\eta^6\text{-}C_6H_6)(\eta^5\text{-}C_6H_7)]^+$ the lone pair of the nucleophile is expected to interact most strongly with the complexes' lowest unoccupied molecular orbitals (LUMO). In the proposed MO scheme, Fig. 1.6, two LUMOs, IV(S) and V(A) which are respectively symmetric (S) and antisymmetric (A) with respect to the cyclohexadienyl ligand mirror plane, lie relatively close together in energy. The largest (and almost equal) contributions to these orbitals come from C_1 and C_3 and so, in the first instance, attack would be expected to occur at either of these positions.

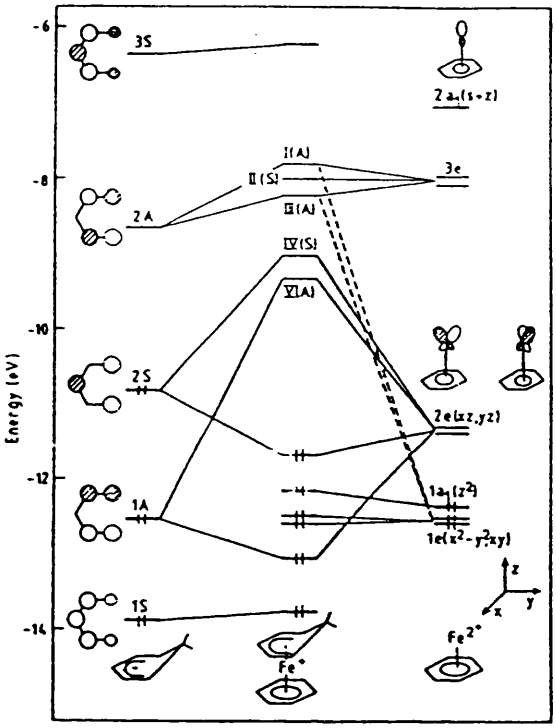

Fig. 1.6: Molecular orbital diagram for $[Fe(\eta^6\text{-}C_6H_6)(\eta^5\text{-}C_6H_7)]^+$ constructed from the combination of basis orbitals from $(C_6H_6)Fe^{2+}$ and $C_6H_7^-$ (taken from ref. 87).

In gauging whether either C_1 or C_3 is a particularly more likely site for nucleophilic addition, the remaining unoccupied molecular orbitals, I(A), II(S) and III(A), must also be taken into consideration. For symmetry reasons C_3 may only contribute to orbitals of the S type. In this group of three only II(S) possesses the appropriate symmetry and this orbital is entirely localised upon the benzene (and not cyclohexadienyl) ring of the complex. Hence C_1 has by far the largest total contribution to the complex's unoccupied molecular orbitals and is therefore the most favoured site for nucleophilic attack.

This rationalisation has been tested by calculation of the interaction energies for H^- with $[Fe(\eta^6\text{-}C_6H_6)(\eta^5\text{-}C_6H_7)]^+$ at a distance of 2.0 Å away from C_1, C_2, C_3 and C_5. These results, unfortunately, are only in accord with attack solely at C_1 if the cyclohexadienyl moiety is assumed to be *planar*, because of unfavourable steric interactions in the more

realistic half-boat geometry. Furthermore, doubt has been cast upon the applicability of the Extended Hückel method to charged compounds, and clearly experimental results indicate that attack at C_3 and C_5 cannot be ruled out.[7,73] Extended Hückel calculations however, can overestimate the magnitude of steric interactions and on balance the model does represent a good qualitative rationalisation of the experimental observations.[87]

1.4 η^3-Allyl Complexes

1.4.1 Simple Allyl Transition Metal Complexes

The first binary allyl metal complex to be isolated was *bis*(η^3-allyl)nickel(II), [Ni(η^3-C_3H_5)$_2$] **28**[88] and complexes of Ni, Pd and Pt are amongst the most common allyl transition metal species. Compound **28** may be synthesised directly from the interaction of $NiBr_2$ with allyl magnesium bromide but the isolation must be performed at low temperature (-10°C) because of the high thermal lability of the complex. Compound **28** also spontaneously inflames in air but is stable to hydrolysis in ether solution. This synthetic route is general and extremely versatile and may be used to form a number of binary species such as [Co(η^3-C_3H_5)$_3$],[23] and [Mo$_2$(μ-η^3-C_3H_5)$_2$(η^3-C_3H_5)$_2$].[89,90] Similarly, action of (allyl)MgCl (allyl = C_3H_5, 2-MeC_3H_4) upon the polymeric ruthenium(II) cyclooctadiene complex [{Ru(C_8H_{12})Cl$_2$}$_n$] gives the *bis*(allyl) compound [Ru(η^4-C_8H_{12})(η^3-allyl)$_2$] **29**.[91] Synthetically useful dichloride dimers such as [{Pd(η^3-allyl)(μ-Cl)}$_2$][23] and [{Rh(η^3-allyl)$_2$(μ-Cl)}$_2$] **30**[92] structurally related to **7**, may also be prepared by a variety of routes such as interaction of metal halide salts with allyl halide or with olefin in the presence of base, or oxidative hydrolysis of CO from carbonyl compounds such as [{RhCl(CO)$_2$}$_2$].[92,93] Further reaction of **30** with allylmagnesium chloride gives *tris*(allyl)rhodium(III), [Rh(C_3H_5)$_3$].[94]

The tri-ruthenium cluster [Ru$_3$(CO)$_{12}$] undergoes oxidative addition of allyl bromide at 60°C over a period of hours to give the mononuclear complex [Ru(η^3-C_3H_5)Br(CO)$_3$][95] while a recent report[96] describes the synthesis of substituted allyl palladium species with good *syn* / *anti* control by the oxidative addition of allyl trifluoroacetates in the presence of hindered phenanthrolines.

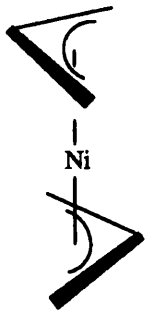

28

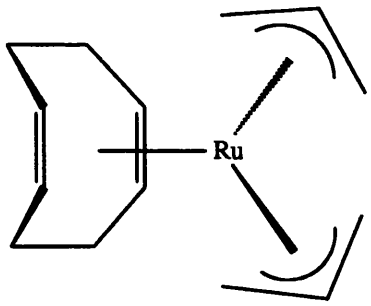

29

Another important route to metal-allyl species is *via* partial hydrogenation of coordinated olefins, often as a result of metal to ligand hydride transfer. Recent work has shown that the η^6-cyclooctatriene, η^4-isoprene complex $[Ru(\eta^6\text{-}C_8H_{10})(\eta^4\text{-}C_5H_8)]$ reacts with $H[BF_4]$ in the presence of CO to generate a 17 : 83 mixture of the 1,1- and 1,2-dimethylallyl complexes $[Ru(\eta^6\text{-}C_8H_{10})(\eta^3\text{-}C_5H_9)(CO)][BF_4]$ **31**.[97] (The η^6-cyclooctatriene ligand along with other non-arene η^6-ligands, is discussed in Section 1.5.) Similarly, dropwise addition of HCl in diethyl ether to the η^4-trimethylenemethane complex $[Ru(\eta^6\text{-}C_6Me_6)\{\eta^4\text{-}C(CH_2)_3\}]$ gives the 2-methylallyl compound $[Ru(\eta^6\text{-}C_6Me_6)(\eta^3\text{-}C_3H_4Me)Cl]$ **32**.[98]

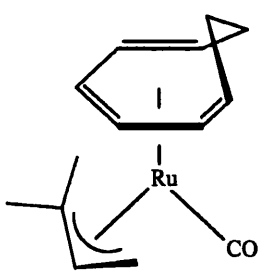

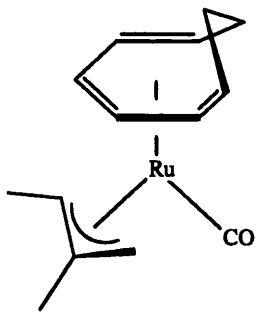

31

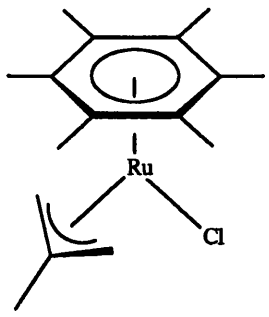

32

Reaction of $[Cr(PR_3)_2Cl_2]$ with allylmagnesium chlorides generates the thermally unstable, red *bis*(allyl)chromium(II) compounds $[Cr(PR_3)_2(\eta^3\text{-}C_3H_4R')_2]$ **33** (R' = H, Me;

PR_3 = PMe_3, PPh_2Me; $(PR_3)_2$ = dmpe, $^iPr_2PC_2H_4P^iPr_2$). These materials decompose above *ca.* -40°C to give low yields of *tetrakis*(allyl)Cr_2 complexes. At -70°C in thf, the 1-methylallyl analogue of **33** (PR_3 = PMe_3) is formed only as a transient and isomerises rapidly *via* an intramolecular reductive coupling to give $[Cr(PMe_3)_2(\eta^2{:}\eta^2\text{-}C_8H_{14})]$ which exists as a mixture of 2,6-octadiene and 3-methyl-1,5-heptadiene isomers.[99]

The vast majority of η^3-allylic complexes exhibit a symmetrical mode of bonding with the two C-C bond lengths equal and all the carbon atoms approximately equidistant from the metal. The dirhodium *bis*(allyl)dimer **30** was initially shown by X-ray crystallography[100] to involve double bond localisation along with unequal Rh-Cl bond distances. A more recent re-determination of the structure has shown that the allyl functionalities are, in fact, symmetrically bound and the Rh-Cl distances are approximately equal.[101] A genuinely asymmetric class of allylic complexes is formed however, by reaction of the hydrido ruthenium(II) compound $[RuCl(CO)(H)(PPh_3)_3]$ **34** with the acetylenes *trans*-$(R^1)CH{=}CHC{\equiv}CR^2$ (R^1, R^2 = Me, Et, ^{t}Bu, $SiMe_3$) to give the highly unsymmetrical, apparently sixteen electron η^3- / η^1-complexes $[Ru\{\eta\text{-}(R^2)CH{=}CCH{=}CHR^1\}Cl(CO)(PPh_3)_2]$ **35**, Fig. 1.7.[102]

Deuteriation studies, in conjunction with X-ray diffraction measurements, indicate that, after coordination of the acetylenes *via* the C≡C bond, the hydride ligand is transferred to the terminal site of the acetylinic functionality while the carbon atom C_3 remains bound to the metal centre, Ru-C_3 2.044(4) Å. The double bond between C_2 and C_1 is only very weakly bound to the ruthenium ion, the metal-carbon distances being 2.336(5) and 2.627(5) Å respectively.

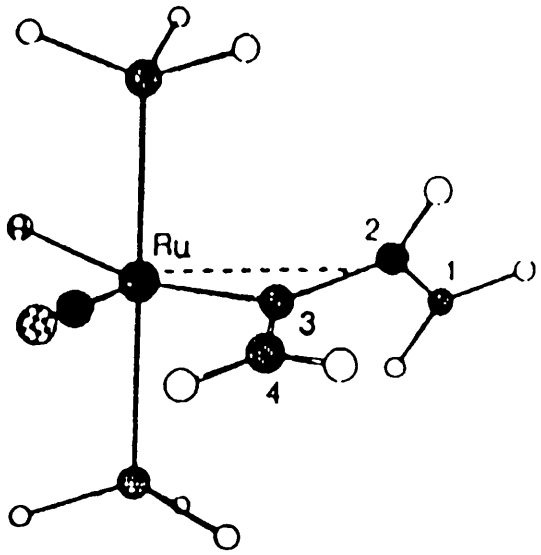

Fig. 1.7: *Ab initio* calculated structure of the highly asymmetric allyl complex $[RuCl(CO)(PPh_3)_2\{\eta\text{-}(R^1)CH{=}CCH{=}CH(R^2)\}]$ **35** ($R^1 = R^2 = H$). (Confirmed by X-ray structure determinations of related examples $R^1 = R^2 = SiMe_3$, Ph and $R^1 = {}^tBu$, $R^2 = Et$[102]).

1.4.2 Reaction of Simple Transition Metal Compounds with Olefins

Some of the most catalytically important allylic transition metal species result from the oxidative coupling of coordinated olefins. Such species are often transients in catalytic cycles but, in some cases may be isolated.[103] Olefin complexes of Ni(0), because of their high thermal lability, are especially good catalysts for olefin polymerisation. For example, the reaction of the cyclododecatriene (cdt) complex $[Ni(\eta^2{:}\eta^2{:}\eta^2\text{-}C_{12}H_{18})]$ **36** (or any other source of "naked" nickel) with butadiene at 20°C results in the formation of free cdt in proportion to the amount of butadiene added.[103] At -40°C exactly three moles of butadiene are taken up per mole of catalyst and the intermediate *bis*(allyl)nickel(II) species $[Ni(\eta^3{:}\eta^2{:}\eta^3\text{-}C_{12}H_{18})]$ **37** may be crystallised. Warming **37** in solution, to room temperature

results in the re-formation of **36**, Scheme 1.4. Addition of donors such as PPh_3 and especially tri(2-biphenyl)phosphite results in a drastic spectator ligand effect. The strongly bound P-donor effectively blocks one of the coordination sites of the active catalyst, allowing only two butadiene molecules to coordinate. These couple in the same way as before to give cyclooctadiene in up to 95% selectivity.

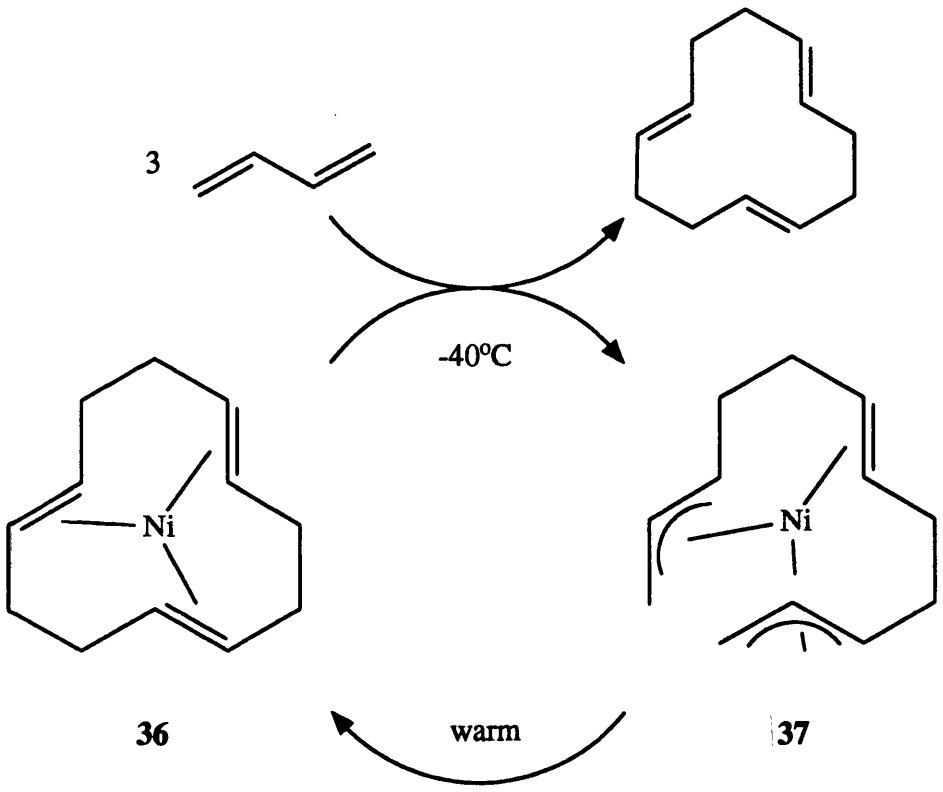

Scheme 1.4: Nickel catalysed cyclotrimerisation of butadiene.

These results are consistent with the reactivity of the sixteen electron compound **28** which also undergoes an intramolecular coupling in the presence of electron donors to give, ultimately, the free organic molecule diallyl (C_6H_{10}). Reaction of the closely related [Pd(η^3-allyl)$_2$] with butadiene in the presence of PMe_3 results in coupling of the butadiene to give the η^1:η^3-octadienediyl Pd(II) complex [Pd(η^1:η^3-C_8H_{12})(PMe_3)] **38**.[88,104] In contrast, the *bis*(allyl)ruthenium complex **29**[91] does not couple in the presence of two electron

ligands, even at elevated temperatures. However, reaction of ruthenium trichloride hydrate with butadiene in refluxing 2-ethoxyethanol (*ca.* 90°C) does result in trimerisation of butadiene to give the *bis*(allyl)ruthenium(IV) species $[Ru(\eta^3:\eta^2:\eta^3\text{-}C_{12}H_{18})Cl_2]$ **39**,[105-107] a reaction exactly analogous to the formation of the Ni(II) complex **37**. Unlike **37** however, **39** is stable and does not yield free cdt under normal laboratory conditions. Its existence and structure, confirmed by X-ray crystallography (Fig. 1.8),[105,107] provides strong evidence for the formulation of the more unstable nickel analogue.

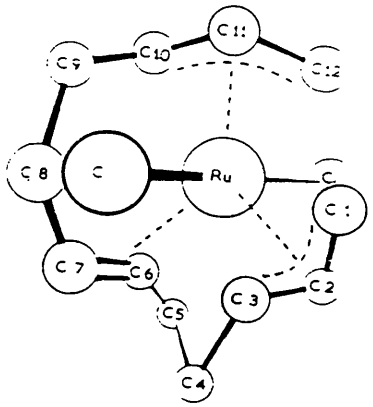

Fig. 1.8: X-ray crystal structure of the *bis*(allyl)ruthenium(IV) complex $[Ru(\eta^3:\eta^2:\eta^3\text{-}C_{12}H_{18})Cl_2]$ **39**.

In contrast to nickel and ruthenium, interaction of $RhCl_3.3H_2O$ with butadiene at low temperature (-10°C) results in neutral coordination of the organic to give the *bis*(butadiene)Rh(I) compound $[RhCl(\eta^4\text{-}C_4H_6)_2]$ **40**.[108,109] At room temperature however, a complex of Rh(III) is obtained, $[Rh_2(\eta^3\text{-}C_4H_7)_2Cl_2(\mu\text{-}Cl)_2(\mu\text{-}C_4H_6)]$ **41**, which contains a butadiene bridge as well as two crotyl (1-methylallyl) ligands.[110]

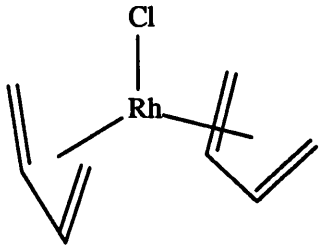

40

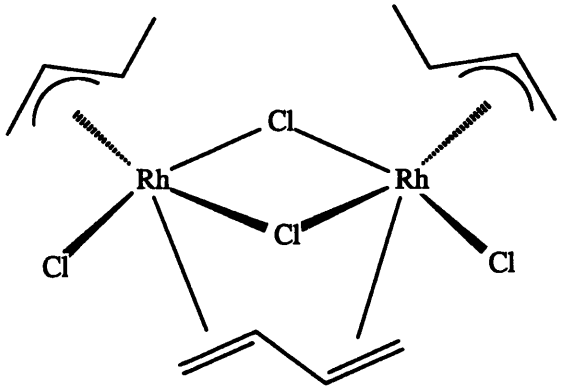

41

Reaction of "$RuCl_3.xH_2O$" with isoprene (2-methylbutadiene) in ethanol at 70°C[12,13] results in the formation of the oxidatively coupled ruthenium(IV) complex $[\{Ru(\eta^3:\eta^3\text{-}C_{10}H_{16})Cl(\mu\text{-}Cl)\}_2]$ **6**, as mentioned in Section 1.1. The reaction is related to the formation of **39** except that the hindered, methylated diene dimerises, rather than trimerises, at the metal, in a tail-to-tail fashion, to give the $\eta^3:\eta^3$-2,7-dimethylocta-2,6-diene-1,8-diyl ligand **2**. Also as in the case of **39**, cyclisation does not readily take place and the complex possesses a high degree of stability.

In spite of their apparent stability **6** and **39** have been examined as catalysts for a number of olefin polymerisations. Complex **6** is known to be an active catalyst for the ring opening polymerisation of norbornene as well as other, non-strained cycloolefins.[111] A number of catalytic applications of **39**, such as acrylonitrile dimerisation, olefin hydrogenation, butane dehydrogenation and methacrylate polymerisation are also known.[112] In the presence of controlled amounts of tertiary phosphine, **6** and **39** catalyse the polymerisation of butadiene to *cis*-1,4-, *trans*-1,4- and 1,2-polybutadiene.[113] The related Ziegler-Natta head-to-tail polymerisation of isoprene is an extremely important step in the synthesis of 1,4-*cis*-polyisoprene which has almost identical properties to natural rubber.[103] It has been suggested that the majority of these catalytic reactions in the ruthenium complexes, take place by metathesis and indeed **6** has recently been shown to be an excellent source of "free" Ru^{2+} ions.[114] In the case of diene polymerisations especially

however, **6** and **39** have been regarded as good models for the growing end of the active catalyst.[113]

Other examples of allyl ruthenium complexes derived from olefins include the dimerisation of ethylene to give the 1-methylallyl complex $[Ru(Cp^*)(\eta^3\text{-}C_4H_7)(\eta^2\text{-}C_2H_4)]$ which has been recently reported to be formed in the reaction of the sixteen electron compounds $[\{Ru(Cp^*)(OMe)\}_2]$ with ethylene under 2 bar pressure at room temperature. The analogous reaction with propylene results in deprotonation to give the unsubstituted $\eta^3\text{-}C_3H_5$ analogue. At low temperature unstable olefin adducts are also observed.[115]

1.4.3 Reactions of Bis*(Allyl)Ruthenium Complexes*

In spite of the catalytic properties of **6** and **39** and the extensive body of knowledge concerning related (arene)ruthenium(II) compounds such as **7**,[41-44] prior to this study only a few sporadic investigations had been made of their chemistry. Like complexes **7**, **6** undergoes bridge rupture in the presence of Lewis bases to generate mononuclear adducts of the form $[Ru(\eta^3{:}\eta^3\text{-}C_{10}H_{16})Cl_2L]$ **42** (L = CO, py, PR_3 and PF_3)[12,15,16] analogous to **9**, with the two electron ligand occupying an equatorial coordination site of the trigonal bipyramidal metal ion.* Similarly, in coordinating solvents, solvato adducts are formed with solvent molecules usually occupying an equatorial site, although in MeCN the predominant species is apparently an axial adduct.[17] In non-coordinating solvents **6** has been shown by ^1H NMR spectroscopy to exist in two diastereomeric forms, **6a** and **6b**, of respectively C_i and C_2 molecular symmetries, as a consequence of the chirality of the "$(\eta^3{:}\eta^3\text{-}C_{10}H_{16})Ru$" fragment.[17] These species are present in approximately equimolar proportions ($[C_2]/[C_i]$ = 1.25 at 25°C) and interconvert at room temperature at a rate k = *ca.* 0.3 s^{-1} *via* bridge rupture and exchange of mononuclear units. During the course of this work a number of other reports concerning the chemistry of **6** have appeared and these will be referred to at the appropriate points.

---

* If the allylic functionalities of the ligand **2** are taken as occupying two coordination sites each then the coordination geometry about the metal centres in **6** and **39** is best described as distorted pentagonal bipyramidal.[107] Current convention however, favours description of the geometry as trigonal bipyramidal which makes the complexes easier to visualise. The latter convention will be adopted in this thesis.

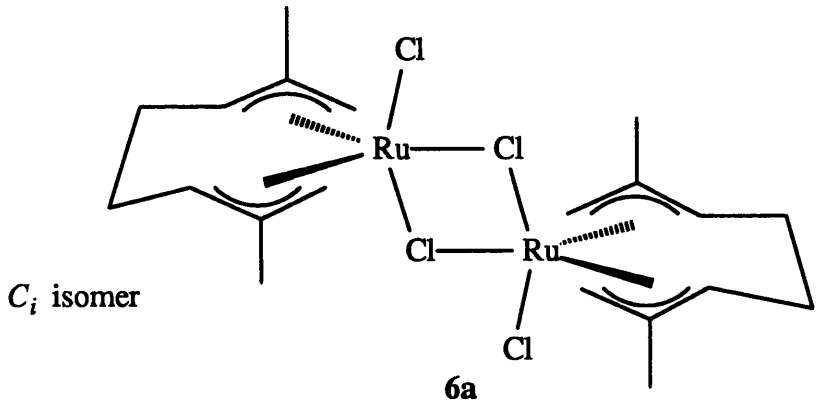

C_i isomer

6a

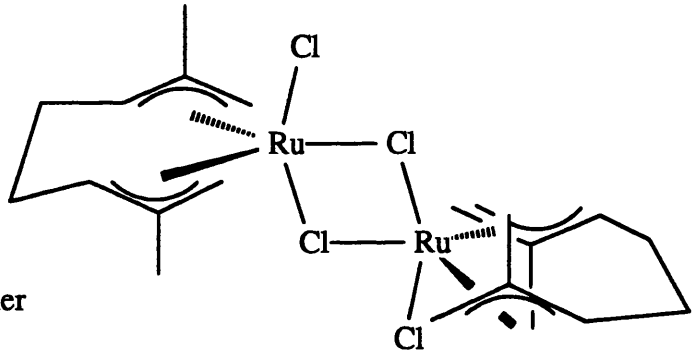

C_2 isomer

6b

A single study[116,117] has also been made into the chemistry of **39** which is found to react with MeMgI to give the mono-methyl complex $[Ru(\eta^3:\eta^2:\eta^3\text{-}C_{12}H_{18})(Me)I]$ **43**, and with MeLi to give the thermally unstable dimethyl analogue. Reaction of **43** with electron donors L (L = CO, ^{t}BuNC or $P(OR)_3$) results in reductive coupling to give the (allyl)ruthenium(II) compound $[Ru\{\eta^3\text{-}C_3H_4(CH_2)_2CH{=}CH(CH_2)_2CH(Me)CH{=}CH_2\}(L)_3I]$ **44**. These results are summarised in Scheme 1.5.

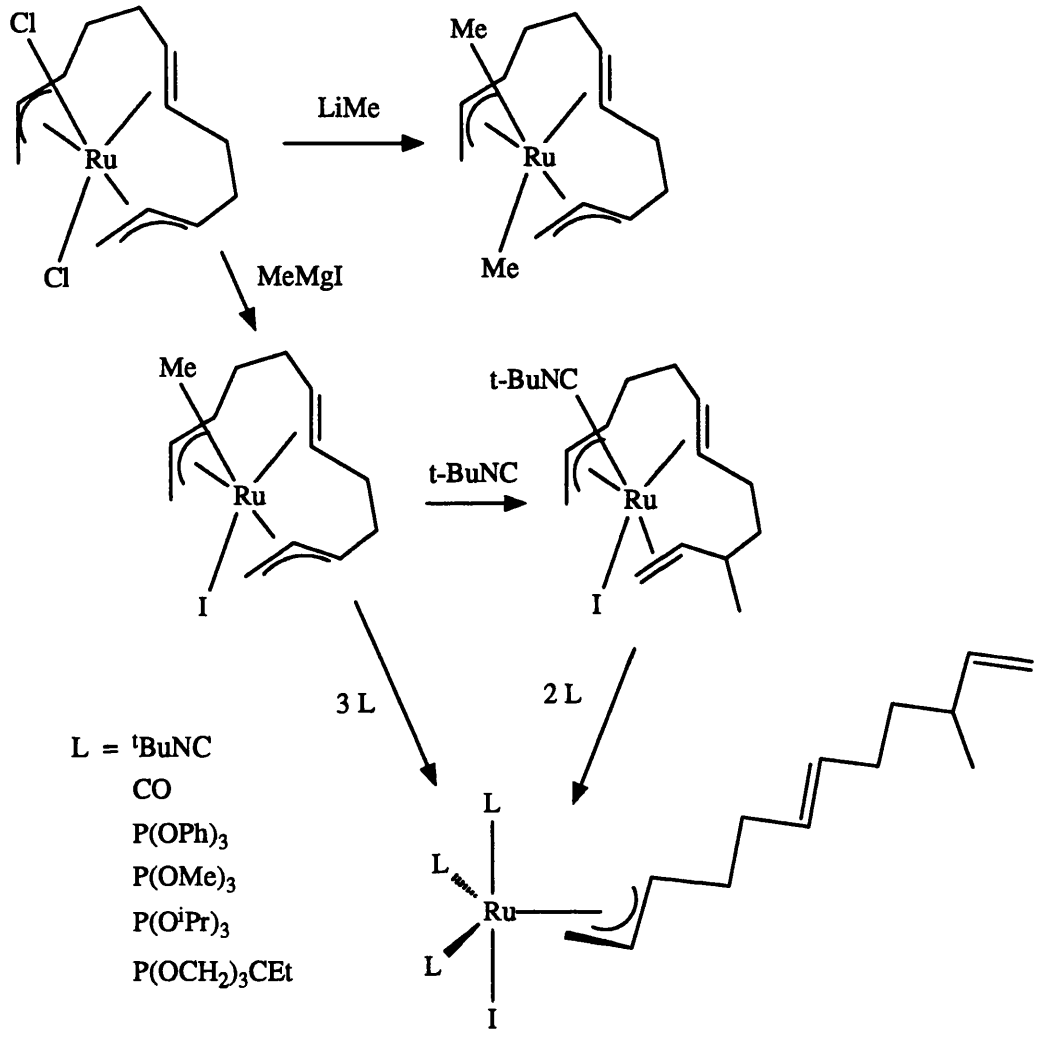

Scheme 1.5: Reactions of $[Ru(\eta^3:\eta^2:\eta^3\text{-}C_{12}H_{18})Cl_2]$ **39**.

1.5 Other η^6-Complexes

1.5.1 Cyclic Trienes and Tetraenes

Reflux of "$RuCl_3.xH_2O$" in ethanol in the presence of 1,3,5-cycloheptatriene (cht) yields dimeric $[\{Ru(\eta^6\text{-}C_7H_8)Cl(\mu\text{-}Cl)\}_2]$ **45** containing an η^6-cht ligand. The reaction of "$RuCl_3.xH_2O$" with 1,3,5,7-cyclooctatetraene (cot) over several days, results in hydrogenation to give $[\{Ru(\eta^6\text{-}C_8H_{10})Cl_2\}_n]$ **46** ($n \geq 2$)[97] (rather than $[\{Ru(C_8H_8)Cl_2\}_n]$ as

previously reported[118,119]). The analogous reactions of norbornadiene (nbd) and 1,5-cyclooctadiene (cod) give related polymeric products $[\{Ru(diene)Cl_2\}_n]$ **47** in which the dienes probably bind in an η^4- fashion.[118] Like the closely related arene compounds **7**, complexes **45** and **46** undergo bridge cleavage reactions to give adducts related to **8**.[97,120] Reduction of **45** and **46** with *iso*-propyl Grignard reagent or Na/Hg amalgam in the presence of dienes such as nbd or cod, or reaction of the diene complexes **47** with $K_2[C_8H_8]$ gives Ru(0) complexes of general form $[Ru(\eta^6\text{-triene})(\eta^4\text{-diene})]$ (triene = cht **48a**, 1,3,5-cyclooctatriene **48b**) analogous to the arene species (Section 1.3).[121] Such complexes are of interest as potential catalyst precursors[122-124] and in the synthesis of new functionalised olefins.[97,125]

Complex **48a** readily undergoes hydride abstraction, to give $[Ru(\eta^7\text{-}C_7H_7)(\eta^4\text{-diene})]^+$ **49** which contains the cycloheptatrienyl (tropylium) ligand.[125]

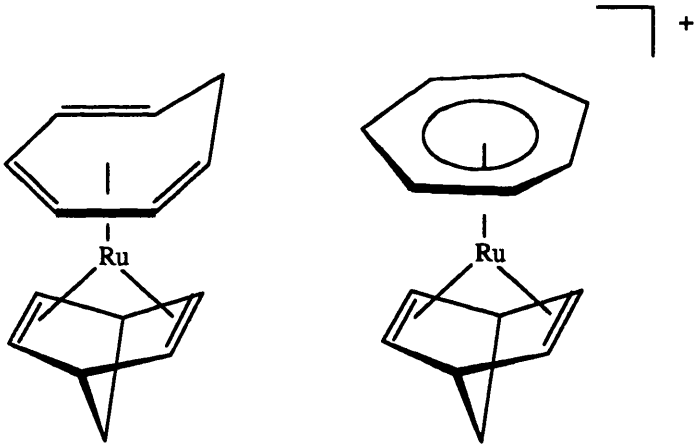

48a **49**

Tropylium, while formally a seven electron ligand, is best described as a cation $[C_7H_7]^+$ giving it an aromatic, six π-electron configuration. This is clearly demonstrated by the crystal structure of the vanadium compound $[V(\eta^7\text{-}C_7H_7)(CO)_3]$, in which all the C-C bond lengths are equal (1.39 Å), and the tropylium ligand is planar.[23] The crystal structure of the isoelectronic η^6-cht Mo(0) complex $[Mo(\eta^6\text{-}C_7H_8)(CO)_3]$ **50** conversely, demonstrates the localised nature of the olefinic functionalities in the neutral triene, with alternating bond lengths of *ca.* 1.34 and 1.43 Å and the obvious out of plane distortion of the CH_2 group. Complexes such as **49** and tropylium containing cations derived from **50**

undergo nucleophilic addition to re-generate η^6-cycloheptatriene species with the nucleophile in the *exo* position.[23,125] Further nucleophilic addition of β-diketonates (L) (as their Tl salts) to the η^6-cht phosphine or arsine adducts $[Ru(\eta^6\text{-}C_7H_8)Cl_2(EPh_3)]$ (E = P, As) gives $[Ru(\eta^5\text{-}C_7H_8L)L(EPh_3)]$ **51** resulting[120] from i) the substitution of both chloride ligands by a chelating β-diketonate and ii) addition of a further $[RC(O)CHC(O)R]^-$ anion at a terminal olefinic site to give an η^5-cycloheptadienyl ligand, consistent with charge control.[11]

Analogous complexes containing the $[C_8H_8]^{2-}$ dianion are rarer for first and second row transition metals because of poor metal-ligand orbital overlap and $[C_8H_8]^{2-}$ species are most commonly found in lanthanide and actinide chemistry, *e.g.* uranocene $[U(\eta^8\text{-}C_8H_8)_2]$, although Ti, Zr and Hf all form quadrivalent, binary species containing two planar $[C_8H_8]^{2-}$ rings. The unusual binuclear complex $[\{Ti(\eta^8\text{-}C_8H_8)\}_2\{\mu\text{-}(1\text{-}4\eta\text{:}3\text{-}6\eta\text{-}C_8H_8)\}]$ in which six atoms of a C_8H_8 ligand bridge the two metal centres, is also known.[23]

In contrast, [Ni(cdt)] **36** reacts with cot at low temperature to give a binuclear analogue of *bis*(allyl)nickel(II), $[\{Ni(C_8H_8)\}_2]$ in which the two metal centres are linked by two bridging $\eta^3\text{:}\eta^3\text{-}C_8H_8$ ligands.[23]

1.5.2 η^6-Aromatic Bridging Ligands

One of the most interesting classes of η^6-ligands is those in which two or more metal centres are bridged by π-arene and related ligands. When only a single arene is involved the resulting species are formally highly unsaturated multidecker complexes such as the mesitylene complex $[\{Cr(C_6Me_3H_3)\}_2(\mu\text{-}C_6Me_3H_3)]$[23] formed by metal-atom ligand-vapour co-condensation, in which each metal atom formally possesses fifteen electrons. Polyaromatic ligands such as cyclophanes have been extensively studied as $\eta^6\text{:}\eta^6$-bridges in which a single external face of each arene is coordinated to a metal centre giving saturated 'cylinder' complexes such as the binuclear, [2.2]paracyclophane cation $[\{Ru(\eta^6\text{-}C_6Me_6)\}_2(\eta^6\text{:}\eta^6\text{-}C_{16}H_{16})]^{4+}$ **52** and the mixed-metal trinuclear complex $[(\eta^6\text{-}C_6H_6)Os(\eta^6\text{:}\eta^6\text{-}C_{16}H_{16})Ru(\eta^6\text{:}\eta^6\text{-}C_{16}H_{16})Os(\eta^6\text{-}C_6H_6)]^{6+}$ **53**.[7,126-128] The delocalised π-electron structure within the cyclophane bridge[129,130] results in extensive redox behaviour with **52** displaying two two-electron reductions to $[\{Ru(\eta^6\text{-}C_6Me_6)\}_2(\eta^6\text{:}\eta^6\text{-}C_{16}H_{16})]^{2+}$ and thence the neutral Ru(0) compound $[\{Ru(\eta^6\text{-}C_6Me_6)\}_2(\eta^6\text{:}\eta^6\text{-}C_{16}H_{16})]$.[7] An eighteen electron configuration is

probably obtained in the Ru(0) case by the slippage of the cyclophane to an η^4-mode of coordination, in contrast to genuinely twenty electron species such as $[Fe(\eta^6\text{-}C_6Me_6)_2]$ **17**. In the partially reduced dication, X-ray crystallography has shown that the cyclophane consists of two cyclohexadienyl anionic decks joined by a particularly long C-C bond of 1.96(3) Å in addition to the two more conventional ethylenic bridges, and hence both metals are in the +2 oxidation state (Scheme 1.6a).[131] In contrast, the closely related complex cation $[Ru(\eta^6\text{-}C_6Me_6)]_2(\eta^6\text{:}\eta^6\text{-}[2_4](1,2,4,5)\text{cyclophane})]^{2+}$ exhibits localised Ru(II) and Ru(0) class IIb mixed valence behaviour with the two sites exchanging rapidly at room temperature (Scheme 1.6b), because of the less flexible nature of the highly bridged cyclophane.[132]

Cyclophane bridged species are also known for elements of the cobalt triad[133] and for iron[134] and chromium, along with $Cr(CO)_3$ capped and *bis*(capped) multi layered [2.2]paracyclophanes, *e.g.* $[\{Cr(CO)_3\}_2(\mu\text{-}\eta^6\text{:}\eta^6\text{-quadruple-layered [2.2]paracyclophane})]$.[135] Such species are of obvious interest in the construction of conducting solid state materials from organometallic building blocks and related oligomers containing up to six ruthenium atoms linked by polyphenyl bridges have been synthesised.[136,137]

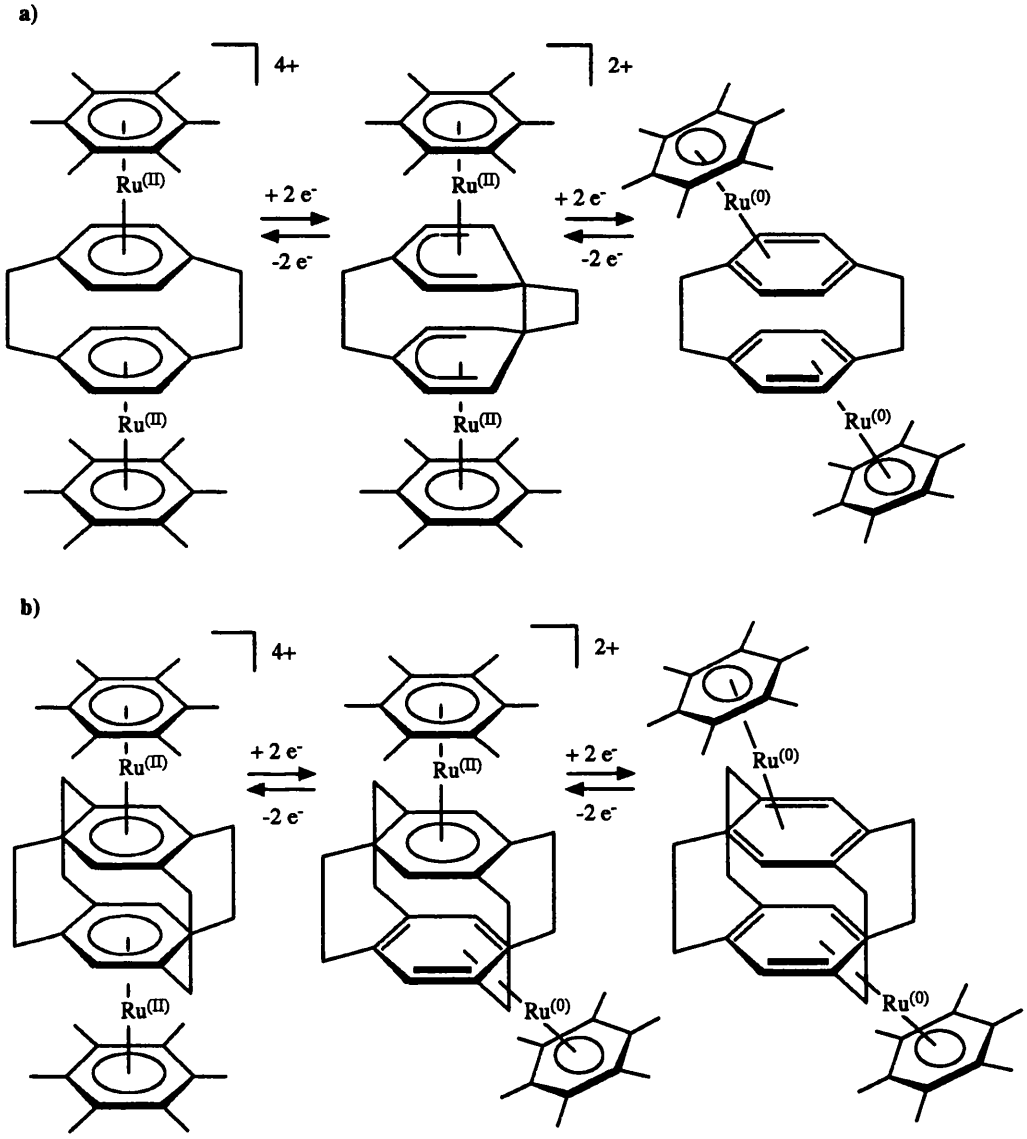

Scheme 1.6: a) Redox chemistry of $[\{Ru(\eta^6\text{-}C_6Me_6)\}_2(\eta^6{:}\eta^6\text{-}[2.2]paracyclophane)]^{n+}$; b) $[\{Ru(\eta^6\text{-}C_6Me_6)\}_2(\eta^6{:}\eta^6\text{-}[2_4](1,2,4,5)cyclophane)]^{n+}$ (n = 0, 2, 4).

1.5.3 Heteroatom η^6-Donors

η^6-π-complexes are not restricted to carbon donor ligands and a number of sandwich and half-sandwich complexes containing heterocyclic ligands such as borabenzene (BBz^-) are known.[138,139] Sandwich compounds such as $[Fe(\eta^6\text{-}C_5H_5B)_2]$ and the nineteen electron $[Co(\eta^6\text{-}C_5H_5B)_2]$ (synthesised from the interaction of the lithium salt of the ligand with the transition metal halide) are formally analogous to metallocenes but, in contrast to the planar, symmetrically bound π-arene and π-Cp moieties, X-ray crystallographic studies have shown that the borabenzene ligands exhibit a significant degree of ring slippage. Bonds from the metal centre to the carbon atom *para* to the boron in the phenylborabenzene complex $[Mn(CO)_3(\eta^6\text{-}PhBBz)]$ for example, are 0.34 Å shorter than the M-B distance.[139] Calculations have shown[140] that this slippage results in the maximisation of π and δ overlaps between metal and ring orbitals and minimisation of the summed energy of the occupied orbitals that are significantly delocalised over the metal-ring system as a whole.

Hexa-hapto π-complexes, analogous to their arene counterparts, also exist for cyclo-trisborazine ("inorganic benzene", $B_3N_3H_6$), *e.g.* $[Cr(CO)_3(\eta^6\text{-}B_3N_3R_6)]$ (R = Me, Et), which may be synthesised from refluxing of $[Cr(CO)_3(MeCN)_3]$ with $B_3N_3R_6$ in the same way as the corresponding arene complexes.[23] The coordinated ring adopts a shallow chair conformation with Cr-B = 2.31 Å and Cr-N = 2.22 Å (R = Et) and the complex is notably less stable than its arene analogues. No sandwich complexes containing two $B_3N_3R_6$ ligands are yet known.[23]

Carborane complexes, such as those of the $[C_2B_{10}H_{12}]^{2-}$ dianion represent particularly exotic examples of η^6-coordination. The cyclopentadienyl cobalt complex $[(\eta^5\text{-}C_5H_5)Co(\eta^6\text{-}C_2B_{10}H_{12})]$ exists in three isomeric forms. At room temperature the red isomer is bound by two carbon and four boron atoms. Warming to 40°C results in rearrangement to form the orange isomer in which one of the carbon atoms has moved to the second (uncoordinated layer) of the carborane. At 70°C another isomerisation takes place involving a further movement of this carbon atom within the carborane framework. The metal remains bound to one carbon and five boron atoms.[141,142] A more recent report deals with the europium(II) sandwich complex $[Eu(\eta^6\text{-}C_2B_{10}H_{12})_2(thf)_2]^{2-}$ in which the europium atom is asymmetrically bound to two carbon and four boron atoms.[143]

Hexa-hapto π-complexes of group V heterocycles (pyridine, phosphabenzene and arsabenzene) are also well established, although many have been synthesised *via* co-condensation techniques. In the case of pyridine, σ-donation through the nitrogen atom lone pair is significantly more favourable than π-bonding and the nitrogen atom must be sterically hindered during the synthesis to prevent this mode of coordination.[144] In contrast the η^1-arsabenzene adduct $[Mo(CO)_5(AsC_5H_5)]$ undergoes decarbonylation at 120°C to give the more stable η^6-complex $[Mo(CO)_3(\eta^6\text{-}AsC_5H_5)]$.[145] This compound may be prepared in much greater yield by refluxing $[Mo(CO)_6]$ with arsabenzene in diglyme, or by treatment of $[Mo(CO)_3(py)_3]$ with $BF_3.Et_2O$ in the presence of AsC_5H_5. Similar π-compounds are also known for SbC_5H_5 but attempts to isolate BiC_5H_5 adducts have been frustrated by the extreme lability of the products.[145]

Finally, reaction of $[Cp^*(CO)_2Mo{\equiv}Mo(CO)_2Cp^*]$ with white phosphorus in refluxing xylene gives the novel triple decker compound $[\{(Cp^*)Mo\}_2(\mu\text{-}\eta^6\text{-}P_6)]$ containing a cyclic P_6 ring derived from the cyclo-trimerisation of three P≡P units.[23]

Chapter 2

Complexes of "(η^3:η^3-$C_{10}H_{16}$)Ru" with N-Donor Ligands

2.1 Introduction

Nitrogen donor ligands such as amines, amides, imides and polypyridines are known in conjunction with a number of high oxidation state transition metal centres. Recently reported examples include Os(VI) amine / pyridyl complexes $[OsO_2(L)(L')]$ (L = *bis*(2-hydroxy-2,2-diphenylethyl)pyridinato, L' = $NH_2{}^tBu$, py, 4-^{t}Bupy),[146] and the Ru(IV) *bis*(imido) compound *trans*-$[Ru(2,6\text{-}{}^iPr_2C_6H_3N)_2(Pme_3)_2]$, formed by air oxidation of an unidentified Ru(II) amido species.[147] Similarly, exposure of the Ru(II) tetraphenylphorphorinato (P) amine complex $[Ru(P)(NH_2{}^tBu)_2]$ to O_2 results in oxidation to the analogous ruthenium(VI) *bis*(imido) compound $[Ru(P)(N^tBu)_2]$.[147] Nitrogen donor ligands are also frequently observed in conjunction with ruthenium(II) compounds, *e.g.* $[Ru(\eta^5\text{-Cp})(NH_2R)(PR'_3)]^+$ (R = H, Me),[148] and the Creutz-Taube ion $[(NH_3)_5Ru(\mu\text{-pyz})Ru(NH_3)_5]^{n+}$ (n = 4, 5, 6).[149]

A great deal of interest, including a considerable amount of very recent work,[150-154] has been expressed in potentially bridging or chelating bifunctional amine ligands such as 1,2-diaminobenzene [*o*-phenylenediamine, *o*-pda, $1,2\text{-}(NH_2)_2C_6H_4$]. Compounds containing neutral *o*-pda are uncommon and are often of limited stability, although stable anionic complexes $[MCl_4(o\text{-pda})]^-$ (M = Cr, V) have recently been reported, along with related Cr(IV) oxidation products such as $[Cr(O_3SCF_3)_4(o\text{-pda})]$.[154] The off-white complex $[Fe(o\text{-pda})_3]X_2$ (X = ClO_4, I) has been known for some years[155] and in the presence of atmospheric oxygen oxidises to the deep blue-black diiminobenzene [*o*-dib, $1,2\text{-}(NH)_2C_6H_4$] complex $[Fe(o\text{-dib})_3]X_2$. Oxidation of coordinated *o*-pda in the presence of oxygen and a catalytic amount of base (often uncomplexed amine) is a well known reaction and a number of compounds are known with *o*-dib coordinated in either chelating or bridging modes (*e.g.* $[Ru(PPh_3)_3(o\text{-dib})]$[152] and $[\{Ru(CO)_2(PPh_3)\}_2(\mu\text{-}o\text{-dib})]$[153] in which the ligand is present as the dianion). Also, a series of compounds of general formula $[M(o\text{-dib})_2]^n$ (M = Ni, Co, Pt, Pd; n = -2 to +2) have been studied in which the *o*-dib ligands may exist as either a neutral, anionic or dianionic chelates, and the dianion is also known to bridge metals in such diverse oxidation states as Ru(I) and W(V).[150,151] In view of this obvious versatility and stability in the presence of metals in high oxidation states, the reactivity of $[\{Ru(\eta^3\text{:}\eta^3\text{-}C_{10}H_{16})Cl(\mu\text{-Cl})\}_2]$ **6** towards amine and polypyridyl[157] ligands has been

examined and special emphasis has been placed on reactions with bifunctional amines related to *o*-pda.

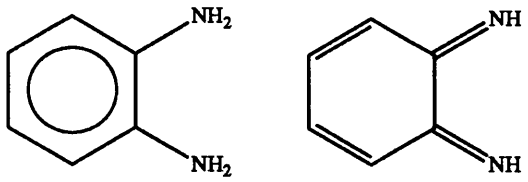

o-diaminobenzene (*o*-pda)

o-diiminobenzene (*o*-dib)

2.2 Reactions with Amines

2.2.1 Reaction with Aniline

Even in a highly polar solvent such as methanol, interaction of **6** with aniline ($PhNH_2$) does not result in deprotonation, rather the adduct $[Ru(\eta^3:\eta^3\text{-}C_{10}H_{16})Cl_2(NH_2Ph)]$ **54** is formed as a bright yellow precipitate over the course of *ca.* 1 h. at room temperature. The complex exhibits a ^1H NMR spectrum characteristic of a simple equatorial adduct (the two axial sites of the approximately trigonal bipyramidal ruthenium ion are equivalent and occupied by terminal chloride ligands, see Appendix I) with only two singlet resonances for the terminal allyl protons (δ 4.15 and 3.76 ppm) and one methyl signal, δ 2.29 ppm (Table 2.1). Because of the chirality of the "$Ru(\eta^3:\eta^3\text{-}C_{10}H_{16})$" fragment the two NH protons of the prochiral NH_2R nitrogen atom are diastereotopic and consequently two broad N*H* resonances (δ 6.13 and 5.67 ppm, $^2J_{H\text{-}H}$ unresolved) are observed. The effect is analogous to that observed for the fluorophosphine compound $[Ru(\eta^3:\eta^3\text{-}C_{10}H_{16})Cl_2(PF_2Me_2N)]$[16] in which two separate ^{19}F NMR resonances are observed for the diastereotopic fluorine atoms attached to phosphorus.* Compound **54** also exhibits two $\nu(NH_2)$ bands in its infrared spectrum (3304 and 3230 cm^{-1}) and a characteristic $\delta(NH_2)$

* At the time the inequivalence of the two fluorine atoms was attributed to a restricted rotation about the Ru-P bond. The phenomenon has since been re-interpreted by Cox and Roulet.[17]

mode at 1598 cm^{-1}.

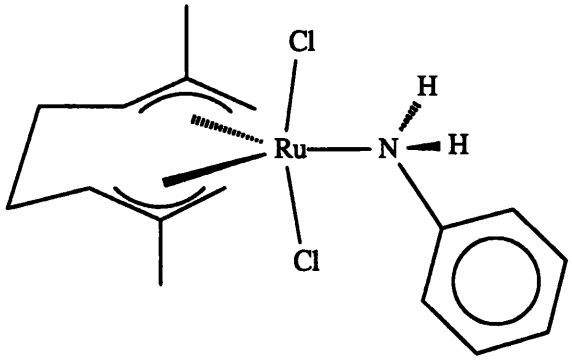

54

The possibility of formation of cationic *bis*(aniline) compounds or deprotonation of the aniline to give amido / imido species was investigated by reaction of **6** with an excess of aniline in methanol over a period of 5 days. This experiment resulted in the isolation of a yellow precipitate of **54** as before. The solution had, however, become a deep blue-black and removal of the solvent *in vacuo* gave a deep blue product soluble in common organic solvents, and in which it gradually decomposed on exposure to atmospheric oxygen to give a purple colouration. However, the ^1H NMR spectrum of this material, even over a very wide spectral window, revealed no signals other than those attributable to **54**, whilst analytical data were also consistent with the formulation of **54**. It was concluded that the unusual colour of this material was caused by small amounts of a highly coloured second product resulting from loss of the *bis*(allyl) ligand and that the bulk of the product was identical to that isolated after short reaction times.

2.2.2 Reactions with 1,2- and 1,4-Diaminobenzene

The analogous reaction of **6** in methanol with 1,4-diaminobenzene (*p*-pda) also results in the formation of a yellow precipitate, analysing closely for the adduct $[Ru(\eta^3:\eta^3\text{-}C_{10}H_{16})Cl_2(1,4\text{-}NH_2C_6H_4NH_2)]$ **55**. As with **54** the diastereotopic N*H* protons of the complexed amine donor occur as two resonances at δ 6.01 and 5.55 (AB, $^2J_{H\text{-}H}$ = 6.1 Hz) ppm whilst the protons of the uncomplexed amine functionality give rise to a broad singlet at δ 3.58 ppm. The infrared spectrum of **55** displays a total of four $\nu(NH_2)$ bands 3429,

3334, 3303 and 3236 cm^{-1}. The formation of **55** contrasts markedly to the difficulty in isolation of the monodentate pyrazene adduct $[Ru(\eta^3:\eta^3\text{-}C_{10}H_{16})Cl_2(N_2C_4H_4)]$ (see Chapter 5 and ref. 158) which is unstable with respect to disproportionation into the binuclear compound $[\{Ru(\eta^3:\eta^3\text{-}C_{10}H_{16})Cl_2\}_2(\mu\text{-}N_2C_4H_4)]$ and free ligand, and is only observed in the presence of a large excess of pyrazene.[158] Interestingly, if **55** is allowed to stand for *ca.* 10 minutes in chloroform solution disproportionation occurs to give a mixture of **55**, free 1,4-diaminobenzene and a new compound displaying a further two terminal allyl resonances (δ 4.17 and 3.74 ppm). *Two* more signals in the methyl region are also observed (δ 2.30 and 2.29 ppm) with a peak separation of only 2.5 Hz. No new signals for uncoordinated N*H* δ *ca.* 3.5 are observed but two broad coordinated N*H* resonances occur at δ 6.12 and 5.67 (AB, $^2J_{H\text{-}H}$ = 7.9 Hz) ppm. The diaminobenzene aromatic protons occur as two singlets (δ 7.27 and 7.26 ppm) again with a very small peak separation (1.8 Hz). The appearance of the latter signals as singlets implies that both amine functionalities of the diamine ligand are complexed and are equivalent, and hence this new material is formulated as the 1,4-diaminobenzene bridged binuclear compound $[\{Ru(\eta^3:\eta^3\text{-}C_{10}H_{16})Cl_2\}_2\{\mu\text{-}1,4\text{-}(NH_2)_2C_6H_4\}]$ **56**. The binuclear nature of the purified complex was confirmed by a FAB mass spectrum [*m/z* 724 (M^+ based on ^{102}Ru and ^{35}Cl, isotope distribution characteristic of two ruthenium and four chlorine atoms), 689 (M^+ - Cl)]. The slight splitting of the methyl and C_6H_4 resonances is explained by the fact that **56** exists as two diastereoisomers in the same way as the parent compound **6**. Unlike **6**, in which the metal centres of the two chiral "$Ru(\eta^3:\eta^3\text{-}C_{10}H_{16})$" fragments are 3.98 Å apart,[13] the much larger bridging ligand in **56** probably results in a distance between the two ruthenium ions in excess of 8 Å and hence the magnetic environment of the protons of one "$Ru(\eta^3:\eta^3\text{-}C_{10}H_{16})$" fragment is very little affected by the handedness of the other *bis*(allyl)ruthenium moiety. Also, the ^1H NMR spectrum of **56** is slightly broad at room temperature probably due to interconversion of the two diastereomeric forms *via* Ru-N bond fission and exchange of mononuclear "$Ru(\eta^3:\eta^3\text{-}C_{10}H_{16})Cl_2$" units. Lowering the temperature in the NMR probe to -60°C resulted in a sharpening of the broad resonances but no further diastereomeric splittings were resolved.

Complex **56** was synthesised free of **55** by reaction of **6** with a one mole equivalent of *p*-pda in CH_2Cl_2. In this medium both reactants and products are soluble and the

reaction proceeds almost instantaneously (colour change from pink to yellow-orange). The most likely mechanism for this reaction is bridge cleavage of **6** to generate the adduct **55**, which is precipitated out of methanol solution. In CH_2Cl_2 **55** remains in solution where the pendant amine functionality reacts with a further molecule of **6** to give **56**.

The reaction of **6** with 1,2-diaminobenzene (*o*-pda) is rather more complicated. Addition of two equivalents of *o*-pda to **6** in methanol results in the formation of a bright orange solution over a period of *ca.* 1 h. Work-up yields orange-red crystals analysing for an adduct $[Ru(\eta^3:\eta^3\text{-}C_{10}H_{16})Cl_2(1,2\text{-}NH_2C_6H_4NH_2)]$ **57** (analogous to **54** and **55**). This compound may also be obtained as one component of a mixture of products from the analogous reaction in CH_2Cl_2. The ^1H NMR spectrum of **57** is sharp at room temperature and closely resembles that of the 1,4-diaminobenzene adduct **55** (Table 2.1). Like **55**, compound **57** rapidly disproportionates into free ligand and the binuclear compound $[\{Ru(\eta^3:\eta^3\text{-}C_{10}H_{16})Cl_2\}_2\{\mu\text{-}1,2\text{-}(NH_2)_2C_6H_4\}]$ **58** reaching an equilibrium at room temperature in which K_{20} = [**57**]/[**58**] = *ca.* 1. Addition of a small quantity of $H[BF_4]$ to an NMR sample containing **57** and **58** resulted in the immediate selective precipitation of **57** from the chloroform-*d* solvent, probably because of protonation of the uncomplexed amine functionality. Complex **58** was not precipitated and was found to be the sole ruthenium species present upon re-examination of the ^1H NMR spectrum. Complexation doubtless greatly reduces the basicity of the amine functionalities.

Compound **58** may also be synthesised in pure form by reaction of **6** with one mole equivalent of *o*-pda in either MeOH or CH_2Cl_2. The binuclear nature of **58** was confirmed by a FAB mass spectrum which showed a clear molecular ion peak *m/z* 724 with isotopic distribution characteristic of two ruthenium ions and four chloride ligands. Fragmentation peaks corresponding to sequential loss of all four chloride ligands are also observed as well as a strong peak (*m/z* 381) corresponding to $[Ru(\eta^3:\eta^3\text{-}C_{10}H_{16})Cl(o\text{-pda})]$. The ^1H NMR spectrum of **58** in acetone-d_6 solution at +50°C is consistent with the proposed formulation, and qualitatively resembles that of **56**. Like **56** and **6**, complex **58** exists as two diastereoisomers which may be distinguished by ^1H NMR spectroscopy. Integration of the ^1H NMR resonances for each isomer gives an equilibrium constant at this temperature, K_{50} = 1.6. The corresponding ratio for **6**, $K_{20} = [C_2]/[C_1]$ is 1.25.[17] In the absence of an X-ray

crystal structure determination it is not possible to assign the resonances for **58** to one particular diastereoisomer but there is clearly a significant preference for one form over the other.

At room temperature in either acetone-d_6 or $CDCl_3$ the resonances for one of the two diastereoisomers of **58** apparently split further dividing into two sets of signals of unequal intensities. Examination of the spectrum down to -80°C in acetone solution resulted in the observation of a very complicated, although sharp, set of resonances. The precise nature of this dynamic behaviour is unclear but examination of molecular models seems to indicate the possibility of several conformers with relatively high barriers to interconversion.

If **6** is stirred with two equivalents of *o*-pda in methanol from which no attempt has been made to exclude atmospheric oxygen, a deep red colouration is observed (in contrast to the bright orange solutions of **57** formed in the absence of O_2). The deep red product which is isolated by addition of diethyl ether to this solution analyses for an adduct of the same empirical formula as **57**, although the FAB mass spectrum of this material displays a molecular ion peak at *m/z* 381 ([Ru($C_{10}H_{16}$)Cl(*o*-pda)]) consistent with the presence of one less chloride ion per metal, suggesting that one of the chloride ions is not strongly associated with the complex. Unlike **57** the new material, **59**, is highly soluble in methanol and even water, but only sparingly so in chloroform and other less polar solvents. The ^{1}H NMR spectrum of **59** displays peaks assignable to coordinated N*H* (δ 8.45, 6.93, 6.42 and 4.79 ppm). Four signals (δ 4.14, 3.88, 3.74 and 3.38 ppm) are observed for the terminal allyl protons of the *bis*(allyl) ligand and for the protons of the aromatic C_6H_4 moiety [δ 7.61 (d, ^3J = 7.8), 7.34 (d, ^3J = 7.1), 7.28 (t, ^3J = 7.3), 7.11 (t, ^3J = 7.3 Hz) ppm]. The fact that two of the aromatic signals occur as triplets indicates that the two halves of the *o*-pda ligand are unique and, in conjunction with the observed inequivalence of the two halves of the *bis*(allyl) ligand implies that **59** should be formulated as an ionic chelate [Ru(η^3:η^3-$C_{10}H_{16}$)Cl{$(NH_2)_2C_6H_4$}]Cl in which the *o*-pda ligand occupies one equatorial and one axial coordination site. Consistent with the proposed formulation, the infrared spectrum of **59** exhibits two ν(NH_2) bands 3359 and 3157 cm^{-1} (complex **58** exhibits two bands at 3199 and 3102 cm^{-1}). The formulation of this product as an ionic material would account for its high solubility in polar solvents.

At room temperature the ^{1}H NMR spectrum of **59** is slightly broad. Lowering the temperature of the NMR probe resulted in significantly greater broadening of all the resonances until, at -90°C (the lowest accessible temperature in CD_2Cl_2) the signals had apparently begun to resolve into two or more new sets of resonances. Interpretation of this spectrum was hampered by its extreme broadness, caused in part by extensive precipitation of the compound from solution. Because of the poor solubility of the compound, lower temperature NMR experiments in freon solvents were not attempted. It is possible that this apparent fluxionality results from H-bond interactions of the amine functionalities with the chloride counterion and extensive ion-pairing, but the precise nature of the process is unknown.

It is interesting to note that complex **59** was *only* formed in solutions which had *not* been deaerated. Use of methanol which had been deoxygenated (by bubbling nitrogen through it for 1 - 2 hours beforehand) as a solvent, resulted in the formation of orange solutions from which only **57** and **58** could be isolated. Such solutions did not become red even on standing under N_2 for several days but gradually decomposed to give a deep purple colouration. As described in Section 2.1, reaction of metal *o*-pda complexes with O_2 frequently results in dehydrogenation / deprotonation of the ligand to give diiminobenzene derivatives which are often highly coloured. In the case of **59** however, all four NH protons are clearly evident in the ^{1}H NMR spectrum of the complex, and similarly two ν(NH) bands are observed in the infrared spectrum. Such an oxidation process may, however, occur during the course of the reaction and may be instrumental in removing one of the axial chloride ligands (by enhancing the nucleophilicity of the uncomplexed amine functionality in adducts such as **57**) to enable chelation to take place. The ligand may then be re-protonated to give **59**.

Consistent with the suggestion that the chloride counterion in **59** is strongly associated with the complex cation we were unable to obtain precipitates of the tetraphenylborate salt $[Ru(\eta^3:\eta^3\text{-}C_{10}H_{16})Cl(o\text{-pda})][BPh_4]$ by mixing a solution of **59** in methanol with methanolic $Na[BPh_4]$. Addition of $[NH_4][PF_6]$ to the reaction mixture formed in the synthesis of **59**, and subsequent stirring for several hours did, however, yield the hexafluorophosphate salt $[Ru(\eta^3:\eta^3\text{-}C_{10}H_{16})Cl(o\text{-pda})][PF_6]$ **60** as a red-orange precipitate on reduction of the volume of the solution. The ^{1}H NMR spectrum of **60** (Table

2.1) was sharp at room temperature and exhibited a much smaller range in the chemical shifts for the N*H* protons, consistent with the fact that these protons are no longer involved in strong hydrogen bonding to the counter ion. In the infrared spectrum **60** displayed a strong, broad band at 1168 cm^{-1} confirming the presence of the hexafluorophosphate anion as well as four bands assignable to ν(NH) 3319, 3288, 3265 (m, sharp) and 3125 (w, br) cm^{-1}, and a strong band at 1576 cm^{-1} assigned to $\delta(NH_2)$. A strong band assigned to ν(RuCl) was observed at 271 cm^{-1}.

Attempted syntheses of amido compounds by reaction of **6** with *o*-pda in the presence of $Na_2[CO_3]$ resulted in the formation of extremely air sensitive deep purple solution from which a brown-black solid could be isolated. The ^1H NMR spectrum of this material indicated that the *bis*(allyl) ligand was no longer present but no further attempts at characterisation were made because of the compound's instability. The possibility of oxidation to amido / imido species was also investigated by examination of the cyclic voltammetric response of **59**. Over a variety of scan speeds (200 - 600 mV s^{-1}) only irreversible waves were observed at *ca.* +1.57, -0.72 and -1.00 V (vs. Ag / AgCl). It seems likely that the electron transfer reactions are followed by rapid chemical decomposition of the complex, and irreversible loss of the *bis*(allyl) ligand. The cyclic voltammogram of the bridged complex **58** was also examined. Like **59** it also displayed only irreversible waves although the observation of a pair of oxidations (+1.60 and +1.76 V) may well be associated with the diamine ligand.

The reactions of **6** with *o*-pda are summarised in Scheme 2.1.

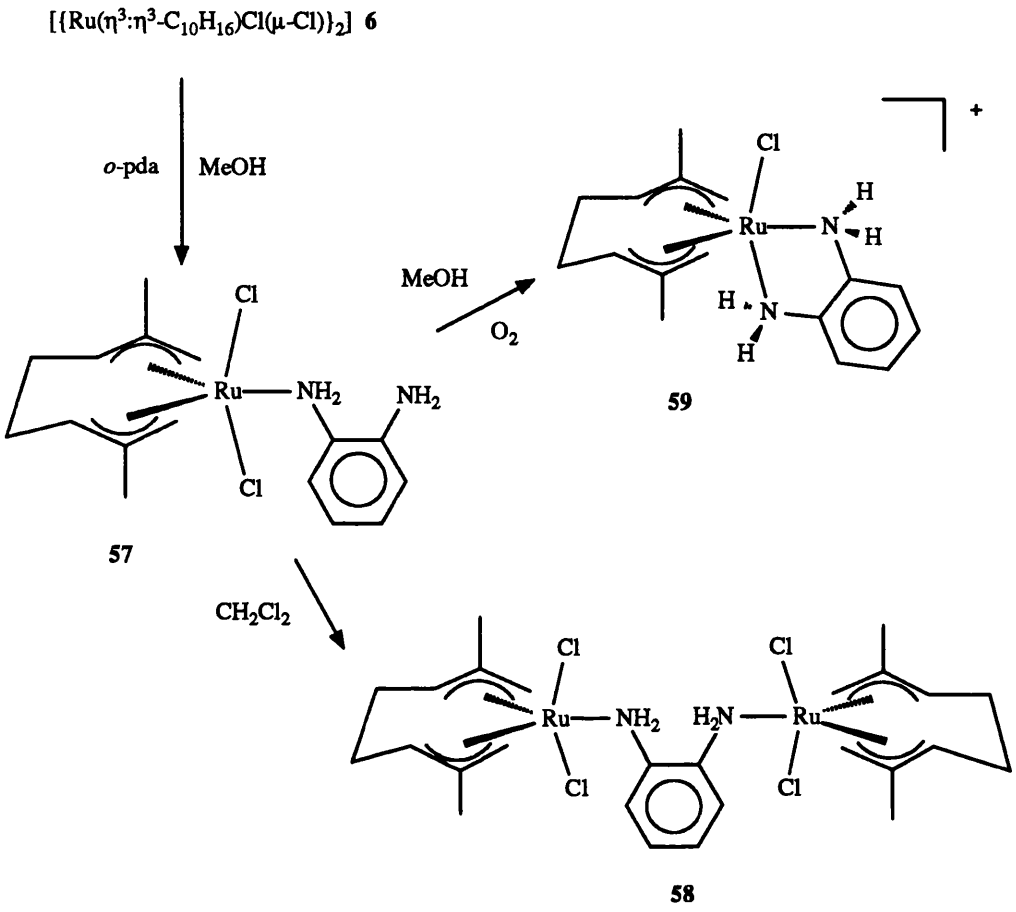

Scheme 2.1: Formation of the amine compounds $[Ru(\eta^3:\eta^3\text{-}C_{10}H_{16})Cl_2(o\text{-}NH_2C_6H_4NH_2)]$ **57**, $[\{Ru(\eta^3:\eta^3\text{-}C_{10}H_{16})Cl_2\}_2\{\mu\text{-}(NH_2)_2C_6H_4\}]$ **58** and $[Ru(\eta^3:\eta^3\text{-}C_{10}H_{16})Cl(1,2\text{-}\{(NH_2)_2C_6H_4\})]Cl$ **59**.

2.2.3 Reactions with Other Potentially Bidentate Amine Ligands

The reaction of **6** with 2,2'-diaminodiphenyl ($NH_2C_6H_4\text{-}C_6H_4NH_2$) was also investigated. Analogously to the preparation of **59**, use of oxygenated methanol as the solvent resulted in the formation of an ionic compound, $[Ru(\eta^3:\eta^3\text{-}C_{10}H_{16})Cl(NH_2C_6H_4C_6H_4NH_2)]Cl$ **61**. The FAB mass spectrum of this material displayed a strong peak at *m/z* 475 corresponding to the expected molecular cation and, as anticipated for an ionic compound, **61** is soluble in methanol and water. The ^1H NMR spectrum of **61**

displays an AB pattern assignable to one set of coordinated N*H* protons [δ 6.10 and 5.47 ($^2J_{H\text{-}H}$ = 9.0 Hz) ppm] and a broad singlet resonance [δ 3.61 (2H) ppm] for the second set. Four terminal allyl and two methyl resonances are observed (Table 2.1) as expected for a chelate complex with inequivalent axial sites, but one methyl and two terminal allyl signals are significantly broadened at room temperature suggesting a fluxional process which is to some degree localised on one side of the molecule. Lowering the temperature in the NMR probe results initially in a general broadening of the spectrum, but at -60°C a pattern of sharp resonances similar to the room temperature spectrum is observed once more, with the only noteworthy difference being the splitting of the broad N*H* resonance at δ 3.61 into two broad singlets at δ 3.69 and 3.52 ppm (probably an unresolved AB pattern). This fluxionality is consistent with that suggested for **59** and may well take the form of exchange between two or more modes of hydrogen bonding interaction between the amino protons and the chloride counterion, Scheme 2.2.

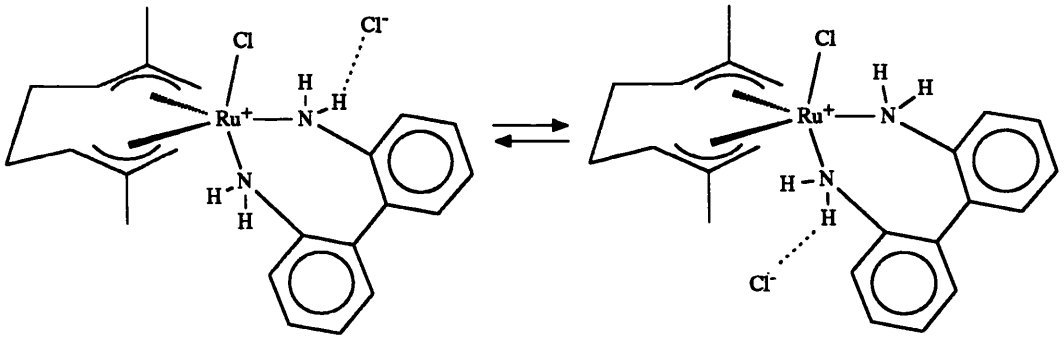

Scheme 2.2: Ion pairing in [Ru(η^3:η^3-$C_{10}H_{16}$)Cl($NH_2C_6H_4C_6H_4NH_2$)]Cl **61**.

Strong evidence both for the formulation of **61** and the nature of the fluxionality involved comes from the synthesis of the tetrafluoroborate salt of the compound [Ru(η^3:η^3-$C_{10}H_{16}$)Cl($NH_2C_6H_4C_6H_4NH_2$)][BF_4] **62** by reaction of an acetone solution of **6** pre-treated with two mole equivalents of Ag[BF_4], with 2,2'-diaminodiphenyl. The ^{1}H NMR spectrum of **62** bears a strong resemblance to that of **61** except the coordinated N*H* protons occur as four sharp, doublet resonances [δ 6.08 (^2J=9.3 Hz), 5.57 (^2J=9.3), 5.09 (^2J=8.3) and 3.81

(^2J=8.3) ppm] and the remainder of the spectrum is sharp at room temperature, consistent with the suggestion that the chloride counterion is involved in the fluxionality of **61**.

The formation of **61** and **62** is surprising in that both complexes possess seven-membered heterocyclic chelate rings which might be expected to exhibit a high degree of steric strain. Examination of molecular models shows unambiguously that the two aromatic rings in these complexes cannot both coordinate to the metal centre *via* their amino functionalities and retain a co-planar arrangement as is invariably observed in related complexes of 2,2'-bipyridyl. An unstrained seven membered heterocyclic ring may be obtained however if the two rings are orientated at *ca.* 90° to one another as shown in Fig. 2.1.

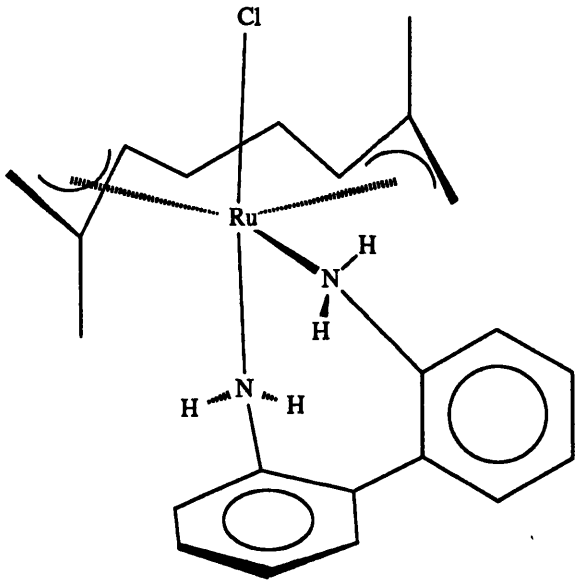

Fig. 2.1: Geometry of the chelate complexes $[Ru(\eta^3:\eta^3\text{-}C_{10}H_{16})Cl(NH_2C_6H_4C_6H_4NH_2)]^+$ **61** and **62** suggested by examination of molecular models

Reaction of **6** with two mole equivalents of 2,2'-diaminodiphenyl in CH_2Cl_2 resulted in the rapid formation of a bright orange solution from which a compound with formula $[Ru(\eta^3:\eta^3\text{-}C_{10}H_{16})Cl(NH_2C_6H_4C_6H_4NH_2)]$ (C,H,N analysis, FAB-MS *m/z* 457) may be isolated. Such a metal to ligand ratio would only result in the metal centre attaining an eighteen

electron configuration if the ligand were coordinated in a bidentate fashion as an anion. The ^{1}H NMR spectrum of this compound is extremely broad at room temperature. At +70°C in benzene-d_6 however, the spectrum is sharp but consistent with a mononuclear material with equivalent axial sites. Strikingly, at temperatures from -20°C to -90°C the spectrum is also well resolved and exhibits *six* singlet signals in the terminal allyl region of the spectrum of equal intensity [δ 4.20, 3.99, 3.86, 3.77, 3.52 and 3.38 ppm] and, confusingly, *two* methyl resonances occurring at very similar frequencies to one another (δ 2.14 and 2.12 ppm). Four doublet resonances, each of only half the intensity of the terminal allyl signals, are also observed [δ 6.74, 6.22, 6.16 and 5.17 (^2J = *ca.* 11 Hz) ppm] and are assigned to coordinated N*H*.

Addition of D_2O to the NMR tube containing this material and re-recording its spectrum several hours later resulted in the complete disappearance not only of the doublet resonances assigned to coordinated N*H*, but also of two of the sharp singlet signals in the terminal allyl region of the spectrum (δ 3.86 and 3.77 ppm) revealing these signals to arise from uncoordinated N*H* protons. The increased polarity of the NMR solvent caused by addition of D_2O also apparently resulted in the partial conversion of the new material, into **61**. Examination of the chemical shifts of the remaining four resonances in the terminal allyl region of the spectrum along with the two methyl signals and the internal allyl resonances revealed their close similarity to those of the simple aniline adduct **54**. Furthermore, the formulation of this compound as a binuclear species [{Ru(η^3:η^3-$C_{10}H_{16}$)Cl_2}$_2$(μ-$NH_2C_6H_4C_6H_4NH_2$)] related to **56** and **58** was ruled out by the reaction of **6** in CH_2Cl_2 with a one mole equivalent of 2,2'-diaminodiphenyl which resulted in the recovery of the same new material along with a large quantity of unreacted starting material. Also, such a binuclear compound would not be expected to exhibit the observed singlet signals due to uncoordinated N*H* (δ 3.86 and 3.77 ppm). This NMR evidence suggests that this material should be formulated as a mononuclear adduct [Ru(η^3:η^3-$C_{10}H_{16}$)Cl_2($NH_2C_6H_4C_6H_4NH_2$)], possibly existing as two isomers giving rise to twice the number expected resonances (such isomerism could arise from different modes of hydrogen bonding of the uncoordinated NH protons with the chloride ligands for example). Such as formulation is however, inconsistent with the observed empirical and molecular formula and, as yet, this discrepancy has not been resolved.

Reaction of **6** with pyrazole (NC_3H_3NH) in toluene, acetone and methanol results in the isolation of the adduct $[Ru(\eta^3:\eta^3\text{-}C_{10}H_{16})Cl_2(NC_3H_3NH)]$ **63** in good yield. From ^1H NMR (δ N*H* 12.10 ppm) and infrared [ν(NH) 3246 cm^{-1}] spectroscopic data we infer the ligand to be bound in a monodentate fashion through the unsaturated nitrogen atom. Reaction of **6** with sodium pyrazolate in acetone at room temperature resulted in decomposition.

2.3 Reactions with Oligopyridines

2.3.1 Synthesis of Chelate Complexes

Complex **6** has recently been reported to form neutral, chelate complexes with ligands such as mercaptopyridines,[159] and semicarbazide[160]. Cationic compounds with monodentate nitrile ligands have also been reported and it has been demonstrated (Section 2.2) that chelate complex cations may be formed with bidentate amine ligands.[114,161] In this section further reactions of **6** to form well defined mono- and dicationic complexes with chelate ligands are reported.

We find that reaction of **6** with 2,2'-bipyridyl (bipy) in CH_2Cl_2 at room temperature proceeds poorly to give low yields and mixtures of products. In general however, pretreatment of dichloride dimers such as **6** with silver salts of non-coordinating anions, such as $[BF_4]^-$, affords mono- and dicationic solvates which are excellent precursors to cationic ruthenium complexes. While some problems are encountered using this procedure with compound **6**, as a consequence of its decomposition in alcoholic solvents in the presence of $Ag[BF_4]$ to form solvato Ru^{2+} ions,[114] air and moisture stable solvates may readily be generated in acetone solution.

By this route we have synthesised the monocationic complexes $[Ru(\eta^3:\eta^3\text{-}C_{10}H_{16})Cl(L\text{-}L)][BF_4]$ (L-L = 2,2'-bipyridyl, **64**; 1,10-phenanthroline, **65**) analogous to **59** - **61**, and the dicationic compound $[Ru(\eta^3:\eta^3\text{-}C_{10}H_{16})(terpy)][BF_4]_2$ **66** (terpy = 2,2':6',2''-terpyridine). The ^1H NMR spectra of complexes **64** and **65** display four resonances for the terminal allyl protons (*e.g.* δ 4.35, 4.02, 3.69 and 2.49 ppm in complex **64**) characteristic

of inequivalent axial sites on the trigonal bipyramidal ruthenium atom. In each case one resonance occurs at an uncharacteristically high field, possibly as a consequence of ring current effects arising from the aromatic moiety. Complex **66** on the other hand, displays only two terminal allyl resonances (δ 3.94 and 2.94 ppm) and a single methyl signal (δ 2.11 ppm), characteristic of equivalent axial sites, and as expected for the proposed terdentate, chelating geometry.

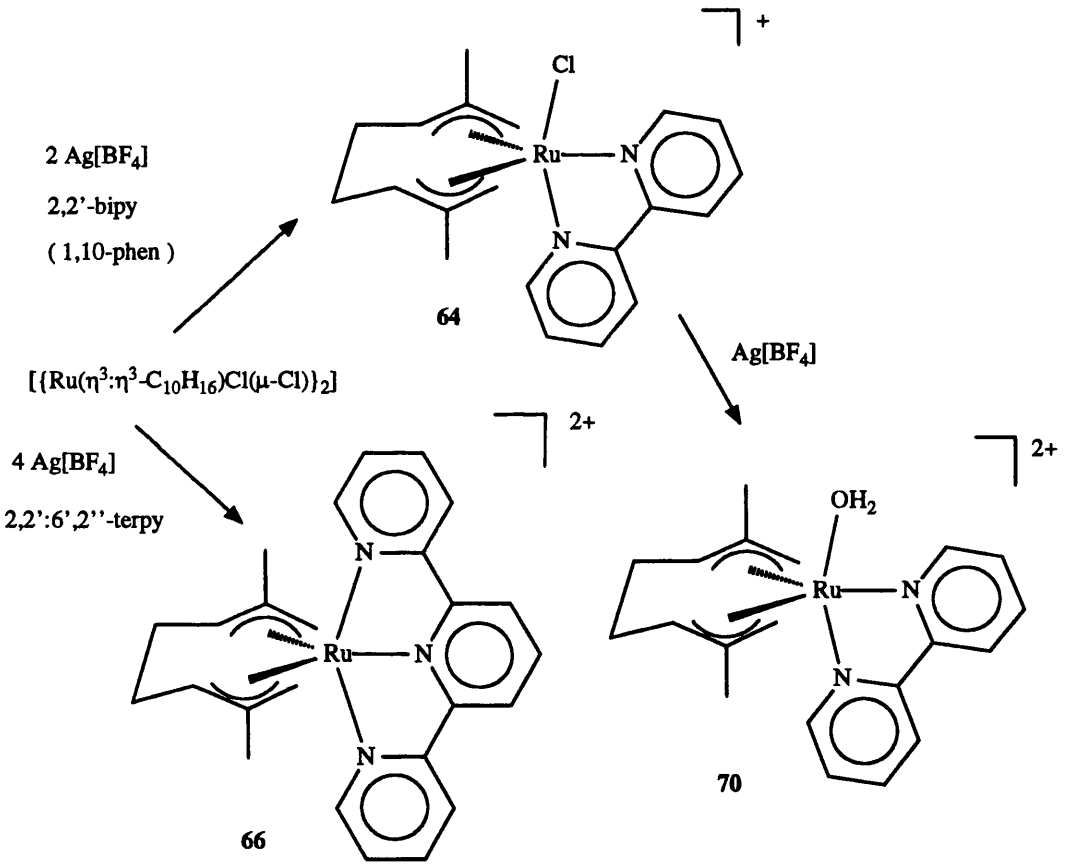

Scheme 2.3: Synthesis and reactions of polypyridyl compounds from $[\{Ru(\eta^3:\eta^3\text{-}C_{10}H_{16})Cl(\mu\text{-}Cl)\}_2]$.

Complexes **64** and **66** have been characterised by X-ray crystallography, Figs. 2.2 and 2.3. In general the structures are related to those reported for **6**, $[Ru(\eta^3:\eta^3\text{-}C_{10}H_{16})Cl_2(PF_3)]$ **67**[15] and, more recently, the benzothiazole-2-thiolate chelate $[Ru(\eta^3:\eta^3\text{-}C_{10}H_{16})Cl(mcbt)]$ **68**,[159] with the *bis*(allyl) ligand adopting the usual local C_2 symmetry and

each Ru-C distance approximately equal within experimental error. The ruthenium chloride distance of 2.433(2) Å in **64** is markedly longer than the corresponding terminal Ru-Cl distance observed in the structure of **6** (2.386 Å) but is similar to that reported for **67** and **68** (2.414 and 2.423 Å respectively). This difference is probably attributable to the poor *trans* influence of the bridging chloride ligand in **6**. The ruthenium-nitrogen distances, 2.140(5) (*equatorial*) and 2.115(4) (*axial*) in **64** and 2.02(1) (*eq.*), 2.17(1) and 2.147(9) Å (*ax.*), are similar to a wide range of Ru-N distances for Lewis base complexes *e.g.* **68** Ru-N 2.147(9) Å, [Ru(*p*-cymene)Cl(pyz)$_2$][PF$_6$] 2.16 Å (av.).[55] The bond from the metal to the central pyridyl ring [Ru-N(2)] in **66** is slightly shorter than the remaining bond distances, a feature common to terpyridines as terdentate ligands,[157] and relates to the small size of the metal ion relative to the optimal ligand cavity. Similarly, the angle N(1)-C(15)-C(16) within the ligand of 110(1)°, is smaller than the analogous parameter in the closely related 4'-phenylterpyridine ligand (116° when uncomplexed; 114° in the Ni(II) complex [Ni(Phterpy)$_2$][PF$_6$]$_2$[157]).

In compound **64**, the angle Cl-Ru-N(1) [89.5(1)°] is large compared to the average "unconstrained" value[13,161] of L_{axial}-Ru-$L_{equatorial}$ of *ca.* 85° but unexceptional in comparison to the value of 96.4(4)° observed by us for the 6-chlorohydroxypyridinate chelate [Ru(η^3:η^3-$C_{10}H_{16}$)Cl(NC_6H_3O-6-Cl)] (see Chapter 4). The most striking feature of the structure of **64** is the distortion of the two aromatic rings of the bipy ligand. While each is planar within experimental error, they are inclined at an angle of 8.2° to one another and the equatorially located ring [N(1)-C(16)-C(17)-C(18)-C(19)-C(20)] is inclined at an angle of 13.9° to the plane containing Cl(1), Ru(1) and N(2). This may be compared to a corresponding deviation of only 6.2° in complex **68**, and presumably arises as a consequence of an imbalance in the steric requirements of the ligand and the metal centre in a way related to that suggested for **61**, Fig. 2.1.

Compound **66** crystallises in the non-centrosymmetric space group Pc (see experimental section) in which the asymmetric unit contains two enantiomeric cations (as well as four [BF$_4$]$^-$ counter ions and two molecules of nitromethane of crystallisation), Fig. 2.4.

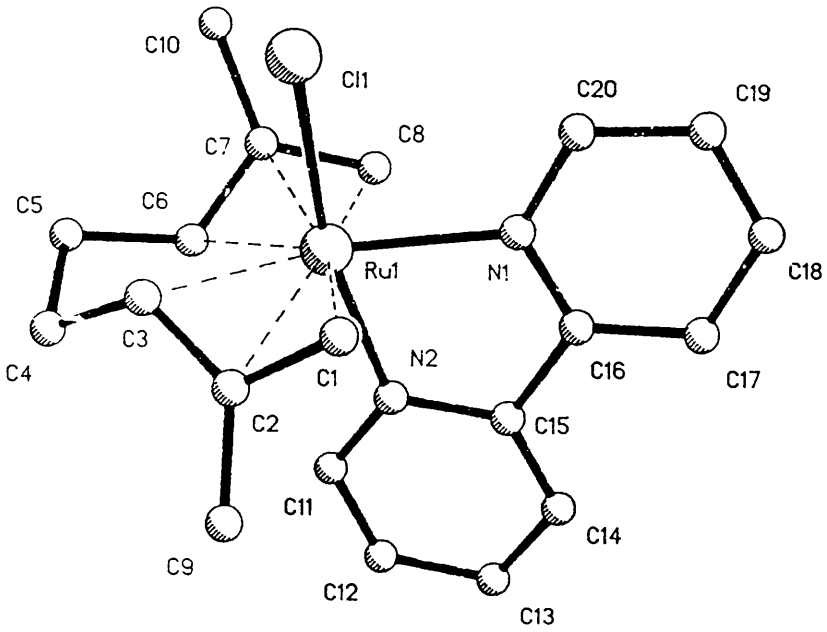

Fig. 2.2: Molecular structure of the cation $[Ru(\eta^3:\eta^3\text{-}C_{10}H_{16})Cl(N_2C_{10}H_8)]^+$ in **64** showing the atom numbering scheme adopted.

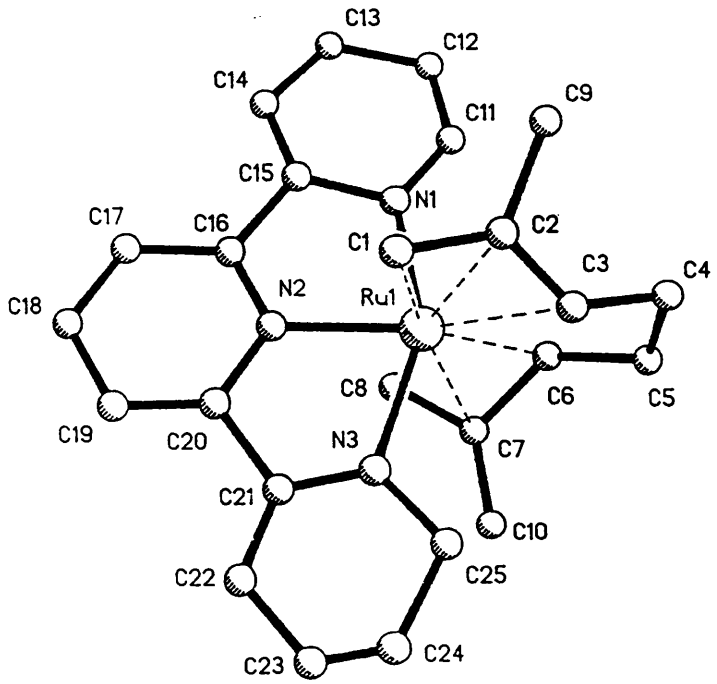

Fig. 2.3: Molecular structure of the cation $[Ru(\eta^3:\eta^3\text{-}C_{10}H_{16})(N_3C_{15}H_{11})]^{2+}$ in **66** showing the atom numbering scheme adopted.

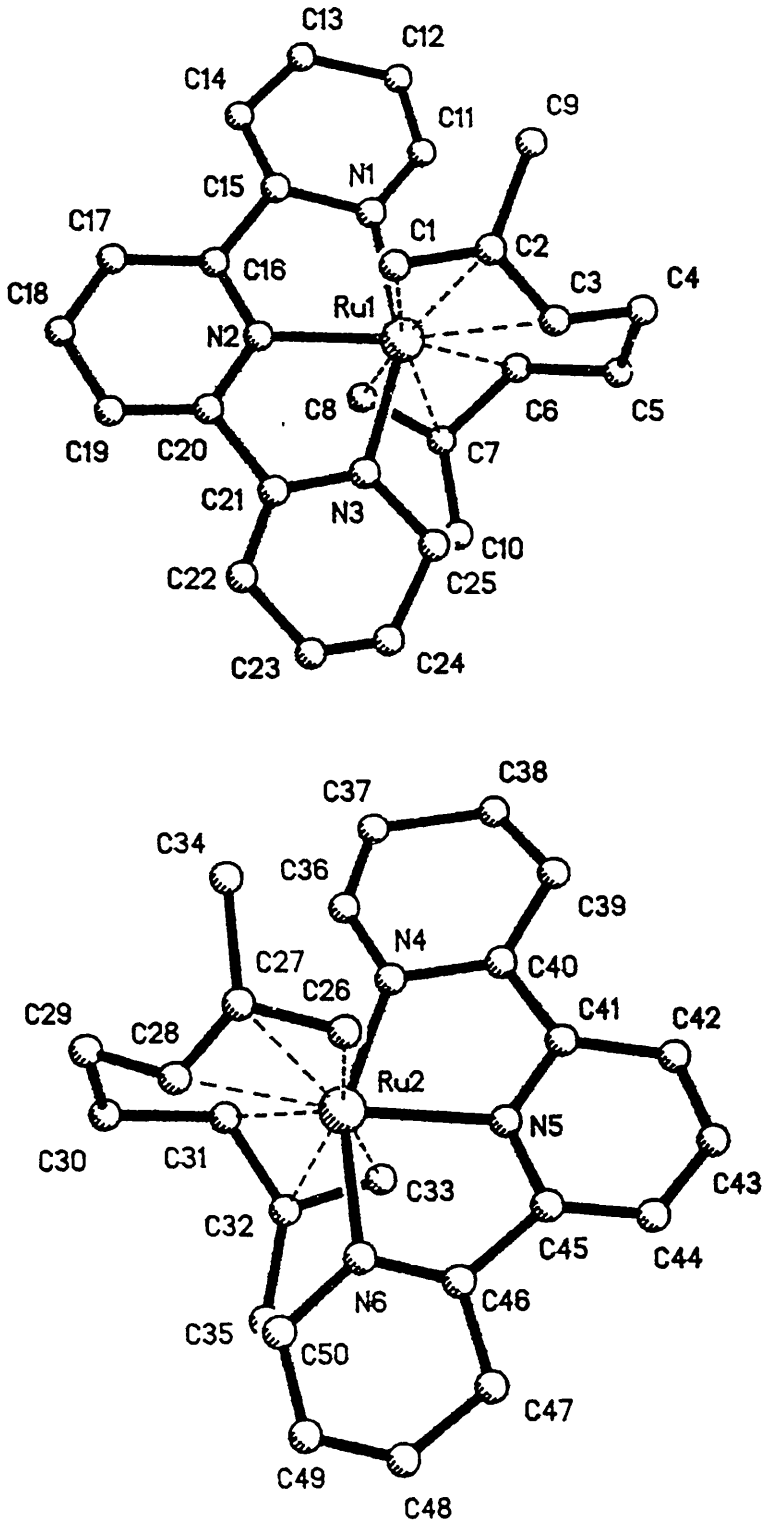

Fig. 2.4: The two enantiomeric cations in the asymmetric unit of $[Ru(\eta^3:\eta^3\text{-}C_{10}H_{16})(N_3C_{15}H_{11})]^{2+}$ **66**.

2.3.2 Reactions to form Aqua Complexes

One of the more striking features of complex **66** and a number of the ionic amine compounds described in Section 2.2, is their high solubility in water. Water soluble organometallic complexes are of considerable current interest[160,162] and the discovery of several water soluble *bis*(allyl) ruthenium(IV) complexes suggests an area of aqueous chemistry and catalysis which merits further investigation. With this in mind we have investigated the reactions of **64** and **65** with additional $Ag[BF_4]$ in undried acetone. Previous work[159] has shown that neutral chelate compounds containing chloride ligands such as $[Ru(\eta^3:\eta^3\text{-}C_{10}H_{16})Cl(mcbt)]$ **68** (mcbt = benzothiazole-2-thiolate) react with AgX (X = BF_4, PF_6) in acetonitrile to form the acetonitrile solvates $[Ru(\eta^3:\eta^3\text{-}C_{10}H_{16})(NCMe)(mcbt)]X$ **69**. In acetone, even in the presence of only trace amounts of water, **64** and **65** react with $Ag[BF_4]$ to form the aqua compounds $[Ru(\eta^3:\eta^3\text{-}C_{10}H_{16})(L\text{-}L)(OH_2)][BF_4]_2$ (L-L = 2,2'-bipyridyl, **70**; 1,10-phenanthroline, **71**). Compound **70** is difficult to isolate because of its high solubility, whereas **71** is readily obtained from acetone solution as greenish yellow crystals. The presence of the coordinated molecule of water is clearly demonstrated by the observation of sharp 2H singlet resonances in the ^1H NMR spectra of both compounds, δ 4.36 (**70**) and 3.92 ppm (**71**). The remainder of the ^1H NMR spectra (Table 2.1) are consistent with the proposed formulation and the infrared spectra demonstrate bands due to $\nu(OH_2)$ *e.g.* 3390 and 3294 cm^{-1} in compound **70**.

A significant amount of recent work has concentrated on (aqua)ruthenium(II) compounds because of their facile electrochemical or chemical oxidation to ruthenium(IV) oxo species.[163,164] High oxidation state ruthenium oxo compounds, typically Ru(IV)[165-168] or Ru(VI),[169-171] are of significant interest as organic oxidants, whilst compounds based on the $Ru^{II}\text{-}OH_2$ / $Ru^{IV}{=}O$ couple have been shown to be effective reagents for the catalytic cleavage of DNA.[172,173] In the hope of producing further high oxidation state ruthenium oxo compounds which might have unusual specificities, the chemical oxidation of **70** and **71** was attempted. Unfortunately treatment with reagents such as 4-methylmorpholine-*N*-oxide, ceric ammonium nitrate and PhIO resulted either in the recovery of unchanged starting material or extensive decomposition, and no oxidised products were isolated.

Reaction of the chloro complex **64** with Ag(I) salts (Ag_2O and $Ag[BF_4]$) did give rise to a quantity of a new compound in which the *bis*(allyl) ligand was still attached,

along with large quantities of unchanged starting material. The new complex was apparently diamagnetic and exhibited a similar ^{1}H NMR spectrum to **64** and **70**. We have been unable to purify this compound and hence it has not been unambiguously determined whether an oxo ligand is present. Reaction of **70** with strong bases such as KO^{t}Bu did not result in isolation of products arising from deprotonation of the water ligand.

2.4 Experimental

Instrumental. - Infrared spectra were recorded on a PE983 grating spectrometer between 4000 and 180 cm^{-1} as either KBr disks or nujol mulls on CsI plates. NMR spectra were recorded either on Varian XL200 and VXR400 spectrometers at University College London. Microanalyses were carried out by the departmental service and mass spectra were recorded by the University of London Intercolliegate Research Service at the School of Pharmacy. Cyclic voltammetric measurements were performed using a Metrohm E506 potentiostat interfaced with a Metrohm E612 VA scanner and a Hewlett Packard 7035B XY recorder. Electrolyte solutions were 0.2 molar in tetra-n-butyl ammonium tetrafluoroborate in CH_2Cl_2. Deaeration of the solution was performed before the experiment and a stream of nitrogen passed throughout. The working electrode was a platinum wire (Metrohm EA285). A platinum wire was used as a *pseudo*-reference electrode and potentials were corrected relative to the ferrocene / ferrocinium couple (ferrocene was added at the end of each experiment). A massive platinum wire was used as the auxiliary electrode. All potentials are reported with respect to the Ag / AgCl couple against which ferrocene is oxidised at a potential of +0.60 V. All manipulations were carried out under nitrogen with degassed solvents using conventional Schlenk line techniques except where otherwise stated. In general isolated products were found to be air stable or to decompose only slowly in solution in the presence of atmospheric oxygen.

Materials. - $[\{Ru(\eta^3:\eta^3\text{-}C_{10}H_{16})Cl(\mu\text{-}Cl)\}_2]$ was prepared by published literature methods.[12,17,159] Ruthenium trichloride hydrate was obtained on loan from Johnson Matthey plc. and was purified before use by repeated dissolution in water and boiling to dryness.

All other reagents and materials were obtained from the usual commercial sources.

Preparations. - $[Ru(\eta^3:\eta^3\text{-}C_{10}H_{16})Cl_2(NH_2Ph)]$ **54.** $[\{Ru(\eta^3:\eta^3\text{-}C_{10}H_{16})Cl(\mu\text{-}Cl)\}_2]$ (0.07 g, 0.11 mmol) was stirred in methanol (5 cm^3) with aniline (0.1 cm^3, excess) for 3 h. The resulting orange-yellow precipitate was recovered by filtration and washed sparingly with diethyl ether. A second crop of the product was obtained by evaporation of the yellow filtrate to *ca.* 2 cm^3. Combined yield 0.06 g, 0.15 mmol, 68% (Found: C, 48.20; H, 5.60; N, 3.65. Calc. for $C_{16}H_{23}NCl_2Ru$: C, 47.90; H, 5.80; N, 3.50%).

$[Ru(\eta^3:\eta^3\text{-}C_{10}H_{16})Cl_2(1,4\text{-}NH_2C_6H_4NH_2)]$ **55.** $[\{Ru(\eta^3:\eta^3\text{-}C_{10}H_{16})Cl(\mu\text{-}Cl)\}_2]$ (0.05 g, 0.08 mmol) was stirred in methanol (5 cm^3) with *p*-$(NH_2)_2C_6H_4$ (0.02 g, 0.18 mmol). Work-up and isolation were carried out in the same way as described for **54.** Yield 0.06 g, 0.14 mmol, 88% (Found: C, 46.15; H, 5.90; N, 6.55; Cl, 17.00. Calc. for $C_{16}H_{24}N_2Cl_2Ru$: C, 46.15; H, 5.80; N, 6.75; Cl, 17.05%).

$[\{Ru(\eta^3:\eta^3\text{-}C_{10}H_{16})Cl_2\}_2\{\mu\text{-}1,4\text{-}(NH_2)_2C_6H_4\}]$ **56.** $[\{Ru(\eta^3:\eta^3\text{-}C_{10}H_{16})Cl(\mu\text{-}Cl)\}_2]$ (0.10 g, 0.16 mmol) was stirred in CH_2Cl_2 (5 cm^3) with *p*-$(NH_2)_2C_6H_4$ (0.02 g, 0.17 mmol) for 1 h. resulting in the formation of a bright yellow precipitate which was collected by filtration. A second crop of precipitate was obtained by concentrating the filtrate to *ca.* 2 cm^3. Combined yield 0.10 g, 0.14 mmol, 86% (Found: C, 42.35; H, 5.50; N, 3.65. Calc. for $C_{26}H_{40}N_2Cl_4Ru_2$: C, 43.10; H, 5.55; N, 3.85%).

$[Ru(\eta^3:\eta^3\text{-}C_{10}H_{16})Cl_2(1,2\text{-}NH_2C_6H_4NH_2)]$ **57.** $[\{Ru(\eta^3:\eta^3\text{-}C_{10}H_{16})Cl(\mu\text{-}Cl)\}_2]$ (0.07 g, 0.11 mmol) was stirred in methanol (5 cm^3) with *o*-$(NH_2)_2C_6H_4$ (0.03 g, 0.24 mmol) for 4 h. resulting in the formation of an orange solution. The solvent was removed *in vacuo* and the product dissolved in the minimum amount of CH_2Cl_2. Trituration with diethyl ether resulted in the formation of an orange-red precipitate which was recovered by filtration and washed with diethyl ether. Yield 0.04 g, 0.10 mmol, 45% (Found: C, 46.20; H, 6.20; N, 6.45. Calc. for $C_{16}H_{24}N_2Cl_2Ru$: C, 46.15; H, 5.80; N, 6.75%).

$[\{Ru(\eta^3:\eta^3\text{-}C_{10}H_{16})Cl_2\}_2\{\mu\text{-}1,2\text{-}(NH_2)_2C_6H_4\}]$ **58.** $[\{Ru(\eta^3:\eta^3\text{-}C_{10}H_{16})Cl(\mu\text{-}Cl)\}_2]$ (0.08

g, 0.13 mmol) was stirred in CH_2Cl_2 (5 cm^3) with *o*-$(NH_2)_2C_6H_4$ (0.015 g, 0.14 mmol) for 2 h. resulting in the formation of a bright orange solution. The solvent was removed *in vacuo* and the resulting orange oil triturated with diethyl ether to give the product as a bright orange precipitate which was isolated by filtration and dried under reduced pressure. Yield 0.08 g, 0.11 mmol, 85% (Found: C, 43.75; H, 5.90; N, 3.75. Calc. for $C_{26}H_{40}N_2Cl_4Ru_2$: C, 43.10; H, 5.55; N, 3.85%).

$[Ru(\eta^3:\eta^3\text{-}C_{10}H_{16})Cl\{1,2\text{-}(NH_2)_2C_6H_4\}]Cl$ **59**. $[\{Ru(\eta^3:\eta^3\text{-}C_{10}H_{16})Cl(\mu\text{-}Cl)\}_2]$ (0.07 g, 0.11 mmol) was stirred in oxygenated methanol (5 cm^3) with *o*-$(NH_2)_2C_6H_4$ (0.03 g, 0.24 mmol) for 2 h. resulting in the formation of a ruby red solution. The solvent was removed *in vacuo* resulting in a deep red oil which was triturated with diethyl ether. The product was obtained as a deep red solid which was recovered by filtration and washed with diethyl ether. Yield 0.08 g, 0.10 mmol, 91% (Found: C, 45.70; H, 6.15; N, 6.50; Cl, 15.45. Calc. for $C_{16}H_{24}N_2Cl_2Ru$: C, 46.15; H, 5.80; N, 6.75; Cl, 17.05%).

$[Ru(\eta^3:\eta^3\text{-}C_{10}H_{16})Cl\{1,2\text{-}(NH_2)_2C_6H_4\}][PF_6]$ **60**. $[\{Ru(\eta^3:\eta^3\text{-}C_{10}H_{16})Cl(\mu\text{-}Cl)\}_2]$ (0.09 g, 0.15 mmol) was stirred in oxygenated methanol (5 cm^3) with *o*-$(NH_2)_2C_6H_4$ (0.036 g, 0.33 mmol) after 1 h. a red colouration was observed and all the starting material had been taken up into solution. A methanolic solution of $[NH_4][PF_6]$ (0.057 g, 0.35 mmol) was added and the mixture stirred for a further hour. The volume of the solvent was reduced to *ca.* 1 cm^3 resulting in the deposition of the product as an orange-red solid which was recovered by filtration and washed with diethyl ether. Yield 0.12 g, 0.23 mmol, 77% (Found: C, 36.55; H, 4.55; N, 5.45. Calc. for $C_{16}H_{24}N_2ClF_6PRu$: C, 36.55; H, 4.60; N, 5.35%).

$[Ru(\eta^3:\eta^3\text{-}C_{10}H_{16})Cl(2,2'\text{-}NH_2C_6H_4C_6H_4NH_2)]Cl$ **61**. $[\{Ru(\eta^3:\eta^3\text{-}C_{10}H_{16})Cl(\mu\text{-}Cl)\}_2]$ (0.10 g, 0.16 mmol) was stirred in methanol (5 cm^3) with 2,2'-diaminodiphenyl (0.06 g, 0.32 mmol) for 3 h. The resulting yellow solution was filtered and the solvent removed *in vacuo* resulting in the deposition of the product as a bright yellow solid. The product was recovered by filtration and washed with diethyl ether. Yield 0.15 g, 0.30 mmol, 94% (Found: C, 52.40; H, 5.80; N, 5.60; Cl, 14.55. Calc. for $C_{22}H_{28}N_2Cl_2Ru$: C, 53.65; H, 5.75;

N, 5.70; Cl, 14.40%).

$[Ru(\eta^3:\eta^3\text{-}C_{10}H_{16})Cl(2,2'\text{-}NH_2C_6H_4C_6H_4NH_2)][BF_4]$ **62.** $[\{Ru(\eta^3:\eta^3\text{-}C_{10}H_{16})Cl(\mu\text{-}Cl)\}_2]$ (0.09 g, 0.14 mmol) was stirred in acetone (5 cm^3) with $Ag[BF_4]$ (0.06 g, 0.31 mmol) for 30 minutes. The resulting orange solution was filtered through Celite to remove the precipitate of AgCl and 2,2'-diaminodiphenyl (0.05 g, 0.27 mmol) was then added resulting in an immediate colour change to greenish-yellow. The mixture was stirred for a further 30 minutes and the solvent removed *in vacuo* to give a greenish oil. Trituration with diethyl ether resulted in the formation of the product as a yellow-brown precipitate. Yield 0.13 g, 0.24 mmol, 86% (Found: C, 47.55; H, 5.30; N, 4.85; Cl, 5.75. Calc. for $C_{22}H_{28}N_2BClF_4Ru$: C, 48.60; H, 5.20; N, 5.15; Cl, 6.50%).

Reaction of **6** with 2,2'-diaminodiphenyl in CH_2Cl_2. $[\{Ru(\eta^3:\eta^3\text{-}C_{10}H_{16})Cl(\mu\text{-}Cl)\}_2]$ (0.10 g, 0.16 mmol) was stirred in CH_2Cl_2 (5 cm^3) with 2,2'-diaminodiphenyl (0.06 g, 0.34 mmol) for 30 minutes resulting in the formation of a bright orange solution. The solvent was removed *in vacuo* and the resulting orange oil triturated with hexane to give the product as a bright orange precipitate. Yield 0.10 g, 0.20 mmol, 63% (Found: C, 57.25; H, 6.05; N, 6.80. Calc. for $C_{22}H_{28}N_2ClRu$: C, 57.80; H, 6.15; N, 6.15%). ^1H NMR data (400 MHz, CD_2Cl_2, -20°C): 4.20 (s, 2H), 3.99 (s, 2H), 3.52 (s, 2H) and 3.38 (s, 2H) - *terminal allyl*; 4.41 (m, 2H) 4.32 (m, 2H) - *internal allyl*; 2.58 - 2.40 (m, 8H) - *ethylinic*; 2.14 (s, 6H) and 2.12 (s, 6H) - *methyl*; 7.32 - 7.14 (m, 12H, C_6H_4), 7.07 (t, 1H, ^3J=7.6, C_6H_4), 6.93 (t, 1H, ^3J=7.4, C_6H_4), 6.87 (d, 1H, ^3J=7.9, C_6H_4), 6.81 (d, 1H, ^3J=8.4, C_6H_4), 6.74 (d, 1H, ^2J=10.8, N*H*), 6.22 (d, 1H, ^2J=11.0, N*H*), 6.16 (d, 1H, ^2J=11.0, N*H*), 5.17 (d, 1H, ^2J=10.8, N*H*), 3.86 (s, 2H, N*H*), 3.77 (s, 2H, N*H*) - *ligand.*

$[Ru(\eta^3:\eta^3\text{-}C_{10}H_{16})Cl_2(NC_3H_3NH)]$ **63.** $[\{Ru(\eta^3:\eta^3\text{-}C_{10}H_{16})Cl(\mu\text{-}Cl)\}_2]$ (0.09 g, 0.15 mmol) was treated with pyrazole (0.02 g, 0.27 mmol) in toluene (5 cm^3) and the mixture stirred for 2 h. Evaporation of the resulting solution to *ca.* 2 cm^3 and addition of hexane gave the product as an orange powder which was washed with diethyl ether and dried *in vacuo*. Yield 0.08 g, 0.20 mmol, 68% (Found: C, 41.70; H, 5.10; N, 7.25. Calc. for $C_{13}H_{20}Cl_2N_2Ru$: C, 41.50; H, 5.35; N, 7.45%).

$[Ru(\eta^3:\eta^3\text{-}C_{10}H_{16})Cl(N_2C_{10}H_8)][BF_4]$ **64**. $[\{Ru(\eta^3:\eta^3\text{-}C_{10}H_{16})Cl(\mu\text{-}Cl)\}_2]$ (0.10 g, 0.16 mmol) was suspended in acetone (5 cm^3) and stirred with $Ag[BF_4]$ (0.06 g, 0.32 mmol) for 1 h. The resulting orange solution was filtered through Celite and treated with 2 mole equivalents (relative to **6**) of 2,2'-bipyridyl (0.05 g, 0.33 mmol) and the mixture stirred for a further 2 h. The resulting red solution was evaporated to dryness *in vacuo* and the residue recrystallised from acetone / hexane (1 : 1 v/v) to give yellow crystals which were isolated by filtration, washed with diethyl ether, and air dried. Yield 0.08 g, 0.15 mmol, 46% (Found: C, 46.10; H, 4.55; N, 5.55. Calc. for $C_{20}H_{24}BClF_4N_2Ru$: C, 46.60; H, 4.70; N, 5.45%).

$[Ru(\eta^3:\eta^3\text{-}C_{10}H_{16})RuCl(N_2C_{12}H_8)][BF_4]$ **65**. $[\{Ru(\eta^3:\eta^3\text{-}C_{10}H_{16})RuCl(\mu\text{-}Cl)\}_2]$ (0.16 g, 0.26 mmol) was suspended in acetone (5 cm^3) and treated with $Ag[BF_4]$ (0.10 g, 0.52 mmol) in a similar way to that described for **64**. The resulting orange solution was treated with 1,10-phenanthroline (0.09 g, 0.52 mmol) and the product isolated as described above. Yield 0.17 g, 0.31 mmol, 61% (Found: C, 48.25; H, 4.55; N, 5.40. Calc. for $C_{22}H_{24}BClF_4N_2Ru$: C, 48.95; H, 4.50; N, 5.20%).

$[Ru(\eta^3:\eta^3\text{-}C_{10}H_{16})(N_3C_{15}H_{11})][BF_4]_2$ **66**. $[\{Ru(\eta^3:\eta^3\text{-}C_{10}H_{16})RuCl(\mu\text{-}Cl)\}_2]$ (0.08 g, 0.12 mmol) was suspended in acetone (5 cm^3) and treated with $Ag[BF_4]$ (0.10 g, 0.50 mmol). The resulting orange solution was filtered through Celite and subsequently treated with 2 mole equivalents (relative to **6**) of 2,2':6',2''-terpyridine (0.05 g, 0.20 mmol). The mixture stirred for a further 2 h. during which time a colour change to deep red and the formation of a yellow precipitate were observed. The yellow precipitate was collected by filtration and washed with acetone and diethyl ether, then air dried. The red solution was concentrated to *ca.* 1 cm^3 to give a further crop of the product. Combined yield 0.11 g, 0.16 mmol, 67% (Found: C, 46.65; H, 4.55; N, 6.05. Calc. for $C_{25}H_{27}B_2F_8N_3Ru$: C, 46.60; H, 4.20; N, 6.50%).

$[Ru(\eta^3:\eta^3\text{-}C_{10}H_{16})(N_2C_{10}H_8)(OH_2)][BF_4]$ **70**. $[Ru(\eta^3:\eta^3\text{-}C_{10}H_{16})Cl(N_2C_{10}H_8)][BF_4]$ (0.06 g, 0.12 mmol) was dissolved in undried acetone (5 cm^3) and stirred with $Ag[BF_4]$ (0.03 g, 0.16 mmol) for 1 h. The resulting orange solution was filtered through Celite and

the filtrate added to diethyl ether (20 cm^3) resulting in the formation of the product as a hygroscopic yellow precipitate which was recovered by filtration and dried *in vacuo*. Yield 0.04 g, 0.07 mmol, 58% (Found: C, 40.55; H, 4.45; N, 4.70. Calc. for $C_{20}H_{26}B_2F_8N_2ORu$: C, 41.05; H, 4.50; N, 4.80%).

$[Ru(\eta^3:\eta^3\text{-}C_{10}H_{16})(N_2C_{12}H_8)(OH_2)][BF_4]$ **71.** $[Ru(\eta^3:\eta^3\text{-}C_{10}H_{16})Cl(N_2C_{12}H_8)][BF_4]$ (0.39 g, 0.72 mmol) was dissolved in undried acetone (5 cm^3) and stirred with $Ag[BF_4]$ (0.15 g, 0.77 mmol) for 1 h. The resulting orange solution was filtered through Celite and the volume reduced to *ca.* 1 cm^3 resulting in the formation of the product as yellow-green microcrystals which were recovered by filtration, washed sparingly with acetone and diethyl ether and air dried. Yield 0.33 g, 0.54 mmol, 75% (Found: C, 43.40; H, 4.30; N, 4.95. Calc. for $C_{22}H_{26}B_2F_8N_2ORu$: C, 43.40; H, 4.30; N, 4.60%).

Crystallography. - General Considerations. Crystals of maximum dimensions 0.8 x 0.8 x 0.8 mm were mounted on a glass fibre using a fast setting epoxy resin. A Nicolet R3mV four-circle diffractometer was used to irradiate the crystal with graphite monochromated Mo-K_α radiation (λ = 0.71073 Å) and to collect geometric and intensity data. Crystals were centred using a minimum of 25 discrete reflections usually in the range $10° \leq 2\theta \leq 30°$, taken from a rotation photograph. Autoindexing was used to determine unit cell dimensions and crystal orientation. Axial photography was used to verify Laue class and confirm unit cell dimensions. The ω-2θ technique used to collect data sets in the range $5° \leq 2\theta \leq 50°$. Three standards were measured every 97 reflections to monitor crystal decay and data sets were corrected for Lorentz and polarisation effects. Empirical absorption corrections were based on azimuthal scans of between 6 and 11 reflections with χ = 270 ± 20° or 90 ± 20°. Space groups were determined from systematically absent data and confirmed by successful refinement, see individual sections. Except where otherwise stated all non-hydrogen atoms were refined anisotropically whilst hydrogen atoms were placed in idealised positions (C-H 0.96 Å) and assigned a common, fixed, isotropic thermal parameter (U_{iso} = 0.08 $Å^2$), and allowed to ride on the atoms to which they were attached. All calculations were carried out using the SHELXTL PLUS program package[174] on a Microvax II computer.

i) $[Ru(\eta^3:\eta^3\text{-}C_{10}H_{16})Cl(N_2C_{10}H_8)][BF_4]$ **64**

Crystal data. - $C_{20}H_{24}N_2BClF_4Ru$, M = 515.79 g mol^{-1}, triclinic, space group $P\bar{1}$, a = 9.464(2), b = 10.493(3), c = 12.070(3), α = 72.93(2), β = 67.10(2), γ = 89.63(2), U = 1047 Å^3 (by least-squares refinement of diffractometer angles for 31 automatically centred reflections in the range $13 \leq 2\theta \leq 25°$), Z = 2, F(000) = 520, D_c = 1.64 g cm^{-3}, μ(Mo-K$_\alpha$) = 9.04 cm^{-1}.

A yellow plate of approximate dimensions 0.4 x 0.3 x 0.05 mm was prepared by layering an acetone solution of the compound with hexane. A primitive data set consisting of 3927 reflections (3685 unique) was collected as described above, 2878 of which were observed to have $I \geq 3\sigma(I)$ and were used in the refinement. Three standard reflections monitored throughout the data collection showed no appreciable change in intensity. An empirical absorption correction was applied. The structure was solved by the conventional Patterson and difference-Fourier techniques. The asymmetric unit was observed to contain one complete cationic molecule, and one tetrafluoroborate anion. The tetrafluoroborate anion was found to be disordered and was modelled as possessing two distinct sets of fluorine atoms, F(1)-F(4) and F(1a)-F(4a), occupancies refined to 0.67 and 0.33 respectively. Full-matrix least-squares refinement gave R = 0.0433, R_w = 0.0461 in the final cycle from 298 parameters. A weighting scheme of the form $w^{-1} = \sigma^2(F)+0.001368F^2$ was applied and the maximum shift to error ratio in the final cycle was 0.327, associated with an anisotropic thermal parameter for one of the disordered fluorine atoms. The largest residual peak was 0.95 e Å^{-3}, associated with the ruthenium atom. No short intermolecular contacts were observed.

ii) $[Ru(\eta^3:\eta^3\text{-}C_{10}H_{16})(N_3C_{15}H_{11})][BF_4]_2.CH_3NO_2$ **66**

Crystal data. - $C_{25}H_{27}N_3B_2F_8Ru.CH_3NO_2$, M = 705.23 g mol^{-1}, monoclinic, space group Pc, a = 7.121(2), b = 31.412(8), c = 13.373(3) Å, β = 101.13(2), U = 2935 Å^3 (by least-squares refinement of diffractometer angles for 28 automatically centred reflections in the range $17 \leq 2\theta \leq 27°$), Z = 4, F(000) = 1424, D_c = 1.60 g cm^{-3}, μ(Mo-K$_\alpha$) = 6.03 cm^{-1}.

A yellow block of approximate dimensions 0.4 x 0.4 x 0.6 mm was prepared by slow evaporation of a nitromethane solution of the compound in air. A data set comprising

5518 unique reflections in the range $5° \leq 2\theta \leq 50°$ was collected. Three standard reflections, monitored throughout, were used to correct the data set for crystal decay (*ca.* 30%). The space group was identified from the systematic absences as either P2/c or Pc although statistical analysis of the data was consistent with the presence of *pseudo*-C centring.

A total of 3689 absorption corrected reflections with $I \geq 3\sigma(I)$ were employed in the analysis. Structure solution and refinement was attempted in space groups C2/c, P2/c and Pc using Direct Methods, Patterson and difference-Fourier techniques. The Patterson solution for the space group Pc was unquestionably the only one to give a chemically reasonable structure and the only solution to refine successfully. Blocked least-squares refinement (two blocks) was carried out upon the Pc solution with two enantiomeric cations, four tetrafluoroborate anions and two nitromethane solvent molecules in the asymmetric unit, apparently related in pairs by a centre of symmetry at (¼, ¼, ¼). The metal atoms were refined anisotropically but an isotropic model was employed for the other non-hydrogen atoms due to lack of data. Refinement gave $R = 0.0640$, $R_w = 0.0717$ in the final cycle from 353 parameters. One of the tetrafluoroborate anions was found to be disordered and was fixed with an idealised tetrahedral geometry; B-F 1.3700 Å, F-F 2.2371 Å. A weighting scheme of the form $w^{-1} = \sigma^2(F)+0.000682F^2$ was applied and the maximum shift to error ratio in the final cycle was 0.14 associated with one of the nitromethane solvent molecules. The largest residual peak was 1.09 electrons $Å^{-3}$ associated with the disordered tetrafluoroborate anion. No short intermolecular contacts were observed.

A further attempt was made to solve the structure in space group P2/c by calculation of the heavy atom coordinates relative to the apparent centre of symmetry at (¼, ¼, ¼) and then correction of those coordinates to place the hypothetical inversion centre at the origin. This solution was unsuccessful, generating two large peaks *ca.* 3.5 Å apart which failed to refine. It was concluded that Pc was indeed the correct space group and that the disorder of only one of the tetrafluoroborate anions, was sufficient to break the symmetry of the crystal and result in a non-centrosymmetric space group.

Table 2.1: ^{1}H NMR Data for New Compounds.[a]

Compound	δ				
	Terminal Allyl	Internal Allyl	Ethylenic	Me	Ligand
[Ru(η^3:η^3-$C_{10}H_{16}$)Cl_2(NH_2Ph)] **54**	4.15 (s, 2H) 3.76 (s, 2H)	4.48 (m, 2H)	2.57 (m, 4H)	2.29 (s, 6H)	7.33 (d, 2H, ^3J=7.4, *o*-C_6H_5), 7.27 (t, 2H, ^3J=7.5, *m*-C_6H_5), 7.16 (t, 1H, ^3J=7.3, *p*-C_6H_5) 6.13 (s, br, N*H*), 5.67 (s, br, N*H*)
[Ru(η^3:η^3-$C_{10}H_{16}$)Cl_2($NH_2C_6H_4NH_2$)] **55**	4.15 (s, 2H) 3.75 (s, 2H)	4.45 (m, 2H)	2.58 (m, 4H)	2.29 (s, 6H)	7.15 (d, 2H, ^3J=6.5, C_6H_4), 6.57 (d, 2H, ^3J=6.5, C_6H_4), 6.01 (d, br, ^2J=6.1, N*H*), 5.55 (d, br, ^2J=6.1, N*H*), 3.58 (s, br, 2H, N*H*)
[{Ru(η^3:η^3-$C_{10}H_{16}$)Cl_2}$_2${μ-1,4-$(NH_2)_2C_6H_4$}] **56**	4.17 (s, 8H) 3.74 (s, 8H)	4.46 (m, 8H)	2.58 (m, 16H)	2.30 (s, 12H) 2.29 (s, 12H)	7.27 (s, 4H, C_6H_4), 7.26 (s, 4H, C_6H_4), 6.12 (d, br, 4H, ^2J=7.9), 5.67 (d, br, 4H, ^2J=7.9)
[Ru(η^3:η^3-$C_{10}H_{16}$)Cl_2(1,2-$NH_2C_6H_4NH_2$)] **57**	4.33 (s, 2H) 4.03 (s, 2H)	4.64 (t, 2H, ^3J=5.3)	2.68 (m, 2H) 2.51 (m, 2H)	2.32 (s, 6H)	7.26 (dd, 1H, ^3J=7.7, ^4J=1.4, C_6H_4), 6.95 (dt, 1H, ^3J=7.7, ^4J=1.4, C_6H_4), 6.72 (dd, 1H, ^3J=7.7, ^4J=1.4, C_6H_4), 6.68 (dt, 1H, ^3J=7.7, ^4J=1.4, C_6H_4), 5.87 (d, br, 1H, ^2J=8.8, N*H*), 5.53 (d, br, 1H, ^2J=8.8, N*H*), 3.40 (s, br, 2H, N*H*)

[{Ru(η^3:η^3-$C_{10}H_{16}$)Cl_2}$_2${μ-1,2-$(NH_2)_2C_6H_4$}] **58**[b] Major diastereoisomer	4.60, 4.48, 4.21[c] 4.18, 4.11, 3.99	4.62 (m, 4H)	2.69 (m, 4H) 2.46 (m, 4H)	2.26 (s, 12H)	8.26 (m, 2H, C_6H_4), 7.49 (d, 1H, ^2J=7.0, N*H*), 7.21 (d, 1H, ^2J=7.0, N*H*), 5.74 (d, 1H, ^2J=9.5, N*H*), 5.33 (d, 1H, ^2J=9.5, N*H*)
[{Ru(η^3:η^3-$C_{10}H_{16}$)Cl_2}$_2${μ-1,2-$(NH_2)_2C_6H_4$}] **58**[b] Minor diastereoisomer		4.62 (m, 4H)	2.69 (m, 4H) 2.46 (m, 4H)	2.31 (s, 6H) 2.24 (s, 6H)	8.36 (m, 2H, C_6H_4), 7.42 (s, 1H, N*H*), 7.25 (s, 1H, N*H*), 5.62 (s, 1H, N*H*), 5.22 (s, 1H, N*H*)
[{Ru(η^3:η^3-$C_{10}H_{16}$)Cl{1,2-$(NH_2)_2C_6H_4$}]Cl **59**[b]	4.14 (s, 1H) 3.88 (s, 1H) 3.74 (s, 1H) 3.38 (s, 1H)	4.44 (m, 1H) 4.37 (m, 1H)	2.90 - 2.54 (m, 4H)	2.25 (s, 6H)	8.45 (s, br, 1H, N*H*), 7.61 (d, 1H, ^3J=7.8, C_6H_4), 7.34 (d, 1H, ^3J=7.1, C_6H_4), 7.28 (t, 1H, ^3J=7.3, C_6H_4), 7.11 (t, 1H, ^3J=7.3, C_6H_4), 6.93 (s, br, 1H, N*H*), 6.42 (s, br, 1H, N*H*), 4.79 (s, br, 1H, N*H*)
[{Ru(η^3:η^3-$C_{10}H_{16}$)Cl{1,2-$(NH_2)_2C_6H_4$}][PF_6] **60**[d]	4.48 (s, 1H) 4.25 (s, 1H) 3.60 (s, 1H) 3.03 (s, 1H)	4.48 (m, 1H) 3.60 (m, 1H)	2.88 - 2.66 (m, 4H)	2.39 (s, 3H) 2.30 (s, 3H)	7.51 (d, 1H, ^3J=7.9, C_6H_4), 7.35 (t, 1H, ^3J=7.5, C_6H_4), 7.29 (t, 1H, ^3J=7.9, C_6H_4), 7.21 (d, 1H, ^3J=7.9, C_6H_4), 6.96 (d, br, 1H, ^2J=12.5, N*H*), 6.64 (d, br, 1H, ^2J=12.5, N*H*), 4.29 (s, br, 2H, N*H*)
[Ru(η^3:η^3-$C_{10}H_{16}$)Cl($NH_2C_6H_4C_6H_4NH_2$)]Cl **61**[b]	4.36 (s, 1H) 4.10 (s, 1H) 3.59 (s, 1H) 3.05 (s, 1H)	4.73 (m, 2H)	2.80 - 2.50 (m, 4H)	2.44 (s, br, 3H) 2.35 (s, 3H)	7.48 (m, br, 3H, C_6H_4), 7.28 (m, 3H, C_6H_4), 7.19 (d, 1H, ^3J=7.6, C_6H_4), 7.12 (d, 1H, ^3J=7.5, C_6H_4), 6.10 (d, 1H, ^2J=9.0, N*H*), 5.47 (d, 1H, ^2J=9.0, N*H*), 3.61 (s, br, 2H, N*H*)

$[Ru(\eta^3:\eta^3\text{-}C_{10}H_{16})Cl(NH_2C_6H_4C_6H_4NH_2)][BF_4]$ **62**	4.41 (s, 1H) 4.13 (s, 1H) 3.60 (s, 1H) 3.04 (s, 1H)	4.79 (dd, 1H, ^3J=8.1 & 3.9) 4.18 (d, 1H, ^3J=7.5)	3.38 (m, 1H) 2.85 (m, 1H) 2.76 (m, 1H) 2.60 (m, 1H)	2.42 (s, 3H) 2.29 (s, 3H)	7.62 (m, 2H, C_6H_4), 7.36 (m, 3H, C_6H_4), 7.26 (d, 1H, ^3J=6.2), 7.21 (dd, 1H, ^3J=7.4, ^4J=1.7, C_6H_4), 7.10 (d, 1H, ^3J=7.8, C_6H_4), 6.08 (d, 1H, ^2J=9.3, N*H*), 5.57 (d, 1H, ^2J=9.3, N*H*), 5.09 (d, 1H, ^2J=8.3, N*H*), 3.81 (d, 1H, ^2J=8.3, N*H*)
$[Ru(\eta^3:\eta^3\text{-}C_{10}H_{16})Cl_2(NC_3H_3NH)]$ **63**	4.45 (s, 2H) 4.35 (s, 2H)	5.18 (m, 2H)	3.07 (m, 2H) 2.43 (m, 2H)	2.33 (s, 6H)	12.10 (d, 1H, ^3J=0.9, N*H*), 8.30 (d, 1H, ^3J=4.8), 7.69 (dd 1H, ^3J=2.4 & 0.9), 6.48 (dd 1H, ^3J=4.8 & 2.4)
$[Ru(\eta^3:\eta^3\text{-}C_{10}H_{16})Cl(N_2C_{10}H_8)][BF_4]$ **64**	4.35 (s, 1H) 4.02 (s, 1H) 3.69 (s, 1H) 2.49 (s, 1H)	5.53 (dd, 1H, ^3J=12.1 & 4.0) 4.79 (dd, 1H, ^3J=11.5 & 4.2)	3.70 (m, 1H) 3.42 (m, 1H) 2.93 (m, 1H) 2.67 (m, 1H)	2.45 (s, 3H) 1.77 (s, 3H)	9.70 (d, 1H, ^3J=5.7), 8.60 (d, 1H, ^3J=7.6), 8.58 (d, 1H, ^3J=5.3), 8.48 (d, 1H, ^3J=8.1), 8.25 (t, 1H, ^3J=7.7), 8.06 (t, 1H, ^3J=7.2), 7.81 (t, 1H, ^3J=6.1), 7.69 (t, 1H, ^3J=6.1)
$[Ru(\eta^3:\eta^3\text{-}C_{10}H_{16})Cl(N_2C_{12}H_8)][BF_4]$ **65**	4.36 (s, 1H) 4.00 (s, 1H) 3.47 (s, 1H) 2.44 (s, 1H)	5.63 (dd, 1H, ^3J=11.9 & 4.0) 5.11 (dd, 1H, ^3J=11.3 & 4.3)	3.89 (m, 1H) 3.48 (m, 1H) 3.06 (m, 1H) 2.74 (m, 1H)	2.50 (s, 3H) 1.76 (s, 3H)	10.06 (d, 1H, ^3J=5.4), 9.15 (d, 1H, ^3J=5.4), 8.71 (d, 1H, ^3J=8.2), 8.58 (d, 1H, ^3J=8.2), 8.26 (t, 1H, ^3J=6.6), 8.15 (s, 2H), 8.05 (t, 1H, ^3J=8.2)
$[Ru(\eta^3:\eta^3\text{-}C_{10}H_{16})(N_3C_{15}H_{11})][BF_4]_2$ **66**[e]	3.94 (s, 2H) 2.94 (s, 2H)	5.08 (m, 2H)	3.91 (m, 2H) 3.18 (m, 2H)	2.11 (s, 6H)	8.69 (d, 2H, ^3J=8.1), 8.61 (t, 1H, ^3J=8.1), 8.55 (d, 2H, ^3J=8.1), 8.48 (d, 2H, ^3J=5.1), 8.32 (t, 2H, ^3J=8.1), 7.82 (t, 2H, ^3J=6.8)

$[Ru(\eta^3:\eta^3\text{-}C_{10}H_{16})(N_2C_{10}H_8)(OH_2)][BF_4]_2$ **70**[e]	4.77 (s, 1H) 4.04 (s, 1H) 3.89 (s, 1H) 2.92 (s, 1H)	5.08 (m, 2H)	3.84 (m, 2H) 3.09 (m, 2H)	2.46 (m, 3H) 1.93 (m, 3H)	8.79 (d, 1H, ^3J=5.7), 8.64 (d, 1H, ^3J=8.4), 8.42 (m, 2H), 8.32 (d, 1H, 5.8), 8.18 (t, 1H, ^3J=8.1), 7.98 (t, 1H, ^3J=6.2), 7.68 (t, 1H, ^3J=6.2), 4.36 (s, 2H, OH_2)
$[Ru(\eta^3:\eta^3\text{-}C_{10}H_{16})(N_2C_{12}H_8)(OH_2)][BF_4]_2$ **71**[e]	4.77 (s, 1H) 4.22 (s, 1H) 3.94 (s, 1H) 3.57 (s, 1H)	5.28 (dd, 1H, ^3J=11.5 & 4.6) 5.17 (dd, 1H, ^3J=11.1 & 3.8)	3.94 (m, 2H) 3.12 (m, 2H)	2.49 (s, 3H) 1.84 (s, 3H)	9.21 (d, 1H, ^3J=5.3), 9.00 (d, 1H, ^3J=8.2), 8.74 (d, 1H, ^3J=8.2) 8.71 (d, 1H, ^3J=5.6), 8.36 (d, 1H, ^3J=8.9), 8.31 (dd, 1H, ^3J=8.2 & 5.4), 8.23 (d, 1H, ^3J=8.9), 7.99 (dd, 1H, ^3J=8.2 & 5.7), 3.92 (s, 2H, OH_2)

a) δ / ppm, $J_{H\text{-}H}$ / Hz, 400 MHz, 20°C, solvent $CDCl_3$ unless otherwise stated, s = singlet, d = doublet, dd = doublet of doublets, t = triplet, se = septet, m = multiplet, br = broad; b) signals broad due to fluxionality; c) overlap and broadness of spectrum makes assignment of resonances to their respective isomers impossible. All resonances are broad singlets of varying intensity, total integral 12H for each diastereoisomer; d) solvent MeCN-d_3; e) solvent *nitromethane*-d_3.

Table 2.2: Fractional atomic coordinates (x 10^4) and equivalent isotropic displacement factors ($Å^2$ x 10^3)* for $[Ru(\eta^3:\eta^3\text{-}C_{10}H_{16})Cl(N_2C_{10}H_8)][BF_4]$ **64**.

	x	y	z	U(eq)
Ru(1)	2353(1)	2197(1)	1831(1)	39(1)
Cl(1)	5160(2)	2348(2)	948(2)	74(1)
N(1)	2478(5)	3813(4)	2547(4)	46(2)
N(2)	5(5)	2491(4)	2652(4)	46(2)
C(1)	2777(9)	3907(6)	94(5)	58(3)
C(2)	1997(8)	2844(6)	-21(5)	61(3)
C(3)	2682(8)	1630(6)	77(5)	68(3)
C(4)	1911(9)	271(6)	283(6)	66(3)
C(5)	2162(8)	-687(6)	1388(7)	64(3)
C(6)	1676(7)	-37(5)	2414(5)	50(2)
C(7)	2552(7)	137(5)	3090(6)	54(3)
C(8)	1998(8)	1003(6)	3817(6)	63(3)
C(9)	484(10)	2993(8)	-129(7)	84(4)
C(10)	4054(9)	-434(7)	2950(8)	82(4)
C(11)	-1242(7)	1753(7)	2795(7)	64(3)
C(12)	-2735(8)	2097(9)	3297(8)	85(4)
C(13)	-2958(9)	3225(9)	3647(9)	85(4)
C(14)	-1693(8)	3996(7)	3513(6)	65(3)
C(15)	-241(7)	3611(6)	3031(5)	49(2)
C(16)	1137(7)	4320(5)	2979(5)	49(2)
C(17)	1081(8)	5460(6)	3367(6)	58(3)
C(18)	2414(9)	6017(6)	3345(6)	70(3)
C(19)	3740(9)	5460(7)	2960(6)	68(3)
C(20)	3763(7)	4364(6)	2542(6)	57(3)
B(1)	7320(9)	-2229(7)	3624(7)	55(3)
F(1)	8451(11)	-2653(14)	4096(13)	100(7)
F(1A)	7822(43)	-3083(31)	4412(25)	153(22)
F(2)	6301(15)	-1727(15)	4485(14)	114(7)
F(2A)	6620(39)	-1280(23)	4064(33)	127(25)
F(3)	6687(22)	-3295(13)	3538(20)	144(10)
F(3A)	6371(27)	-2822(21)	3233(25)	86(10)
F(4)	8114(24)	-1210(14)	2531(17)	130(8)
F(4A)	8348(54)	-1776(49)	2568(29)	213(26)

* U_{iso} defined as ⅓ of the trace of the orthogonalised U_{ij} tensor

Table 2.3: Bond lengths (Å) and angles (°) for $[Ru(\eta^3:\eta^3\text{-}C_{10}H_{16})Cl(N_2C_{10}H_8)][BF_4]$ **64**.

Ru(1)-Cl(1)	2.433 (2)	Ru(1)-N(1)	2.140 (5)
Ru(1)-N(2)	2.115 (4)	Ru(1)-C(1)	2.219 (5)
Ru(1)-C(2)	2.294 (7)	Ru(1)-C(3)	2.270 (7)
Ru(1)-C(6)	2.259 (5)	Ru(1)-C(7)	2.303 (5)
Ru(1)-C(8)	2.246 (6)	N(1)-C(16)	1.344 (8)
N(1)-C(20)	1.346 (9)	N(2)-C(11)	1.340 (9)
N(2)-C(15)	1.369 (8)	C(1)-C(2)	1.410 (11)
C(2)-C(3)	1.420 (10)	C(2)-C(9)	1.491 (13)
C(3)-C(4)	1.515 (10)	C(4)-C(5)	1.519 (11)
C(5)-C(6)	1.503 (10)	C(6)-C(7)	1.415 (11)
C(7)-C(8)	1.405 (10)	C(7)-C(10)	1.507 (11)
C(11)-C(12)	1.397 (10)	C(12)-C(13)	1.359 (14)
C(13)-C(14)	1.378 (13)	C(14)-C(15)	1.378 (9)
C(15)-C(16)	1.476 (10)	C(16)-C(17)	1.401 (10)
C(17)-C(18)	1.381 (12)	C(18)-C(19)	1.352 (11)
C(19)-C(20)	1.382 (11)	B(1)-F(1)	1.410 (17)
B(1)-F(1A)	1.334 (37)	B(1)-F(2)	1.351 (17)
B(1)-F(2A)	1.320 (31)	B(1)-F(3)	1.322 (22)
B(1)-F(3A)	1.388 (34)	B(1)-F(4)	1.363 (15)
B(1)-F(4A)	1.218 (30)		

Cl(1)-Ru(1)-N(1)	89.5(1)	Cl(1)-Ru(1)-N(2)	166.9(2)
N(1)-Ru(1)-N(2)	77.7(2)	Cl(1)-Ru(1)-C(1)	83.3(2)
N(1)-Ru(1)-C(1)	81.1(2)	N(2)-Ru(1)-C(1)	91.7(2)
Cl(1)-Ru(1)-C(2)	99.1(2)	N(1)-Ru(1)-C(2)	113.8(2)
N(2)-Ru(1)-C(2)	83.8(2)	C(1)-Ru(1)-C(2)	36.4(3)
Cl(1)-Ru(1)-C(3)	82.2(2)	N(1)-Ru(1)-C(3)	145.3(2)
N(2)-Ru(1)-C(3)	106.7(2)	C(1)-Ru(1)-C(3)	64.6(2)
C(2)-Ru(1)-C(3)	36.3(2)	Cl(1)-Ru(1)-C(6)	101.6(2)
N(1)-Ru(1)-C(6)	143.4(2)	N(2)-Ru(1)-C(6)	90.5(2)
C(1)-Ru(1)-C(6)	134.4(3)	C(2)-Ru(1)-C(6)	98.9(3)
C(3)-Ru(1)-C(6)	71.2(2)	Cl(1)-Ru(1)-C(7)	82.4(2)
N(1)-Ru(1)-C(7)	113.8(2)	N(2)-Ru(1)-C(7)	105.2(2)
C(1)-Ru(1)-C(7)	159.2(2)	C(2)-Ru(1)-C(7)	132.4(3)
C(3)-Ru(1)-C(7)	98.5(2)	C(6)-Ru(1)-C(7)	36.1(3)
Cl(1)-Ru(1)-C(8)	95.7(2)	N(1)-Ru(1)-C(8)	80.7(2)
N(2)-Ru(1)-C(8)	85.1(2)	C(1)-Ru(1)-C(8)	161.8(3)
C(2)-Ru(1)-C(8)	159.2(3)	C(3)-Ru(1)-C(8)	133.5(2)
C(6)-Ru(1)-C(8)	63.7(3)	C(7)-Ru(1)-C(8)	36.0(2)
Ru(1)-N(1)-C(16)	114.2(4)	Ru(1)-N(1)-C(20)	125.8(4)
C(16)-N(1)-C(20)	119.9(5)	Ru(1)-N(2)-C(11)	128.1(4)
Ru(1)-N(2)-C(15)	114.8(4)	C(11)-N(2)-C(15)	117.1(5)
Ru(1)-C(1)-C(2)	74.7(3)	Ru(1)-C(2)-C(1)	68.9(4)
Ru(1)-C(2)-C(3)	71.0(4)	C(1)-C(2)-C(3)	115.8(7)
Ru(1)-C(2)-C(9)	125.9(4)	C(1)-C(2)-C(9)	120.3(7)
C(3)-C(2)-C(9)	123.7(7)	Ru(1)-C(3)-C(2)	72.8(4)

Ru(1)-C(3)-C(4)	117.2(4)	C(2)-C(3)-C(4)	125.8(7)
C(3)-C(4)-C(5)	105.3(7)	C(4)-C(5)-C(6)	106.2(5)
Ru(1)-C(6)-C(5)	117.6(3)	Ru(1)-C(6)-C(7)	73.6(3)
C(5)-C(6)-C(7)	125.7(6)	Ru(1)-C(7)-C(6)	70.2(3)
Ru(1)-C(7)-C(8)	69.8(3)	C(6)-C(7)-C(8)	114.8(6)
Ru(1)-C(7)-C(10)	124.3(4)	C(6)-C(7)-C(10)	123.4(7)
C(8)-C(7)-C(10)	121.5(8)	Ru(1)-C(8)-C(7)	74.2(4)
N(2)-C(11)-C(12)	122.5(7)	C(11)-C(12)-C(13)	119.8(8)
C(12)-C(13)-C(14)	118.7(7)	C(13)-C(14)-C(15)	119.7(7)
N(2)-C(15)-C(14)	122.3(6)	N(2)-C(15)-C(16)	115.4(5)
C(14)-C(15)-C(16)	122.2(6)	N(1)-C(16)-C(15)	116.9(5)
N(1)-C(16)-C(17)	120.4(6)	C(15)-C(16)-C(17)	122.8(6)
C(16)-C(17)-C(18)	118.8(6)	C(17)-C(18)-C(19)	120.1(7)
C(18)-C(19)-C(20)	119.4(8)	N(1)-C(20)-C(19)	121.3(6)
F(1)-B(1)-F(2)	105.1(12)	F(1A)-B(1)-F(2A)	113.6(24)
F(1)-B(1)-F(3)	107.4(12)	F(2)-B(1)-F(3)	112.2(11)
F(1A)-B(1)-F(3A)	115.0(20)	F(2A)-B(1)-F(3A)	108.4(22)
F(1)-B(1)-F(4)	103.6(12)	F(2)-B(1)-F(4)	109.6(11)
F(3)-B(1)-F(4)	117.8(15)	F(1A)-B(1)-F(4A)	111.3(28)
F(2A)-B(1)-F(4A)	112.4(27)	F(3A)-B(1)-F(4A)	94.8(28)

Table 2.4: Anisotropic displacement factors ($Å^2$ x 10^3) for $[Ru(\eta^3:\eta^3\text{-}C_{10}H_{16})Cl(N_2C_{10}H_8)][BF_4]$ **64.**

	U_{11}	U_{22}	U_{33}	U_{23}	U_{13}	U_{12}
Ru(1)	43(1)	36(1)	36(1)	-30(1)	-14(1)	-4(1)
Cl(1)	51(1)	72(1)	90(1)	-34(1)	-14(1)	-3(1)
N(1)	53(3)	40(2)	38(2)	-12(2)	-13(2)	-9(2)
N(2)	44(2)	49(2)	45(2)	-18(2)	-15(2)	3(2)
C(1)	91(5)	42(3)	40(3)	-3(2)	-17(3)	-1(3)
C(2)	87(5)	63(4)	29(3)	-10(3)	-25(3)	11(3)
C(3)	77(4)	60(4)	37(3)	-23(3)	-17(3)	6(3)
C(4)	84(5)	64(4)	70(4)	-37(3)	-41(4)	13(3)
C(5)	83(5)	41(3)	84(4)	-29(3)	-45(4)	9(3)
C(6)	58(3)	40(3)	53(3)	-7(2)	-28(3)	-6(2)
C(7)	65(4)	33(3)	57(3)	0(2)	-29(3)	-7(3)
C(8)	84(5)	57(4)	48(3)	0(3)	-38(3)	-18(3)
C(9)	132(7)	75(5)	79(5)	-28(4)	-74(5)	30(5)
C(10)	93(5)	57(4)	118(6)	-16(4)	-75(5)	2(4)
C(11)	53(4)	63(4)	88(5)	-30(3)	-35(3)	2(3)
C(12)	49(4)	102(6)	111(6)	-36(5)	-39(4)	-3(4)
C(13)	65(5)	100(6)	103(6)	-44(5)	-38(4)	25(4)
C(14)	64(4)	66(4)	68(4)	-25(3)	-28(3)	14(3)
C(15)	52(3)	51(3)	44(3)	-16(2)	-17(3)	4(3)
C(16)	65(4)	36(3)	40(3)	-9(2)	-16(3)	-1(2)
C(17)	81(4)	48(3)	58(4)	-23(3)	-22(3)	3(3)
C(18)	101(6)	42(3)	61(4)	-17(3)	-25(4)	-15(3)
C(19)	74(5)	66(4)	63(4)	-23(3)	-24(3)	-21(3)
C(20)	56(4)	56(3)	58(3)	-19(3)	-20(3)	-17(3)
B(1)	57(4)	54(4)	59(4)	-25(3)	-24(3)	0(3)
F(1)	72(5)	105(9)	136(11)	-41(7)	-53(6)	43(5)
F(1A)	315(45)	101(19)	96(15)	-45(13)	-127(24)	95(24)
F(2)	65(5)	203(15)	104(7)	-97(9)	-32(5)	51(7)
F(2A)	200(32)	66(10)	246(41)	-101(17)	-189(32)	84(15)
F(3)	163(12)	79(8)	248(17)	-72(9)	-129(10)	27(7)
F(3A)	85(12)	71(13)	136(15)	-55(12)	-63(10)	-1(10)
F(4)	178(13)	91(6)	109(10)	14(5)	-77(10)	-52(7)
F(4A)	186(31)	303(56)	53(16)	-12(24)	19(17)	-56(36)

The anisotropic displacement exponent takes the form:

$-2\pi^2(h^2a^{*2}U_{11} + \ldots + 2hka^*b^*U_{12})$

Table 2.5: Fractional atomic coordinates (x 10^4) and equivalent isotropic displacement factors ($Å^2$ x 10^3) for $[Ru(\eta^3:\eta^3\text{-}C_{10}H_{16})(N_3C_{15}H_{11})][BF_4]_2.CH_3NO_2$ **66**.

	x	y	z	U(eq)
Ru(1)	0	1116(1)	0	36(1)
C(1)	2584(26)	1467(5)	-374(11)	57(4)
C(2)	1855(21)	1147(4)	-1174(9)	37(3)
C(3)	2008(25)	684(5)	-869(12)	60(4)
C(4)	908(32)	415(6)	-1687(15)	83(6)
C(5)	-345(43)	236(8)	-1136(22)	130(9)
C(6)	-1733(23)	533(5)	-642(11)	50(4)
C(7)	-1823(18)	576(4)	468(8)	29(3)
C(8)	-2559(21)	980(4)	646(9)	36(3)
C(9)	1330(28)	1256(6)	-2280(12)	68(5)
C(10)	-1215(26)	294(5)	1293(11)	58(4)
N(1)	-2077(17)	1506(3)	-1002(8)	38(3)
N(2)	-51(16)	1656(3)	813(7)	35(2)
N(3)	1934(16)	972(3)	1399(7)	33(2)
C(11)	-2942(26)	1425(6)	-2032(12)	63(5)
C(12)	-4214(20)	1719(4)	-2531(10)	36(3)
C(13)	-4254(30)	2038(6)	-2258(13)	70(5)
C(14)	-3247(37)	2205(8)	-1111(18)	112(8)
C(15)	-2227(21)	1899(4)	-696(9)	37(3)
C(16)	-1187(20)	1948(4)	408(9)	33(3)
C(17)	-1132(27)	2339(6)	1045(12)	64(4)
C(18)	-193(21)	2321(4)	2047(10)	42(3)
C(19)	1039(23)	2003(5)	2413(11)	49(4)
C(20)	1090(22)	1631(5)	1812(10)	47(3)
C(21)	2146(26)	1261(5)	2177(12)	57(4)
C(22)	3189(22)	1198(5)	3029(10)	46(3)
C(23)	4281(29)	807(6)	3232(14)	71(5)
C(24)	3924(23)	562(5)	2673(11)	50(4)
C(25)	2940(19)	586(4)	1591(9)	33(3)
C(52)	5988(53)	3647(10)	99(23)	185(15)
N(8)	6755(49)	3686(12)	1289(23)	158(11)
O(3)	7434(40)	3440(8)	1536(19)	167(9)
O(4)	6136(32)	3990(7)	1447(15)	138(7)
B(1)	4604(14)	564(3)	6167(6)	157(15)
F(1)	6199(19)	773(4)	5993(9)	168(7)
F(2)	4840(19)	460(4)	7178(6)	118(4)
F(3)	3037(19)	823(4)	5904(10)	196(8)
F(4)	4339(19)	200(3)	5591(8)	127(5)
B(2)	2557(75)	2287(16)	5225(37)	164(16)
F(5)	3796(18)	2551(3)	5779(8)	87(3)
F(6)	3654(20)	2000(4)	4893(9)	101(4)
F(7)	1234(22)	2084(4)	5795(10)	112(4)
F(8)	1484(17)	2556(3)	4454(7)	77(3)

Ru(2)	4929(2)	3894(1)	4930(1)	39(1)
C(26)	7379(28)	4094(6)	4265(13)	68(5)
C(27)	6637(30)	4462(6)	4644(14)	76(5)
C(28)	6483(23)	4507(5)	5501(11)	51(4)
C(29)	5466(22)	4864(4)	5858(10)	44(3)
C(30)	3975(24)	4663(5)	6383(11)	50(4)
C(31)	3157(21)	4239(4)	5817(10)	42(3)
C(32)	2941(28)	3835(5)	6103(13)	66(5)
C(33)	2505(24)	3563(5)	5352(11)	50(4)
C(34)	5846(31)	4798(6)	3739(13)	78(5)
C(35)	3821(25)	3643(5)	7169(11)	53(4)
N(4)	3006(21)	4051(4)	3593(10)	62(4)
N(5)	5072(19)	3365(4)	4062(8)	48(3)
N(6)	6853(18)	3521(3)	5962(8)	43(3)
C(36)	1963(29)	4364(6)	3208(14)	77(5)
C(37)	764(27)	4492(5)	2429(12)	60(4)
C(38)	1001(26)	4128(5)	1528(12)	57(4)
C(39)	1990(30)	3767(6)	1765(15)	77(5)
C(40)	2972(19)	3720(4)	2875(8)	31(3)
C(41)	4135(19)	3317(4)	3128(8)	31(3)
C(42)	4256(27)	2951(5)	2586(12)	59(4)
C(43)	5379(28)	2606(6)	3073(13)	71(5)
C(44)	6467(20)	2662(4)	3979(9)	37(3)
C(45)	6248(26)	3017(5)	4455(12)	59(4)
C(46)	7175(23)	3140(4)	5478(10)	46(3)
C(47)	8407(19)	2815(4)	6116(9)	33(3)
C(48)	9363(24)	2879(5)	6982(11)	50(4)
C(49)	8893(29)	3351(6)	7541(15)	77(5)
C(50)	7905(20)	3608(4)	6829(10)	38(3)
C(51)	8985(41)	1195(8)	4991(17)	119(9)
N(7)	8471(23)	1268(5)	3965(11)	67(4)
O(1)	8553(30)	1058(6)	3300(14)	131(6)
O(2)	7725(30)	1645(7)	3616(15)	145(7)
B(3)	2618(19)	2729(4)	9638(9)	18(2)
F(9)	1502(21)	2449(4)	9058(9)	109(4)
F(10)	3297(20)	2914(4)	8884(9)	110(4)
F(11)	1812(20)	3055(4)	10097(9)	106(4)
F(12)	3967(17)	2555(3)	10350(8)	84(3)
B(4)	460(22)	4461(4)	8767(10)	27(3)
F(13)	2338(28)	4500(5)	8657(13)	152(6)
F(14)	-855(22)	4580(4)	7867(10)	118(4)
F(15)	212(21)	4071(4)	9105(10)	110(4)
F(16)	307(17)	4793(3)	9479(8)	84(3)

Table 2.6: Bond lengths (Å) and angles (°) for $[Ru(\eta^3:\eta^3\text{-}C_{10}H_{16})(N_3C_{15}H_{11})][BF_4]_2.CH_3NO_2$ **66.**

Ru(1)-C(1)	2.283 (18)	Ru(1)-C(2)	2.241 (15)
Ru(1)-C(3)	2.423 (18)	Ru(1)-C(6)	2.281 (15)
Ru(1)-C(7)	2.294 (12)	Ru(1)-C(8)	2.203 (15)
Ru(1)-N(1)	2.172 (10)	Ru(1)-N(2)	2.018 (10)
Ru(1)-N(3)	2.147 (9)	C(1)-C(2)	1.486 (19)
C(2)-C(3)	1.509 (20)	C(2)-C(9)	1.493 (20)
C(3)-C(4)	1.482 (25)	C(4)-C(5)	1.381 (39)
C(5)-C(6)	1.593 (34)	C(6)-C(7)	1.504 (19)
C(7)-C(8)	1.409 (17)	C(7)-C(10)	1.417 (18)
N(1)-C(11)	1.420 (18)	N(1)-C(15)	1.313 (16)
N(2)-C(16)	1.273 (16)	N(2)-C(20)	1.426 (16)
N(3)-C(21)	1.368 (19)	N(3)-C(25)	1.406 (16)
C(11)-C(12)	1.374 (21)	C(12)-C(13)	1.067 (22)
C(13)-C(14)	1.648 (28)	C(14)-C(15)	1.266 (28)
C(15)-C(16)	1.525 (17)	C(16)-C(17)	1.491 (21)
C(17)-C(18)	1.378 (20)	C(18)-C(19)	1.359 (20)
C(19)-C(20)	1.422 (20)	C(20)-C(21)	1.419 (22)
C(21)-C(22)	1.249 (20)	C(22)-C(23)	1.449 (23)
C(23)-C(24)	1.070 (23)	C(24)-C(25)	1.483 (17)
C(52)-N(8)	1.584 (42)	N(8)-O(3)	0.937 (43)
N(8)-O(4)	1.090 (43)	B(1)-F(1)	1.370 (17)
B(1)-F(2)	1.370 (11)	B(1)-F(3)	1.370 (16)
B(1)-F(4)	1.370 (13)	B(2)-F(5)	1.328 (50)
B(2)-F(6)	1.324 (55)	B(2)-F(7)	1.467 (57)
B(2)-F(8)	1.434 (48)	Ru(2)-C(26)	2.197 (21)
Ru(2)-C(27)	2.234 (20)	Ru(2)-C(28)	2.276 (14)
Ru(2)-C(31)	2.180 (15)	Ru(2)-C(32)	2.314 (20)
Ru(2)-C(33)	2.180 (17)	Ru(2)-N(4)	2.090 (13)
Ru(2)-N(5)	2.040 (12)	Ru(2)-N(6)	2.104 (11)
C(26)-C(27)	1.405 (27)	C(27)-C(28)	1.180 (25)
C(27)-C(34)	1.622 (25)	C(28)-C(29)	1.465 (21)
C(29)-C(30)	1.520 (23)	C(30)-C(31)	1.585 (19)
C(31)-C(32)	1.343 (22)	C(32)-C(33)	1.309 (22)
C(32)-C(35)	1.564 (21)	N(4)-C(36)	1.279 (23)
N(4)-C(40)	1.413 (18)	N(5)-C(41)	1.306 (15)
N(5)-C(45)	1.415 (20)	N(6)-C(46)	1.401 (18)
N(6)-C(50)	1.282 (16)	C(36)-C(37)	1.278 (24)
C(37)-C(38)	1.692 (23)	C(38)-C(39)	1.341 (25)
C(39)-C(40)	1.520 (21)	C(40)-C(41)	1.513 (17)
C(41)-C(42)	1.370 (20)	C(42)-C(43)	1.427 (24)
C(43)-C(44)	1.318 (20)	C(44)-C(45)	1.309 (21)
C(45)-C(46)	1.452 (20)	C(46)-C(47)	1.500 (18)
C(47)-C(48)	1.241 (18)	C(48)-C(49)	1.722 (24)
C(49)-C(50)	1.341 (22)	C(51)-N(7)	1.369 (26)
N(7)-O(1)	1.118 (25)	N(7)-O(2)	1.345 (25)
B(3)-F(9)	1.329 (17)	B(3)-F(10)	1.335 (19)
B(3)-F(11)	1.376 (18)	B(3)-F(12)	1.332 (15)
B(4)-F(13)	1.379 (26)	B(4)-F(14)	1.425 (18)
B(4)-F(15)	1.331 (19)	B(4)-F(16)	1.430 (17)

C(1)-Ru(1)-C(2)	38.3(5)	C(1)-Ru(1)-C(3)	65.8(6)
C(2)-Ru(1)-C(3)	37.5(5)	C(1)-Ru(1)-C(6)	134.9(6)
C(2)-Ru(1)-C(6)	97.0(5)	C(3)-Ru(1)-C(6)	72.4(6)
C(1)-Ru(1)-C(7)	160.0(5)	C(2)-Ru(1)-C(7)	131.7(4)
C(3)-Ru(1)-C(7)	97.8(5)	C(6)-Ru(1)-C(7)	38.4(5)
C(1)-Ru(1)-C(8)	160.4(5)	C(2)-Ru(1)-C(8)	158.0(4)
C(3)-Ru(1)-C(8)	133.5(5)	C(6)-Ru(1)-C(8)	64.1(5)
C(7)-Ru(1)-C(8)	36.4(4)	C(1)-Ru(1)-N(1)	94.2(5)
C(2)-Ru(1)-N(1)	88.1(5)	C(3)-Ru(1)-N(1)	114.5(5)
C(6)-Ru(1)-N(1)	88.1(4)	C(7)-Ru(1)-N(1)	103.4(4)
C(8)-Ru(1)-N(1)	80.5(4)	C(1)-Ru(1)-N(2)	79.1(5)
C(2)-Ru(1)-N(2)	114.5(5)	C(3)-Ru(1)-N(2)	143.3(5)
C(6)-Ru(1)-N(2)	144.3(5)	C(7)-Ru(1)-N(2)	113.8(4)
C(8)-Ru(1)-N(2)	81.3(5)	N(1)-Ru(1)-N(2)	77.1(4)
C(1)-Ru(1)-N(3)	83.4(5)	C(2)-Ru(1)-N(3)	104.7(5)
C(3)-Ru(1)-N(3)	87.8(5)	C(6)-Ru(1)-N(3)	111.6(4)
C(7)-Ru(1)-N(3)	84.7(4)	C(8)-Ru(1)-N(3)	93.3(4)
N(1)-Ru(1)-N(3)	154.5(4)	N(2)-Ru(1)-N(3)	77.5(4)
Ru(1)-C(1)-C(2)	69.3(9)	Ru(1)-C(2)-C(1)	72.3(9)
Ru(1)-C(2)-C(3)	77.8(9)	C(1)-C(2)-C(3)	117.4(11)
Ru(1)-C(2)-C(9)	129.4(11)	C(1)-C(2)-C(9)	123.0(12)
C(3)-C(2)-C(9)	118.7(12)	Ru(1)-C(3)-C(2)	64.7(8)
Ru(1)-C(3)-C(4)	113.4(13)	C(2)-C(3)-C(4)	110.6(13)
C(3)-C(4)-C(5)	98.2(18)	C(4)-C(5)-C(6)	119.9(20)
Ru(1)-C(6)-C(5)	107.0(13)	Ru(1)-C(6)-C(7)	71.3(7)
C(5)-C(6)-C(7)	127.6(14)	Ru(1)-C(7)-C(6)	70.3(7)
Ru(1)-C(7)-C(8)	68.3(8)	C(6)-C(7)-C(8)	109.6(10)
Ru(1)-C(7)-C(10)	124.9(10)	C(6)-C(7)-C(10)	130.2(12)
C(8)-C(7)-C(10)	120.1(11)	Ru(1)-C(8)-C(7)	75.3(8)
Ru(1)-N(1)-C(11)	127.8(10)	Ru(1)-N(1)-C(15)	115.2(8)
C(11)-N(1)-C(15)	115.2(11)	Ru(1)-N(2)-C(16)	116.9(8)
Ru(1)-N(2)-C(20)	113.1(8)	C(16)-N(2)-C(20)	129.7(11)
Ru(1)-N(3)-C(21)	118.8(9)	Ru(1)-N(3)-C(25)	124.0(7)
C(21)-N(3)-C(25)	117.2(10)	N(1)-C(11)-C(12)	118.2(14)
C(11)-C(12)-C(13)	121.6(15)	C(12)-C(13)-C(14)	125.5(18)
C(13)-C(14)-C(15)	106.1(19)	N(1)-C(15)-C(14)	130.6(15)
N(1)-C(15)-C(16)	110.0(10)	C(14)-C(15)-C(16)	118.7(15)
N(2)-C(16)-C(15)	119.3(11)	N(2)-C(16)-C(17)	114.0(11)
C(15)-C(16)-C(17)	126.1(11)	C(16)-C(17)-C(18)	118.5(14)
C(17)-C(18)-C(19)	122.6(14)	C(18)-C(19)-C(20)	119.1(12)
N(2)-C(20)-C(19)	114.4(12)	N(2)-C(20)-C(21)	122.4(12)
C(19)-C(20)-C(21)	123.2(12)	N(3)-C(21)-C(20)	108.0(12)
N(3)-C(21)-C(22)	123.2(15)	C(20)-C(21)-C(22)	128.7(15)
C(21)-C(22)-C(23)	120.5(15)	C(22)-C(23)-C(24)	115.6(17)
C(23)-C(24)-C(25)	130.5(16)	N(3)-C(25)-C(24)	110.5(10)
C(52)-N(8)-O(3)	110.2(34)	C(52)-N(8)-O(4)	100.8(27)
O(3)-N(8)-O(4)	148.7(38)	F(1)-B(1)-F(2)	109.5(9)
F(1)-B(1)-F(3)	109.5(10)	F(2)-B(1)-F(3)	109.5(10)
F(1)-B(1)-F(4)	109.5(10)	F(2)-B(1)-F(4)	109.5(9)
F(3)-B(1)-F(4)	109.5(9)	F(5)-B(2)-F(6)	103.9(36)
F(5)-B(2)-F(7)	114.0(35)	F(6)-B(2)-F(7)	110.9(35)
F(5)-B(2)-F(8)	103.8(32)	F(6)-B(2)-F(8)	115.3(37)
F(7)-B(2)-F(8)	108.9(35)	C(26)-Ru(2)-C(27)	37.0(7)
C(26)-Ru(2)-C(28)	61.4(6)	C(27)-Ru(2)-C(28)	30.3(6)
C(26)-Ru(2)-C(31)	131.8(6)	C(27)-Ru(2)-C(31)	95.0(7)
C(28)-Ru(2)-C(31)	72.1(6)	C(26)-Ru(2)-C(32)	159.1(6)

C(27)-Ru(2)-C(32)	127.2(7)	C(28)-Ru(2)-C(32)	99.3(6)
C(31)-Ru(2)-C(32)	34.6(6)	C(26)-Ru(2)-C(33)	166.2(6)
C(27)-Ru(2)-C(33)	155.5(7)	C(28)-Ru(2)-C(33)	132.4(6)
C(31)-Ru(2)-C(33)	61.7(5)	C(32)-Ru(2)-C(33)	33.7(6)
C(26)-Ru(2)-N(4)	91.6(6)	C(27)-Ru(2)-N(4)	87.4(6)
C(28)-Ru(2)-N(4)	106.5(5)	C(31)-Ru(2)-N(4)	89.8(5)
C(32)-Ru(2)-N(4)	102.3(6)	C(33)-Ru(2)-N(4)	85.0(6)
C(26)-Ru(2)-N(5)	82.6(6)	C(27)-Ru(2)-N(5)	117.7(6)
C(28)-Ru(2)-N(5)	143.6(6)	C(31)-Ru(2)-N(5)	144.3(5)
C(32)-Ru(2)-N(5)	115.1(6)	C(33)-Ru(2)-N(5)	83.6(5)
N(4)-Ru(2)-N(5)	78.6(5)	C(26)-Ru(2)-N(6)	87.5(6)
C(27)-Ru(2)-N(6)	104.5(6)	C(28)-Ru(2)-N(6)	92.1(5)
C(31)-Ru(2)-N(6)	106.9(5)	C(32)-Ru(2)-N(6)	85.2(5)
C(33)-Ru(2)-N(6)	90.7(5)	N(4)-Ru(2)-N(6)	158.2(5)
N(5)-Ru(2)-N(6)	79.8(4)	Ru(2)-C(26)-C(27)	72.9(12)
Ru(2)-C(27)-C(26)	70.1(11)	Ru(2)-C(27)-C(28)	76.8(13)
C(26)-C(27)-C(28)	124.0(18)	Ru(2)-C(27)-C(34)	121.7(13)
C(26)-C(27)-C(34)	111.5(16)	C(28)-C(27)-C(34)	124.3(18)
Ru(2)-C(28)-C(27)	72.8(12)	Ru(2)-C(28)-C(29)	121.2(11)
C(27)-C(28)-C(29)	123.5(15)	C(28)-C(29)-C(30)	105.3(12)
C(29)-C(30)-C(31)	110.8(12)	Ru(2)-C(31)-C(30)	118.6(10)
Ru(2)-C(31)-C(32)	78.2(11)	C(30)-C(31)-C(32)	135.2(13)
Ru(2)-C(32)-C(31)	67.2(10)	Ru(2)-C(32)-C(33)	67.5(11)
C(31)-C(32)-C(33)	114.9(15)	Ru(2)-C(32)-C(35)	117.3(12)
C(31)-C(32)-C(35)	125.2(14)	C(33)-C(32)-C(35)	116.2(14)
Ru(2)-C(33)-C(32)	78.8(11)	Ru(2)-N(4)-C(36)	139.3(12)
Ru(2)-N(4)-C(40)	109.3(9)	C(36)-N(4)-C(40)	111.1(13)
Ru(2)-N(5)-C(41)	124.4(9)	Ru(2)-N(5)-C(45)	120.6(9)
C(41)-N(5)-C(45)	115.0(12)	Ru(2)-N(6)-C(46)	108.4(8)
Ru(2)-N(6)-C(50)	131.9(9)	C(46)-N(6)-C(50)	118.7(12)
N(4)-C(36)-C(37)	144.5(19)	C(36)-C(37)-C(38)	103.0(15)
C(37)-C(38)-C(39)	121.6(14)	C(38)-C(39)-C(40)	115.8(16)
N(4)-C(40)-C(39)	122.4(12)	N(4)-C(40)-C(41)	121.7(10)
C(39)-C(40)-C(41)	115.4(12)	N(5)-C(41)-C(40)	105.9(10)
N(5)-C(41)-C(42)	122.0(12)	C(40)-C(41)-C(42)	132.1(11)
C(41)-C(42)-C(43)	118.9(14)	C(42)-C(43)-C(44)	119.8(16)
C(43)-C(44)-C(45)	117.1(14)	N(5)-C(45)-C(44)	126.6(13)
N(5)-C(45)-C(46)	105.9(12)	C(44)-C(45)-C(46)	127.5(14)
N(6)-C(46)-C(45)	125.3(13)	N(6)-C(46)-C(47)	116.7(11)
C(45)-C(46)-C(47)	117.7(12)	C(46)-C(47)-C(48)	125.1(12)
C(47)-C(48)-C(49)	115.3(13)	C(48)-C(49)-C(50)	109.2(14)
N(6)-C(50)-C(49)	130.5(13)	C(51)-N(7)-O(1)	130.8(19)
C(51)-N(7)-O(2)	120.5(18)	O(1)-N(7)-O(2)	108.7(17)
F(9)-B(3)-F(10)	96.4(11)	F(9)-B(3)-F(11)	119.9(13)
F(10)-B(3)-F(11)	104.7(11)	F(9)-B(3)-F(12)	114.5(11)
F(10)-B(3)-F(12)	113.8(13)	F(11)-B(3)-F(12)	107.0(10)
F(13)-B(4)-F(14)	112.3(13)	F(13)-B(4)-F(15)	108.2(13)
F(14)-B(4)-F(15)	114.8(12)	F(13)-B(4)-F(16)	101.9(12)
F(14)-B(4)-F(16)	104.4(11)	F(15)-B(4)-F(16)	114.4(12)

Table 2.7: Anisotropic displacement factors ($Å^2$ x 10^3) for $[Ru(\eta^3:\eta^3\text{-}C_{10}H_{16})(N_3C_{15}H_{11})][BF_4]_2.CH_3NO_2$ **66.**

	U_{11}	U_{22}	U_{33}	U_{23}	U_{13}	U_{12}
Ru(1)	39(1)	30(1)	36(1)	1(1)	2(1)	1(1)
Ru(2)	36(1)	41(1)	39(1)	-5(1)	2(1)	-1(1)

Chapter 3

Mono- and Bidentate Carboxylato Complexes of Ruthenium(IV)

3.1 Introduction

Carboxylato compounds of the platinum metals are of interest because of their extensive chemistry and catalytic applications.[175-177] A great deal of work has been carried out on the synthesis and reactions of carboxylato complexes of (pentamethylcyclopentadienyl)rhodium(III) and -iridium(III) and their isoelectronic (arene)ruthenium(II) analogues.[55,178,179] In this chapter the chemistry of **6** with carboxylato and related ligands is examined and, where appropriate, contrasted with that of its ruthenium(II) analogues. Much of this work has been carried out in collaboration with Mr. Brian Kavanagh whose insight and experience is gratefully acknowledged.

3.2 Reactions with Acetate and Trifluoroacetate Anions

Previous work[55] has demonstrated that (arene)ruthenium(II) carboxylato complexes may be synthesised by one or more of the three general methods listed below:

i) Refluxing the appropriate (arene)ruthenium(II) chloro-bridged dimer **7** in a mixture of the neat carboxylic acid and the acid anhydride.
ii) Treatment of $[\{Ru(arene)Cl(\mu\text{-}Cl)\}_2]$ with two mole equivalents of the silver salt of the carboxylic in acetone or benzene.
iii) Reaction of $[\{Ru(arene)Cl(\mu\text{-}Cl)\}_2]$ with an excess of the sodium salt of the carboxylic acid in acetone.

The greater solubility of complexes derived from **6**, in comparison to their (arene)ruthenium(II) analogues, makes method (i) unsuitable for all but the most insoluble products and it is found that, in general, reaction of **6** with silver or sodium carboxylates is most likely to lead to the formation and isolation of the desired products.

The reaction of **6** with $Ag[O_2CMe]$ proceeds rapidly at room temperature in acetone to give an orange-red solution from which the chelate complex $[Ru(\eta^3\text{:}\eta^3\text{-}C_{10}H_{16})Cl(O_2CMe)]$ **72**, analogous to the (arene)ruthenium(II) complexes

previously synthesised,[55] may be isolated in good yield. The reaction also proceeds, albeit more slowly, with sodium acetate but we were unable to recover any complexes from the direct interaction of **6** with refluxing acetic acid because of the high solubility of the products in this medium. The solid state infrared spectrum of **72** (Table 3.2) displays two strong bands (1517 and 1461 cm^{-1}), assignable respectively to $\nu_{asymm}(OCO)$ and $\nu_{symm}(OCO)$[180] (*cf.* 1510, 1470 cm^{-1} for $[Ru(\eta^6\text{-}C_6H_6)Cl(O_2CMe)]$[55]). The value of $\Delta\nu$ (= $\nu_{asymm} - \nu_{symm}$) of 56 cm^{-1} clearly indicates a chelate mode of coordination for the carboxylate ligand [values of $\Delta\nu$ are expected to be small (*ca.* 50 - 100 cm^{-1}) for chelating carboxylato functionalities, and larger (*ca.* 150 - 250 cm^{-1}) for unidentate coordination).[180] Medium intensity bands at 345 cm^{-1} and 273 cm^{-1} are assigned to ν(RuO) and ν(RuCl) respectively. An electron impact mass spectrum of this material displayed peaks centred on *m/z* 332 ($[Ru(\eta^3\text{:}\eta^3\text{-}C_{10}H_{16})Cl(O_2CMe)]^+$ - based on ^{102}Ru and ^{35}Cl), 297 ($[Ru(\eta^3\text{:}\eta^3\text{-}C_{10}H_{16})(O_2CMe)]^+$) and 238 ($[Ru(\eta^3\text{:}\eta^3\text{-}C_{10}H_{16})]^+$) with isotope distribution patterns consistent with the presence of one ruthenium atom. The ^1H NMR spectrum of **72** displays a pattern of $\eta^3\text{:}\eta^3\text{-}C_{10}H_{16}$ resonances similar to those already reported for the chelate benzothiazole-2-thiolate complex $[Ru(\eta^3\text{:}\eta^3\text{-}C_{10}H_{16})Cl(mcbt)]$[159] and the bipyridine complex $[Ru(\eta^3\text{:}\eta^3\text{-}C_{10}H_{16})Cl(bipy)][BF_4]$ (Chapter 2). The terminal allylic protons of the dimethyloctadienediyl ligand give rise to four singlet signals (δ 5.51, 4.65, 4.63 and 3.56 ppm) while the methyl substituents resonate at δ 2.29 and 2.12 ppm; a spectrum consistent with inequivalent axial sites on the trigonal bipyramidal ruthenium ion. A further singlet resonance, observed at δ 1.85 ppm, is due to the acetate methyl group. The formulation and structure of **72** was unequivocally confirmed by a single crystal X-ray structure determination, Fig. 3.1 (*vide infra*).

The formation of **72** contrasts sharply with that of the more acetone insoluble deep orange trifluoroacetate compound $[Ru(\eta^3\text{:}\eta^3\text{-}C_{10}H_{16})(O_2CCF_3)_2(OH_2)]$ **73**,* readily obtained by methods (i) and (ii) described above. Indeed we have been unable to isolate the corresponding 1 : 1 chelate complex $[Ru(\eta^3\text{:}\eta^3\text{-}C_{10}H_{16})Cl(O_2CCF_3)]$ since the interaction of **6** with only two mole equivalents of $Ag[O_2CCF_3]$ gives a low yield of **73** along with

* A trifluoroacetato bridged complex, $[\{Ru(\eta^3\text{:}\eta^3\text{-}C_{10}H_{16})(O_2CCF_3)(\mu\text{-}O_2CCF_3)\}_2]$, has been reported[111] to be formed from the reaction of thallium trifluoroacetate with **6** although no spectroscopic data were quoted and we find no evidence for the existence of this material.

a large quantity of unreacted starting material. Similarly, refluxing **72** in trifluoroacetic acid results in the replacement of both the chloride and acetate ligands to form **73**. These observations contrast with those made in the area of (arene)ruthenium(II) chemistry where the compounds [Ru(η^6-arene)Cl(O_2CCF_3)] (arene = C_6H_6, C_6Me_6) can be readily synthesised by methods (i) and (ii).[55] Interestingly the reaction of the *bis*(acetato) complexes [Ru(η^6-arene)($O_2CMe)_2$] with trifluoroacetic acid gives *bis*(trifluoroacetato) complexes, tentatively formulated as [Ru(η^6-arene)($O_2CCF_3)_2$].H_2O, which crystallise as monohydrates.[55] The water of crystallisation in these complexes occurs as a broad resonance at *ca.* 6 ppm in the ^1H NMR spectrum and is thought to be only loosely associated with the metal atom.

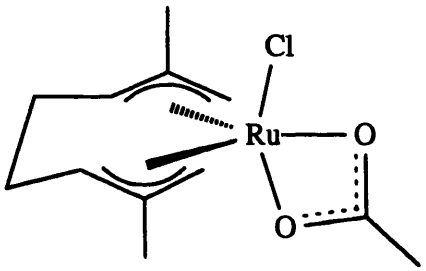

72

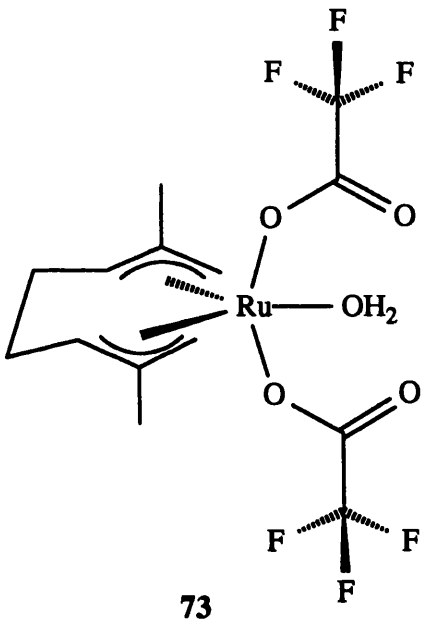

73

The ^1H NMR spectrum of **73**, in $CDCl_3$, displays only half the number of η^3:η^3-$C_{10}H_{16}$ resonances of **72**, *viz* two terminal allyl singlets (δ 5.68 and 4.23 ppm) and a single methyl resonance (δ 2.12 ppm) indicative of equivalent axial sites on the trigonal bipyramidal ruthenium atom and inconsistent with a compound containing both monodentate and bidentate carboxylate ligands. The water ligand occurs as a sharp singlet resonance at δ 7.11 ppm, broadening somewhat in nitromethane-d_3 solution. The ^{19}F NMR spectrum displays a single singlet resonance at δ -76.50 ppm (relative to $CFCl_3$), close to

the value observed for the free acid (δ -76.41 ppm) but somewhat upfield of the corresponding signal in the fluxional arene complex $[Ru(\eta^6\text{-}C_6H_6)(O_2CCF_3)_2].H_2O$ (δ -74.71 ppm).[55] This latter resonance represents a time averaged signal between mono- and bidentate coordination modes. In the infrared spectrum, **73** displays a strong, broad band at 3362 cm^{-1} assignable to ν(OH) and indicative of hydrogen bonding in the solid state. The trifluoroacetate ligands give rise to $\nu(CF_3)$ bands at 1196, 1143 cm^{-1}, $\nu_{asymm}(OCO)$ at 1703, 1670 cm^{-1}, and $\nu_{symm}(OCO)$ at 1421 cm^{-1}. The much larger value of Δν (249-282 cm^{-1}) is suggestive of a monodentate mode of coordination.[180]

Compound **73** will sublime intact at *ca.* 100°C under reduced pressure with no trace of displacement of the water molecule and similarly refluxing **73** in dry dichloromethane containing anhydrous magnesium sulphate results in the recovery of the unchanged material. These observations suggest that the water molecule in **73** is strongly bound and actually forms part of the coordination sphere of the metal ion with the two trifluoroacetate ligands bonding in a monodentate mode at the axial sites, consistent with ^1H NMR data. This contention is apparently further supported by the low substitutional lability of the water ligand which is slowly displaced by pyrazene over a period of days at room temperature, to give the adduct $[Ru(\eta^3\text{:}\eta^3\text{-}C_{10}H_{16})(O_2CCF_3)_2(N_2C_4H_4)]$ **74** along with a quantity of residual **73**. It should be noted, however, that this is probably an equilibrium effect since addition of D_2O to a chloroform-*d* solution in an NMR tube results in the complete disappearance of the resonance due to coordinated water (δ 7.11 ppm) after *ca.* 30 minutes.

The formulation of **73** was confirmed by a single crystal X-ray structure determination. Fig. 3.2 shows the water molecule to occupy one of the equatorial coordination sites of the trigonal bipyramidal ruthenium ion while the two trifluoroacetato ligands are bound in a monodentate fashion in the axial positions. The Ru-OH_2 distance, 2.146(4) Å, is only slightly longer than the Ru-O bond lengths to the axial trifluoroacetate ligands, 2.100(3) Å and is even somewhat shorter than other Ru-$L_{equatorial}$ distances [2.15 - 2.20 Å, L = acetate **72**, pyrazene (Chapter 5), 2,2':6',2''-terpyridine **66** (Chapter 2)] and suggests clearly that the water molecule is relatively strongly bound to the metal centre. Similarly, the 1,5-cyclooctadiene complex $[Ru(COD)(OH_2)_4][OTs]_2$[181] exhibits Ru-OH_2 distances of 2.158(1) Å *trans* to the COD ligand and 2.095(2) Å *trans* to water, while the

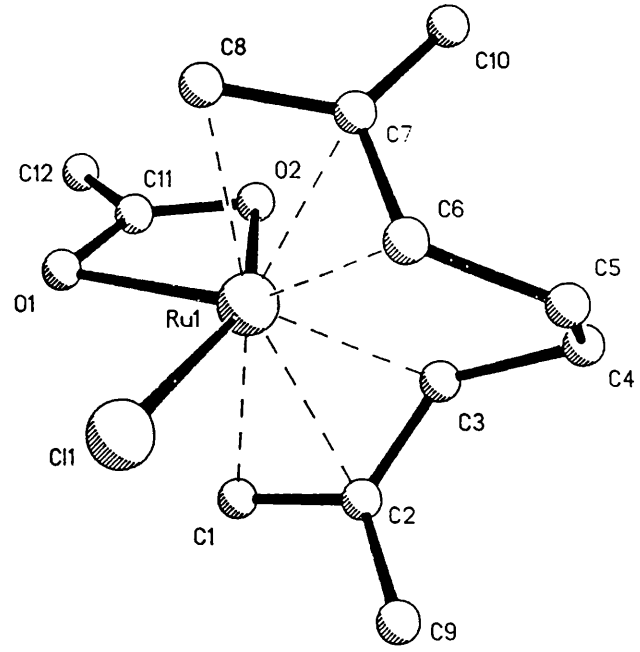

Fig. 3.1: Crystal structure of $[Ru(\eta^3:\eta^3\text{-}C_{10}H_{16})Cl(O_2CCH_3)]$ **72** showing the atom numbering scheme adopted.

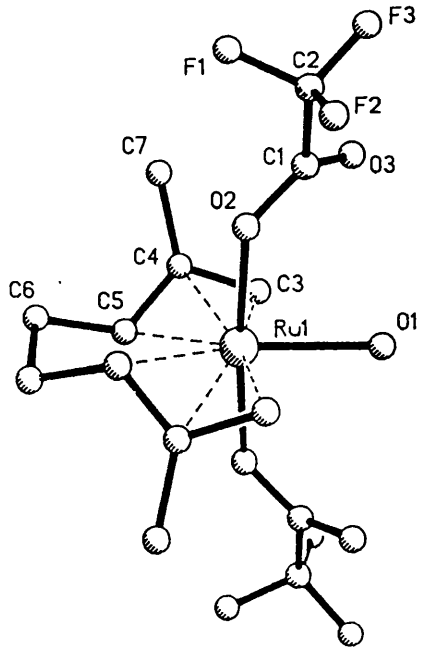

Fig. 3.2: Crystal structure of $[Ru(\eta^3:\eta^3\text{-}C_{10}H_{16})(O_2CCF_3)_2(OH_2)]$ **73** showing the atom numbering scheme adopted.

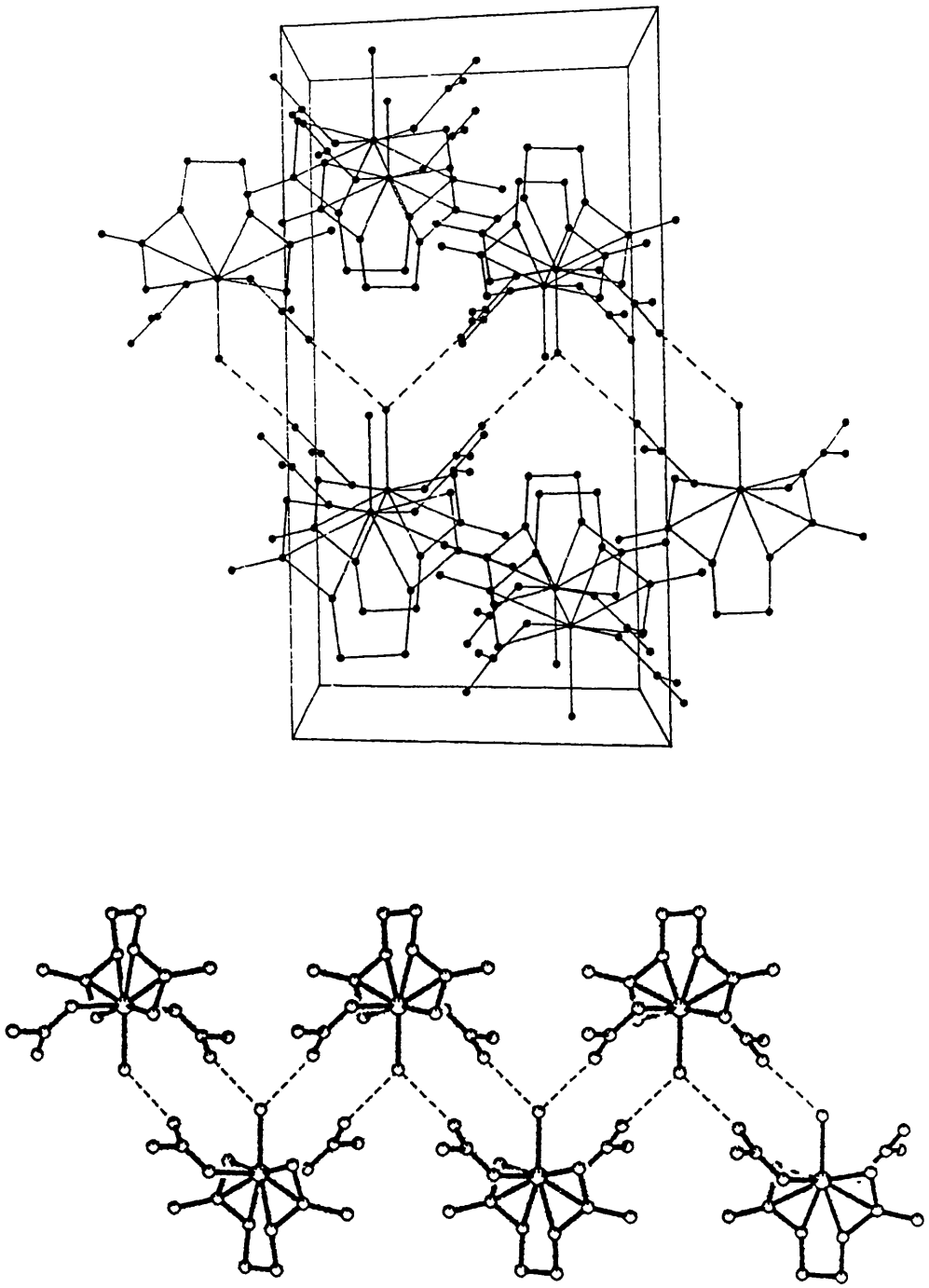

Fig. 3.3: Crystal packing diagram of $[Ru(\eta^3:\eta^3\text{-}C_{10}H_{16})(O_2CCF_3)_2(OH_2)]$ **73**, viewed down the *a* axis (fluorine atoms omitted for clarity, dashed lines represent short intermolecular contacts).

Fe(II)-OH_2 distance in the 2,6-diacetylpyridine *bis*(semicarbazone) complex $[Fe(dapsc)(H_2O)_2]^{2+}$ is 2.214 Å.[182]

In solution the aqua ligand is presumably intramolecularly hydrogen bonded to the trifluoroacetato ligands. In the solid state however, an infinite intermolecular hydrogen bonded network exists (Fig. 3.3) with short contacts between oxygen of the aqua ligand and the uncoordinated trifluoroacetato oxygen on adjacent molecules, O(1)...O(3)', of 2.70 Å, implying relatively strong[183] interactions.

3.3 The Cross-over Between Mono- and Bidentate Coordination

The differences in the reactivity of **6** towards acetate and trifluoroacetate ligands are presumably a consequence of the differing electronic properties of the $-CH_3$ and $-CF_3$ substituents. These electronic properties may be quantified, either i) simply by consideration of the p*K*a of the neutral acid (a parameter which contains both inductive and resonance components), or ii) by examination of substituent polarity parameters such as the $\mathcal{F}$ parameter of Swain and Lupton[184] (a wide variety of $\mathcal{F}$ values are available, derived from the Hammett constants σ_m and σ_p[185]) which deals solely with the field (*i.e.* inductive as opposed to resonance) effects of substituent groups [$\mathcal{F}(CF_3) = 0.38$, $\mathcal{F}(CH_3) = -0.052$[186]]. Logically there must be a certain value of $\mathcal{F}$ (or p*K*a) where the cross-over from monodentate to bidentate coordination occurs. With this in mind, a range of simple chloro- and fluorocarboxylates has been examined in the hope determining that point and perhaps of finding a ligand exhibiting both types of coordination.

We find that interaction of **6** with an excess of the sodium salts of trichloro-, dichloro- and difluoroacetic acids ($\mathcal{F}_{\text{acid substituent}} = 0.31, 0.17, 0.27$;[186] acid p*K*a = 0.52, 1.35 and 1.34[187]) gives the complexes $[Ru(\eta^3{:}\eta^3\text{-}C_{10}H_{16})(O_2CCH_{3-n}X_n)_2(OH_2)]$ (X = Cl, n = 3, **75**; X = Cl, n = 2, **76**; X = F, n = 2, **77**) which are structurally related to **73**. The ^1H NMR spectra of these complexes are all consistent with a geometry incorporating equivalent axial sites. In addition complex **76** displays a single, singlet resonance at δ 5.45 ppm assigned to the $CHCl_2$- group, while the corresponding CHF_2- resonance in **77** appears as a triplet (δ 5.34 ppm, $^2J_{H\text{-}F} = 54.8$ Hz).

In analogous reactions involving the sodium salts of monochloro- and monofluoroacetic acids mixtures of two complexes are formed, namely $[Ru(\eta^3:\eta^3\text{-}C_{10}H_{16})Cl(O_2CCH_2X)]$ (X = Cl **78a**, F **79a**) and $[Ru(\eta^3:\eta^3\text{-}C_{10}H_{16})(O_2CCH_2X)_2(OH_2)]$ **78b**, **79b**. In both cases the complex with chelating ligands (**78a**, **79a**) forms the bulk of the isolated yields [product ratios: 7 : 1 (**78a** : **78b**), 6 : 1 (**79a** : **79b**)]. The ^1H NMR spectra of **78a** and **79a** exhibit the expected four singlet resonances for the terminal allylic protons of the dimethyloctadienediyl ligand and two signals for the methyl groups, indicative of inequivalent axial sites. In addition the ^1H NMR spectrum of **78a** at room temperature displays a closely spaced AB pattern (δ 3.80 and 3.74 ppm, $^2J_{H\text{-}H}$ = 14.3 Hz) assigned to the protons of the chloroacetate ligand. These protons are diastereotopic and the presence of the chiral metal centre results in the splitting of the expected singlet into the observed AB pattern. The analogous protons in **79a** give rise to an eight line pattern because of additional coupling to fluorine ($^2J_{H\text{-}F}$ = 48.1 Hz). The effect is analogous to that observed in the ^{19}F NMR spectrum of the adduct $[Ru(\eta^3:\eta^3\text{-}C_{10}H_{16})Cl_2(Me_2NPF_2)]$ where the diastereotopic fluorine atoms give rise to an eight line pattern due to coupling to phosphorus.[16]

At 20°C two of the terminal allyl resonances in the ^1H NMR spectra of both **78a** and **79a** are broad whilst the other two are much sharper, implying a fluxional process may be occurring in which the major changes take place on only one side of the molecule. In both cases raising the temperature to 50°C in the NMR probe results in sharp, four line patterns for the terminal allyl protons, consistent with inequivalent axial sites, even in a rapid exchange regime. Lowering the temperature results in a gradual broadening of all the lines in the spectrum until, at -20°C, they are significantly flattened into the baseline. At -50°C eight sharp singlet resonances are observed in the allylic region of the spectra, half of them four times the intensity of the other four. Similarly, four methyl signals can now be observed. In addition new broad peaks occur at δ 6.39 (**78a**) and 6.52 ppm (**79a**) [close to the value of *ca.* 6 ppm for the exchanging water of crystallisation in the related (carboxylato)(arene) ruthenium(II) compounds[55]]. Other new resonances corresponding to the carboxylates and the remainder of the *bis*(allyl) ligands are also apparent. Complete NMR data are given in Table 3.1.

These temperature dependent NMR spectra are interpreted in terms of a equilibrium

involving monodentate and bidentate coordination of the $[O_2CCH_2X]^-$ ligands analogous to that observed in the *tris*phosphine complex *fac*-$[RuCl(O_2CMe)\{PhP(C_3H_6PCy_2)_2\}]$,[175] and activated by residual water in the chloroform-*d* solvent. Thus we believe complexes **78a** and **79a** are each in equilibrium with further aqua complexes, $[Ru(\eta^3:\eta^3\text{-}C_{10}H_{16})Cl(\eta^1\text{-}O_2CCH_2X)(OH_2)]$ **78c**, **79c** each of which also possesses inequivalent axial sites, Scheme 3.1. The equilibrium constant at -50°C for this process (K = [*N***a**]/[*N***c**]) is *ca.* 5 in both cases.

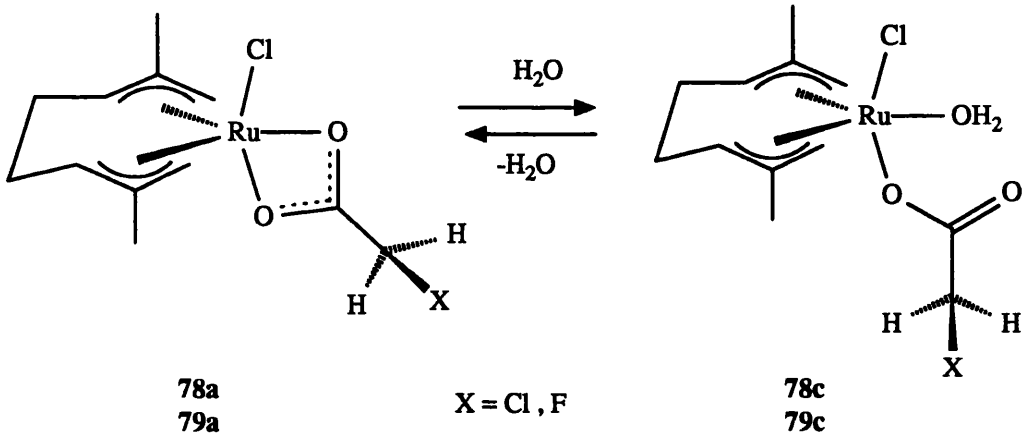

78a **79a** X = Cl, F **78c** **79c**

Scheme 3.1: Fluxional behaviour of the haloacetateo complexes $[Ru(\eta^3:\eta^3\text{-}C_{10}H_{16})Cl(O_2CCH_2X)]$ (X = Cl, **78a**; F, **79a**).

The ^1H NMR spectra of the *bis*(carboxylato) aqua complexes **78b** and **79b** also display evidence of fluxionality. Raising the temperature to 50°C results in a gradual broadening of all the resonances in the spectra, most notably those corresponding to the water ligands. At 0°C however, all the resonances are sharp, as in the case of **73**. Further lowering of the temperature produces no additional changes in the spectra. These observations are consistent with a simple exchange of coordinated water with that in the bulk solvent, consistent with the exchange of H_2O for D_2O in the presence of D_2O in **73**. Close examination of the room temperature (20°C) ^1H NMR spectra for **73**, **75** - **77**, **78b** and **79b** reveals a noticeable increase in the broadness of the resonance due to the aqua

ligands as $\mathcal{F}$ (*i.e.* the substituent electron withdrawing power) decreases. This suggests that the exchange of coordinated water with bulk solvent is slower in the case of **73** than the less strongly electron withdrawing carboxylates, and implies that the rate of exchange may well be dependent upon the electron charge density at the metal. This in turn suggests a significant electrostatic component to the Ru-OH_2 bond. Another possible factor which may influence the binding of the water molecule to the complex as a whole is intramolecular hydrogen bonding to the uncoordinated carboxylato oxygen atoms. The H-bond basicity of these acceptors would, however, be expected to *decrease* with increasing substituent $\mathcal{F}$ implying weaker H-bonding in **73** than in **77** for example. Thus this interaction probably does not dominate the trend in aqua ligand lability.

In summary, the more electron withdrawing carboxylates favour the formation of complexes with monodentate ligands and equatorially coordinated water molecules. Increasing the electron releasing properties of the substituent group on the carboxylate leads to fluxional behaviour involving monodentate and bidentately coordinated ligands. In the limiting case (R = CH_3 **72**) the second carboxylate oxygen atom is a sufficiently good donor to bind more rigidly to the metal centre resulting in the formation of only the 1 : 1 chelate complex. It would thus appear that the "cross over" between these two bonding modes occurs gradually over acid p*K*a values of *ca.* 1.3 to 2.9; $\mathcal{F}$ of *ca.* 0.1 to 0.27.

3.4 X-ray Crystal Structure Determinations of Representative Compounds

The X-ray crystal structures of complexes **72** and **73** are shown in Figs. 3.1 and 3.2 respectively. In both compounds the geometry about the ruthenium atom may be loosely described as approximately trigonal bipyramidal with the *bis*(allyl) ligands occupying two of the equatorial coordination sites and possessing the usual local C_2 symmetry.[13,158-161] No significant variation is observed in the Ru-C bond lengths. The bonds to the two axial oxygen atoms, O(2), are virtually identical in length in the two complexes (2.10 Å) and are somewhat shorter than the corresponding distances in the fluxional Ru(II) complex *fac*-[RuCl(O_2CMe)(PhP{$C_3H_6PCy_2$}$_2$)], (2.21 - 2.23 Å) possibly as a consequence of the

larger size of the Ru(II) centre, or weaker binding of the acetate ligand.[175] In complex **73**, the equatorial Ru-OH_2 bond, 2.146(4) Å, is actually somewhat shorter than the Ru-O(1) distance in **72**, 2.205(6) Å. This arises as a consequence of the strained nature of the four membered heterocyclic ring in the latter compound which is evinced in the characteristically small bite angle, O(1)-Ru-O(2) 60.7(2)°, comparable to the value observed in *fac*-[RuCl(O_2CMe){PhP($C_3H_6PCy_2$)$_2$}],[175] 58.9(1)°, and in the 6-chloro-2-hydroxypyridinate compound [Ru(η^3:η^3-$C_{10}H_{16}$)Cl(NC_5H_3O-6-Cl)] (Chapter 4), 61.9(4)°. The large Cl-Ru-O(1) angle in complex **72**, 93.7(2)°, is also indicative of the strained nature of the chelate ring. The angles between axial and equatorial ligands normally fall in the region of *ca.* 85° [13,158] The analogous unstrained angle in complex **73** is 87.4(1)°. The endocyclic, O(1)-C(11)-O(2) angle in **72** is 118.0(8) whereas the corresponding parameter in complex **73** is 127.7(5)° (this is similar to the analogous parameters in [Hg(terpy)(O_2CCF_3)$_2$] and [Ti(Cp)$_2$(O_2CCF_3)$_2$][188,189] and is therefore unaffected by the hydrogen bonding interactions present in **73**). This might be indicative of the fact that the acetate ligand is distorting significantly in order to chelate the small Ru(IV) centre, although similar angles are noted in related chelate and bridging acetato complexes of ruthenium(II).[175,190]

This lengthening of the equatorial Ru-O bond in the chelate complex as a result of strain in the heterocyclic ring is almost certainly a contributatory factor in the formation of aqua complexes as the donor ability of the carboxylato ligand decreases. The small size of the ruthenium(IV) centre exacerbates the effect, thus resulting in the observed differences in reactivity, compared to the analogous carboxylates of ruthenium(II).[55]

3.5 Conclusions

It has been demonstrated that the small size of the ruthenium(IV) centre, coupled with the inherently strained nature of four membered heterocyclic rings acts to destabilise the formation of bidentate carboxylates containing the "(η^3:η^3-$C_{10}H_{16}$)Ru" moiety, resulting in fluxionality and, ultimately, the formation of aqua species beyond a threshold in the electron withdrawing properties of the carboxylate substituent group.

3.6 Further Aqua Complexes of Ruthenium(IV)

The apparent strength and stability of the Ru(IV)-OH_2 bond augurs well for the potential synthesis of oxo species derived from aqua complexes of ruthenium(IV) which may, given the unusual stereochemical requirements of the dimethyloctadienediyl ligand, exhibit interesting selectivity in organic oxidations, and in the oxidative cleavage of DNA (see Section 2.3.2). An investigation was therefore undertaken into further systematic methods for the synthesis of *bis*(allyl) complexes of ruthenium(IV) containing coordinated water ligands in the hope that the possibility of η^1 and η^2-coordination of the carboxylato ligands might result in greater electronic and stereochemical flexibility at the metal centre than that found in the bipyridyl and phenanthroline compounds reported in Section 2.3.2, and hence result in redox activity.

3.4.1 β-*Diketonate Complexes*

In a further attempt to observe aqua complexes we have investigated the reaction of **6** with other electron withdrawing ligands such as the hexafluoroacetylacetonate anion, $[CF_3C(O)CHC(O)CF_3]^-$. We find that in this case a chelate complex $[Ru(\eta^3:\eta^3\text{-}C_{10}H_{16})Cl\{F_3CC(O)CHC(O)CF_3\}]$ **80** is formed, analogous to the ruthenium(II) complex $[Ru(\eta^6\text{-}C_6H_6)Cl(acac)]$.[55] Mr. Dietrich Schreiber has also synthesised the trifluoroacetylacetonate and acetylacetonate analogues of **80**, $[Ru(\eta^3:\eta^3\text{-}C_{10}H_{16})Cl\{R_3CC(O)CHC(O)Me\}]$ (R = F, **81**; H, **82**) which exhibit similar chelating geometries (verified by a single crystal X-ray structure determination in the case of **81**).[191] The less strained nature of the six membered heterocyclic ring no doubt stabilises the bidentate coordination mode.

Reaction of **82** with $Ag[BF_4]$ in "wet" acetone results in the precipitation of AgCl and the formation of an orange-brown solution presumably containing the cationic aqua complex $[Ru(\eta^3:\eta^3\text{-}C_{10}H_{16})(acac)(H_2O)][BF_4]$. Unfortunately, this complex could not be isolated because of its extremely high solubility. This contrasts to the successful isolation of the dicationic bipyridyl and phenanthroline complexes **70** and **71** reported in Section 2.3.2, although high solubility was also a problem in the isolation of **70**.

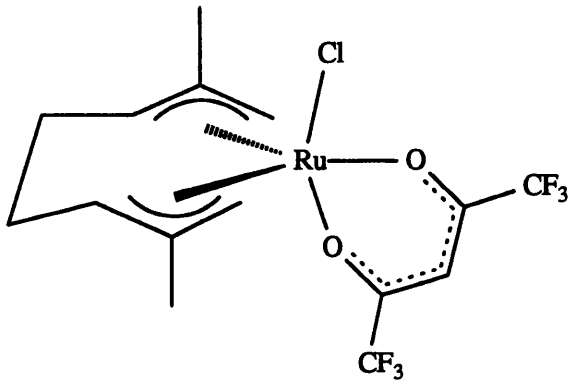

80

3.4.2 Reactions of [Ru(η^3:η^2:η^3-$C_{12}H_{18}$)Cl_2]

In an attempt to determine whether the apparent high affinity of *bis*(allyl)ruthenium(IV) species for water was general, the reaction of the related butadiene-derived compound [Ru(η^3:η^2:η^3-$C_{12}H_{18}$)Cl_2] **39** (Section 1.4.2)[105-107] with Ag[BF_4] was examined. In the case of a reaction involving a 1 : 1 mole ratio of **39** : Ag[BF_4] in acetone, the aqua cation [Ru(η^3:η^2:η^3-$C_{12}H_{18}$)Cl(H_2O)][BF_4] **83** was isolated by slow crystallisation from liquid diffusion of hexane into an acetone solution of the complex. The analogous diaqua dication could not be isolated, due to solubility constraints, although is probably stable in solution.

Like **6**, compounds **39** and **83** contain a *bis*(allyl) ligand in a rigid "up-down" (C_2) orientation in which each of the allylic functionalities is *pseudo*-eclipsed with one of the *axial* chloride ligands. This results in ^{1}H and ^{13}C-{^{1}H} NMR spectra of compounds derived from **39** also exhibiting a doubling of the usual number of resonances (Appendix I) when the *axial* sites are inequivalent, as is the case for **83**. Thus the ^{1}H NMR spectrum of **39** (Table 3.1) exhibits two terminal allyl resonances [δ 4.89 (d, ^3J = 7.7) and 3.76 (d, ^3J = 11.8) ppm] whereas all four terminal allyl protons are unique in **83** [δ 5.30 (m), 5.15 (dd, ^2J=2.0, ^3J=8.0), 3.87 (d, ^3J=12.0), 3.39 (d, ^3J=12.0) ppm]. The effect is also observed in the ^{13}C-{^{1}H} spectra of the compounds (Table 3.3) which were assigned with the aid of APT and INEPT experiments. Interestingly the resonances corresponding to the terminal

allyl carbon atoms resonate at much higher field than either of the internal allylic nuclei (*e.g.* δ 65.8 ppm as against 111.5 and 105.7 ppm in **39**) possibly implying a high degree of σ-bonding character in the terminal sites. The presence of the coordinated water molecule in **83** was confirmed by the observation of bands due to ν(OH) in the infrared spectrum of the complex (3369 and 3169 cm^{-1}) and a peak at δ 2.21 ppm in its ^1H NMR spectrum.

Complex **83** was also examined by X-ray crystallography, Fig. 3.4. As with the compounds previously reported in this thesis containing the "$Ru(\eta^3:\eta^3\text{-}C_{10}H_{16})$" fragment, the geometry about the metal centre is best described as a distorted trigonal (or pentagonal) bipyramid with two allylic and one olefinic functionalities occupying the equatorial plane. A chloride ion and a water molecule each occupy the axial sites [Ru-Cl 2.396(2), Ru-O 2.165(5) Å]. The bonds to these ligands are not collinear but subtend an angle of 169.0(1)° at the metal centre [*cf.* 168.2(2)° for **39**]. Unlike compounds containing the "$Ru(\eta^3:\eta^3\text{-}C_{10}H_{16})$" fragment, the six carbon atoms of the two η^3-allylic functionalities are not equidistant from the metal centre but form two distinct sets [av. Ru-C(1), C(2), C(11) and C(12) 2.206(6), av. Ru-C(2), C(10) 2.301(5) Å] indicative of an imbalance between the steric requirements of the metal and those of the ligand. The distortions in the organic ligand which arise on coordination to the metal also result in long bonds to the olefinic functionality [Ru-C(6) 2.314(5), Ru-C(7) 2.291(5) Å]. In the crystalline solid pairs of cations are hydrogen bonded together *via* bridging tetrafluoroborate anions. Each anion forms two relatively short hydrogen bonds [av. O...F 2.71(3) Å] to coordinated water molecules (Fig. 3.5).

Compound **83** is readily re-dissolved in aqueous solution and these solutions are stable in air for prolonged periods. Such an observation augers well for the development of aqueous chemistry involving compounds such as **83** as organic oxidants or in the oxidative cleavage of DNA.

3.4.3 Attempted Oxidations

Syntheses of oxo compounds derived from the trifluoroacetato aqua complex **73**, the chloro aqua complex **83** and the dichloro complex **39** were attempted. The reactions of **73** with KOH and the organic base DBU (1,8-diazabicyclo[5.4.0]undec-7-ene) gave

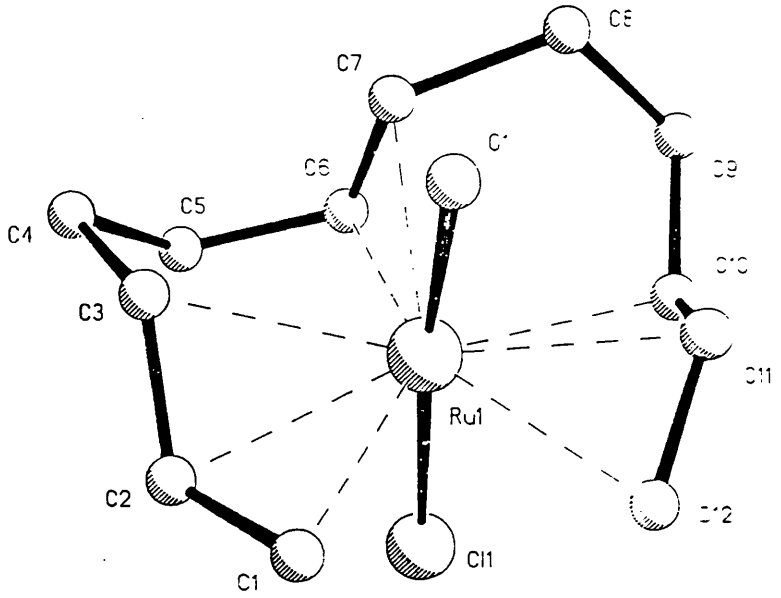

Fig. 3.4: Crystal structure of the molecular cation in $[Ru(\eta^3:\eta^2:\eta^3\text{-}C_{12}H_{18})Cl(OH_2)][BF_4]$ **83** showing the atom numbering scheme adopted.

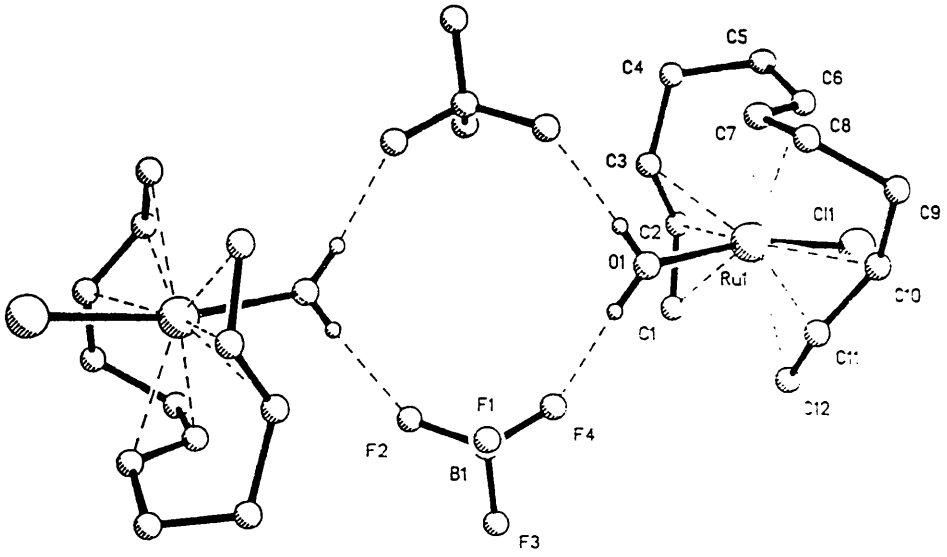

Fig. 3.5: Pairwise association of $[Ru(\eta^3:\eta^2:\eta^3\text{-}C_{12}H_{18})Cl(OH_2)][BF_4]$ **83** units in the solid state (dashed lines represent hydrogen bonding interactions).

colour changes from orange to red but no well characterised products could be isolated. Attempted oxidation of **83** with Ce(IV) resulted in recovery of the unchanged starting material whilst action of IOPh and Ag_2O upon **39** resulted in either no reaction or decomposition respectively.

3.7 Reactions with Thiocarboxylic Acids

Reaction of **6** with a small excess of thioacetic acid in acetone rapidly produces a bright orange solution from which may be isolated a complex of formula $[Ru(\eta^3:\eta^3\text{-}C_{10}H_{16})Cl_2\{S(OH)CMe\}]$ **84**, containing a neutral coordinated thioacetic acid molecule. The infrared spectrum of this molecule shows two broad bands of medium intensity at surprisingly low wavenumber (2606, 2458 cm^{-1}) which fall in the region expected for ν(SH) or for hydrogen bonded carboxylic acid dimers.[192] No bands assignable to coordinated C=O in the region[61] of 1600 cm^{-1} were observed, instead the complex exhibits two strong bands at 1437 and 1347 cm^{-1} assignable to ν(O-C=S) in addition to the usual weaker bands arising from the *bis*(allyl) ligand. The far infrared spectrum contains two strong absorptions at 310 and 239 cm^{-1} The assignment of these bands definitively to ν(RuCl) or ν(RuS) is uncertain, but 239 cm^{-1} is at remarkably low wavenumber for a terminal Ru-Cl vibration and may be indicative of a strong hydrogen bonding interaction at one of the chloride ligands. The ^1H NMR spectrum of **84** displays two resonances arising from the terminal allyl protons of the dimethyloctadienediyl ligand, (δ 4.76 and 4.00 ppm), the latter signal being noticeably broader than the former at room temperature, perhaps indicating a hydrogen bonding interaction involving one of the axial chloride ligands. In addition, an extremely sharp singlet resonance is observed at δ 13.99 ppm assignable to a strongly hydrogen bonded acidic proton. This evidence leads us to suggest that the thioacetic acid molecule is S-bound with the hydroxyl proton involved in a strong hydrogen bonding interaction with one of the axial chloride ligands both in the solid state and in solution, giving rise to ν(O..H..Cl) at anomalously low wavenumber.

Reaction of **6** with thioacetic acid over longer reaction times, up to 24 hours, gives the chelate complex $[Ru(\eta^3:\eta^3\text{-}C_{10}H_{16})Cl(OSCMe)]$ **85**, analogous to **72**. Because of the

asymmetry of the thioacetate ligand the existence of axial and / or equatorial isomers arises. In this case **85** is found to exist as both possible geometrical isomers **85a** and **85b** (distinguished by their ^{1}H NMR spectra) in a ratio of approximately 4 : 1. It is unclear whether the major isomer has the sulphur atom equatorially or axially bound but it seems likely that the more bulky donor atom occupies an equatorial position in order to minimise unfavourable axial ligand - methyl substituent steric interactions. A number of examples of the related 2-hydroxypyridinate complexes [Ru(η^3:η^3-$C_{10}H_{16}$)Cl(pyrO)] exhibit analogous isomerism, and have been studied in some detail (Chapter 4).

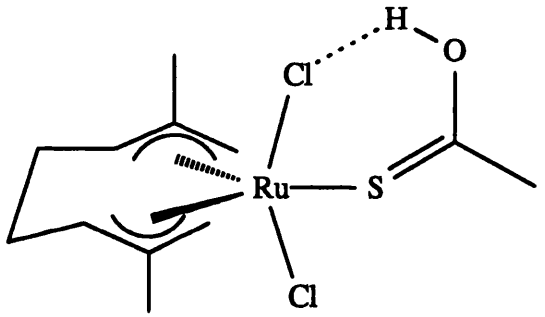

84

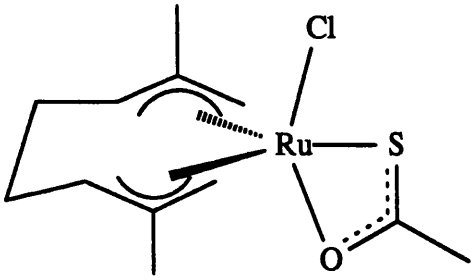

85a

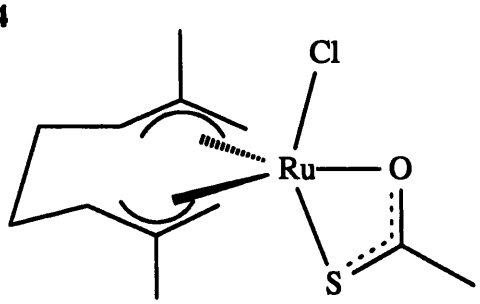

85b

The two-step mechanism of coordination of thioacids, initially proceeding *via* adducts such as **84**, is analogous to the reaction of **6** with 2-thiopyridinol (pyrSH)[159] which proceeds initially *via* the adduct [Ru(η^3:η^3-$C_{10}H_{16}$)Cl_2(pyrSH)] before base-induced deprotonation occurs to form the chelate compound [Ru(η^3:η^3-$C_{10}H_{16}$)Cl(pyrS)].

Reaction of **6** with thiopivalic and thiobenzoic acids also gives chelate species [Ru(η^3:η^3-$C_{10}H_{16}$)Cl(OSCR)] (R = ^{t}Bu **86**, Ph **87**), although in these cases we have been

unable to observe the formation of simple adduct intermediates related to **84**. We infer that the chelation step in these instances is more rapid than in the former case. Also the high solubility of the complexes makes it difficult to isolate them quickly and chelation may well occur during the recrystallisation procedure. As with **85**, complexes **86** and **87** exist as *axial* and *equatorial* isomers, each possessing similar, but distinct, ^{1}H NMR spectra (Table 3.1). Isolated isomer ratios were 25 : 1 and 6 : 1 for **86** and **87** respectively. In the absence of competing steric interactions the major isomers are again assigned S-equatorial structures for reasons outlined above.

3.8 Synthesis and Structures of Nitrato Complexes

The nitrate anion, $[NO_3]^-$, is structurally closely related to the carboxylato ligands described in Sections 3.2 and 3.3 and we have also investigated the reaction of **6** with $Ag[NO_3]$. Interaction of **6** with two mole equivalence of $Ag[NO_3]$ in acetone over a period of *ca.* 12 h, results in the formation of the chelate complex $[Ru(\eta^3:\eta^3\text{-}C_{10}H_{16})Cl(NO_3)]$ **88** exactly analogous to the acetate compound **72**. At room temperature the ^{1}H NMR spectrum of **88** is sharp and exhibits the expected four resonances (δ 5.59, 4.84, 4.62 and 3.70 ppm) for the terminal allyl protons and two methyl signals, δ 2.33 and 2.18 ppm. The IR spectrum of **88** displays bands ν(N=O) 1526, $\nu_{asymm}(NO_2)$ 1223, $\nu_{symm}(NO_2)$ 994 cm^{-1}, Δν (= ν_1 - ν_2) = 303 cm^{-1} (for comparable compounds Δν, the separation between the two highest energy bands in nitrato complexes, is expected to be larger in the case of bidentate, rather than monodentate coordination[193]). A medium intensity band attributable to ν(RuCl) is observed at 288 cm^{-1}.

Treatment of **6** with four molar equivalents of $Ag[NO_3]$ even in "wet" acetone results in the formation of an orange solution from which orange crystals are deposited analyzing closely for the formulation $[Ru(\eta^3:\eta^3\text{-}C_{10}H_{16})(NO_3)_2]$ **89**. Such a complex might reasonably be expected to contain one chelating and one monodentate nitrato group and thus be formally analogous to the chelate complexes **72** and **88** (with the chloride ligand simply replaced by a monodentate nitrate ligand). Unlike the chelate compounds however, **89** exhibits a very simple ^{1}H NMR spectrum (Table 3.1) characteristic of a complex such

as the *bis*(trifluoroacetato) compound **73**, with equivalent axial sites. Thus **89** displays only two singlet resonances assigned to the terminal allyl protons of the dimethyloctadienediyl ligand (δ 5.68 and 4.21 ppm) and a single methyl signal. Unlike complex **73** however, no signals were observed at δ *ca.* 7 in the spectrum of **89** which could be assigned to a coordinated water molecule.

The infrared spectrum (KBr disk) of **89** displays three very strong bands $\nu_{asymm}(NO_2)$ 1502, $\nu_{symm}(NO_2)$ 1284 and ν(N-O) 987 cm^{-1} suggesting monodentate nitrato ligands, $\Delta\nu$ = 218 cm^{-1} (*cf. cis*-$[Pt(NH_3)_2(NO_3)_2]$ 1510, 1275 and 997 cm^{-1}, $K[Au(NO_3)_4]$ 1570, 1286 and 920 cm^{-1}, monodentate; $[Sn(NO_3)_4]$ 1629, 1250 and 973 cm^{-1}, $[Ti(NO_3)_4]$ 1635, 1225 and 993 cm^{-1} symmetrically bidentate).[193,194] Two bands attributable to ν(RuO) are also observed at 345 and 328 cm^{-1}.

These data would seem to imply a four coordinate,* formally sixteen electron complex containing two equivalent, axially bound nitrato ligands. To fully characterise this material a single crystal X-ray structure determination was undertaken.

The crystal and molecular structure of **89** together with the atom numbering scheme adopted is shown in Fig. 3.6. The geometry about the metal centre is broadly similar to that observed for other structures containing the "$(\eta^3:\eta^3\text{-}C_{10}H_{16})Ru$" unit and is based on a distorted trigonal bipyramid with the *bis*(allyl) ligand occupying two of the three equatorial coordination sites. As implied by the room temperature ^1H NMR spectrum, the axial sites are equivalent on the X-ray timescale, and each is occupied by a "semi-chelating" nitrato ligand, Ru-O(1) 2.091(5) Å. Unlike previous structures such as **73** however, the remaining equatorial site does not contain an additional two electron ligand (such as a water molecule). Instead the axial nitrato ligands "wrap round" such that the oxygen atoms O(2) and O(2a) each form long bonds to the metal, Ru-O(2) 2.548(8) Å, resulting in an overall coordination number of six (as opposed to the usual number of five observed in all previously characterised examples of complexes containing the "$(\eta^3:\eta^3\text{-}C_{10}H_{16})Ru$" moiety). This asymmetric chelating mode of bonding is reflected in the bond lengths within the nitrato ligand itself: the distance from the nitrogen atom to the axially coordinated oxygen atoms is relatively long, N(1)-O(1) 1.290(8) as would be expected for a single N-O bond whereas N(1)-O(3) is significantly shorter 1.187(8) Å, more consistent

* Counting each allylic functionality as occupying one coordination site.

with a N=O double bond. The distance N(1)-O(2) of 1.240(10) Å falls somewhere in between, implying a bond order between 1 and 2. [*cf.* the corresponding distances in the bridged bidentate nitrato ligand in *cis*-[$Pt(NH_3)_2$(methyluracilato)(methylcytosine) $Ag(OH_2)(NO_3)]^+$ 1.26(2), 1.24(1) and 1.22(1) Å,[195] and in the mixed mono- / bidentate complex [Ni{diacetylpyridine *bis*(anil)}$(O_2NO)(ONO_2)$] 1.271(5), 1.276(8) and 1.223(8) (chelating), and 1.279(7), 1.225(6) and 1.205(8) Å (monodentate).[196]] The "semi-chelating" mode of coordination is also reflected in the angle O(1)-Ru-O(1a) which, in the case of unidentate ligands, has a value of *ca.* 175° [*e.g.* **73** 174.8(2)°]. In **89** this angle is reduced to 167.1(3)° reflecting the movement of the nitrato ligands towards the "vacant" equatorial site. The relatively close approach of O(2) to O(2a) (*ca.* 2.5 Å) results in slight unfavourable steric interactions such that each nitrato ligand is distorted some 2.4° out of the plane containing Ru(1), O(1) and O(1a). Each ligand itself is planar within experimental error. Asymmetrically bound bidentate nitrato ligands such as those observed in complex **89** are known in the literature[194] although they are rare and their occurrence is normally confined to paramagnetic complexes of Cu(II) or Co(II) such as $[Cu(NO_3)_2(MeCN)_2]$ and $[Co(NO_3)_4]^{2-}$ in which there is an asymmetric charge distribution about the metal centre, or to complexes where there is ligand exerting a strong *trans* influence.

It is possible that static or dynamic disorder within the crystal might serve to render the two nitrato ligands equivalent on average and indeed a close examination of the anisotropic thermal ellipsoids for O(2) and O(3) reveals them to be very slightly elongated in the Ru-NO_3 plane, implying, at least, a slightly anisotropic thermal motion. Even at temperatures down to -135°C in mixed CD_2Cl_2 / CHF_2Cl solvent however, the ^1H NMR spectrum of the complex remains sharp with the two axial sites equivalent on the NMR timescale, implying that any fluxional process involving monodentate / bidentate exchange is extremely rapid even at very low temperatures. Determined attempts were made to refine the structure of **89** in terms of disordered contributions from symmetrically bidentate and monodentate nitrato ligands but we were unable to refine alternative positions in spite of relatively good data quality (final *R* factor 4.2%), indicating that if the structure is disordered then there is little difference in the positions of the nitrato ligands in the two coordination modes. We reasoned however, that such a difference should be very large and

easily resolved by a modern diffractometer, given, for example, the expected M-O(2) bond lengths: *ca.* 2.8 Å - unidentate, 2.1 Å - symmetrically bidentate.[194]

For comparison the X-ray crystal structure of **88** was also examined, Fig. 3.7. As anticipated, the complex is isostructural with the acetato compound **72**. The nitrate ligand adopts a much more symmetric mode of chelation than **89**: Ru-O(1) 2.104(4) Å, Ru-O(2) 2.237(4) Å although the same elongation of the Ru-O(2) bond as found in **72** is evidenced. Thus the difference in Ru-O(2) between the approximately symmetric bidentate complex **88** and the unsymmetric **89** is 0.31 Å, a difference which should be easily resolved in the event of disorder in the latter case, and certainly greatly exceeds the compass of the slightly elongated thermal ellipsoid for O(2) in the structure of **89**. Given this evidence and the fact that **88** is also apparently non-fluxional it seems likely that **89** is indeed genuinely six coordinate (albeit with two very long Ru-ligand bonds) in spite of the small size of the ruthenium(IV) centre, and contains two asymmetrically bidentate nitrato ligands.

This observation contrasts to the *bis*(nitrato)ruthenium(II) compound $[Ru(ONO_2)(O_2NO)(CO)(PPh_3)_2]$[197] in which the two nitrato ligands are equivalent at room temperature, but exchange between mono- and bidentate coordination is slow on the ^{31}P NMR timescale below *ca.* -90°C revealing a mixed mono- bidentate complex. In this material however, the two nitrato ligands are *cis* to one another which may mitigate against the adoption of a semi-chelating geometry for steric reasons. Mono- / bidentate exchange is also observed in the monohaloacetato compounds described in Section 3.3 but the fluxionality was slow on the ^1H NMR timescale at -50°C and the spectra were broad even at room temperature.

Given the apparently weak nature of the long bonds to the two equatorial oxygen atoms O(2) and O(2a) in **89** it might be anticipated that the complex should readily react with two electron ligands to generate more conventional five coordinate compounds containing two unidentate nitrato ligands, and related to the trifluoroacetato complexes **73** and **74**. To this end the reaction of **89** with CO was investigated. Shaking a dichloromethane solution of **89** in an atmosphere of CO for *ca.* 15 minutes resulted in an obvious colour change from deep orange to pale yellow. Removal of the solvent *in vacuo* resulted in the isolation of the bright yellow adduct $[Ru(\eta^3{:}\eta^3\text{-}C_{10}H_{16})(ONO_2)_2(CO)]$ **90**. The presence of the carbonyl ligand was confirmed by the observation of ν(CO) 2080 cm^{-1}

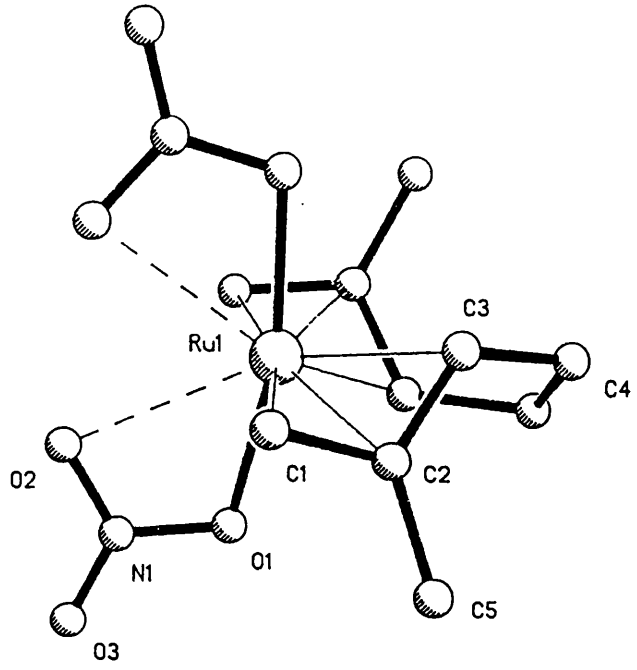

Fig. 3.6: Crystal structure of $[Ru(\eta^3:\eta^3\text{-}C_{10}H_{16})(NO_3)_2]$ **89** showing the atom numbering scheme adopted.

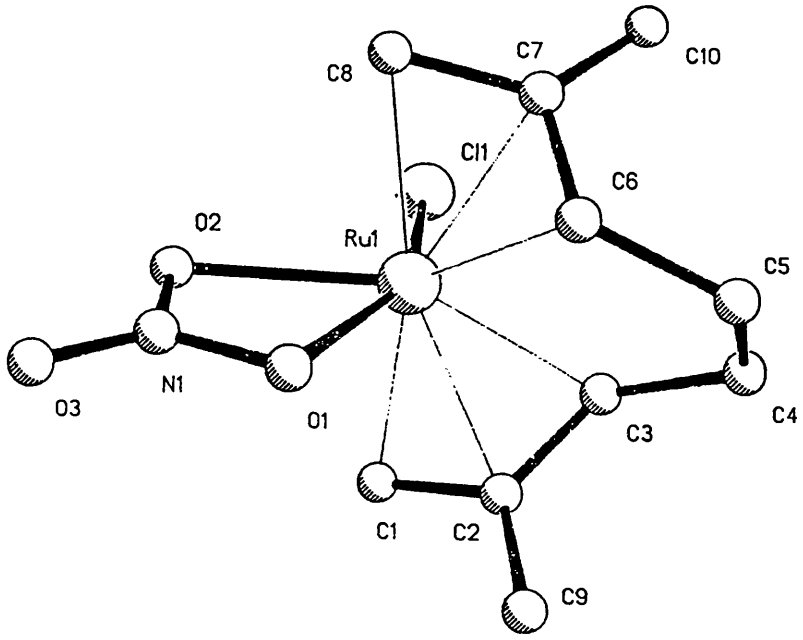

Fig. 3.7: Crystal structure of $[Ru(\eta^3:\eta^3\text{-}C_{10}H_{16})Cl(NO_3)]$ **88** showing the atom numbering scheme adopted.

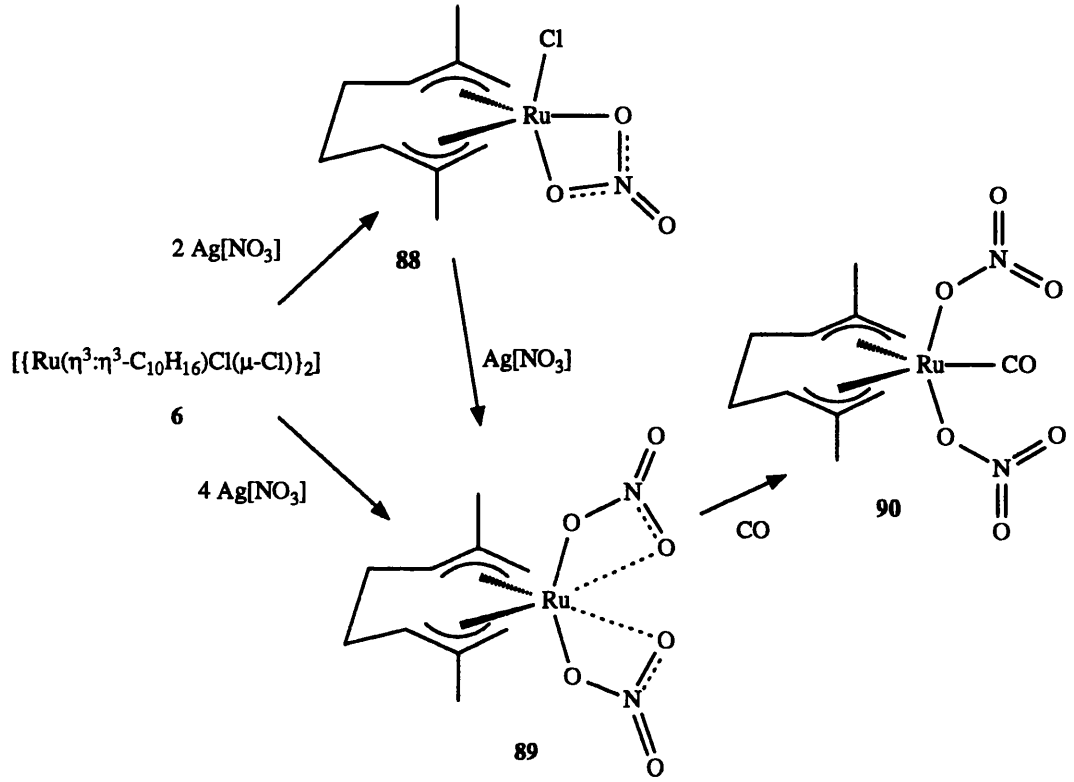

Scheme 3.2: Synthesis and reactions of nitrato compounds derived from $[\{Ru(\eta^3:\eta^3\text{-}C_{10}H_{16})Cl(\mu\text{-}Cl)\}_2]$.

with in the infrared spectrum of the complex (the relatively high wavenumber suggesting little metal to ligand π back-donation by the Ru(IV) centre), whilst the unidentate nitrato ligands gave rise to bands at 1491, 1259 and 975 cm^{-1}, $\Delta\nu$ = 232 cm^{-1} consistent with unidentate coordination of the nitrato ligands. The ^1H NMR spectrum of **90** was completely consistent with the proposed formulation, and clearly indicated that the carbonyl ligand occupies an equatorial coordination site. Similar reactions were also attempted using pyridine and PPh_3. Rapid colour changes from orange to yellow were also noted in these cases but, on work-up a further colour change to deep green occurred, apparently as a result of high air sensitivity, and in the case of the triphenylphosphine adduct no clean products were obtained. The ^1H NMR spectrum of the pyridine product was again

consistent with the formation of an equatorial adduct, $[Ru(\eta^3:\eta^3\text{-}C_{10}H_{16})(ONO_2)_2(NC_5H_5)]$ **91** analogous to **90** although it was noted that a large amount of **89** and free pyridine were also present in the sample possibly as a result of disproportionation of the complex. In a separate experiment a fivefold excess of pyridine was added to an NMR sample of pure **89** in chloroform-*d*. An instant colour change to bright yellow was noted and in the resulting sample it was found that all of the compound **89** present had been cleanly converted to **91**. On standing for *ca.* 10 minutes this sample too gradually became deep green. The instability of the phosphine and pyridine adducts is possibly a consequence of unfavourable steric interactions between the more bulky Lewis bases and the nitrato ligands, forcing them into close proximity with the sterically demanding *bis*(allyl) ligand, although no such problems were noted in the case of the pyrazene adduct **74** which presumably possesses a similar structure.

The apparent ease with which the semi-chelating nitrato ligands are displaced to leave an unsaturated metal centre has interesting possibilities for the application of **89** as a catalyst in olefin polymerisation for example. It has already been demonstrated[111] that both **6** and a trifluoroacetate compound (probably **73**) are active catalysts for the polymerisation of norbornene as well as other, less strained, olefins, and it seems likely that **89** may show similar activity. To test this idea, **89** was warmed at 70°C in acetone with a large excess of butadiene. After 12 h a large quantity of brownish precipitate had formed. Recrystallisation of this material from diethyl ether gave a white solid exhibiting a simple ^{1}H NMR spectrum, consistent with either *cis*- or *trans*-polybutadiene (δ 5.41 and 2.03 ppm, ratio 1 : 2). At room temperature however, it was found that **89** did not react with ethylene or diphenylacetylene.

3.9 Experimental

General experimental and instrumental considerations are outlined in Section 2.4. All manipulations were carried out under nitrogen with degassed solvents using conventional Schlenk line techniques, although no significant air sensitivity of the products was noted. Sodium carboxylates were prepared by reaction of sodium metal with solutions

of the acids in dry thf, or alternatively with the neat acid, for those that are liquids. Silver salts were prepared by the reaction of the aqueous acid with Ag_2O.[198] All other reagents and materials were obtained from the usual commercial sources.

Preparations. - $[Ru(\eta^3:\eta^3\text{-}C_{10}H_{16})Cl(O_2CMe)]$ **72.** a) The compound $[\{Ru(\eta^3:\eta^3\text{-}C_{10}H_{16})Cl(\mu\text{-}Cl)\}_2]$ (0.04 g, 0.07 mmol) was suspended in acetone (5 cm^3), $Ag[O_2CMe]$ (0.02 g, 0.13 mmol) was added and the mixture stirred for 1 h. The resulting orange-red solution was filtered through Celite to remove the precipitate of AgCl and the solvent removed *in vacuo* to give an orange oil which was recrystallised from diethyl ether. Yield: 0.03 g, 0.08 mmol, 60% (Found: C, 43.65; H, 5.85. Calc. for $C_{14}H_{19}ClO_2Ru$: C, 43.45; H, 5.75%).

b) The compound $[\{Ru(\eta^3:\eta^3\text{-}C_{10}H_{16})Cl(\mu\text{-}Cl)\}_2]$ (0.20 g, 0.32 mmol) was suspended in acetone (5 cm^3), $Na[O_2CMe]$ (0.05 g, excess) was added and the mixture stirred for 24 h. The resulting product was recovered in a similar manner to (a). Yield: 0.19 g, 0.56 mmol, 86%.

c) Attempts to prepare **72** by refluxing **6** in acetic acid resulted in the formation of a dark brown colouration over a period of *ca.* 4 h. However no product could be isolated probably due to high solubility in this reaction mixture.

$[Ru(\eta^3:\eta^3\text{-}C_{10}H_{16})(O_2CCF_3)_2(OH_2)]$ **73.** a) The compound $[\{Ru(\eta^3:\eta^3\text{-}C_{10}H_{16})Cl(\mu\text{-}Cl)\}_2]$ (0.10 g, 0.16 mmol) was suspended in 'wet' acetone (5 cm^3). $Ag[CF_3CO_2]$ (0.13 g, 0.57 mmol) was added and the mixture stirred for 1 h. The resulting orange solution was filtered through Celite to remove the precipitate of AgCl and the volume reduced to *ca.* one quarter resulting in the precipitation of the orange product which was isolated by filtration, washed with acetone and diethyl ether and air dried. Yield: 0.10 g, 0.20 mmol, 64% (Found: C, 35.10; H, 3.75. Calc. for $C_{14}H_{18}O_5F_6Ru$: C, 34.95; H, 3.75%).

b) $[\{Ru(\eta^3:\eta^3\text{-}C_{10}H_{16})Cl(\mu\text{-}Cl)\}_2]$ (0.20 g, 0.32 mmol) was refluxed in trifluoroacetic acid (15 cm^3) in the presence of trifluoroacetic anhydride (3 cm^3) for 4 h. The resulting red brown solution was filtered through Celite to remove particulate matter, evaporated to *ca.* half volume and layered with hexane. The product separated out as large, orange

crystals after standing for 48 h at *ca.* -20°C. Yield: 0.22 g, 0.45 mmol, 71%.

c) The product may also be prepared in near-quantitative yield by refluxing of the acetate complex $[Ru(\eta^3:\eta^3\text{-}C_{10}H_{16})Cl(O_2CMe)]$ **72** in neat CF_3CO_2H, followed by work up in a similar manner as described in (b).

$[Ru(\eta^3:\eta^3\text{-}C_{10}H_{16})(O_2CCF_3)_2(N_2C_4H_4)]$ **74**. To $[Ru(\eta^3:\eta^3\text{-}C_{10}H_{16})(O_2CCF_3)_2(OH_2)]$ (0.08 g, 0.17 mmol) was added pyrazene (0.02 g, 0.21 mmol) and the mixture stirred in CH_2Cl_2 (5 cm^3) for 72 h. The resulting orange solution was evaporated to *ca.* one quarter volume and hexane added to precipitate the product as an orange, microcrystalline solid which was isolated by filtration, washed with diethyl ether and air dried. Yield: 0.07 g, 0.13 mmol, 76% (Found: C, 39.55; H, 3.60; N, 5.15. Calc. for $C_{18}H_{20}N_2O_4F_6Ru$: C, 39.80; H, 3.70; N, 5.15%).

$[Ru(\eta^3:\eta^3\text{-}C_{10}H_{16})(O_2CCCl_3)_2(OH_2)]$ **75**. To a solution of $[\{Ru(\eta^3:\eta^3\text{-}C_{10}H_{16})Cl(\mu\text{-}Cl)\}_2]$ (0.12 g, 0.20 mmol) in CH_2Cl_2 (4 cm^3) was added an acetone (4 cm^3) suspension of $Na[O_2CCCl_3]$ (0.18 g, 0.98 mmol). The mixture was stirred for 12 h at room temperature. The resulting brown-orange solution was filtered through Celite to remove the precipitate of NaCl and the solvents removed *in vacuo* to give a dark solid. Recrystallisation from chloroform / diethyl ether (1 : 1 v/v) yielded bright yellow crystals which were isolated by filtration and air dried. Yield: 0.10 g, 0.18 mmol, 45% (Found: C, 28.75; H, 3.25; Cl, 37.45. Calc. for $C_{14}H_{18}O_5Cl_6Ru$: C, 29.00; H, 3.15; Cl, 36.65%).

$[Ru(\eta^3:\eta^3\text{-}C_{10}H_{16})(O_2CCHCl_2)_2(OH_2)]$ **76**. A similar procedure to that employed for **75** was followed using $[\{Ru(\eta^3:\eta^3\text{-}C_{10}H_{16})Cl(\mu\text{-}Cl)\}_2]$ (0.12 g, 0.20 mmol) and $Na[O_2CCHCl_2]$ (0.15 g, 0.97 mmol). Yield: 0.10 g, 0.20 mmol, 50% (Found: C, 32.80; H, 4.00; Cl, 27.75. Calc. for $C_{14}H_{20}O_5Cl_4Ru$: C, 32.90; H, 3.90; Cl, 28.50%).

$[Ru(\eta^3:\eta^3\text{-}C_{10}H_{16})(O_2CCHF_2)_2(OH_2)]$ **77**. A similar procedure to that employed for **75** was followed using $[\{Ru(\eta^3:\eta^3\text{-}C_{10}H_{16})Cl(\mu\text{-}Cl)\}_2]$ (0.06 g, 0.10 mmol) and $Na[O_2CCHF_2]$ (0.06 g, 0.49 mmol). The product was purified by dry flash column chromatography and recrystallised from CH_2Cl_2 / diethyl ether (1 : 1 v/v). Yield: 0.02 g,

0.05 mmol, 23% (Found: C, 37.80; H, 4.75. Calc. for $C_{14}H_{20}O_5F_4Ru$: C, 37.75; H, 4.55%).

$[Ru(\eta^3:\eta^3\text{-}C_{10}H_{16})Cl(O_2CCH_2Cl)]$ **78a** and $[Ru(\eta^3:\eta^3\text{-}C_{10}H_{16})(O_2CCH_2Cl)_2(OH_2)]$ **78b**. To a solution of $[\{Ru(\eta^3:\eta^3\text{-}C_{10}H_{16})Cl(\mu\text{-}Cl)\}_2]$ (0.12 g, 0.20 mmol) in CH_2Cl_2 (4 cm^3) was added $Na[O_2CCH_2Cl]$ (0.17 g, 1.00 mmol) in acetone (4 cm^3). The mixture stirred at room temperature for 12 h. Removal of the solvents *in vacuo* gave a yellow oily product which was recrystallised from diethyl ether / hexane (1 : 4 v/v) to give 0.06 g of orange-yellow crystals which were shown by ^1H NMR spectroscopy to be a mixture of **78a**, **78b** and unreacted starting material. Pure samples of **78a** and **78b** were isolated by dry flash column chromatography. (Found **78a**: C, 39.75; H, 5.25. Calc. for $C_{12}H_{18}O_2Cl_2Ru$: C, 39.35; H, 4.95%; **78b**: C, 36.80; H, 5.20. Calc. for $C_{14}H_{22}O_5Cl_2Ru$: C, 38.00; H, 5.00%).

$[Ru(\eta^3:\eta^3\text{-}C_{10}H_{16})Cl(O_2CCH_2F)]$ **79a** and $[Ru(\eta^3:\eta^3\text{-}C_{10}H_{16})(O_2CCH_2F)_2(OH_2)]$ **79b**. A similar procedure to that adopted for **78a** and **78b** was employed using $[\{Ru(\eta^3:\eta^3\text{-}C_{10}H_{16})Cl(\mu\text{-}Cl)\}_2]$ (0.12 g, 0.20 mmol) and $Na[O_2CCH_2F]$ (0.10 g, 1.00 mmol) to give 0.02 g of a yellow material shown by ^1H NMR to be a mixture of **79a** and **79b**. The products were separated by dry flash column chromatography. (Found **79a**: C, 40.40; H, 5.55. Calc. for $C_{12}H_{18}O_2F_2Ru$: C, 41.20; H, 5.20%; **79b**: C, 39.85; H, 5.70. Calc. for $C_{14}H_{22}O_5F_2Ru$: C, 41.05; H, 5.40%).

$[Ru(\eta^3:\eta^3\text{-}C_{10}H_{16})Cl\{F_3CC(O)CHC(O)CF_3\}]$ **80**. a) The compound $[\{Ru(\eta^3:\eta^3\text{-}C_{10}H_{16})Cl(\mu\text{-}Cl)\}_2]$ (0.04 g, 0.07 mmol) was suspended in acetone (5 cm^3), $Ag[CF_3CC(O)CHC(O)CF_3]$ (0.1 g, excess) was added and the mixture stirred for 24 h. The resulting pale orange solution was filtered through Celite to remove the precipitate of AgCl and unreacted starting material and the solvent removed *in vacuo* to give an orange oil which was recrystallised from diethyl ether. Yield: 0.02 g, 0.03 mmol, 22% (Found: C, 36.90; H, 3.50. Calc. for $C_{15}H_{17}ClO_2F_6Ru$: C, 37.55; H, 3.55%). Some difficulty was noted in the separation of the product from the excess of silver hexafluoroacetylacetonate.

b) The compound $[\{Ru(\eta^3:\eta^3\text{-}C_{10}H_{16})Cl(\mu\text{-}Cl)\}_2]$ (0.05 g, 0.09 mmol) was suspended in acetone (5 cm^3), $Na[F_3CC(O)CHC(O)CF_3]$ (0.04 g, 0.19 mmol) was added and the mixture stirred at room temperature for 2 weeks. The product was isolated as in

(a). Yield: 0.03 g, 0.06 mmol, 34%.

$[Ru(\eta^3:\eta^2:\eta^3\text{-}C_{12}H_{18})Cl(H_2O)]$ **83**. The compound $[Ru(\eta^3:\eta^2:\eta^3\text{-}C_{12}H_{18})Cl_2]$ (0.06 g, 0.18 mmol) was stirred in acetone (5 cm^3) with $Ag[BF_4]$ (0.04 g, 0.18 mmol) in a 1 : 1 mole ratio for 3 h. The resulting brown solution was filtered through Celite and the volume reduced to *ca.* 2 cm^3 *in vacuo*. Hexane (3 cm^3) was layered over the remaining solution resulting in the formation of the compound as straw brown needles over the course of *ca.* 4 h which were isolated by filtration and air dried. Yield: 0.02 g, 0.05 mmol, 28% (Found: C, 35.90; H, 4.85. Calc. for $C_{12}H_{20}BClF_4ORu$: C, 35.70; H, 5.00%).

$[Ru(\eta^3:\eta^3\text{-}C_{10}H_{16})Cl_2\{SC(OH)Me\}]$ **84**. $[\{Ru(\eta^3:\eta^3\text{-}C_{10}H_{16})Cl(\mu\text{-}Cl)\}_2]$ (0.07 g, 0.12 mmol) was stirred in acetone (5 cm^3) containing a small excess of thioacetic acid (0.2 cm^3) for 15 min during which time the solution became bright orange. The solvent was removed *in vacuo* to give an orange oil from which the product was deposited as orange crystals. These were filtered off and washed with hexane, then air dried. Yield: 0.07 g, 0.19 mmol, 82% (Found: C, 37.60; H, 5.50. Calc. for $C_{12}H_{20}Cl_2ORuS$: C, 37.50; H, 5.25%).

$[Ru(\eta^3:\eta^3\text{-}C_{10}H_{16})Cl(SOCMe)]$ **85a, 85b**. $[\{Ru(\eta^3:\eta^3\text{-}C_{10}H_{16})Cl(\mu\text{-}Cl)\}_2]$ (0.11 g, 0.18 mmol) was stirred in CH_2Cl_2 (5 cm^3) with a small excess of thioacetic acid (0.2 cm^3) for 24 h during which time the bright orange colouration initially formed darkened to a deep brown. The reaction mixture was evaporated to *ca.* one quarter volume and diethyl ether added to precipitate the product as a red-brown solid which was isolated by filtration and air dried. Yield: 0.07 g, 0.20 mmol, 54% (Found: C, 42.40; H, 5.55. Calc. for $C_{12}H_{19}ClORuS$: C, 41.45; H, 5.50%).

$[Ru(\eta^3:\eta^3\text{-}C_{10}H_{16})Cl(SOCBu^t)]$ **86a, 86b**. $[\{Ru(\eta^3:\eta^3\text{-}C_{10}H_{16})Cl(\mu\text{-}Cl)\}_2]$ (0.06 g, 0.09 mmol) was stirred in acetone (5 cm^3) with a small excess of thiopivalic acid (0.2 cm^3) for 1 h during which time a deep orange solution formed. The reaction mixture was evaporated to an orange oil which yielded an orange precipitate on trituration with methanol / hexane (1 : 2 v/v). The product was isolated by filtration and air dried. Yield: 0.06 g, 0.16 mmol, 88% (Found: C, 47.15; H, 6.90. Calc. for $C_{15}H_{25}ClORuS$: C, 46.20; H, 6.45%).

$[Ru(\eta^3:\eta^3\text{-}C_{10}H_{16})Cl(SOCPh)]$ **87a, 87b.** $[\{Ru(\eta^3:\eta^3\text{-}C_{10}H_{16})Cl(\mu\text{-}Cl)\}_2]$ (0.07 g, 0.12 mmol) was stirred in acetone (5 cm^3) with a small excess of thiobenzoic acid (0.1 cm^3) for 1 h resulting in the formation of a bright orange solution. The solvent was removed *in vacuo* and the residue dissolved in diethyl ether (1 cm^3) and layered with hexane resulting in the formation of a deep red crystalline product over a period of *ca.* 12 h. This product was collected by filtration and air dried. Yield: 0.06 g, 0.14 mmol, 60% (Found: C, 49.65; H, 5.00. Calc. for $C_{17}H_{21}ClORuS$: C, 49.80; H, 5.15%).

$[Ru(\eta^3:\eta^3\text{-}C_{10}H_{16})Cl(NO_3)]$ **88.** $[\{Ru(\eta^3:\eta^3\text{-}C_{10}H_{16})Cl(\mu\text{-}Cl)\}_2]$ (0.07 g, 0.11 mmol) was suspended in acetone (5 cm^3), $Ag[NO_3]$ (0.03 g, 0.20 mmol) was added and the mixture stirred for 12 h. The resulting pale pink solution was filtered through Celite to remove the precipitate of AgCl and the solvent reduced to *ca.* one quarter volume to give pinkish-purple crystals. which were isolated by filtration and air dried. Yield: 0.06 g, 0.18 mmol, 82% (Found: C, 35.70; H, 4.90; N, 4.10. Calc. for $C_{10}H_{16}NClO_3Ru$: C, 35.90; H, 4.80; N, 4.20%).

$[Ru(\eta^3:\eta^3\text{-}C_{10}H_{16})(NO_3)_2]$ **89.** $[\{Ru(\eta^3:\eta^3\text{-}C_{10}H_{16})Cl(\mu\text{-}Cl)\}_2]$ (0.34 g, 0.54 mmol) was suspended in acetone (5 cm^3), $Ag[NO_3]$ (0.38 g, 2.21 mmol) was added and the mixture stirred for 2 h. The resulting pale orange solution was filtered through Celite to remove the precipitate of AgCl. The Celite was washed with CH_2Cl_2 (2 x 10 cm^3) and the washings combined with the filtrate. Reduction of the volume of the solution *in vacuo* to *ca.* 2 cm^3 gave orange crystals which were isolated by filtration, washed with diethyl ether (1 cm^3) and air dried. Yield: 0.34 g, 0.94 mmol, 87% (Found: C, 33.25; H, 4.45; N, 7.50. Calc. for $C_{10}H_{16}N_2O_6Ru$: C, 33.25; H, 4.45; N, 7.75%).

$[Ru(\eta^3:\eta^3\text{-}C_{10}H_{16})(ONO_2)_2(CO)]$ **90.** $[Ru(\eta^3:\eta^3\text{-}C_{10}H_{16})(NO_3)_2]$ (0.04 g, 0.10 mmol) was dissolved in CH_2Cl_2 (5 cm^3) in a 20 cm^3 round bottomed flask. Gaseous CO was bubbled through the solution for one minute and the flask was then stoppered and shaken for 15 minutes during which time a colour change from orange to yellow was observed. The solution was filtered and the solvent removed *in vacuo* to give the product as a bright yellow powder. Yield: 0.03 g, 0.08 mmol, 80% (Found: C, 33.40; H, 3.95; N, 6.70. Calc.

for $C_{11}H_{16}N_2O_7Ru$: C, 33.95; H, 4.15; N, 7.20%).

$[Ru(\eta^3:\eta^3\text{-}C_{10}H_{16})(ONO_2)_2(NC_5H_5)]$ **91**. $[Ru(\eta^3:\eta^3\text{-}C_{10}H_{16})(NO_3)_2]$ (0.06 g, 0.15 mmol) was dissolved in CH_2Cl_2 (5 cm^3) in a 20 cm^3 round bottomed flask. Pyridine (0.01 cm^3, excess) was added and the solution stirred for one minute until all the starting material had been taken up into solution. During this time a colour change from orange to yellow was observed. The solution was filtered and the solvent rapidly removed *in vacuo* to give the product as a greenish-yellow solid which was washed with diethyl ether and dried under vacuum. Yield: 0.06 g, 0.14 mmol, 93% (Found: C, 40.20; H, 4.65; N, 9.45. Calc. for $C_{11}H_{16}N_2O_7Ru$: C, 40.90; H, 4.80; N, 9.55%).

X-ray Crystal Structure Determinations

A summary of general considerations in the following X-ray crystal structure determinations may be found in Section 2.4

i) $[Ru(\eta^3:\eta^3\text{-}C_{10}H_{16})Cl(O_2CMe)]$ **72**

Crystal data. - $C_{12}H_{19}ClO_2Ru$, M = 331.80 g mol^{-1}, orthorhombic, space group Pbca, a = 12.742(6), b = 14.082(6), c = 14.614(6), U = 2622 $Å^3$ (by least-squares refinement of diffractometer angles for 30 automatically centred reflections in the range $10 \leq 2\theta \leq 23°$), Z = 8, F(000) = 1344, D_c = 1.68 g cm^{-3}, μ(Mo-K_α) = 13.63 cm^{-1}.

A pink plate of approximate dimensions 0.4 x 0.3 x 0.05 mm was prepared by evaporation of an acetone solution of the compound. A primitive data set of 2576 reflections was collected (2270 unique), 1381 of which were observed to have $I \geq 3\sigma(I)$. Three standard reflections monitored throughout the data collection showed no appreciable change in intensity. An empirical absorption correction was applied. The structure was solved by the conventional Direct Methods and difference-Fourier techniques. The asymmetric unit was observed to contain one complete molecule. Full-matrix least-squares refinement gave R = 0.0447, R_w = 0.0458 in the final cycle from 145 parameters. A weighting scheme of the form $w^{-1} = \sigma^2(F)+0.000338F^2$ was applied and the maximum shift to error ratio in the final cycle was 0.02. The largest residual peak was 0.52 electrons $Å^{-3}$. No short intermolecular contacts were observed.

ii) $[Ru(\eta^3:\eta^3\text{-}C_{10}H_{16})(O_2CCF_3)_2(H_2O)]$ **73**

Crystal data. - $C_{14}H_{18}O_5F_6Ru$, M = 481.39 g mol^{-1}, monoclinic, space group C2/c, a = 12.191(3), b = 17.318(5), c = 9.314(2), β = 105.14(2)°, U = 1898 Å^3 (by least-squares refinement diffractometer angles for 46 automatically centred reflections in the range 15 ≤ 2θ ≤ 30°), Z = 4, F(000) = 960, D_c = 1.68 g cm^{-3}, μ(Mo-K$_\alpha$) = 8.80 cm^{-1}.

An orange wedge shaped crystal of approximate dimensions 0.6 x 0.25 x 0.2 mm was prepared by cooling an acetone solution containing the compound to *ca.* -20°C for 24 h. A total of 2116 (1675 unique) data were collected. Three standard reflections were monitored throughout the data collection but showed no appreciable change in intensity. A total of 1568 absorption corrected reflections with I ≥ 3σ(I) were employed in the analysis. The structure was solved by the conventional Patterson and difference-Fourier techniques. The asymmetric unit containing half of the molecule situated on a crystallographic two-fold axis at (¼, y, ¼). Full-matrix least-squares refinement gave R = 0.0384, R_w = 0.0395 in the final cycle from 146 parameters. Hydrogen atoms were not included for the water molecule due to the difficulty in predicting their positions. The fluorine atoms of the trifluoroacetate group were found to be disordered and each was modeled as having two positions, each of 50% occupancy. A weighting scheme of the form $w^{-1} = \sigma^2(F)+0.000350F^2$ was applied and the maximum shift to error ratio in the final cycle was 0.116, which was associated with a thermal parameter for one of the disordered fluorine atoms. The largest residual peak was 0.81 electrons Å^{-3}. Short intermolecular contacts were observed between carboxylate oxygen atoms and the water ligand on adjacent molecules (see discussion). Attempts to refine the molecule in the non-centrosymmetric space group Cc (in which disorder need not be present) were unsuccessful.

iii) $[Ru(\eta^3:\eta^3\text{-}C_{10}H_{16})Cl(NO_3)]$ **88**

Crystal data. - $C_{10}H_{16}NClO_3Ru$, M = 334.79 g mol^{-1}, orthorhombic, space group Pcab, a = 11.968(3), b = 13.647(2), c = 15.310(4), U = 2501 Å^3 (by least-squares refinement of diffractometer angles for 32 automatically centred reflections in the range 19 ≤ 2θ ≤ 29°), Z = 8, F(000) = 1344, D_c = 1.78 g cm^{-3}, μ(Mo-K$_\alpha$) = 14.37 cm^{-1}.

An purple needle of approximate dimensions 0.5 x 0.25 x 0.2 mm was prepared by

slow liquid diffusion of hexane into a diethyl ether solution of the compound and used to collect a total of 4817 data (2208 unique). Three standards monitored every 97 reflections showed no appreciable change in intensity throughout the data collection. Omission of intensities of $I \leq 3\sigma(I)$ gave 1847 observed, absorption corrected data which were employed in the analysis. The structure was solved by a combination of conventional direct methods and difference-Fourier techniques. The asymmetric unit contained one complete molecule. The final cycle of full matrix least squares refinement included 145 parameters (weighting scheme applied: $w^{-1} = \sigma^2(F)+0.000506F^2$) and the largest shift to error ratio was 0.001, $R = 0.0384$, $R_w = 0.0433$. The largest residual peak was 0.79 electrons $Å^{-3}$ and no intermolecular short contacts were observed.

iv) $[Ru(\eta^3:\eta^3\text{-}C_{10}H_{16})(NO_3)_2]$ **89**

Crystal data. - $C_{10}H_{16}N_2O_6Ru$, $M = 361.35$ g mol^{-1}, monoclinic, space group C2/c, $a = 7.560(3)$, $b = 14.145(7)$, $c = 12.512(3)$, $\beta = 91.31(3)°$, $U = 1337.6$ $Å^3$ (by least-squares refinement of diffractometer angles for 24 automatically centred reflections in the range $6 \leq 2\theta \leq 22°$), $Z = 4$, F(000) = 728, $D_c = 1.79$ g cm^{-3}, $\mu(Mo\text{-}K_\alpha) = 11.71$ cm^{-1}.

An orange needle of dimensions 0.4 x 0.1 x 0.05 mm was prepared by slow diffusion of diethyl ether vapour into a chloroform solution of the compound and was used to collect a total of 2530 (1173 unique) data. Three standards monitored every 97 reflections showed no appreciable change in intensity throughout the data collection. Omission of intensities of $I \leq 3\sigma(I)$ gave 966 observed, absorption corrected data which were employed in the analysis. The structure was solved by a combination of conventional direct methods and difference-Fourier techniques. Refinement was attempted in space groups C2/c and Cc. In both cases similar gross structures were observed, refinement proceeded more smoothly in the former space group, the asymmetric unit of which contained half of one complete molecule which resides on a two-fold axis (0, y, ¾). Attempts were made to model the nitrato ligands as being disordered over two positions of fractional occupancy but this proved unsatisfactory and it was concluded that the structure was not disordered. The final cycle of full matrix least squares refinement included 87 parameters (weighting scheme applied: $w^{-1} = \sigma^2(F)+0.000590F^2$) and the largest shift to error ratio was 0.02. The final residuals were $R = 0.0423$, $R_w = 0.0440$ and

the the largest peak in the final difference electron density map was 0.62 electrons $Å^{-3}$. No short intermolecular contacts were observed.

v) $[Ru(\eta^3:\eta^2:\eta^3\text{-}C_{12}H_{18})Cl(OH_2)][BF_4]$ **83.**

Crystal data. - $C_{12}H_{20}BClF_4ORu$, M = 403.65 g mol^{-1}, monoclinic, space group $P2_1/n$, a = 7.366(1), b = 14.132(3), c = 14.510(3), β = 101.22(2)°, U = 1482 $Å^3$ (by least-squares refinement of diffractometer angles for 30 automatically centred reflections in the range $16 \leq 2\theta \leq 27°$), Z = 4, F(000) = 808, D_c = 1.81 g cm^{-3}, μ(Mo-K_α) = 12.50 cm^{-1}.

An brown needle of dimensions 0.4 x 0.1 x 0.05 mm was prepared by slow liquid diffusion of hexane into an acetone solution of the compound and was used to collect a total of 2915 (2582 unique) data. Three standards monitored every 97 reflections showed no appreciable change in intensity throughout the data collection. Omission of intensities of $I \leq 3\sigma(I)$ gave 1803 observed, absorption corrected data which were employed in the analysis. The structure was solved by a combination of conventional Patterson methods and difference-Fourier techniques. All non-hydrogen atoms were refined anisotropically. The hydrogen atoms on the water molecule were located in the final difference map and their coordinates refined, while remaining hydrogens were placed in idealised positions (C-H 0.96 Å), assigned a common, isotropic displacement parameter (U_{iso} 0.08 $Å^2$) and allowed to ride on the atoms to which they were attached. The fluorine atoms of the $[BF_4]^-$ ions were disordered over two sets of positions (occupancy refined to 50%). The final cycle of full matrix least squares refinement included 87 parameters (weighting scheme applied: $w^{-1} = \sigma^2(F)+0.000752F^2$) and the largest shift to error ratio was 0.02. The final residuals were R = 0.0323, R_w = 0.0372 and the largest peak in the final difference electron density map was 0.47 electrons $Å^{-3}$. Short intermolecular contacts were observed between the oxygen atom, O(1), and fluorine atoms of the $[BF]^-$ anion F(2), F(2a), F(4) and F(4a) of 2.70 Å av..

Table 3.1: ^{1}H NMR Data for New Complexes.[a]

Compound	δ				
	Terminal allyl	Internal allyl	Ethylinic	Methyl	Ligand
$[Ru(\eta^3:\eta^3\text{-}C_{10}H_{16})Cl(O_2CMe)]$ **72**	5.51 (s, 1H), 4.65 (s, 1H) 4.63 (s, 1H), 3.56 (s, 1H)	4.20 (m, 1H) 3.49 (m, 1H)	2.53 (m, 4H)	2.29 (s, 3H) 2.12 (s, 3H)	1.85 (s, 3H, C*H*$_3$)
$[Ru(\eta^3:\eta^3\text{-}C_{10}H_{16})(O_2CCF_3)_2(OH_2)]$ **73**	5.68 (s, 2H), 4.23 (s, 2H)	4.42 (m, 2H)	3.07 (m, 2H) 2.47 (m, 2H)	2.12 (s, 6H)	7.11 (s, 2H, O*H*$_2$)
$[Ru(\eta^3:\eta^3\text{-}C_{10}H_{16})(O_2CCF_3)_2(N_2C_4H_4)]$ **74**	5.22 (s, 2H), 4.16 (s, 2H)	6.17 (m, 2H)	3.47 (m, 2H) 2.71 (m, 2H)	2.15 (s, 6H)	8.72, 8.44 (AB, 4H, ^3J=3.2, $N_2C_4H_4$)
$[Ru(\eta^3:\eta^3\text{-}C_{10}H_{16})(O_2CCCl_3)_2(OH_2)]$ **75**	5.77 (s, 2H), 4.29 (s, 2H)	4.56 (m, 2H)	3.11 (m, 2H) 2.50 (m, 2H)	2.23 (s, 6H)	7.13 (s, 2H, O*H*$_2$)
$[Ru(\eta^3:\eta^3\text{-}C_{10}H_{16})(O_2CCHCl_2)_2(OH_2)]$ **76**	5.67 (s, 2H), 4.29 (s, 2H)	4.52 (m, 2H)	3.09 (m, 2H) 2.48 (m, 2H)	2.17 (s, 6H)	7.52 (s, 2H, O*H*$_2$) 5.45 (s, 2H, C*H*Cl$_2$)
$[Ru(\eta^3:\eta^3\text{-}C_{10}H_{16})(O_2CCHF_2)_2(OH_2)]$ **77**	5.65 (s, 2H), 4.22 (s, 2H)	4.38 (m, 2H)	3.08 (m, 2H) 2.48 (m, 2H)	2.15 (s, 6H)	7.68 (s, br, 2H, O*H*$_2$) 5.34 (t, 2H, $^2J_{H\text{-}F}$ = 54.8, C*H*F$_2$)

[Ru(η^3:η^3-$C_{10}H_{16}$)Cl(O_2CCH_2Cl)] **78a** i) 20°C (average between **78a** and **78c**)	5.59 (s,1H), 4.74 (s, br, 1H) 4.70 (s, 1H), 3.69 (s, br, 1H)	4.31 (m, br, 1H) 3.71 (m, br, 1H)	2.58 (m, 4H)	2.30 (s, 3H) 2.15 (s, 3H)	3.80, 3.74 (AB, 2H, ^2J=14.3, CH_2Cl)
ii) -50°C	5.61 (s, 1H), 4.75 (s, 1H) 4.66 (s, 1H), 3.71 (s, 1H)	4.29 (m, 1H) 3.73 (m, 1H)	2.58 (m, 4H)	2.30 (s, 3H) 2.17 (s, 3H)	3.80, 3.74 (AB, 2H, ^2J=14.3, CH_2Cl)
[Ru(η^3:η^3-$C_{10}H_{16}$)(O_2CCH_2Cl)$_2$(OH_2)] **78b**	5.56 (s, 2H), 4.16 (s, 2H)	4.28 (m, br, 2H)	3.02 (m, br, 2H) 2.48 (m, br, 2H)	2.12 (s, 6H)	8.10 (s, br, 2H, OH_2) 3.64 (s, br, 2H, CH_2Cl)
[Ru(η^3:η^3-$C_{10}H_{16}$)Cl(O_2CCH_2Cl)(OH_2)] **78c** -50°C	5.46 (s, 1H), 5.34 (s, 1H) 4.87 (s, 1H), 4.10 (s, 1H)	4.98 (m, 1H) 4.32 (m, 1H)	2.92 (m, 4H)	2.39 (s, 3H) 2.06 (s, 3H)	6.39 (s, br, 2H, OH_2) 3.78 (s, 2H, CH_2Cl)
[Ru(η^3:η^3-$C_{10}H_{16}$)Cl(O_2CCH_2F)] **79a** i) 20°C (average between **79a** and **79c**)	5.56 (s, br, 1H), 4.89 (s, br, 1H) 4.75 (s, 1H), 3.86 (s, br, 1H)	4.46 (m, br, 1H) 3.86 (m, br, 1H)	2.50 (m, br, 4H)	2.32 (s, 3H) 2.13 (s, 3H)	4.58 (d, br, $^2J_{H\text{-}F}$=47.1, CH_2F)
ii) -50°C	5.63 (s, 1H), 4.83 (s, 1H) 4.69 (s, 1H), 3.80 (s, 1H)	4.42 (m, 1H) 3.79 (m, 1H)	2.50 (m, 4H)	2.30 (s, 3H) 2.17 (s, 3H)	4.61, 4.55 (dAB, $^2J_{H\text{-}H}$ = 8.2, $^2J_{H\text{-}F}$ = 47.1, CH_2F)
[Ru(η^3:η^3-$C_{10}H_{16}$)(O_2CCH_2F)$_2$(OH_2)] **79b**	5.58 (s, 2H), 4.21 (s, 2H)	4.37 (m, 2H)	3.01 (m, 2H) 2.50 (m, 2H)	2.10 (s, 6H)	8.18 (s, br, 2H, OH_2), 4.32 (d, 2H, $^2J_{H\text{-}F}$=48.3, CH_2F)
[Ru(η^3:η^3-$C_{10}H_{16}$)Cl(O_2CCH_2F)(OH_2)] **79c** -50°C	5.47 (s, 1H), 5.37 (s, 1H) 4.79 (s, 1H), 4.13 (s, 1H)	5.00 (m, 1H) 4.59 (m, 1H)	2.90 (m, 4H)	2.41 (s, 3H) 2.05 (s, 3H)	6.52 (s, br, 2H, OH_2), 4.30 (m, br, 2H, CH_2F)

$[Ru(\eta^3:\eta^3\text{-}C_{10}H_{16})Cl\{CF_3C(O)CHC(O)CF_3\}]$ **80**	6.08 (s, 1H), 4.92 (s, 1H) 4.89 (s, 1H), 3.50 (s, 1H)	5.19 (m, 1H) 4.44 (m, 1H)	3.04 (m, 2H) 2.43 (m, 2H)	2.45 (s, 3H) 1.99 (s, 3H)	4.96 (s, 1H, $CF_3COCHCOCF_3$)[b]
$[Ru(\eta^3:\eta^2:\eta^3\text{-}C_{12}H_{18})Cl(H_2O)]$ **83**	5.30 (m, 1H), 5.15 (dd, 1H, ^2J=2.0, ^3J=8.0), 3.87 (d, 1H, ^3J=12.0), 3.39 (d, 1H, ^3J=12.0)	5.93 (dd, ^3J=13.0 & 4.5, -*H*C=CH-) 5.78 (d, ^3J=13.0, -HC=C*H*-) 5.68 (m, 1H) 5.26 (m, 2H) 4.40 (m, 1H)	3.19 (m, 2H) 3.16 (m, 1H) 2.82 (m, 1H) 2.63 (m, 2H) 2.45 (m, 2H)	-	2.21 (s, 2H, OH_2)
$[Ru(\eta^3:\eta^2:\eta^3\text{-}C_{12}H_{18})Cl_2]$ **39**[c]	4.89 (d, 2H, ^3J=7.7) 3.76 (d, 2H, ^3J=11.8)	5.50 (t, 2H, ^3J=1.5,-*H*C=C*H*-) 5.56 (m, 2H) 5.01 (m, 2H)	3.26 (m, 2H) 3.07 (dd, 2H, ^2J=16.0, ^3J=6.1) 2.35 (m, 4H)	-	-
$[Ru(\eta^3:\eta^3\text{-}C_{10}H_{16})Cl_2\{SC(OH)Me\}]$ **84**	4.76 (s, 2H), 4.00 (s, 2H)[d]	5.08 (m, 2H)	3.26 (m, 2H) 2.57 (m, 2H)	2.30 (s, 6H)	13.99 (s, 1H, O*H*), 2.69 (s, 3H, CH_3)
S-equatorial-$[Ru(\eta^3:\eta^3\text{-}C_{10}H_{16})Cl(OSCMe)]$ **85a**	5.28 (s, 1H), 4.24 (s, 1H) 4.06 (s, 1H), 2.61 (s, 1H)	4.31 (m, 1H) 3.30 (m, 1H)	2.83 (m, 4H)	2.32 (s, 3H) 2.07 (s, 3H)	1.66 (s, 3H, CH_3)
S-axial-$[Ru(\eta^3:\eta^3\text{-}C_{10}H_{16})Cl(OSCMe)]$ **85b**	5.28 (s, 1H), 4.68 (s, 1H) 4.36 (s, 1H), 3.52 (s, 1H)	4.41 (m, 1H) 3.67 (m, 1H)	2.65 (m, 4H)	2.21 (s, 3H) 2.13 (s, 3H)	1.68 (s, 3H, CH_3)

S-equatorial-[Ru(η^3:η^3-$C_{10}H_{16}$)Cl(OSCBu^t)] **86a**	5.27 (s, 1H), 4.05 (s, 1H) 4.04 (s, 1H), 2.36 (s, 1H)	4.32 (m, 1H) 3.27 (m, 1H)	2.88 (m, 4H)	2.36 (s, 3H) 2.09 (s, 3H)	1.05 (s, 9H, C(CH_3)$_3$)
S-axial-[Ru(η^3:η^3-$C_{10}H_{16}$)Cl(OSCBu^t)] **86b**	5.21 (s, 1H), 4.66 (s, 1H) 4.18 (s, 1H), 3.20 (s, 1H)	4.43 (m, 1H) 3.63 (m, 1H)	2.69 (m, 4H)	2.44 (s, 3H) 2.19 (s, 3H)	1.14 (s, 9H, C(CH_3)$_3$)
S-equatorial-[Ru(η^3:η^3-$C_{10}H_{16}$)Cl(OSCPh)] **87a**	5.33 (s, 1H), 4.28 (s, 1H) 4.11 (s, 1H), 2.69 (s, 1H)	4.30 (m, 1H) 3.50 (m, 1H)	2.93 (m, 4H)	2.39 (s, 3H) 2.17 (s, 3H)	7.84 (dd, 2H, ^3J=8.4, ^4J=1.2, *o*-C$_6H_5$), 7.54 (dt, 1H, ^3J=7.5, ^4J=1.2, *p*-C$_6H_5$), 7.37 (t, 2H, ^3J=7.9, *m*-C$_6H_5$)
S-axial-[Ru(η^3:η^3-$C_{10}H_{16}$)Cl(OSCPh)] **87b**	5.33 (s, 1H), 4.69 (s, 1H) 4.38 (s, 1H), 3.45 (s, 1H)	4.51 (m, 1H) 3.79 (m, 1H)	2.44 (m, 4H)	2.48 (s, 3H) 2.26 (s, 3H)	7.96 (dd, 2H, ^3J=7.8, ^4J=0.6, *o*-C$_6H_5$), 7.55 (dt, 1H, ^3J=7.6, ^4J=1.3, *p*-C$_6H_5$), 7.42 (t, 2H, ^3J=7.5, *m*-C$_6H_5$)
[Ru(η^3:η^3-$C_{10}H_{16}$)Cl(NO_3)] **88**	5.59 (s, 1H), 4.84 (s, 1H) 4.62 (s, 1H), 3.70 (s, 1H)	4.41 (m, 1H) 3.84 (m, 1H)	2.66 (m, 3H) 2.51 (m, 1H)	2.33 (s, 3H) 2.18 (s, 3H)	-
[Ru(η^3:η^3-$C_{10}H_{16}$)(NO_3)$_2$] **89**	5.68 (s, 2H), 4.21 (s, 2H)	4.42 (t, 2H, $^3J_{H\text{-}H}$=7.2)	2.94 (m, 2H) 2.55 (m, 2H)	2.27 (s, 6H)	-

$[Ru(\eta^3:\eta^3\text{-}C_{10}H_{16})(ONO_2)_2(CO)]$ **90**	5.51 (s, 2H), 3.14 (s, 2H)	4.83 (m, 2H)	3.82 (m, 2H) 3.07 (m, 2H)	1.98 (s, 6H)	-
$[Ru(\eta^3:\eta^3\text{-}C_{10}H_{16})(ONO_2)_2(NC_5H_5)]$ **91**	5.88 (s, 2H), 4.17 (s, 2H)	4.81 (m, 2H)	3.41 (m, 2H) 2.69 (m, 2H)	2.20 (s, 6H)	8.18 (d, 2H, ^3J=6.6), 7.86 (t, 1H, ^3J=6.1), 7.39 (t, 2H, ^3J=6.2)

a) Solvent $CDCl_3$, δ / ppm, $J_{H\text{-}H}$ / Hz, 400 MHz, 20°C, s = singlet, d = doublet, dd = doublet of doublets, t = triplet, dt = doublet of triplets, AB = AB pattern, dAB = doublet of AB patterns, m = multiplet, br = broad; b) unambiguous assignment of this resonance is not possible since it occurs at a very similar chemical shift to two other 1H singlet signals arising from the *bis*(allyl) ligand; c) first synthesised by Nicholson and Shaw[105-107]; d) signals noticeably broader than the corresponding resonances for the other half of the *bis*(allyl) ligand.

Table 3.2: Selected Infrared Data for New Complexes.[a]

Compound	ν_{asymm}(OCO)	ν_{symm}(OCO)	$\Delta\nu$	$\nu(OH_2)$	ν(RuCl)	Other
$[Ru(\eta^3:\eta^3\text{-}C_{10}H_{16})Cl(O_2CMe)]$ **72**	1517s	1461s	56	-	273m	-
$[Ru(\eta^3:\eta^3\text{-}C_{10}H_{16})(O_2CCF_3)_2(OH_2)]$ **73**	1703vs, 1670vs	1421m	249-282	3362s,br	-	1196s, 1143s ν(CF)
$[Ru(\eta^3:\eta^3\text{-}C_{10}H_{16})(O_2CCCl_3)_2(OH_2)]$ **75**	1702vs, 1680vs	1323s	379-357	3390s,br	-	844s, 831s ν(CCl)
$[Ru(\eta^3:\eta^3\text{-}C_{10}H_{16})(O_2CCHCl_2)_2(OH_2)]$ **76**	1671s, 1629s	1359s, 1341s	270-330	3372s	-	814s, 787s ν(CCl)
$[Ru(\eta^3:\eta^3\text{-}C_{10}H_{16})(O_2CCHF_2)_2(OH_2)]$ **77**	1660s, 1625s	1436	189-224	3317s	-	1117s, 1064s ν(CF)
$[Ru(\eta^3:\eta^3\text{-}C_{10}H_{16})Cl(O_2CCH_2Cl)]$ **78a**	1526s, 1519s	1452s, 1441s	67-85	-	b	790m ν(CCl)
$[Ru(\eta^3:\eta^3\text{-}C_{10}H_{16})(O_2CCH_2Cl)_2(OH_2)]$ **78b**	1612s	1374s	238	3326s	-	784m ν(CCl)
$[Ru(\eta^3:\eta^3\text{-}C_{10}H_{16})Cl(O_2CCH_2F)]$ **79a**	1556s, 1536s	1466s, 1454s	70-102	-	b	1076s, 1066s ν(CF)
$[Ru(\eta^3:\eta^3\text{-}C_{10}H_{16})Cl(O_2CCH_2F)_2(OH_2)]$ **79b**	1617s	1419s	198	3328s	-	1085s ν(CF)
$[Ru(\eta^3:\eta^3\text{-}C_{10}H_{16})Cl\{F_3CC(O)CHC(O)CF_3\}]$ **80**	1655m, 1623s ν(CO)	-	-	-	317s	1258s,br, 1205s,br, 1143s,br ν(CF)

a) Wavenumber / cm^{-1}, spectra run in nujol mulls or as KBr disk. Abbreviations: s = strong, m = medium, w = weak, v = very, br = broad; b) impossible to unambiguously assign.

Table 3.3: ^{13}C-{^{1}H} NMR Data for Compounds $[Ru(\eta^3:\eta^2:\eta^3\text{-}C_{12}H_{18})ClX]^{n+}$ (X = Cl, n=0 **39**; X = OH_2, n=1 **83**).[a]

Compound	δ			
	C_1	$C_{2,3}$	$C_{4,5}$	C_6
$[Ru(\eta^3:\eta^2:\eta^3\text{-}C_{12}H_{18})Cl_2]$ **39**	65.8	111.5, 105.7	35.3, 23.7	121.7
$[Ru(\eta^3:\eta^2:\eta^3\text{-}C_{12}H_{18})Cl(OH_2)][BF_4]$ **83**[b]	66.4	109.0, 108.5,	37.0, 36.3	128.6
	63.3	113.2 118.2	24.6, 24.2	122.2

a) Solvent $CDCl_3$, δ / ppm, 100.6 MHz, 20°C; b) solvent CD_3CN.

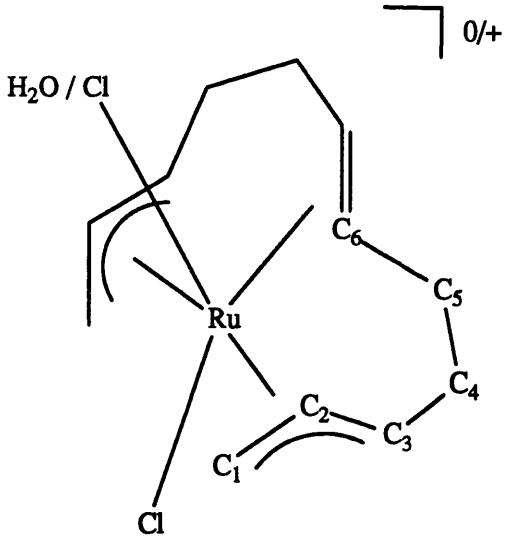

Table 3.4: Fractional atomic coordinates (x 10^4) and equivalent isotropic displacement factors ($Å^2$ x 10^3) for [Ru(η^3:η^3-$C_{10}H_{16}$)Cl(O_2CMe)] **72**

	x	y	z	U(eq)
Ru(1)	872(1)	1555(1)	1185(1)	34(1)
Cl(1)	-870(2)	1787(2)	630(2)	55(1)
O(1)	1494(5)	1150(5)	-168(4)	48(2)
O(2)	2468(5)	1226(4)	1051(4)	45(2)
C(1)	563(7)	-1(6)	1231(6)	48(3)
C(2)	278(7)	389(6)	2076(6)	42(3)
C(3)	1106(7)	884(6)	2506(6)	41(3)
C(4)	962(8)	1473(7)	3374(6)	53(3)
C(5)	315(9)	2375(8)	3184(7)	61(4)
C(6)	411(7)	2646(6)	2175(6)	42(3)
C(7)	1358(8)	2936(6)	1752(7)	44(3)
C(8)	1283(8)	3016(7)	798(7)	53(3)
C(9)	-832(8)	383(7)	2417(7)	58(3)
C(10)	2392(8)	3025(8)	2240(7)	66(4)
C(11)	2376(8)	1045(6)	192(6)	41(3)
C(12)	3283(7)	682(8)	-350(8)	65(4)

Table 3.5: Bond lengths (Å) and angles (°) for [Ru(η^3:η^3-$C_{10}H_{16}$)Cl(O_2CMe)] **72**

Ru(1)-Cl(1)	2.385 (3)	Ru(1)-O(1)	2.205 (6)
Ru(1)-O(2)	2.095 (6)	Ru(1)-C(1)	2.227 (8)
Ru(1)-C(2)	2.227 (9)	Ru(1)-C(3)	2.169 (9)
Ru(1)-C(6)	2.191 (9)	Ru(1)-C(7)	2.203 (9)
Ru(1)-C(8)	2.197 (10)	Ru(1)-C(11)	2.509 (9)
O(1)-C(11)	1.249 (11)	O(2)-C(11)	1.287 (10)
C(1)-C(2)	1.399 (13)	C(2)-C(3)	1.412 (13)
C(2)-C(9)	1.499 (13)	C(3)-C(4)	1.527 (12)
C(4)-C(5)	1.540 (15)	C(5)-C(6)	1.527 (13)
C(6)-C(7)	1.417 (13)	C(7)-C(8)	1.402 (14)
C(7)-C(10)	1.504 (14)	C(11)-C(12)	1.491 (14)

Cl(1)-Ru(1)-O(1)	93.7(2)	Cl(1)-Ru(1)-O(2)	154.4(2)
O(1)-Ru(1)-O(2)	60.7(2)	Cl(1)-Ru(1)-C(1)	88.9(2)
O(1)-Ru(1)-C(1)	80.6(3)	O(2)-Ru(1)-C(1)	87.6(3)
Cl(1)-Ru(1)-C(2)	89.1(2)	O(1)-Ru(1)-C(2)	117.1(3)
O(2)-Ru(1)-C(2)	102.8(3)	C(1)-Ru(1)-C(2)	36.6(3)
Cl(1)-Ru(1)-C(3)	119.4(3)	O(1)-Ru(1)-C(3)	129.5(3)
O(2)-Ru(1)-C(3)	81.6(3)	C(1)-Ru(1)-C(3)	64.5(3)
C(2)-Ru(1)-C(3)	37.4(3)	Cl(1)-Ru(1)-C(6)	83.0(3)
O(1)-Ru(1)-C(6)	150.5(3)	O(2)-Ru(1)-C(6)	118.5(3)
C(1)-Ru(1)-C(6)	128.5(3)	C(2)-Ru(1)-C(6)	92.3(3)
C(3)-Ru(1)-C(6)	75.8(3)	Cl(1)-Ru(1)-C(7)	105.5(3)
O(1)-Ru(1)-C(7)	117.7(3)	O(2)-Ru(1)-C(7)	87.5(3)
C(1)-Ru(1)-C(7)	155.1(4)	C(2)-Ru(1)-C(7)	121.8(3)
C(3)-Ru(1)-C(7)	90.7(3)	C(6)-Ru(1)-C(7)	37.6(3)
Cl(1)-Ru(1)-C(8)	90.3(3)	O(1)-Ru(1)-C(8)	85.7(3)
O(2)-Ru(1)-C(8)	87.2(3)	C(1)-Ru(1)-C(8)	166.2(4)
C(2)-Ru(1)-C(8)	157.2(4)	C(3)-Ru(1)-C(8)	127.2(4)
C(6)-Ru(1)-C(8)	65.0(4)	C(7)-Ru(1)-C(8)	37.1(4)
Cl(1)-Ru(1)-C(11)	123.6(2)	O(1)-Ru(1)-C(11)	29.9(3)
O(2)-Ru(1)-C(11)	30.8(3)	C(1)-Ru(1)-C(11)	82.6(3)
C(2)-Ru(1)-C(11)	112.8(3)	C(3)-Ru(1)-C(11)	106.6(3)
C(6)-Ru(1)-C(11)	142.0(3)	C(7)-Ru(1)-C(11)	104.8(3)
C(8)-Ru(1)-C(11)	86.4(3)	Ru(1)-O(1)-C(11)	88.7(5)
Ru(1)-O(2)-C(11)	92.7(5)	Ru(1)-C(1)-C(2)	71.7(5)
Ru(1)-C(2)-C(1)	71.7(5)	Ru(1)-C(2)-C(3)	69.0(5)
C(1)-C(2)-C(3)	113.1(8)	Ru(1)-C(2)-C(9)	121.2(6)
C(1)-C(2)-C(9)	122.4(8)	C(3)-C(2)-C(9)	124.0(8)
Ru(1)-C(3)-C(2)	73.5(5)	Ru(1)-C(3)-C(4)	119.1(6)
C(2)-C(3)-C(4)	123.3(8)	C(3)-C(4)-C(5)	111.2(7)
C(4)-C(5)-C(6)	109.7(8)	Ru(1)-C(6)-C(5)	118.9(6)
Ru(1)-C(6)-C(7)	71.7(5)	C(5)-C(6)-C(7)	124.2(9)
Ru(1)-C(7)-C(6)	70.7(5)	Ru(1)-C(7)-C(8)	71.2(5)
C(6)-C(7)-C(8)	113.5(9)	Ru(1)-C(7)-C(10)	119.9(6)
C(6)-C(7)-C(10)	124.3(9)	C(8)-C(7)-C(10)	121.7(9)
Ru(1)-C(8)-C(7)	71.7(5)	Ru(1)-C(11)-O(1)	61.5(5)
Ru(1)-C(11)-O(2)	56.5(4)	O(1)-C(11)-O(2)	118.0(8)
Ru(1)-C(11)-C(12)	175.7(7)	O(1)-C(11)-C(12)	121.0(8)
O(2)-C(11)-C(12)	121.0(8)		

Table 3.6: Anisotropic displacement factors ($Å^2$ x 10^3) for [Ru(η^3:η^3-$C_{10}H_{16}$)Cl(O_2CMe)] **72**

	U_{11}	U_{22}	U_{33}	U_{23}	U_{13}	U_{12}
Ru(1)	35(1)	36(1)	29(1)	-1(1)	-4(1)	4(1)
Cl(1)	44(1)	64(2)	57(1)	-7(1)	-15(1)	8(1)
O(1)	51(4)	55(4)	37(4)	-8(3)	-4(3)	0(3)
O(2)	37(3)	62(4)	37(3)	-4(3)	-4(3)	12(3)
C(1)	58(6)	30(4)	57(6)	-3(5)	-3(5)	-1(4)
C(2)	50(5)	30(5)	46(6)	1(4)	2(5)	3(4)
C(3)	56(6)	32(4)	35(4)	7(4)	3(4)	7(4)
C(4)	74(6)	54(6)	30(4)	-2(4)	-6(5)	6(6)
C(5)	73(7)	68(7)	41(6)	-17(5)	-7(5)	11(6)
C(6)	52(5)	34(5)	38(5)	1(4)	-5(5)	20(4)
C(7)	50(6)	29(5)	52(6)	-4(4)	0(5)	6(4)
C(8)	55(6)	32(5)	72(7)	14(5)	11(5)	1(4)
C(9)	55(6)	59(6)	60(6)	-2(5)	21(6)	-10(6)
C(10)	58(7)	57(6)	81(8)	-26(6)	-23(6)	0(5)
C(11)	53(6)	28(5)	42(5)	1(4)	6(5)	-1(4)
C(12)	51(6)	77(8)	67(7)	-8(6)	19(6)	9(6)

Table 3.7: Fractional atomic coordinates (x 10^4) and equivalent isotropic displacement factors ($Å^2$ x 10^3) for [Ru(η^3:η^3-$C_{10}H_{16}$)(O_2CCF_3)$_2$(OH_2)] **73**

	x	y	z	U(eq)
Ru(1)	5000	6634(1)	2500	37(1)
O(1)	5000	5394(2)	2500	64(2)
O(2)	6282(3)	6578(2)	1373(3)	47(1)
O(3)	5630(4)	5654(3)	-281(5)	102(2)
C(1)	6375(4)	6081(3)	448(6)	60(2)
C(2)	7505(5)	6075(4)	70(8)	75(2)
C(3)	3488(4)	6436(3)	560(5)	51(1)
C(4)	3918(3)	7167(3)	388(4)	49(1)
C(5)	3996(3)	7676(2)	1587(4)	47(1)
C(6)	4586(5)	8456(3)	1728(6)	64(2)
C(7)	4383(4)	7351(3)	-924(5)	66(2)
F(1)	7778(17)	6749(7)	-321(32)	132(8)
F(2)	8283(15)	5875(20)	1143(22)	170(11)
F(3)	7538(15)	5640(15)	-1008(27)	145(9)
F(1A)	7424(17)	6353(22)	-1238(24)	182(11)
F(2A)	8337(13)	6396(16)	1007(25)	134(8)
F(3A)	7893(15)	5360(9)	-25(41)	172(12)

Table 3.8: Bond lengths (Å) and angles (°) for $[Ru(\eta^3:\eta^3\text{-}C_{10}H_{16})(O_2CCF_3)_2(OH_2)]$ **73**

Ru(1)-O(1)	2.146 (4)	Ru(1)-O(2)	2.100 (3)
Ru(1)-C(3)	2.245 (4)	Ru(1)-C(4)	2.260 (4)
Ru(1)-C(5)	2.221 (4)	Ru(1)-O(2A)	2.100 (3)
Ru(1)-C(3A)	2.245 (4)	Ru(1)-C(4A)	2.260 (4)
Ru(1)-C(5A)	2.221 (4)	O(2)-C(1)	1.244 (6)
O(3)-C(1)	1.229 (6)	C(1)-C(2)	1.509 (9)
C(2)-F(1)	1.292 (18)	C(2)-F(2)	1.234 (20)
C(2)-F(3)	1.264 (27)	C(2)-F(1A)	1.290 (26)
C(2)-F(2A)	1.279 (19)	C(2)-F(3A)	1.337 (19)
C(3)-C(4)	1.395 (7)	C(4)-C(5)	1.406 (6)
C(4)-C(7)	1.509 (7)	C(5)-C(6)	1.521 (6)
C(6)-C(6A)	1.526 (10)		

O(1)-Ru(1)-O(2)	87.4(1)	O(1)-Ru(1)-C(3)	81.2(1)
O(2)-Ru(1)-C(3)	98.8(1)	O(1)-Ru(1)-C(4)	114.1(1)
O(2)-Ru(1)-C(4)	85.7(1)	C(3)-Ru(1)-C(4)	36.1(2)
O(1)-Ru(1)-C(5)	144.3(1)	O(2)-Ru(1)-C(5)	104.7(1)
C(3)-Ru(1)-C(5)	64.0(2)	C(4)-Ru(1)-C(5)	36.6(2)
O(1)-Ru(1)-O(2A)	87.4(1)	O(2)-Ru(1)-O(2A)	174.8(1)
C(3)-Ru(1)-O(2A)	80.4(1)	C(4)-Ru(1)-O(2A)	96.5(1)
C(5)-Ru(1)-O(2A)	79.7(1)	O(1)-Ru(1)-C(3A)	81.2(1)
O(2)-Ru(1)-C(3A)	80.4(1)	C(3)-Ru(1)-C(3A)	162.5(2)
C(4)-Ru(1)-C(3A)	158.9(2)	C(5)-Ru(1)-C(3A)	133.4(2)
O(2A)-Ru(1)-C(3A)	98.8(1)	O(1)-Ru(1)-C(4A)	114.1(1)
O(2)-Ru(1)-C(4A)	96.5(1)	C(3)-Ru(1)-C(4A)	158.9(2)
C(4)-Ru(1)-C(4A)	131.8(2)	C(5)-Ru(1)-C(4A)	98.0(1)
O(2A)-Ru(1)-C(4A)	85.7(1)	C(3A)-Ru(1)-C(4A)	36.1(2)
O(1)-Ru(1)-C(5A)	144.3(1)	O(2)-Ru(1)-C(5A)	79.7(1)
C(3)-Ru(1)-C(5A)	133.4(2)	C(4)-Ru(1)-C(5A)	98.0(1)
C(5)-Ru(1)-C(5A)	71.4(2)	O(2A)-Ru(1)-C(5A)	104.7(1)
C(3A)-Ru(1)-C(5A)	64.0(2)	C(4A)-Ru(1)-C(5A)	36.6(2)
Ru(1)-O(2)-C(1)	126.3(3)	O(2)-C(1)-O(3)	127.7(5)
O(2)-C(1)-C(2)	114.8(4)	O(3)-C(1)-C(2)	117.0(5)
C(1)-C(2)-F(1)	112.2(11)	C(1)-C(2)-F(2)	111.6(12)
F(1)-C(2)-F(2)	106.4(18)	C(1)-C(2)-F(3)	114.2(10)
F(1)-C(2)-F(3)	104.5(18)	F(2)-C(2)-F(3)	107.4(17)
C(1)-C(2)-F(1A)	111.6(10)	C(1)-C(2)-F(2A)	116.6(11)
F(1A)-C(2)-F(2A)	109.5(17)	C(1)-C(2)-F(3A)	112.4(11)
F(1A)-C(2)-F(3A)	103.0(23)	F(2A)-C(2)-F(3A)	102.5(15)
Ru(1)-C(3)-C(4)	72.6(2)	Ru(1)-C(4)-C(3)	71.4(2)
Ru(1)-C(4)-C(5)	70.2(2)	C(3)-C(4)-C(5)	115.2(4)
Ru(1)-C(4)-C(7)	122.3(3)	C(3)-C(4)-C(7)	121.1(4)
C(5)-C(4)-C(7)	123.3(4)	Ru(1)-C(5)-C(4)	73.2(2)
Ru(1)-C(5)-C(6)	119.2(3)	C(4)-C(5)-C(6)	123.9(4)
C(5)-C(6)-C(6A)	105.2(3)		

Table 3.9: Anisotropic displacement factors ($Å^2$ x 10^3) for $[Ru(\eta^3:\eta^3\text{-}C_{10}H_{16})(O_2CCF_3)_2(OH_2)]$ **73**

	U_{11}	U_{22}	U_{33}	U_{23}	U_{13}	U_{12}
Ru(1)	36(1)	44(1)	28(1)	0	6(1)	0
O(1)	104(4)	43(2)	43(2)	0	13(2)	0
O(2)	48(2)	54(2)	43(2)	-6(1)	17(1)	-4(1)
O(3)	110(3)	113(3)	98(3)	-56(3)	55(3)	-39(3)
C(1)	61(3)	64(3)	61(3)	-18(2)	28(2)	-18(2)
C(2)	68(4)	84(4)	81(4)	-17(3)	34(3)	1(3)
C(3)	41(2)	69(3)	36(2)	1(2)	-2(2)	-4(2)
C(4)	42(2)	64(3)	37(2)	13(2)	0(2)	3(2)
C(5)	37(2)	54(2)	48(2)	10(2)	6(2)	7(2)
C(6)	63(3)	52(3)	76(3)	10(2)	16(3)	4(2)
C(7)	67(3)	86(3)	43(2)	21(2)	14(2)	5(3)
F(1)	135(12)	119(8)	182(16)	-4(10)	115(13)	-36(7)
F(2)	85(10)	243(24)	175(16)	16(18)	21(10)	57(13)
F(3)	117(12)	188(19)	166(15)	-109(13)	101(12)	-29(11)
F(1A)	175(15)	291(25)	107(11)	91(14)	85(12)	46(20)
F(2A)	70(7)	194(16)	160(16)	-108(15)	67(9)	-62(10)
F(3A)	100(9)	95(8)	324(29)	-54(14)	60(15)	23(7)

Table 3.10: Fractional atomic coordinates (x 10^4) and equivalent isotropic displacement factors ($Å^2$ x 10^3) for $[Ru(\eta^3:\eta^2:\eta^3\text{-}C_{12}H_{18})Cl(OH_2)][BF_4]$ **83**

	x	y	z	U(eq)
Ru(1)	8701(1)	-2489(1)	9842(1)	33(1)
Cl(1)	11540(2)	-1614(1)	10089(1)	69(1)
O(1)	6239(6)	-3303(3)	9909(3)	60(2)
C(1)	10236(9)	-3600(4)	10725(4)	65(2)
C(2)	10698(9)	-3652(4)	9832(5)	66(2)
C(3)	9329(8)	-3822(4)	9072(4)	59(2)
C(4)	9574(9)	-3634(5)	8060(5)	74(3)
C(5)	9952(9)	-2611(5)	7921(5)	72(3)
C(6)	8652(7)	-1971(4)	8324(4)	51(2)
C(7)	6913(7)	-2233(4)	8385(3)	45(2)
C(8)	5415(8)	-1536(4)	8523(4)	63(2)
C(9)	6206(9)	-667(4)	9071(4)	64(2)
C(11)	7126(8)	-1539(4)	10609(4)	53(2)
C(10)	7554(8)	-971(4)	9941(4)	56(2)
C(12)	8493(8)	-2000(4)	11267(4)	56(2)
B(1)	5641(10)	-4924(5)	11838(6)	59(3)
F(1)	4008(17)	-4592(8)	11538(20)	163(9)
F(2)	5792(25)	-5877(7)	11613(12)	77(4)
F(3)	6378(34)	-4920(10)	12749(8)	143(11)
F(4)	6821(27)	-4390(12)	11506(12)	150(8)
F(1A)	4260(24)	-5033(8)	12288(13)	117(6)
F(2A)	5917(28)	-5708(15)	11394(17)	170(10)
F(3A)	7083(22)	-4586(13)	12306(27)	220(15)
F(4A)	5022(39)	-4313(19)	11167(17)	254(14)

Table 3.11: Bond lengths (Å) and angles (°) for $[Ru(\eta^3:\eta^2:\eta^3\text{-}C_{12}H_{18})Cl(OH_2)][BF_4]$ **83**

Ru(1)-Cl(1)	2.396 (2)	Ru(1)-O(1)	2.165 (5)
Ru(1)-C(1)	2.196 (6)	Ru(1)-C(2)	2.207 (6)
Ru(1)-C(3)	2.282 (6)	Ru(1)-C(6)	2.314 (5)
Ru(1)-C(7)	2.291 (5)	Ru(1)-C(11)	2.210 (6)
Ru(1)-C(10)	2.320 (5)	Ru(1)-C(12)	2.214 (6)
O(1)-H(1)	0.833 (72)	O(1)-H(2)	0.719 (74)
C(1)-C(2)	1.404 (10)	C(2)-C(3)	1.363 (8)
C(3)-C(4)	1.538 (9)	C(4)-C(5)	1.494 (9)
C(5)-C(6)	1.514 (9)	C(6)-C(7)	1.353 (8)
C(7)-C(8)	1.521 (8)	C(8)-C(9)	1.516 (8)
C(9)-C(10)	1.509 (8)	C(10)-C(11)	1.342 (8)
C(11)-C(12)	1.405 (7)	B(1)-F(1)	1.286 (14)
B(1)-F(2)	1.396 (13)	B(1)-F(3)	1.328 (14)
B(1)-F(4)	1.311 (21)	B(1)-F(1A)	1.320 (21)
B(1)-F(2A)	1.317 (24)	B(1)-F(3A)	1.239 (21)
B(1)-F(4A)	1.314 (26)		

Cl(1)-Ru(1)-O(1)	169.0(1)	Cl(1)-Ru(1)-C(1)	86.9(2)
O(1)-Ru(1)-C(1)	86.3(2)	Cl(1)-Ru(1)-C(2)	79.7(2)
O(1)-Ru(1)-C(2)	99.8(2)	C(1)-Ru(1)-C(2)	37.2(3)
Cl(1)-Ru(1)-C(3)	104.2(2)	O(1)-Ru(1)-C(3)	80.5(2)
C(1)-Ru(1)-C(3)	64.2(2)	C(2)-Ru(1)-C(3)	35.3(2)
Cl(1)-Ru(1)-C(6)	80.2(1)	O(1)-Ru(1)-C(6)	110.6(2)
C(1)-Ru(1)-C(6)	133.8(2)	C(2)-Ru(1)-C(6)	96.7(2)
C(3)-Ru(1)-C(6)	76.3(2)	Cl(1)-Ru(1)-C(7)	112.6(1)
O(1)-Ru(1)-C(7)	77.8(2)	C(1)-Ru(1)-C(7)	142.1(2)
C(2)-Ru(1)-C(7)	112.1(2)	C(3)-Ru(1)-C(7)	79.3(2)
C(6)-Ru(1)-C(7)	34.2(2)	Cl(1)-Ru(1)-C(11)	98.0(2)
O(1)-Ru(1)-C(11)	76.9(2)	C(1)-Ru(1)-C(11)	113.7(2)
C(2)-Ru(1)-C(11)	150.5(2)	C(3)-Ru(1)-C(11)	157.4(2)
C(6)-Ru(1)-C(11)	112.0(2)	C(7)-Ru(1)-C(11)	96.0(2)
Cl(1)-Ru(1)-C(10)	80.3(2)	O(1)-Ru(1)-C(10)	99.8(2)
C(1)-Ru(1)-C(10)	141.0(2)	C(2)-Ru(1)-C(10)	160.0(2)
C(3)-Ru(1)-C(10)	154.7(2)	C(6)-Ru(1)-C(10)	80.1(2)
C(7)-Ru(1)-C(10)	76.1(2)	C(11)-Ru(1)-C(10)	34.3(2)
Cl(1)-Ru(1)-C(12)	85.2(2)	O(1)-Ru(1)-C(12)	85.0(2)
C(1)-Ru(1)-C(12)	78.4(2)	C(2)-Ru(1)-C(12)	113.9(2)
C(3)-Ru(1)-C(12)	140.5(2)	C(6)-Ru(1)-C(12)	143.0(2)
C(7)-Ru(1)-C(12)	132.9(2)	C(11)-Ru(1)-C(12)	37.0(2)
C(10)-Ru(1)-C(12)	64.0(2)	Ru(1)-O(1)-H(1)	124.7(42)
Ru(1)-O(1)-H(2)	115.5(61)	H(1)-O(1)-H(2)	109.7(74)
Ru(1)-C(1)-C(2)	71.8(3)	Ru(1)-C(2)-C(1)	71.0(4)
Ru(1)-C(2)-C(3)	75.4(4)	C(1)-C(2)-C(3)	118.8(6)
Ru(1)-C(3)-C(2)	69.4(4)	Ru(1)-C(3)-C(4)	113.4(4)
C(2)-C(3)-C(4)	122.4(6)	C(3)-C(4)-C(5)	110.8(5)
C(4)-C(5)-C(6)	112.2(6)	Ru(1)-C(6)-C(5)	106.6(4)
Ru(1)-C(6)-C(7)	72.0(3)	C(5)-C(6)-C(7)	122.7(5)
Ru(1)-C(7)-C(6)	73.8(3)	Ru(1)-C(7)-C(8)	106.4(3)

C(6)-C(7)-C(8)	123.5(5)	C(7)-C(8)-C(9)	112.3(5)
C(8)-C(9)-C(10)	109.3(4)	Ru(1)-C(11)-C(10)	77.3(4)
Ru(1)-C(11)-C(12)	71.6(3)	C(10)-C(11)-C(12)	122.0(6)
Ru(1)-C(10)-C(9)	113.6(4)	Ru(1)-C(10)-C(11)	68.3(3)
C(9)-C(10)-C(11)	124.4(6)	Ru(1)-C(12)-C(11)	71.3(3)
F(1)-B(1)-F(2)	112.6(11)	F(1)-B(1)-F(3)	120.7(17)
F(2)-B(1)-F(3)	101.6(10)	F(1)-B(1)-F(4)	108.0(13)
F(2)-B(1)-F(4)	112.4(13)	F(3)-B(1)-F(4)	101.1(13)
F(1A)-B(1)-F(2A)	110.5(12)	F(1A)-B(1)-F(3A)	115.8(20)
F(2A)-B(1)-F(3A)	113.3(15)	F(1A)-B(1)-F(4A)	104.7(15)
F(2A)-B(1)-F(4A)	104.8(16)	F(3A)-B(1)-F(4A)	106.8(18)

Table 3.12: Anisotropic displacement factors ($Å^2 \times 10^3$) for $[Ru(\eta^3:\eta^2:\eta^3\text{-}C_{12}H_{18})Cl(OH_2)][BF_4]$ **83**

	U_{11}	U_{22}	U_{33}	U_{23}	U_{13}	U_{12}
Ru(1)	30(1)	32(1)	35(1)	-1(1)	3(1)	0(1)
Cl(1)	39(1)	75(1)	88(1)	-11(1)	4(1)	-20(1)
O(1)	63(3)	61(3)	58(3)	1(2)	18(2)	-24(2)
C(1)	76(4)	55(3)	59(4)	8(3)	1(3)	24(3)
C(2)	52(3)	55(4)	83(4)	-10(3)	-4(3)	28(3)
C(3)	56(3)	42(3)	75(4)	-12(3)	4(3)	14(3)
C(4)	70(4)	86(5)	67(4)	-29(4)	16(3)	28(4)
C(5)	58(4)	103(6)	60(4)	-11(4)	27(3)	2(3)
C(6)	60(3)	59(4)	38(3)	9(3)	17(3)	0(3)
C(7)	52(3)	49(3)	31(2)	1(2)	-1(2)	2(2)
C(8)	53(3)	79(4)	50(3)	1(3)	-3(3)	26(3)
C(9)	86(4)	44(3)	58(4)	3(3)	6(3)	26(3)
C(11)	59(3)	56(3)	46(3)	-17(3)	12(3)	12(3)
C(10)	72(4)	37(3)	60(4)	-14(3)	12(3)	9(3)
C(12)	68(4)	59(3)	39(3)	-6(3)	9(3)	4(3)
B(1)	53(4)	60(4)	66(5)	2(4)	15(4)	-1(3)
F(1)	58(6)	80(8)	319(25)	0(11)	-37(10)	8(6)
F(2)	94(9)	31(4)	90(7)	2(5)	-15(6)	-19(5)
F(3)	284(29)	73(8)	61(6)	6(5)	8(10)	-19(11)
F(4)	123(12)	168(13)	151(12)	88(11)	7(10)	-73(11)
F(1A)	137(11)	81(7)	160(12)	-27(7)	93(11)	-26(7)
F(2A)	69(9)	250(22)	182(18)	-150(16)	-1(10)	24(13)
F(3A)	97(10)	102(15)	406(39)	-107(19)	-92(21)	-29(9)
F(4A)	190(20)	330(26)	271(22)	249(21)	113(19)	103(19)

Table 3.13: Fractional atomic coordinates (x 10^4) and equivalent isotropic displacement factors ($Å^2$ x 10^3) for [Ru(η^3:η^3-$C_{10}H_{16}$)Cl(NO_3)] **88**

	x	y	z	U(eq)
Ru(1)	2272(1)	897(1)	3658(1)	30(1)
Cl(1)	458(1)	231(1)	3469(1)	56(1)
O(1)	4012(3)	808(3)	3841(3)	48(1)
O(2)	3109(4)	-551(3)	3863(3)	51(1)
O(3)	4932(4)	-562(4)	4029(3)	78(2)
N(1)	4061(4)	-137(4)	3915(3)	48(2)
C(1)	2556(5)	654(4)	2241(3)	47(2)
C(2)	2597(5)	1650(4)	2401(3)	40(2)
C(3)	1627(5)	2044(4)	2780(4)	46(2)
C(4)	1566(6)	3082(4)	3137(4)	58(2)
C(5)	2265(6)	3225(5)	3930(4)	60(2)
C(6)	2474(5)	2243(4)	4400(4)	51(2)
C(7)	1632(5)	1687(4)	4821(3)	45(2)
C(8)	2003(5)	775(4)	5094(4)	46(2)
C(9)	3676(5)	2212(4)	2286(4)	58(2)
C(10)	436(6)	2009(5)	4905(4)	65(2)

Table 3.14: Bond lengths (Å) and angles (°) for [Ru(η^3:η^3-$C_{10}H_{16}$)Cl(NO_3)] **88**

Ru(1)-Cl(1)	2.372 (2)	Ru(1)-O(1)	2.104 (4)
Ru(1)-O(2)	2.237 (4)	Ru(1)-C(1)	2.221 (5)
Ru(1)-C(2)	2.216 (5)	Ru(1)-C(3)	2.204 (5)
Ru(1)-C(6)	2.174 (6)	Ru(1)-C(7)	2.218 (5)
Ru(1)-C(8)	2.228 (6)	O(1)-N(1)	1.297 (6)
O(2)-N(1)	1.274 (7)	O(3)-N(1)	1.206 (7)
C(1)-C(2)	1.382 (8)	C(2)-C(3)	1.405 (8)
C(2)-C(9)	1.512 (8)	C(3)-C(4)	1.520 (8)
C(4)-C(5)	1.487 (10)	C(5)-C(6)	1.541 (9)
C(6)-C(7)	1.417 (8)	C(7)-C(8)	1.386 (8)
C(7)-C(10)	1.503 (9)		

Cl(1)-Ru(1)-O(1)	154.2(1)	Cl(1)-Ru(1)-O(2)	95.1(1)
O(1)-Ru(1)-O(2)	59.2(2)	Cl(1)-Ru(1)-C(1)	87.9(2)
O(1)-Ru(1)-C(1)	88.3(2)	O(2)-Ru(1)-C(1)	86.4(2)
Cl(1)-Ru(1)-C(2)	103.4(2)	O(1)-Ru(1)-C(2)	88.2(2)
O(2)-Ru(1)-C(2)	116.9(2)	C(1)-Ru(1)-C(2)	36.3(2)
Cl(1)-Ru(1)-C(3)	82.9(2)	O(1)-Ru(1)-C(3)	117.9(2)
O(2)-Ru(1)-C(3)	150.4(2)	C(1)-Ru(1)-C(3)	64.1(2)
C(2)-Ru(1)-C(3)	37.1(2)	Cl(1)-Ru(1)-C(6)	119.3(2)
O(1)-Ru(1)-C(6)	82.5(2)	O(2)-Ru(1)-C(6)	128.6(2)
C(1)-Ru(1)-C(6)	128.3(2)	C(2)-Ru(1)-C(6)	92.4(2)
C(3)-Ru(1)-C(6)	75.9(2)	Cl(1)-Ru(1)-C(7)	88.2(1)
O(1)-Ru(1)-C(7)	105.3(2)	O(2)-Ru(1)-C(7)	118.2(2)
C(1)-Ru(1)-C(7)	155.4(2)	C(2)-Ru(1)-C(7)	122.1(2)
C(3)-Ru(1)-C(7)	91.3(2)	C(6)-Ru(1)-C(7)	37.6(2)
Cl(1)-Ru(1)-C(8)	87.7(2)	O(1)-Ru(1)-C(8)	90.5(2)
O(2)-Ru(1)-C(8)	82.0(2)	C(1)-Ru(1)-C(8)	167.1(2)
C(2)-Ru(1)-C(8)	156.5(2)	C(3)-Ru(1)-C(8)	127.2(2)
C(6)-Ru(1)-C(8)	64.1(2)	C(7)-Ru(1)-C(8)	36.3(2)
Ru(1)-O(1)-N(1)	96.5(3)	Ru(1)-O(2)-N(1)	91.0(3)
O(1)-N(1)-O(2)	113.3(5)	O(1)-N(1)-O(3)	122.0(5)
O(2)-N(1)-O(3)	124.7(5)	Ru(1)-C(1)-C(2)	71.7(3)
Ru(1)-C(2)-C(1)	72.0(3)	Ru(1)-C(2)-C(3)	71.0(3)
C(1)-C(2)-C(3)	114.9(5)	Ru(1)-C(2)-C(9)	119.1(4)
C(1)-C(2)-C(9)	120.6(5)	C(3)-C(2)-C(9)	124.0(5)
Ru(1)-C(3)-C(2)	72.0(3)	Ru(1)-C(3)-C(4)	117.4(4)
C(2)-C(3)-C(4)	123.0(5)	C(3)-C(4)-C(5)	112.8(5)
C(4)-C(5)-C(6)	111.0(5)	Ru(1)-C(6)-C(5)	118.2(4)
Ru(1)-C(6)-C(7)	72.9(3)	C(5)-C(6)-C(7)	124.2(5)
Ru(1)-C(7)-C(6)	69.5(3)	Ru(1)-C(7)-C(8)	72.2(3)
C(6)-C(7)-C(8)	113.0(5)	Ru(1)-C(7)-C(10)	122.7(4)
C(6)-C(7)-C(10)	124.0(5)	C(8)-C(7)-C(10)	122.8(5)
Ru(1)-C(8)-C(7)	71.4(3)		

Table 3.15: Anisotropic displacement factors ($Å^2$ x 10^3) for $[Ru(\eta^3:\eta^3\text{-}C_{10}H_{16})Cl(NO_3)]$ **88**

	U_{11}	U_{22}	U_{33}	U_{23}	U_{13}	U_{12}
Ru(1)	32(1)	28(1)	29(1)	0(1)	2(1)	0(1)
Cl(1)	44(1)	65(1)	57(1)	-6(1)	3(1)	-19(1)
O(1)	40(2)	47(2)	56(3)	7(2)	4(2)	3(2)
O(2)	60(3)	35(2)	58(3)	8(2)	8(2)	6(2)
O(3)	62(3)	88(3)	84(4)	17(3)	-1(3)	41(3)
N(1)	49(3)	49(3)	47(3)	12(2)	4(2)	17(2)
C(1)	43(3)	46(3)	34(3)	0(2)	4(2)	1(2)
C(2)	49(3)	41(3)	31(3)	5(2)	2(2)	-2(2)
C(3)	48(3)	43(3)	46(3)	6(2)	-4(3)	0(3)
C(4)	69(4)	42(3)	65(4)	-1(3)	-4(3)	9(3)
C(5)	78(5)	36(3)	67(4)	-11(3)	3(4)	-3(3)
C(6)	45(3)	51(4)	56(4)	-20(3)	-3(3)	-2(3)
C(7)	44(3)	56(3)	36(3)	-11(3)	2(2)	-1(3)
C(8)	54(3)	51(3)	34(3)	1(2)	4(3)	-1(3)
C(9)	49(3)	61(4)	64(4)	19(3)	5(3)	-11(3)
C(10)	56(4)	82(5)	58(4)	-15(4)	9(3)	6(4)

Table 3.16: Fractional atomic coordinates (x 10^4) and equivalent isotropic displacement factors ($Å^2$ x 10^3) for $[Ru(\eta^3:\eta^3\text{-}C_{10}H_{16})(NO_3)_2]$ **89**

	x	y	z	U(eq)
Ru(1)	0	3674(1)	7500	32(1)
N(1)	-271(9)	2610(4)	5657(5)	55(2)
O(1)	-226(6)	3507(3)	5842(4)	51(2)
O(2)	-255(11)	2120(5)	6478(6)	108(3)
O(3)	-402(9)	2326(5)	4766(5)	95(3)
C(1)	2881(8)	3472(5)	7355(6)	52(2)
C(2)	2510(9)	4418(5)	7119(6)	49(2)
C(3)	1622(11)	4905(5)	7940(6)	59(3)
C(4)	827(16)	5870(6)	7851(8)	103(5)
C(5)	2803(12)	4825(6)	6033(6)	67(3)

Table 3.17: Bond lengths (Å) and angles (°) for $[Ru(\eta^3:\eta^3\text{-}C_{10}H_{16})(NO_3)_2]$ **89**

Ru(1)-O(1)	2.091 (5)	Ru(1)-C(1)	2.208 (6)
Ru(1)-C(2)	2.230 (7)	Ru(1)-C(3)	2.193 (8)
Ru(1)-O(1A)	2.091 (5)	Ru(1)-C(1A)	2.208 (6)
Ru(1)-C(2A)	2.230 (7)	Ru(1)-C(3A)	2.193 (8)
N(1)-O(1)	1.290 (8)	N(1)-O(2)	1.240 (10)
N(1)-O(3)	1.187 (8)	C(1)-C(2)	1.397 (10)
C(2)-C(3)	1.419 (10)	C(2)-C(5)	1.497 (10)
C(3)-C(4)	1.495 (11)	C(4)-C(4A)	1.512 (22)

O(1)-Ru(1)-C(1)	87.8(2)	O(1)-Ru(1)-C(2)	83.8(2)
C(1)-Ru(1)-C(2)	36.7(3)	O(1)-Ru(1)-C(3)	111.8(2)
C(1)-Ru(1)-C(3)	64.9(3)	C(2)-Ru(1)-C(3)	37.4(3)
O(1)-Ru(1)-O(1A)	167.1(3)	C(1)-Ru(1)-O(1A)	90.5(2)
C(2)-Ru(1)-O(1A)	102.4(2)	C(3)-Ru(1)-O(1A)	78.9(2)
O(1)-Ru(1)-C(1A)	90.5(2)	C(1)-Ru(1)-C(1A)	165.2(4)
C(2)-Ru(1)-C(1A)	157.5(3)	C(3)-Ru(1)-C(1A)	129.0(3)
O(1A)-Ru(1)-C(1A)	87.8(2)	O(1)-Ru(1)-C(2A)	102.4(2)
C(1)-Ru(1)-C(2A)	157.5(3)	C(2)-Ru(1)-C(2A)	123.7(4)
C(3)-Ru(1)-C(2A)	92.6(3)	O(1A)-Ru(1)-C(2A)	83.8(2)
C(1A)-Ru(1)-C(2A)	36.7(3)	O(1)-Ru(1)-C(3A)	78.9(2)
C(1)-Ru(1)-C(3A)	129.0(3)	C(2)-Ru(1)-C(3A)	92.6(3)
C(3)-Ru(1)-C(3A)	74.8(4)	O(1A)-Ru(1)-C(3A)	111.8(2)
C(1A)-Ru(1)-C(3A)	64.9(3)	C(2A)-Ru(1)-C(3A)	37.4(3)
O(1)-N(1)-O(2)	113.7(6)	O(1)-N(1)-O(3)	120.2(6)
O(2)-N(1)-O(3)	126.0(7)	Ru(1)-O(1)-N(1)	106.9(4)
Ru(1)-C(1)-C(2)	72.5(4)	Ru(1)-C(2)-C(1)	70.8(4)
Ru(1)-C(2)-C(3)	69.9(4)	C(1)-C(2)-C(3)	114.1(6)
Ru(1)-C(2)-C(5)	121.3(5)	C(1)-C(2)-C(5)	121.8(7)
C(3)-C(2)-C(5)	123.5(7)	Ru(1)-C(3)-C(2)	72.7(4)
Ru(1)-C(3)-C(4)	119.0(6)	C(2)-C(3)-C(4)	125.9(7)
C(3)-C(4)-C(4A)	111.6(5)		

Table 3.18: Anisotropic displacement factors ($Å^2$ x 10^3) for $[Ru(\eta^3:\eta^3\text{-}C_{10}H_{16})(NO_3)_2]$ **89**

	U_{11}	U_{22}	U_{33}	U_{23}	U_{13}	U_{12}
Ru(1)	33(1)	28(1)	35(1)	0	1(1)	0
N(1)	67(4)	50(3)	47(3)	-11(3)	1(3)	-14(3)
O(1)	53(3)	55(3)	46(3)	-12(2)	-1(2)	-4(2)
O(2)	121(6)	93(5)	109(6)	47(4)	-13(5)	-30(5)
O(3)	104(5)	115(5)	66(4)	-60(4)	10(4)	-17(4)
C(1)	24(3)	72(5)	60(4)	10(4)	3(3)	1(3)
C(2)	44(4)	55(4)	47(4)	6(3)	0(3)	-17(3)
C(3)	69(5)	56(4)	53(4)	-13(3)	6(4)	-25(4)
C(4)	165(12)	40(4)	101(9)	-27(5)	58(7)	-31(6)
C(5)	76(5)	68(5)	57(4)	7(4)	23(4)	-9(4)

Chapter 4

Geometrical Isomerism in Hydroxypyridinate and Pyridinethiolate Complexes of Ruthenium(IV)

4.1 Introduction

A recent report[159] has described the reactions of **6** with the heterocyclic thiols benzothiazole-2-thiol (mcbtH) and pyridine-2-thiol (pyrSH), a class of ligand which is of considerable interest in its own right.[199,200] Complex **6** reacts with mcbtH and pyrSH *via* a two step process initially involving bridge cleavage to give neutral complexes [Ru(η^3:η^3-$C_{10}H_{16}$)Cl_2(LH)] (LH = mcbtH **92a**, pyrSH **92b**) similar to compounds of type **42**, exhibiting equatorial coordination of the pyridyl nitrogen atom. Refluxing of **92a** and **92b** in solutions containing $Na_2[CO_3]$ brings about the intramolecular loss of HCl and gives [Ru(η^3:η^3-$C_{10}H_{16}$)Cl(L)] (L = SNC_7H_4S **93a**, NC_5H_4S **93b**) containing mcbt and pyrS as anionic chelates. A number of similar complexes of 6-substituted-2-hydroxypyridines (RpyrOH) [Ru(η^6-arene)Cl(NC_5H_3O-6-R)] (arene = C_6H_6, R = H **94a**, Cl **94b**, Me **94c**; arene = *p*-$MeC_6H_4CHMe_2$, R = H **94d**) have been reported in (arene)ruthenium(II) chemistry.[61,62]

Ligands related to 2-hydroxypyridine and pyridine-2-thiol are subject to tautomerism such that in polar reaction media the pyridinol form is converted to the pyridone tautomer, Fig. 4.1.

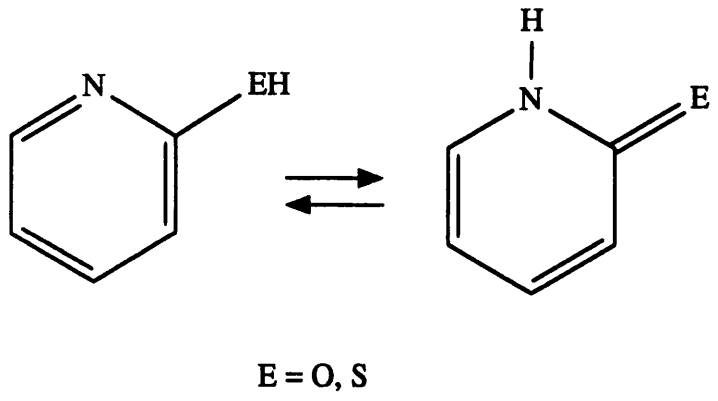

Fig. 4.1: Tautomerism in 2-hydroxypyridines and Pyridine-2-thiols

In the case of complexes of type **94**, 2-hydroxypyridine ligands have been shown[61] to coordinate initially through the pyridone oxygen atom at room temperature in methanol,

to give adducts such as $[Ru(\eta^6\text{-}C_6H_6)Cl_2(OC_5H_4NH)]$ **95**. Subsequent deprotonation on refluxing gives the corresponding chelate complexes. The reaction of 2-hydroxypyridine (pyrOH) with **6** has also been investigated[159] but the products could not be identified.

The following chapter reports the results of our re-investigation of the interaction of **6** with pyrOH and describes the examination of a number of related reactions.

4.2 Reactions with 2-Hydroxypyridines

4.2.1 Reaction with 2-Hydroxypyridine

In previous work it has been shown that labile trifluoroacetate complexes such as $[Ru(\eta^6\text{-}C_6H_6)Cl(O_2CCF_3)]$ are useful synthetic precursors to hydroxypyridinate chelates such as **94a**. This synthetic route is not available in the case of the *bis*(allyl)ruthenium(IV) system since the reaction of **6** with trifluoroacetic acid or silver trifluoroacetate gives the relatively inert aquo complex $[Ru(\eta^3\text{:}\eta^3\text{-}C_{10}H_{16})(O_2CCF_3)_2(OH_2)]$ (Chapter 3). However, direct interaction of **6** with pyrOH in CH_2Cl_2 at room temperature gives a good yield (*ca.* 70%) of an orange-red complex **96**. The infrared spectrum of **96** showed no bands attributable to ν(OH) or to ν(NH) but did display a band at 1596 cm^{-1} (*cf.* 1585 cm^{-1} for $Tl[NC_5H_4O]$ and 1635 cm^{-1} for the free ligand[192]) which is tentatively attributed to ν_{asymm}(OCN) of the coordinated hydroxypyridinate anion. Assignment of ν_{symm}(OCN) at lower wavenumber is ambiguous due to the presence of bands arising from the pyridyl ring. A weak band is also observed at 317 cm^{-1} and is assigned to ν(RuCl). The ^1H NMR spectrum of **96** (Table 4.1) shows the characteristic four line pattern for the terminal allyl protons of the *bis*(allyl) ligand (δ 5.05, 4.24, 4.07 and 3.00 ppm) and two relatively widely separated signals for the methyl substituents (δ 2.38 and 2.24 ppm) indicative of inequivalent axial sites on the trigonal bipyramidal ruthenium atom. A FAB mass spectrum displayed a strong molecular ion peak at *m/z* = 367 (based on ^{102}Ru and ^{35}Cl) with the expected isotope distribution pattern. Fragmentation peaks associated with loss of a single chloride ligand and loss of both chloride and hydroxypyridinate ligands were also observed, and a peak at *m/z* = 136 is assigned to the *bis*(allyl) ligand. These observations, in conjunction with analytical data, leads us to formulate **96** as the chelate complex $[Ru(\eta^3\text{:}\eta^3\text{-}C_{10}H_{16})Cl(NC_5H_4O)]$, which is

structurally related to **94a** and to the thiolate complexes **92**.[159] It was also noted that the ^{1}H NMR spectrum of crude **96**, showed small traces of a second compound with only two terminal allyl resonances (δ 4.90 and 4.04 ppm) and a broad peak at δ 10.40 ppm. We were unable to isolate this second product but tentatively suggest it to be an analogue of the ruthenium(II) monodentate pyridone adduct $[Ru(\eta^6\text{-}C_6H_6)Cl_2(OC_5H_4NH)]$, in which the amine proton is observed at δ 11.56 ppm. The ready formation of chelate complexes such as **96** markedly contrasts with studies on the pyridine-2-thiolate analogues,[159] and may be related to the relative hardness of the ruthenium(IV) centre.

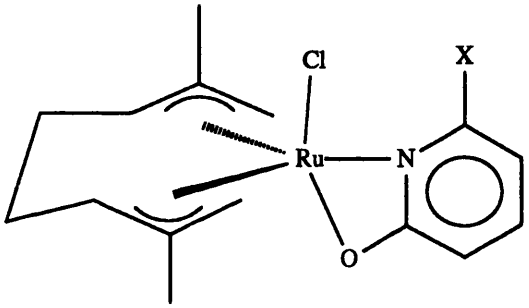

(**a**) *Equatorial* isomer

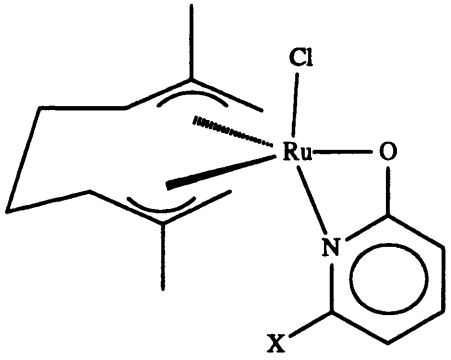

(**b**) *Axial* isomer

96a	X = H	**96b**
97a	Cl	**97b**
99a	Me	**99b**

Unlike its (arene)ruthenium(II) analogues, **96** might be expected to exist as two geometrical isomers (**96a**, **96b**), distinguishable by ^{1}H NMR spectroscopy, as a consequence of the stereochemical inequivalence of the axial and equatorial sites of the trigonal bipyramidal ruthenium ion. However, both $[Ru(\eta^3\text{:}\eta^3\text{-}C_{10}H_{16})Cl(mcbt)]$ and $[Ru(\eta^3\text{:}\eta^3\text{-}C_{10}H_{16})Cl(pyrS)]$[159] are reported to exist solely as *equatorial* isomers (type **a**), with the pyridyl nitrogen atom occupying the equatorial site of the trigonal bipyramidal ruthenium atom. The ^{1}H NMR spectrum of **96** (obtained as described above from a sample synthesised by direct interaction of **6** with the non-deprotonated 2-hydroxypyridine ligand) is interpreted in terms of a single isomer, possessing a set of resonances qualitatively similar, in the allyl, region to those exhibited by $[Ru(\eta^3\text{:}\eta^3\text{-}C_{10}H_{16})Cl(mcbt)]$ and $[Ru(\eta^3\text{:}\eta^3\text{-}$

$C_{10}H_{16}$)Cl(pyrS)].[159]

It might be supposed that, analogously to the ruthenium(II)arene system,[192] 2-hydroxypyridine would react with **6** in a two step process, coordinating initially *via* the pyridone oxygen atom at the equatorial site of the "Ru(η^3:η^3-$C_{10}H_{16}$)Cl_2" unit (as observed in all previous cases of monodentate coordination in adducts derived from **6** [16,17,158] and suggested by the ^{1}H NMR spectrum of the trace product described above). Subsequent loss of HCl from such an adduct would then be expected to give a complex exhibiting a pyridyl ring in one of the axial coordination sites of the metal ion, a geometry at variance with that observed crystallographically for [Ru(η^3:η^3-$C_{10}H_{16}$)Cl(mcbt)].[159] However, at some stage in the reaction a rearrangement must take place such that the relatively unhindered pyridone oxygen atom of the 2-hydroxypyridinate ligand preferentially occupies the more hindered axial site. This proposal is consistent with the isomerisation of **6** in CH_3CN solution,[17,161] where the predominant species is observed to be a monomeric, bridge cleaved complex with a chloride ligand in the equatorial position and the acetonitrile axially located.

Indirect evidence for an intramolecular rearrangement of a pyridone intermediate in the formation of **96** comes from reaction of **6** with sodium 2-hydroxypyridinate. The major product (95% - evaluated by integration of the ^{1}H NMR spectrum) consists of the isomer **96a** however smaller quantities of an alternative geometric isomer, **96b**, are also observed. The ^{1}H NMR spectrum of **96b** is described in Table 4.1. This reaction, which uses the preformed anionic ligand, presumably increases the rate of the chelation step in the reaction such that there is insufficient time for the equatorial-axial rearrangement to occur completely and hence a significant quantity of the less stable *axial* isomer is observed.

4.2.2 Reactions with 6-Substituted 2-Hydroxypyridines

In an attempt to confirm the formulation of **96a** and **96b** and synthesise further compounds displaying both *axial* and *equatorial* pyridyl fragments, we investigated the reaction of **6** with 2-hydroxy-6-chloropyridine, 2-hydroxy-4-methylquinoline and 2-hydroxy-6-methylpyridine. These ligands contain bulky *ortho*-substituents which might be expected to interact unfavourably with the remaining axial chloride ligand in complexes

of type **a** and thus may display less preference for the *equatorial* form. Reaction with the neutral pyridinols was found to be slow at room temperature and significantly more efficient conversions were obtained through use of the sodium salts of the ligands or addition of anhydrous sodium carbonate to the reaction mixtures. In this way compounds of formulae $[Ru(\eta^3:\eta^3\text{-}C_{10}H_{16})Cl(NC_5H_3O\text{-}6\text{-}Cl)]$ **97**, $[Ru(\eta^3:\eta^3\text{-}C_{10}H_{16})Cl(NC_9H_5O\text{-}4\text{-}Me)]$ **98** and $[Ru(\eta^3:\eta^3\text{-}C_{10}H_{16})Cl(NC_5H_3O\text{-}6\text{-}Me)]$ **99** were obtained in good yields. Like **96**, complexes **97**, **98** and **99** display no bands attributable to ν(OH) or ν(NH) in their infrared spectra but possess peaks at 1589 cm^{-1} (**97**), 1550 cm^{-1} (**98**) and 1558 cm^{-1} (**99**) tentatively assigned to ν_{asymm}(OCN) as well as peaks arising as a consequence of pyridyl C=C modes (see experimental section) and bands due to ν(RuCl). The ^1H NMR spectra of these materials proved complex, each possessing two sets of signals, present in a ratio of approximately 3 : 1 in the case of **97**, 6 : 1 for **98** and 3 : 2 for **99**. The spectrum of **97** for example, displays four singlets for the major product, due to terminal allyl protons (δ 5.25, 4.36, 4.27 and 4.96 ppm), and two methyl resonances (δ 2.32 and 2.16 ppm) and similarly, the minor product, **97b**, displays resonances at δ 4.95, 4.66, 4.56 and 3.73 (terminal allyl), and 2.49 and 2.37 ppm (methyl). These spectra could conceivably be attributed to pairs of diastereoisomers of **97**, **98** and **99** if the compounds were dimeric, since binuclear compounds containing two "$\eta^3:\eta^3\text{-}C_{10}H_{16}Ru$" units have been shown to display a total of eight terminal allyl resonances and four methyl signals (Appendix I).[17] However, electron impact mass spectra exhibit strong molecular ion peaks at *m/z* 401 (**97**), 431 (**98**), and 381 (**99**) with isotope distribution patterns consistent with the presence of a single ruthenium atom and one chloride ligand in each case, implying mononuclear complexes. The mononuclear nature of **97** was confirmed by a single crystal X-ray structure determination (*vide infra*). Fractional crystallisation of **97** from an acetone solution gave red-brown crystals of a single isomer which was shown to be the major isomer, **97a**, by low temperature dissolution of the crystalline material and simultaneous recording its ^1H NMR spectrum (-80°C). The structure determination (Fig. 4.2) showed **97a** to be a mononuclear chelate compound, with the nitrogen atom equatorially located, closely related to the *equatorial* structure assigned to **96a**, and observed crystallographically in the case of $[Ru(\eta^3:\eta^3\text{-}C_{10}H_{16})Cl(mcbt)]$.[159] Complex **97b** is therefore assigned a similar structure with the pyridyl nitrogen atom axially located. By analogy,

similar isomeric structures are assigned to **98a, 98b** and **99a, 99b**. The major products are assigned the structures with the nitrogen atoms equatorially coordinated, allowing the bulky pyridyl fragments to avoid the axial sites which are sterically crowded by the methyl groups of the, dimethyloctadienediyl ligand.

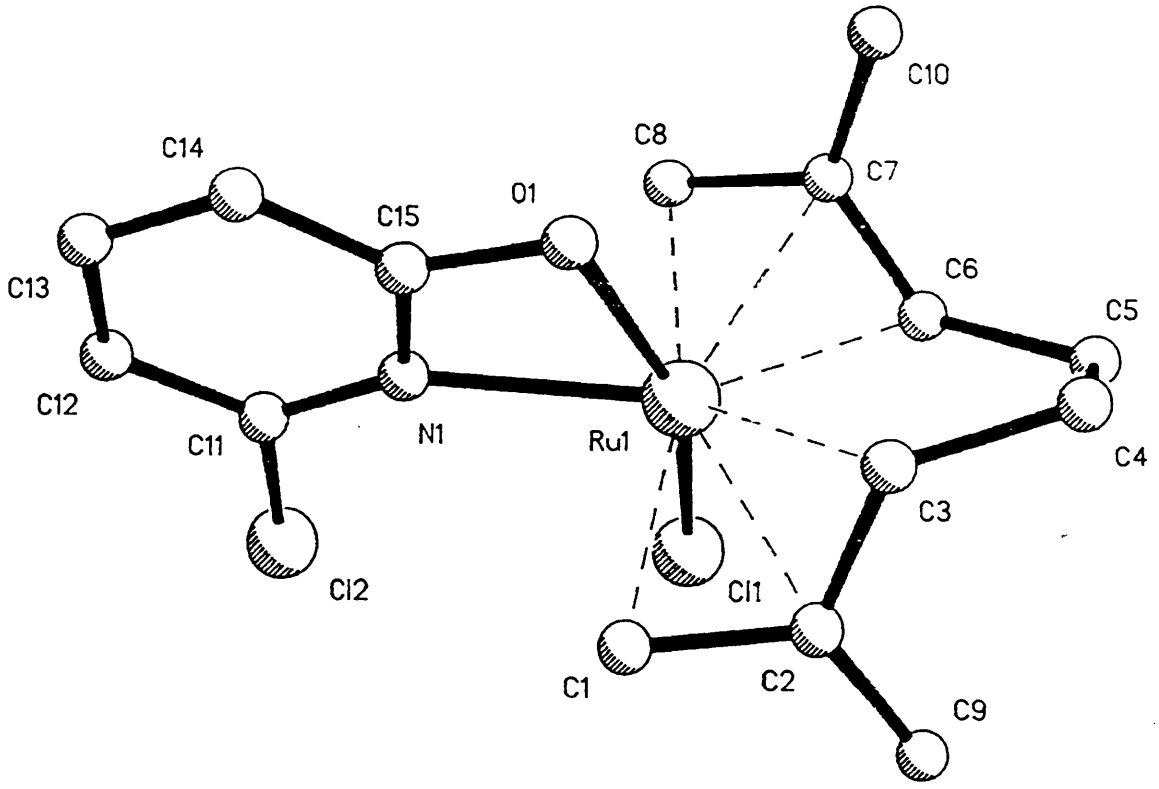

Fig. 4.2: X-ray crystal structure of $[Ru(\eta^3:\eta^3\text{-}C_{10}H_{16})Cl(NC_5H_3O\text{-}6\text{-}Cl)]$ **97a** showing the atom numbering scheme adopted.

Good evidence for the *equatorial* nature of **96a - 99a** comes from their ^1H NMR spectra which, in common with those of $[Ru(\eta^3:\eta^3\text{-}C_{10}H_{16})Cl(mcbt)]$ and $[Ru(\eta^3:\eta^3\text{-}C_{10}H_{16})Cl(pyrS)]$,[159] have the two central resonances, due to the terminal allyl protons,

occurring at very similar chemical shifts. The pattern differs markedly from that observed for **96b** - **99b** and $[Ru(\eta^3:\eta^3\text{-}C_{10}H_{16})Cl(L\text{-}L)][BF_4]$ (L-L = 2,2'-bipyridyl **64**, 1,10-phenanthroline **65** - Chapter 2), where one of the terminal allylic proton resonances is shifted significantly upfield relative to the other three, possibly as a consequence of ring current effects of the aromatic moiety. Another observation which may serve to distinguish between the two possible isomers is the differences in the resonances assigned to the internal allyl protons. In the case of **96a** - **99a** these occur as two broad, poorly resolved, singlet-like resonances at δ *ca.* 4.3 and 3.5 ppm. Conversely, the spectra of **96b** - **99b** display the corresponding resonances as much sharper signals at δ *ca.* 4.7 and 4.2 - 4.5 ppm, one occurring as a pseudo triplet and the other as a well resolved five line multiplet.

4.2.3 Other O,N-Donor Complexes Exhibiting Isomerism

To confirm these observations the reaction of **6** with 8-hydroxyquinoline (NC_9H_6OH) was examined. Both isomers resulting from this reaction might be expected to possess an aromatic ring in the axial site and so display ^1H NMR spectra typical of type **b** compounds. Two products were indeed obtained, $[Ru(\eta^3:\eta^3\text{-}C_{10}H_{16})Cl(NC_9H_6O)]$ (**100a, 100b**) although, presumably due to the relatively unhindered nature of the ligand, the isomer ratio was in excess of 20 : 1 (in retrospect an unsurprising result given the observation of only a single isomer of **96** arising from reaction with the neutral ligand). The mononuclear nature of these materials was confirmed by a FAB mass spectrum. The ^1H NMR spectra of both these materials displayed the expected four line patterns for the terminal allyl protons [δ 4.34, 3.98, 3.87 and 2.70 (major isomer, **100a**); 4.87, 4.58, 4.02 and 3.09 ppm (minor isomer **100b**)] which are qualitatively similar to those of type **b** complexes. The signals attributed to the internal allyl protons occurred a sharp resonances strongly resembling those observed for the cationic bipyridine and phenanthroline complexes (Chapter 2). Logically, and by analogy with **96a** and **96b**, the major product will be of the N-equatorial, O-axial type. Evidence for this comes from the consistent upfield shift of the signals due to the allyl protons of the major isomer relative to the minor one, presumably as a consequence of the closer proximity of the aromatic ring to the *bis*(allyl) ligand when the pyridyl fragment occupies the axial site.

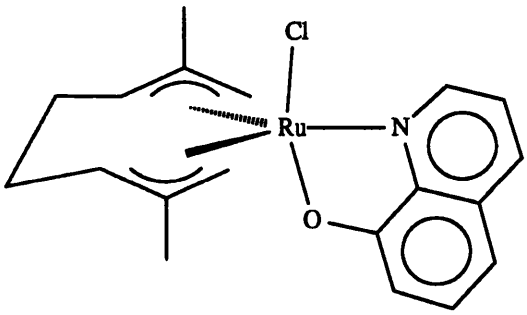

100a

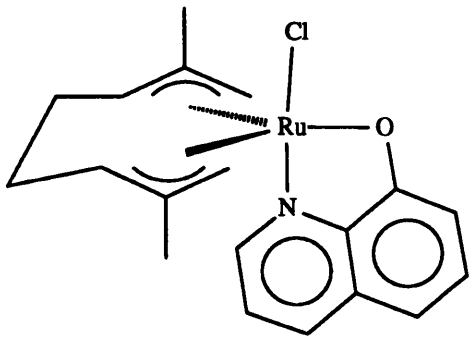

100b

Reaction of **6** with α-pyrrolidinone, HNC_4H_6O, also gives rise to *axial* and *equatorial* isomers, related to **97**, **98** and **99**, namely $[Ru(\eta^3:\eta^3\text{-}C_{10}H_{16})Cl(NC_4H_6O)]$ (**101a**, **101b**). The solid state infrared spectrum of **101** displays strong, broad peaks at 1540 and 1407 cm^{-1} (signals due to individual isomers not resolved) corresponding to the antisymmetric and symmetric ν(OCN) modes (in this particular case the assignment may be made with confidence due to the absence of pyridyl C=C stretching bands). The ^1H NMR spectra of **101a** and **101b** are described in Table 4.1. It is unclear from this data which isomer is *equatorial* and which is *axial* although the major product (*ca.* 70%) does display a pattern of four terminal allyl proton resonances reminiscent of an *equatorial* isomer whilst the relatively abundant minor isomer exhibits an NMR spectrum slightly more similar to those of complexes of type **b**. Clearly isomerism in **101** is unlikely to be a consequence of unfavourable steric interactions between the chloride ligand and bulky *ortho* ring substituents, which are absent in this case. The formation of substantial quantities of the *axial* isomer is rather attributed to the stereochemical non-rigidity of the saturated five membered ring of the hydroxypyrrolidinate ligand which allows the relief of otherwise unfavourable steric interactions between the coordinated ligands.

4.3 Reactions with Pyridine-2-thiols

Sterically hindered ligands such as 2-hydroxy-6-chloropyridine, 2-hydroxy-4-methylquinoline and 2-hydroxy-6-methylpyridine are often observed to bridge across two metal centres[190] rather than form strained four membered chelate rings. Nevertheless it has been described above how the reaction of **6** with these ligands leads to the formation of mononuclear complexes **97**, **98** and **99**. We reasoned though, that reaction of **6** with ligands containing larger donor atoms such as sulphur, as well as a sterically hindering *ortho* substituent might lead to the formation of bridged, binuclear complexes. It should be noted however that pyridine-2-thiol has already been observed to form a mononuclear compound on reaction with **6**,[159] this mode of coordination being attributed to the slowness of the deprotonation step relative to the rate of coordination of the ligand in a monodentate fashion *via* the pyridyl nitrogen atom.[159]

We have investigated the reaction of the more hindered pyridinethiols, quinoline-2-thiol and 6-methylpyridine-2-thiol and of their sodium salts with **6** in an attempt to prepare binuclear compounds. The reactions involving the free ligands, gave only mononuclear bridge cleaved adducts $[Ru(\eta^3:\eta^3\text{-}C_{10}H_{16})Cl_2(NC_9H_6SH)]$ **102** and $[Ru(\eta^3:\eta^3\text{-}C_{10}H_{16})Cl_2(NC_5H_3MeSH)]$ **103** in which the ligands are probably coordinated in a monodentate fashion *via* the pyridyl nitrogen atom, by analogy with $[Ru(\eta^3:\eta^3\text{-}C_{10}H_{16})Cl(mcbt)]$ and $[Ru(\eta^3:\eta^3\text{-}C_{10}H_{16})Cl(pyrS)]$.[159] The infrared spectra (nujol) of both of these complexes display several strong bands in the region 1600 - 1400 cm^{-1} corresponding to ν(C=C) and ν(C=N) ring modes, and ν(RuCl) bands are observed at 316, 289 and 317, 297 cm^{-1} for **102** and **103** respectively. No bands unambiguously assignable to ν(SH) or ν(NH) were seen, as was the case in Toerien and van Rooyen's study,[159] although one or the other would be expected to be present.

Reaction of **6** with the pre-formed sodium salt of quinoline-2-thiol led to a compound displaying a ^1H NMR spectrum containing a four line pattern for the terminal allyl protons (δ 5.00, 4.57, 4.19 and 3.14 ppm), which was difficult to unambiguously assign unequivocally to either *axial* or *equatorial* coordination but consistent with the chelate complex $[Ru(\eta^3:\eta^3\text{-}C_{10}H_{16})Cl(NC_9H_6S)]$ **104a**. The internal allyl resonances, which consist of two sharp, narrow multiplets, occurring at δ 4.88 and 4.06 ppm, however imply

equatorial coordination. The solid state infrared spectrum of **104a** (KBr disc) displays similar bands to **102** at 1608, 1589, 1498 and 1421 cm^{-1}. In addition, two bands of medium intensity are observed at 1545 and 1448 cm^{-1} and are tentatively assigned to ν(S-C=N). The nujol mull spectrum displays ν(RuCl) 303 cm^{-1} and a FAB mass spectrum of **104a** exhibits a strong molecular ion peak at *m/z* 433 along with fragmentation peaks consistent with the proposed structure. A quantity of a second isomer, **104b**, was also observed (**104a** : **104b**, 5 : 1). A single crystal X-ray structure determination revealed a complex posessing an *equatorial* structure (Fig. 4.3), very similar to that of **97a** and [Ru(η^3:η^3-$C_{10}H_{16}$)Cl(mcbt)].[159] Low temperature dissolution of the crystalline sample and simultaneous recording of its ^{1}H NMR spectrum showed this structure to be **104a**, the form strongly predominant in solution.

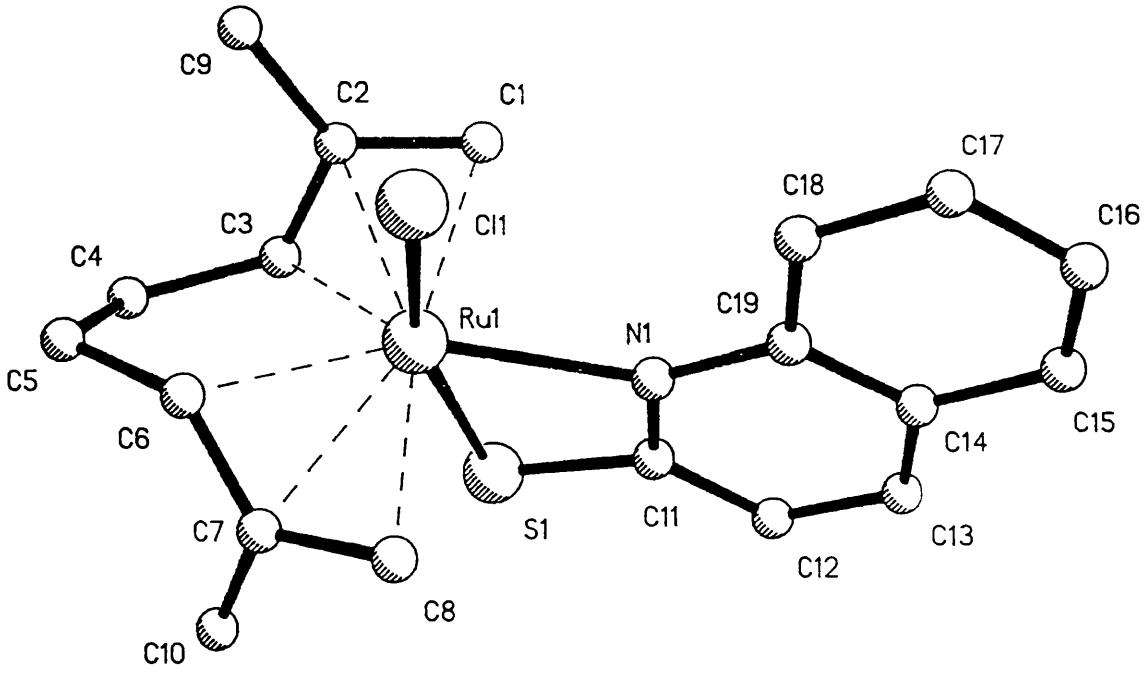

Fig. 4.3: X-ray crystal structure of [Ru(η^3:η^3-$C_{10}H_{16}$)Cl(NC_9H_6S)] **104a** showing the atom numbering scheme adopted.

The above data indicate that the relationship between mode of ligand coordination and the ^{1}H NMR spectral pattern is less well defined for the pyridinethiolate complexes than for hydroxypyridinates, especially in terms of the positions of the terminal allyl resonances (the anomaly is, to some extent, shared by the pyridine-2-thiolate complex [Ru(η^3:η^3-$C_{10}H_{16}$)Cl(pyrS)][159]) to the extent that it is not possible to unambiguously assign structure for a given isomer in the absence of supplementary data. A comparison of the spectra of two isomers of the same compound may however, provide a worthwhile indication as to the likely geometry.

Reaction of **6** with the sodium salt of 6-methylpyridine-2-thiol also led to a mononuclear compound (FAB mass spectrum, molecular ion *m/z* 397), [Ru(η^3:η^3-$C_{10}H_{16}$)Cl(NC_5H_3S-6-Me)] (**105a, 105b**; in a ratio of 1 : 3), directly analogous to **99a, 99b**.

4.4 Factors Affecting Isomer Ratios

If a model invoking two sets of competing steric interactions i) between axial ligand fragments and dimethyloctadienediyl methyl substituents, and ii) between *ortho*-pyridyl substituents and axial chloride ligands is assumed, it becomes possible to rationalise the observed preferences in isomer ratio. The unsubstituted 2-hydroxypyridinate and pyridine-2-thiolate[159] ligands display uniquely equatorial pyridyl coordination (type **a**). When bulky ring substituents are introduced *ortho* to the pyridyl nitrogen atom (*e.g.* complexes **97, 98, 99**) the interactions of these substituents with the axial chloride ligands destabilise the type **a** form relative to the type **b** and thus two isomers are observed. The *axial* (type **b**) form would thus be expected to become more predominant as the size of the ring substituent increases. This argument is qualitatively compatible with the observed isomer ratios for complexes **96** - **99**.

In the case of **105a, 105b** the isomer ratio was observed to be 1 : 3 *i.e.* for **105** it is the *N-axial* (type **b**) form which predominates. Evidence for this comes from comparison of the allyl region of the ^{1}H NMR spectra of **99** and **105**. The terminal allyl signals for the *major* isomer in the spectrum of **105** display a grouping characteristic of an *axial* isomer with three signals between 4.5 - 5 ppm and the fourth shifted upfield to δ 3.88 (*cf.* **99b** δ

5.10, 4.77, 4.51, and 3.70 ppm). The signals for the minor isomer are much more evenly distributed (δ 4.91, 4.45, 4.15 and 3.10; *cf.* **99a** 5.21, 4.31, 4.30 and 2.91 ppm). Turning to the internal allyl resonances **96a**, **97a** and **98a** (*equatorial* isomers) display poorly resolved, "singlet-like" multiplets (δ 4.19 and 3.46, **96**; 4.32 and 3.59, **97a**; 4.37 and 3.56 ppm, **99a**) as does the *minor* product in the case of **105** (δ 4.79 and 3.96 ppm), although the actual values are shifted downfield by 0.5 ppm (an observation consistent with most of the other signals on changing to the sulphur donor atom of the pyridinethiolate ligand). In contrast the corresponding signals for **97b** and **99b** occur as a sharp triplet and sharp, five line multiplet (δ 4.81 and 4.56, **97b**; 4.61 and 4.14 ppm, **99b**) as do the corresponding resonances for the major isomer in the case of **105**, again with an overall downfield chemical shift (δ 5.02 and 4.66 ppm).

Conclusive proof for these deductions of the identity of the **105a**, **105b** pair must await a single crystal X-ray structure determination and concomitant low temperature NMR experiment, but the evidence would seem to point towards a consistent relationship between *equatorial : axial* isomer ratio and the relative magnitudes of the various steric interactions.

4.5 X-ray Crystal Structure Determinations of Representative Compounds

The crystal structures of **97a** and **104a** are shown in Figs. 4.2 and 4.3. Fractional atomic coordinates, thermal parameters and bond lengths and angles are given along with details of the structure solutions and refinement in the experimental section. As observed in previous structures containing the "Ru(η^3:η^3-$C_{10}H_{16}$)" unit[13,158,160] the geometry about the ruthenium ions in both **97a** and **104a** is conveniently described as a distorted trigonal bipyramid, although a pentagonal bipyramidal description can also be justified in this type of *bis*(allyl)ruthenium(IV) system.[105-107] The η^3:η^3-$C_{10}H_{16}$ ligand shows the usual local C_2 symmetry and there is no significant variation in the Ru-C distances. The ruthenium chloride distances in **97a** and **104a** are 2.381(3) Å and 2.461(2) Å respectively. The former is similar to that observed for Ru-$Cl_{terminal}$ (2.386 Å) in the parent chloro-bridged dimer[13] but rather shorter than the norm for other "Ru(η^3:η^3-$C_{10}H_{16}$)" systems (2.40 - 2.42 Å),[158]

although similar to that observed in [Ru(η^6-C_6H_6)Cl(NC_5H_3O-6-Me)],[61] 2.392(2) Å. The longer Ru-Cl bond in **104a** may be attributed to the *trans* influence of the sulphur donor atom. The ruthenium-oxygen distance is rather short in **97a** [2.099(8) Å when compared to 2.120(5) Å[61] and 2.153(6) Å[62] in related (arene)ruthenium(II) systems] whereas the ruthenium-nitrogen distance is somewhat longer (2.166(6) Å as against 2.091(5) Å[61] and 2.084(7) Å).[62] In general the structure of **97a** is closely related to that of [Ru(η^6-C_6H_6)Cl(NC_5H_3O-6-Me)][61] with one important difference. In the latter structure the *ortho* methyl group possesses apparently little stereochemical consequence and resides on the opposite side of the molecule to the chloride ligand. The more sterically demanding nature of the *bis*(allyl) ligand in **97a** causes the chloride ligand and the *ortho* chloride ring substituent to lie virtually eclipsed with one another (the pyridyl ring is inclined at an angle of 6.2° to the plane containing the chlorine, nitrogen and oxygen atoms), the chlorine-chlorine non-bonded distance being 3.48 Å. As a result the Ru(1)-N(1)-C(11) angle is opened up to 149(1)°, compared to 143.4(5)° in the case of **3**[61] and 124(1)° when the 2-hydroxy-6-methylpyridinate ion is in the less sterically demanding bridging mode,[190] and is indicative of significant steric strain in the complex. Steric strain is also apparent in the very large Cl(1)-Ru(1)-N(1) angle, 96.4(4)°. In undistorted structures this angle averages *ca.* 85° [161] and indeed the Cl-Ru-S angle in [{Ru(η^3:η^3-$C_{10}H_{16}$)Cl(μ-SCN)}$_2$] (see Chapter 5) is only 80.3(1)°. Values of up to 88.6(3)° in [Ru(η^3:η^3-$C_{10}H_{16}$)Cl(mcbt)][159] and 90.3(1)° [{(η^3:η^3-$C_{10}H_{16}$)Cl_2}$_2$(μ-dppm)] (dppm = diphenylphosphinomethane)[158] have also been found.

The steric strain in this complex is a significant contributory factor in the observation of appreciable quantities of the *axial* isomer **97b**, where no strong chlorine-chlorine interactions would be apparent. However, steric interactions between the *bis*(allyl) ligand and the chloride substituent in **97b** mean that **97a** is still the predominant isomer observed.

For **104a**, the Ru-S distance [2.386(2) Å] significantly shorter than the equivalent bond lengths in [Ru(η^3:η^3-$C_{10}H_{16}$)Cl(mcbt)],[159] 2.425(3) Å, and in [{Ru(η^3:η^3-$C_{10}H_{16}$)Cl(μ^2-SCN)}$_2$], 2.490(4) Å (where the sulphur atom occupies the equatorial site, Chapter 5). In the former case a geometrical factor may be involved since the sulphur atom in **104a** is attached to a six membered ring, as opposed to five membered one in the mcbt complex.

This is also reflected in the angle Cl(1)-Ru(1)-S(1) which is opened out to 160.0(1)° compared to 156.4(1)° in [Ru(η^3:η^3-$C_{10}H_{16}$)Cl(mcbt)].[159] The ruthenium-nitrogen distance, 2.221(5) Å, is remarkably long when compared to the bond lengths noted above (2.09 - 2.16 Å). This is probably a geometrical effect arising from the short Ru-S distance.

4.6 Conclusions

In spite of the use of pre-formed salts of ligands expected to bring about bridged, binuclear complexation, only mononuclear species have been observed. It has been shown that ligands related to 2-hydroxypyridine show two distinct chelate coordination geometries when bound to the "Ru(η^3:η^3-$C_{10}H_{16}$)" moiety. These isomers may be distinguished from one another by analysis of the allyl regions of their ^{1}H NMR spectra. By variation of the substitution of the *ortho* site of the ligand and the identities of the donor atoms it is possible to selectively synthesise a predominance of either coordination geometry.

4.7 Experimental

General experimental and instrumental considerations are outlined in Section 2.4. All manipulations were carried out under nitrogen with degassed solvents using conventional Schlenk line techniques, although no significant air sensitivity of the products was noted. Sodium salts were prepared from reaction of sodium metal with the relevant ligand in dry thf, or in the neat ligand. All other reagents and materials were obtained from the usual commercial sources, with the exception of 6-methylpyridine-2-thiol which was synthesised by the literature method.[201,202]

Preparations. - [Ru(η^3:η^3-$C_{10}H_{16}$)Cl(NC_5H_4O)] **96.** [{Ru(η^3:η^3-$C_{10}H_{16}$)Cl(μ-Cl)}$_2$] (0.10 g, 0.16 mmol) was dissolved in dichloromethane (5 cm^3) and 2-hydroxypyridine (0.10 g, 1.07 mmol) added. After stirring for 5 h. the reaction mixture was evaporated to *ca.* ¼ volume and the solution diluted with hexane (5 cm^3). The product separated on

standing at *ca.* -20°C for a further hour and was isolated by filtration and washed with hexane. Yield: 0.08 g, 0.23 mmol, 73%. (Found: C, 49.70; H, 5.70; N, 4.50; Cl, 10.80% Calc. for $C_{15}H_{20}ClNORu$: C, 49.10; H, 5.50; N, 3.80; Cl, 9.70%). Infrared: ν_{asymm}(OCN) 1596 cm^{-1}, ν(RuCl) 317 cm^{-1}. The product may also be prepared more cleanly, in comparable yield, by suspension of **6** in acetone (5 cm^3) and addition of sodium 2-hydroxypyridinate. The reaction mixture was stirred for 5 h. during which time a colour change from pink to orange was observed and the starting material is taken up into solution. The mixture was filtered through Celite and evaporated to an oil. This oil was dissolved in diethyl ether (1 cm^3) and layered with hexane (1 cm^3) from which the product separates as orange crystals after 12 h as a 95 : 5 mixture of **96a** : **96b**.

[Ru(η^3:η^3-$C_{10}H_{16}$)Cl(NC_5H_3O-6-Cl)] **97**. [{Ru(η^3:η^3-$C_{10}H_{16}$)Cl(μ-Cl)}$_2$] (0.07 g, 0.12 mmol) was suspended in acetone (5 cm^3) and sodium 2-hydroxy-6-chloropyridinate (0.04 g, 0.24 mmol) added. The reaction mixture was stirred for 36 h. during which time a colour change from pink to orange was observed and the starting material was taken up into solution. The mixture was filtered through Celite and evaporated to an oil. This oil was dissolved in diethyl ether (1 cm^3) and layered with hexane (1 cm^3) from which the product separated as deep red crystals after a further 12 h. Yield: 0.05g, 0.11 mmol, 48%. (Found: C, 44.85; H, 4.50; N, 3.35% Calc. for $C_{15}H_{19}Cl_2NORu$: C, 44.90; H, 4.75; N, 3.50%). Infrared: 1589, 1437 cm^{-1}; ν(RuCl) 312 cm^{-1}.

[Ru(η^3:η^3-$C_{10}H_{16}$)Cl(NC_9H_5O-4-Me)] **98**. Following a procedure analogous to that described for **97** using sodium 2-hydroxy-4-methylquinolinate an orange / yellow powder was isolated. Yield: 0.10 g, 0.24 mmol, 67%. (Found: C, 56.15; H, 6.15; N, 2.85% Calc. for $C_{20}H_{24}ClNORu$: C, 55.75; H, 5.60; N, 3.25%). Infrared: 1657, 1600, 1550, 1507, 1465, 1446, 1416, 1403 cm^{-1}; ν(RuCl) 310 cm^{-1}.

[Ru(η^3:η^3-$C_{10}H_{16}$)Cl(NC_5H_3O-6-Me)] **99**. [{Ru(η^3:η^3-$C_{10}H_{16}$)Cl(μ-Cl)}$_2$] (0.09 g, 0.15 mmol) was dissolved in dichloromethane (5 cm^3) and 2-hydroxy-6-methylpyridine (0.03 g, 0.30 mmol) added. The mixture was stirred with $Na_2[CO_3]$ (0.05 g, excess) for 24 h. during which time an orange colouration was observed to form. The reaction mixture was

filtered through Celite and the filtrate evaporated to an orange oil. The product was obtained as orange crystals by recrystallisation from diethyl ether. Yield: 0.08 g, 0.22 mmol, 73%. (Found: C, 50.30; H, 5.80; N, 3.55% Calc. for $C_{14}H_{22}ClNORu$: C, 50.45; H, 5.80; N, 3.70%). Infrared: 1558, 1464 cm^{-1}; ν(RuCl) 322 cm^{-1}. The complex was also synthesised in similar yield by use of the sodium salt of the ligand as outlined for **96**.

$[Ru(\eta^3:\eta^3\text{-}C_{10}H_{16})Cl(NC_9H_6O)]$ **100**. $[\{Ru(\eta^3:\eta^3\text{-}C_{10}H_{16})Cl(\mu\text{-}Cl)\}_2]$ (0.07 g, 0.12 mmol) was suspended in acetone (5 cm^3) and 8-hydroxyquinoline (0.04 g, 0.25 mmol) added. The reaction mixture was stirred for 2 h. in the presence of $Na_2[CO_3]$ (0.05 g, excess) during which time a colour change from pink to orange was observed and the starting material was taken up into solution. The mixture was filtered through Celite and evaporated to an oil which was recrystallised from diethyl ether to give an orange product. Yield: 0.08g, 0.18 mmol, 74%. (Found: C, 54.40; H, 5.65; N, 3.40% Calc. for $C_{19}H_{22}ClNORu$: C, 54.75; H, 5.30; N, 3.35%). Infrared: 1591, 1562, 1493 cm^{-1}; ν(RuCl) 318 cm^{-1}.

$[Ru(\eta^3:\eta^3\text{-}C_{10}H_{16})Cl(NC_4H_6O)]$ **101**. $[\{Ru(\eta^3:\eta^3\text{-}C_{10}H_{16})Cl(\mu\text{-}Cl)\}_2]$ (0.12 g, 0.19 mmol) was dissolved in dichloromethane (5 cm^3) and α-pyrrolidinone (0.05 cm^3, 0.6 mmol) added. The mixture was stirred with $Na_2[CO_3]$ (0.05 g, excess) 24 h. during which time a dark colouration was observed to form. The reaction mixture was filtered through Celite and the filtrate evaporated to an oil. The product was obtained as yellow crystals by recrystallisation from diethyl ether. Yield: 0.03 g, 0.08 mmol, 20%. (Found: C, 45.85; H, 6.50; N, 4.00% Calc. for $C_{14}H_{22}ClNORu$: C, 47.10; H, 6.20; N, 3.95%). Infrared: ν(OCN) 1540, 1407 cm^{-1}; ν(RuCl) 313 cm^{-1}.

$[Ru(\eta^3:\eta^3\text{-}C_{10}H_{16})Cl_2(NC_9H_6SH)]$ **102**. $[\{Ru(\eta^3:\eta^3\text{-}C_{10}H_{16})Cl(\mu\text{-}Cl)\}_2]$ (0.11 g, 0.17 mmol) was suspended in acetone (5 cm^3) and quinoline-2-thiol (0.06 g, 0.35 mmol) added. The reaction mixture was stirred for 3 h. during which time a colour change from pink to orange was observed and the starting material was taken up into solution. The mixture was filtered and evaporated to *ca.* ¼ volume. Diethylether (4 cm^3) was added and the product obtained as an orange precipitate. Yield: 0.09 g, 0.19 mmol, 53%. (Found: C, 48.60; H,

4.75; N, 2.90% Calc. for $C_{19}H_{23}Cl_2NRuS$: C, 48.60; H, 4.95; N, 3.00%). Infrared: 1617, 1585 cm^{-1}; ν(RuCl) 289, 316 cm^{-1}.

[Ru(η^3:η^3-$C_{10}H_{16}$)Cl_2(NC_5H_3SH-6-Me)] **103**. Following a procedure analogous to that outlined for **102** above using 6-methylpyridine-2-thiol over a period of 24 h. an orange-brown product was obtained. Yield: 0.08 g, 0.21 mmol, 88%. (Found: C, 43.35; H, 5.05; N, 2.60% Calc. for $C_{16}H_{23}Cl_2NRuS$: C, 44.30; H, 5.35; N, 3.23%). Infrared: 1612, 1589 cm^{-1}; ν(RuCl) 297, 317 cm^{-1}.

[Ru(η^3:η^3-$C_{10}H_{16}$)Cl(NC_9H_6S)] **104**. Following a procedure analogous to that described for **98** using sodium quinoline-2-thiolate an orange-brown powder was isolated. Yield: 0.05 g, 0.12 mmol, 46%. (Found: C, 52.10; H, 5.15; N, 3.20% Calc. for $C_{20}H_{24}ClNORu$: C, 52.70; H, 5.10; N, 3.25%). Infrared: ν(C=C) 1608, 1589, 1498 1421 cm^{-1}; ν(S-C=N) 1545, 1448 cm^{-1}; ν(RuCl) 303 cm^{-1}.

[Ru(η^3:η^3-$C_{10}H_{16}$)Cl(NC_5H_3S-6-Me)] **105**. Following a procedure analogous to that described for **98** using sodium 6-methylpyridine-2-thiolate an orange-brown powder was isolated. Yield: 0.05 g, 0.12 mmol, 66%. (Found: C, 48.50; H, 6.10; N, 2.95% Calc. for $C_{16}H_{22}ClNRuS$: C, 48.40; H, 5.60; N, 3.50%). Infrared: 1597, 1583, 1545 cm^{-1}; ν(RuCl) 303 cm^{-1}.

X-ray Crystal Structure Determinations

A summary of general considerations for X-ray crystal structure determinations may be found in Section 2.4.

i) [Ru(η^3:η^3-$C_{10}H_{16}$)Cl(NC_5H_3O-6-Cl)] **98a**

Crystal data. - $C_{15}H_{19}NCl_2ORu$, M = 401.32, orthorhombic, space group $Pc2_1n$, a = 7.636(3) Å, b = 11.519(3) Å, c = 18.054(8) Å, U = 1588 $Å^3$ (by least-squares refinement of diffractometer angles for 32 automatically centred reflections in the range 14° ≤ 2θ ≤ 24°), F(000) = 808, D_c = 1.68 g cm^{-3}, μ(Mo-K_α) = 13.0 cm^{-1}, Z = 4. Orange block, 0.35 x 0.20 x 0.20 mm.

The crystal was prepared by slow evaporation of an acetone solution of the compound. A primitive data set of 1715 reflections was collected (1455 unique), 1302 of which were observed to have $I \geq 1.5\sigma(I)$ and were used in the refinement. Three standard reflections monitored throughout the data collection showed no appreciable change in intensity. An empirical absorption correction was applied. The structure was solved by the conventional Direct Methods and difference-Fourier technique. Refinement was attempted in the space groups Pcmn and $Pc2_1n$ and proceeded most smoothly in the latter, the asymmetric unit being observed to contain one complete molecule. Full-matrix least-squares refinement gave $R = 0.0386$, $R_w = 0.0439$ in the final cycle from 180 parameters. A weighting scheme of the form $w^{-1} = \sigma^2(F)+0.003058F^2$ was applied and the maximum shift to error ratio in the final cycle was 0.03. The largest residual peak was 0.51 electrons $Å^{-3}$. No short intermolecular contacts were observed.

ii) $[Ru(\eta^3:\eta^3\text{-}C_{10}H_{16})Cl(NC_9H_6S)]$ **104**

Crystal data. - $C_{19}H_{22}NClRuS$, $M = 433.0$, monoclinic, space group $P2_1/c$, $a = 10.434(3)$, $b = 12.518(2)$, $c = 14.561(4)$ Å, $\beta = 108.30(2)$ °, $U = 1805.6$ $Å^3$ (by least-squares refinement of diffractometer angles for 29 reflections in the range $13° \leq 2\theta \leq 28°$), $F(000) = 880$, $D_c = 1.59$ g cm^{-3}, $\mu(Mo\text{-}K_\alpha) = 11.1$ cm^{-1}, $Z = 4$. Orange block, 0.50 x 0.40 x 0.25 mm.

The crystal was prepared by slow evaporation of an acetone solution of the compound. A primitive data set of 3491 reflections was collected (3148 unique), 2314 of which were observed to have $I \geq 3\sigma(I)$ and were used in the refinement. Three standard reflections monitored throughout the data collection showed no appreciable change in intensity. An empirical absorption correction was applied. The structure was solved by the conventional Direct Methods and difference-Fourier techniques. The asymmetric unit was observed to contain one complete molecule. Hydrogen atoms were placed in idealised positions (C-H 0.96 Å) and assigned a common isotropic temperature factor U_{iso} which refined to 0.0896 $Å^2$, and were allowed to ride on the atoms to which they were attached. Full-matrix least-squares refinement gave $R = 0.0435$, $R_w = 0.0503$ in the final cycle from 209 parameters. A weighting scheme of the form $w^{-1} = \sigma^2(F)+0.003564F^2$ was applied and the maximum shift to error ratio in the final cycle was 0.06. The largest residual peak was

0.90 electrons $Å^{-3}$ associated with the ruthenium atom. No short intermolecular contacts were observed.

Table 4.1: ^{1}H NMR Data for new complexes.[a]

Compound	δ				
	Terminal allyl	Internal allyl	Ethylinic	Me	Ligand
$[Ru(\eta^3:\eta^3\text{-}C_{10}H_{16})Cl(NC_5H_4O)]$ **96a**	5.05 (s, 1H)	4.19 (m, 1H)	2.78 (m, 4H)	2.38 (s, 3H)	8.30 (d, 1H, ^3J=5.4), 7.48 (t, 1H, ^3J=8.6), 6.66 (t, 1H,
	4.24 (s, 1H)	3.46 (m, 1H)		2.24 (s, 3H)	^3J=6.0), 5.94 (d, 1H, ^3J=8.6)
(N equatorial)	4.07 (s, 1H)				
	3.00 (s, 1H)				
$[Ru(\eta^3:\eta^3\text{-}C_{10}H_{16})Cl(NC_5H_4O)]$ **96b**	5.24 (s, 1H)	4.40 (m, 1H)	2.78 (m, 4H)	2.42 (s, 3H)	7.43 (t, 1H)[b], 7.08 (d, 1H, ^3J=5.9), 6.32 (t, 1H, ^3J=6.1),
	4.69 (s, 1H)	3.31 (m, 1H)		2.12 (s, 3H)	6.16 (d, 1H, ^3J=8.7)
(O equatorial)	4.36 (s, 1H)				
	3.24 (s, 1H)				
$[Ru(\eta^3:\eta^3\text{-}C_{10}H_{16})Cl(NC_5H_4O\text{-}6\text{-}Cl)]$ **98a**	5.25 (s, 1H)	4.32 (m, 1H)	2.69 (m, 4H)	2.32 (s, 3H)	7.48 (dd, 1H, ^3J=8.4, 7.6), 6.62 (d, 1H, ^3J=7.6), 5.92 (d,
	4.36 (s, 1H)	3.59 (m, 1H)		2.16 (s, 3H)	1H, ^3J=8.4)
(N equatorial) [c]	4.27 (s, 1H)				
	2.96 (s, 1H)				
$[Ru(\eta^3:\eta^3\text{-}C_{10}H_{16})Cl(NC_5H_4O\text{-}6\text{-}Cl)]$ **98b**	4.95 (s, 1H)	4.81 (m, 1H)	2.69 (m, 4H)	2.49 (s, 3H)	7.45 (dd, 1H, ^3J=7.6, 8.6), 6.35 (d, ^3J=7.6), 6.08 (d, ^3J=8.6)
	4.66 (s, 1H)	4.56 (t, 1H,		2.37 (s, 3H)	
(O equatorial) [c]	4.56 (s, 1H)	^3J=5.4)			
	3.73 (s, 1H)				

[Ru(η^3:η^3-$C_{10}H_{16}$)Cl(NC_9H_5O-4-Me)] **98a**	5.31 (s, 1H) 4.43 (s, 1H)	4.43 (m, 1H) 3.64 (m, 1H)	2.76 (m, 4H)	2.39 (s, 3H) 2.21 (s, 3H)	8.49 (d, 1H, ^3J=8.4), 7.76 (d, 1H, ^3J=8.2), 7.54 (t, 1H, ^3J=7.0), 7.28 (t, 1H, ^3J=7.0), 6.01 (s, 1H), 2.54 (s, 3H, CH_3)
(N equatorial)	4.36 (s, 1H) 2.97 (s, 1H)				
[Ru(η^3:η^3-$C_{10}H_{16}$)Cl(NC_9H_5O-4-Me)] **98b**	5.15 (s, 1H) 4.80 (s, 1H)	4.62 (t, 1H, ^3J=5.6)	2.65 (m, 4H)	2.45 (s, 3H) 2.30 (s, 3H)	7.73 (d, 1H, ^3J=8.2), 7.39 (t, 1H, ^3J=7.0), 7.18 (t, 1H, ^3J=7.6), 6.88 (d, 1H, ^3J=8.4), 6.32 (s, 1H), 2.52 (s, 3H, CH_3)
(O equatorial)	4.56 (s, 1H) 3.53 (s, 1H)	4.39 (m, 1H)			
[Ru(η^3:η^3-$C_{10}H_{16}$)Cl(NC_5H_4O-6-Me)] **99a**	5.21 (s, 1H) 4.31 (s, 1H)	4.37 (m, 1H) 3.56 (m, 1H)	2.73 (m, 4H)	2.36 (s, 3H) 2.17 (s, 3H)	7.28 (dd, 1H, ^3J=8.4, 7.6), 6.33 (d, 1H, ^3J=7.6), 5.71 (d, 1H, ^3J=8.4)
(N equatorial)	4.30 (s, 1H) 2.91 (s, 1H)				
[Ru(η^3:η^3-$C_{10}H_{16}$)Cl(NC_5H_4O-6-Me)] **99b**	5.10 (s, 1H) 4.77 (s, 1H)	4.61 (t, 1H, ^3J=6.2)	2.59 (m, 4H)	2.11 (s, 3H) 2.33 (s, 3H)	6.07 (virtual t, 2H), 7.28 (m, 1H)
(O equatorial)	4.51 (s, 1H) 3.70 (s, 1H)	4.14 (m, 1H)			
[Ru(η^3:η^3-$C_{10}H_{16}$)Cl(NC_9H_6O)] **100a**	4.34 (s, 1H) 3.98 (s, 1H)	4.95 (m, 1H) 4.37 (m, 1H)	3.22 (m, 2H) 2.72 (m, 1H)	2.41 (s, 3H) 2.08 (s, 3H)	9.28 (dd, 1H, ^3J=4.9, ^4J=1.3), 8.13 (dd, 1H, ^3J=8.4, ^4J=1.2), 7.39 (dd, 1H, ^3J=5.0, 5.0), 7.24 (t, 1H, ^3J=7.9), 6.85 (d, 1H, ^3J=7.9), 6.67 (d, 1H, ^3J=8.0)
(N equatorial)	3.87 (s, 1H) 2.70 (s, 1H)		2.64 (m, 1H)		

$[Ru(\eta^3:\eta^3\text{-}C_{10}H_{16})Cl(NC_9H_6O)]$ **100b**	4.87 (s, 1H) 4.58 (s, 1H) 4.02 (s, 1H) 3.09 (s, 1H)	5.13 (m, 1H) 4.15 (m, 1H)	3.22 (m, 2H) 2.72 (m, 1H) 2.64 (m, 1H)	2.54 (s, 3H) 1.71 (s, 3H)	7.99 (d, 1H, ^3J=8.4), 7.78 (d, 1H, ^3J=4.9), 7.36 (t, 1H, ^3J=7.9), 7.12 (dd, 1H, ^3J=5.0, 5.0), 6.83 (d, 1H, ^3J=7.9), 6.67 (d, 1H, ^3J=8.0)
(O equatorial)					
$[Ru(\eta^3:\eta^3\text{-}C_{10}H_{16})Cl(NC_4H_6O)]$ **101a**	5.14 (s, 1H) 4.25 (s, 1H) 4.16 (s, 1H) 2.81 (s, 1H)	4.06 (m, 1H) 3.29 (m, 1H)	2.70 (m, 4H)	2.29 (s, 3H) 2.18 (s, 3H)	3.83 (m, 2H), 3.38 (t, 4H, ^3J=7.0)
(N equatorial)					
$[Ru(\eta^3:\eta^3\text{-}C_{10}H_{16})Cl(NC_4H_6O)]$ **101b**	5.22 (s, 1H) 4.63 (s, 1H) 4.51 (s, 1H)[d] 3.15 (s, 1H)[d]	4.32 (m, 1H) 3.72 (m, 1H)	2.47 (m, 4H)	2.36 (s, 3H) 2.27 (s, 3H)	3.83 (m, 2H), 3.38 (t, 4H, ^3J=7.0)
(O equatorial)					
$[Ru(\eta^3:\eta^3\text{-}C_{10}H_{16})Cl_2(NC_9H_6SH)]$ **102**	4.85 (s, 2H) 4.17 (s, 2H)[d]	5.16 (m, 2H)	3.24 (m, 2H) 2.54 (m, 2H)	2.33 (s, 6H)	7.38 (t, 1H, ^3J=8.1), 7.43 (d, 1H, ^3J=7.9), 7.58 (t, 1H, ^3J=7.8), 7.65 (m, 3H), 13.96 (s, 1H, S*H*)
$[Ru(\eta^3:\eta^3\text{-}C_{10}H_{16})Cl_2(NC_5H_3SH\text{-}6\text{-}Me)]$ **103**	4.80 (s, 2H) 4.16 (s, 2H)[d]	5.09 (m, 2H)	3.20 (m, 2H) 2.52 (m, 2H)	2.29 (s, 6H)	7.59 (d, 1H, ^3J=8.7), 7.25 (t, 1H, ^3J=8.5), 6.56 (d, 1H, ^3J=7.0), 2.35 (s, 3H, CH_3), 13.81 (s, 1H, S*H*)

[Ru(η^3:η^3-$C_{10}H_{16}$)Cl(NC_9H_6S)] **104a**	5.00 (s, 1H)	4.88 (m, 1H)	2.68 (m, 1H)	2.53 (s, 3H)	9.35 (d, 1H, ^3J=8.6), 7.70 (d, 1H, ^3J=8.7), 7.58 (d, 1H,
	4.57 (s, 1H)	4.06 (m, 1H)	2.49 (m, 3H)	2.36 (s, 3H)	^3J=7.0), 7.56 (t, 1H, ^3J=8.7), 7.33 (t, 1H, ^3J=8.0), 6.63 (d,
(N equatorial)	4.19 (s, 1H)				1H, ^3J=8.6)
	3.14 (s, 1H)				
[Ru(η^3:η^3-$C_{10}H_{16}$)Cl(NC_9H_6S)] **104b**	4.95 (s, 1H)	4.63 (m, 1H)	2.68 (m, 1H)	2.46 (s, 3H)	7.70 (d, 1H)[b], 7.56 (m, 2H), 7.50 (t, 1H, ^3J=6.9), 7.30 (d,
	4.49 (s, 1H)	4.43 (m, 1H)	2.49 (m, 3H)	2.05 (s, 3H)	1H, ^3J=8.7), 6.71 (d, 1H, ^3J=8.8)
(S equatorial)	4.31 (s, 1H)				
	3.45 (s, 1H)				
[Ru(η^3:η^3-$C_{10}H_{16}$)Cl(NC_5H_4S-6-Me)] **105a**	4.91 (s, 1H)	4.79 (m, 1H)	2.36 (m, 4H)	2.64 (s, 3H)	7.20 (t, 1H, ^3J=7.8), 6.49 (d, 1H, ^3J=7.6), 6.43 (d, 1H,
	4.45 (s, 1H)	3.96 (m, 1H)		2.31 (s, 3H)	^3J=8.2), 2.48 (s, 3H, CH_3)
(N equatorial)	4.15 (s, 1H)				
	3.10 (s, 1H)				
[Ru(η^3:η^3-$C_{10}H_{16}$)Cl(NC_5H_4S-6-Me)] **105b**	5.02 (s, 1H)	5.02 (t, 1H,	2.72 (m, 2H)	2.79 (s, 3H)	7.79 (t, 1H, ^3J=7.9), 7.25 (m, 2H), 2.48 (s, 3H, CH_3)
	4.88 (s, 1H)	^3J=3.9)	2.58 (m, 2H)	2.48 (s, 3H)	
(S equatorial)	4.65 (s, 1H)	4.66 (m, 1H)			
	3.88 (s, 1H)				

a) Solvent $CDCl_3$, δ / ppm, $J_{H\text{-}H}$ / Hz, 400 MHz, 20°C, s = singlet, d = doublet, dd = doublet of doublets, t = triplet, m = multiplet; b) coupling constant unmeasureable due to overlapping signals of major isomer; c) solvent $(CD_3)_2CO$; d) singlets noticably broader than those arising from other terminal allyl protons on the same molecule.

Table 4.2: Fractional atomic coordinates (x 10^4) and equivalent isotropic displacement factors ($Å^2$ x 10^3) for [Ru(η^3:η^3-$C_{10}H_{16}$)Cl(NC_5H_3O-6-Cl)] **97a**.

	x	y	z	U(eq)
Ru(1)	1896(1)	3798	5763(1)	34(1)
Cl(1)	2024(3)	5845(2)	5592(2)	51(1)
Cl(2)	-1071(6)	5917(4)	7002(2)	97(2)
N(1)	88(8)	3826(12)	6687(4)	50(2)
O(1)	1224(11)	2211(7)	6259(4)	60(2)
C(1)	-608(10)	3783(15)	5139(4)	49(2)
C(2)	800(10)	3695(12)	4615(4)	42(3)
C(3)	1904(12)	2728(8)	4757(6)	46(3)
C(4)	3572(15)	2528(12)	4347(5)	54(3)
C(5)	4938(12)	3403(10)	4566(6)	55(3)
C(6)	4596(10)	3930(12)	5312(5)	45(3)
C(7)	4638(13)	3283(10)	5981(6)	50(3)
C(8)	3977(10)	3926(14)	6596(4)	51(3)
C(9)	1113(14)	4573(11)	4045(6)	55(4)
C(10)	5103(19)	2038(12)	6050(7)	70(4)
C(11)	-924(13)	4446(12)	7145(6)	63(4)
C(12)	-1843(13)	3941(25)	7705(6)	79(7)
C(13)	-1728(18)	2740(19)	7782(7)	88(7)
C(14)	-710(18)	2108(13)	7319(6)	74(5)
C(15)	202(17)	2650(11)	6744(6)	64(4)

Table 4.3: Bond lengths (Å) and angles (°) for [Ru(η^3:η^3-$C_{10}H_{16}$)Cl(NC_5H_3O-6-Cl)] **97a**.

Ru(1)-Cl(1)	2.381 (3)	Ru(1)-N(1)	2.166 (6)
Ru(1)-O(1)	2.099 (8)	Ru(1)-C(1)	2.219 (8)
Ru(1)-C(2)	2.239 (8)	Ru(1)-C(3)	2.195 (10)
Ru(1)-C(6)	2.222 (8)	Ru(1)-C(7)	2.211 (10)
Ru(1)-C(8)	2.193 (8)	Ru(1)-C(15)	2.561 (12)
Cl(2)-C(11)	1.718 (15)	N(1)-C(11)	1.338 (15)
N(1)-C(15)	1.361 (18)	C(1)-C(15)	1.278 (14)
C(1)-C(2)	1.436 (11)	C(2)-C(3)	1.421 (15)
C(2)-C(9)	1.461 (16)	C(3)-C(4)	1.492 (14)
C(4)-C(5)	1.504 (16)	C(5)-C(6)	1.499 (14)
C(6)-C(7)	1.419 (15)	C(7)-C(8)	1.427 (15)
C(7)-C(10)	1.483 (18)	C(11)-C(12)	1.362 (19)
C(12)-C(13)	1.392 (36)	C(13)-C(14)	1.355 (21)
C(14)-C(15)	1.396 (17)		

Cl(1)-Ru(1)-N(1)	96.4(4)	Cl(1)-Ru(1)-O(1)	158.1(2)
N(1)-Ru(1)-O(1)	61.9(4)	Cl(1)-Ru(1)-C(1)	88.7(4)
N(1)-Ru(1)-C(1)	80.9(3)	O(1)-Ru(1)-C(1)	90.0(5)
Cl(1)-Ru(1)-C(2)	87.0(4)	N(1)-Ru(1)-C(2)	118.4(3)
O(1)-Ru(1)-C(2)	104.9(4)	C(1)-Ru(1)-C(2)	37.6(3)
Cl(1)-Ru(1)-C(3)	116.7(3)	N(1)-Ru(1)-C(3)	130.4(4)
O(1)-Ru(1)-C(3)	82.2(3)	C(1)-Ru(1)-C(3)	65.0(4)
C(2)-Ru(1)-C(3)	37.4(4)	Cl(1)-Ru(1)-C(6)	81.2(4)
N(1)-Ru(1)-C(6)	150.8(3)	O(1)-Ru(1)-C(6)	116.3(4)
C(1)-Ru(1)-C(6)	127.9(3)	C(2)-Ru(1)-C(6)	90.6(3)
C(3)-Ru(1)-C(6)	74.5(4)	Cl(1)-Ru(1)-C(7)	104.5(3)
N(1)-Ru(1)-C(7)	118.1(3)	O(1)-Ru(1)-C(7)	85.5(4)
C(1)-Ru(1)-C(7)	154.7(4)	C(2)-Ru(1)-C(7)	120.3(4)
C(3)-Ru(1)-C(7)	89.7(4)	C(6)-Ru(1)-C(7)	37.3(4)
Cl(1)-Ru(1)-C(8)	89.5(4)	N(1)-Ru(1)-C(8)	86.1(3)
O(1)-Ru(1)-C(8)	86.7(4)	C(1)-Ru(1)-C(8)	166.7(3)
C(2)-Ru(1)-C(8)	155.4(3)	C(3)-Ru(1)-C(8)	127.1(4)
C(6)-Ru(1)-C(8)	64.8(3)	C(7)-Ru(1)-C(8)	37.8(4)
Cl(1)-Ru(1)-C(15)	128.4(3)	N(1)-Ru(1)-C(15)	32.1(5)
O(1)-Ru(1)-C(15)	29.8(3)	C(1)-Ru(1)-C(15)	85.0(4)
C(2)-Ru(1)-C(15)	115.1(4)	C(3)-Ru(1)-C(15)	106.5(4)
C(6)-Ru(1)-C(15)	139.2(4)	C(7)-Ru(1)-C(15)	102.5(4)
C(8)-Ru(1)-C(15)	85.8(4)	Ru(1)-N(1)-C(11)	148.5(10)
Ru(1)-N(1)-C(15)	90.2(7)	C(11)-N(1)-C(15)	121.4(10)
Ru(1)-O(1)-C(15)	95.6(7)	Ru(1)-C(1)-C(2)	72.0(4)
Ru(1)-C(2)-C(1)	70.5(4)	Ru(1)-C(2)-C(3)	69.6(5)
C(1)-C(2)-C(3)	112.3(10)	Ru(1)-C(2)-C(9)	123.6(8)
C(1)-C(2)-C(9)	122.5(11)	C(3)-C(2)-C(9)	124.9(8)
Ru(1)-C(3)-C(2)	73.0(5)	Ru(1)-C(3)-C(4)	120.0(7)
C(2)-C(3)-C(4)	122.5(9)	C(3)-C(4)-C(5)	111.0(9)
C(4)-C(5)-C(6)	112.8(8)	Ru(1)-C(6)-C(5)	117.6(6)
Ru(1)-C(6)-C(7)	70.9(5)	C(5)-C(6)-C(7)	123.2(11)
Ru(1)-C(7)-C(6)	71.7(5)	Ru(1)-C(7)-C(8)	70.4(5)
C(6)-C(7)-C(8)	112.4(10)	Ru(1)-C(7)-C(10)	120.1(8)
C(6)-C(7)-C(10)	125.8(10)	C(8)-C(7)-C(10)	121.4(10)
Ru(1)-C(8)-C(7)	71.8(5)	Cl(2)-C(11)-N(1)	118.1(9)
Cl(2)-C(11)-C(12)	119.9(13)	N(1)-C(11)-C(12)	121.9(16)
C(11)-C(12)-C(13)	117.7(15)	C(12)-C(13)-C(14)	120.6(13)
C(13)-C(14)-C(15)	120.3(15)	Ru(1)-C(15)-N(1)	57.7(5)
Ru(1)-C(15)-O(1)	54.7(6)	N(1)-C(15)-O(1)	112.4(10)
Ru(1)-C(15)-C(14)	175.1(10)	N(1)-C(15)-C(14)	118.0(11)
O(1)-C(15)-C(14)	129.5(12)		

Table 4.4: Anisotropic displacement factors ($Å^2 \times 10^3$) for $[Ru(\eta^3:\eta^3\text{-}C_{10}H_{16})Cl(NC_5H_3O\text{-}6\text{-}Cl)]$ **97a**.

	U_{11}	U_{22}	U_{33}	U_{23}	U_{13}	U_{12}
Ru(1)	32(1)	31(1)	40(1)	0(1)	-1(1)	-3(1)
Cl(1)	60(2)	30(1)	64(1)	-3(1)	5(1)	-2(1)
Cl(2)	112(3)	100(3)	78(2)	-5(2)	28(2)	53(2)
N(1)	39(3)	66(5)	46(3)	18(6)	2(3)	-6(3)
O(1)	68(4)	45(4)	66(4)	4(4)	1(4)	-12(4)
C(1)	35(3)	57(4)	56(4)	-1(8)	-10(3)	-5(7)
C(2)	37(4)	43(5)	45(4)	2(5)	-12(3)	-17(5)
C(3)	43(5)	45(6)	49(5)	-16(4)	-8(4)	-6(4)
C(4)	53(6)	61(6)	49(5)	-18(5)	-4(4)	8(6)
C(5)	40(5)	77(8)	48(5)	-9(5)	6(4)	1(5)
C(6)	30(3)	49(6)	58(5)	-11(5)	0(3)	-3(5)
C(7)	43(5)	56(5)	50(5)	-11(5)	-10(4)	10(5)
C(8)	43(4)	65(7)	43(4)	-13(6)	-12(3)	0(6)
C(9)	53(6)	68(7)	45(5)	11(5)	-4(4)	16(5)
C(10)	77(8)	75(8)	57(6)	-1(6)	4(6)	22(7)
C(11)	41(5)	100(9)	47(5)	6(6)	5(5)	4(5)
C(12)	49(5)	133(18)	54(6)	-3(9)	5(4)	-1(9)
C(13)	75(9)	151(18)	39(6)	26(8)	-5(6)	-38(9)
C(14)	88(9)	86(10)	48(6)	20(6)	-1(7)	-37(8)
C(15)	73(8)	54(6)	64(7)	16(5)	-5(6)	-27(6)

Table 4.5: Fractional atomic coordinates (x 10^4) and equivalent isotropic displacement factors ($Å^2$ x 10^3) for [Ru(η^3:η^3-$C_{10}H_{16}$)Cl(NC_9H_6S)] **104.**

	x	y	z	U(eq)
Ru(1)	2539(1)	842(1)	2926(1)	34(1)
S(1)	1601(2)	1212(2)	4190(1)	55(1)
Cl(1)	3717(2)	-113(2)	1950(1)	61(1)
N(1)	2364(5)	-601(4)	3765(4)	44(2)
C(1)	619(7)	211(6)	1946(5)	54(3)
C(2)	936(7)	1167(6)	1551(5)	50(2)
C(3)	1014(6)	2061(6)	2170(5)	49(2)
C(4)	1517(8)	3168(6)	2016(6)	66(3)
C(5)	2973(8)	3144(6)	2016(5)	62(3)
C(6)	3727(7)	2185(5)	2593(5)	50(2)
C(7)	4069(6)	2102(6)	3618(5)	50(2)
C(8)	4567(7)	1101(6)	4000(6)	59(3)
C(9)	1208(9)	1233(7)	580(5)	66(3)
C(10)	3841(8)	2997(6)	4239(6)	56(3)
C(11)	1892(6)	-144(6)	4435(4)	47(2)
C(12)	1653(8)	-696(6)	5195(5)	60(3)
C(13)	1894(8)	-1765(7)	5265(5)	67(3)
C(14)	2342(7)	-2304(6)	4565(6)	60(3)
C(15)	2555(9)	-3421(7)	4580(7)	74(3)
C(16)	2954(10)	-3910(7)	3892(8)	84(4)
C(17)	3155(8)	-3325(7)	3136(7)	76(4)
C(18)	2959(8)	-2217(6)	3092(6)	63(3)
C(19)	2561(7)	-1715(5)	3801(5)	50(2)

Table 4.6: Bond lengths (Å) and angles (°) for [Ru(η^3:η^3-$C_{10}H_{16}$)Cl(NC_9H_6S)] **104.**

Ru(1)-S(1)	2.386 (2)	Ru(1)-Cl(1)	2.461 (2)
Ru(1)-N(1)	2.221 (5)	Ru(1)-C(1)	2.209 (6)
Ru(1)-C(2)	2.206 (6)	Ru(1)-C(3)	2.229 (6)
Ru(1)-C(6)	2.231 (7)	Ru(1)-C(7)	2.245 (6)
Ru(1)-C(8)	2.225 (7)	S(1)-C(11)	1.741 (7)
N(1)-C(11)	1.351 (9)	N(1)-C(19)	1.408 (8)
C(1)-C(2)	1.412 (10)	C(2)-C(3)	1.422 (10)
C(2)-C(9)	1.529 (11)	C(3)-C(4)	1.523 (11)
C(4)-C(5)	1.519 (12)	C(5)-C(6)	1.533 (10)
C(6)-C(7)	1.426 (10)	C(7)-C(8)	1.403 (10)
C(7)-C(10)	1.504 (11)	C(11)-C(12)	1.392 (11)
C(12)-C(13)	1.360 (12)	C(13)-C(14)	1.419 (12)
C(14)-C(15)	1.414 (11)	C(14)-C(19)	1.412 (11)
C(15)-C(16)	1.347 (16)	C(16)-C(17)	1.391 (16)
C(17)-C(18)	1.400 (11)	C(18)-C(19)	1.380 (12)

S(1)-Ru(1)-Cl(1)	160.0(1)	S(1)-Ru(1)-N(1)	67.0(2)
Cl(1)-Ru(1)-N(1)	93.7(2)	S(1)-Ru(1)-C(1)	93.4(2)
Cl(1)-Ru(1)-C(1)	88.3(2)	N(1)-Ru(1)-C(1)	81.4(2)
S(1)-Ru(1)-C(2)	106.7(2)	Cl(1)-Ru(1)-C(2)	86.5(2)
N(1)-Ru(1)-C(2)	118.7(2)	C(1)-Ru(1)-C(2)	37.3(3)
S(1)-Ru(1)-C(3)	81.2(2)	Cl(1)-Ru(1)-C(3)	117.1(2)
N(1)-Ru(1)-C(3)	131.3(2)	C(1)-Ru(1)-C(3)	64.2(2)
C(2)-Ru(1)-C(3)	37.4(3)	S(1)-Ru(1)-C(6)	114.4(2)
Cl(1)-Ru(1)-C(6)	80.1(2)	N(1)-Ru(1)-C(6)	151.7(2)
C(1)-Ru(1)-C(6)	125.6(2)	C(2)-Ru(1)-C(6)	88.8(2)
C(3)-Ru(1)-C(6)	74.7(2)	S(1)-Ru(1)-C(7)	85.6(2)
Cl(1)-Ru(1)-C(7)	100.8(2)	N(1)-Ru(1)-C(7)	119.6(2)
C(1)-Ru(1)-C(7)	156.1(2)	C(2)-Ru(1)-C(7)	120.5(3)
C(3)-Ru(1)-C(7)	92.1(2)	C(6)-Ru(1)-C(7)	37.2(3)
S(1)-Ru(1)-C(8)	87.7(2)	Cl(1)-Ru(1)-C(8)	86.5(2)
N(1)-Ru(1)-C(8)	87.5(2)	C(1)-Ru(1)-C(8)	167.3(3)
C(2)-Ru(1)-C(8)	153.3(3)	C(3)-Ru(1)-C(8)	128.4(3)
C(6)-Ru(1)-C(8)	64.7(3)	C(7)-Ru(1)-C(8)	36.6(2)
Ru(1)-S(1)-C(11)	83.2(3)	Ru(1)-N(1)-C(11)	99.5(4)
Ru(1)-N(1)-C(19)	142.2(5)	C(11)-N(1)-C(19)	118.4(6)
Ru(1)-C(1)-C(2)	71.2(4)	Ru(1)-C(2)-C(1)	71.5(3)
Ru(1)-C(2)-C(3)	72.2(3)	C(1)-C(2)-C(3)	112.5(7)
Ru(1)-C(2)-C(9)	122.8(5)	C(1)-C(2)-C(9)	123.9(6)
C(3)-C(2)-C(9)	123.6(7)	Ru(1)-C(3)-C(2)	70.4(4)
Ru(1)-C(3)-C(4)	118.0(4)	C(2)-C(3)-C(4)	125.2(7)
C(3)-C(4)-C(5)	111.9(6)	C(4)-C(5)-C(6)	110.9(7)
Ru(1)-C(6)-C(5)	119.0(5)	Ru(1)-C(6)-C(7)	72.0(4)
C(5)-C(6)-C(7)	123.2(6)	Ru(1)-C(7)-C(6)	70.9(4)
Ru(1)-C(7)-C(8)	70.9(4)	C(6)-C(7)-C(8)	114.8(7)
Ru(1)-C(7)-C(10)	124.6(5)	C(6)-C(7)-C(10)	122.7(6)
C(8)-C(7)-C(10)	122.4(7)	Ru(1)-C(8)-C(7)	72.5(4)
S(1)-C(11)-N(1)	110.2(5)	S(1)-C(11)-C(12)	125.7(6)
N(1)-C(11)-C(12)	124.1(7)	C(11)-C(12)-C(13)	118.3(8)
C(12)-C(13)-C(14)	120.5(8)	C(13)-C(14)-C(15)	123.0(8)
C(13)-C(14)-C(19)	119.3(7)	C(15)-C(14)-C(19)	117.7(8)
C(14)-C(15)-C(16)	121.4(9)	C(15)-C(16)-C(17)	120.5(8)
C(16)-C(17)-C(18)	120.1(10)	C(17)-C(18)-C(19)	119.4(8)
N(1)-C(19)-C(14)	119.2(7)	N(1)-C(19)-C(18)	119.9(7)
C(14)-C(19)-C(18)	120.9(6)		

Table 4.7: Anisotropic displacement factors (Å x 10^3) for $[Ru(\eta^3:\eta^3\text{-}C_{10}H_{16})Cl(NC_9H_6S)]$ **104**.

	U_{11}	U_{22}	U_{33}	U_{23}	U_{13}	U_{12}
Ru(1)	37(1)	29(1)	37(1)	1(1)	11(1)	0(1)
S(1)	73(1)	47(1)	53(1)	-6(1)	31(1)	0(1)
Cl(1)	76(1)	46(1)	72(1)	-2(1)	40(1)	6(1)
N(1)	52(3)	29(3)	45(3)	4(2)	8(2)	-3(2)
C(1)	44(4)	54(4)	54(4)	1(3)	1(3)	-13(3)
C(2)	49(4)	48(4)	44(4)	5(3)	2(3)	-2(3)
C(3)	40(3)	54(4)	49(4)	11(3)	8(3)	7(3)
C(4)	74(5)	42(4)	73(5)	0(4)	9(4)	10(4)
C(5)	79(5)	45(4)	55(4)	7(3)	13(4)	-9(4)
C(6)	48(4)	42(4)	60(4)	7(3)	18(3)	-10(3)
C(7)	34(3)	47(4)	60(4)	-3(3)	-1(3)	-9(3)
C(8)	46(4)	52(4)	64(5)	8(3)	-5(3)	-5(3)
C(9)	91(6)	56(5)	45(4)	7(3)	11(4)	-4(4)
C(10)	82(5)	44(4)	67(5)	-11(4)	17(4)	-17(4)
C(11)	39(3)	62(4)	39(3)	1(3)	12(3)	-12(3)
C(12)	65(5)	60(5)	52(4)	-3(3)	14(4)	-18(4)
C(13)	60(4)	77(6)	54(5)	24(4)	5(4)	-22(4)
C(14)	45(4)	59(5)	64(5)	18(4)	1(3)	-14(3)
C(15)	68(5)	53(5)	83(6)	28(5)	-1(4)	-3(4)
C(16)	73(6)	36(4)	129(9)	13(5)	13(6)	-4(4)
C(17)	64(5)	46(4)	115(7)	-1(5)	25(5)	6(4)
C(18)	72(5)	33(4)	84(5)	-7(3)	27(4)	-1(3)
C(19)	47(4)	29(3)	65(4)	5(3)	4(3)	-5(3)

Chapter 5

Bi- and Trinuclear Complexes of Ruthenium(IV)

5.1 Introduction

Mention has already been made of the diastereoisomerism inherent in binuclear complexes such as **6**, containing the chiral "Ru(η^3:η^3-$C_{10}H_{16}$)" fragment (see Chapter 2). Cox and Roulet[17] have demonstrated by isolation of the C_i diastereoisomer of **6** (**6a**, observed crystallographically[13]) and assignment of its ^{1}H NMR spectrum, that the isomer of C_2 molecular symmetry (**6b**) is slightly more stable in solution at 25°C; $K_{25} = [C_2]/[C_i] = 1.25$. The two compounds interconvert at room temperature, although this process is slow on the ^{1}H NMR timescale [rate constant, $k_{25} = (3 \pm 2) \times 10^{-1}$ s^{-1}, $\Delta G^{\ddagger}_{25} = 76 \pm 2$ kJ mol^{-1}]. Other binuclear compounds reported in Chapter 2 also exhibit diastereoisomerism to a greater or lesser extent. In this section a range of binuclear compounds has been prepared and their diastereoisomerism studied in detail. In addition, the possibility of electron transfer between two "Ru(η^3:η^3-$C_{10}H_{16}$)" fragments is studied by the construction of binuclear compounds with π-delocalised bridging ligands and their examination by cyclic voltammetry.

5.2 Bridge Cleavage Reactions

5.2.1 Reaction with Pyrazene

Reaction of **6** with a single mole equivalent of pyrazene (pyz) in CH_2Cl_2 at room temperature results in the immediate formation of a bright orange solution from which the pyrazene bridged binuclear complex [{Ru(η^3:η^3-$C_{10}H_{16}$)Cl_2}$_2$(μ-pyz)] **106** may be isolated.* The ^{1}H and ^{13}C-{^{1}H} NMR spectra of **106** clearly demonstrate that, in solution, the material exists in two diastereomeric forms analogous to the C_i (*meso*) and C_2 (*rac*) isomers of **6**,[17] although the linear bridge geometry results in the analogous forms of **106** possessing approximate C_{2h} and D_2 symmetries (*meso* and *rac* respectively). For the sake of convenience and consistency these materials will be referred to as "C_i" and "C_2" isomers. The ^{1}H NMR spectrum of a mixture of the C_i and C_2 forms of **106** (Fig. 5.1) thus

* During the course of this work complex **106** was also reported independently by Toerien and van Rooyen.[158]

displays two singlet resonances (δ 9.32 and 9.24 ppm, each 4H) corresponding to the pyrazene protons of the two diastereoisomers. Similarly, each isomer displays two singlet resonances due to the terminal allyl protons (δ 4.66, 4.34, C_2 and 4.61, 4.39 ppm, C_i). In the ^{13}C-{^1H} NMR spectrum the resonances assigned to the pyrazene carbon atoms in the two isomers occur at δ 149.43 and 149.20 ppm. Likewise twice as many signals as would have been expected for a non-diastereomeric material are observed for the carbon atoms of the *bis*(allyl) ligand.

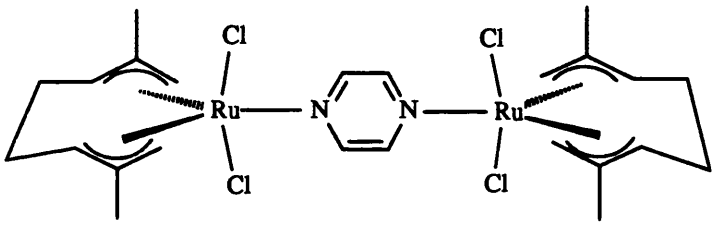

106

The geometry of **106** was confirmed by a single crystal X-ray study, Fig. 5.2. The structure determination (of the chloroform solvate) shows that in the crystal the complex possesses C_i type symmetry, as does **6**. In general the structure is similar to those reported elsewhere in this thesis with the usual distorted trigonal bipyramidal geometry about the metal ion and local C_2 symmetry of the *bis*(allyl) ligand. The angle Cl(1)-Ru-Cl(2), 170.2(1)°, is an example of the expected "unconstrained" distortion of the L_{axial}-Ru-L_{axial} vector. Such small distortions away from the ideal 180° are probably caused by unfavourable chloride-methyl steric interactions. More acute angles are observed in "constrained" systems where factors such as the bite angle of chelating ligands also play a part, *e.g.* [Ru(η^3:η^3-$C_{10}H_{16}$)Cl(O_2CCMe)] **72** and [Ru(η^3:η^3-$C_{10}H_{16}$)Cl(bipy)][BF_4] **64** [respectively 154.4(2)° (Chapter 3) and 166.9(2)° (Chapter 2)]. The Ru-N(1) distance is long, 2.19(1) Å, in comparison both to the range of pyrazene bridged compounds [$(NH_3)_5$Ru(μ-pyz)Ru$(NH_3)_5$]$^{n+}$ (n = 4, 5, 6)[149] of 1.99 - 2.11 Å and even the Ru-OH_2 bond length in the trifluoroacetato compound **73**, 2.146(4) Å although it is comparable to that observed for the *bis*(pyrazene)(arene)ruthenium(II) complex [Ru(η^6-*p*-$MeC_6H_4CHMe_2$)Cl$(pyz)_2$][PF_6], 2.17 Å.

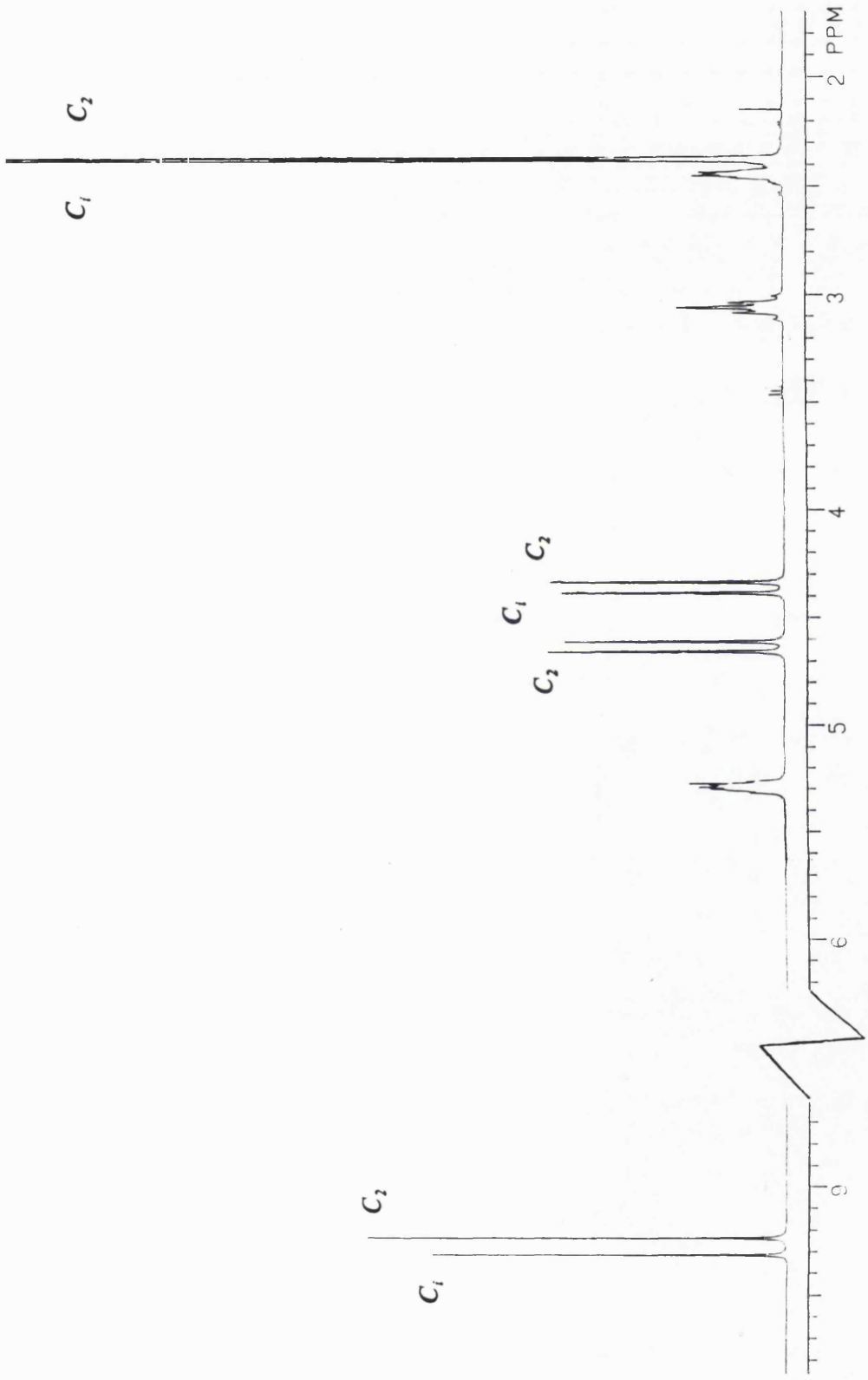

Fig. 5.1: Room temperature ^{1}H NMR spectrum of $[\{Ru(\eta^3:\eta^3\text{-}C_{10}H_{16})Cl_2\}_2(\mu\text{-}N_2C_4H_4)]$ **106** showing the peak assignment to the C_1 and C_2 forms.

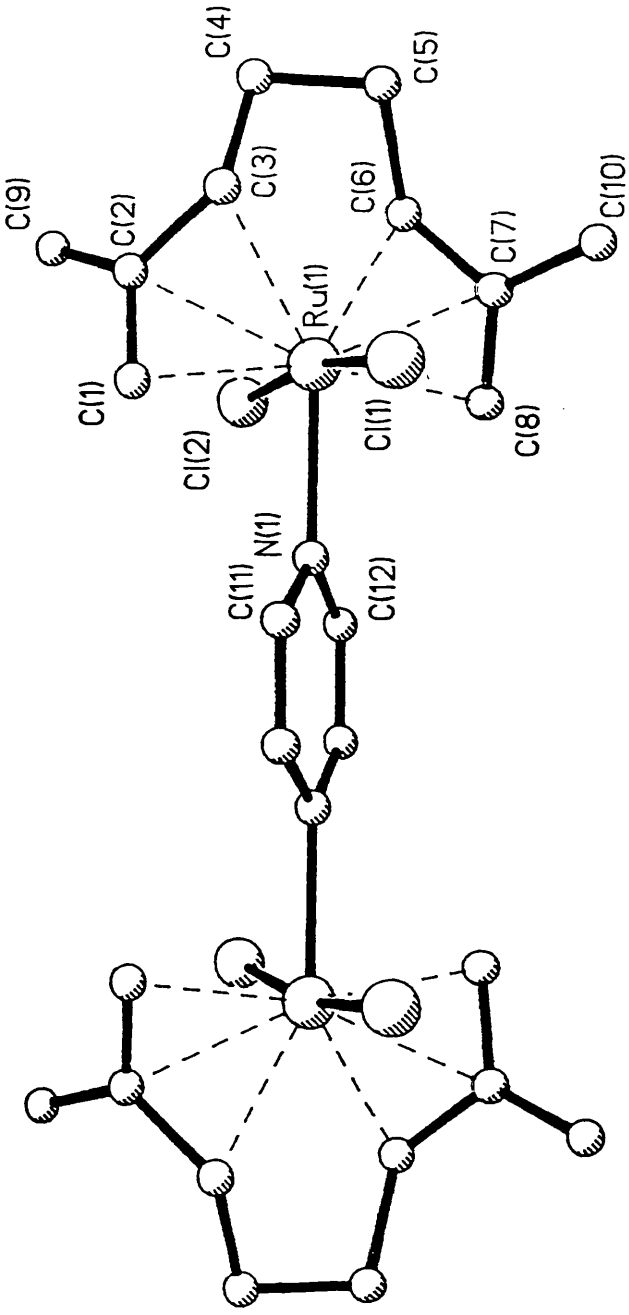

Fig. 5.2: Crystal structure of *meso*-[{Ru(η^3:η^3-$C_{10}H_{16}$)Cl_2}$_2$(μ-$N_2C_4H_4$)] **106a** showing the atom numbering scheme adopted.

Crystals of **106** grown from a chloroform / diethyl ether solution, were dissolved in $CDCl_3$ cooled in a toluene / solid CO_2 slush and the ^1H NMR spectrum of the sample immediately recorded (-60°C). Under these conditions only half the number of resonances present in the room temperature spectrum were observed indicating the presence of only a single diastereoisomer (the *meso* form of approximate C_i symmetry). This experiment thus allowed unequivocal assignment of the signals observed in the room temperature spectrum, Table 5.1. At room temperature (20°C) the ^1H NMR spectrum of the crystalline sample displayed resonances corresponding to two diastereoisomers as before, K_{20} = [*rac*]/[*meso*] = 1.14 (*cf.* 1.25 in the case of **6**[17]). This is interpreted in terms of an *intermolecular* exchange between the *meso* and *rac* forms of **106**. At higher temperatures (above *ca.* 50°C) the signals for the two diastereoisomers are observed to broaden and merge to produce a single, averaged set of resonances.[158] It seems likely that this is due to rapid Ru-N bond fission and interchange of chiral "(η^3:η^3-$C_{10}H_{16}$)Ru" units between isomers, as opposed to an increase in the rate of rotation about the Ru-N single bond suggested by Toerien and van Rooyen,[158] which is presumably rapid over all the temperature ranges studied. Diastereoisomers may only interconvert by a change in handedness at one of the chiral centres responsible for the isomerism. For this process to occur intramolecularly would require breakage of the metal carbon bonds between the ruthenium ion and the *bis*(allyl) ligand and re-complexation with the metal situated on the opposite faces of the allylic functionalities, a process for which we have never found any evidence. This suggestion is further supported by the fluxionality observed in the triazine complexes **108**, **109** and **110** (*vide infra*).

In contrast to the straightforward isolation of **106**, the mononuclear adduct [Ru(η^3:η^3-$C_{10}H_{16}$)Cl_2(pyz)] **107** has only been observed by us in solution, by ^1H NMR spectroscopy, in the presence of *ca.* 15 mole equivalents of free pyrazene. In **107** the two singlet resonances of the pyrazene ligand in **106** are replaced by an AA'BB' pattern [δ 9.29 and 8.63 ppm, $^3J_{H\text{-}H}$ = 3.25, $^5J_{H\text{-}H}$ = 1.0 Hz (*cf.* the multiplet resonance centred on 8.72 observed for the terminal *bis*(pyrazene) complex [Ru(η^6-C_6H_6)Cl(pyz)$_2$][PF_6][55])]. The relative instability of **107** with respect to disproportionation into free pyrazene and **106** has also been noted by Toerien and van Rooyen who estimate[158] the equilibrium constant for the process to be *ca.* 6.8 at ambient temperatures.

The observation of two metal centres linked by a delocalised π-electron ligand raises the possibility of electronic interactions between the two metal ions. The degree of communication might, in favourable circumstances, be estimated by the cyclic voltammetric response of the compound. Consequently the cyclic voltammogram of **106** was examined (CH_2Cl_2 / $[^nBu_4N][BF_4]$). A single, irreversible reduction was observed (*ca.* -1.12 V, vs. Ag / AgCl) over a variety of scan speeds (50 - 500 mV s^{-1}). On the return scan a coupled irreversible oxidation was apparent (+0.53 V). Such behaviour is suggestive of an ECE process but implies that there is no reversible electron transfer between the two metal centres. Hence the behaviour of **106** differs markedly from the rich electrochemistry of the class of mixed valence complexes $[(NH_3)_5Ru(\mu\text{-pyz})Ru(NH_3)_5]^{n+}$ (n = 4, 5, 6).[149] We have also established that the parent complex **6** exhibits two irreversible reductions at -0.63 and -0.87 V (ν = 200 mV s^{-1}) and an irreversible oxidation on the return scan (+0.88 V). Such behaviour is consistent with the observed irreversible chemical reduction of **6** to solvated ruthenium(II) ions by action of $Ag[BF_4]$ in alcoholic solvents, reported by Cox and Roulet.[114]

5.2.2 Reaction with 1,3,5-Triazine

In contrast to the ready formation of **106** by reaction with pyrazene, interaction of **6** with 1,3,5-triazine (tra) leads to a mixture of products, *viz* $[Ru(\eta^3{:}\eta^3\text{-}C_{10}H_{16})Cl_2(tra)]$ **108**, $[\{Ru(\eta^3{:}\eta^3\text{-}C_{10}H_{16})Cl_2\}_2(\mu^2\text{-tra})]$ **109** and $[\{Ru(\eta^3{:}\eta^3\text{-}C_{10}H_{16})Cl_2\}_3(\mu^3\text{-tra})]$ **110**. Fractional crystallisation of this mixture by slow diffusion of diethyl ether into a chloroform solution led to the isolation of a pure sample of the trinuclear complex **110**. At room temperature the ^1H NMR spectrum ($CDCl_3$) of **110** displays a single broad resonance (δ 10.70 ppm) due to the protons of the triazine ligand and two broad terminal allyl signals (δ 4.91 and 4.46 ppm) consistent with the presence of only one diastereoisomer. Lowering the temperature of the NMR probe causes the resonances to split until, at -50°C, four sharp singlet resonances of approximately equal intensity are observed in the triazine region of the spectrum (δ 10.53, 10.52, 10.47 and 10.40 ppm) consistent with the appearance of four isomeric forms of **110**.

The binuclear complex **109** is more readily isolated than **110** (short reaction time and 1 : 1 mole ratio of **6** to triazine). Like **6**, the ^1H NMR spectrum of complex **109**

displays broad lines at room temperature, ostensibly consistent with the presence of a single diastereoisomer [*e.g.* δ 10.64 (s, 1H) and 9.85 (s, 2H) ppm]. At -50°C however, the peaks are resolved and reveal the presence of two diastereoisomers (δ 10.52, 10.39 and 9.81, 9.75 ppm), analogous to those of **106.**

Treatment of **6** with excess triazine over several hours, gives a mixture of **109, 110** and a third complex, which displays two new peaks in the triazine region of its ^{1}H NMR spectrum (δ 9.87 and 9.21 ppm, 2H and 1H respectively) which do not split at low temperature. These signals are ascribed to the mononuclear adduct [Ru(η^3:η^3-$C_{10}H_{16}$)Cl_2(tra)] **108.**

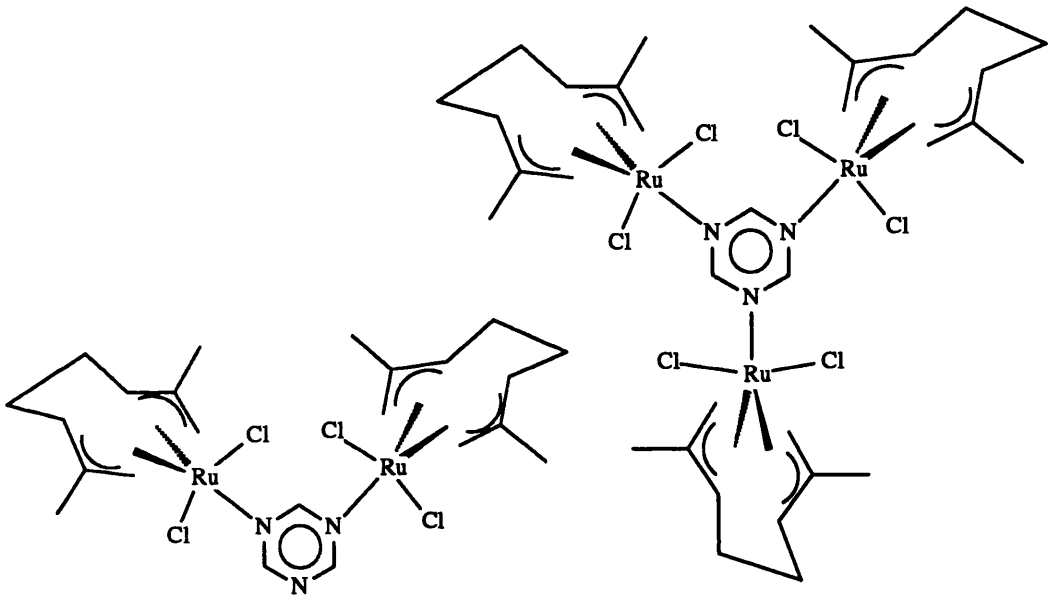

109 **110**

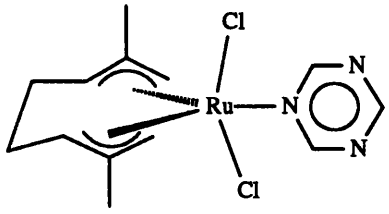

108

On warming an NMR sample containing a mixture of **108, 109,** and **110,** to 55°C the triazine signals broaden further and eventually merge into the baseline. The upfield region of the spectrum is more informative however, with coalescence clearly occurring

between all three sets of allyl resonances to give an averaged spectrum exhibiting only two terminal allyl signals (δ 4.81 and 4.29 ppm), one internal allyl resonance (δ 5.19 ppm), two ethylenic multiplets (δ 2.98 and 2.47 ppm) and a single methyl resonance (δ 2.40 ppm).

The coalescence of the signals for all three complexes present is due to intermolecular exchange of "(η^3:η^3-$C_{10}H_{16}$)Ru" units such that not only are the diastereomeric forms of one complex averaged, but the mono-, bi- and trinuclear species themselves are in dynamic equilibrium with each other. The observed temperature dependence is analogous to that observed for **106**[158] and lends strong support to the suggestion that such an intermolecular exchange is also occurring for that complex, albeit as a slightly slower rate, presumably as a consequence of the better donor abilities of the pyrazene ligand, or reduced steric crowding.

5.2.3 Synthesis and Electrochemistry of Mixed Valence Compounds

In view of the limited electrochemical activity displayed by **106** we attempted the synthesis of the mixed valence, pyrazene bridged ruthenium complexes such as the Ru(IV)-Ru(II) complexes [(η^3:η^3-$C_{10}H_{16}$)Cl_2Ru(μ-pyz)RuCl_2(η^6-arene)] (arene = benzene, **111a**; *p*-cymene, **111b**) in the hope that they might display a more versatile electrochemistry. The preparation of **111a** and **111b** proved tedious because of the limited availability of monodentate pyrazene precursors to such compounds. Also it is known that the complexes [Ru(η^6-arene)Cl(pyz)$_2$][PF_6] display a very limited reactivity of the non-complexed pyrazene nitrogen atoms.[55]

In attempting to prepare a complex of type **111** efforts were made to optimise the conditions necessary for the formation of the mixed valence species, as opposed to **106** and known[55] Ru(II)-Ru(II) pyrazene bridged complexes such as [{Ru(*p*-$MeC_6H_4CHMe_2$)Cl_2}$_2$(μ-pyz)] **112**. To this end the ruthenium(II) *p*-cymene complex [Ru(*p*-$MeC_6H_4CHMe_2$)Cl_2(pyz)] **113** was chosen as the precursor because of the greater solubility in organic solvents conferred by the alkylated arene (more comparable with that of complex **6**). A crude sample of **113** was treated with a small excess of **6** in toluene and the mixture stirred at room temperature for half an hour to give a brown precipitate which was found to be an approximately equimolar mixture of **111b** and **112**. A pure sample of **111b** was obtained by fractional crystallisation (see experimental section).

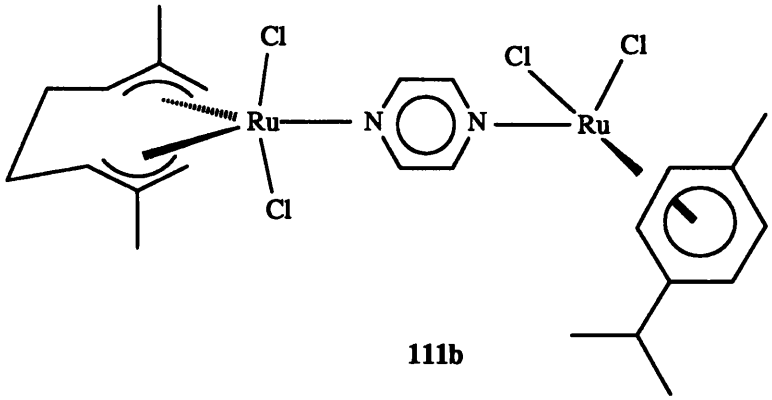

111b

In contrast to **106** and **112**, the pyrazene resonances in the ^{1}H NMR spectrum of **111b** do not appear as singlets but rather as an AA'BB' pattern (δ 8.99, 8.83 ppm, $^3J_{H\text{-}H}$ = 5.3, $^5J_{H\text{-}H}$ = 1.5) similar to that observed for the adduct **107** and indicative of the inequivalence of the two termini of the complex.

Disappointingly, the cyclic voltammogram of **111b** proved to be similar to that of **106** with a single irreversible reduction at *ca.* -1.44 V (ν = 400 - 100 mV s^{-1}) and irreversible oxidations observed at +1.08 and +1.35 V. This observation would seem to indicate that the complex is a class I mixed valence species with each metal ion in a discrete oxidation state (+2 or +4) with no interaction between them on the cyclic voltammetric timescale, in spite of the delocalised bonding in the bridging ligand. Complex **111b** is thus electronically analogous to the diphenylphosphinomethane ($Ph_2PCH_2PPh_2$, dppm) bridged mixed valence complex $[(\eta^6\text{-}C_6H_6)Cl_2Ru(\mu\text{-dppm})RuCl_2(\eta^3\text{:}\eta^3\text{-}C_{10}H_{16})]$ prepared by Toerien and van Rooyen.[158]

5.3 Reaction with Silver Thiocyanate

In alcoholic solvents the chloro-bridged dimer **6** is reduced to solvated Ru^{2+} ions by the action of $Ag[BF_4]$.[114] However, in less reducing media the abstraction of chloride ions results in the formation of stable solutions containing the "$(\eta^3\text{:}\eta^3\text{-}C_{10}H_{16})RuCl^+$" and "$(\eta^3\text{:}\eta^3\text{-}C_{10}H_{16})Ru^{2+}$" moieties, which readily react with Lewis bases such as nitriles[161] and

polypyridines (Chapter 2). Other silver salts will also abstract halide ions from **6** and, if the counterion is a coordinating one, it can be directly introduced onto the metal centre. In mixed acetone / water solvent, over short reaction times, Ag[SCN] reacts with **6** to give a yellow material, $[\{Ru(\eta^3:\eta^3\text{-}C_{10}H_{16})Cl(\mu\text{-}SCN)\}_2]$ **114**, in *ca* 50% yield, displaying a ν(CN) band at 2141 cm^{-1} in the solid state infrared spectrum, indicative of an S,N-bridged complex[193] [*cf.* $[Bu_4N]_2[Re_2(NCS)_6(PEt_2Ph)_2(\mu\text{-}SCN)_2]$, ν(CN) = 2120 (bridging), 2070, 2048 and 2025 (terminal) cm^{-1}, $[Bu_4N]_2[Re(NCS)_3(PEt_2Ph)(dppe)]$ ν(CN) = 2080, 2020 and 1995 (terminal) cm^{-1} [203]]. The binuclear nature of the complex was confirmed by an electron impact mass spectrum which showed a molecular ion peak at m/z 662 ($[C_{22}H_{32}Cl_2N_2Ru_2S_2]^+$) with an isotope distribution characteristic of two ruthenium and two chlorine atoms. The ^1H NMR spectrum of this material showed a typical eight line pattern for the terminal allyl protons of the dimethyloctadienediyl ligand (δ 4.81, 4.77, 4.70, 4.65, 4.13, 4.05, 3.68 and 3.56 ppm) and four line pattern for the methyl groups (δ 2.35, 2.29, 2.26 and 2.26 ppm) similar to that observed[17] for the parent compound **6**, and characteristic of a binuclear, diastereomeric material with inequivalent axial sites on the distorted trigonal bipyramidal ruthenium ions. Over reaction times of several hours the product displayed progressively less of one subset of these signals until, after 24h, the spectrum contained predominantly only four terminal allyl signals (δ 4.81, 4.65, 4.05 and 3.68 ppm) and two methyl resonances (δ 2.29 and 2.26 ppm) consistent with the survival of only one of the diastereoisomers. In order to characterise fully this material a single crystal structure determination was undertaken.

Fractional crystallisation of a reaction mixture containing **114** gave a single isomer (NMR evidence) a crystal of which was examined by X-ray diffraction. The results of that study show, in contrast to those on **6**,[13] and **106**, the isomer in the crystal to be of C_2 symmetry (Fig. 5.3). The molecule consists of two distorted trigonal bipyramidal ruthenium ions with two of the equatorial coordination sites occupied by the *bis*(allyl) ligand which exhibits the usual local C_2 symmetry[13,158,161] and one axial site occupied by a chloride ligand, Ru-Cl 2.409(3) and 2.412(3) Å. The two ruthenium ions are linked by two S,N-bound thiocyanate bridges, Ru-S 2.490(4) and 2.483(4) Å, Ru-N 2.039(8) and 2.004(8) Å, with the more bulky sulphur atoms occupying the less hindered, equatorial coordination

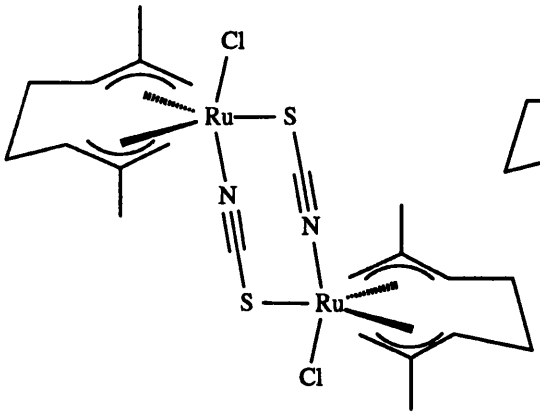

114a

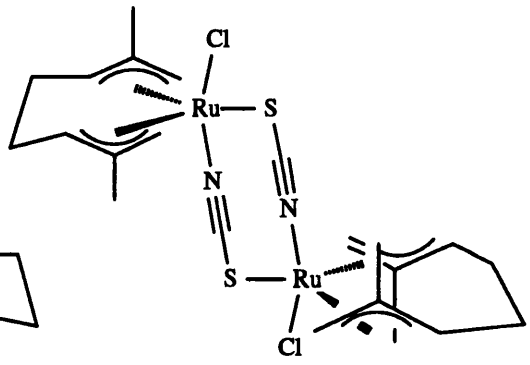

114b

site.

In contrast to most, if not all, other structures containing two thiocyanate ligands bridging a pair of metal ions[204-206] the two halves of the molecule in **114b** are not related by a crystallographic inversion centre because the atoms of the thiocyanate bridge do not lie in the same plane. Instead, a puckered "butterfly" type conformation is adopted by the eight-membered ring. This results in a torsion angle in the Cl-Ru-Ru-Cl linkage which deviates from the ideal value 180° by 9.4°. It has been suggested[204,207,208] that π-overlap renders a planar conformation for thiocyanate bridged structures significantly more stable and it therefore seems likely that it is the large steric requirement of the dimethyloctadienediyl ligand which, in this instance, causes the distortions from planarity. Steric interactions between the methyl substituents on the *bis*(allyl) ligand and the axial chloride ligands cause a significant reduction in the Cl-Ru-(equatorial ligand) angle in all compounds of this type[13,158,161] and the Cl-Ru-S angles in this case are significantly compressed, 80.3(1)° and 80.7(1)°, in spite of the bulk of the sulphur atom. The corresponding angle in the pyrazene compound **106**, (Cl-Ru-N) is 85.4(2)°. The puckering of the ring system is thus due to the increased Cl-S interactions which, synergically, cause further chloride / methyl interactions.

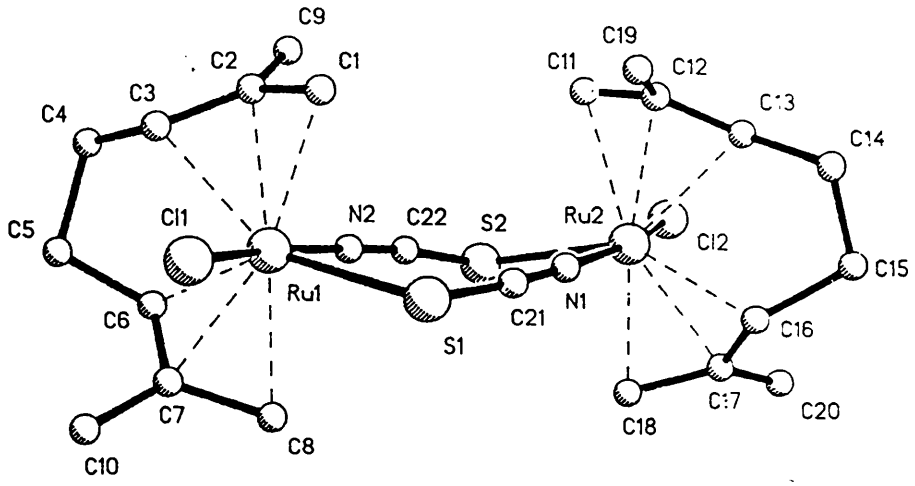

Fig. 5.3: Crystal structure of *rac*-[{Ru(η^3:η^3-$C_{10}H_{16}$)Cl(μ-SCN)}$_2$] **114b** showing the atom labelling scheme adopted.

From these observations it is easy to rationalise the thermodynamic preference for the C_2 isomer. The chloride ligands are constrained by the geometry of the "Ru(SCN)$_2$Ru" unit to adopt a transoid configuration and, in the *rac* form, their out of plane distortion is angled away from the methyl groups of the *bis*(allyl) ligand. In the C_i isomer the opposite effect would be in evidence and so give rise to greater unfavourable chloride / methyl steric interactions which destabilise the *meso*, **114a**, form.

Low temperature dissolution of crystalline **114b** allowed the unequivocal assignment of the resonances observed in the room temperature ^{1}H NMR spectrum. Attempts were also made to crystallise the less stable C_i isomer **114a** in order to compare the distortions within the "Ru$_2$(SCN)$_2$" ring. A second set of crystals (yellow-orange, needle-like plates) was obtained and characterised by X-ray crystallography. Surprisingly this sample proved to be

this sample proved to be of an allotrope (monoclinic form) of **114b**, and not **114a** as hoped. Representative crystal packing diagrams for both allotropes are shown in Fig. 5.4. The triclinic structure adopts an arrangement in the solid state in which adjacent molecules lie parallel to one another, resulting in no significant intermolecular contacts (sulphur-to-sulphur distance in excess of 7 Å). In contrast the monoclinic form exhibits a "herring bone" packing arrangement resulting in significantly closer intermolecular approaches, *e.g.* an intermolecular sulphur-sulphur contact of 3.55 Å. Reassuringly, in spite of these very different packing arrangements, the puckered "butterfly" conformation observed for triclinic **114b** is also present in the monoclinic form; torsion angle Cl-Ru-Ru-Cl 173.8° (*cf.* 170.4° in the triclinic form). Other intramolecular bond lengths and angles are also approximately the same within experimental error.

The reaction of **6** with silver cyanate (Ag[OCN]) has been investigated by Mr. Matthew Rowley within this group.[209] In contrast to **114**, up to three products may be formed depending upon the stoichiometry of the reagents employed. It seems likely that one of these products is analogous to **114** and exhibits N / O - linkage isomerism. Analytical data indicate the remaining two materials possess a 2 : 1 stoichiometry of $[OCN]^-$: Ru and while one may be a fluxional binuclear complex the other is probably a mononuclear solvate.

In parallel work Mr. Gary Belchem[210] has prepared the well characterised compounds $[\{Ru(\eta^3:\eta^3\text{-}C_{10}H_{16})Cl(\mu\text{-}SR)\}_2]$ (R = Et, Ph) from interaction of **6** with the appropriate thiol, RSH, in methanol. In contrast to all the compounds previously studied the cyclic voltammograms of these materials exhibit well defined, reversible oxidations to compounds formulated as $[\{Ru(\eta^3:\eta^3\text{-}C_{10}H_{16})Cl(\mu\text{-}SR)\}_2]^{n+}$ (n = 1, 2), which are apparently (allyl)Ru(V) species. Further work on these compounds is in progress.

a)

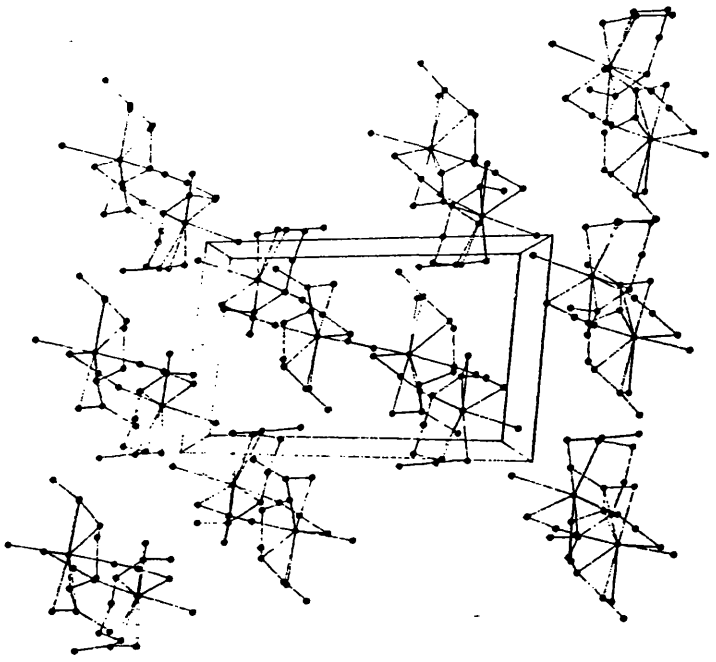

b)

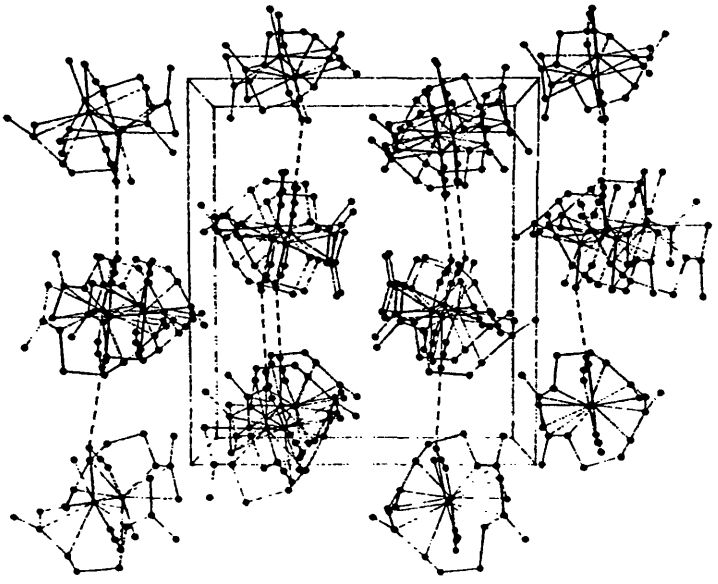

Fig. 5.4: Crystal packing diagrams for *rac*-[{Ru(η^3:η^3-$C_{10}H_{16}$)Cl(μ-SCN)}$_2$] **114b**
a) triclinic form, view down the *c* axis; b) monoclinic form, view down the *a* axis.

5.4 Binuclear Carboxylato Bridged Complexes

Given the fluxional nature of **106**, **109** and **110** which contain ligands which bind to each metal centre *via* a single donor functionality, we turned our attention to potentially chelating, π-delocalised bridging ligands. It was anticipated that chelate bridges may serve to bind the two metal centres together more strongly and result in non-fluxional compounds with strong metal-ligand bonds, which may be more electrochemically active. With this in mind the reactions of **6** with oxalate and malonate anionshavebeen examined. We were also interested to observed what effect the -CH_2- spacer group in the latter ligand would have i) on the binding mode of the carboxylato functionalities and ii) on the differences in chemical shift between the ^{1}H NMR resonances for the anticipated two diastereoisomers (*i.e.* as the bridge becomes longer do the diastereoisomers experience more similar magnetic environments?).

5.4.1 Reaction with Oxalate Ions

Reaction of **6** in a mixed acetone / water solvent with either a one or two mole ratio of silver oxalate gives the oxalato bridged complex [{Ru(η^3:η^3-$C_{10}H_{16}$)Cl}$_2$(μ-O_4C_2)] **115** in almost quantitative yield. The presence of the oxalato ligand is confirmed by the observation of a strong, broad band in the IR spectrum assignable to ν_{asymm}(OCO) at 1627 cm^{-1}. Compound **115** might be expected to exist as up to four different isomers distinguishable by NMR spectroscopy, *viz* two pairs of diastereoisomers with respectively *cisoid* (**115c**, **115d**) and *transoid* (**115a**, **115b**) configurations of the terminal chloride ligands as shown in Fig. 5.5.

In practice the ^{1}H NMR spectrum of **115** is qualitatively similar to that of **6**, *i.e.* eight singlet resonances attributable to the terminal allyl protons of the dimethyloctadienediyl ligand (δ 5.32, 5.19, 4.53, 4.44, 4.34, 4.19, 3.37 and 3.24 ppm) and four assigned to the methyl groups (δ 2.33, 2.30, 2.20 and 2.15 ppm). This observation is consistent with the formation of only two isomers. A pure sample of a single isomer was obtained by fractional crystallisation from chloroform / diethylether and was dissolved in chloroform-*d* at -60°C. The ^{1}H NMR spectrum of this solution displayed essentially only half the number of resonances of the bulk sample [δ 5.32, 4.44, 4.19, 3.37 (terminal allyl), 2.33, 2.15 ppm (methyl)]. A single crystal X-ray structure determination (*vide infra*), Fig. 5.6, showed these resonances to be due to isomer **115a** possessing a *transoid* configuration

and overall C_i molecular symmetry (with only half of the molecule being crystallographically unique). Raising the temperature of the NMR probe from -60°C to +50°C did not bring about the conversion of **115a** into **115b** indicating that, in contrast to the parent compound **6**, interconversion of isomers by bridge rupture is slow even at higher temperatures.

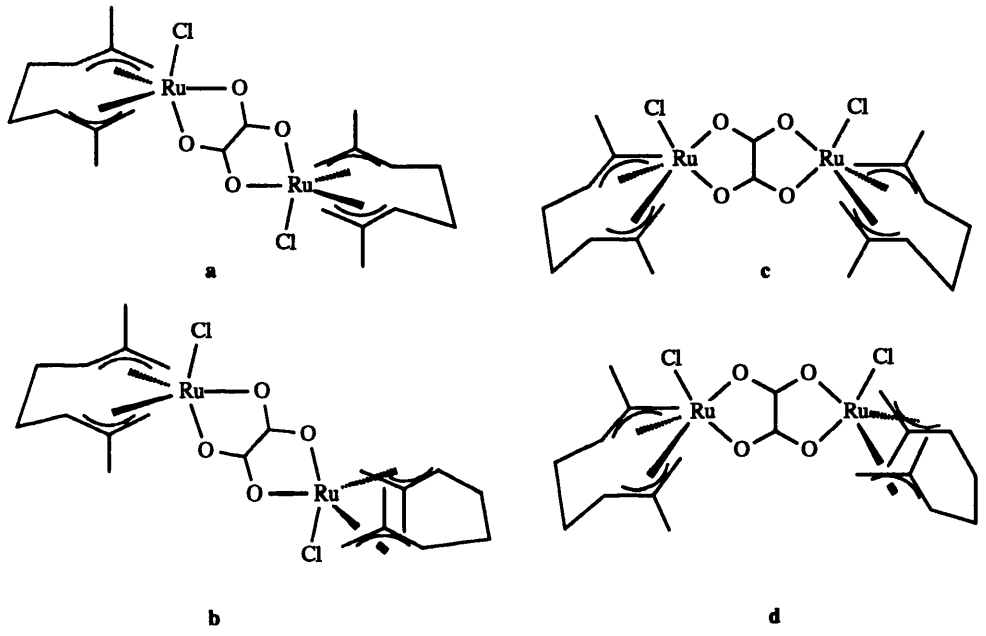

Fig. 5.5: Four possible isomers of $[\{Ru(\eta^3:\eta^3\text{-}C_{10}H_{16})Cl\}_2(\mu\text{-}O_4C_2)]$ **115**.

The NMR tube containing **115a** was sealed and allowed to stand at room temperature for several weeks. Spectra were recorded periodically during this time and showed the gradual partial conversion of **115a** into **115b**. Close examination of the spectra revealed that there were also additional weak resonances: eight singlet signals due to terminal allylic protons (δ 5.38, 5.32, 4.66, 4.56, 4.38, 4.27, 3.43 and 3.19 ppm), four methyl resonances (δ 2.33, 2.32, 2.15, 2.02 ppm), as well as additional multiplets (δ 4.56, 3.95 and 2.64 ppm). The appearance of these signals is completely consistent with the accumulation of small quantities of the *cisoid* isomers **115c** and **115d**. After *ca.* one

month, nearly equimolar quantities of **115a** and **115b** were present in the sample, together with small amounts of **115c** and **115d**, which never constituted more than 20% of any of the samples studied. It is unclear whether this represents the true equilibrium concentrations of the four isomers.

The observation of two metal centres linked by a potentially delocalised bridging ligand, as is the case here, again raises the question of whether the metal centres can communicate with one another electronically. The cyclic voltammogram of **115** recorded in CH_2Cl_2 with tetrabutylammonium tetrafluoroborate supporting electrolyte is unencouraging however, displaying a single, irreversible reduction at -0.92 V along with a partial oxidation wave on the return scan at +1.04 V (ν = 200 mV s^{-1}), possibly indicative of an ECE process.

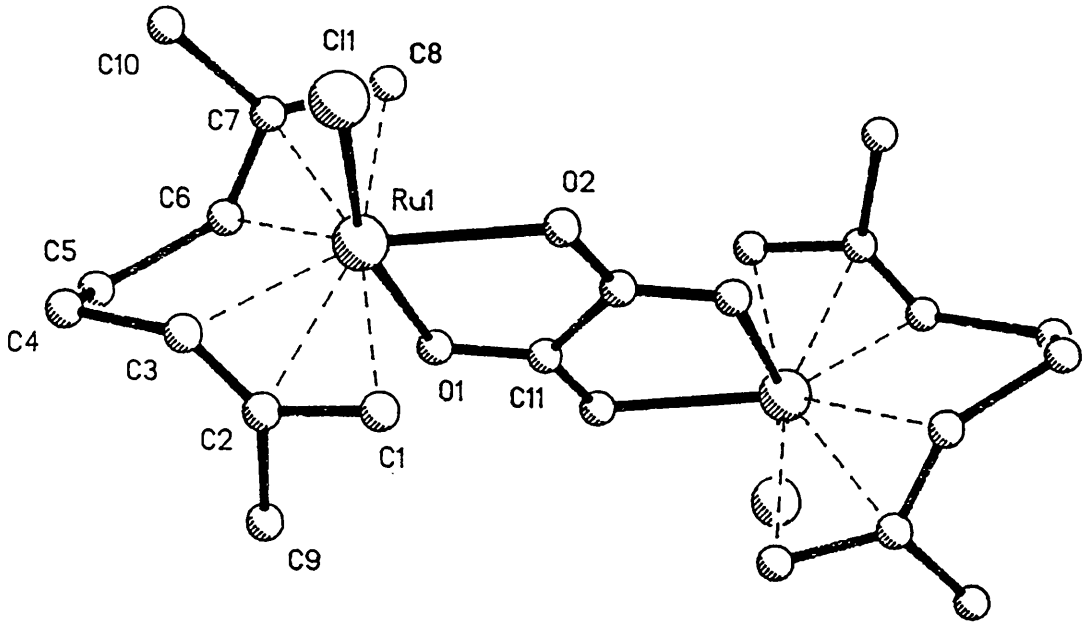

Fig. 5.6: X-ray crystal structure of *meso*-[{Ru(η^3:η^3-$C_{10}H_{16}$)Cl}$_2$(μ-O_4C_2)] **115a**

5.4.2 Reaction with Malonate Ions

The orange product formed from the reaction of **6** with $K_2[O_2CCH_2CO_2]$ was found to decompose slowly in chlorinated methane solvents to re-form **6**, possibly as a consequence of the presence of trace quantities of HCl in the solvent. The complex was sufficiently stable however, to permit an examination of its ^1H NMR spectrum in $CDCl_3$. The spectrum is a surprising one in that it displays only six resonances for the terminal allyl protons (δ 5.54, 5.53, 4.83, 4.82, 4.64 and 3.74 ppm) and three resonances for the methyl hydrogen atoms (δ 2.29, 2.15 and 2.10 ppm) as opposed to the eight and four respectively which is expected for a binuclear compound. The infrared spectrum of the material displays a band at 1516 cm^{-1} assigned to $\nu_{asymm}(OCO)$ (*cf.* 1516 cm^{-1} for $[Ru(\eta^3:\eta^3\text{-}C_{10}H_{16})Cl(O_2CMe)]$ **72** and 1510 cm^{-1} for the ruthenium(II) arene compound $[Ru(\eta^6\text{-}C_6H_6)Cl(O_2CCMe)]$[55]). Analytical data are fully consistent with a binuclear compound $[\{Ru(\eta^3:\eta^3\text{-}C_{10}H_{16})Cl\}_2(\mu\text{-}O_4C_3H_2)]$ **116**. It is believed that the reduced number of ^1H NMR signals is due to the accidental degeneracy of some of the resonances, thus two terminal allyl and one methyl resonance have twice the integral of their counterparts where the separate peaks are resolved. This conclusion is further supported by the observation of only a single second order multiplet resonance approximating to a singlet, arising from the two protons of the malonate ligand (*cf.* the case of $[\{Ru(\eta^3:\eta^3\text{-}C_{10}H_{16})Cl_2\}_2\{\mu\text{-}1,4\text{-}(NH_2)_2C_6H_4\}]$ **56** where the two singlet resonances for the protons of the bridging ligand occur at very similar chemical shifts). Such degeneracy indicates that there is little difference in magnetic environment between the two diastereoisomers of **116** and is consistent with the fact that the two chiral fragments are linked by a ligand containing a long continuous chain of five atoms. Although it is possible that the linkage between the two metal ions consists of two fused six membered heterocyclic rings, this seems unlikely from our examination of molecular models which show that such a mode of coordination would result in severe steric congestion. Certainly the similarity of the frequencies in $\nu_{asymm}(OCO)$ for **116** and **72** (both 1516 cm^{-1}), compared to the much greater value for **115** (1627 cm^{-1}), suggests that they are both similarly bound and implies that **116** contains four membered heterocyclic rings. When malonates contain six membered rings with metal ions the separation between symmetric and asymmetric stretching frequencies is expected to be somewhat larger.[211,212] Assuming the bridging malonate to act as two essentially independent chelating carboxylate

functionalities and assuming free rotation about the two interconnecting carbon-carbon bonds, the possibility of *cisoid* and *transoid* geometries for the terminal chloride ligands does not need to be considered, hence the experimental evidence is consistent with **116** possessing the diastereomeric structures shown in Fig. 5.7.

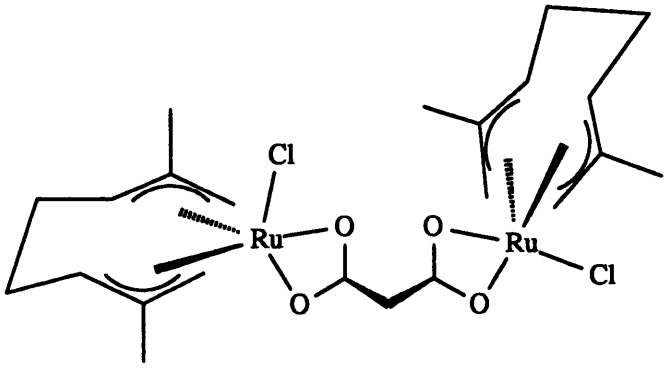

116a

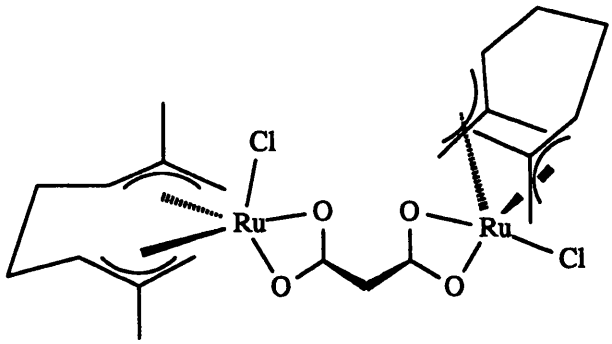

116b

Fig. 5.7: Two diastereomeric forms of $[\{Ru(\eta^3:\eta^3\text{-}C_{10}H_{16})Cl\}_2(\mu\text{-}O_4C_3H_2)]$ **116.**

5.4.3 X-ray Crystal Structure Determination

The single crystal X-ray structure of **115** is shown in Fig. 5.6. Atomic coordinates, bond length and angles and technical considerations are summarised in the experimental section. The asymmetric unit of the crystal was observed to contain half of one binuclear molecule, the remainder being generated by an inversion operation centred at the origin. Due to the presence of a significant disorder of the *bis*(allyl) ligand taking the form of two

alternative positions for the carbon atoms C(2) to C(7), it was not possible to determine crystallographically whether the sample consisted uniquely of C_1 or C_2 diastereoisomers or a mixture of the two. Given that the disordered molecule was symmetric about an inversion centre however, it seemed likely that the former diastereoisomer was predominant. This was confirmed by low temperature dissolution of the crystalline sample which possessed an ^{1}H NMR spectrum consistent with a predominance of only a single diastereoisomer.

The *bis*(allyl) ligands show the usual local C_2 symmetry and the metal adopts an approximately trigonal bipyramidal geometry as previously observed in related systems. The central portion of the molecule consists of two fused five membered heterocyclic rings (a geometry typical of the oxalato ligand in the bridging mode[213,214]) consisting of one bridging oxalato ligand and the two metal centres, Ru-O_{axial} 2.144(5) Å, Ru-$O_{equatorial}$ 2.182(6) Å [*cf.* 2.120(5) Å for [Ru(η^6-C_6H_6)Cl(NC_6H_6O)][61]], ∠O(1)-Ru(1)-O(2) 77.0(2)°. The ruthenium chloride distance is 2.368(2) Å which is short compared with Ru-Cl distances in related compounds which normally fall in the range 2.38 - 2.42 Å.[13,158-161] The angle Cl(1)-Ru(1)-O(1) is 161.8(2), and is more acute than that observed for unconstrained systems such as [{Ru(η^3:η^3-$C_{10}H_{16}$)Cl_2}$_2$(μ-pyz)] [170.2(1)°, Section 5.2.1] but typical of the significant distortions from the ideal 180° observed in other related *bis*(allyl)ruthenium(IV) systems containing chelate rings.[160] The angle is notably larger than the corresponding Cl-Ru-S angle in the benzothiazole-2-thiolate complex [Ru(η^3:η^3-$C_{10}H_{16}$)Cl(mcbt)][159] [156.4(1)°] which contains a four membered heterocyclic ring, but is roughly similar to the Cl-Ru-N angle in the bipyridine complex [Ru(η^3:η^3-$C_{10}H_{16}$)Cl(bipy)][BF_4] **64** [166.9(2)°, Chapter 2]. The metal-carbon distances, while not particularly precise, are all approximately equal and fall into the range 2.19 - 2.25 Å while the two metal centres are 5.59 Å apart.

5.5 Reactions with Nicotinic Acids

Continuing the theme of compounds with potentially chelating bridging ligands with delocalised π-systems, the reactions of **6** with nicotinic acids (carboxylato pyridines) was

examined. Recent work has shown that nicotinato analogues of the pyrazene bridged Creutz-Taubé ion display an extensive electrochemistry.[215] In addition, nicotinic acids were regarded as being especially attractive because of the difficulties previously encountered by us in the synthesis of mononuclear precursors to mixed valence binuclear compounds (*e.g.* the unstable pyrazene adducts **107** or **113** may be regarded as precursors to the mixed valence complex **111b**). The unsymmetrical nature of nicotinic acids suggested that it may be possible to generate mononuclear compounds bound *via* the pyridyl nitrogen atom before deprotonation of the carboxylate functionality in the presence of a second metal complex to give an unsymmetrically bridged compound.

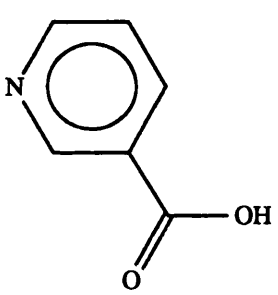

Nicotinic acid

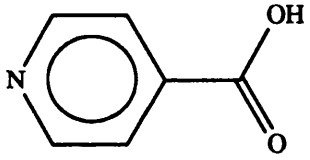

Isonicotinic acid

In contrast to the case of the mononuclear pyrazene adduct **107**, reaction of **6** with two molar equivalents of isonicotinic acid (*p*-$NC_5H_4CO_2H$) results in the clean formation of the adduct [$Ru(\eta^3:\eta^3\text{-}C_{10}H_{16})Cl_2$(*p*-$NC_5H_4CO_2H$)] **117** in 80% yield. This is consistent with recent results reported by Creutz[215] in which isonicotinate and isonicotinamidate bridged analogues of the Creutz-Taubé ion are readily prepared from mononuclear precursors. The ^1H NMR spectrum of **117** was consistent with its formulation as an equatorial adduct, with the only noteworthy feature being the surprisingly similar chemical shifts of the two terminal allyl signals (δ 4.62 and 4.46 ppm). The infrared spectrum of the complex showed a strong ν_{asymm}(OCO) at 1732 cm^{-1} and ν_{symm}(OCO) 1414 and 1369 cm^{-1}, similar to the values for free carboxylic acids and implying the complex to be N-bound.[192] If the reaction is carried out with a single mole equivalent of nicotinic (*m*-$NC_5H_4CO_2H$) or isonicotinic acid in the presence of excess $Na_2[CO_3]$ an equally smooth reaction occurs

to give the unsymmetrical binuclear complexes $[Ru_2(\eta^3:\eta^3\text{-}C_{10}H_{16})_2Cl_3(\mu\text{-}m\text{-}NC_5H_4CO_2)]$ **118** and $[Ru_2(\eta^3:\eta^3\text{-}C_{10}H_{16})_2Cl_3(\mu\text{-}p\text{-}NC_5H_4CO_2)]$ **119** respectively in *ca.* 70% yield. Unlike **117**, the infrared spectra of **118** and **119** no longer display a band at *ca.* 1700 cm^{-1}, instead two new bands at lower wavenumber, assignable to $\nu_{asymm}(OCO)$ are apparent [1607 and 1509 cm^{-1} in **118** and 1509 and 1496 cm^{-1} in **119**]. Bands assignable to $\nu_{symm}(OCO)$ also occur in both complexes [1444 and 1381 (**118**) and 1429 and 1383 cm^{-1} (**119**)]. The difference in frequency between ν_{asymm} and ν_{symm}, $\Delta\nu$ is ambiguous, and hence from this data the coordination mode of the carboxylato functionalities is uncertain, although the chelate mode is suspected. The binuclear nature of **118** was confirmed by a FAB mass spectrum which exhibited a clear molecular ion peak centred on *m/z* 703 with isotope distribution characteristic of two ruthenium and three chlorine atoms along with a fragmentation peak corresponding to loss of chloride *m/z* 668.

The ^1H NMR spectra of **118** and **119** strongly reflect the asymmetric, binuclear nature of the compounds. In the spectrum of **118** for example, the N-bound "$Ru(\eta^3:\eta^3\text{-}C_{10}H_{16})$" fragment demonstrates sharp resonances similar to the N-bound adduct **117**, the terminal allyl resonances again occurring at similar chemical shifts to one another. In common with other binuclear complexes containing the "$Ru(\eta^3:\eta^3\text{-}C_{10}H_{16})$" moiety, **118** is expected to exist as two diastereoisomers. The linkage between the two metal atoms is long however (6 atoms), and thus only small chemical shift differences are anticipated in the ^1H NMR resonances for the two forms. In reality the diastereoisomers are resolved on only one of the terminal allyl signals for the N-bound side of the molecule: δ 4.60 and 4.59 ppm. The other two terminal allyl signals are coincident, δ 4.41 ppm. In contrast to the N-bound side of the molecule, the O-bound "$Ru(\eta^3:\eta^3\text{-}C_{10}H_{16})$" fragment exhibits four terminal allyl signals at room temperature, δ 5.61, 4.73, 4.70 and 3.75 ppm, all of which are broad implying a fluxional process that apparently has most effect on the O-bound end of the molecule. The remainder of the spectrum of the O-bound fragment resembles strongly that of carboxylato complexes such as **72**.

At -20°C all the resonances in the spectrum of **118** are sharp (Fig. 5.8) and consistent with the proposed formulation with signals for individual diastereoisomers resolved on some of the resonances due to the terminal allylic protons on the O-bound end of the molecule. Interestingly, a number of additional resonances of very low intensity (*ca.*

5% of the total sample) are observed, including a broad signal at δ 6.46 ppm. It seems likely that this second species contains a unidentate carboxylato group with the vacant coordination site at the carboxylate bound metal centre occupied by a water molecule. An ^{1}H NMR spectrum exhibiting similar features is observed for **119** and it would thus appear that the carboxylatopyridines exhibit behaviour related to that of the fluoro- and chloroacetato complexes **78** and **79** (reported in Chapter 3), with chelating compounds in equilibrium with aqua species containing unidentate carboxylato ligands (Scheme 5.1).

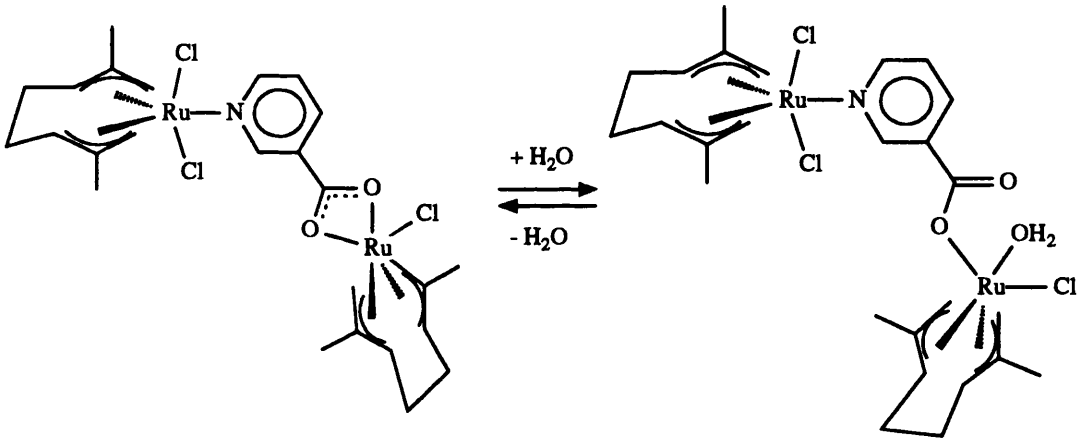

Scheme 5.1: Fluxionality in the nicotinato bridged compound $[Ru_2(\eta^3{:}\eta^3\text{-}C_{10}H_{16})_2Cl_3(\mu\text{-}NC_5H_4CO_2)]$ **118**.

Attempts were made to use **117** to synthesise mixed valence compounds such as $[(\eta^3{:}\eta^3\text{-}C_{10}H_{16})Cl_2Ru(\mu\text{-}NC_5H_4CO_2)RuCl(\eta^6\text{-}p\text{-}MeC_6H_4CHMe_2)]$ **120**, related to **111**, by reaction with $[\{Ru(\eta^6\text{-}p\text{-}MeC_6H_4CHMe_2)Cl(\mu\text{-}Cl)\}_2]$ **7c**. On carrying out the reaction the mixed-valence compound represented *ca.* 50% of the isolated yield (by ^{1}H NMR spectroscopy) but was contaminated by significant amounts of **119** and the analogous Ru(II)-Ru(II) species. Similar results were obtained from the reaction of $[Ru(\eta^6\text{-}p\text{-}MeC_6H_4CHMe_2)Cl_2(m\text{-}NC_5H_4CO_2H)]$ with **6** whilst an extremely complicated mixture of products was obtained from the reaction of **117** with $[PdCl_2(PhCN)_2]$.

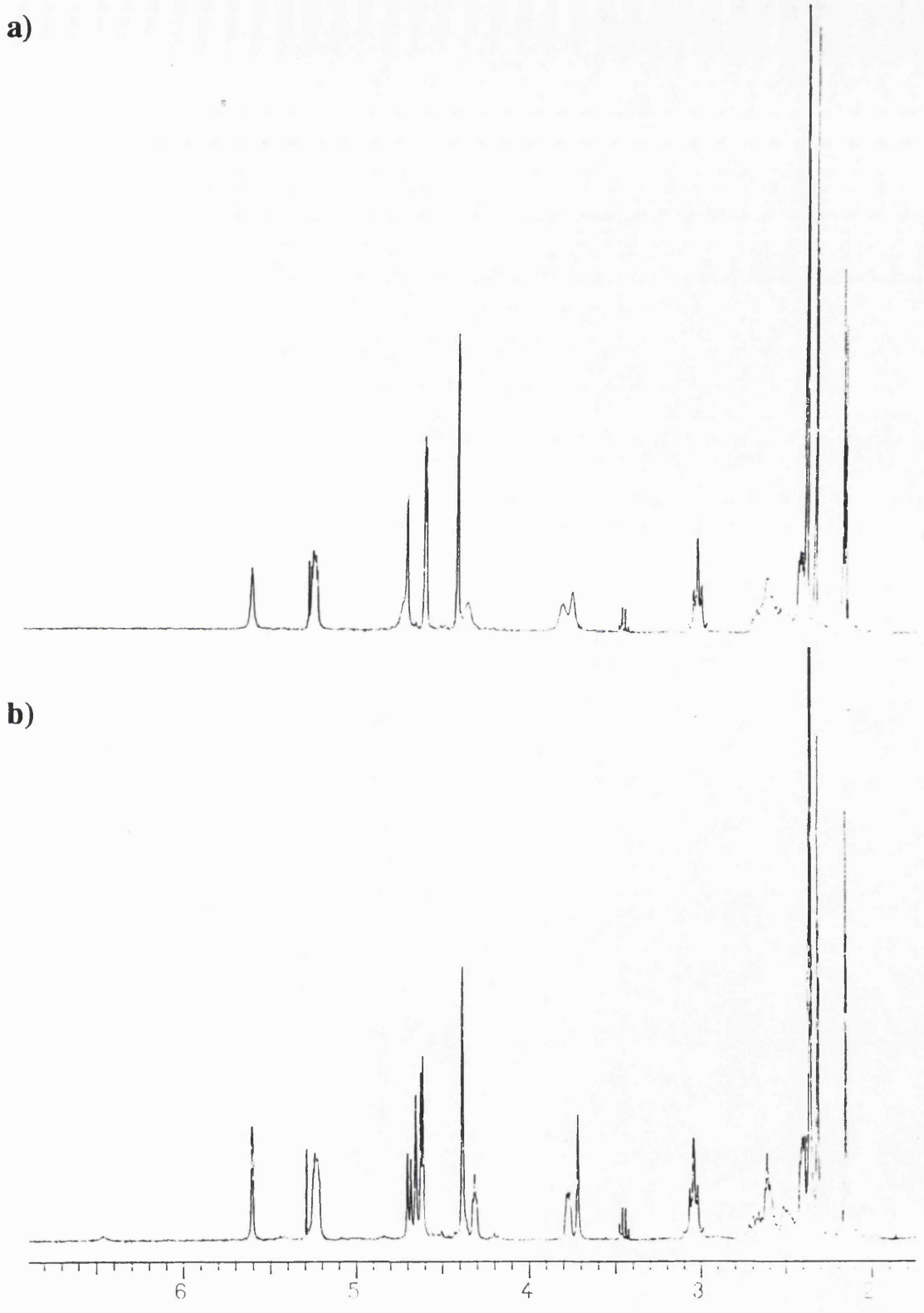

Fig. 5.8: ^{1}H NMR spectrum of the binuclear compound $[Ru_2(\eta^3:\eta^3\text{-}C_{10}H_{16})_2Cl_3(\mu\text{-}m\text{-}NC_5H_4CO_2)]$ **118** a) recorded at +20°C; b) -20°C.

5.6 Experimental

General experimental considerations are outlined in Section 2.4.

Preparations. - $[\{Ru(\eta^3:\eta^3\text{-}C_{10}H_{16})Cl_2\}_2(\mu\text{-}N_2C_4H_4)]$ **106**. The complex $[\{Ru(\eta^3:\eta^3\text{-}C_{10}H_{16})RuCl(\mu\text{-}Cl)\}_2]$ (0.08 g, 0.13 mmol) was stirred in CH_2Cl_2 (5 cm^3) with pyrazene (0.01 g, 0.13 mmol) for 1 h. during which time a colour change from pink to orange was observed. Evaporation to *ca.* 1 cm^3 and slow addition of n-hexane (10 cm^3) gave the product as an orange powder which was isolated by filtration, washed with diethyl ether and air dried. Yield 0.08 g, 0.11 mmol, 83% (Found: C, 41.10; H, 5.05; N, 3.55. Calc. for $C_{24}H_{36}Cl_4N_2Ru_2$: C, 41.40; H, 5.20; N, 4.00%).

$[\{Ru(\eta^3:\eta^3\text{-}C_{10}H_{16})Cl_2\}_2(\mu^2\text{-}N_3C_3H_3)]$ **109**. $[\{Ru(\eta^3:\eta^3\text{-}C_{10}H_{16})Cl(\mu\text{-}Cl)\}_2]$ (0.10 g, 0.16 mmol) was treated with 1,3,5-triazine (0.015 g, 0.17 mmol) following a procedure analogous to that outlined for **106**. Reaction time 15 minutes. Yield 0.09 g, 0.13 mmol, 79% (Found: C, 39.80; H, 5.05; N, 6.00. Calc. for $C_{23}H_{35}Cl_4N_3Ru_2$: C, 39.60; H, 5.05; N, 6.00%).

$[\{Ru(\eta^3:\eta^3\text{-}C_{10}H_{16})Cl_2\}_3(\mu^3\text{-}N_3C_3H_3)]$ **110**. $[\{Ru(\eta^3:\eta^3\text{-}C_{10}H_{16})Cl(\mu\text{-}Cl)\}_2]$ (0.15 g, 0.25 mmol) was treated with 1,3,5-triazine (0.03 g, 0.37 mmol) following a procedure analogous to that outlined for **106**. The resulting orange solution was concentrated under reduced pressure to *ca.* 2 cm^3 and diethyl ether vapour was allowed to diffuse slowly into it within a closed system. After 24 h. small, well formed crystals were formed and were filtered off and dried under vacuum. Microanalysis and ^1H NMR spectroscopy showed the product to consist solely of **110**. Yield 0.06 g, 0.06 mmol, 20% (Found: C, 38.90; H, 5.38; N, 4.15. Calc. for $C_{33}H_{51}Cl_6N_3Ru_3$: C, 39.40; H, 5.10; N, 4.20%).

$[(\eta^3:\eta^3\text{-}C_{10}H_{16})Cl_2Ru(\mu\text{-}N_2C_4H_4)RuCl_2(\eta^6\text{-}MeC_6H_4CHMe_2)]$ **111b**. i) $[\{Ru(\eta^6\text{-}p\text{-}MeC_6H_4CHMe_2)Cl(\mu\text{-}Cl)\}_2]$ (0.10 g, 0.16 mmol) was stirred in acetone (5 cm^3) with pyrazene (0.27 g, 3.39 mmol) for 5 h. to give a brown precipitate of the known ruthenium(II) complex $[\{Ru(p\text{-cymene})Cl_2\}_2(\mu\text{-pyz})]$ **112**, and a red solution. The filtered

solution was concentrated to *ca.* half volume and diethyl ether added to give a red precipitate (shown by ^{1}H NMR spectroscopy to be an approximately 2 : 1 mixture of **112** and [Ru(*p*-cymene)Cl_2(pyz)] **113**) which was used without further purification.

ii) To the product from (i) (0.06 g) in toluene (5 cm^3) was added [{Ru(η^3:η^3-$C_{10}H_{16}$)Cl(μ-Cl)}$_2$] (0.04 g, 0.07 mmol) and the mixture stirred for 30 minutes to give a brown precipitate. The filtered solid was dissolved in toluene / acetone (1 : 10 v/v) and filtered through Celite to remove excess **6**. Diethyl ether (5 cm^3) was added to precipitate unreacted **112** as a brown solid. After filtration, the remaining orange-red solution was evaporated to *ca.* one quarter volume and n-hexane slowly added to give the product as red microcrystals. (^{1}H NMR spectroscopy showed this material to consist of pure **111b** with one molecule of toluene of crystallisation.) Yield 0.03 g, 0.04 mmol, 13% based on [{Ru(η^6-*p*-$MeC_6H_4CHMe_2$)Cl(μ-Cl)}$_2$] (Found C, 48.05; H, 5.55; N, 3.60. Calc. for $C_{31}H_{42}Cl_4N_2Ru_2$ C, 47.35; H, 5.40; N, 3.55%).

[{Ru(η^3:η^3-$C_{10}H_{16}$)Cl(μ-SCN)}$_2$] **114**. [{Ru(η^3:η^3-$C_{10}H_{16}$)Cl(μ-Cl)}$_2$] (0.11 g, 0.18 mmol) was suspended in a degassed mixture of acetone (2.5 cm^3) and water (2.5 cm^3). Ag[SCN] (0.06 g, 0.37 mmol) was added and the mixture stirred for a further hour. The resulting yellow solution was filtered through celite to remove the precipitate of AgCl and the volume was reduced to *ca.* 1 cm^3, resulting in the precipitation of the yellow product which was isolated by filtration, washed with acetone and diethyl ether, and air dried. Yield: 0.05 g, 0.08 mmol, 43%. (Found: C, 40.0; H, 4.9; N, 3.9. Calc. for $C_{22}H_{32}Cl_2N_2Ru_2S_2$: C, 39.9; H, 4.9; N, 4.2%). Infrared Spectrum: ν(CN) 2141 cm^{-1}, ν(CS) 723 cm^{-1}, ν(RuCl) 280 cm^{-1}, ν(RuS) 251 cm^{-1}.

Orange, diamond shaped crystals of isomerically pure **114b** (triclinic) were obtained by fractional crystallisation from a nitromethane solution. The monoclinic form of **114b** crystallised from nitromethane / acetone (1 : 1 v/v) on standing the solution in air, as long, flattened, orange needles.

[{Ru(η^3:η^3-$C_{10}H_{16}$)Cl}$_2$(μ-O_4C_2)] **115**. [{Ru(η^3:η^3-$C_{10}H_{16}$)Cl(μ-Cl)}$_2$] (0.09 g, 0.16 mmol) was suspended in acetone (2.5 cm^3) and water (2.5 cm^3). $Ag_2[O_4C_2]$ (0.09 g, 0.32 mmol) was added and the mixture stirred for 1 h. The resulting orange solution was

filtered through Celite to remove the precipitate of AgCl which formed and the volume of the filtrate reduced to *ca.* 1.5 cm^3 resulting in the deposition of the yellow product, which was isolated by filtration, washed with acetone and diethyl ether and air dried. Yield: 0.08 g, 0.13 mmol, 83% (Found: C, 42.30; H, 5.30. Calc. for $C_{22}H_{32}Cl_2O_4Ru_2$: C, 41.70; H, 5.10%).

$[\{Ru(\eta^3:\eta^3\text{-}C_{10}H_{16})Cl\}_2(\mu\text{-}O_4C_3H_2)]$ **116.** $[\{Ru(\eta^3:\eta^3\text{-}C_{10}H_{16})Cl(\mu\text{-}Cl)\}_2]$ (0.06 g, 0.10 mmol) was suspended in acetone (5 cm^3). $K_2[O_4C_3H_2]$ (0.02 g, 0.12 mmol) was added and the mixture stirred for 24 h. The resulting orange solution was filtered through Celite to remove the precipitate of KCl and any unreacted starting materials. The solvent was removed *in vacuo* giving a pinkish residue which was recrystallised from diethyl ether. Yield: 0.05 g, 0.06 mmol, 62% (Found: C, 42.80; H, 5.20. Calc. for $C_{23}H_{34}Cl_2O_4Ru_2$: C, 42.70; H, 5.30%).

$[Ru(\eta^3:\eta^3\text{-}C_{10}H_{16})Cl_2(p\text{-}NC_5H_4CO_2H)]$ **117.** $[\{Ru(\eta^3:\eta^3\text{-}C_{10}H_{16})Cl(\mu\text{-}Cl)\}_2]$ (0.24 g, 0.38 mmol) was stirred as an acetone (5 cm^3) suspension with isonicotinic acid (0.09 g, 0.77 mmol) for 2 h, during which time the gradual formation of an orange colouration was observed as the starting material was taken up into solution. The solution was evaporated to an orange oil and triturated resulting in the deposition of the product as an orange precipitate which was washed with diethyl ether and air dried. Yield: 0.26 g, 0.61 mmol, 80% (Found: C, 44.15; H, 5.05; N, 2.95. Calc. for $C_{16}H_{21}NCl_2O_2Ru$: C, 44.55; H, 4.90; N, 3.25%).

$[Ru_2(\eta^3:\eta^3\text{-}C_{10}H_{16})_2Cl_3(\mu\text{-}m\text{-}NC_5H_4CO_2)]$ **118.** $[\{Ru(\eta^3:\eta^3\text{-}C_{10}H_{16})Cl(\mu\text{-}Cl)\}_2]$ (0.08 g, 0.12 mmol) was stirred with nicotinic acid (0.015 g, 0.12 mmol) in acetone (5 cm^3) in the presence of $Na_2[CO_3]$ (0.1 g, excess) for 2 h. The resulting orange solution was filtered to remove excess base and evaporated to an orange oil. Addition of diethyl ether (4 cm^3) resulted in the formation of the product as an orange precipitate which was isolated by filtration and air dried. Evaporation of the filtrate and trituration with hexane resulted in a further crop of product. Combined yield: 0.06 g, 0.09 mmol, 71% (Found: C, 43.75; H,

5.40; N, 1.85. Calc. for $C_{26}H_{36}NCl_3O_2Ru_2$: C, 44.40; H, 5.15; N, 2.00%).

$[Ru_2(\eta^3{:}\eta^3\text{-}C_{10}H_{16})_2Cl_3(\mu\text{-}p\text{-}NC_5H_4CO_2)]$ **119**. $[\{Ru(\eta^3{:}\eta^3\text{-}C_{10}H_{16})Cl(\mu\text{-}Cl)\}_2]$ (0.06 g, 0.10 mmol) was treated with isonicotinic acid (0.012 g, 0.10 mmol) and excess anhydrous sodium carbonate as described for **118**. Combined yield: 0.05 g, 0.07 mmol, 70% (Found: C, 44.35; H, 5.40; N, 1.75. Calc. for $C_{26}H_{36}NCl_3O_2Ru_2$: C, 44.40; H, 5.15; N, 2.00%).

Crystallography. - A summary of general X-ray crystallographic considerations is given in section 2.4.

i) $[\{Ru(\eta^3{:}\eta^3\text{-}C_{10}H_{16})Cl_2\}_2(\mu\text{-}N_2C_4H_4)].2CHCl_3$ **106a** (C_i diastereoisomer)

Crystal data. - $C_{26}H_{38}N_2Ru_2Cl_{10}$, M = 935.27, triclinic, space group $P\bar{1}$, a = 7.297(2), b = 9.889(2), c = 13.411(4) Å, α = 70.77(2), β = 83.29(2), γ = 89.70(2)°, U = 906.9 Å^3 (by least-squares refinement of diffractometer angles for 30 automatically centred reflections in the range 11° ≤ 2θ ≤ 24°), Z = 1, F(000) = 664, D_c = 1.71 g cm^{-3}, μ(Mo-K$_\alpha$) = 15.3 cm^{-1}.

An orange crystal of approximate dimensions 0.3 x 0.17 x 0.1 mm was prepared by diffusion of diethyl ether into a chloroform solution of the compound and was used to obtain a primitive data set of 3383 (3122 unique) reflections. A correction was applied to allow for crystal decomposition (*ca.* 40%) but no correction was made for absorption (collection of the necessary data based on azimuthal scans was impossible because of crystal decomposition). Omission of reflections with $I \leq 3\sigma(I)$ gave 1864 observed reflections which were employed in the analysis. The structure was solved by the conventional Patterson and difference-Fourier techniques. The asymmetric unit contained half of one binuclear molecule (related to the other half by an inversion operation centred at the origin) and a molecule of chloroform of solvation. Full-matrix least-squares refinement gave R = 0.0640, R_w = 0.0659 in the final cycle from 181 parameters. A weighting scheme of the form $w^{-1} = \sigma^2(F)+0.000807F^2$ was applied and the maximum shift to error ratio in the final cycle was 0.001. The largest residual peak was 1.05 electrons Å^{-3} close to the metal atom. No short intermolecular contacts were observed.

ii) [{Ru(η^3:η^3-$C_{10}H_{16}$)Cl(μ-SCN)}$_2$] **114b** (C_2 diastereoisomer, triclinic form)

Crystal data. - $C_{22}H_{32}NCl_2Ru_2S_2$, M = 661.67, triclinic, space group $P\bar{1}$, a = 7.831(3), b = 12.882(3), c = 14.109(6) Å, α = 112.48(3), β = 100.52(3), γ = 91.45(3)°, U = 1285(1) Å^3 (by least-squares refinement of diffractometer angles for 29 automatically centred reflections in the range 13° ≤ 2θ ≤ 22°), Z = 2, F(000) = 664, D_c = 1.71 g cm^{-3}, μ(Mo-K$_\alpha$) = 15.3 cm^{-1}.

An orange block of approximate dimensions 0.5 x 0.2 x 0.1 mm was prepared by slow evaporation of a nitromethane solution of the compound and was used to collect a primitive data set of 4448 reflections (all unique). An empirical absorption correction was applied. Three standard reflections monitored throughout the data collection showed no loss in intensity. A total 2772 reflections were observed with I ≥ 3σ(I) and were employed in the analysis. The structure was solved by the conventional Patterson and difference-Fourier techniques. The asymmetric unit contained one complete molecule. Full-matrix least-squares refinement gave R = 0.0557, R_w = 0.0596 in the final cycle from 271 parameters. A weighting scheme of the form $w^{-1} = \sigma^2(F)+0.0012167F^2$ was applied and the maximum shift to error ratio in the final cycle was 0.002. The largest residual peak was 1.21 electrons Å^{-3} associated with one of the metal atoms. No short intermolecular contacts were observed.

iii) [{Ru(η^3:η^3-$C_{10}H_{16}$)Cl(μ^2-SCN)}$_2$] **114b** (C_2 diastereoisomer, monoclinic form)

Crystal data. - $C_{22}H_{32}N_2Cl_2Ru_2S_2$, M = 661.67, monoclinic, space group $P2_1/c$, a = 13.494(6), b = 13.069(6), c = 14.582(4) Å, β = 95.99(3), U = 2557 Å^3 (by least-squares refinement of diffractometer angles for 23 automatically centred reflections in the range 10° ≤ 2θ ≤ 24°), Z = 4, F(000) = 1382, D_c = 1.72 g cm^{-3}, μ(Mo-K$_\alpha$) = 15.4 cm^{-1}.

An orange plate of approximate dimensions 0.6 x 0.3 x 0.04 mm was prepared by slow evaporation of a nitromethane / acetone (1 : 1 v/v) solution of the compound and was used to collect a primitive data set of 4741 (4349 unique) reflections. Three standards monitored throughout the data collection showed no appreciable loss in intensity and an empirical absorption correction was applied. A total of 2250 Reflections were observed with I ≥ 3σ(I) and were employed in the refinement. The structure was solved by the conventional Patterson and difference Fourier techniques. The asymmetric unit contained

one complete molecule. Full-matrix least-squares refinement gave R = 0.0497, R_w = 0.0515 in the final cycle from 272 parameters. A weighting scheme of the form $w^{-1} = \sigma^2(F)+0.000617F^2$ was applied and the maximum shift to error ratio in the final cycle was 0.001. The largest residual peak was 0.84 electrons $Å^{-3}$ associated with one of the metal atoms. Short intermolecular contacts, 3.55 Å, were observed between thiocyanato sulphur atoms on adjacent molecules in the lattice.

iv) $[\{Ru(\eta^3:\eta^3\text{-}C_{10}H_{16})Cl\}_2(\mu\text{-}O_4C_2)]$ **115a**

Crystal data. - $C_{22}H_{32}Cl_2O_4Ru_2$, M = 633.58 g mol^{-1}, monoclinic, space group $P2_1/n$, a = 7.636(2), b = 20.168(5), c = 7.902(2), β = 90.74(2)°, U = 1216.9 $Å^3$ (by least-squares refinement diffractometer angles for 30 automatically centred reflections in the range 12 ≤ 2θ ≤ 25°), Z = 2, F(000) = 636, D_c = 1.73 g cm^{-3}, μ(Mo-K_α) = 14.64 cm^{-1}.

A deep red block of approximate dimensions 0.4 x 0.3 x 0.2 mm was prepared by diffusion of diethyl ether into a chloroform solution of the compound. A primitive data set of 2377 reflections (2134 unique) was collected, 1669 of which were observed to have $I \geq 3\sigma(I)$ and were employed in the analysis. Three standard reflections monitored throughout the data collection showed no appreciable change in intensity. An empirical absorption correction was applied. The structure was solved by the conventional Patterson and difference Fourier techniques. The asymmetric unit was observed to contain half of one binuclear molecule, related to the other half by a crystallographic inversion centre at the origin. Heavy atoms were refined anisotropically but an isotropic model was adopted for the light atoms due to the presence of significant disorder in the crystal which took the form of two alternative positions for all the carbon atoms of the *bis*(allyl) ligand except C(1) and C(8). This disorder was modelled satisfactorily by two ligand positions of fractional occupancy. The occupancy was refined and converged on a value of 0.6 for the major position. Hydrogen atoms were not included in the model due to the disorder. Full-matrix least-squares refinement gave R = 0.0541, R_w = 0.0648 in the final cycle from 104 parameters. A weighting scheme of the form $w^{-1} = \sigma^2(F)+0.005368F^2$ was applied and the maximum shift to error ratio in the final cycle was 0.006. The largest residual peak was 1.00 electrons $Å^{-3}$ close to the metal atom. No short intermolecular contacts were observed.

Table 5.1: ^{1}H NMR Data for New Complexes.[a]

Compound	δ				
	Terminal Allyl	Internal Allyl	$-CH_2-$	Me	Other
[{Ru(η^3:η^3-$C_{10}H_{16}$)Cl_2}$_2$(μ-pyz)] **106a** C_i diastereoisomer	4.61 (s, 4H) 4.39 (s, 4H)	5.29 (m, 4H)	3.07 (m, 4H) 2.44 (m, 4H)	2.37 (s, 12H)	9.32 (s, 4H)
[{Ru(η^3:η^3-$C_{10}H_{16}$)Cl_2}$_2$(μ-pyz)] **106b** C_2 diastereoisomer	4.66 (s, 4H) 4.34 (s, 4H)	5.29 (m, 4H)	3.07 (m, 4H) 2.44 (m, 4H)	2.38 (s, 12H)	9.24 (s, 4H)
[Ru(η^3:η^3-$C_{10}H_{16}$)Cl_2(pyz)] **107**	4.59 (s, 2H) 4.40 (s, 2H)	5.29 (m, 2H)	3.06 (m, 2H) 2.43 (m, 2H)	2.38 (s, 6H)	9.29, 8.63 (AA'BB', 4H, ^3J=3.25, ^5J=1.0)
[{Ru(η^3:η^3-$C_{10}H_{16}$)Cl_2}$_2$(μ^2-tra)] **109**[b]	4.76 (s, 4H) 4.42 (s, 4H)	5.20 (m, 4H)	2.97 (m, 4H)	2.41 (s, 12H)	9.85 (s, 2H), 10.63 (s, 1H)
[{Ru(η^3:η^3-$C_{10}H_{16}$)Cl_2}$_3$(μ^3-tra)] **110**[b]	4.91 (s, 6H) 4.46 (s, 6H)	5.20 (m, 6H)	2.97 (m, 6H) 2.50 (m, 6H)	2.41 (s, 18H)	10.70 (s, 3H)

[Ru(η^3:η^3-$C_{10}H_{16}$)Cl_2(μ-pyz) RuCl$_2$(η^6-*p*-MeC_6H_4CHMe$_2$)] **111**	4.59 (s, 2H) 4.44 (s, 2H)	5.26 (m, 2H)	3.04 (m, 2H) 2.39 (m, 2H)	2.38 (s, 6H)	8.99, 8.83 (AA'BB', 4H, ^3J=5.3, ^5J=1.5, $N_2C_4H_4$), 5.40, 5.18 (AB, 4H, ^3J=6.1, MeC_6H_4CHMe$_2$), 2.97 (se, 1H, ^3J=7.0, MeC_6H_4C*H*Me$_2$), 2.08 (s, 3H, *Me*C_6H_4CHMe$_2$), 1.28 (d, 6H, ^3J=7.0, MeC_6H_4CH*Me*$_2$)
[{Ru(η^3:η^3-$C_{10}H_{16}$)Cl(μ-SCN)}$_2$] **114a** C_i diastereoisomer	4.81 (s, 2H) 4.65 (s, 2H) 4.05 (s, 2H) 3.68 (s, 2H)	4.90 (m, 2H) 4.68 (m, 2H)	3.14 (m, 4H) 2.57 (m, 4H)	2.29 (s, 6H) 2.26 (s, 6H)	-
[{Ru(η^3:η^3-$C_{10}H_{16}$)Cl(μ-SCN)}$_2$] **114b** C_2 diastereoisomer	4.77 (s, 2H) 4.70 (s, 2H) 4.13 (s, 2H) 3.56 (s, 2H)	4.90 (m, 2H) 4.68 (m, 2H)	3.14 (m, 4H) 2.57 (m, 4H)	2.35 (s, 6H) 2.26 (s, 6H)	-
[{Ru(η^3:η^3-$C_{10}H_{16}$)Cl}$_2$(μ-O_4C_2)] **115a** C_i isomer	5.32 (s, 2H) 4.44 (s, 2H) 4.19 (s, 2H) 3.37 (s, 2H)	4.49 (m, 2H) 4.13 (m, 2H)	2.65 (m, 8H)	2.33 (s, 6H) 2.15 (s, 6H)	-

[{Ru(η^3:η^3-$C_{10}H_{16}$)Cl}$_2$(μ-O_4C_2)] **115b** C_2 isomer	5.19 (s, 2H) 4.53 (s, 2H) 4.34 (s, 2H) 3.24 (s, 2H)	4.49 (m, 2H) 4.08 (m, 2H)	2.65 (m, 8H)	2.30 (s, 6H) 2.20 (s, 6H)	-
[{Ru(η^3:η^3-$C_{10}H_{16}$)Cl}$_2$(μ-$O_4C_3H_2$)] **116** 2 diastereoisomers	5.54 (s, 2H) 5.53 (s, 2H) 4.83 (s, 2H) 4.82 (s, 2H) 4.62 (s, 4H) 3.74 (s, 4H)	4.26 (m, 4H) 3.60 (m, 4H)	2.55 (m, 16H)	2.29 (s, 12H) 2.15 (s, 6H) 2.10 (s, 6H)	2.94 (virtual s, 4H, $O_2CCH_2CO_2$)
[Ru(η^3:η^3-$C_{10}H_{16}$)Cl$_2$(*p*-$NC_5H_4CO_2H$)] **117**	4.62 (s, 2H) 4.46 (s, 2H)	5.31 (m, 2H)	3.06 (m, 2H) 2.43 (m, 2H)	2.39 (s, 6H)	9.42 & 7.88 (AA'BB', 4H, ^3J=5.4, ^5J=1.5, $NC_5H_4CO_2H$)
[Ru$_2$(η^3:η^3-$C_{10}H_{16}$)$_2$Cl$_3$(μ-*m*-$NC_5H_4CO_2$)] **118** i) 20°C (Two diastereoisomers)	5.61 (s, br, 2H) 4.73 (s, br, 2H) 4.70 (s, br, 2H) 4.60 (s, 2H) 4.59 (s, 2H) 4.41 (s, 4H) 3.75 (s, br, 2H)	5.26 (m, 4H) 4.35 (s, br, 2H) 3.80 (s, br, 2H)	3.02 (m, 4H) 2.61 (m, 8H) 2.41 (m, 4H)	2.38 (s, 12H) 2.33 (s, 6H) 2.17 (s, 3H) 2.16 (s, 3H)	9.59 (d, 1H, ^4J=1.8), 9.58 (d, 1H, ^4J=1.8), 9.31 (d, 2H, ^3J=5.8), 8.36 (d, 2H, ^3J=7.4), 7.37 (dd, 2H, ^3J=5.8 & 7.4)

ii) -50°C (Two diastereoisomers)	5.59 (s, 2H) 4.69 (s, 1H) 4.67 (s, 1H) 4.64 (s, 2H) 4.62 (s, 2H) 4.61 (s, 2H) 4.38 (s, 4H) 3.72 (s, 2H)	5.22 (m, 4H) 4.30 (m, 2H) 3.76 (m, 2H)	3.06 (m, 4H) 2.69 (m, 2H) 2.62 (m, 4H) 2.50 (m, 2H) 2.38 (m, 4H)	2.34 (s, 12H) 2.31 (s, 6H) 2.16 (s, 3H) 2.15 (s, 3H)	9.51 (s, 1H), 9.49 (s, 1H), 9.26 (d, 1H, ^3J=5.8), 9.25 (d, 1H, ^3J=5.8), 8.38 (d, 2H, ^3J=7.8), 7.39 (dd, 2H, ^3J=5.8 & 7.8)
$[Ru_2(\eta^3:\eta^3\text{-}C_{10}H_{16})_2Cl_3(\mu\text{-}p\text{-}NC_5H_4CO_2)]$ **119**	5.63 (s, 2H) 4.72 (s, 2H) 4.69 (s, br, 2H) 4.58 (s, 2H) 4.57 (s, 2H) 4.43 (s, 2H) 4.42 (s, 2H) 3.68 (s, br, 2H)	5.27 (m, 4H) 4.37 (m, 2H) 3.79 (m, 2H)	3.04 (m, 4H) 2.63 (m, 8H) 2.41 (m, 4H)	2.38 (s, 6H) 2.37 (s, 6H) 2.34 (s, 6H) 2.18 (s, 6H)	9.32 (t, 4H, ^3J=6.5), 7.76 (d, 4H, ^3J=6.5)

a) In $CDCl_3$, δ / ppm, $J_{H\text{-}H}$ / Hz, 400 MHz, 20°C, s = singlet, d = doublet, dd = doublet of doublets, t = triplet, se = septet, m = multiplet; b) Room temperature (20°C) spectrum, all signals broad due to exchange; c) solvent nitromethane-d_3

Table 5.2: Fractional atomic coordinates (x 10^4) and equivalent isotropic displacement factors ($Å^2$ x 10^3) for [{Ru(η^3:η^3-$C_{10}H_{16}$)Cl_2}$_2$(μ-$N_2C_4H_4$)].2$CHCl_3$ **106**.

	x	y	z	U(eq)
Ru(1)	1764(2)	1177(1)	1989(1)	41(1)
Cl(1)	4456(5)	1985(4)	703(2)	65(1)
Cl(2)	-1148(5)	222(3)	3059(2)	58(1)
C(1)	3093(21)	-935(12)	2372(9)	63(6)
C(2)	2938(19)	-596(14)	3329(9)	57(5)
C(3)	3818(20)	740(16)	3182(10)	69(6)
C(4)	3570(24)	1515(16)	4020(11)	82(7)
C(5)	3051(25)	2971(17)	3471(12)	87(8)
C(6)	1529(21)	2805(14)	2824(11)	67(6)
C(7)	1467(21)	3548(14)	1712(11)	66(6)
C(8)	120(19)	3089(12)	1267(9)	53(5)
C(9)	1907(22)	-1472(14)	4363(9)	73(6)
C(10)	2921(24)	4753(15)	1067(12)	88(7)
N(1)	692(14)	439(10)	790(6)	45(4)
C(11)	1766(17)	-121(12)	155(8)	46(4)
C(12)	-1111(17)	556(13)	618(8)	50(5)
C(50)	2193(26)	3281(15)	-2974(11)	88(8)
Cl(50)	2622(14)	3269(7)	-1768(4)	195(5)
Cl(51)	4195(11)	3814(8)	-3861(6)	172(4)
Cl(52)	548(12)	4412(7)	-3501(8)	193(5)

Table 5.3: Bond lengths (Å) and angles (°) for [{Ru(η^3:η^3-$C_{10}H_{16}$)Cl_2}$_2$(μ-$N_2C_4H_4$)].2$CHCl_3$ **106**.

Ru(1)-Cl(1)	2.406 (3)	Ru(1)-Cl(2)	2.425 (3)
Ru(1)-C(1)	2.226 (13)	Ru(1)-C(2)	2.303 (12)
Ru(1)-C(3)	2.256 (15)	Ru(1)-C(6)	2.240 (16)
Ru(1)-C(7)	2.264 (14)	Ru(1)-C(8)	2.235 (12)
Ru(1)-N(1)	2.191 (10)	C(1)-C(2)	1.422 (20)
C(2)-C(3)	1.416 (21)	C(2)-C(9)	1.487 (15)
C(3)-C(4)	1.550 (24)	C(4)-C(5)	1.456 (21)
C(5)-C(6)	1.527 (25)	C(6)-C(7)	1.435 (18)
C(7)-C(8)	1.360 (22)	C(7)-C(10)	1.553 (19)
N(1)-C(11)	1.341 (15)	N(1)-C(12)	1.360 (16)
C(11)-C(12A)	1.379 (18)	C(12)-C(11A)	1.379 (18)
C(50)-Cl(50)	1.678 (18)	C(50)-Cl(51)	1.737 (18)
C(50)-Cl(52)	1.690 (19)		

Cl(1)-Ru(1)-Cl(2)	170.2(1)	Cl(1)-Ru(1)-C(1)	83.8(3)
Cl(2)-Ru(1)-C(1)	94.7(3)	Cl(1)-Ru(1)-C(2)	101.7(3)
Cl(2)-Ru(1)-C(2)	82.4(3)	C(1)-Ru(1)-C(2)	36.5(5)
Cl(1)-Ru(1)-C(3)	84.0(3)	Cl(2)-Ru(1)-C(3)	104.1(3)
C(1)-Ru(1)-C(3)	63.3(6)	C(2)-Ru(1)-C(3)	36.2(5)
Cl(1)-Ru(1)-C(6)	103.9(4)	Cl(2)-Ru(1)-C(6)	84.3(4)
C(1)-Ru(1)-C(6)	131.8(5)	C(2)-Ru(1)-C(6)	96.3(5)
C(3)-Ru(1)-C(6)	70.3(6)	Cl(1)-Ru(1)-C(7)	83.3(4)
Cl(2)-Ru(1)-C(7)	100.8(4)	C(1)-Ru(1)-C(7)	158.5(6)
C(2)-Ru(1)-C(7)	131.2(5)	C(3)-Ru(1)-C(7)	98.2(6)
C(6)-Ru(1)-C(7)	37.1(5)	Cl(1)-Ru(1)-C(8)	95.0(3)
Cl(2)-Ru(1)-C(8)	83.7(3)	C(1)-Ru(1)-C(8)	164.1(5)
C(2)-Ru(1)-C(8)	156.9(5)	C(3)-Ru(1)-C(8)	132.5(6)
C(6)-Ru(1)-C(8)	63.9(5)	C(7)-Ru(1)-C(8)	35.2(5)
Cl(1)-Ru(1)-N(1)	85.4(2)	Cl(2)-Ru(1)-N(1)	84.8(2)
C(1)-Ru(1)-N(1)	81.8(5)	C(2)-Ru(1)-N(1)	114.7(4)
C(3)-Ru(1)-N(1)	144.4(5)	C(6)-Ru(1)-N(1)	145.4(5)
C(7)-Ru(1)-N(1)	114.2(5)	C(8)-Ru(1)-N(1)	82.3(4)
Ru(1)-C(1)-C(2)	74.7(8)	Ru(1)-C(2)-C(1)	68.8(7)
Ru(1)-C(2)-C(3)	70.1(7)	C(1)-C(2)-C(3)	112.0(10)
Ru(1)-C(2)-C(9)	126.5(10)	C(1)-C(2)-C(9)	125.5(13)
C(3)-C(2)-C(9)	122.4(13)	Ru(1)-C(3)-C(2)	73.7(8)
Ru(1)-C(3)-C(4)	117.4(10)	C(2)-C(3)-C(4)	123.3(11)
C(3)-C(4)-C(5)	106.8(12)	C(4)-C(5)-C(6)	105.1(14)
Ru(1)-C(6)-C(5)	119.8(11)	Ru(1)-C(6)-C(7)	72.3(9)
C(5)-C(6)-C(7)	126.0(12)	Ru(1)-C(7)-C(6)	70.5(8)
Ru(1)-C(7)-C(8)	71.2(8)	C(6)-C(7)-C(8)	115.8(11)
Ru(1)-C(7)-C(10)	125.8(10)	C(6)-C(7)-C(10)	121.0(14)
C(8)-C(7)-C(10)	123.2(12)	Ru(1)-C(8)-C(7)	73.6(8)
Ru(1)-N(1)-C(11)	122.7(8)	Ru(1)-N(1)-C(12)	122.1(8)
C(11)-N(1)-C(12)	115.2(11)	N(1)-C(11)-C(12A)	123.1(11)
N(1)-C(12)-C(11A)	121.7(11)	Cl(50)-C(50)-Cl(51)	109.1(11)
Cl(50)-C(50)-Cl(52)	114.7(11)	Cl(51)-C(50)-Cl(52)	106.5(8)

Table 5.4: Anisotropic displacement factors ($Å^2$ x 10^3) for $[\{Ru(\eta^3:\eta^3\text{-}C_{10}H_{16})Cl_2\}_2(\mu\text{-}N_2C_4H_4)].2CHCl_3$ **106.**

	U_{11}	U_{22}	U_{33}	U_{23}	U_{13}	U_{12}
Ru(1)	33(1)	57(1)	35(1)	-20(1)	-1(1)	6(1)
Cl(1)	49(2)	85(2)	59(2)	-27(2)	8(2)	-1(2)
Cl(2)	51(2)	74(2)	50(2)	-25(2)	3(2)	0(2)
C(1)	77(10)	54(7)	71(8)	-28(6)	-42(8)	40(8)
C(2)	47(9)	68(8)	55(7)	-18(7)	-14(7)	13(7)
C(3)	46(9)	103(11)	63(8)	-32(8)	-16(7)	14(9)
C(4)	90(13)	103(12)	70(9)	-43(9)	-40(9)	14(10)
C(5)	97(14)	92(11)	82(10)	-43(9)	-17(10)	0(10)
C(6)	65(10)	77(9)	78(9)	-52(8)	-8(8)	7(8)
C(7)	58(10)	67(8)	72(9)	-26(7)	3(8)	18(8)
C(8)	51(9)	58(7)	52(7)	-19(6)	-9(7)	5(7)
C(9)	83(12)	75(9)	50(7)	-3(7)	-15(8)	7(9)
C(10)	94(13)	71(9)	92(10)	-25(8)	10(10)	-1(10)
N(1)	40(6)	66(6)	34(4)	-24(4)	-3(5)	6(5)
C(11)	41(8)	68(7)	33(5)	-22(5)	-6(5)	12(6)
C(12)	37(8)	70(8)	45(6)	-26(6)	2(6)	13(7)
C(50)	123(16)	63(9)	85(10)	-32(8)	-19(11)	20(10)
Cl(50)	366(12)	137(5)	78(3)	-37(3)	-7(5)	-32(6)
Cl(51)	152(6)	173(6)	167(6)	-44(5)	36(5)	5(5)
Cl(52)	176(7)	137(5)	309(10)	-107(6)	-102(7)	69(5)

Table 5.5: Fractional atomic coordinates (x 10^4) and equivalent isotropic displacement factors ($Å^2$ x 10^3) for triclinic *rac*-[{Ru(η^3:η^3-$C_{10}H_{16}$)Cl(μ-SCN)}$_2$] **114b**.

	x	y	z	U(eq)
Ru(1)	1733(1)	1543(1)	2919(1)	46(1)
Ru(2)	4561(1)	3529(1)	7276(1)	40(1)
Cl(1)	783(5)	-335(3)	1610(3)	69(1)
Cl(2)	5187(5)	5420(3)	8612(3)	67(1)
S(1)	2941(5)	414(3)	3929(3)	58(1)
S(2)	4456(4)	4606(3)	6138(3)	57(1)
N(1)	3961(13)	2106(8)	5976(8)	51(4)
N(2)	2713(13)	2990(8)	4193(9)	56(5)
C(1)	-674(17)	1295(13)	3538(13)	74(7)
C(2)	-836(16)	2233(12)	3240(13)	69(7)
C(3)	-754(16)	2010(12)	2191(14)	74(7)
C(4)	-583(25)	2903(15)	1716(15)	105(10)
C(5)	884(24)	2652(14)	1208(14)	95(9)
C(6)	2425(21)	2504(13)	1975(12)	75(7)
C(7)	3414(22)	1628(14)	1783(13)	78(8)
C(8)	4488(16)	1523(15)	2669(13)	79(8)
C(9)	-983(21)	3398(13)	4008(14)	98(9)
C(10)	3303(25)	755(15)	703(14)	102(10)
C(11)	1766(16)	3868(11)	7176(11)	60(6)
C(12)	1911(16)	2993(11)	7490(11)	58(6)
C(13)	3165(17)	3171(11)	8401(10)	55(6)
C(14)	3806(20)	2260(12)	8767(12)	72(7)
C(15)	5792(20)	2380(12)	8924(11)	74(7)
C(16)	6170(18)	2472(11)	7953(10)	63(6)
C(17)	7323(18)	3314(12)	7965(11)	65(6)
C(18)	7273(16)	3449(13)	7026(11)	68(7)
C(19)	886(18)	1856(11)	6829(11)	72(7)
C(20)	8452(19)	4128(13)	8938(11)	81(7)
C(21)	3593(14)	1392(9)	5147(10)	45(5)
C(22)	3431(16)	3661(10)	4970(10)	53(6)

Table 5.6: Bond lengths (Å) and angles (°) for triclinic *rac*-[{Ru(η^3:η^3-$C_{10}H_{16}$)Cl(μ-SCN)}$_2$] **114b.**

Ru(1)-Cl(1)	2.409 (3)	Ru(1)-S(1)	2.490 (4)
Ru(1)-N(2)	2.039 (8)	Ru(1)-C(1)	2.280 (16)
Ru(1)-C(2)	2.271 (13)	Ru(1)-C(3)	2.239 (15)
Ru(1)-C(6)	2.255 (20)	Ru(1)-C(7)	2.283 (20)
Ru(1)-C(8)	2.248 (14)	Ru(2)-Cl(2)	2.412 (3)
Ru(2)-S(2)	2.483 (4)	Ru(2)-N(1)	2.004 (8)
Ru(2)-C(11)	2.232 (13)	Ru(2)-C(12)	2.278 (14)
Ru(2)-C(13)	2.257 (16)	Ru(2)-C(16)	2.236 (16)
Ru(2)-C(17)	2.273 (14)	Ru(2)-C(18)	2.214 (13)
S(1)-C(21)	1.671 (11)	S(2)-C(22)	1.666 (11)
N(1)-C(21)	1.158 (14)	N(2)-C(22)	1.136 (14)
C(1)-C(2)	1.425 (26)	C(2)-C(3)	1.410 (27)
C(2)-C(9)	1.500 (20)	C(3)-C(4)	1.551 (30)
C(4)-C(5)	1.442 (29)	C(5)-C(6)	1.535 (25)
C(6)-C(7)	1.354 (24)	C(7)-C(8)	1.429 (26)
C(7)-C(10)	1.493 (22)	C(11)-C(12)	1.360 (24)
C(12)-C(13)	1.404 (19)	C(12)-C(19)	1.511 (17)
C(13)-C(14)	1.514 (24)	C(14)-C(15)	1.525 (22)
C(15)-C(16)	1.500 (24)	C(16)-C(17)	1.386 (22)
C(17)-C(18)	1.394 (25)	C(17)-C(20)	1.475 (16)

Cl(1)-Ru(1)-S(1)	80.3(1)	Cl(1)-Ru(1)-N(2)	169.9(4)
S(1)-Ru(1)-N(2)	89.6(4)	Cl(1)-Ru(1)-C(1)	84.7(3)
S(1)-Ru(1)-C(1)	81.3(5)	N(2)-Ru(1)-C(1)	93.5(5)
Cl(1)-Ru(1)-C(2)	102.3(3)	S(1)-Ru(1)-C(2)	115.5(5)
N(2)-Ru(1)-C(2)	81.7(4)	C(1)-Ru(1)-C(2)	36.5(7)
Cl(1)-Ru(1)-C(3)	85.1(3)	S(1)-Ru(1)-C(3)	143.5(5)
N(2)-Ru(1)-C(3)	103.1(4)	C(1)-Ru(1)-C(3)	64.2(7)
C(2)-Ru(1)-C(3)	36.4(7)	Cl(1)-Ru(1)-C(6)	103.2(3)
S(1)-Ru(1)-C(6)	143.6(4)	N(2)-Ru(1)-C(6)	85.2(5)
C(1)-Ru(1)-C(6)	135.0(6)	C(2)-Ru(1)-C(6)	99.4(7)
C(3)-Ru(1)-C(6)	72.4(6)	Cl(1)-Ru(1)-C(7)	83.5(4)
S(1)-Ru(1)-C(7)	112.4(5)	N(2)-Ru(1)-C(7)	100.8(5)
C(1)-Ru(1)-C(7)	160.1(6)	C(2)-Ru(1)-C(7)	132.0(7)
C(3)-Ru(1)-C(7)	98.7(7)	C(6)-Ru(1)-C(7)	34.7(6)
Cl(1)-Ru(1)-C(8)	94.5(4)	S(1)-Ru(1)-C(8)	80.0(5)
N(2)-Ru(1)-C(8)	84.0(5)	C(1)-Ru(1)-C(8)	161.1(7)
C(2)-Ru(1)-C(8)	158.7(6)	C(3)-Ru(1)-C(8)	134.7(7)
C(6)-Ru(1)-C(8)	63.6(7)	C(7)-Ru(1)-C(8)	36.7(7)
Cl(2)-Ru(2)-S(2)	80.7(1)	Cl(2)-Ru(2)-N(1)	169.1(4)
S(2)-Ru(2)-N(1)	88.5(4)	Cl(2)-Ru(2)-C(11)	85.4(3)
S(2)-Ru(2)-C(11)	81.8(5)	N(1)-Ru(2)-C(11)	91.9(4)
Cl(2)-Ru(2)-C(12)	101.5(3)	S(2)-Ru(2)-C(12)	115.0(4)
N(1)-Ru(2)-C(12)	81.9(4)	C(11)-Ru(2)-C(12)	35.1(6)
Cl(2)-Ru(2)-C(13)	84.8(3)	S(2)-Ru(2)-C(13)	143.1(4)
N(1)-Ru(2)-C(13)	103.4(4)	C(11)-Ru(2)-C(13)	63.2(6)
C(12)-Ru(2)-C(13)	36.1(5)	Cl(2)-Ru(2)-C(16)	104.9(3)

S(2)-Ru(2)-C(16)	144.7(4)	N(1)-Ru(2)-C(16)	84.7(4)
C(11)-Ru(2)-C(16)	132.9(6)	C(12)-Ru(2)-C(16)	98.3(6)
C(13)-Ru(2)-C(16)	71.9(5)	Cl(2)-Ru(2)-C(17)	84.2(3)
S(2)-Ru(2)-C(17)	113.3(5)	N(1)-Ru(2)-C(17)	101.4(4)
C(11)-Ru(2)-C(17)	159.8(6)	C(12)-Ru(2)-C(17)	131.6(6)
C(13)-Ru(2)-C(17)	98.6(6)	C(16)-Ru(2)-C(17)	35.8(6)
Cl(2)-Ru(2)-C(18)	93.2(3)	S(2)-Ru(2)-C(18)	80.5(5)
N(1)-Ru(2)-C(18)	86.2(4)	C(11)-Ru(2)-C(18)	162.2(7)
C(12)-Ru(2)-C(18)	160.0(6)	C(13)-Ru(2)-C(18)	134.4(6)
C(16)-Ru(2)-C(18)	64.6(6)	C(17)-Ru(2)-C(18)	36.2(6)
Ru(1)-S(1)-C(21)	102.9(5)	Ru(2)-S(2)-C(22)	102.8(6)
Ru(2)-N(1)-C(21)	169.7(12)	Ru(1)-N(2)-C(22)	167.0(12)
Ru(1)-C(1)-C(2)	71.4(5)	Ru(1)-C(2)-C(1)	72.1(8)
Ru(1)-C(2)-C(3)	70.5(8)	C(1)-C(2)-C(3)	115.7(13)
Ru(1)-C(2)-C(9)	124.2(9)	C(1)-C(2)-C(9)	122.2(16)
C(3)-C(2)-C(9)	122.0(16)	Ru(1)-C(3)-C(2)	73.0(9)
Ru(1)-C(3)-C(4)	116.8(10)	C(2)-C(3)-C(4)	126.2(12)
C(3)-C(4)-C(5)	106.1(16)	C(4)-C(5)-C(6)	108.4(17)
Ru(1)-C(6)-C(5)	115.4(12)	Ru(1)-C(6)-C(7)	73.8(12)
C(5)-C(6)-C(7)	126.9(13)	Ru(1)-C(7)-C(6)	71.5(11)
Ru(1)-C(7)-C(8)	70.3(10)	C(6)-C(7)-C(8)	117.1(14)
Ru(1)-C(7)-C(10)	125.0(13)	C(6)-C(7)-C(10)	122.0(16)
C(8)-C(7)-C(10)	120.7(16)	Ru(1)-C(8)-C(7)	72.9(9)
Ru(2)-C(11)-C(12)	74.3(8)	Ru(2)-C(12)-C(11)	70.6(8)
Ru(2)-C(12)-C(13)	71.2(8)	C(11)-C(12)-C(13)	116.7(11)
Ru(2)-C(12)-C(19)	123.9(9)	C(11)-C(12)-C(19)	121.0(12)
C(13)-C(12)-C(19)	122.0(14)	Ru(2)-C(13)-C(12)	72.8(9)
Ru(2)-C(13)-C(14)	116.9(10)	C(12)-C(13)-C(14)	125.5(11)
C(13)-C(14)-C(15)	106.6(14)	C(14)-C(15)-C(16)	105.6(12)
Ru(2)-C(16)-C(15)	118.2(10)	Ru(2)-C(16)-C(17)	73.6(9)
C(15)-C(16)-C(17)	123.7(11)	Ru(2)-C(17)-C(16)	70.6(8)
Ru(2)-C(17)-C(18)	69.6(8)	C(16)-C(17)-C(18)	117.5(11)
Ru(2)-C(17)-C(20)	125.8(10)	C(16)-C(17)-C(20)	122.7(15)
C(18)-C(17)-C(20)	119.4(14)	Ru(2)-C(18)-C(17)	74.2(8)
S(1)-C(21)-N(1)	175.7(11)	S(2)-C(22)-N(2)	177.2(15)

Table 5.7: Anisotropic displacement factors ($Å^2$ x 10^3) for triclinic *rac*-[{Ru(η^3:η^3-$C_{10}H_{16}$)Cl(μ-SCN)}$_2$] **114b**.

	U_{11}	U_{22}	U_{33}	U_{23}	U_{13}	U_{12}
Ru(1)	45(1)	37(1)	51(1)	17(1)	-1(1)	-3(1)
Ru(2)	40(1)	34(1)	44(1)	12(1)	9(1)	3(1)
Cl(1)	90(2)	46(2)	55(2)	9(2)	0(2)	-5(2)
Cl(2)	83(2)	45(2)	58(2)	5(2)	13(2)	-4(2)
S(1)	79(2)	35(2)	49(2)	10(1)	3(2)	9(1)
S(2)	67(2)	42(2)	56(2)	20(1)	-3(2)	-17(1)
N(1)	57(6)	39(6)	48(6)	14(5)	-2(5)	7(5)
N(2)	60(6)	37(6)	66(7)	25(5)	-11(5)	-20(5)
C(1)	51(8)	77(10)	88(11)	25(9)	14(7)	-3(7)
C(2)	38(7)	57(9)	90(12)	14(8)	-3(7)	10(6)
C(3)	41(7)	53(8)	103(13)	21(8)	-23(8)	-8(6)
C(4)	108(15)	76(12)	104(14)	28(10)	-33(12)	27(10)
C(5)	115(15)	62(10)	106(14)	52(10)	-21(12)	-14(10)
C(6)	88(11)	63(9)	81(10)	47(8)	-1(8)	-26(8)
C(7)	94(12)	73(10)	76(11)	38(9)	23(9)	-11(9)
C(8)	36(7)	109(13)	108(13)	56(11)	24(8)	8(7)
C(9)	78(11)	70(10)	113(14)	5(10)	7(10)	25(8)
C(10)	134(16)	98(13)	98(14)	49(11)	60(12)	13(11)
C(11)	56(8)	48(7)	77(9)	25(7)	19(7)	4(6)
C(12)	49(7)	60(8)	74(9)	32(7)	25(7)	3(6)
C(13)	68(8)	51(7)	60(8)	26(6)	34(7)	17(6)
C(14)	90(11)	67(9)	73(10)	41(8)	25(8)	7(8)
C(15)	109(12)	59(9)	55(9)	27(7)	11(8)	31(8)
C(16)	73(9)	50(8)	57(8)	14(6)	7(7)	27(7)
C(17)	60(8)	70(9)	51(8)	14(7)	-1(7)	18(7)
C(18)	41(7)	74(9)	77(10)	15(8)	20(7)	5(6)
C(19)	69(9)	67(9)	88(11)	37(8)	26(8)	-16(7)
C(20)	67(9)	85(11)	69(10)	17(8)	-6(8)	-4(8)
C(21)	42(6)	39(6)	65(8)	30(6)	13(6)	15(5)
C(22)	56(7)	41(7)	64(8)	28(6)	7(6)	-3(6)

Table 5.8: Fractional atomic coordinates (x 10^4) and equivalent isotropic displacement factors ($Å^2$ x 10^3) for monoclinic *rac*-[{Ru(η^3:η^3-$C_{10}H_{16}$)Cl(μ-SCN)}$_2$] **114b.**

	x	y	z	U(eq)
Ru(1)	6674(1)	2350(1)	1186(1)	38(1)
Ru(2)	10869(1)	2652(1)	914(1)	32(1)
Cl(1)	5655(3)	2079(3)	2439(2)	59(1)
Cl(2)	11913(2)	3058(3)	-291(2)	55(1)
S(1)	7951(2)	2248(3)	2525(2)	55(1)
S(2)	9584(2)	2932(3)	-410(2)	44(1)
N(1)	9762(7)	2371(8)	1731(6)	42(3)
N(2)	7784(7)	2540(8)	338(6)	46(4)
C(1)	6876(12)	656(9)	1173(10)	60(6)
C(2)	6354(11)	915(10)	319(9)	49(5)
C(3)	5454(11)	1433(11)	395(9)	55(5)
C(4)	4844(12)	1908(12)	-433(11)	68(6)
C(5)	4734(11)	3036(14)	-177(11)	77(7)
C(6)	5752(10)	3397(11)	213(10)	57(5)
C(7)	5953(11)	3926(10)	1066(11)	59(6)
C(8)	6958(13)	4046(10)	1426(10)	63(6)
C(9)	6807(12)	768(12)	-567(10)	72(6)
C(10)	5138(12)	4296(12)	1638(13)	85(8)
C(11)	10477(11)	4287(10)	1220(9)	56(5)
C(12)	11501(9)	4153(9)	1575(8)	41(4)
C(13)	11680(9)	3320(10)	2215(8)	47(4)
C(14)	12712(10)	2900(11)	2531(9)	58(5)
C(15)	12656(11)	1742(10)	2403(11)	63(6)
C(16)	12118(10)	1584(9)	1442(9)	44(4)
C(17)	11259(12)	972(10)	1237(10)	55(6)
C(18)	10797(11)	1106(9)	305(10)	57(5)
C(19)	12308(12)	4777(11)	1177(10)	67(6)
C(20)	10799(11)	380(11)	1901(11)	74(7)
C(21)	9048(9)	2300(11)	2079(7)	46(4)
C(22)	8511(9)	2698(10)	14(7)	41(4)

Table 5.9: Bond lengths (Å) and angles (°) for monoclinic *rac*-[{Ru(η^3:η^3-$C_{10}H_{16}$)Cl(μ-SCN)}$_2$] **114b**.

Ru(1)-Cl(1)	2.425 (4)	Ru(1)-S(1)	2.470 (3)
Ru(1)-N(2)	2.054 (10)	Ru(1)-C(1)	2.230 (12)
Ru(1)-C(2)	2.277 (13)	Ru(1)-C(3)	2.254 (14)
Ru(1)-C(6)	2.251 (14)	Ru(1)-C(7)	2.277 (14)
Ru(1)-C(8)	2.271 (13)	Ru(2)-Cl(2)	2.424 (4)
Ru(2)-S(2)	2.484 (3)	Ru(2)-N(1)	2.038 (9)
Ru(2)-C(11)	2.256 (13)	Ru(2)-C(12)	2.310 (12)
Ru(2)-C(13)	2.264 (12)	Ru(2)-C(16)	2.261 (12)
Ru(2)-C(17)	2.295 (13)	Ru(2)-C(18)	2.205 (12)
S(1)-C(21)	1.679 (13)	S(2)-C(22)	1.661 (12)
N(1)-C(21)	1.139 (16)	N(2)-C(22)	1.152 (16)
C(1)-C(2)	1.407 (19)	C(2)-C(3)	1.405 (20)
C(2)-C(9)	1.497 (20)	C(3)-C(4)	1.520 (20)
C(4)-C(5)	1.532 (24)	C(5)-C(6)	1.506 (20)
C(6)-C(7)	1.424 (21)	C(7)-C(8)	1.411 (22)
C(7)-C(10)	1.527 (24)	C(11)-C(12)	1.435 (19)
C(12)-C(13)	1.439 (17)	C(12)-C(19)	1.523 (20)
C(13)-C(14)	1.523 (18)	C(14)-C(15)	1.526 (20)
C(15)-C(16)	1.523 (19)	C(16)-C(17)	1.414 (19)
C(17)-C(18)	1.446 (20)	C(17)-C(20)	1.431 (22)

Cl(1)-Ru(1)-S(1)	78.5(1)	Cl(1)-Ru(1)-N(2)	167.9(3)
S(1)-Ru(1)-N(2)	89.4(3)	Cl(1)-Ru(1)-C(1)	86.6(4)
S(1)-Ru(1)-C(1)	83.0(4)	N(2)-Ru(1)-C(1)	91.0(5)
Cl(1)-Ru(1)-C(2)	102.1(4)	S(1)-Ru(1)-C(2)	118.1(3)
N(2)-Ru(1)-C(2)	82.7(5)	C(1)-Ru(1)-C(2)	36.4(5)
Cl(1)-Ru(1)-C(3)	82.4(4)	S(1)-Ru(1)-C(3)	142.0(4)
N(2)-Ru(1)-C(3)	107.2(4)	C(1)-Ru(1)-C(3)	63.4(5)
C(2)-Ru(1)-C(3)	36.1(5)	Cl(1)-Ru(1)-C(6)	104.1(4)
S(1)-Ru(1)-C(6)	145.6(4)	N(2)-Ru(1)-C(6)	86.4(5)
C(1)-Ru(1)-C(6)	131.2(5)	C(2)-Ru(1)-C(6)	95.2(5)
C(3)-Ru(1)-C(6)	71.0(5)	Cl(1)-Ru(1)-C(7)	85.3(4)
S(1)-Ru(1)-C(7)	111.5(4)	N(2)-Ru(1)-C(7)	100.2(5)
C(1)-Ru(1)-C(7)	161.6(5)	C(2)-Ru(1)-C(7)	130.3(5)
C(3)-Ru(1)-C(7)	99.1(5)	C(6)-Ru(1)-C(7)	36.6(5)
Cl(1)-Ru(1)-C(8)	97.2(4)	S(1)-Ru(1)-C(8)	80.7(4)
N(2)-Ru(1)-C(8)	81.5(5)	C(1)-Ru(1)-C(8)	162.0(6)
C(2)-Ru(1)-C(8)	155.3(5)	C(3)-Ru(1)-C(8)	134.4(5)
C(6)-Ru(1)-C(8)	64.9(5)	C(7)-Ru(1)-C(8)	36.1(5)
Cl(2)-Ru(2)-S(2)	79.4(1)	Cl(2)-Ru(2)-N(1)	168.5(3)
S(2)-Ru(2)-N(1)	89.2(3)	Cl(2)-Ru(2)-C(11)	95.8(4)
S(2)-Ru(2)-C(11)	81.7(4)	N(1)-Ru(2)-C(11)	81.6(5)
Cl(2)-Ru(2)-C(12)	84.2(3)	S(2)-Ru(2)-C(12)	113.4(3)
N(1)-Ru(2)-C(12)	99.8(4)	C(11)-Ru(2)-C(12)	36.6(5)
Cl(2)-Ru(2)-C(13)	104.9(3)	S(2)-Ru(2)-C(13)	146.3(3)
N(1)-Ru(2)-C(13)	84.2(4)	C(11)-Ru(2)-C(13)	64.7(5)

C(12)-Ru(2)-C(13)	36.7(4)	Cl(2)-Ru(2)-C(16)	85.0(3)
S(2)-Ru(2)-C(16)	142.2(3)	N(1)-Ru(2)-C(16)	104.8(4)
C(11)-Ru(2)-C(16)	134.4(5)	C(12)-Ru(2)-C(16)	98.8(4)
C(13)-Ru(2)-C(16)	71.0(4)	Cl(2)-Ru(2)-C(17)	102.7(4)
S(2)-Ru(2)-C(17)	115.3(4)	N(1)-Ru(2)-C(17)	82.8(5)
C(11)-Ru(2)-C(17)	156.7(5)	C(12)-Ru(2)-C(17)	131.3(5)
C(13)-Ru(2)-C(17)	96.7(5)	C(16)-Ru(2)-C(17)	36.1(5)
Cl(2)-Ru(2)-C(18)	85.0(4)	S(2)-Ru(2)-C(18)	79.9(4)
N(1)-Ru(2)-C(18)	93.8(5)	C(11)-Ru(2)-C(18)	161.0(5)
C(12)-Ru(2)-C(18)	160.9(5)	C(13)-Ru(2)-C(18)	133.5(5)
C(16)-Ru(2)-C(18)	64.6(5)	C(17)-Ru(2)-C(18)	37.4(5)
Ru(1)-S(1)-C(21)	105.2(4)	Ru(2)-S(2)-C(22)	104.4(4)
Ru(2)-N(1)-C(21)	168.7(9)	Ru(1)-N(2)-C(22)	167.1(9)
Ru(1)-C(1)-C(2)	73.6(7)	Ru(1)-C(2)-C(1)	70.0(7)
Ru(1)-C(2)-C(3)	71.0(8)	C(1)-C(2)-C(3)	113.8(12)
Ru(1)-C(2)-C(9)	120.9(10)	C(1)-C(2)-C(9)	121.4(13)
C(3)-C(2)-C(9)	124.3(12)	Ru(1)-C(3)-C(2)	72.8(8)
Ru(1)-C(3)-C(4)	119.7(10)	C(2)-C(3)-C(4)	122.3(12)
C(3)-C(4)-C(5)	104.9(12)	C(4)-C(5)-C(6)	106.7(12)
Ru(1)-C(6)-C(5)	118.0(10)	Ru(1)-C(6)-C(7)	72.7(8)
C(5)-C(6)-C(7)	124.5(14)	Ru(1)-C(7)-C(6)	70.7(8)
Ru(1)-C(7)-C(8)	71.7(8)	C(6)-C(7)-C(8)	117.9(14)
Ru(1)-C(7)-C(10)	124.8(10)	C(6)-C(7)-C(10)	123.2(13)
C(8)-C(7)-C(10)	118.7(14)	Ru(1)-C(8)-C(7)	72.2(8)
Ru(2)-C(11)-C(12)	73.7(7)	Ru(2)-C(12)-C(11)	69.7(7)
Ru(2)-C(12)-C(13)	69.9(7)	C(11)-C(12)-C(13)	114.6(11)
Ru(2)-C(12)-C(19)	122.9(9)	C(11)-C(12)-C(19)	119.8(11)
C(13)-C(12)-C(19)	125.1(11)	Ru(2)-C(13)-C(12)	73.4(7)
Ru(2)-C(13)-C(14)	117.5(9)	C(12)-C(13)-C(14)	123.7(11)
C(13)-C(14)-C(15)	106.7(11)	C(14)-C(15)-C(16)	105.1(11)
Ru(2)-C(16)-C(15)	119.7(9)	Ru(2)-C(16)-C(17)	73.2(8)
C(15)-C(16)-C(17)	124.9(12)	Ru(2)-C(17)-C(16)	70.6(7)
Ru(2)-C(17)-C(18)	67.9(7)	C(16)-C(17)-C(18)	113.2(12)
Ru(2)-C(17)-C(20)	123.3(11)	C(16)-C(17)-C(20)	124.6(13)
C(18)-C(17)-C(20)	121.8(13)	Ru(2)-C(18)-C(17)	74.7(7)
S(1)-C(21)-N(1)	175.6(11)	S(2)-C(22)-N(2)	177.6(10)

Table 5.10: Anisotropic displacement factors ($Å^2$ x 10^3) for monoclinic *rac*-[{Ru(η^3:η^3-$C_{10}H_{16}$)Cl(μ-SCN)}$_2$] **114b.**

	U_{11}	U_{22}	U_{33}	U_{23}	U_{13}	U_{12}
Ru(1)	27(1)	49(1)	38(1)	5(1)	4(1)	-2(1)
Ru(2)	28(1)	38(1)	29(1)	-1(1)	3(1)	1(1)
Cl(1)	45(2)	88(3)	47(2)	5(2)	16(2)	-10(2)
Cl(2)	41(2)	82(2)	43(2)	0(2)	14(1)	8(2)
S(1)	32(2)	97(3)	35(2)	6(2)	4(1)	-3(2)
S(2)	33(2)	69(2)	31(2)	8(1)	2(1)	3(2)
N(1)	22(5)	67(7)	36(5)	11(5)	-4(4)	-10(5)
N(2)	37(6)	66(7)	35(5)	4(5)	7(4)	7(5)
C(1)	64(10)	34(7)	83(11)	2(7)	7(9)	6(7)
C(2)	51(9)	50(8)	44(8)	-11(6)	-8(7)	-4(7)
C(3)	49(9)	77(10)	37(7)	8(7)	-5(7)	-23(8)
C(4)	49(10)	81(11)	73(11)	-3(9)	7(8)	-14(8)
C(5)	40(9)	127(16)	62(10)	31(10)	-5(8)	-4(9)
C(6)	47(9)	59(9)	65(10)	8(7)	8(7)	-2(7)
C(7)	59(10)	39(8)	83(12)	8(7)	25(8)	5(7)
C(8)	90(13)	44(8)	55(9)	-8(7)	8(9)	-26(8)
C(9)	69(11)	90(11)	54(9)	-33(8)	-7(8)	2(9)
C(10)	64(11)	61(10)	135(17)	11(10)	31(11)	24(9)
C(11)	81(11)	46(8)	43(8)	-1(6)	12(8)	2(7)
C(12)	40(8)	46(7)	35(7)	-4(5)	1(6)	4(5)
C(13)	38(7)	64(9)	36(7)	-20(6)	-3(6)	0(6)
C(14)	39(8)	93(12)	40(7)	19(7)	-3(6)	-8(7)
C(15)	38(8)	51(9)	93(12)	17(8)	-21(8)	7(7)
C(16)	42(8)	43(7)	48(7)	4(6)	7(6)	21(6)
C(17)	51(9)	45(8)	71(11)	-1(7)	15(9)	15(7)
C(18)	72(10)	31(7)	64(9)	-17(6)	-2(8)	8(7)
C(19)	87(12)	56(9)	55(9)	3(7)	-7(9)	-19(8)
C(20)	55(10)	65(10)	105(14)	32(9)	23(9)	7(8)
C(21)	42(7)	71(8)	24(5)	2(6)	0(5)	-7(7)
C(22)	32(6)	60(8)	29(6)	13(6)	-10(5)	5(6)

Table 5.11: Fractional atomic coordinates (x 10^4) and equivalent isotropic displacement factors ($Å^2$ x 10^3) for [{Ru(η^3:η^3-$C_{10}H_{16}$)Cl}$_2$(μ-O_4C_2)] **115.**

	x	y	z	U(eq)
Ru(1)	2203(1)	948(1)	1483(1)	37(1)
Cl(1)	4625(3)	1422(1)	86(3)	59(1)
O(1)	-59(7)	355(3)	2001(7)	47(1)
O(2)	1810(8)	395(3)	-864(7)	51(1)
C(1)	3868(13)	86(5)	2178(13)	59(2)
C(2)	3346(23)	350(8)	3580(20)	53(4)
C(3)	3930(22)	1038(8)	3712(22)	57(4)
C(4)	3433(35)	1544(13)	5189(34)	106(7)
C(5)	1526(27)	1706(10)	5074(26)	75(5)
C(6)	785(23)	1579(9)	3354(22)	65(4)
C(7)	1140(26)	1947(9)	1817(22)	55(4)
C(8)	474(13)	1681(5)	226(13)	63(2)
C(9)	2250(24)	60(9)	4877(25)	69(4)
C(10)	2284(24)	2589(10)	1885(25)	76(5)
C(11)	-520(10)	-18(4)	821(10)	39(2)
C(2A)	4050(27)	592(11)	3541(25)	41(4)
C(3A)	2390(30)	802(11)	4265(29)	50(5)
C(4A)	2168(31)	1393(12)	5415(29)	51(5)
C(5A)	2422(33)	2036(12)	4483(32)	59(6)
C(6A)	2181(28)	1941(11)	2599(27)	45(5)
C(7A)	446(33)	1802(11)	1762(28)	46(5)
C(9A)	5840(37)	950(12)	3953(39)	65(7)
C(10A)	-1161(33)	1754(13)	2845(32)	63(6)

Table 5.12: Bond lengths (Å) and angles (°) for [{Ru(η^3:η^3-$C_{10}H_{16}$)Cl}$_2$(μ-O_4C_2)] **115.**

Ru(1)-Cl(1)	2.368 (2)	Ru(1)-O(1)	2.144 (5)
Ru(1)-O(2)	2.182 (6)	Ru(1)-C(1)	2.219 (10)
Ru(1)-C(2)	2.219 (16)	Ru(1)-C(3)	2.194 (17)
Ru(1)-C(6)	2.240 (18)	Ru(1)-C(7)	2.189 (18)
Ru(1)-C(8)	2.209 (10)	Ru(1)-C(2A)	2.256 (20)
Ru(1)-C(3A)	2.221 (23)	Ru(1)-C(6A)	2.189 (21)
Ru(1)-C(7A)	2.196 (24)	O(1)-C(11)	1.245 (9)
C(1)-C(2)	1.297 (19)	C(1)-C(2A)	1.489 (23)
C(2)-C(3)	1.461 (24)	C(2)-C(9)	1.454 (25)
C(3)-C(4)	1.600 (32)	C(4)-C(5)	1.494 (34)
C(5)-C(6)	1.488 (27)	C(6)-C(7)	1.453 (25)
C(7)-C(8)	1.453 (20)	C(7)-C(10)	1.562 (27)
C(8)-C(7A)	1.239 (25)	C(11)-C(11A)	1.532 (15)
C(2A)-C(3A)	1.460 (31)	C(2A)-C(9A)	1.576 (34)
C(3A)-C(4A)	1.510 (32)	C(4A)-C(5A)	1.505 (33)
C(5A)-C(6A)	1.510 (33)	C(6A)-C(7A)	1.500 (32)
C(7A)-C(10A)	1.508 (35)		

Cl(1)-Ru(1)-O(1)	161.8(2)	Cl(1)-Ru(1)-O(2)	84.8(2)
O(1)-Ru(1)-O(2)	77.0(2)	Cl(1)-Ru(1)-C(1)	89.0(3)
O(1)-Ru(1)-C(1)	88.7(3)	O(2)-Ru(1)-C(1)	83.2(3)
Cl(1)-Ru(1)-C(2)	105.4(5)	O(1)-Ru(1)-C(2)	82.2(5)
O(2)-Ru(1)-C(2)	113.9(5)	C(1)-Ru(1)-C(2)	34.0(5)
Cl(1)-Ru(1)-C(3)	82.9(5)	O(1)-Ru(1)-C(3)	111.7(5)
O(2)-Ru(1)-C(3)	143.0(5)	C(1)-Ru(1)-C(3)	61.9(5)
C(2)-Ru(1)-C(3)	38.7(6)	Cl(1)-Ru(1)-C(6)	117.8(5)
O(1)-Ru(1)-C(6)	78.1(5)	O(2)-Ru(1)-C(6)	142.1(5)
C(1)-Ru(1)-C(6)	124.2(5)	C(2)-Ru(1)-C(6)	90.3(6)
C(3)-Ru(1)-C(6)	73.4(6)	Cl(1)-Ru(1)-C(7)	88.7(5)
O(1)-Ru(1)-C(7)	100.9(5)	O(2)-Ru(1)-C(7)	121.7(5)
C(1)-Ru(1)-C(7)	154.6(5)	C(2)-Ru(1)-C(7)	123.6(6)
C(3)-Ru(1)-C(7)	92.7(6)	C(6)-Ru(1)-C(7)	38.3(6)
Cl(1)-Ru(1)-C(8)	89.2(3)	O(1)-Ru(1)-C(8)	88.9(3)
O(2)-Ru(1)-C(8)	83.4(3)	C(1)-Ru(1)-C(8)	166.6(4)
C(2)-Ru(1)-C(8)	157.9(5)	C(3)-Ru(1)-C(8)	130.9(5)
C(6)-Ru(1)-C(8)	68.0(5)	C(7)-Ru(1)-C(8)	38.6(5)
Cl(1)-Ru(1)-C(2A)	88.8(5)	O(1)-Ru(1)-C(2A)	100.5(6)
O(2)-Ru(1)-C(2A)	121.8(6)	C(1)-Ru(1)-C(2A)	38.8(6)
Cl(1)-Ru(1)-C(3A)	118.3(6)	O(1)-Ru(1)-C(3A)	77.2(6)
O(2)-Ru(1)-C(3A)	141.3(6)	C(1)-Ru(1)-C(3A)	67.8(6)
C(2A)-Ru(1)-C(3A)	38.1(8)	Cl(1)-Ru(1)-C(6A)	80.1(6)
O(1)-Ru(1)-C(6A)	115.0(6)	O(2)-Ru(1)-C(6A)	144.0(6)
C(1)-Ru(1)-C(6A)	128.7(6)	C(2A)-Ru(1)-C(6A)	90.5(8)
C(3A)-Ru(1)-C(6A)	73.9(8)	Cl(1)-Ru(1)-C(7A)	102.2(6)
O(1)-Ru(1)-C(7A)	85.6(7)	O(2)-Ru(1)-C(7A)	114.2(6)
C(1)-Ru(1)-C(7A)	159.8(6)	C(2A)-Ru(1)-C(7A)	123.7(8)
C(3A)-Ru(1)-C(7A)	92.1(8)	C(6A)-Ru(1)-C(7A)	40.0(8)
Ru(1)-O(1)-C(11)	114.5(5)	Ru(1)-O(2)-C(11A)	112.9(5)
Ru(1)-C(1)-C(2)	73.0(9)	Ru(1)-C(1)-C(2A)	71.9(9)
Ru(1)-C(2)-C(1)	73.0(8)	Ru(1)-C(2)-C(3)	69.7(9)
C(1)-C(2)-C(3)	110.7(14)	Ru(1)-C(2)-C(9)	121.4(13)
C(1)-C(2)-C(9)	128.6(15)	C(3)-C(2)-C(9)	120.7(15)
Ru(1)-C(3)-C(2)	71.6(9)	Ru(1)-C(3)-C(4)	119.5(13)
C(2)-C(3)-C(4)	125.6(16)	C(3)-C(4)-C(5)	109.6(19)
C(4)-C(5)-C(6)	112.1(18)	Ru(1)-C(6)-C(5)	121.3(13)
Ru(1)-C(6)-C(7)	69.0(10)	C(5)-C(6)-C(7)	127.0(16)
Ru(1)-C(7)-C(6)	72.8(10)	Ru(1)-C(7)-C(8)	71.5(8)
C(6)-C(7)-C(8)	117.9(14)	Ru(1)-C(7)-C(10)	124.0(13)
C(6)-C(7)-C(10)	120.4(15)	C(8)-C(7)-C(10)	121.7(14)
Ru(1)-C(8)-C(7)	70.0(8)	O(1)-C(11)-O(2A)	124.4(7)
O(1)-C(11)-C(11A)	117.5(8)	O(2A)-C(11)-C(11A)	118.1(8)
Ru(1)-C(2A)-C(1)	69.2(8)	C(1)-C(2A)-C(3A)	114.2(17)
Ru(1)-C(2A)-C(9A)	122.4(16)	C(1)-C(2A)-C(9A)	122.4(18)
C(3A)-C(2A)-C(9A)	122.8(20)	Ru(1)-C(3A)-C(2A)	72.3(12)
Ru(1)-C(3A)-C(4A)	119.0(15)	C(2A)-C(3A)-C(4A)	124.8(20)
C(3A)-C(4A)-C(5A)	111.7(19)	C(4A)-C(5A)-C(6A)	111.0(19)
Ru(1)-C(6A)-C(5A)	120.8(15)	Ru(1)-C(6A)-C(7A)	70.3(12)
C(5A)-C(6A)-C(7A)	123.7(19)	Ru(1)-C(7A)-C(8)	74.2(12)
Ru(1)-C(7A)-C(6A)	69.8(12)	C(8)-C(7A)-C(6A)	116.3(20)
Ru(1)-C(7A)-C(10A)	120.6(16)	C(8)-C(7A)-C(10A)	124.6(21)
C(6A)-C(7A)-C(10A)	118.8(19)		

Table 5.13: Anisotropic displacement factors ($Å^2$ x 10^3) for $[\{Ru(\eta^3:\eta^3\text{-}C_{10}H_{16})Cl\}_2(\mu\text{-}O_4C_2)]$ **115**.

	U_{11}	U_{22}	U_{33}	U_{23}	U_{13}	U_{12}
Ru(1)	40(1)	40(1)	30(1)	-3(1)	1(1)	-4(1)
Cl(1)	60(1)	65(1)	53(1)	2(1)	9(1)	-22(1)

Chapter 6

Single Nucleophilic Addition Reactions of (Arene)([2.2]Paracyclophane)Ruthenium(II) Complexes

6.1 Introduction

Both single and double nucleophilic addition to coordinated arenes are of significant interest as a synthetic route to arene functionalisation[8] and a single nucleophilic attack is a key initial step in the recently reported synthesis of (±)-dihydroxyserrulatic acid.[216] While *bis*(arene)ruthenium complexes are expected[84] to be around thirty times less electrophilic than their iron analogues they display a number of advantages which make them an attractive alternative in this type of work. These advantages include (a) the ready availability, *via* the Bennett[35] and Rybinskaya[38,217] syntheses, of unsymmetrical *bis*(arene)Ru^{2+} complexes and (b) the elimination of interfering electron transfer reactions[25,72,79] which can occur on the addition of carbon donor nucleophiles and result in the formation, and often rapid decomposition, of unstable nineteen and twenty electron species. Single nucleophilic addition reactions give rise to functionalised cyclohexadienyl complexes[11,58,73,79] from which functionalised arenes may be generated by oxidative decomplexation (possibly preceded by hydride abstraction by $[Ph_3C]^+$).[125,218] Double nucleophilic additions to $[Ru(arene)_2]^{2+}$ complexes can, in principle, give useful functionally disubstituted 1,3- or 1,4-cyclohexadiene complexes of Ru(0) from which the free cyclohexadiene might be liberated by oxidative decomplexation.[87] In practice however, all nucleophilic additions so far studied, except some reactions with hydride ions,[8-10,44,217] give rise to *bis*(cyclohexadienyl) complexes even when one of the arenes is the sterically congested 1,3,5-tri*iso*-propylbenzene ligand.[8] These results contrast sharply to the iron analogues in which double nucleophilic additions frequently occur at the same arene ring and in which nucleophilic additions have been used successfully as a route to the synthesis of free, functionalised 1,3-cyclohexadienes.[71,87] It is noteworthy however, that Boekelheide[7] has demonstrated that the action of the hydride source Red-Al upon [Ru(η^6-[2.2]paracyclophane)(η^6-arene)][BF_4]$_2$ (arene = C_6H_6 **3a** and C_6Me_6 **3b**) gives solely diene products. Reduction of the benzene complex **3a** gives the 1,3-diene compound [Ru(η^6-$C_{16}H_{16}$)(η^4-C_6H_8)] whereas a 1,4-double addition occurs in the case of **3b** to give the 1,4-diene complex [Ru(η^6-$C_{16}H_{16}$)(η^4-*exo,exo*-3,6-$C_6Me_6H_2$)]. Double addition of nucleophiles *para* to one another is consistent with charge control[11,87] but contrasts to the iron analogues in which additions are thought to be frontier orbital controlled[71,87] and occur

ortho to one another (see Section 1.3.3). These results suggest that [2.2]paracyclophane may be relatively inert towards nucleophilic addition and may therefore be suitable as a spectator ligand, complexing the vacant coordination sites in moieties such as "(arene)Ru^{2+}", and directing nucleophiles on to the coordinated arene ligand. Other, more conventional, candidates for spectator ligands such as CO are themselves susceptible to nucleophilic addition. Nitrogen donors such as polypyridines are poor π-acceptors and do not stabilise the zero valent metal centres which result from double nucleophilic additions to ruthenium(II) compounds. Phosphine ligands may be susceptible to oxidation during the oxidative decomplexation phase in which the free functionalised diene is liberated. The formation of the 1,4-diene complex [Ru(η^6-$C_{16}H_{16}$)(η^4-*exo,exo*-3,6-$C_6Me_6H_2$)] also suggests that double nucleophilic additions to ruthenium cyclophane compounds may offer the possibility of synthesis of the less readily obtainable, functionalised 1,4-dienes.

In this chapter the use of [2.2]paracyclophane as a non-innocent spectator ligand, to direct *single* nucleophilic attack onto a number of η^6-arenes is reported and the question of *exo* or *endo* addition addressed by a study of the effects of deuterium isotopic substitution on solid state infrared and solution ^1H NMR spectra.

6.2 Reactions of the (Benzene)([2.2]Paracyclophane)Ruthenium(II) Cation

Treatment of an methanolic suspension of [Ru(η^6-$C_{16}H_{16}$)(η^6-C_6H_6)][BF_4]$_2$ **3a** with Na[BH_4] results in a rapid darkening to give a greenish solution. Extraction of the reaction mixture with dichloromethane and precipitation gives the stable bright yellow cyclohexadienyl compound [Ru(η^6-$C_{16}H_{16}$)(η^5-C_6H_7)][BF_4] **121** in *ca.* 40% yield as the sole product (Scheme 6.1). A similar synthetic procedure utilising KCN gives the very mildly air sensitive complex [Ru(η^6-$C_{16}H_{16}$)(η^5-C_6H_6CN)][BF_4] **122.** ^1H NMR data for these compounds are summarised in Table 6.1. The singlet resonance for the benzene ligand in the parent compound is replaced with one multiplet and three triplet resonances covering a wide chemical shift range (*e.g.* δ 6.20, 4.86, 3.33 and 2.32 ppm in compound **121**) consistent with previous observations[85] and indicative of the formation of a cyclohexadienyl ligand. In addition a doublet resonance ($^2J_{H\text{-}H}$ = 13.5 Hz) is observed at

δ 2.06 ppm and is assigned to H_{exo} (Fig. 6.1). Vicinal coupling to H_c is not observed since the dihedral angle between the two protons H_c and H_{exo} is close to 90°. In the infrared spectrum, **121** exhibits strong bands at 2926 cm^{-1} and 2813 cm^{-1} which may be assigned as $\nu(CH_{endo})$ and $\nu(CH_{exo})$ respectively.[7,74] A similar $\nu(CH_{endo})$ band is observed in the infrared spectrum of **122** at 2923 cm^{-1} but in that compound there are no bands in the ν(CH) region below 2850 cm^{-1}. The $^{13}C-\{^1H\}$ NMR spectrum of **122** (Table 6.2) displays a peak at δ 119.3 ppm which is assigned as the resonance due to the CN carbon atom.

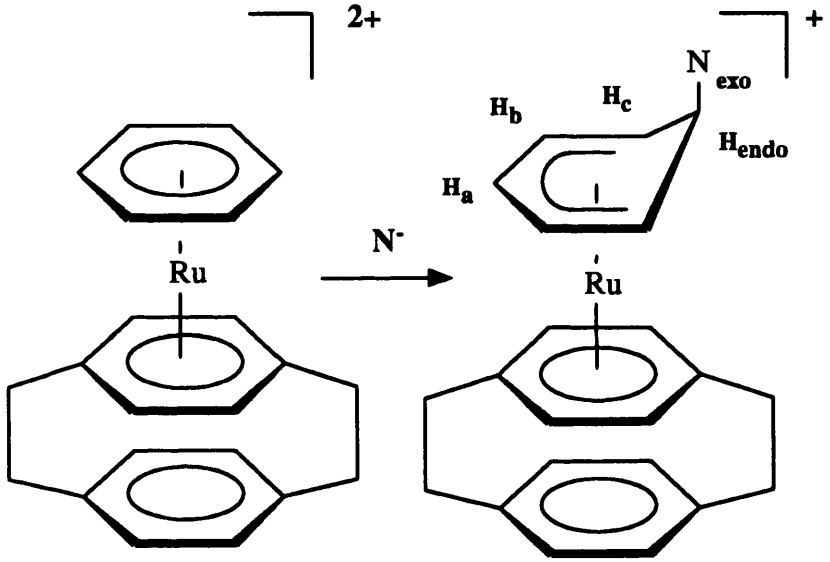

N = H **121**
CN **122**
OMe **123**
Me **124**

Scheme 6.1: Nucleophilic addition to $[Ru([2.2]paracyclophane)(benzene)]^{2+}$.

Treatment of **3a** with $Na[BD_4]$ gives the product, $[Ru(\eta^6-C_{16}H_{16})(\eta^5-C_6H_6D)][BF_4]$ **121'**, which exhibits a very similar ^1H NMR spectrum to **121** except for the absence of the

doublet resonance at δ 2.06 ppm. The infrared spectrum of this material displays $\nu(CH_{endo})$ at 2925 cm^{-1} but the band observed at 2813 cm^{-1} in **121**, occurs at 2113 cm^{-1}, a typical deuterium isotope shift.[74,219]

The anomalously low wavenumber of the band assigned to the $\nu(CH_{exo})$ vibration in cyclohexadienyl complexes such as **121** is a well documented phenomenon.[39,74-77] Deuteriation and substitution studies have firmly established that the vibration is associated with the *exo* C-H bond of the CH_2 group of the cyclohexadienyl ligand but the reason for the position of the band is still poorly understood. Although an agostic type of interaction in which C-H σ-electron density is donated to the metal centre is unlikely given the *exo* nature of the bond, we wondered if the low wavenumber of the vibration might be caused by a reduction in C-H σ-electron density of some other kind and consequent lowering of the force constant of the vibration. In order to test this hypothesis the ^1H coupled ^{13}C NMR spectrum of complex **121** was examined. A reduction in σ-bond electron density might be expected to result in a reduced value of $^1J_{C\text{-}H}$ for the *exo* CH bond. In fact, the resonance corresponding to the aliphatic carbon atom of the cyclohexadienyl ligand occurs as a triplet at δ 27.9 ppm (*cf.* δ 27.5 ppm for $[Ru(\eta^5\text{-}C_6H_7)(PMe_2Ph)(phen)][PF_6]$[58]). The coupling constant, $^1J_{C\text{-}H}$ = 136.0 Hz, suggesting no difference in bond strength between $C\text{-}H_{exo}$ and $C\text{-}H_{endo}$, and no reduced C-H bond order.

Reaction of **3a** with MeLi / Et_2O in methanol results in the deprotonation of the solvent by the alkyl lithium reagent followed by methoxide addition to give the methoxy compound $[Ru(\eta^6\text{-}C_{16}H_{16})(\eta^5\text{-}C_6H_6OMe)][BF_4]$ **123** in excellent yield. Complex **123** is characterised by the singlet ^1H NMR resonance due to the OMe group at δ 2.88 ppm and the high field chemical shift of H_{endo}, δ 3.38 ppm. The analogous reaction in dry thf results in the isolation of the methyl adduct $[Ru(\eta^6\text{-}C_{16}H_{16})(\eta^5\text{-}C_6H_6Me)][BF_4]$ **124**, characterised by a doublet resonance due to the methyl substituent at δ 0.30 ppm (^3J = 6.6 Hz), along with a similar pattern of resonances to compounds **121** - **123** indicating the formation of a cyclohexadienyl product. Unfortunately the reaction is not a clean one, and the product exhibits poor crystallinity and is difficult to precipitate from solution hence an analytically pure compound could not be isolated.

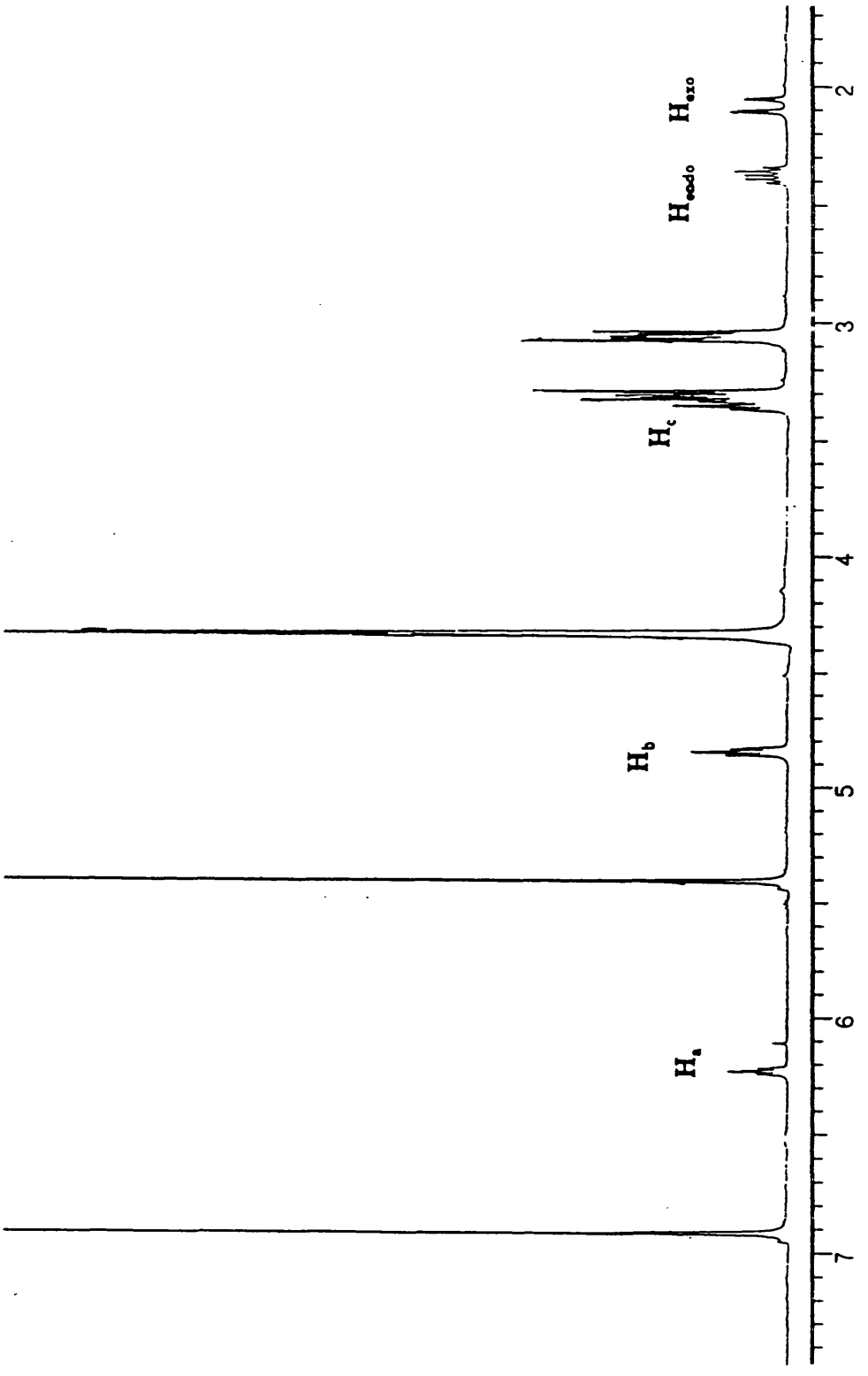

Fig. 6.1: ^{1}H NMR spectrum (NO_2CD_3) of $[Ru(\eta^6\text{-}C_{16}H_{16})(\eta^5\text{-}C_6H_7)][BF_4]$ 121.

The reaction of $Na[BH_4]$ with $[Os(\eta^6\text{-}C_{16}H_{16})(\eta^6\text{-}C_6H_6)][BF_4]_2$[128] proceeds cleanly to give a product $[Os(\eta^6\text{-}C_{16}H_{16})(\eta^5\text{-}C_6H_7)][BF_4]$ **125** analogous to **121**, with no obvious decrease in rate in spite of the presumed lower electrophilicity of the osmium complex.[84]

These results clearly indicate that single nucleophilic attack occurs on the less alkylated ring (expected to possess the most partial positive charge as a consequence of the +I inductive effect of the alkyl substituents), to give a monocationic product with the added nucleophile in the *exo* position. This observation is consistent with the ideas of Davies *et al.* and suggests the reactions may be charge controlled.[11]

6.3 Nucleophilic Additions to Alkylated Arenes

If single nucleophilic additions in (arene)(paracyclophane)ruthenium(II) cations are charge controlled increasing the degree of alkylation upon the arene ligand should, ultimately, result in the greatest partial positive charges residing on the carbon atoms of the paracyclophane coordinated deck. In principle, this should result in nucleophilic addition occurring on the cyclophane ligand and not the other coordinated arene. In order to determine whether the paracyclophane ligand could indeed be activated in this way and,if so, to what degree the arene ligand needs to be alkylated to achieve this change in regioselectivity, we have examined the reactions of a number of alkylated (arene)([2.2]paracyclophane)ruthenium(II) cations towards nucleophiles.

*6.3.1 Addition to the ([2.2]Paracyclophane)(*p*-cymene)ruthenium(II) Cation*

The action of $Na[BH_4]$ on the *p*-cymene complex $[Ru(\eta^6\text{-}C_{16}H_{16})(\eta^6\text{-}4\text{-}MeC_6H_4CHMe_2)][BF_4]_2$ **3c** gives two compounds in a ratio of 5 : 2, which may be distinguished by their ^1H NMR spectra (Table 6.1). The infrared spectrum of a mixture of these two materials (which could not be separated) exhibits $\nu(CH_{endo})$ 2928 cm^{-1} and $\nu(CH_{exo})$ 2804 cm^{-1}. Extensive homonuclear ^1H NMR decoupling experiments showed these compounds to be two isomers of $[Ru(\eta^6\text{-}C_{16}H_{16})(\eta^5\text{-}MeC_6H_5CHMe_2)][BF_4]$ **126a** and **126b** in which nucleophilic addition has occurred exclusively on the *p*-cymene ligand. The major isomer (evaluated by ^1H NMR spectral integration of the resonances due to the substituents

on the cyclohexadienyl ring) is assigned the structure **126b**, with nucleophilic attack occurring at the site *ortho* to the methyl (as opposed to *iso*-propyl) substituent.*

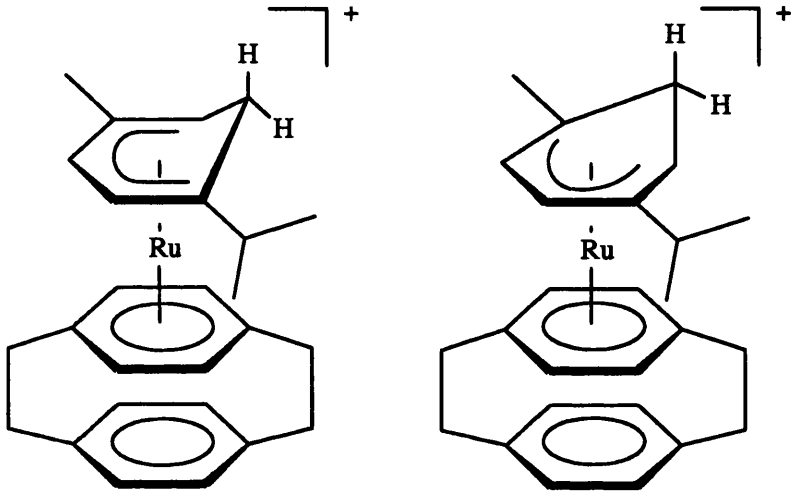

126a **126b**

An interesting feature of the ^{1}H NMR spectra of **126a** and **126b** is that in each case the resonances corresponding to the four coordinated ring protons of the [2.2]paracyclophane ligand are not singlets as has been previously observed for metal-[2.2]paracyclophane complexes[7,128] but form a widely spaced AB (or, more strictly, AA'BB') pattern (*e.g.* δ 5.02 and 5.61 ppm for the major isomer). The reason for this would appear to be the sensitivity of the [2.2]paracyclophane ligand to chirality at the metal centre[220] caused, for example, by the presence of three different ligands in addition to the cyclophane, coordinated to the ruthenium ion (see Appendix I). Recently it has been noted[47] that the presence of two different *ortho*-related substituents on a six-membered coordinated ring causes the formation of a chiral centre and is thus capable of rendering

* The assignment of the structures **126a, 126b** is made on the basis of i) the chemical shifts of the methyl substituents; the high field resonance for the major isomer (δ 1.36) suggests that the methyl substituent is adjacent to the aliphatic site (*cf.* δ 1.71 for the minor isomer). This chemical shift difference is also observed in reverse for the *iso*-propyl substituents. ii) The chemical shift difference in the signals for the diastereotopic methyl groups of the *iso*-propyl substituent; the splitting is larger for the minor isomer in which the *iso*-propyl group is closer to the (asymmetric) aliphatic site.

the cyclophane aromatic protons magnetically inequivalent in spite of the rapid rotation of the ligand. In these particular cases, **126a** and **126b**, either the *iso*-propyl or methyl group is ortho to the attack site. In effect the alkyl substituent and the sp^3 attack site may be regarded as two very different ring substituents and hence, due to the chirality when coordinated to a metal centre, cause a large splitting of the cyclophane resonances, as has been observed in other [2.2]paracyclophane systems.[220] A fuller account of the characteristic ^1H NMR spectra of the metal coordinated [2.2]paracyclophane ligand is given in Appendix I.

The tetraphenylborate salts of **126a** and **126b**, $[Ru(\eta^6\text{-}C_{16}H_{16})(\eta^5\text{-}MeC_6H_5CHMe_2)][BPh_4]$ **127a** and **127b**, were also prepared and their ^1H NMR spectra recorded. Surprisingly, while the general form of the spectrum remained the same, the splitting patterns were significantly more complex than those observed for the corresponding tetrafluoroborate salts (Fig. 6.2) and the resonances due to both cyclophane decks occurred at significantly higher field. This is probably due to specific cation-anion interactions, possibly as a consequence of π-π stacking between the phenyl substituents of the $[BPh_4]^-$ anion and the cationic complex, but the precise nature of the effects is unknown. The changes are consistent with those which occur on changing to a $[BPh_4]^-$ counterion[220] in related chiral systems.

The reaction of **3c** with KCN was also investigated and analogous products $[Ru(\eta^6\text{-}C_{16}H_{16})(\eta^5\text{-}MeC_6H_4CHMe_2CN)][BF_4]$, **128a** and **128b**, obtained in a similar isomer ratio, the most favourable site of attack again being *ortho* to the smaller (methyl) substituent. A steric dependence in the formation of isomers of this kind has also been observed in nucleophilic addition to cations of the type $[Mn(\eta^6\text{-}4\text{-}MeC_6H_4X)(CO)_3]^+$. The larger the substituent, X, the more nucleophilic attack is favoured *ortho* to the methyl group.[221] It should be noted that this preference may also be rationalised on electronic grounds. Also, a recent theoretical investigation has suggested that the regioselectivity of single nucleophilic additions to related substituted (arene)iron(II) complexes is dependent solely on changes in the classical, statistical probability of the nucleophile to contact different regions of the molecular surface.[222]

Action of $Na[BD_4]$ upon **3c** gave the expected deuterio complexes $[Ru(\eta^6\text{-}C_{16}H_{16})(\eta^5\text{-}MeC_6H_4DCHMe_2)][BF_4]$ **126a'** and **126b'** which exhibited $\nu(CD_{exo})$ in their

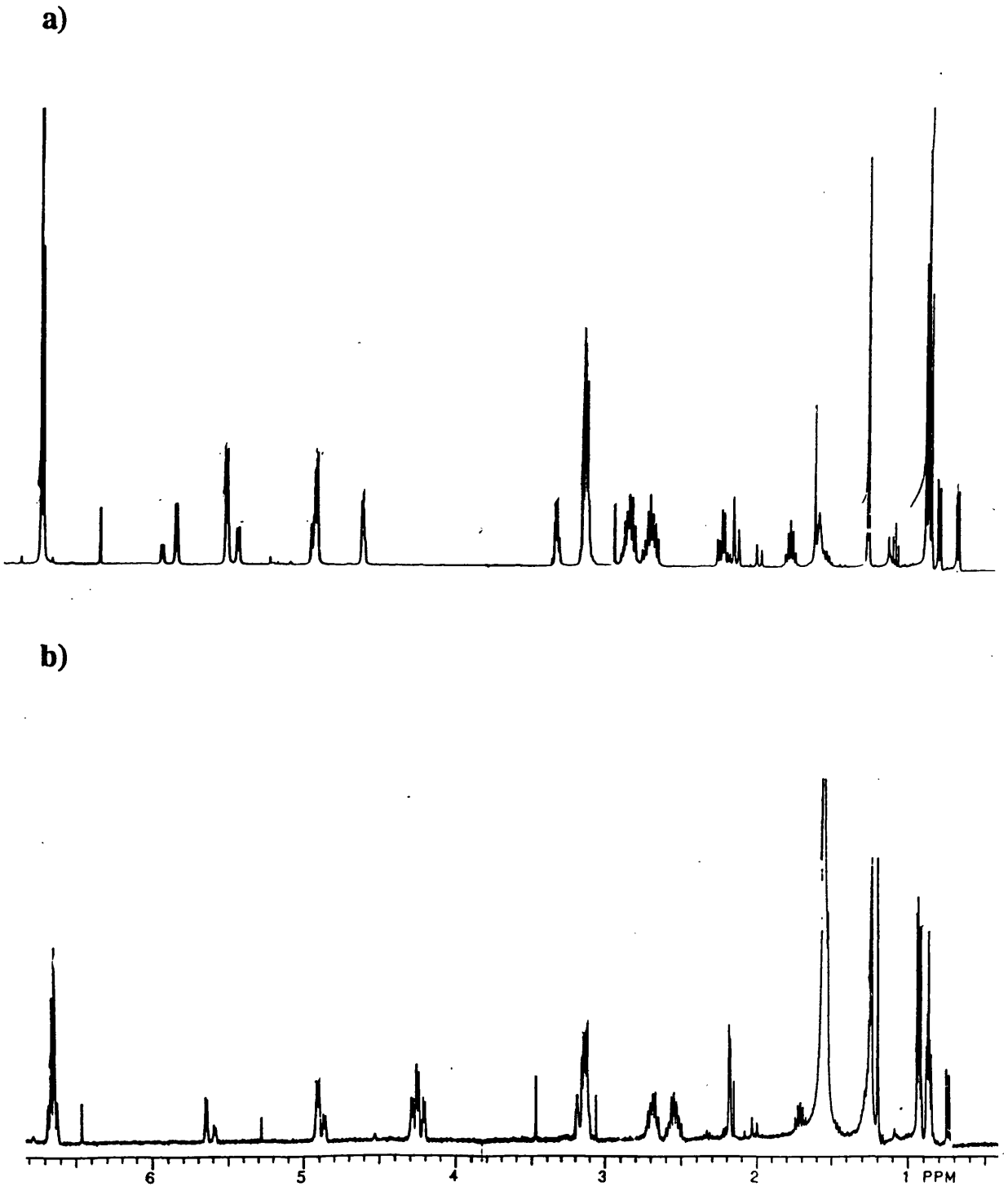

Fig. 6.2: Partial ^1H NMR spectra of $[Ru(\eta^6\text{-}C_{16}H_{16})(\eta^5\text{-}MeC_6H_5CHMe_2)]^+$ a) tetrafluoroborate salt **126**; b) tetraphenylborate salt **127**.

infrared spectra at 2129 cm^{-1}, confirming *exo* addition. The infrared spectral results of the deuteriation studies are summarised in Table 6.3.

The proposed structures for **126a** and **126b** were further confirmed by an examination of the action of $Na[BH_4]$ on the 1,4-di-*iso*-propylbenzene derivative $[Ru(\eta^6\text{-}C_{16}H_{16})\{\eta^6\text{-}1,4\text{-}(CHMe_2)_2C_6H_4\}][BF_4]_2$ which was synthesised from di-*iso*-propylbenzene and $[Ru(\eta^6\text{-}C_{16}H_{16})(OCMe_2)_3][BF_4]_2$ using the general method reported by Boekelheide *et al.*[7] The product of this reaction, $[Ru(\eta^6\text{-}C_{16}H_{16})\{\eta^5\text{-}1,4\text{-}(CHMe_2)_2C_6H_5\}][BF_4]$ **129**, took the form of a single isomer and exhibited a ^1H NMR spectrum consistent with the expected single addition of hydride to one of the non-alkylated sites of the di-*iso*-propylbenzene ring. As in the case of **126a**, **126b** and **128a**, **128b** the proton resonances for the coordinated cyclophane deck took the form of an AA'BB' pattern (δ 5.04 and 5.59 ppm, ^3J = 6.3 Hz) indicating the presence of two different *ortho* related substituents on the cyclohexadienyl ring, and the four methyl groups of the *iso*-propyl groups occurred as four separate doublet resonances (δ 1.04, 0.94, 0.92 and 0.80 ppm) indicating a unique environment for each substituent.

6.3.2 Addition to the (Hexamethylbenzene)([2.2]Paracyclophane)Ruthenium(II) Cation

The reaction of $[Ru(\eta^6\text{-}C_{16}H_{16})(\eta^6\text{-}C_6Me_6)][BF_4]_2$ **3b** with H^-, CN^- and Me^- under the conditions described above, results in isolation of compounds of formula $[Ru(\eta^6\text{-}C_{16}H_{16})(\eta^5\text{-}C_6Me_6R)][BF_4]$ (R = H, **130**; CN, **131**; Me, **132**). In each case attack occurs solely on the hexamethylbenzene ligand. Compound **130** displays a band in the infrared spectrum assigned to $\nu(CH_{exo})$ at 2813 cm^{-1}, this appears at 2107 cm^{-1} in the deuteriated analogue but is absent in the spectra of both **131** and **132**. The ^1H NMR spectrum of **130** (Table 6.1) clearly shows a quartet resonance (^3J = 6.8 Hz) for the added hydrogen atom (δ 2.00 ppm) and a corresponding methyl doublet at δ 1.01 ppm. The $^{13}C\text{-}\{^1H\}$ NMR spectrum of **131** displays a resonance at δ 120.6 ppm due to the CN carbon atom. In **132** the *exo* methyl substituent occurs at δ 0.15 ppm (*cf.* δ 0.30 for **124**). The kinetic products of charge controlled[10,11] reactions are predicted to arise from attack at the less alkylated ring (*i.e.* [2.2]paracyclophane), yet this is clearly not the case in this instance. This may be readily rationalised in terms of i) the steric bulk of the [2.2]paracyclophane ligand - the uncoordinated aromatic deck shields the *exo* attack sites on the coordinated ring, and ii)

the deactivation of the coordinated deck of the cyclophane *via* π-overlap with the uncoordinated ring; interannular interactions within [2_n]cyclophanes are a well documented phenomenon.[129,130,223]

Reaction of **3b** with KOH or with alkyllithium reagents in methanol, in a manner analogous to the synthesis of **123**, does not result in the formation of either hydroxide or methoxide addition products. Instead, the presence of a strong base results in deprotonation of one of the methyl substituents of the hexamethylbenzene ring to generate the exomethylene complex [Ru(η^6-$C_{16}H_{16}$){η^5-$C_6Me_5(CH_2)$}] **133**. The uncoordinated, olefinic =CH_2 group exhibits a ^{1}H NMR resonance at δ 3.72 ppm integrating for two protons and the infrared spectrum of the complex exhibits a band corresponding to the uncoordinated double bond at 1592 cm^{-1}. Complex **133** was also synthesised by action of one mole of KO^{t}Bu upon **3b** in dry thf precluding the possibility of the formation of a hydroxide or methoxide species. The formation of **133** is consistent with a range of methylene complexes recently reported by Gladfelter *et al.*[80-82] such as [Ru(η^6-C_6Me_6){η^5-$C_6Me_5(CH_2)$}]$^+$, although it should be noted that action of KOH upon non-alkylated arenes has been shown to give hydroxide addition products.[58]

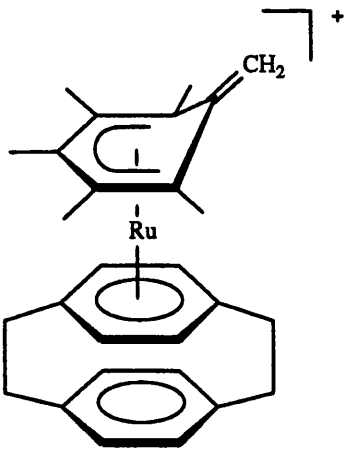

133

6.3.3 Addition to the Bis*([2.2]paracyclophane)ruthenium(II) Cation*

Reduction of **3b** with aluminium metal followed by protonation with HCl has been observed[7] to produce an isomer of **130** containing an η^5-cyclophane with the added proton

in the *endo* position (Scheme 6.2).

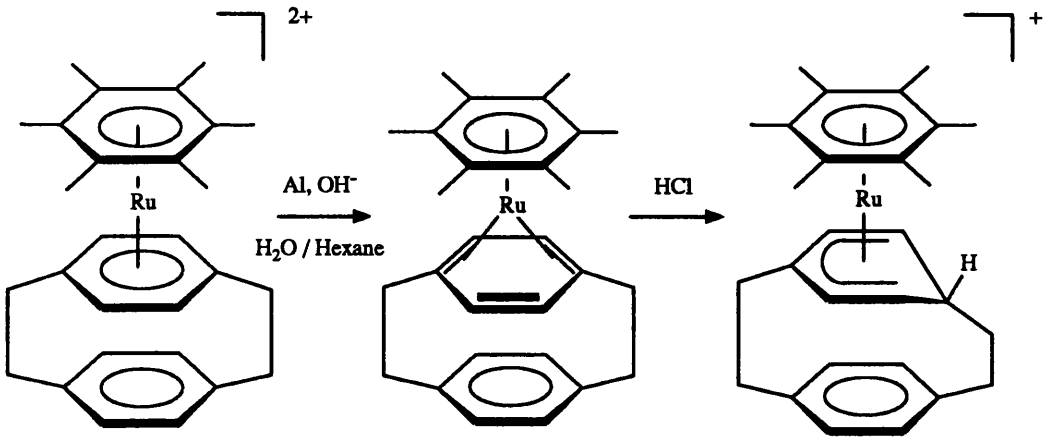

Scheme 6.2: Reduction-protonation synthesis of $[Ru(\eta^6\text{-}C_6Me_6)(\eta^5\text{-}C_{16}H_{17})][HCl_2]$, a complex containing an η^5-cyclophane ligand

It was of obvious importance to test whether nucleophilic addition is at all possible at the "Ru([2.2]paracyclophane)" fragment and to this end the action of $Na[BH_4]$ on the *bis*([2.2]paracyclophane) complex $[Ru(\eta^6\text{-}C_{16}H_{16})_2][BF_4]_2$ **3f** was examined. If cyclohexadienyl products could be isolated it was also of interest to determine whether addition would occur at an alkylated site as expected if the reaction were charge controlled, or at a bridgehead site, to give a compound related to the protonation product shown in Scheme 6.2. The reaction is not a clean one and proceeds with much decomposition and we were unable to isolate any pure product. However, crude samples exhibited clean ^1H NMR spectra (Fig. 6.3) related to those observed by Boekelheide *et al.* for $[Ru(\eta^6\text{-}C_6Me_6)(\eta^5\text{-}C_{16}H_{17})][HCl_2]$,[7] consistent with a single *endo* addition of hydride to the (more alkylated) *bridgehead* site of one of the coordinated aromatic decks, to give $[Ru(\eta^6\text{-}C_{16}H_{16})(\eta^5\text{-}C_{16}H_{17})][BF_4]$ **134**. The reason for this surprising reactivity might well lie in the geometry of the coordinated cyclophane ligand which, in contrast to conventional η^6-arenes, is bent into a shallow boat conformation, the distortion being some 13° in the

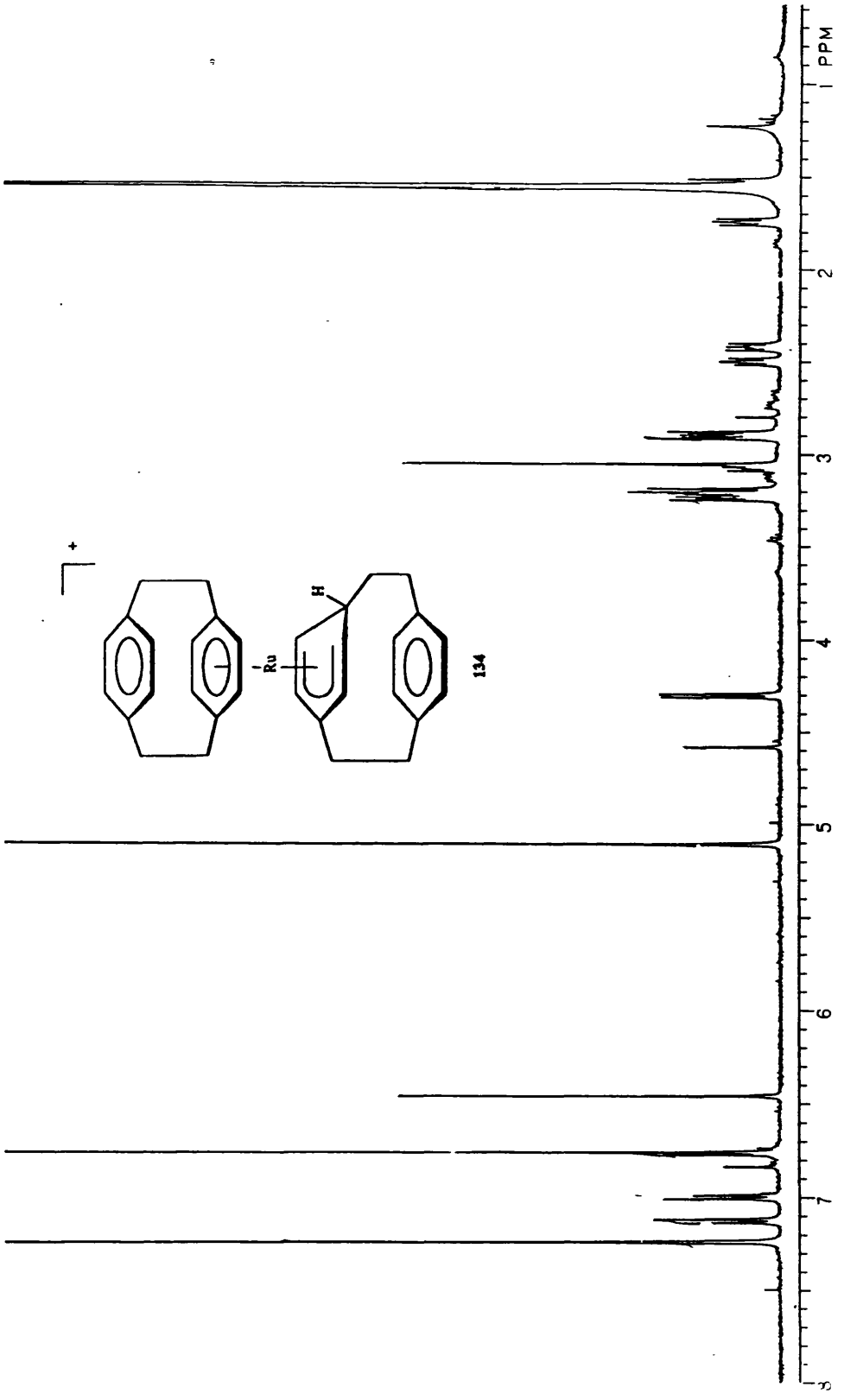

Fig. 6.3: ^{1}H NMR Spectrum of $[Ru(\eta^6\text{-}C_{16}H_{16})(\eta^5\text{-}C_{16}H_{17})][BF_4]$ **134.**

free ligand,[224] although this is reduced somewhat on coordination.[220] This may well result in a component of the LUMO on the bridgehead atoms pointing outwards away from the metal ion and available to interact with an incoming nucleophile, hence an *endo* attack pathway could be less sterically unfavourable than in planar systems, especially since *exo* attack pathways are all blocked by the uncoordinated deck of the [2.2]paracyclophane ligand.

Although it may seem surprising that reaction of $Na[BH_4]$ with these dications give monocationic, rather than a neutral species, there is a well established precedent for such a reaction in (arene)ruthenium(II) chemistry,[58] where treatment of the mesitylene complex $[Ru(\eta^6\text{-}C_6H_3Me_3)(PMe_2Ph)(1,10\text{-phen})][PF_6]_2$ with $Na[BH_4]$ in methanol gives $[Ru(\eta^5\text{-}C_6H_4Me_3)(PMe_2Ph)(1,10\text{-phen})][PF_6]$. Similarly $[Fe(\eta^6\text{-}1,3,5\text{-}C_6H_3Me_3)_2]^{2+}$ reacts with KCN in acetone to form $[Fe(\eta^6\text{-}1,3,5\text{-}C_6H_3Me_3)(\eta^5\text{-}C_6H_3Me_3CN)]^+$.[73] Conversely, reactions of a number of $[Ru(\eta^6\text{-arene})_2]^{2+}$ ions with $Na[BH_4]$ in anhydrous THF are consistent with the formation of neutral arene-cyclohexadiene complexes in high yield although it was noted that in water, low yields of monocationic arene-cyclohexadienyl complexes could be obtained.[10] It has also been noted that reaction of $[Fe(\eta^6\text{-}C_6Me_6)_2]^{2+}$ with LiMe will give both η^5- and η^4-products, depending upon the precise reaction conditions employed.[25] Hence it seems likely that the choice of methanol as a solvent for this study is largely responsible for the observation of only single hydride attack, leading to the formation of monocationic products.

6.4 Experimental

General experimental and instrumental considerations are outlined in Section 2.4. All manipulations were carried out under nitrogen with degassed solvents using conventional Schlenk line techniques, although in general, little significant air sensitivity of the products was noted. The compounds $[M(\eta^6\text{-}C_{16}H_{16})(\eta^6\text{-arene})][BF_4]_2$ (M = Ru, Os) were prepared by published literature methods[35,14,225,226] or simple modifications thereof.

Preparations. - $[Ru(\eta^6\text{-}C_{16}H_{16})(\eta^5\text{-}C_6H_7)][BF_4]$ **121.** $[Ru(\eta^6\text{-}C_{16}H_{16})(\eta^6\text{-}C_6H_6)][BF_4]_2$ (0.11 g, 0.19 mmol) was suspended in methanol (5 cm^3) and to the stirred mixture excess $Na[BH_4]$ (0.05 g) was gradually added over 15 minutes during which time a rapid colour change from yellow to pale green was observed. Water (5 cm^3) was added to destroy any remaining $Na[BH_4]$ and the mixture was extracted with one aliquot of dichloromethane (20 cm^3). The separated organic layer was dried over magnesium sulphate, filtered and evaporated to dryness. The residue was recrystallised from acetone, isolated by filtration and washed with a few drops of acetone and diethylether to give a pale yellow product. Yield 0.04 g, 0.08 mmol, 42% (Found: C, 55.10; H, 4.35. Calc. for $C_{22}H_{23}BF_4Ru$: C, 55.60; H, 4.90%).

$[Ru(\eta^6\text{-}C_{16}H_{16})(\eta^5\text{-}C_6H_6CN)][BF_4]$ **122.** $[Ru(\eta^6\text{-}C_{16}H_{16})(\eta^6\text{-}C_6H_6)][BF_4]_2$ (0.10 g, 0.18 mmol) was suspended in methanol (5 cm^3) and KCN (0.01 g, 0.18 mmol) added. The mixture was stirred for 15 minutes until a bright yellow solution was obtained. The mixture was filtered and diethylether added to give a pale yellow precipitate. This was filtered off and the residue dissolved in dichloromethane (5 cm^3). After further filtration the solution was evaporated to dryness to give a bright yellow product. Yield 0.05 g, 0.10 mmol, 65% (Found: C, 54.85; H, 4.70; N, 2.40. Calc. for $C_{23}H_{22}BF_4NRu$: C, 55.20; H, 4.45; N, 2.80%).

$[Ru(\eta^6\text{-}C_{16}H_{16})(\eta^5\text{-}C_6H_6OMe)][BF_4]$ **123.** The compound $[Ru(\eta^6\text{-}C_{16}H_{16})(\eta^6\text{-}C_6H_6)][BF_4]_2$ (0.13 g, 0.24 mmol) was stirred in MeOH (5 cm^3) while LiMe / Et_2O (1.6 M, 1 cm^3) was added dropwise over a period of *ca.* 5 minutes. The resulting yellow solution was evaporated to *ca.* 1 cm^3 resulting in the deposition of the product as orange crystals. Yield 0.11 g, 0.21 mmol, 88% (Found: C, 54.25; H, 5.35. Calc. for $C_{23}H_{25}BF_4ORu$: C, 54.65; H, 5.00%).

$[Ru(\eta^6\text{-}C_{16}H_{16})(\eta^5\text{-}C_6H_6Me)][BF_4]$ **124.** The compound $[Ru(\eta^6\text{-}C_{16}H_{16})(\eta^6\text{-}C_6H_6)][BF_4]_2$ (0.16 g, 0.30 mmol) was stirred in dry thf (10 cm^3) for 1 h with LiMe / Et_2O (1.6 M, 2 cm^3) at -78°C. The resulting brown suspension was allowed to warm slowly to 0°C and was stirred for a further 1 h. Solvents were removed *in vacuo* and the resulting

brown residue washed with hexane and re-dissolved in acetone. Reduction of the volume of the resulting yellow solution to *ca.* 1 cm^3 and trituration with diethyl ether resulted in the formation of the product as a yellow precipitate which was isolated by filtration, washed with diethyl ether and air dried. Analytically pure products could not be isolated because of the high solubility of the compound. Yield 0.07 g, 0.14 mmol, 47%

$[Os(\eta^6\text{-}C_{16}H_{16})(\eta^5\text{-}C_6H_7)][BF_4]$ **125**. Using an analogous method to that for **121** $[Os(\eta^6\text{-}C_{16}H_{16})(\eta^6\text{-}C_6H_6)][BF_4]_2$ (0.07 g, 0.11 mmol) was reacted with $Na[BH_4]$ to give an off white solid. Yield 0.03 g, 0.05 mmol, 48% (Found: C, 46.85; H, 3.85. Calc. for $C_{22}H_{23}BF_4Os$: C, 46.80; H, 4.10%).

$[Ru(\eta^6\text{-}C_{16}H_{16})(^5\text{-}MeC_6H_5CHMe_2)][BF_4]$ **126a** and **126b**. Using an analogous method to that for **121** $[Ru(\eta^6\text{-}C_{16}H_{16})(\eta^6\text{-}4\text{-}MeC_6H_4CHMe_2)][BF_4]_2$ (0.14 g, 0.22 mmol) was reacted with $Na[BH_4]$ to give a yellow solid containing two isomer **126a** : **126b**, 2 : 5 (NMR evidence). Yield 0.07 g, 0.13 mmol, 59% (Found: C, 58.95; H, 5.80. Calc. for $C_{26}H_{31}BF_4Ru$: C, 58.80; H, 5.90%).

$[Ru(\eta^6\text{-}C_{16}H_{16})(\eta^5\text{-}MeC_6H_5CHMe_2)][BPh_4]$ **127a** and **127b**. To a solution of **126** (0.07 g, 0.14 mmol) in methanol (3 cm^3) was added a solution containing an excess of sodium tetraphenylborate (0.1 g) in methanol (3 cm^3). The resulting yellow precipitate was isolated by filtration, washed with methanol and diethylether, and air dried. Yield 0.10 g, 0.13 mmol, 94% (Found: C, 78.40; H, 6.75. Calc. for $C_{50}H_{51}BRu$: C, 78.60; H, 6.70%).

$[Ru(\eta^6\text{-}C_{16}H_{16})(\eta^5\text{-}4\text{-}MeC_6H_4CHMe_2CN)][BF_4]$ **128a** and **128b**. Using the method described for **122** $[Ru(\eta^6\text{-}C_{16}H_{16})(\eta^6\text{-}4\text{-}MeC_6H_4CHMe_2)][BF_4]_2$ (0.14 g, 0.22 mmol) was reacted with KCN to give an off-white product consisting of two isomers **128a** : **128b**, 2 : 5 (NMR evidence). Yield 0.07 g, 0.13 mmol, 54% (Found: C, 57.75; H, 5.30; N, 2.50. Calc. for $C_{27}H_{30}BF_4NRu$: C, 58.30; H, 5.45; N, 2.50%).

$[Ru(^6\text{-}C_{16}H_{16})\{\eta^5\text{-}1,4\text{-}(CHMe_2)_2C_6H_5\}][BF_4]$ **129**. Using a similar method to that described for **121** $[Ru(\eta^6\text{-}C_{16}H_{16})\{\eta^6\text{-}1,4\text{-}(CHMe_2)_2C_6H_4\}][BF_4]_2$ (0.35 g, 0.54 mmol) was

reacted with $Na[BH_4]$ to give a yellow solid. Yield 0.07 g, 0.12 mmol, 22% (Found: C, 60.30; H, 6.25. Calc. for $C_{28}H_{35}BF_4Ru$: C, 60.10; H, 6.30%).

$[Ru(\eta^6\text{-}C_{16}H_{16})(\eta^5\text{-}C_6Me_6H)][BF_4]$ **130**. Using an analogous method to that for **121** $[Ru(^6\text{-}C_{16}H_{16})(\eta^6\text{-}C_6Me_6)][BF_4]_2$ (0.10 g, 0.16 mmol) was reacted with $Na[BH_4]$ to give a yellow solid. Yield 0.04 g, 0.07 mmol, 44% (Found: C, 59.95; H, 6.10. Calc. for $C_{28}H_{35}BF_4Ru$: C, 60.10; H, 6.30%).

$[Ru(\eta^6\text{-}C_{16}H_{16})(\eta^5\text{-}C_6Me_6CN)][BF_4]$ **131**. $[Ru(\eta^6\text{-}C_{16}H_{16})(\eta^6\text{-}C_6Me_6)][BF_4]_2$ (0.10 g, 0.15 mmol) was suspended in methanol (5 cm^3) and KCN (0.013 g, 0.20 mmol) added. The mixture was stirred for 15 minutes until a bright yellow solution was obtained. The mixture was filtered and diethylether added to precipitate a pale yellow solid which was filtered off and then extracted into dichloromethane (5 cm^3). Filtration of this solution followed by evaporation gave a bright yellow product. Yield 0.03 g, 0.05 mmol, 34% (Found: C, 59.65; H, 6.05; N, 2.70. Calc. for $C_{29}H_{34}BF_4Ru$: C, 59.60; H, 5.85; N, 2.40%).

$[Ru(\eta^6\text{-}C_{16}H_{16})(\eta^5\text{-}C_6Me_7)][BF_4]$ **132**. The compound $[Ru(\eta^6\text{-}C_{16}H_{16})(\eta^6\text{-}C_6Me_6)][BF_4]_2$ (0.17 g, 0.26 mmol) was stirred in thf (10 cm^3) for 1 h. with LiMe / Et_2O (1.6 M, 1 cm^3) at -78°C. The resulting bright yellow-orange suspension was allowed to warm slowly to room temperature and was stirred for a further 1 h. A further aliquot of LiMe / Et_2O was added (1 cm^3) such that the solution became a clear orange. Degassed water (5 cm^3) was added to destroy the excess alkylating reagent and the organic layer separated. The aqueous phase was washed with a further portion of CH_2Cl_2 (5 cm^3) and the washings combined with the organic phase and dried over $Mg[SO_4]$. After removal of solvent *in vacuo* the yellow oily residue was triturated with Et_2O (10 cm^3) to give the product as a yellow solid. Yield 0.07 g, 0.12 mmol, 46% (Found: C, 59.50; H, 6.35. Calc. for $C_{29}H_{37}BF_4Ru$: C, 60.75; H, 6.50%).*

---

* The poor analytical data for this compound is probably due to contamination by traces of lithium salts which could not be seperated because of the high solubility of the complex. FAB-MS data clearly establish the proposed formulation however, with a molecular cation peak centred on *m/z* 487 (based on ^{102}Ru) and a strong peak corresponding to the C_6Me_7 ligand *m/z* 177.

$[Ru(\eta^6\text{-}C_{16}H_{16})\{\eta^5\text{-}C_6Me_5(CH_2)\}][BF_4]$ **133**. The compound $[Ru(\eta^6\text{-}C_{16}H_{16})(\eta^6\text{-}C_6Me_6)][BF_4]_2$ (0.08 g, 0.12 mmol) was stirred in MeOH (5 cm^3) while Li^nBu / Et_2O (1.6 M, 1 cm^3) was added dropwise over a period of *ca.* 5 minutes. The resulting yellow solution was evaporated to *ca.* 1 cm^3 resulting in the deposition of the product as yellow crystals. Yield 0.05 g, 0.09 mmol, 75% (Found: C, 60.05; H, 5.90. Calc. for $C_{28}H_{33}BF_4Ru$: C, 60.35; H, 5.95%). This compound was also prepared in poorer yields (*ca.* 50%) by reaction of **3b** with a 1 : 1 equivalence of KO^tBu in dry thf, and with KOH (using a similar method to that described for **131**).

The deuterides of **121**, **126**, and **130** were prepared in an identical fashion to their undeuterated counterparts substituting sodium borodeuteride for sodium borohydride in the preparative method.

121' Found: C, 55.50; H, 5.00. Calc. for $C_{22}H_{22}DBF_4Ru$: C, 55.50; H, 5.10%.

126' Found: C, 59.70; H, 6.00. Calc. for $C_{26}H_{30}DBF_4Ru$: C, 60.00; H, 6.50%.

130' Found: C, 58.60; H, 5.85. Calc. for $C_{28}H_{34}DBF_4Ru$: C, 58.65; H, 6.05%.

Table 6.1: ^{1}H NMR data for new compounds[a]

Compound	δ		
	Cyclophane Ring	Cyclophane Bridge	Cyclohexadienyl ligand
$[Ru(\eta^6\text{-}C_{16}H_{16})(\eta^5\text{-}C_6H_7)][BF_4]$ **121**	6.84 (s, 4H) 5.36 (s, 4H)	3.26 & 3.02 (AA'XX', 8H)	6.20 (t, 1H, ^3J=5.1), 4.86 (t, 2H, ^3J=5.6), 3.33 (t, 2H, ^3J=6.6), 2.32 (m, 1H, *endo-H*), 2.06 (d, 1H, ^2J=13.5, *exo-H*)
$[Ru(\eta^6\text{-}C_{16}H_{16})(\eta^5\text{-}C_6H_6D)][BF_4]$ **121'**	6.84 (s, 4H) 5.31 (s, 4H)	3.29 & 3.00 (AA'XX', 8H)	6.21 (t, 1H, ^3J=5.2), 4.87 (t, 2H, ^3J=5.5), 3.35 (t, 2H[c]), 2.29 (t, 1H, ^3J=5.4, *endo-H*)
$[Ru(\eta^6\text{-}C_{16}H_{16})(\eta^5\text{-}C_6H_6CN)][BF_4]$ **122**[b]	6.84(s, 4H) 5.42 (s, 4H)	3.23 & 2.92 (AA'XX', 8H)	6.30 (t, 1H, ^3J=4.9), 4.94 (t, 2H, ^3J=5.7), 3.47 (t, 2H, ^3J=6.3), 3.43 (t, 1H, ^3J=6.0, *endo-H*)
$[Ru(\eta^6\text{-}C_{16}H_{16})(\eta^5\text{-}C_6H_6OMe)][BF_4]$ **123**[c]	6.92 (s, 4H) 5.50 (s, 4H)	3.31 & 3.06 (AA'XX', 8H)	6.01 (t, 1H, ^3J=5.2), 4.99 (t, 2H, ^3J=6.0), 4.04 (t, 2H, ^3J=6.8), 3.38 (t, 1H, ^3J=5.9, *endo-H*), 2.88 (s, 3H, O*Me*)
$[Ru(\eta^6\text{-}C_{16}H_{16})(\eta^5\text{-}C_6H_6Me)][BF_4]$ **124**	6.85 (s, 4H) 5.36 (s, 4H)	3.26 & 3.02 (AA'XX', 8H)	6.14 (t, 1H, ^3J=5.1), 4.79 (t, 2H, ^3J=5.5), 3.61 (t, 2H, ^3J=6.7), 2.23 (m, 1H, *endo-H*), 0.30 (d, 3H, ^3J=6.6, *Me*)

$[Os(\eta^6\text{-}C_{16}H_{16})(\eta^5\text{-}C_6H_7)][BF_4]$ **125**	6.95 (s, 4H) 5.57 (s, 4H)	3.34 & 2.97 (AA'XX', 8H)	6.58 (t, 1H, ^3J=5.1), 5.19 (t, 2H, ^3J=5.4), 3.63 (t, 2H, ^3J=5.9), 3.58 (d, 1H, ^2J=12.4, *exo-H*), 2.33 (m, 1H, *endo-H*)
$[Ru(\eta^6\text{-}C_{16}H_{16})(\eta^5\text{-}1\text{-}MeC_6H_5\text{-}4\text{-}CHMe_2)][BF_4]$ **126b** Major isomer	6.84 (s, 4H) 5.02 & 5.61 (AB, 4H, ^3J=6.1)	3.23 (m, 4H) 2.94 (m, 2H) 2.82 (m, 2H)	5.95 (d, 1H, ^3J=4.4), 4.71 (d, 1H, ^3J=4.8), 3.44 (d, 1H, ^3J=6.2), 2.34 (dd, 1H, ^3J=6.2, ^2J=13.2, *endo-H*), 2.24 (d, 1H, ^2J=13.2, *exo-H*), 1.36 (s, 3H, *Me*), 1.88 (se, 1H, ^3J=7.1, C*H*Me$_2$), 0.97 (d, 3H, ^3J=7.1, CH*Me*$_2$), 0.95 (d, 3H, ^3J=7.1, CH*Me*$_2$)
$[Ru(\eta^6\text{-}C_{16}H_{16})(\eta^5\text{-}2\text{-}MeC_6H_5\text{-}5\text{-}CHMe_2)][BF_4]$ **126a** Minor isomer	6.83 (s, 4H) 5.04 & 5.54 (AB, 4H, ^3J=6.7)	3.23 (m, 4H) 2.94 (m, 2H) 2.82 (m, 2H)	6.05 (d, 1H, ^3J=4.6), 4.70 (d, 1H[d]), 3.44 (d, 1H[d]), 2.32 (dd, 1H[d], *endo-H*), 2.08 (d, 1H, ^2J=13.2, *exo-H*), 1.71 (s, 3H, *Me*), 1.65 (se, 1H, ^3J=6.8, C*H*Me$_2$), 0.90 (d, 3H, ^3J=6.8, CH*Me*$_2$), 0.78 (d, 3H, ^3J=6.8, CH*Me*$_2$)
$[Ru(\eta^6\text{-}C_{16}H_{16})(\eta^5\text{-}1\text{-}MeC_6H_5\text{-}4\text{-}CHMe_2)][BPh_4]$ **127b**[e] Major isomer	6.63 & 6.67 (AB, 4H, ^3J=7.1) 4.90 & 4.25 (AB, 4H, ^3J=5.7)	3.13 (m, 4H) 2.68 (m, 2H) 2.55 (m, 2H)	5.64 (d, 1H, ^3J=5.4), 4.20 (d, 1H, ^3J=5.3), 3.19 (s, br, 1H), 2.17 (m, 1H, *endo-H*), 2.17 (d, 1H, ^2J=12.4, *exo-H*), 1.19, (s, 3H, *Me*), 1.71 (se, 1H, ^3J=6.8, C*H*Me$_2$), 0.92 (dd, 3H, ^3J=3.7, CH*Me*$_2$), 0.86 (m, 3H, CH*Me*$_2$)
$[Ru(\eta^6\text{-}C_{16}H_{16})(\eta^5\text{-}2\text{-}MeC_6H_5\text{-}5\text{-}CHMe_2)][BPh_4]$ **127a**[e] Minor isomer	6.63 & 6.67 (AB, 4H, ^3J=7.1) 4.86 & 4.28 (AB, 4H, ^3J=6.0)	3.13 (m, 4H) 2.68 (m, 2H) 2.55 (m, 2H)	5.58 (d, 1H ^3J=5.0), 4.28 (d, 1H[d]), 3.19 (s, br, 1H), 2.17 (m, 1H, *endo-H*), 2.02 (d, 1H, ^2J=13.1, *exo-H*), 1.52 (s, 3H, *Me*), 1.46 (se, 1H, ^3J=5.3, C*H*Me$_2$), 0.85 (d, 3H, ^3J=7.0, CH*Me*$_2$), 0.74 (d, 3H, ^3J=6.9, CH*Me*$_2$)

[Ru(η^6-$C_{16}H_{16}$)(η^5-1-MeC_6H_4D-4-CHMe$_2$)][BF_4] **126b'** Major isomer	6.88 (s, 4H) 5.09 & 5.70 (AB, 4H, ^3J=5.8)	3.28 (m, 4H) 2.86 (m, 2H) 2.90 (m, 2H)	6.01 (d, 1H, ^3J=4.7), 4.83 (d, 1H, ^3J=4.4), 3.36 (d, 1H, ^3J=8.9), 2.34 (d, 1H, ^3J=6.0, *endo-H*), 1.41 (s, 3H, *Me*), 1.91 (se, 1H, ^3J=6.7, C*H*Me$_2$), 1.01 (d, 3H, ^3J=6.7, CH*Me*$_2$), 0.98 (d, 3H, ^3J=6.6, CH*Me*$_2$)
[Ru(η^6-$C_{16}H_{16}$)(η^5-2-MeC_6H_4D-5-CHMe$_2$)][BF_4] **126a'** Minor isomer	6.87 (s, 4H) 5.09 & 5.63 (AB, 4H, ^3J=5.8)	3.28 (m, 4H) 2.86 (m, 2H) 2.90 (m, 2H)	6.13 (d, 1H, ^3J=5.0), 4.77 (d, 1H, ^3J=4.7), 3.36 (d, 1H, ^3J=6.7), 2.30 (d, 1H, ^3J=6.0, *endo-H*), 1.76 (s, 3H, *Me*), 1.66 (se, 1H, ^3J=6.5, C*H*Me$_2$), 0.93 (d, 3H, ^3J=7.0, CH*Me*$_2$), 0.81 (d, 3H, ^3J=6.9, CH*Me*$_2$)
[Ru(η^6-$C_{16}H_{16}$)(η^5-1-MeC_6H_4CN-4-CHMe$_2$)][BF_4] **128b** Major isomer	6.86 (s, 4H) 5.22 & 5.83 (AB, 4H, ^3J=6.4)	3.26 (m, 4H) 2.98 (m, 2H) 2.84 (m, 2H)	6.13 (d, 1H, ^3J=5.5), 4.91 (d, 1H, ^3J=5.4), 3.70 (d, 1H, ^3J=6.2), 3.54 (d, 1H, ^3J=6.2), 1.52 (s, 3H), 2.01 (se, 1H, ^3J=6.8), 1.05 (d, 3H, ^3J=6.9), 1.04 (d, 3H, ^3J=6.9)
[Ru(η^6-$C_{16}H_{16}$)(η^5-2-MeC_6H_4CN-5-CHMe$_2$)][BF_4] **128a** Minor isomer	6.86 (s, 4H) 5.22 & 5.82 (AB, 4H[d])	3.26 (m, 4H) 2.98 (m, 2H) 2.84 (m, 2H)	6.28 (d, 1H ^3J=5.6), 5.01 (d, 1H ^3J=5.4), 3.74 (d, 1H[d]), 3.48 (d, 1H ^3J=6.0), 1.85 (s, 3H), 1.80 (m, 1H), 1.01 (m, 6H)
[Ru(η^6-$C_{16}H_{16}$)(η^5-1,4-(CHMe$_2$)$_2$$C_6H_5$)][$BF_4$] **129**	6.82 (s, 4H) 5.04 & 5.59 (AB, 4H, ^3J=6.3)	3.24 (m, 4H) 2.96 (m, 2H) 2.82 (m, 2H)	6.05 (d, 1H, ^3J=5.1), 4.78 (d, 1H, ^3J=5.1), 3.38 (d, 1H, ^3J=6.5), 2.36 (dd, 1H, ^3J=6.5, ^2J=13.4, *endo-H*), 2.10 (d, 1H, ^2J=13.4, *exo-H*), 1.92 (se, 1H, ^3J=6.7, C*H*Me$_2$), 1.68 (se, 1H, ^3J=6.7, C*H*Me$_2$), 1.04 (d, 3H, ^3J=6.8, CH*Me*$_2$), 0.94 (d, 3H, ^3J=6.7, CH*Me*$_2$), 0.92 (d, 3H, ^3J=6.7, CH*Me*$_2$), 0.80 (d, 3H, ^3J=6.7, CH*Me*$_2$)

$[Ru(\eta^6\text{-}C_{16}H_{16})(\eta^5\text{-}C_6Me_6H)][BF_4]$ **130**	5.04 (s, 4H) 6.81 (s, 4H)	2.86 & 3.23 (AA'XX', 8H)	2.28 (s, 3H), 2.00 (q, 1H, ^3J=6.7, *exo-H*), 1.87 (s, 6H), 1.34 (s, 6H), 1.01 (d, 3H, ^3J=7.0)
$[Ru(\eta^6\text{-}C_{16}H_{16})(\eta^5\text{-}C_6Me_6D)][BF_4]$ **130'**	5.10 (s, 4H) 6.83 (s, 4H)	2.88 & 3.26 (AA'XX', 8H)	2.30 (s, 3H), 1.89 (s, 6H), 1.36 (s, 6H), 1.02 (s, 3H)
$[Ru(\eta^6\text{-}C_{16}H_{16})(\eta^5\text{-}C_6Me_6CN)][BF_4]$ **131**	5.30 (s, 4H) 6.87 (s, 4H)	2.90 & 3.30 (AA'XX', 8H)	2.37 (s, 3H), 2.01 (s, 6H), 1.50 (s, 6H), 1.46 (s, 3H)
$[Ru(\eta^6\text{-}C_{16}H_{16})(\eta^5\text{-}C_6Me_7)][BF_4]$ **129**	6.80 (s, 4H) 5.03 (s, 4H)	3.22 & 2.86 (AA'XX', 8H)	2.28 (s, 3H), 1.86 (s, 6H), 1.39 (s, 6H), 1.04 (s, 3H, Me_{endo}), 0.15 (s, 3H, Me_{exo})
$[Ru(\eta^6\text{-}C_{16}H_{16})\{\eta^5\text{-}C_6Me_5(CH_2)\}][BF_4]$ **133**	5.10 (s, 4H) 6.84 (s, 4H)	2.88 & 3.24 (AA'XX', 8H)	3.72 (s, 2H, =CH_2), 2.23 (s, 3H), 1.99 (s, 6H), 1.76 (s, 6H)
$[Ru(\eta^6\text{-}C_{16}H_{16})(\eta^5\text{-}C_{16}H_{17})][BF_4]$ **134**	6.80 (s, 4H) 5.14 (s, 4H)	3.28 & 2.92 (AA'XX', 8H)	7.17 & 6.95 (AB, 4H, ^3J=8.1, uncoord. ring H), 4.33 (d, 2H, ^3J=7.3, coord. ring H), 3.10 (t, 2H, ^3J=7.8, coord. ring H), 3.22 (m, 2H, bridge), 2.45 (t, 2H, ^3J=7.4, bridge), 2.53 (t, 2H, ^3J=6.4, bridge), 1.78 (t, 2H, ^3J=6.7, bridge), 3.28 (m, 1H, nucleophile)[f]

a) Solvent $CDCl_3$ unless otherwise stated, 200 or 400 MHz, 20°C, δ / ppm, $J_{H\text{-}H}$ / Hz, s = singlet, d = doublet, t = triplet, q = quartet, se = septet, br = broad; b) Solvent CD_3CN; c) Solvent NO_2CD_3; d) coupling masked by overlapping signals from major isomer; e) $[BPh_4]^-$: 6.99 (t, ^3J=7.1, 4H), 7.13 (t, ^3J=7.6, 8H), 7.49 (s, br 8H); f) assigned by analogy with $[Ru(\eta^6\text{-}C_6Me_6)(\eta^5\text{-}C_{16}H_{17})][HCl_2]$.[7]

Table 6.2: ^{13}C-{^{1}H} NMR data for selected compounds.[a]

Compound	δ				
	Ring	Bridge head	-CH_2-	Cyclohexadienyl	CN
$[Ru(\eta^6\text{-}C_{16}H_{16})(\eta^5\text{-}C_6H_7)][BF_4]$ **121**[b]	133.6 86.2	139.2 125.2	34.4 32.4	87.2, 85.9 36.7, 27.9	-
$[Ru(\eta^6\text{-}C_{16}H_{16})(\eta^5\text{-}C_6H_6CN)][BF_4]$ **122**	133.9 87.7	139.8 127.5	34.0 32.1	89.5, 84.6 32.8, 26.4	119.3
$[Ru(\eta^6\text{-}C_{16}H_{16})(\eta^5\text{-}C_6Me_6H)][BF_4]$ **130**	133.6 88.0	139.2 124.5	34.2 31.8	101.7, 100.5 52.7, 38.4, 29.7 18.1, 16.5, 16.0	-
$[Ru(\eta^6\text{-}C_{16}H_{16})(\eta^5\text{-}C_6Me_6CN)][BF_4]$ **131**[c]	133.8 89.3	139.1 126.6	34.1 31.7	99.9, 49.9, 21.1 21.0, 17.0, 16.9	120.6

a) δ / ppm, 100.6 MHz, 20°C, solvent $CDCl_3$ unless otherwise stated, s = singlet, d = doublet, dd = doublet of doublets, t = triplet, se = septet, m = multiplet, br = broad; b) assignment confirmed by ^{1}H coupled ^{13}C spectrum; c) solvent CD_3CN.

Table 6.3: Deuterium isotope shifts of $\nu(CH_{exo})$

Compound	$\nu(C\text{-}H_{exo})$ / cm^{-1}	
	X=H	X=D
$[Ru(\eta^6\text{-}C_{16}H_{16})(\eta^5\text{-}C_6H_6X)][BF_4]$ **121**	2813	2113
$[Ru(\eta^6\text{-}C_{16}H_{16})(\eta^5\text{-}1\text{-}MeC_6H_4X\text{-}4\text{-}CHMe_2)][BF_4]$ **126**[a]	2804	2129
$[Ru(\eta^6\text{-}C_{16}H_{16})(\eta^5\text{-}C_6Me_6X)][BF_4]$ **130**	2813	2107

a) Signals for individual isomers unresolved.

Chapter 7

Synthesis and Reactivity of Diene Complexes of Ruthenium(0)

7.1 Introduction

In Chapter 6 it was demonstrated that the steric properties of the polyaromatic [2.2]paracyclophane ligand are suitable for inducing single nucleophilic addition reactions at other arenes coordinated to the same metal centre, even in the case of poorly electrophilic arenes such as hexamethylbenzene. In this chapter the extension of these studies to the formation of (diene)ruthenium(0) complexes from double nucleophilic addition reactions of (arene)ruthenium(II) complexes containing [2.2]paracyclophane as a non-innocent spectator ligand is reported. The reactivity of the resulting compounds towards $H[BF_4]$ is also investigated.

7.2 Double Nucleophilic Addition Reactions of Hydride

Work by Boekelheide[7] has shown that the reduction of the hexamethylbenzene complex $[Ru(\eta^6\text{-}C_{16}H_{16})(\eta^6\text{-}C_6Me_6)][BF_4]_2$ **3b** with Red-Al [sodium *bis*(methoxyethoxy) aluminium hydride] gives the cyclohexa-1,4-diene ruthenium(0) compound $[Ru(\eta^6\text{-}C_{16}H_{16})(\eta^4\text{-}exo,exo\text{-}3,6\text{-}C_6Me_6H_2)]$ **5**. Conversely, the analogous reduction of the benzene complex **3a** results in the formation of a cyclohexa-1,3-diene complex $[Ru(\eta^6\text{-}C_{16}H_{16})(\eta^4\text{-}5,6\text{-}C_6H_8)]$ **4**. It has been proposed that in both instances 1,4-dienes are the products initially formed, but in the latter case the availability of *endo*-hydrogen atoms on the diene ring enables the complex to rearrange to form a more thermodynamically stable 1,3-diene product *via* a metal-hydride intermediate, Scheme 7.1a.[7] Double nucleophilic additions at sites *para* to one another are consistent with charge control of the reaction but contrast markedly to double nucleophilic additions to the analogous *bis*(arene)iron complexes, in which the products of reaction are governed by frontier molecular orbital control, and result from 1,2-double addition.[71,78,87]

7.2.1 Re-examination of the Hydride Reduction of $[Ru(\eta^6\text{-}C_{16}H_{16})(\eta^6\text{-}C_6Me_6)]^{2+}$

In our hands the reduction of **3b** with Red-Al gives rise to three isomeric products. The major component (67% of the isolated yield) was identified as **5** by its ^1H NMR

spectrum (Table 7.1), and results, as previously reported, from a 1,4-double addition of hydride to the hexamethylbenzene ring.[7] The two minor products were identified as i) the 1,3-diene isomer of **5**, [Ru(η^6-$C_{16}H_{16}$)(η^4-*exo,exo*-5,6-$C_6Me_6H_2$)] **135** (8% of the isolated yield) and ii) the *meta*-dihydro ruthenium(II) compound [Ru(η^6-$C_{16}H_{16}$)(1-σ-3-5-η-*exo,exo*-2,6-$C_6Me_6H_2$)] **136** (25%), *vide infra*. Recrystallisation of this mixture gave only pure **5** as reported by Boekelheide *et. al.*

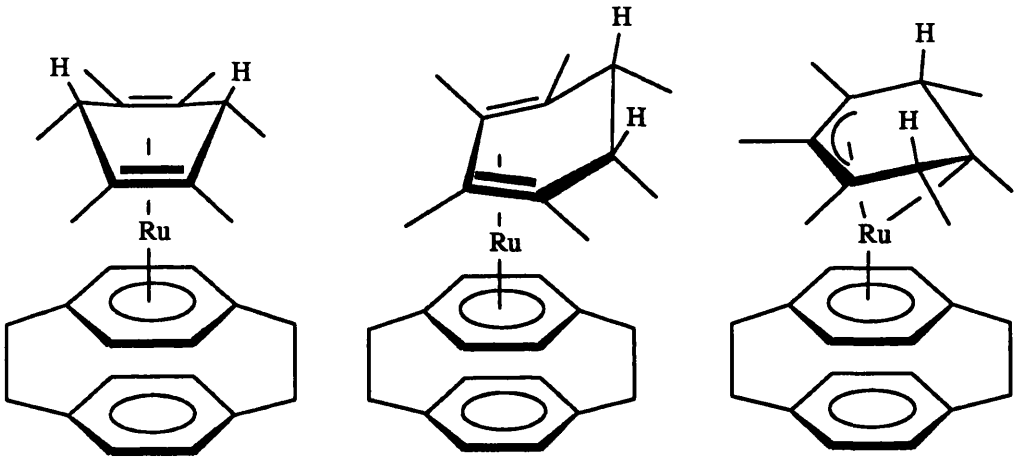

5 **135** **136**

Surprisingly, on carrying out the sodium borohydride reduction of **3b** we find that the 1,3-diene isomer **135** is formed as the sole product. Complex **135** (FAB-MS *m/z* 474 based on ^{102}Ru) is readily identified by its ^{1}H NMR spectrum which exhibits a singlet resonance for the coordinated deck of the paracyclophane ligand at δ 4.09, a chemical shift characteristic of a neutral ruthenium(0) species (*cf.* complex **5**: δ 3.95). Three methyl resonances are observed and a quartet for the *exo* hydrogen atoms [δ 1.74, 1.10 and 0.56 (d, ^3J=6.8), CH_3; 1.18 (q, ^3J = 6.8) ppm, *exo-H**]. In contrast, **5** displays only two methyl signals[7] and the resonance arising from the *exo* hydrogen atoms [δ 1.27 (d, ^3J=7.0) and 1.00 (s), CH_3; 3.41 (q, ^3J = 7.0) ppm, *exo-H*]. The infrared spectrum of **135** exhibits a

* Resonances assigned with the aid of homonuclear decoupling experiments where appropriate. ^{1}H NMR spectrum of **5** re-measured in $CDCl_3$ for comparative purposes.

strong band due to $\nu(CH_{exo})$ at 2808 cm^{-1}, shifting to 2083 cm^{-1} in the dideuterio complex $[Ru(\eta^6\text{-}C_{16}H_{16})(\eta^4\text{-}exo,exo\text{-}5,6\text{-}C_6Me_6D_2)]$ **135'** confirming *exo* addition. The $\nu(CH_{exo})$ vibration in compound **5** occurs at 2751 cm^{-1}.

Complex **135** is structurally similar to the cyclohexa-1,3-diene compound **4**[7] and a wide range of (1,3-diene)iron(0) species formed by direct 1,2-double addition under conditions of frontier orbital control.[71,78,87] The question of whether **135** (and also **4**) is formed as a consequence of direct 1,2-double addition (Scheme 7.1b) or results from a rearrangement of **5** (which might be the kinetic product) has important consequences for the validity of the charge control model for nucleophilic additions to ruthenium. Unlike the case of **4**, complex **5** cannot isomerise to form **135** *via* an *endo*, metal-hydride mediated rearrangement pathway (Scheme 7.1a) because no *endo* hydrogen atoms are available. Formation of **135** must therefore proceed *via* an *exo* pathway such as an intramolecular [1,3]- or series of [1,2]-sigmatropic shifts (Scheme 7.1c) or by direct 1,2-double addition (Scheme 7.1b).

The *meta*-dihydro complex **136** exhibits a singlet ^1H NMR resonance at δ 4.31 for the coordinated paracyclophane deck and, whilst this material could not be isolated in an isomerically pure form, the remainder of its ^1H NMR spectrum is consistent with the proposed ene-diyl formulation. Such a product could result either from a direct 1,3-double nucleophilic addition or possibly a [1,2]-H atom shift rearrangement of complex **5**. The complex exhibits four methyl resonances and a 2H quartet resonance due to H_{exo} [δ 1.49 (s, 3H), 1.46 (s, 6H), 0.80 (d, 6H, ^3J = 6.8) and 0.27 (s, 3H), CH_3; 2.65 (q, ^3J = 6.8) ppm, *exo-H*]. The methyl resonance at δ 0.27 occurs at surprisingly high field and models show that the half-boat conformation of the proposed structure would bring the unique methyl substituent attached to the σ-coordinated site into close proximity to the metal centre. Such upfield shifts have also been noted in related ene-diyl compounds which are formed along with *ortho*-addition products on nucleophilic additions of H^- and CN^- to tri(carbonyl)(cyclohexadienyl)osmium(II) cations[227] and as the sole products of hydride addition to $[Mn(6\text{-}exo\text{-}PhC_6H_6)(NO)(L\text{-}L)]^+$ (L-L = dppe, dppen).[228] The chemical shift of the protons of the coordinated deck of the paracyclophane ligand in **136** is at higher field than that observed for **5** and **135** consistent with a ruthenium(II) centre but lower than the values observed for cationic and dicationic ruthenium(II) complexes (δ 4.31, *cf. ca.*

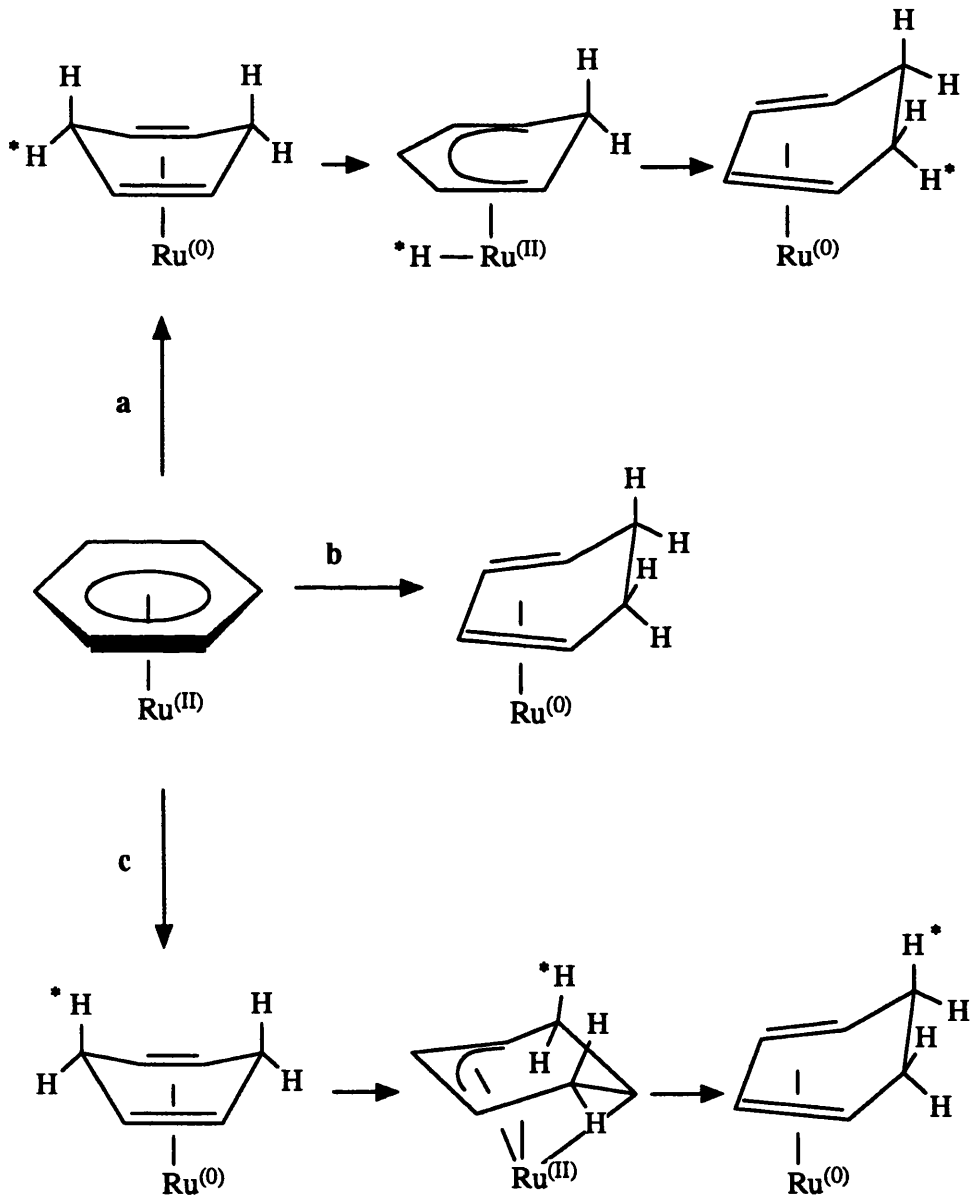

Scheme 7.1: Mechanisms for the formation of cyclohexa-1,3-diene complexes (a) Metal-hydride mediated *endo*-rearrangement of a cyclohexa-1,4-diene; (b) Direct 1,2-double nucleophilic addition; (c) *exo*-sigmatropic shift of a cyclohexa-1,4-diene. (starred hydrogen atoms are undergoing rearrangement).

δ 5 and 6 respectively) suggesting a neutral compound. The chemical shift of H_{exo} is intermediate between that of **5** and **135** [δ 2.65, *cf.* 3.41 (**5**) and 1.18 ppm (**135**)].

In the synthesis of **135**, the relatively poor electrophilicity of complexed hexamethylbenzene coupled with the mild reducing nature of $Na[BH_4]$ has made it necessary for us to employ reaction times of *ca.* 72 h at room temperature in order to obtain good yields, as opposed to *ca.* 2 h in the case of **5**. We considered the possibility that this longer reaction time might result in a slow rearrangement of **5** and **136** to form **135**. However, stirring of **3b** with excess Red-Al over a period of one week gives no change in the relative proportions of **5**, **135** and **136**. Isolation of **5** and subsequent stirring in thf either alone, or in the presence of excess $Na[BH_4]$ for 7 days also does not result in isomerisation. Similarly, action of neither NaOH, $Na[BF_4]$, $B(OH)_3$, $BF_3.Et_2O$, water nor heat (refluxing thf) results in conversion of **5** or **136** into **135**. This contrasts to the ene-diyl osmium compound $[Os(\eta^3{:}\eta^1\text{-}C_6H_8)(CO_3)]$[227] which isomerises in refluxing hexane over a period of 5 hours to the 1,3-diene analogue *via.* a proposed *endo* mechanism analogous to that suggested to be responsible for the formation of **4** (Scheme 7.1a). In the case of **136** however, *endo* hydrogen atoms are absent.

We have noted that the formation of **135** is sensitive to aqueous quenching. If water is *not* added to destroy excess $Na[BH_4]$ during work-up, mixtures containing 20 - 40 % **5** along with **135** (although no **136**) are formed instead of pure **135** in the case of the quenched reaction. Aqueous quenching is also a necessary feature of the Red-Al reduction of **3b** but in that case does not result in the formation of a single isomer. In light of the fact that we find neither water, NaOH, $B(OH)_3$ nor water / $Na[BH_4]$ / $Na[BF_4]$ mixtures bring about the conversion of **5** into **135** once it has been isolated we suggest that the effect of the water in the synthesis of **135** is simply to decompose or otherwise (for reasons of solubility) prevent the extraction of **5**, resulting solely in the isolation of **135**.

In general we conclude that the action of hydrides upon **3b** results in direct 1,2-, 1,3- and 1,4-double nucleophilic additions to form **135**, **136** and **5** respectively and that *no* rearrangement of **5** to form **135** occurs. The ratio in which **5**, **135** and **136** are produced is determined primarily by the choice of reducing agent, thus the bulky Red-Al gives a second attack predominantly *para* to the more hindered sp^3 site[87] on the cyclohexadienyl

ligand (formed after the first addition) resulting in formation of **5**. Use of the less sterically bulky reagent $Na[BH_4]$ results in a preponderance of 1,2-double addition to give **135** (Scheme 7.1b). We have also examined the reduction of **3b** with $Na[Et_2AlH_2]$, a reagent structurally similar to Red-Al but with a slightly more bulky substituent directly adjacent to the aluminium ($-CH_2-$ as opposed to -O-). This reagent also gives **5** as the major product (75%), along with **136** (25%) and essentially no **135**.

7.2.2 Regioselectivity of the Hydride Reduction of $[Ru(\eta^6\text{-}C_{16}H_{16})(\eta^6\text{-}C_6H_6)]^{2+}$

In an attempt to determine the viability of the *endo* hydride transfer mechanism[7,227] (Scheme 7.1a) we have examined the reaction of the benzene complex **3a** with sodium borodeuteride, $Na[BD_4]$. Reaction of **3a** with Red-Al gives the 1,3-diene complex **4**. If the formation of **4** occurs as a result of 1,4-double nucleophilic addition, followed by metal-hydride mediated rearrangement as previously suggested,[7] the product of the analogous $Na[BD_4]$ reduction would be a 1,3-diene exhibiting deuterons in the 2 and 5 positions (Fig. 7.1a), since the incoming nucleophile would finish in an olefinic site after rearrangement. Alternatively (Fig. 7.1b), direct 1,2-double nucleophilic addition would result in deuterons occupying the 5 and 6 positions.

In the case of **3a** theborodeuteridereduction proceeds much more efficiently than in that of **3b** as a consequence of the greater electrophilicity of the non-alkylated ring, and a good yield may be isolated after reaction times of *ca.* 4 h. Under these conditions the resulting yellow solid, $[Ru(\eta^6\text{-}C_{16}H_{16})(\eta^4\text{-}C_6H_6D_2)]$ **4'**, exhibits the expected ^1H NMR spectrum (C_6D_6) similar to that of **4** although the resonance due to the *exo* protons (δ 1.79 ppm) is greatly reduced in intensity. Similar results are obtained after 7 days' stirring of **4'** in the presence of $Na[BD_4]$ and no dependence upon aqueous quenching is observed. The incorporation of deuterium solely into the *exo* aliphatic sites (consistent with direct 1,2-double addition) was confirmed by the ^2H NMR spectrum of the complex (Fig. 7.2) which exhibited a strong signal at δ 1.71 ppm (*exo* CH_2) with very little evidence for deuterium incorporation at the olefinic sites δ 3.09 and 4.76 ppm. Similarly, the infrared spectrum of **4'** displays a single ν(CD) at 2112 cm^{-1} (shifted from 2824 cm^{-1} in **4**) consistent with exo addition to give the isomer shown in Fig. 7.1b.

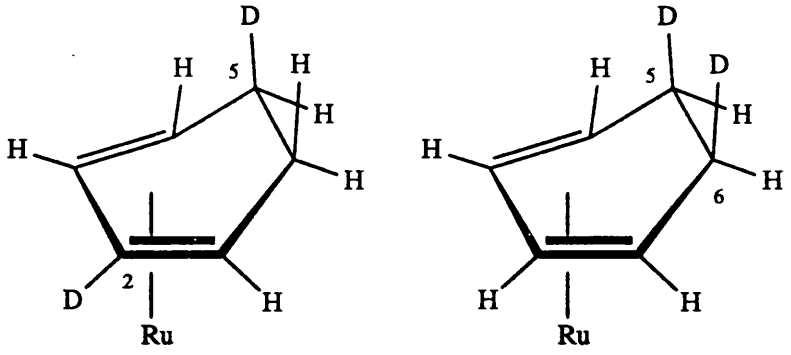

Fig. 7.1: Possible products arising from the action of $Na[BD_4]$ upon the benzene complex **3a** (a) 1,4-addition followed by *endo*-rearrangement; (b) 1,2-addition.

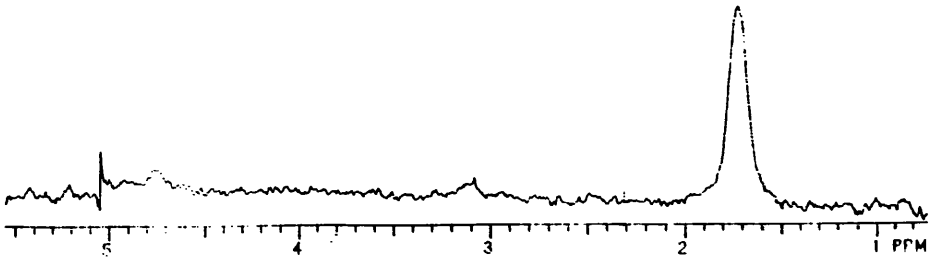

Fig. 7.2: ^2H NMR spectrum of $[Ru(\eta^6\text{-}C_{16}H_{16})(\eta^4\text{-}C_6H_6D_2)]$ **4'**.

7.2.3 Action of Hydride upon Other [Ru(η^6-$C_{16}H_{16}$)(η^6-arene)]$^{2+}$ Complexes

In an attempt to gain a greater understanding of the factors governing the regioselectivities and possible rearrangement pathways of these reactions we have examined the action of hydride upon related [Ru(η^6-$C_{16}H_{16}$)(η^6-arene)][BF_4]$_2$ compounds (arene = *p*-cymene **3c**, durene **3d** and pentamethylbenzene **3e**). In the case of **3e** we envisage the formation of up to three possible products, shown in Fig. 7.3. The 1,4-diene product (Fig. 7.3a) is unlikely given the possibility of an *endo* hydride transfer rearrangement because the availability of an *endo* hydrogen atom (assuming at least one nucleophilic addition takes place, as expected,[11] at the unmethylated site) should enable an *endo* rearrangement to a 1,3-diene, shown in Fig. 7.3b, to take place. Formation of this 1,3-diene *via* the mechanism depicted in Scheme 7.1a would involve an intramolecular nucleophilic addition of hydride from the suggested M-H intermediate to one of the *methylated* sites of the intermediate cyclohexadienyl ring. Formation of the alternative 1,3-diene complex, Fig. 7.3c would occur by direct 1,2-double addition, Scheme 7.1b.

These three possible isomers should be readily distinguishable from each other by their ^{1}H NMR spectra: The 1,4-diene complex, Fig. 7.3a, is symmetrical and would therefore give rise to a singlet resonance for the prochiral protons of the cyclophane coordinated deck. The 1,3-diene species are both asymmetric and would cause a splitting of the coordinated ring resonance into an AA'BB' pattern as observed in other chiral [2.2]paracyclophane compounds (see Chapter 6 and ref. 220). In practice we find that the reaction of **3e** with *both* Red-Al and Na[BH_4] gives a yellow solid [Ru(η^6-$C_{16}H_{16}$)(η^4-$C_6Me_5H_3$)] **137** displaying an AA'BB' quartet for the protons of the coordinated cyclophane ring in its ^{1}H NMR spectrum (δ 4.15 & 4.11 ppm, ^3J=5.9 Hz) clearly indicating a chiral 1,3-diene product. Interestingly however, no resonances are observed in the olefinic region of the spectrum which would correspond to the *endo*-rearranged product (Fig. 7.3b). Also, a resonance observed at δ 0.44 ppm (^2J=13.1, ^3J=3.3 Hz) assigned to the *endo* hydrogen atom of the diene ring, is not a doublet as would be expected from the complex shown in Fig. 7.3b. Instead this signal is a doublet of doublets displaying coupling constants typical of both geminal and vicinal coupling. The endo hydrogen atom could only be coupled to *both exo* protons in this way if the complex possessed the structure shown in Fig. 7.3c, *i.e.* the formation of **137** results from a direct 1,2-

double addition in the same way as **135** in spite of the availability of an *endo* hydrogen atom.

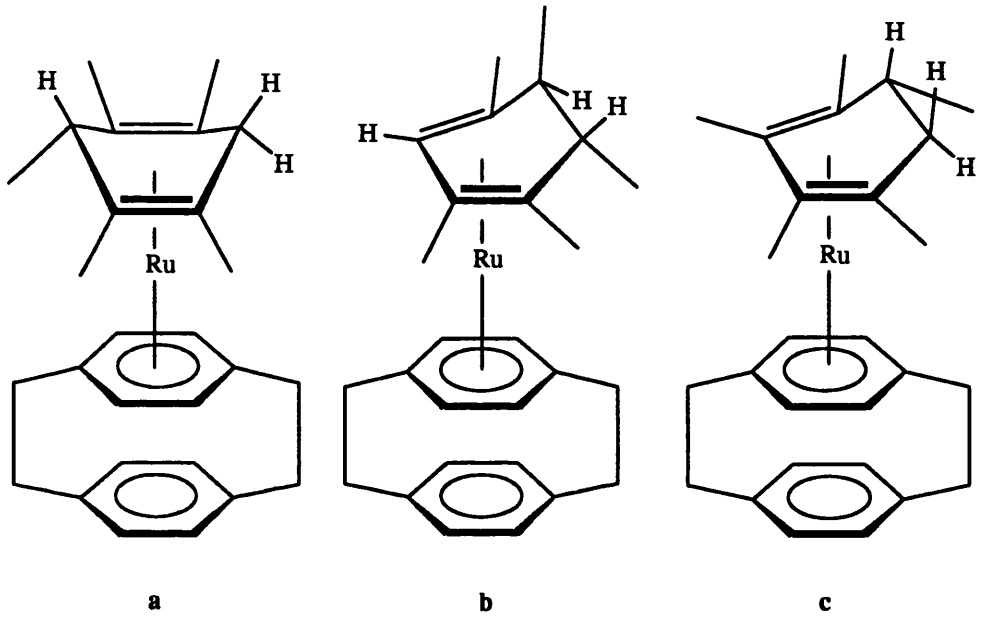

Fig. 7.3: Possible isomers of $[Ru(\eta^6\text{-}C_{16}H_{16})(\eta^4\text{-}C_6Me_5H_3)]$ **137** resulting from a) 1,4-double addition; b) *endo*- rearrangement; c) 1,2-double addition or *exo*-rearrangement.

The ^1H NMR assignments for **137** were confirmed by preparation of the dideuteriated analogue, $[Ru(\eta^6\text{-}C_{16}H_{16})(\eta^4\text{-}exo\text{-}D_2C_6Me_5H)]$ **137'** (by treatment of **3e** with $Na[BD_4]$). In the ^1H NMR spectrum of **137'** the resonances at δ 1.35 and 1.10 ppm, arising from the *exo* protons on the undeuteriated analogue were absent, while the resonance corresponding to H_{endo} (δ 0.44 ppm) occurred as a singlet, as did the resonance corresponding to the *endo* methyl substituent, δ 0.66 ppm. The infrared spectrum of **137** displays $\nu(CH_{exo})$ at 2738 cm^{-1}. In **137'** this band shifted to 2093 cm^{-1} whilst the remainder of the region 2700 - 3100 cm^{-1} remained unchanged. Both **137** and **137'** displayed a band at 2925 cm^{-1} tentatively assigned to $\nu(CH_{endo})$.

Small quantities of a second product representing *ca.* 4% of the overall reaction yield in both the Red-Al and borohydride syntheses of **137** was also observed. This product

was not isolated but, since it exhibits a singlet resonance for the cyclophane coordinated deck at δ 3.97 (*cf.* δ 3.95 for **5**) and a multiplet resonance at δ 3.46 assigned to the *exo* hydrogen atoms from the incoming nucleophile (*cf.* **5** δ 3.41), we suggest it to be the 1,4-diene isomer of **137** shown in Fig. 7.3a.

Action of $Na[BH_4]$ upon the durene (1,2,4,5-tetramethylbenzene) complex **3d** in thf over a period of *ca.* 12 h again results in the formation of a (diene)ruthenium(0) compound, $[Ru(\eta^6\text{-}C_{16}H_{16})(\eta^4\text{-}C_6Me_4H_4)]$ **138** (FAB-MS *m/z* 446). According to arguments based on the accumulation of partial positive charges on the arene carbon atoms[11,78] initial nucleophilic additions should be more likely to occur *para* to one another to give a 1,4-diene product, since the two unmethylated sites should be the most electrophilic. In practice though, an asymmetric 1,3-diene product is obtained as is apparent from the large splitting of the ^1H NMR resonance arising from the protons of the coordinated cyclophane deck. The remainder of the spectrum bears a strong resemblance to that of **137** and selective homonuclear decoupling experiments along with analysis of coupling constants implies that, like **137**, **138** possesses an *endo* methyl group attached to an aliphatic ring site and therefore also results from 1,2-double addition and not an *endo* hydride transfer. Also in common with **137**, a small quantity (*ca.* 2%) of a symmetric (cyclophane)ruthenium(0) species is observed in the crude reaction product (coordinated cyclophane ring δ 3.96 ppm, singlet) suggestive of the presence of a small quantity of the 1,4-diene isomer of **138**.

Reduction of the *p*-cymene complex **3c** with Red-Al and $Na[BH_4]$ (in the absence of aqueous quenching) also results in the formation of a chiral 1,3-diene complex of formula $[Ru(\eta^6\text{-}C_{16}H_{16})\{\eta^4\text{-}1\text{-}Me\text{-}4\text{-}(CHMe_2)C_6H_6\}]$ **139a**, as would be expected from the product of a direct 1,2-double hydride addition at the least alkylated sites. The methyl and *iso*-propyl substituents occupy the two terminal olefinic sites, C(1) & C(4), whilst the two olefinic hydrogen atoms occur as an AB quartet in the ^1H NMR spectrum, δ 4.21 & 4.07 ($^3J_{H\text{-}H}$ = 3.4 Hz consistent with the *cis* geometry). Surprisingly, if the reduction is carried out with $Na[BH_4]$ and water added to the reaction mixture a different isomer is obtained, $[Ru(\eta^6\text{-}C_{16}H_{16})\{\eta^4\text{-}2\text{-}(CHMe_2)\text{-}5\text{-}MeC_6H_6\}]$ **139b**. Complex **139b** is characterised by the observation of a single internal olefinic doublet (δ 4.24 ppm) in place of the AB quartet observed for **139a** and the appearance of a multiplet corresponding to the terminal olefinic

hydrogen atoms on C(1) and C(4) (δ 2.49 ppm, 2H). Strong evidence for the aliphatic nature of the methyl substituent on C(5) is the doublet resonance at δ 0.72 ppm (^3J = 6.7 Hz, 3H). In **139a** the methyl substituent is attached to the terminal olefinic site C(1) and occurs as a singlet (δ 1.22 ppm). The assignment of the ^{1}H NMR spectrum of **139b** was confirmed by an extensive series of homonuclear decoupling experiments which, in conjunction with analysis of coupling constant data, suggested that the methyl substituent on C(5) adopts an *endo* stereochemistry. This would imply that **139b** could result from a net *exo* [1,3] H-shift of **139a**, but not an *endo* metal-hydride mediated rearrangement. The relationship between **139a** and **139b** is in some ways similar to that between **5** and **135**.

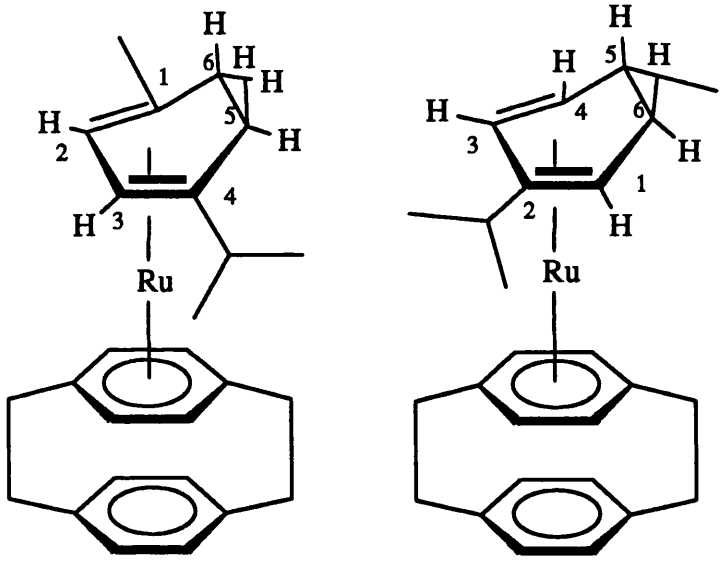

139a **139b**

The observation of 1,2-double additions in complexes **3a** - **3e** is consistent with the chemistry of related *bis*(arene)iron dications, where deuteriation studies and reactions with nucleophiles other than hydride have also shown that double nucleophilic additions occur in a 1,2-fashion and thus the thermodynamic and kinetic products are one and the same.[78,87] Extended Hückel calculations on the cation $[Fe(\eta^6\text{-}C_6H_6)(\eta^5\text{-}C_6H_7)]^+$ have demonstrated that the greatest partial positive charges reside on the η^6-benzene ring (+0.04 to +0.08) and thus, under charge controlled conditions a second nucleophilic addition should give a *bis*(cyclohexadienyl)iron(II) complex, as frequently observed in non-cyclophane ruthenium

compounds.[8] Within the cyclohexadienyl ring itself the greatest partial positive charges reside upon the carbon atoms *meta* (+0.06) and *para* (+0.05) to the saturated site (see Introduction, Fig. 1.5) and so 1,4- or 1,3- double additions would be expected (as observed in the Red-Al reduction of **3b**). The carbon atom, C_1 (Fig. 1.5), *ortho* to the sp^3 site has a small nett negative charge (-0.01). Hence it has been concluded that in the case of the iron complexes, nucleophilic additions do not occur under charge control and a frontier molecular orbital model for the reaction is more satisfactory.[78,87]

Clearly a fine balance exists between the factors affecting regioselectivity in double nucleophilic addition reactions. The observation of 1,3- and 1,4-additions at a given ring, when Red-Al is used as the reducing agent, could be a result of both the steric bulk of the reagent and its strongly reducing nature, resulting in a change from orbital to charge controlled reactivity. Use of the inert spectator ligand [2.2]paracyclophane has enabled us to show that for practical purposes products of 1,2-double additions at a given ring are the norm in the case of ruthenium as well as the iron and osmium[227] analogues and hence occur under frontier molecular orbital control. However it should be noted that the use of water in the 'work-up' has a significant impact on the identity of the *isolated* product.

7.3 Attempted Synthesis of Substituted (Diene)Ruthenium(0) Complexes

Direct interaction of complexes of type **3** with nucleophiles other than hydride in dry thf proved to be inefficient in generating difunctionalised (diene)ruthenium(0) complexes. As described in Chapter 6, it was found that LiMe was insufficiently nucleophilic to effect a second addition to the hexamethylbenzene complex **3b** and only the heptamethyl cyclohexadienyl compound $[Ru(\eta^6\text{-}C_{16}H_{16})(\eta^5\text{-}C_6Me_7)][BF_4]$ **132** was obtained. Action of excess LiMe upon the more electrophilic benzene complex **3a**, however, and extraction into hexane gave an air sensitive yellow oil which was shown by ^1H NMR spectroscopy to consist of at least two major species. Two coordinated cyclophane ring resonances were observed [δ 3.96 (s) and 4.07 (AA'BB' quartet) ppm] whilst the remainder of the spectrum was consistent with a mixture of isomers of formula

$[Ru(\eta^6\text{-}C_{16}H_{16})(\eta^4\text{-}C_6H_6Me_2)]$. Pure samples of these materials could not be isolated.

The generation of monofunctionalised diene species *via* a stepwise strategy (Scheme 7.2) involving $Na[BH_4]$ reduction of functionalised cyclohexadienyl complexes such as $[Ru(\eta^6\text{-}C_{16}H_{16})(\eta^5\text{-}C_6Me_6CN)][BF_4]$ **131** (see Chapter 6) was also attempted. Reduction of the cyano complex **131** with $Na[BH_4]$ proceeds slowly at room temperature over a period of days to generate small quantities (*ca.* 20% of the isolated product) of the functionalised 1,3-diene complex $[Ru(\eta^6\text{-}C_{16}H_{16})\{\eta^4\text{-}C_6Me_6H(CN)\}]$ **140** as well as large quantities of **135** as a contaminant. The formation of **135** must result from loss of cyanide, which is clearly a better leaving group than hydride. Because **140** was only obtained in low yield and was relatively air sensitive it was not isolated. Its existence was however, confirmed by its ^1H NMR spectrum which exhibits an AA'BB' pattern for the coordinated ring protons of the cyclophane ligand (δ 4.28 & 4.17 ppm, ^3J = 6.6 Hz) indicating that the complex is chiral and thus possesses a 1,3-diene structure analogous to **135**.

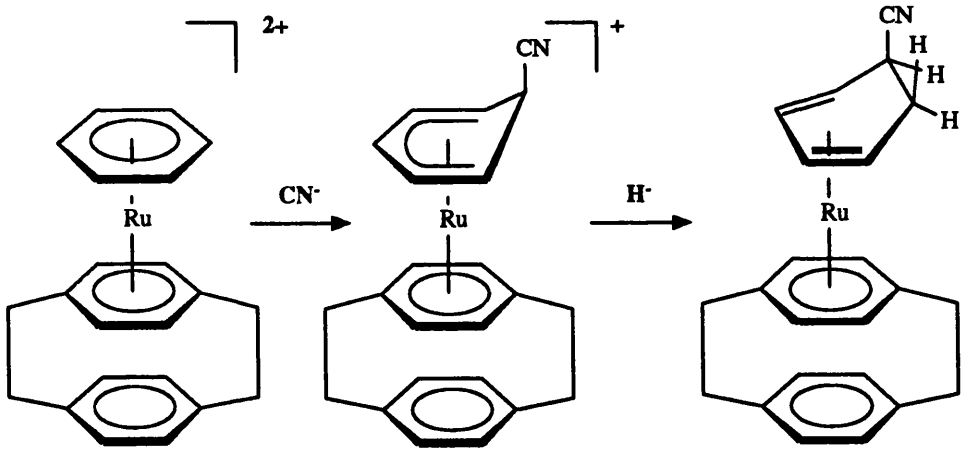

Scheme 7.2: Stepwise strategy for the generation of functionalised (diene)ruthenium(0) species.

In Chapter 6 the compound $[Ru(\eta^6\text{-}C_{16}H_{16})\{\eta^5\text{-}C_6Me_5(CH_2)\}][BF_4]$ **133** was reported to be formed from the deprotonation the hexamethylbenzene complex **3b**. This reaction has

been extended by examination of the reaction of **3b** with two equivalents of KO^{t}Bu. We find that this results in the double deprotonation of the hexamethylbenzene ligand to give the mildly air sensitive tetramethyl *o*-xylyene complex [Ru(η^6-$C_{16}H_{16}$){η^4-$C_6Me_4(CH_2)_2$}] **141** (FAB-MS *m/z* 470) with no trace of deprotonation of the cyclophane ligand observed. Complex **141** exhibits two resonances for the terminal olefinic protons, δ 4.64 and 4.20 ppm, characteristic of binding of the ligand through the endocyclic double bonds.[80,81] In contrast exocyclic complexes exhibit resonances due to H_{anti} and H_{syn} at much higher field, *e.g.* [Ru{η^4-$C_6Me_4(CH_2)_2$}{P(OMe)$_3$}], δ 2.54 and 0.23 ppm.[83] The singlet resonance for the coordinated cyclophane deck is observed at δ 4.23, consistent with a neutral Ru(0) complex whilst the infrared spectrum of **141** exhibits a band of medium intensity at 1590 cm^{-1} (*cf. ca.* 1600 cm^{-1} for [Mn{$C_6Me_4(CH_2)_2$}(CO)$_3$]$^+$ [82]) assigned to the exomethylene C=C bonds.

The synthesis of **141** is reversible and addition of H[BF_4] (aq., 40%) to a hexane solution of **141** re-generates **3b**. Careful addition of H[BF_4].Et_2O to an ether solution of **141** at low temperature also results in the re-formation of **3b** along with a little **133**.

Formation of complexes such as **133** and **141** result from the enhanced acidity of benzylic hydrogen atoms (*e.g.* on methyl substituents) of coordinated arenes and is a well documented phenomenon.[71,80-82] In the case of *bis*(arene) metal cations it has been demonstrated that either one or two protons (from substituents *ortho* to one another) may be abstracted, to generate respectively cyclohexadienyl complexes with one exocyclic double bond, such as **133**, or *o*-xylylene species in which the reduced metal centre is bound to the endocyclic double bonds.[80-82] In contrast to these results however, Bennett *et al.*[83] have recently demonstrated that double deprotonation of the (hexamethylbenzene) ruthenium(II) phosphine complexes [Ru(η^6-C_6Me_6)(ONO_2)(PR_3)$_2$][NO_3] in the presence of phosphine generates the (*o*-xylyene)ruthenium(0) compounds [Ru{η^4-$C_6Me_4(CH_2)_2$}(PR_3)$_3$], in which the metal atom is bound to the exocyclic double bonds.

A similar deprotonation mechanism has been suggested to be responsible for the observed exchange of the pentamethylcyclopentadienyl methyl protons for deuterium in [{Rh(η^5-C_5Me_5)}$_2$(OH)$_3$]Cl to give [{Rh(η^5-$C_5(CD_3)_5$)}$_2$(OD)$_3$]Cl on warming in D_2O in the presence of OD^-.[178]

7.4 Protonation of Ruthenium(0) Complexes

7.4.1 Protonation of [Ru(η^6-$C_{16}H_{16}$)(η^4-5,6-$C_6Me_6H_2$)]

Reaction of the electron rich ruthenium(0) 1,3-diene complex **135** with H[BF_4] (40% aq.) with vigorous stirring in hexane results in the formation of a pale yellow, air and moisture stable precipitate of [Ru(η^6-$C_{16}H_{16}$)($C_6Me_6H_3$)][BF_4] **142**. Analytical data indicated the presence of one mole of water and this was confirmed by the observation of ν(OH) in the infrared spectrum of the complex. The FAB mass spectrum of the material displays only a single peak *m/z* 475 (with the expected isotope distribution characteristic of ruthenium) as expected for the cation in **142**, with no trace of fragmentation peaks of measurable intensity, implying that the water is not strongly associated with the complex. Retention of water was found to be common to a number of [BF_4]$^-$ salts of similar species (*vide infra*) and the related protonolysis product [Ru{η^3-(HCH_2)(CH_2)C_6H_4)}(PMe_2Ph)$_3$][PF_6] also exists as a hydrate.[83] The presence of the [BF_4]$^-$ anion was confirmed by the observation of ν(BF) in the infrared spectrum. The room temperature ^{1}H NMR spectrum of **142** exhibits three resonances of equal intensity arising from the methyl substituents of the $C_6Me_6H_3$ ring. A further aliphatic resonance was assigned to H_{exo} and a high field "hydridic" signal was also observed [δ 1.95 (s), 1.38 (d, J_{obs} 2.5) and 0.72 (d, J_{obs} 6.6), CH_3; 1.22 (d of q, J_{obs} 6.6 & 4.1), *exo-H*; -10.80 (t of sp, J_{obs} 4.1 & 2.5 Hz) ppm]. The peak due to the coordinated deck of the [2.2]paracyclophane ligand occurred as a singlet (implying an apparent plane of symmetry in the $C_6Me_6H_3$ ligand) at δ 4.80. This is at the lower field end of the chemical shift range expected for a monocationic ruthenium(II) species.[220] The symmetrical nature of the spectrum apparently implies that **142** exists as a metal hydride in its ground state, and contains an η^4-$C_6Me_6H_2$ 1,3-diene ligand, consistent with protonation and oxidation of the metal centre [*cf.* oxidation of the ruthenium(0) *bis*(phosphine) compounds [Ru(η^6-C_6Me_6)(PR_3)$_2$] with [NH_4][PF_6] to give the ruthenium(II) hydrido complexes [Ru(η^6-C_6Me_6)(PR_3)$_2$H][PF_6]].[54,56,65] However, a series of homonuclear decoupling experiments revealed significant coupling of the hydridic resonance with i) the *exo* ring protons (δ 1.22, 4.1 Hz) and ii) the methyl signal at δ 1.38, 2.5 Hz, possibly implying an agostic[229] interaction.

The room temperature ^{1}H coupled ^{13}C spectrum of **142** (Fig. 7.4) is also relatively

simple, displaying three resonances for the C_6 ring carbon atoms [δ 91.51 (s, C_c & C_c'), 59.25 (d, J_{obs} 36.0, C_b & C_b') and 38.45 (d, J_{obs} 129.8, C_a & C_a') - for labelling scheme see Scheme 7.3]. The observed $^1J_{C\text{-}H}$ on the resonance at δ 38.45 is typical of an sp^3 aliphatic coupling[230] and this resonance is assigned to the saturated carbon atoms C_a and C_a'. The resonance at δ 59.25 is assigned to C_b / C_b' on the basis of a selective heteronuclear decoupling experiment: continuous irradiation of the ^1H signal at δ -10.80 resulted in the collapse of the 36 Hz doublet at δ 59.25 into a singlet resonance displaying a strong NOE enhancement in intensity with respect to the remainder of the peaks in the spectrum, indicating that the hydridic proton does indeed form part of an agostic CH bond. The observed coupling of 36.0 Hz is too large for the formulation of **142** as a full hydride (it is estimated that hydridic couplings generally fall in the region 0 - 10 Hz[229]) but is also atypical of an agostic CH bond for which a value of 60 - 100 Hz would be expected.[229,231] The fluxional *bis*(ethylene) cobalt(III) complex $[Co(Cp^*)(\eta\text{-}C_2H_4)_2H]^+$ [229] however, exhibits a very similar low $^1J_{C\text{-}H}$ coupling constant (33.5 Hz) as a result of the dynamic averaging of two degenerate agostic modes. The small coupling of 36.0 Hz in **142** is thus rationalised as a dynamic average (Scheme 7.3) of the two static couplings of the agostic proton with C_b and C_b', *i.e.* in a slow exchange regime $^1J(C_b\text{-H}) \approx 72$ and $^1J(C_b'\text{-H}) \approx 0$ Hz.

Attempts were made to freeze out this rapid exchange by low temperature ^1H NMR spectroscopy but the spectrum remained relatively unchanged in the temperature range +50 to -90°C although at the latter temperature considerable broadening of a number of resonances had occurred. This was most noticeable on the signal due to the coordinated deck of the [2.2]paracyclophane ligand. In the static complex this resonance would be expected to exhibit an AA'BB' pattern (or eight line signal if rotation about the Ru-cyclophane bond is slow) as a consequence of the loss of the dynamic plane of symmetry in the agostic ligand. Rapid exchange is not unexpected for systems of this kind and has previously been observed in related compounds.[232] Use of a mixed CD_2Cl_2 / CHF_2Cl solvent allowed examination of the spectrum down to -135°C, Fig. 7.5 (the more convenient CD_2Cl_2 / CF_2Cl_2 mixture was unsuitable because of the low solubility of the complex in this medium). Between -90°C and -110°C the resonances due to H_{exo} and those arising from the methyl groups attached to the olefinic sites C_b / C_b' and C_c / C_c'

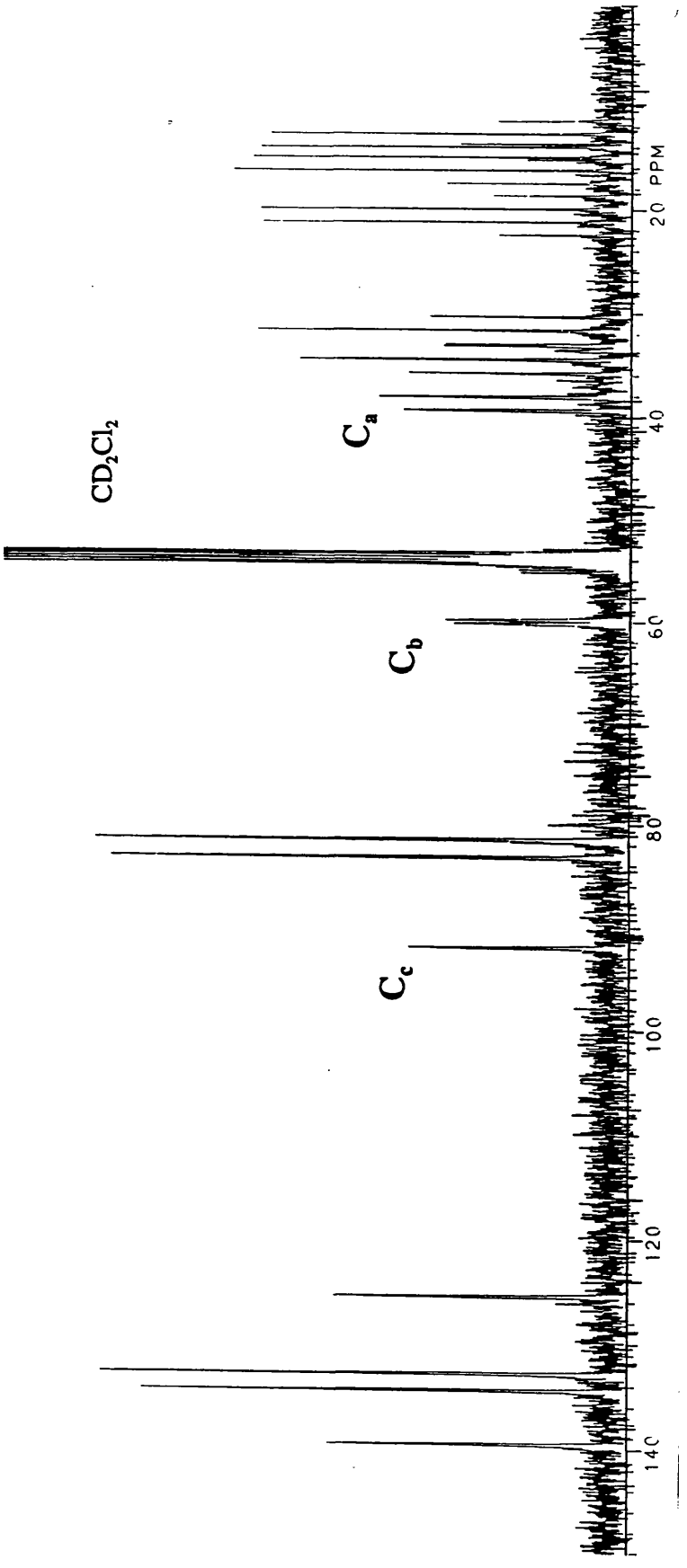

Fig. 7.4: Room temperature ^1H coupled ^{13}C NMR spectrum of the fluxional agostic complex $[Ru(\eta^6\text{-}C_{16}H_{16})(\eta^3\text{-}C_6Me_6H_3)][BF_4]$ **142.**

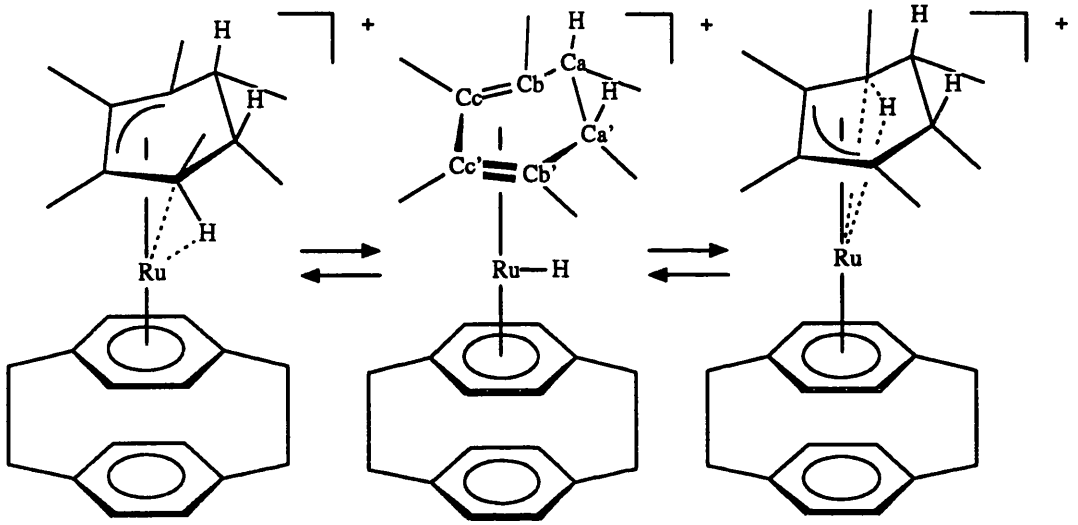

Scheme 7.3: Fluxionality in the agostic complex $[Ru(\eta^6\text{-}C_{16}H_{16})(\eta^3\text{-}C_6Me_6H_3)][BF_4]$ **142.**

(δ 1.95 and 1.38) broadened markedly, whilst the *endo* methyl substituents (δ 0.72) remained relatively unaffected. At -110°C the resonance due to the coordinated [2.2]paracyclophane deck was also barely visible as a broad peak in the baseline. Lowering the temperature even further resulted in the growth of a new set of signals strongly indicative of the loss of the dynamic plane of symmetry in the $C_6Me_6H_3$ ligand. At -135°C four distinct resonances could be distinguished due to the methyl substituents on C_c', C_c, C_b' and C_b (δ 2.01, 1.62, 1.49 and 1.06 ppm respectively). The latter peak exhibited traces of doublet coupling as expected in the static structure although the spectrum was rather broad as a consequence of precipitation and increasing solvent viscosity. Individual signals were also observed for the two protons H_{exo} (δ 1.39 and 0.95 ppm) whilst the methyl substituents on C_a and C_a' both occur at the same chemical shift (δ 0.61 ppm) near their averaged, room temperature position.

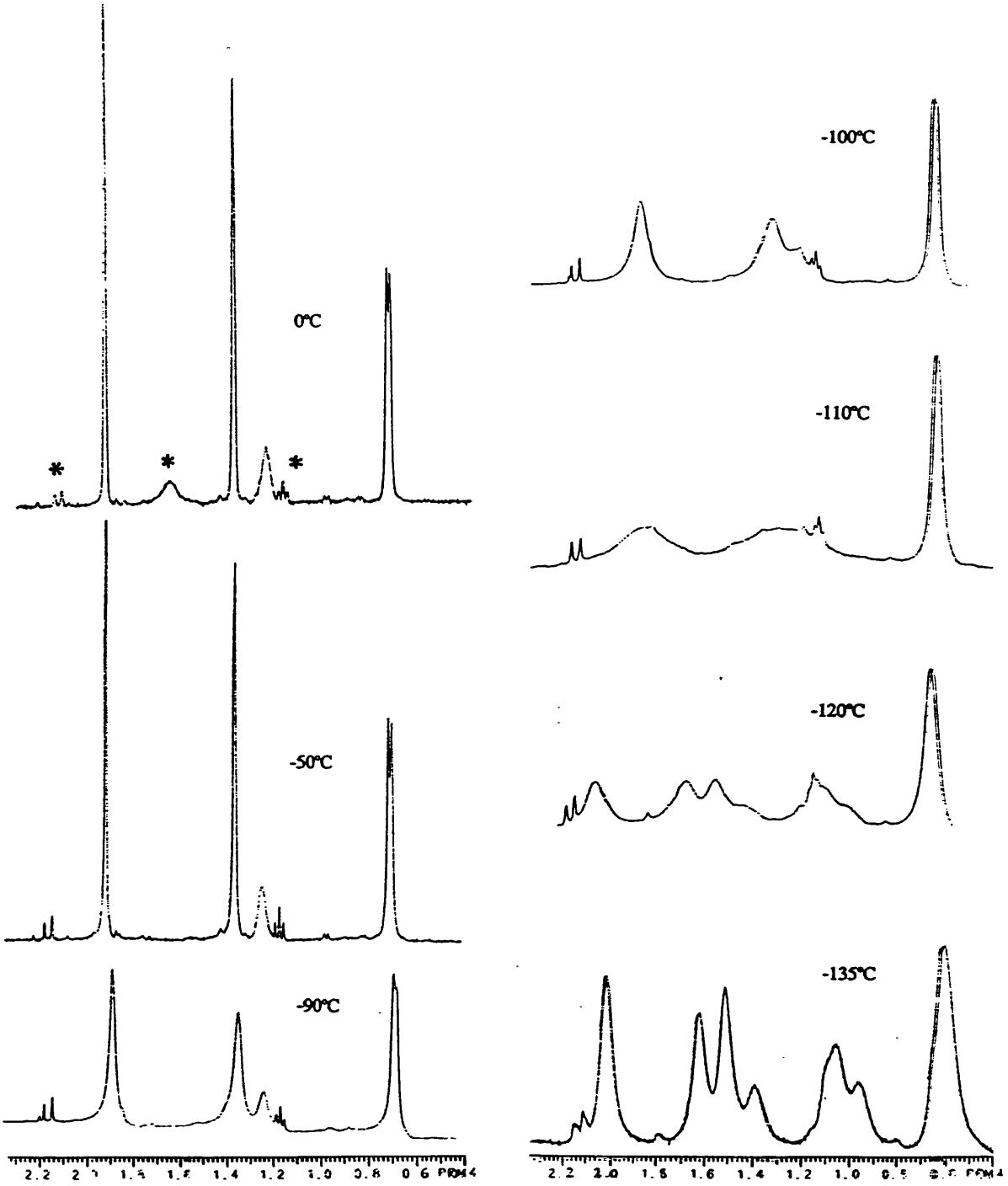

Fig. 7.5: Partial variable temperature ^1H NMR spectrum of $[Ru(\eta^6\text{-}C_{16}H_{16})(\eta^3\text{-}C_6Me_6H_3)][BF_4]$ **142**. Peaks marked (*) are due to impurities.

The origins of the *exo* and agostic protons in **142** were confirmed by a series of deuteriation experiments. Reaction of the *exo*-dideuterio complex **135'** with $H[BF_4]$ led to the formation of the *exo*-dideuteriated agostic compound $[Ru(\eta^6\text{-}C_{16}H_{16})(\eta^3\text{-}D_2C_6Me_6H)][BF_4]$ **142'**. The *exo* nature of the deuterons was established by the observation of ν(CD) in the infrared spectrum at 2113 cm^{-1} and more importantly by the absence of the resonance due to H_{exo} in the ^1H NMR spectrum of the material (δ 1.22 ppm). Reaction of **135** with $D[BF_4]$ [synthesised by stirring $H[BF_4]$ (40% aq.) in D_2O] resulted in the *endo*-deuterio complex $[Ru(\eta^6\text{-}C_{16}H_{16})(\eta^3\text{-}H_2C_6Me_6D)][BF_4]$ **142''** which did not exhibit an obvious ν(CD) band in its infrared spectrum. The ^1H NMR spectrum of **142''** displayed a quartet resonance at δ 1.22 whilst the hydridic signal was *ca.* 40% of its intensity in the undeuteriated analogue **142**, as a result of protonation by residual $H[BF_4]$. Protonation of **135** was also carried out with CF_3CO_2D to give $[Ru(\eta^6\text{-}C_{16}H_{16})(\eta^3\text{-}H_2C_6Me_6D)][H(CF_3CO_2)_2]$ **143** which exhibited *ca.* 75% deuterium incorporation into the agostic site. The presence of the $[H(O_2CCF_3)_2]^-$ anion was confirmed by the observation of a resonance due to the acidic proton (resulting from H / D exchange during work up) in the ^1H NMR spectrum, δ 8.80, and signals for the trifluoroacetate carbon atoms in the ^{13}C NMR spectrum (Table 7.2).

7.4.2 Protonation of $[Ru(\eta^6\text{-}C_{16}H_{16})(\eta^4\text{-}3,6\text{-}C_6Me_6H_2)]$

Protonation of the 1,4-diene complex **5** with $H[BF_4]$ results in the formation of the agostic compound $[Ru(\eta^6\text{-}C_{16}H_{16})\{\eta^3\text{-}(HCH_2)(CH_2)C_6Me_4H_4\}][BF_4]$ **144** which is an isomer of **142** (FAB-MS *m/z* 475, very little fragmentation). Complex **144** may be left in chloroform solution in air for several hours without appreciable decomposition and may be stored in air in the solid state for extended periods. Like **142**, the ^1H NMR spectrum of **144** is deceptively simple at room temperature. Two methyl resonances are observed, coupled to two 2H multiplets assigned to H_d and H_e by selective homonuclear decoupling experiments [δ 0.95 (d, 6H, ^3J=6.6) and 0.82 (d, 6H, ^3J=6.8), CH_3; 2.08 (d of q, 2H, ^3J=4.9 & 6.8), H_d and 1.43 (d of q, 2H, ^3J=4.9 & 6.6) ppm, H_e - for labelling scheme see Scheme 7.4]. A broad 5H singlet was also observed at δ -1.52 which produces no change in the remaining resonances on selective irradiation. The singlet due to the coordinated cyclophane deck implies the existence of a dynamic plane of symmetry in the molecule.

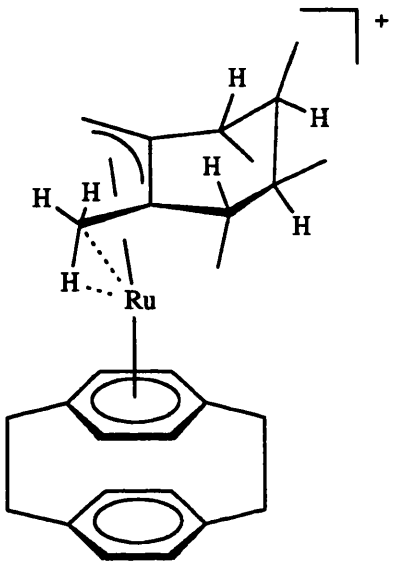

144

Raising the temperature of the NMR probe to 50°C results in a sharpening of the resonance at δ -1.52 confirming that the compound is in a fast exchange regime. Low temperature experiments down to -135°C suggest that the complex is undergoing two dynamic processes (Scheme 7.4):

a) Exchange of the agostic hydrogen atom between the terminal sites C_a / C_a' (analogous to the dynamic process described for **142**) resulting in the molecule's exhibiting a dynamic plane of symmetry at higher temperatures.
b) Agostic methyl group rotation resulting in the averaging of the signals for H_a, H_b and H_c.

The slower of these two exchange processes is process *b*, agostic methyl rotation. At -50°C the 5H resonance at δ -1.52 was replaced by two broad signals at δ -0.90 (2H) and -9.92 (1H) ppm. A further 2H resonance would be expected in the region of δ *ca.* 2.5 but was apparently too broad to be observable at this temperature. The resonance at δ -9.92 ppm occurs at a very similar chemical shift to the agostic signal for C_b-H in **142** and by analogy is assigned to the agostic proton H_a, whilst the resonance at δ -0.90 ppm probably corresponds to the *syn* protons H_c and H_c'. At this temperature the resonance due to the

protons of the coordinated deck of the cyclophane ligand remained a sharp singlet implying that the molecule retains a dynamic plane of symmetry. Lowering the temperature to -80°C results in the sharpening of the "hydridic" resonance due to H_a and its splitting into a quintet consistent with coupling to all four protons H_b, H_b', H_c and H_c' confirming the freezing out of process *b*, although not process *a*. In addition, between -50°C and -80°C the resonance at δ -0.90 ppm disappears once more to be replaced by two broad 1H signals δ 0.10 and -1.85 ppm whilst the resonances due to Me_d / Me_d' and the *endo*-protons H_e / H_e' as well as the signal for the coordinated cyclophane deck broaden significantly. At -100°C process *a* is also slow on the NMR timescale and the loss of the dynamic plane of symmetry is reflected by the splitting of the resonances due to the coordinated deck of the cyclophane ligand into two broad signals (δ 5.10 and 4.65). The hydridic resonance at δ -9.92 ppm now occurs as a triplet due to coupling to H_b and H_c (δ 0.10 and -1.85 ppm respectively) with a $^2J_{H\text{-}H}$ = *ca.* 14 Hz, consistent with geminal coupling (unlike $^1J_{C\text{-}H}$, no reduction is expected in $^2J_{H\text{-}H}$ in agostic systems[223]). The *exo*-protons H_d and H_d' occur at δ 2.18 and 2.09 ppm whilst the difference in chemical shift of the *endo*-protons H_e and H_e' is somewhat larger (δ 1.59 and 1.26 ppm). The *anti* olefinic proton H_b' is apparently masked by the signals for the cyclophane ethylenic bridges, whilst H_c' is observed at δ 0.67 ppm. All four methyl groups are also unique (δ 0.99, 0.96, 0.89 and 0.52 ppm).

These results contrast sharply with the fluxional processes observed by Bennett *et al.*[83] in the closely related agostic diphosphine compound $[Ru\{\eta^3\text{-}(HCH_2)(CH_2)C_6Me_4\}\{(Z)\text{-}Ph_2PCH{=}CHPPh_2\}(PMe_2Ph)][PF_6]$ and related examples. In these complexes agostic methyl rotation (analogous to process *b* in **144**) is extremely rapid and could not be frozen out at temperatures down to -90°C; the protons analogous to $H_{a,b,c}$ occurring as a 3H multiplet at δ -2.20 ppm. In contrast, the process of type *a* (metal-hydride mediated exchange of H_a between the two terminal olefinic sites) was *slow* on the NMR timescale at temperatures below +60°C. These large differences in exchange rates may be rationalised by arguing that the agostic interaction in **144** is much stronger than in the *o*-xylylene-phosphine analogues,[83] where long range interactions between the uncoordinated, endocyclic olefinic functionalities may serve to provide additional stabilisation to the metal centre. A stronger agostic interaction would inhibit methyl group rotation (process *b*) because M-H bond

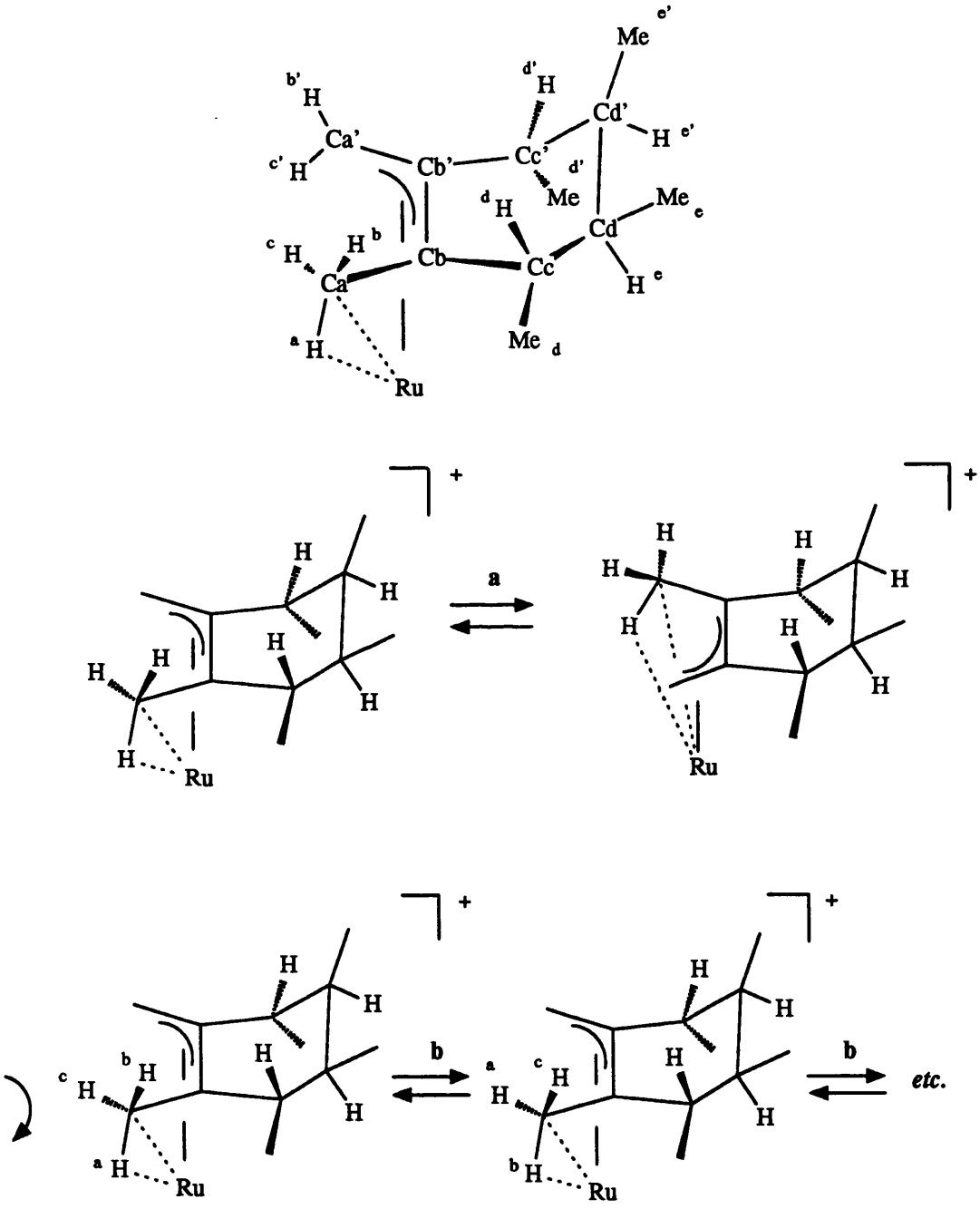

Scheme 7.4: Fluxionality in the agostic complex $[Ru(\eta^6\text{-}C_{16}H_{16})\{\eta^3\text{-}(HCH_2)(CH_2)C_6Me_4H_4\}][BF_4]$ **144**. (a) Terminal agostic exchange; (b) methyl rotation.

breaking is involved, whilst process *a* would be facilitated as a consequence of the more hydridic nature of the M-H bond and corresponding weakening of the C-H_a interaction.

Further evidence for the agostic nature of **144** comes from its room temperature ^{1}H coupled ^{13}C NMR spectrum (Table 7.2). Consistent with the proposed formulation, the unsaturated ring carbon atoms C_b / C_b' exhibit a singlet resonance at δ 100.62 whereas the sp^3 carbons C_c, C_c', C_d and C_d' display two doublet signals at typically aliphatic chemical shifts with one bond coupling constants consistent with non-agostic binding of the ring hydrogen atoms (δ 36.62 and 36.06 ppm, $^1J_{C\text{-}H}$ = *ca.* 127 Hz). Similarly, two quartet resonances exhibiting typically aliphatic couplings are observed for Me_c and Me_d. A further broad quartet (δ 17.45 ppm, $^1J_{obs}$ = 77.5 Hz), is also observed with a significantly reduced observed coupling constant which again represents and average value over the dynamic processes described above. This resonance is assigned to the agostic methyl carbon atoms C_a and C_a'.

The structure of **144** is a surprising one and we propose the mechanism of its formation from **5** to be of the type shown in Scheme 7.5. Steps I - IV are shown as sequential but since this would involve a 14 electron intermediate the mechanism is probably concerted and involves further agostic stabilisation. Step I consists of protonation and oxidation of the metal centre followed by partial hydride transfer to the organic ligand to give an unstable ene-yl intermediate analogous to **142**. Unlike **142** however, the complex undergoes a second protonation (*cf.* the facile double re-protonation of **141** to re-generate **3b**) to relieve the strain inherent in the intermediate ene-yl structure (step II) resulting in a formally 14 electron dicationic complex. This second protonation could occur in either an *exo* or *endo* fashion but is apparently *endo* since an *exo* protonation would result in H_e and H_e' being inequivalent even in a fast exchange regime. In step III the dicationic intermediate rapidly deprotonates at one of the methyl groups on the opposite side of the molecule to give a more stable sixteen electron allyl complex and finally (step IV) the metal attains an 18 electron configuration by a new agostic interaction with the methyl group adjacent to the newly formed exocyclic allylic functionality.

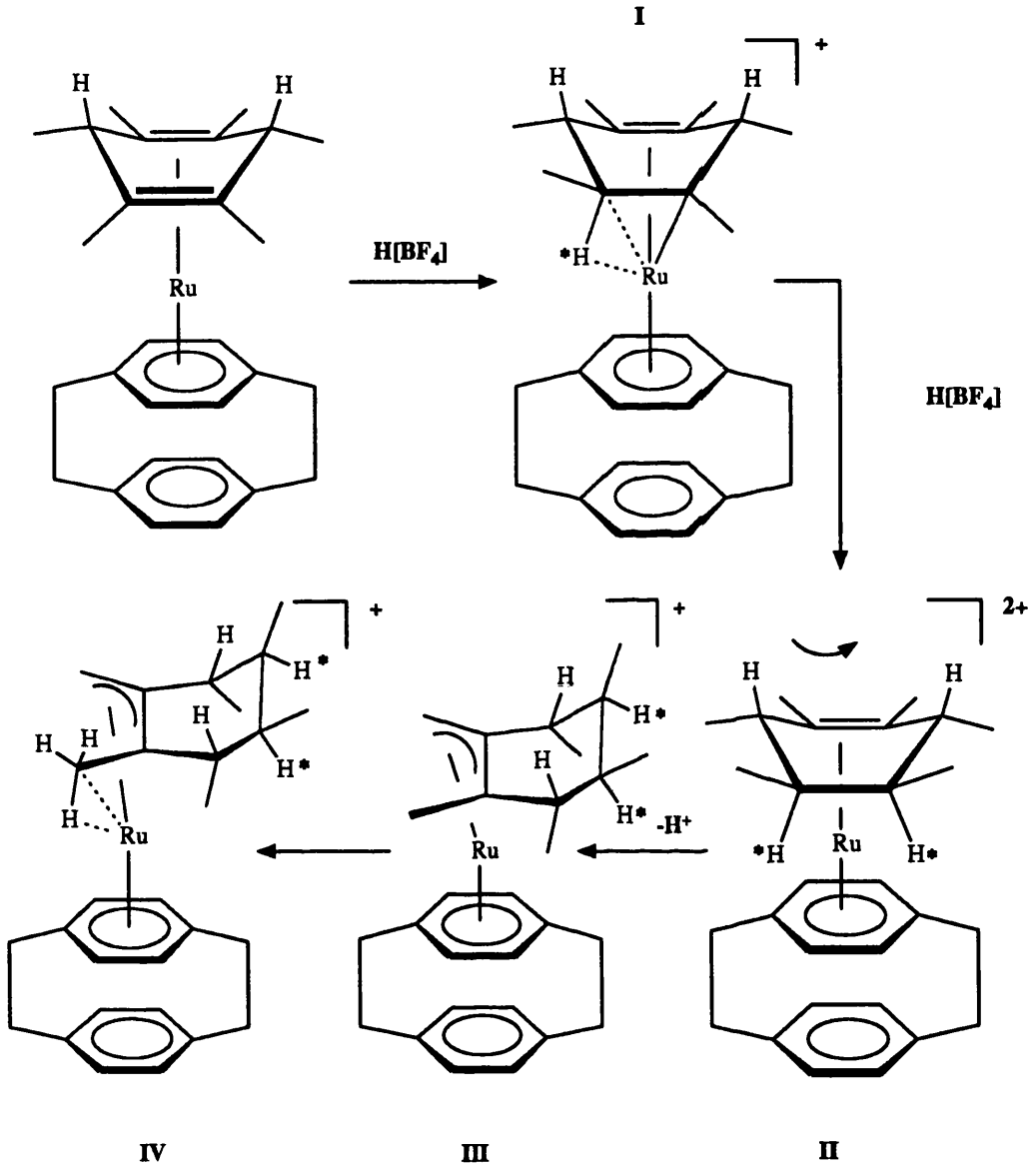

Scheme 7.5: Proposed mechanism for the formation of the agostic complex $[Ru(\eta^6\text{-}C_{16}H_{16})\{\eta^3\text{-}C_6Me_4H_5(CH_2)_2\}][BF_4]$ **144** (starred atoms originate from $H[BF_4]$).

In an attempt to establish the validity of this mechanism we attempted the preparation of the dideuterio analogue of **5**, [Ru(η^6-$C_{16}H_{16}$)(η^4-3,6-$C_6Me_6D_2$)] **5'** from the reaction of **3b** with Na[BD_4]. In favourable cases, in the absence of aqueous quenching, *ca.* 2 : 1 mixtures of **135'** and **5'** could be generated. Due to the air sensitivity of the (diene)ruthenium(0) complexes these mixtures were not separated but were protonated with H[BF_4] to give approximately 5 : 1 mixtures of **142'** and the *exo* dideuterio analogue of **144**, [Ru(η^6-$C_{16}H_{16}$){η^3-(HCH_2)(CH_2)$C_6Me_4H_2D_2$}][BF_4] **144'**. In spite of the low relative concentration of **144'**, the ^{1}H NMR spectrum of the mixture clearly demonstrated the inclusion of deuterons exclusively at H_d and H_d' consistent with the suggestion that H_e and H_e' both come from the H[BF_4].

Deprotonation of **144** with Li^{n}Bu results in the rapid formation of a further isomer of **5** and **135**, namely [Ru(η^6-$C_{16}H_{16}$){η^4-$(CH_2)_2C_6Me_4H_4$}] **145**, in 89% yield. Firm evidence for the binding of the metal centre to exocyclic olefinic functionalities comes from the relatively high field chemical shifts of the *anti* and *syn* =CH_2 protons which resonate at δ 1.45 and -0.71 ppm respectively [*cf.* the unbound exocyclic olefinic functionalities in **141** (δ 4.64 and 4.20 ppm)]. The remainder of the ^{1}H NMR spectrum of **145** strongly resembles the room temperature spectrum of **144** and provides good evidence for the proposed formulation.

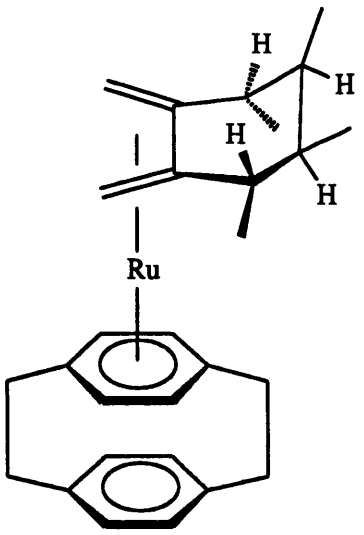

145

7.4.3 Synthesis of Additional Agostic Cyclohexenyl Compounds

Reaction of the pentamethyl and tetramethyl complexes **137** and **138** with $H[BF_4]$ also results in the formation of agostic protonolysis products $[Ru(\eta^6\text{-}C_{16}H_{16})(\eta^3\text{-}C_6Me_{5-n}H_{4+n})][BF_4]$ (n = 0, **146**; 1, **147**). Consistent with the proposed 1,3-diene structures of **137** and **138**, the metal atoms in **146** and **147** are coordinated *via* endocyclic allylic functionalities. All the methyl groups in both compounds are magnetically unique in their ^1H NMR spectra with only one in each case exhibiting a slightly lowered averaged $^3J_{H\text{-}H}$ [δ 1.05 ($^3J_{obs}$ = 4.8), **146**; 0.91 ($^3J_{obs}$ = 5.8) ppm, **147**; *cf.* 6.7 and 6.4 Hz for the methyl groups coupled to H_{exo} in the same compounds). The coordinated deck of the paracyclophane ligands occur as AA'BB' quartets consistent with the asymmetric structures of the complexes. More importantly, both complexes exhibit two broad high field resonances in their room temperature ^1H NMR spectra indicating that both *endo* protons are involved in agostic interactions. In the case of **146** these protons occur at similar chemical shifts (δ -4.56 and -5.25 ppm) and it would seem likely that each spends an approximately equal proportion of their time in agostic coordination to the metal centre. In contrast, one resonance in compound **147** occurs at much higher field than the other (δ -7.68 *cf.* -1.88 ppm) indicating a strong thermodynamic preference for agostic binding on one side of the asymmetric organic ligand. Moreover, the remainder of the ^1H NMR spectrum of **147**, in conjunction with homonuclear decoupling experiments, indicates that the highest field resonance is assignable to the *endo* proton of the CH_2 (as opposed to CHMe) group and does not correspond to the proton ostensibly from the $H[BF_4]$ (although the actual origins of the each of the *endo* hydrogen atoms is likely to be unknowable as a result of rapid scrambling). These results are summarised in Scheme 7.6 which presents the two fluxional processes (processes *a* and *b*) responsible for the observed exchange in **146** and **147**. Protonation of **137** and **138** doubtless proceeds initially in a manner analogous to that observed for **135** to give a complex of type I or type II analogous to **142**, which equilibrate *via* H-atom exchange between the terminal olefinic sites. Because of the availability of a second *endo* hydrogen atom however, complexes of type II may access another, non-degenerate structure (type III, process *b*) involving interaction of the metal centre with a different C-H bond. Like those of type II, molecules of type III may also undergo exchange of the agostic proton between terminal olefinic sites (process *a'*) to give

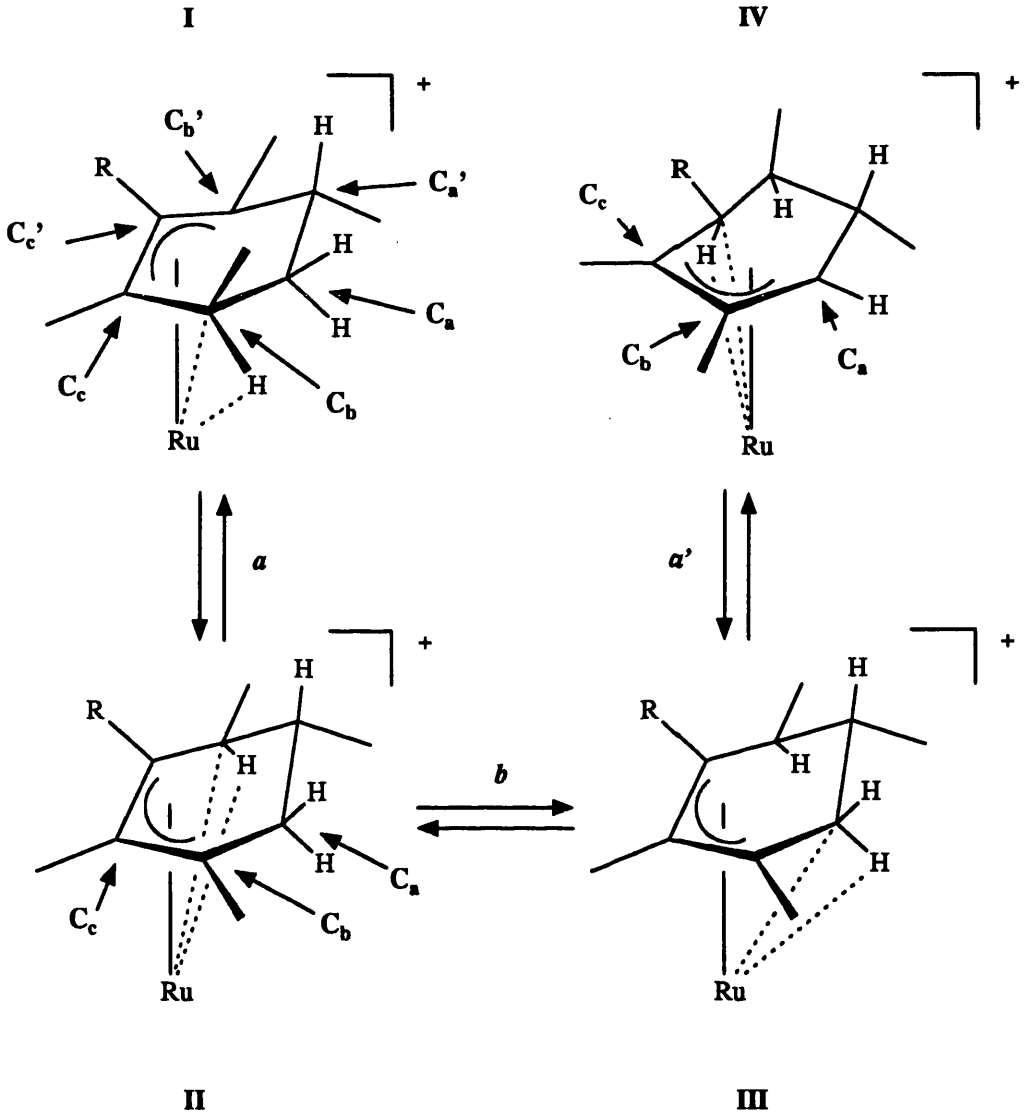

Scheme 7.6: Fluxionality in the agostic complexes $[Ru(\eta^6\text{-}C_{16}H_{16})(\eta^3\text{-}C_6Me_5RH_4)][BF_4]$ (R = Me **146**, H **147**): (a, a') exchange of agostic proton; (b) transfer of agostic interaction.

complexes of type IV. In the case of **146** the *exo* methyl substituent on one side of the molecule makes only a slight difference to the donor abilities of one C-H bond over the other and so molecules of type I / II and type III / IV are present in roughly equimolar amounts. In contrast, equilibrium *b* in the case of **147** significantly favours molecules of type III / IV with the *endo* proton of the CH_2 group taking part in an agostic interaction with the metal centre. Such a preference may be rationalised in terms of the relative π-donor abilities of the allylic functionality in complexes of type II and III. In the case of **146** all three allylic carbon atoms (C_b, C_c and C_c') are methylated and undoubtedly C_b and C_c' have similar donor abilities. In **147** however, there is no methyl substituent on C_c' and therefore C_b is likely to be the better donor of the two. Hence the relatively electron deficient metal centre is more stabilised in complexes of type III, in which it is situated on the more electron rich side of the organic ligand.

The geometries of complexes **146** and **147** and the nature of the exchange processes involved have been confirmed by ^{13}C and variable temperature ^1H NMR spectroscopy.

Raising the temperature of the NMR probe to +50°C results only in a sharpening of the two high field ^1H NMR resonances implying rapid dynamic exchange. Between 0°C and -80°C all the resonances except those due to the methyl groups bonded to C_c and C_a' in both **146** and **147** broaden markedly. At -80°C the resonances due to the two agostic protons in **146** (δ -4.56 and -5.25 ppm) have been replaced by two new signals in a ratio of *ca.* 3 : 4 (δ -10.55 and -11.01 ppm) close to the chemical shifts observed for the agostic protons in **142** and **144**. At -100°C these signals sharpen with one (δ -10.55) exhibiting a doublet structure $^2J_{H\text{-}H}$ = *ca.* 9 Hz consistent with the *endo* proton of the C_aH_2 group. The resonance at δ -11.01 should be a quartet, corresponding to the *endo* proton of the C_b'HMe section of the ring but the coupling is not resolved. Similarly the remainder of the spectrum of **146** is split into two sets of resonances with even two sets of AA'BB' type resonances being observed of the protons of the coordinated cyclophane deck and a total of ten signals (allowing for the accidental overlap of some resonances) for the methyl substituents of the agostic ligand. These observations suggest that at -100°C both processes *a* and *b* are slow and two isomers of **146** have been resolved corresponding to the structures shown as Types II and III in Scheme 7.6. Consistent with the room temperature ^1H and ^{13}C NMR (*vide infra*) data the isomers are of similar energy and are present in

approximately equimolar amounts at low temperature. Signals assignable to structures I and IV were not observed at low temperature indicating that these are less stable.

In contrast to **146**, the ^{1}H NMR spectrum of **147** at -80°C indicates the presence of only a single isomer. The chemical shift and coupling constant of the agostic resonance is consistent with the Type III structure.

The room temperature ^{1}H coupled ^{13}C spectra of **146** and **147** (Table 7.2) are also consistent with the proposed geometries. In the case of **146** the resonance due to C_a' (δ 34.34 ppm) occurs as a doublet with a typical aliphatic coupling constant whilst the resonances due to C_b' and C_a [δ 52.76 (d, J_{obs} = 87.0) and 41.94 (dd, J_{obs} = 95.5 & 141.2) ppm respectively] exhibit agostic couplings to the *endo* protons. The similarity in the magnitudes of these two couplings is consistent with there being little thermodynamic preference between species of type II and type III in **146**. The slightly lower value of $^1J_{obs}(C_b'$-H) is consistent with the higher field chemical shift of this hydrogen atom in the ^{1}H spectrum and implies that agostic interaction at C_b'-H (type I / II) is a marginally more significant mode of coordination. In **147** the situation is reversed [$^1J_{obs}(C_b'$-H) = 101.6, $^1J_{obs}(C_a$-H) = 69.1 Hz], and the preference is for agostic interaction at C_a-H. As might be expected the ^{13}C spectra of **146** and **147** are very similar to one another in most other respects with the only other striking dissimilarity being the chemical shifts of the resonances assigned due to C_c' in the two complexes. In **146** C_c' bears a methyl substituent and is observed at δ 73.83 ppm. In **147** the resonance occurs as a doublet (δ 64.30 ppm, ^1J = 161.0) consistent with the hydrogen atom substituent but, counter intuitively, at a relatively *upfield* chemical shift. Clearly the different shielding effects of R = H / Me is outweighed by the fact that in **147** there is a significant contribution to the average environment of this carbon atom by the type IV geometry in which it adopts an sp^3 hybridisation and consequently resonates at a significantly more aliphatic chemical shift. Further evidence for the complexes spending part of their time as structure IV comes from the signals due to the aliphatic carbon atoms C_a in **146** and **147** which exhibit a unexpectedly high coupling to one of the *exo* protons [141.2 (**146**) and 143.6 (**147**) Hz], possibly indicative of a partial olefinic character. This suggestion is supported by the relatively downfield chemical shifts of these resonances (δ 41.94 and 42.88 ppm respectively), suggesting that the carbon atoms spend some time in an sp^2 state of

hybridisation, as expected from the occurrence of process *a'* and the accessing of structure IV [*cf.* C_a' δ 34.34 (J_{obs} 128.8), **146** and 34.25 (J_{obs} 128.2) ppm, **147**].

7.5 Experimental

General experimental consideration are outlined in Sections 2.4 and 6.4.

Preparations. - $[Ru(\eta^6\text{-}C_{16}H_{16})(\eta^4\text{-}C_6H_6D_2)]$ **4'**. The compound $[Ru(\eta^6\text{-}C_{16}H_{16})(\eta^6\text{-}C_6H_6)][BF_4]_2$ (0.15 g, 0.27 mmol) was suspended in tetrahydrofuran (thf) with $Na[BD_4]$ (0.05 g, excess) and the mixture stirred for 4 h. The solvent was removed *in vacuo* and the product extracted into hexane (2 x 20 cm^3) and filtered. Slow evaporation of the filtrate and cooling resulted in the formation of the product as air sensitive yellow microcrystals. Yield 0.06 g, 0.15 mmol, 56% (Found: C, 68.35; H, 6.30. Calc. for $C_{22}H_{24}D_2Ru$: C, 67.50; H, 6.70%). The identity of the complex was confirmed by ^1H NMR spectroscopy by comparison with a sample of the undeuteriated counterpart $[Ru(\eta^6\text{-}C_{16}H_{16})(\eta^4\text{-}C_6H_8)]$ **4**.[7]

$[Ru(\eta^6\text{-}C_{16}H_{16})(\eta^4\text{-}5,6\text{-}C_6Me_6H_2)]$ **135**. The compound $[Ru(\eta^6\text{-}C_{16}H_{16})(\eta^6\text{-}C_6Me_6)][BF_4]_2$ (0.09 g, 0.15 mmol) was stirred in thf (10 cm^3) for 4 days with $Na[BH_4]$ (0.05 g, excess). Water (0.5 cm^3) was added to destroy the excess reducing agent and the mixture evaporated to dryness. The resulting yellow residue was extracted into hexane (40 cm^3) and filtered. Slow evaporation of the yellow filtrate and cooling gave the product as bright mildly air sensitive yellow crystals. Yield 0.04 g, 0.08 mmol, 53% (Found: C, 70.50; H, 7.85. Calc. for $C_{28}H_{36}Ru$: C, 71.00; H, 7.65%).

$[Ru(\eta^6\text{-}C_{16}H_{16})(1\text{-}\sigma\text{-}3\text{-}5\text{-}\eta\text{-}C_6Me_6H_2)]$ **136**. Treatment of the compound $[Ru(\eta^6\text{-}C_{16}H_{16})(\eta^6\text{-}C_6Me_6)][BF_4]_2$ (0.12 g, 0.19 mmol) in thf (10 cm^3) with Red-Al / toluene (0.5 cm^3, 3.4 M, 1.7 mmol) as previously described[7] followed by evaporation of the solvents, extraction into hexane (2 x 20 cm^3) and pumping to dryness resulted in the isolation of a 67 : 8 : 25 mixture of complexes **5**, **135** and **136** respectively. Compound **136** was not isolated in pure form.

[Ru(η^6-$C_{16}H_{16}$)(η^4-$C_6Me_5H_3$)] **137**. The compound [Ru(η^6-$C_{16}H_{16}$)(η^6-C_6Me_5H)][BF_4]$_2$ (0.13 g, 0.20 mmol) was treated with Na[BH_4] (0.05 g) as described for **135**. Extraction into hexane (40 cm^3) followed by removal of the solvent *in vacuo* resulted in the deposition of the product as a mildly air sensitive yellow powder. Yield 0.05 g, 0.12 mmol, 60% (Found: C, 71.15; H, 7.70. Calc. for $C_{27}H_{34}Ru$: C, 70.55; H, 7.45%).

[Ru(η^6-$C_{16}H_{16}$)(η^4-$C_6Me_4H_4$)] **138**. The compound [Ru(η^6-$C_{16}H_{16}$)(η^6-$C_6Me_4H_2$)][BF_4]$_2$ (0.10 g, 0.16 mmol) was treated with Na[BH_4] (0.05 g) as described for **135**. Extraction into hexane followed by removal of the solvent *in vacuo* resulted in the deposition of the product as an air sensitive yellow powder contaminated with *ca.* 20% free [2.2]paracyclophane. Removal of free ligand by sublimation under vacuum at 100°C followed by recrystallisation from hexane gave the pure product. Yield 0.03 g, 0.09 mmol, 56% (Found: C, 71.05; H, 7.40. Calc. for $C_{26}H_{32}Ru$: C, 70.10; H, 7.25%).

[Ru(η^6-$C_{16}H_{16}$){η^4-1-Me-4-($CHMe_2$)C_6H_6}] **139a**. The compound [Ru(η^6-$C_{16}H_{16}$)(η^6-*p*-$MeC_6H_4CHMe_2$)][BF_4]$_2$ (0.27 g, 0.44 mmol) was treated with Na[BH_4] (0.10 g) over a period of 24 h in a similar manner to that described for **135**. Extraction into hexane without addition of water, followed by removal of the solvent *in vacuo* resulted in the deposition of the product as an air sensitive yellow powder. Yield 0.10 g, 0.22 mmol, 50% (Found: C, 71.85; H, 7.45. Calc. for $C_{26}H_{32}Ru$: C, 70.10; H, 7.25%).* An identical product was obtained from the analogous reduction with Red-Al, which was carried out as previously described for **4**.[7]

[Ru(η^6-$C_{16}H_{16}$){η^4-2-($CHMe_2$)-5-MeC_6H_6}] **139b**. The compound [Ru(η^6-$C_{16}H_{16}$)(η^6-

---

* The product **139a** was shown by ^{1}H NMR to be contaminated by *ca.* 20% free [2.2]paracyclophane, analogously *ca.* 25% in the case of **139b**. Attempts to remove this impurity by sublimation were unsuccessful because of decomposition of the complex at higher temperatures, which generated additional free cyclophane impurity. Chromatographic separation was ruled out because of the complexes' high air sensitivity. Similar problems were found in the case of **3**.[7] Anal. Recalc. for $C_{26}H_{32}Ru.0.2C_{16}H_{16}$ **139a**: C, 72.00; H, 7.30. Recalc for $C_{26}H_{32}Ru.¼C_{16}H_{16}$ **139b**: C, 72.40; H, 7.30. The formulation of both complexes was confirmed by a FAB mass spectrum. In each case molecular ion peaks were observed at *m/z* 446 (based on ^{102}Ru) with little fragmentation.

p-$MeC_6H_4CHMe_2$)][BF_4]$_2$ (0.10 g, 0.16 mmol) was treated with Na[BH_4] (0.05 g) over a period of 24 h. in a similar manner to that described for **135**. Quenching with water (0.5 cm^3), extraction into hexane (2 x 20 cm^3), followed by removal of the solvent *in vacuo*, resulted in the deposition of the product as an air sensitive yellow powder. Yield 0.05 g, 0.11 mmol, 68% (Found: C, 72.25; H, 7.90. Calc. for $C_{26}H_{32}Ru$: C, 70.10; H, 7.25%).

[Ru(η^6-$C_{16}H_{16}$){η^4-$C_6Me_4(CH_2)_2$}] **141**. The compound [Ru(η^6-$C_{16}H_{16}$)(η^6-C_6Me_6)][BF_4]$_2$ (0.17 g, 0.27 mmol) was stirred in thf (10 cm^3) with KO^{t}Bu / ^{t}BuOH (1.0 cm^3, 1.0 M) for 4 h. The resulting bright yellow solution was evaporated to dryness and extracted into warm hexane (2 x 40 cm^3). The solution was filtered and evaporated to dryness. Recrystallisation from acetone gave the product as mildly air sensitive yellow crystals. Yield 0.12 g, 0.26 mmol, 96% (Found: C, 71.00; H, 6.95. Calc. for $C_{28}H_{32}Ru$: C, 71.60; H, 6.85%).

[Ru(η^6-$C_{16}H_{16}$)(η^3-$C_6Me_6H_3$)][BF_4] **142**. To a hexane (30 cm^3) solution of [Ru(η^6-$C_{16}H_{16}$)(η^4-5,6-$C_6Me_6H_2$)] **135** prepared from [Ru(η^6-$C_{16}H_{16}$)(η^6-C_6Me_6)][BF_4]$_2$ (0.19 g, 0.30 mmol) was added H[BF_4] (0.2 cm^3, 40% aq.) and the mixture stirred vigorously for 1 h. The colourless organic layer was decanted off and the aqueous layer washed with diethyl ether to give the product as the pale yellow monohydrate which was isolated by filtration and air dried. Yield 0.08 g, 0.13 mmol, 43% based on **3b** (Found: C, 57.75; H, 6.50. Calc. for $C_{28}H_{37}BF_4Ru.H_2O$*: C, 58.05; H, 6.80%).

[Ru(η^6-$C_{16}H_{16}$)(η^3-$C_6Me_6H_2D$)][BF_4] **142''**. To a hexane (30 cm^3) solution of [Ru(η^6-$C_{16}H_{16}$)(η^4-5,6-$C_6Me_6H_2$)] **135** prepared from [Ru(η^6-$C_{16}H_{16}$)(η^6-C_6Me_6)][BF_4]$_2$ **3b** (0.16 g, 0.24 mmol) was added a pre-mixed solution of H[BF_4] (0.1 cm^3, aq., 40%) / D_2O (1 cm^3) and the mixture stirred vigorously for 7 days. The product was isolated as described for **142**. Yield 0.08 g, 0.14 mmol, 58% based on **3b** (Found: C, 58.60; H, 6.55. Calc. for $C_{28}H_{36}DBF_4Ru.H_2O$*: C, 57.95; H, 6.95%).

---

* Presence of water of crystallisation confirmed by the observation of ν(OH) in the infrared spectra of the complexes.

$[Ru(\eta^6\text{-}C_{16}H_{16})(\eta^3\text{-}C_6Me_6H_2D)][H(O_2CCF_3)_2]$ **143**. To a hexane (30 cm^3) solution of $[Ru(\eta^6\text{-}C_{16}H_{16})(\eta^4\text{-}5,6\text{-}C_6Me_6H_2)]$ **135** prepared from $[Ru(\eta^6\text{-}C_{16}H_{16})(\eta^6\text{-}C_6Me_6)][BF_4]_2$ **3b** (0.11 g, 0.17 mmol) was added CF_3CO_2D (0.2 cm^3) and the mixture stirred for 15 minutes. The colourless organic layer was decanted off and the yellow acid layer stirred with diethyl ether (10 cm^3) to give the product as yellow crystals. Yield 0.06 g, 0.09 mmol, 53% based on **3b** (Found: C, 54.50; H, 5.15. Calc. for $C_{32}H_{37}DF_6O_4Ru$: C, 54.70; H, 5.60%).

$[Ru(\eta^6\text{-}C_{16}H_{16})\{\eta^3\text{-}(HCH_2)(CH_2)C_6Me_4H_4\}][BF_4]$ **144**. To a hexane (30 cm^3) solution of $[Ru(\eta^6\text{-}C_{16}H_{16})(\eta^4\text{-}3,6\text{-}C_6Me_6H_2)]$ **5** (0.11 g, 0.23 mmol) prepared as previously reported[7] was added $H[BF_4].Et_2O$ (0.05 cm^3, 54%) and the mixture stirred for 20 min resulting in the deposition of the product as a pale yellow monohydrate. Yield 0.10 g, 0.17 mmol, 74% (Found: C, 58.50; H, 6.55. Calc. for $C_{28}H_{37}BF_4Ru.H_2O$*: C, 58.05; H, 6.80%). The same product is also obtained less cleanly from the analogous reaction with aqueous $H[BF_4]$.

$[Ru(\eta^6\text{-}C_{16}H_{16})\{\eta^4\text{-}(CH_2)_2C_6Me_4H_4\}]$ **145**. To a thf (30 cm^3) solution of $[Ru(\eta^6\text{-}C_{16}H_{16})\{\eta^3\text{-}(HCH_2)(CH_2)C_6Me_4H_4\}][BF_4]$ **144** (0.05 g, 0.09 mmol) was added Li^nBu / hexane (0.1 cm^3, 1.6 M, 0.16 mmol) initially at -80°C. The mixture was stirred and allowed to warm to room temperature over a period of *ca.* 20 minutes resulting in the formation of a bright yellow solution and a small quantity of a fine brown precipitate. Water (0.2 cm^3) was added to destroy unreacted Li^nBu and the mixture evaporated to dryness. The product was extracted with hexane (2 x 20 cm^3) and the solvent removed *in vacuo* resulting in the formation of a yellow oil from which bright yellow crystals were deposited. Yield 0.04 g, 0.08 mmol, 89% (Found: C, 71.05; H, 7.95. Calc. for $C_{28}H_{36}Ru$: C, 71.00; H, 7.65%).

$[Ru(\eta^6\text{-}C_{16}H_{16})(\eta^3\text{-}C_6Me_5H_4)][BF_4]$ **146**. A hexane (30 cm^3) solution of $[Ru(\eta^6\text{-}C_{16}H_{16})(\eta^4\text{-}C_6Me_5H_3)]$ **137** prepared from $[Ru(\eta^6\text{-}C_{16}H_{16})(\eta^6\text{-}C_6Me_5H)][BF_4]_2$ **3e** (0.10 g, 0.15 mmol) was treated with $H[BF_4]$ (0.2 cm^3, 40% aq.) as described for **142**. Yield 0.03 g, 0.05 mmol, 33% based on **3e** (Found: C, 58.25; H, 6.50. Calc. for $C_{27}H_{35}BF_4Ru.\frac{1}{2}H_2O$*: C,

* Presence of water of crystallisation confirmed by the observation of ν(OH) in the infrared spectra of the complexes.

58.30; H, 6.50%).

[Ru(η^6-$C_{16}H_{16}$)(η^3-$C_6Me_4H_5$)][BF_4] **147**. A diethyl ether (30 cm^3) solution of [Ru(η^6-$C_{16}H_{16}$)(η^4-$C_6Me_4H_4$)] **138** prepared from [Ru(η^6-$C_{16}H_{16}$)(η^6-$C_6Me_4H_2$)][BF_4]$_2$ **3d** (0.11 g, 0.17 mmol) was treated with H[BF_4].Et_2O (0.1 cm^3, 54%) and the mixture stirred for 20 minutes resulting in the deposition of a grey precipitate. Recrystallisation from chloroform / diethyl ether, liquid / vapour diffusion gave the product as feathery yellow crystals. Yield 0.04 g, 0.07 mmol, 41% based on **3d** (Found: C, 56.50; H, 5.65. Calc. for $C_{26}H_{33}BF_4Ru.H_2O$*: C, 56.65; H, 6.40%).

The deuterides of compounds **135**, **137**, and **142** were prepared in an identical fashion to their undeuteriated counterparts substituting Na[BD_4] for Na[BH_4] in the procedure, and their identities confirmed by infrared and ^{1}H NMR spectroscopy. (Found: C, 71.35; H, 8.25. Calc. for $C_{28}H_{34}D_2Ru$. **135'**: C, 70.70; H, 8.05%. Found: C, 69.35; H, 7.95. Calc. for $C_{27}H_{32}D_2Ru$. **137'**: C, 70.25; H, 7.86%. Found: C, 58.40; H, 6.20. Calc. for $C_{28}H_{35}D_2BF_4Ru.H_2O$* **142'**: C, 57.85; H, 7.11%)

* Presence of water of crystallisation confirmed by the observation of ν(OH) in the infrared spectra of the complexes.

Table 7.1: ^{1}H NMR Data for New Compounds[a]

Compound	δ *Cyclophane Ring*	*Cyclophane Bridge*	*Ligand*
$[Ru(\eta^6\text{-}C_{16}H_{16})(\eta^4\text{-}3,6\text{-}C_6Me_6H_2)]$[b] **5**	6.65 (s, 4H) 3.95 (s, 4H)	3.04 & 2.69 (AA'XX', 8H)	3.41 (q, 2H, ^3J=7.0, *exo-H*), 1.27 (d, 6H, ^3J=7.0, CH_3), 1.00 (s, 12H, CH_3)
$[Ru(\eta^6\text{-}C_{16}H_{16})(\eta^4\text{-}3,6\text{-}C_6Me_6D_2)]$ **5'**	6.65 (s, 4H) 3.95 (s, 4H)	3.04 & 2.69 (AA'XX', 8H)	1.27 (s, 6H, CH_3), 1.00 (s, 12H, CH_3)
$[Ru(\eta^6\text{-}C_{16}H_{16})(\eta^4\text{-}5,6\text{-}C_6Me_6H_2)]$ **135**	6.63 (s, 4H) 4.09 (s, 4H)	3.04 & 2.67 (AA'XX', 8H)	1.74 (s, 6H, CH_3), 1.18 (q, 2H, ^3J=6.8, *exo-H*), 1.10 (s, 6H, CH_3), 0.56 (d, 6H, ^3J=6.8, CH_3)
$[Ru(\eta^6\text{-}C_{16}H_{16})(\eta^4\text{-}5,6\text{-}C_6Me_6D_2)]$ **135'**	6.64 (s, 4H) 4.10 (s, 4H)	3.04 & 2.67 (AA'XX', 8H)	1.74 (s, 6H, CH_3), 1.10 (s, 6H, CH_3), 0.56 (s, 6H, CH_3)
$[Ru(\eta^6\text{-}C_{16}H_{16})(\eta^3\text{:}\eta^1\text{-}C_6Me_6H_2)]$ **136**	6.71 (s, 4H) 4.31 (s, 4H)	3.04 & 2.56 (AA'XX', 8H)	2.65 (q, 2H, ^3J=6.8, *exo-H*), 1.49 (s, 3H, CH_3), 1.46 (s, 6H, CH_3), 0.80 (d, 6H, ^3J=6.8, CH_3), 0.27 (s, 3H, CH_3)

[Ru(η^6-$C_{16}H_{16}$)(η^4-$C_6Me_5H_3$)] **137**	6.66 (s, 4H) 4.15 & 4.11 (AA'BB', 4H, ^3J=5.9)	3.06 & 2.68 (AA'XX', 8H)	1.75 (s, 3H, CH_3), 1.74 (s, 3H, CH_3), 1.35 (dd, 1H, ^2J=13.1, ^3J=5.8, *exo-H*(5)), 1.26 (s, 3H, CH_3), 1.16 (s, 3H, CH_3), 1.10 (m, 1H, *exo-H*(6)), 0.66 (d, 3H, ^3J=6.4, CH_3), 0.44 (dd, 1H, ^2J=13.1, ^3J=3.3, *endo-H*(5))
[Ru(η^6-$C_{16}H_{16}$)(η^4-$C_6Me_5D_2H$)] **137'**	6.66 (s, 4H) 4.15 & 4.11 (AA'BB', 4H, ^3J=5.9)	3.06 & 2.68 (AA'XX', 8H)	1.76 (s, 3H, CH_3), 1.75 (s, 3H, CH_3), 1.26 (s, 3H, CH_3), 1.17 (s, 3H, CH_3), 0.66 (s, 3H, CH_3), 0.43 (s, 1H, *endo-H*(5)[c])
[Ru(η^6-$C_{16}H_{16}$)(η^4-$C_6Me_4H_4$)] **138**	6.68 (s, 4H) 4.33 & 4.04 (AA'BB', 4H, ^3J=5.8)	3.10 & 2.74 (AA'XX', 8H)	4.11 (s, 1H, *H*(2)), 1.68 (s, 3H, CH_3), 1.40 (dd, 1H, ^2J=13.2, ^3J=7.6, *exo-H*(5)), 1.25 (s, 3H, CH_3), 1.15 (qdd, 1H, ^3J=7.6, 6.6 & 3.0, *exo-H*(6)), 1.05 (s, 3H, CH_3), 0.64 (d, 3H, ^3J=6.6, CH_3), 0.46 (dd, 1H, ^2J=13.2, ^3J=3.0, *endo-H*(5))
[Ru(η^6-$C_{16}H_{16}$){η^4-1-Me-4-(CHMe$_2$)C_6H_6}] **139a**	6.70 (s, 4H) 4.37 & 4.16 (AA'BB', 4H, ^3J=5.8)	3.09 & 2.78 (AA'XX', 8H)	4.21 & 4.07 (AB, 2H, ^3J=3.4, *H*(2) & *H*(3)), 1.42 - 1.15 (m, 4H, *H*(5) & *H*(6)), 1.32 (se, 1H, ^3J=6.8, C*H*Me$_2$), 1.22 (s, 3H, CH_3), 0.92 (d, 3H, ^3J=6.8, CH*Me$_2$*), 0.89 (d, 3H, ^3J=6.8, CH*Me$_2$*)
[Ru(η^6-$C_{16}H_{16}$){η^4-2-(CHMe$_2$)-5-MeC_6H_6}] **139b**	6.71 & 6.70 (AA'BB', 4H, ^3J=3.3) 4.47 & 4.22 (AA'BB', 4H, ^3J=5.8)	3.09 & 2.78 (AA'XX', 8H)	4.24 (d, 1H, ^3J=5.6, *H*(3)), 2.49 (m, 2H, *H*(1) & *H*(4)), 1.89 (se, 1H, ^3J=6.8, C*H*Me$_2$), 1.63 (m, 1H, *exo-H*(5)), 1.53 (ddd, 1H, ^2J=12.8, ^3J=4.2 & 10.7, *exo-H*(6)), 0.94 (d, 3H, ^3J=6.8, CH*Me$_2$*), 0.90 (d, 3H, ^3J=6.8, CH*Me$_2$*), 0.76 (ddd, 1H, ^2J=12.8, ^3J=1.7 & 4.2, *endo-H*(6)), 0.72 (d, 3H, ^3J=6.7, CH_3)

$[Ru(\eta^6\text{-}C_{16}H_{16})\{\eta^4\text{-}C_6Me_4(CH_2)_2\}]$ **141**	6.65 (s, 4H) 4.23 (s, 4H)	3.08 & 2.71 (AA'XX', 8H)	4.64 (s, 2H, $=CH_2$), 4.20 (s, 2H, $=CH_2$), 1.85 (s, 6H, CH_3), 1.54 (s, 6H, CH_3)
$[Ru(\eta^6\text{-}C_{16}H_{16})(\eta^3\text{-}C_6Me_6H_3)][BF_4]$ **142**	6.85 (s, 4H) 4.80 (s, 4H)	3.24 & 2.98 (AA'XX', 8H)	1.95 (s, 6H, CH_3), 1.38 (d, 6H, ^3J 2.5 av., *exo*-CH_3), 1.22 (d of q, 2H, ^3J=6.6 & 4.1 av., H_{exo}), 0.72 (d, 6H, ^3J=6.6, *endo*-CH_3), -10.80 (t of sp, 1H, ^3J 4.1 & 2.5 av.)
$[Ru(\eta^6\text{-}C_{16}H_{16})(\eta^3\text{-}exo\text{-}D_2C_6Me_6H)][BF_4]$ **142'**	6.86 (s, 4H) 4.80 (s, 4H)	3.22 & 2.96 (AA'XX', 8H)	1.93 (s, 6H, CH_3), 1.36 (d, 6H, ^3J 2.3 av., *exo*-CH_3), 0.68 (s, 6H, *endo*-CH_3), -10.91 (sp, 1H, ^3J=2.3 av.)
$[Ru(\eta^6\text{-}C_{16}H_{16})(\eta^3\text{-}endo\text{-}DC_6Me_6H_2)][BF_4]$ **142''**	6.86 (s, 4H) 4.80 (s, 4H)	3.23 & 2.97 (AA'XX', 8H)	1.93 (s, 6H, CH_3), 1.36 (s, 6H, *exo*-CH_3), 1.22 (q, 2H, ^3J=6.2, H_{exo}), 0.70 (d, 6H, ^3J=6.2, *endo*-CH_3)
$[Ru(\eta^6\text{-}C_{16}H_{16})(\eta^3\text{-}endo\text{-}C_6Me_6H_2D)][H(CF_3CO_2)_2]$ **143**	6.79 (s, 4H) 4.72 (s, 4H)	3.22 & 2.95 (AA'XX', 8H)	8.80 (s, br, 1H, $H(CF_3CO_2)_2$), 1.91 (s, 6H, CH_3), 1.34 (s, 6H, *exo*-CH_3), 1.18 (q, 2H, ^3J=6.0, *exo-H*), 0.69 (d, 6H, ^3J=6.0 av., *endo*-CH_3)
$[Ru(\eta^6\text{-}C_{16}H_{16})\{\eta^3\text{-}(HCH_2)(CH_2)C_6Me_4H_4\}][BF_4]$ **144**	6.88 (s, 4H) 5.03 (s, 4H)	3.25 & 3.10 (AA'XX', 8H)	2.08 (d of q, 2H, ^3J=4.9 & 6.8, H_d & H_d'), 1.43 (d of q, 2H, ^3J=4.9 & 6.6, H_e & H_e'), 0.95 (d, 6H, ^3J=6.6, Me_e & Me_e'), 0.82 (d, 6H, ^3J=6.8, Me_d & Me_d'), -1.52 (s, br, 5H, $H_{a,b,c}$ & $H_{b,c}$')
$[Ru(\eta^6\text{-}C_{16}H_{16})\{\eta^4\text{-}(CH_2)_2C_6Me_4H_4\}]$ **145**	6.70 (s, 4H) 4.46 (s, 4H)	3.11 & 2.80 (AA'XX', 8H)	1.92 (d of q, 2H, ^3J=4.9 & 6.7, *exo-H*), 1.45 (s, 2H, H_{anti}), 1.19 (d of q, 2H, ^3J=4.9 & 6.7, *endo-H*), 0.86 (d, 6H, ^3J=6.7, *exo*-CH_3), 0.60 (d, 6H, ^3J=6.7, *endo*-CH_3), -0.71 (s, 2H, H_{syn})

$[Ru(\eta^6\text{-}C_{16}H_{16})(\eta^3\text{-}C_6Me_5H_4)][BF_4]$ **146**	6.86 (s, 4H) 4.88 & 4.83 (AA'BB', 4H, ^3J=6.6)	3.23 & 2.97 (AA'XX', 8H)	1.86 (s, 3H, CH_3), 1.77 (s, 3H, CH_3), 1.75 (s, 3H, CH_3), 1.73 (m, 1H, *exo-H*), 1.05 (d, 3H, ^3J=4.8 av., *exo*-CH_3), 0.91 (m, 1H, *exo-H*), 0.75 (d, 3H, 6.7, *endo*-CH_3), -4.56 (s, br, 1H, *endo-H*), -5.25 (s, br, 1H, *endo-H*)
$[Ru(\eta^6\text{-}C_{16}H_{16})(\eta^3\text{-}C_6Me_4H_5)][BF_4]$ **147**	6.86 (s, 4H) 4.94 & 4.80 (AA'BB', 4H, ^3J=6.3)	3.23 & 3.03 (AA'XX', 8H)	3.60 (dd, 1H, J=3.7 & 1.8, H_c'), 2.12 (dd, 1H, J=14.0 & 2.1 av., *exo*-H_a), 1.89 (s, 3H, CH_3), 1.86 (s, 3H, CH_3), 0.91 (d, 3H, ^3J=5.8 av., *exo*-CH_3), 0.75 (m, 1H, *exo*-H_a'), 0.70 (d, 3H, ^3J=6.4, *endo*-CH_3), -1.88 (s, br, 1H, *endo*-H_b'), -7.68 (s, br, 1H, *endo*-H_a)

a) Solvent $CDCl_3$ unless otherwise stated, δ / ppm, $J_{H\text{-}H}$ / Hz, 400 MHz, 20°C, s = singlet, d = doublet, t = triplet, q = quartet, se = septet, m = multiplet, dd = doublet of doublets, dt = doublet of triplets, ddd = doublet of doublets of doublets, br = broad; b) Previously synthesised by Boekelheide *et al.*[7]; c) Deuterium coupling not resolved; d) Solvent NO_2Me-d_3.

Table 7.2: ^{1}H Coupled ^{13}C NMR Data for Agostic Compounds[a]

Compound	δ *Ring*	*Bridgehead*	*Bridge*	*Ligand*
$[Ru(\eta^6\text{-}C_{16}H_{16})(\eta^3\text{-}C_6Me_6H_3)][BF_4]$ **142**	133.43 (d, *J*=160.8) 82.18 (d, *J*=174.6)	139.08 (s) 125.07 (s)	34.22 (t, *J*=131.2) 31.35 (t, *J*=129.9)	91.51 (s, C_c & C_c'), 59.25 (d, *J*=36.0 av., C_b & C_b') 38.45 (d, *J*=129.8 av., C_a & C_a'), 20.43 (q, *J*=127.6, CH_3), 15.47 (q, *J*=128.0, CH_3), 13.20 (q, *J*=126.8, CH_3)
$[Ru(\eta^6\text{-}C_{16}H_{16})(\eta^3\text{-}C_6Me_6HD_2)][BF_4]$ **142'**	133.40 (d, *J*=158.1) 82.12 (d, *J*=176.1)	139.06 (s) 124.96 (s)	34.12 (t, *J*=131.1) 31.24 (t, *J*=132.5)	91.41 (s, C_c & C_c'), 59.03 (d, *J*=37.5 av., C_b & C_b') 37.79 (s^b, C_a & C_a'), 20.32 (q, *J*=128.6, CH_3), 15.38 (q, *J*=128.2, CH_3), 13.20 (q, *J*=126.4, CH_3)
$[Ru(\eta^6\text{-}C_{16}H_{16})(\eta^3\text{-}C_6Me_6H_2D)][BF_4]$ **142''**	133.45 (d, *J*=158.3) 82.08 (d, *J*=178.4)	139.06 (s) 124.99 (s)	34.15 (t, *J*=130.4) 31.27 (t, *J*=131.2)	91.50 (s, C_c & C_c'), 59.28 (s^b, C_b & C_b'), 38.36 (d, *J*=130.3 av., C_a & C_a'), 20.32 (q, *J*=128.6, CH_3) 15.43 (q, *J*=128.2, CH_3), 13.18 (q, *J*=126.7, CH_3)
$[Ru(\eta^6\text{-}C_{16}H_{16})(\eta^3\text{-}C_6Me_6H_2D)][H(CF_3CO_2)_2]$ **143**	133.32 (d, *J*=158.3) 82.00 (d, *J*=174.8)	159.82 (s) 125.16 (s)	34.16 (t, *J*=131.6) 31.28 (t, *J*=132.8)	160.37 (q, $^2J_{C\text{-}F}$=36.8, $H(CF_3CO_2)_2$), 116.20 (q, $^1J_{C\text{-}F}$=289.7, $H(CF_3CO_2)_2$), 91.54 (s, C_c & C_c'), 58.90 (s^b, C_b & C_b'), 38.32 (d, *J*=130 av., C_a & C_a'), 20.35 (q, *J*=127.4, CH_3), 15.38 (q, *J*=128.2, CH_3), 13.13 (q, *J*=126.4, CH_3)

$[Ru(\eta^6\text{-}C_{16}H_{16})\{\eta^3\text{-}(HCH_2)(CH_2)C_6Me_4H_4\}][BF_4]$ **144**	133.35 (d, *J*=158.2) 80.66 (d, *J*=176.4)	139.01 (s) 125.53 (s)	34.52 (t, *J*=132.9) 33.20 (t, *J*=137.5)	100.62 (s, C_b & C_b'), 36.62 (d, *J*=128.7, C_c & C_c'), 36.06 (d, *J*=127.0, C_d & C_d'), 20.77 (q, *J*=127.3, Me_c & Me_c'), 17.45 (q, br, *J*=77.5 av., C_a & C_a'), 15.94 (dq, *J*=125.2 & 3.6, Me_d & Me_d')
$[Ru(\eta^6\text{-}C_{16}H_{16})(\eta^3\text{-}C_6Me_5H_4)][BF_4]$ **146**	133.43 (d, *J*=157.6) 82.85 (d, *J*=175.4) 82.43 (d, *J*=175.5)	139.07 (s) 125.30 (s)	34.20 (t, *J*=132.0) 31.40 (t, *J*=132.0)	91.19 (s, C_c), 80.67 (s, C_b), 73.83 (s, C_c'), 52.76 (d, *J*=87.0 av., C_b'), 41.94 (dd, *J*=95.5 & 141.2 av., C_a) 34.34 (d, *J*=128.8, C_a'), 21.62 (q, *J*=128.2, CH_3) 19.27 (q, *J*=126.5, CH_3), 19.10 (q, *J*=125.8, CH_3) 18.55 (q, *J*=128.2, CH_3), 14.91 (q, *J*=128.2, CH_3)
$[Ru(\eta^6\text{-}C_{16}H_{16})(\eta^3\text{-}C_6Me_4H_5)][BF_4]$ **147**	133.45 (dd, *J*=158.6 & 5.0) 82.21 (dd, *J*=176.3 & 6.2) 81.36 (dd, *J*=175.2 & 6.1)	139.08 (s) 126.05 (s)	34.41 (t, *J*=128.8) 31.79 (t, *J*=131.4)	90.20 (s, C_c), 80.67 (s, C_b), 64.30 (d, *J*=161.0, C_c'), 48.24 (d, *J*=101.6, C_b'), 42.88 (dd, *J*=143.6 & 69.1, C_a), 34.25 (d, *J*=128.2, C_a'), 21.36 (q, *J*= 128.5, CH_3), 19.77 (q, *J*= 127.4, CH_3), 19.56 (q, *J*= 128.3, CH_3), 18.59 (q, *J*= 128.2, CH_3)

a) Solvent $CDCl_3$ unless otherwise stated, δ / ppm, $J_{C\text{-}H}$ / Hz, 100.6 MHz, 20°C, s = singlet, d = doublet, t = triplet, q = quartet, dd = doublet of doublets, dq = doublet of quartets, br = broad; b) $^1J_{C\text{-}D}$ unresolved.

Chapter 8

Overview and Conclusions

8.1 Nucleophilic Addition Reactions

8.1.1 Conclusions

Incorporation of [2.2]paracyclophane in complexes of the form $[Ru(arene)(arene')]^{2+}$ as a non-innocent spectator ligand results in the observation of reactions in which selective nucleophilic additions of a range of nucleophiles occur solely to the non-cyclophane ring. In the case where methanol is used as a solvent over short reaction times, the compounds undergo single nucleophilic additions except where the nucleophile is a strong base, in which case deprotonation of the ring alkyl substituents occurs. In thf double nucleophilic additions of hydride are observed with good regioselectivity, which may be tuned by judicious choice of reaction conditions. (Diene)ruthenium(0) complexes resulting from these reactions react with sources of H^+ to give a range of interesting agostic species which might be oxidatively cleaved to give unusual organic cyclohexenes. Attempts to extend the synthetic approach to generate functionalised diene species from attack by nucleophiles other than hydride are complicated by the formation of complex mixtures of products and the relatively poor electrophilicity of the more highly alkylated arenes.

8.1.2 Future Work

In the current work it has been demonstrated that [2.2]paracyclophane is a suitably inert spectator ligand for the synthesis of Ru(0) diene complexes by double nucleophilic addition reactions. Some ideas have also been gleaned concerning the regioselectivities of such reactions in this system. Effort is now required to extent this work to the synthesis of functionalised dienes in order to explore the limitations of the reactions in terms of reagent electrophilicity and isomeric purity of the resulting products. Once suitable functionalised diene compounds have been synthesised it will be necessary to examine their removal from the metal centre by a range of oxidising agents (*e.g.* O_2, I_2, Ce(IV) salts, aqueous Cu(II) or $FeCl_3$). The reactions of agostic cyclohexenyl compounds towards nucleophiles may also be investigated. Single nucleophilic additions to these species should result in functionalised cyclohexene complexes which may spontaneously release the new olefin ligand or may also require oxidative cleavage of the M-C bonds. Other methods of organic functionalisation may also be explored such as reaction of (diene)Ru(0) compounds

with electrophiles such as acetyl chloride. Also, the stability of the metal compounds may be improved by use of a more sterically bulky spectator ligand such as octamethyl[2.2]paracyclophane.

8.2 *Bis*(Allyl)Ruthenium(IV) Complexes

In general similar reactivities are observed for [{Ru(η^3:η^3-$C_{10}H_{16}$)Cl(μ-Cl)}$_2$] **6** and its isoelectronic ruthenium(II) analogues [{Ru(η^6-arene)Cl(μ-Cl)}$_2$] **7** and, in many respects, the related (pentamethylcyclopentadienyl)rhodium(III) species [{Rh(η^5-Cp*)Cl(μ-Cl)}$_2$]. Principal differences in the ruthenium(IV) case arise as a consequence of the unusual, sterically crowded geometry about the metal centre and the chirality of the "Ru(η^3:η^3-$C_{10}H_{16}$)" fragment. A few subtle effects may also be attributed to the small size of the Ru(IV) centre and its electronic properties. In addition, compounds derived from **6** are in general more soluble in organic solvents than their (arene)ruthenium(II) analogues and hence may be readily studied by solution techniques without recourse to strongly coordinating solvents such as dmso.

8.2.1 Geometry

Compound **6** reacts with a wide range of Lewis bases (L) in non-polar solvents to give simple adducts [Ru(η^3:η^3-$C_{10}H_{16}$)Cl_2L], in much the same way as complexes of type **7**. The existence of inequivalent axial and equatorial sites in the case of **6** results in the possibility of axial / equatorial isomerism. In general the ligand L occupies the equatorial site but small, linear donors such as MeCN exist as predominantly L-axial isomers.[17,161] This type of isomerism is also prevalent in compounds containing unsymmetric bidentate ligands such as the 2-hydroxypyridinate anion (Chapter 4), and may be controlled by manipulation of the various steric interactions taking place around the metal centre.

The sterically hindered nature of the "Ru(η^3:η^3-$C_{10}H_{16}$)" fragment [the cone angle of the *bis*(allyl) ligand may be estimated from crystallographic data to be around 190° (*cf.* a maximum of *ca.* 120° even in (hexamethylbenzene)ruthenium(II) compounds)] also gives rise to some unusual geometries, most notably the puckering of the $Ru_2(SCN)_2$ ring in the

thiocyanato bridged complex [{Ru(η^3:η^3-$C_{10}H_{16}$)(μ-SCN)}$_2$] **114.**

In binuclear compounds such as the oxalato bridged complex [{Ru(η^3:η^3-$C_{10}H_{16}$)Cl}$_2$(μ-O_4C_2)] **115** the stereochemical inequivalence of the two types of coordination suggests the possibility of *cisoid* and *transoid* arrangements of the terminal chloride ligands. This type of isomerism is also, in principle, possible in the analogous octahedral (arene)ruthenium(II) species but, unless the separation between the metal centres were large the *cisoid* form would be precluded by unfavourable steric interactions between the terminal chloride ligands. In contrast, *cisoid* forms of **115** are observed and, in very recent work, we have crystallographically characterised the ethanethiolate bridged compound [{Ru(η^3:η^3-$C_{10}H_{16}$)Cl}$_2$(μ-SEt)(μ-Cl)] which exists solely as the *cisoid* pair of diastereoisomers.

8.2.2 Chirality

The chirality of the "Ru(η^3:η^3-$C_{10}H_{16}$)" fragment[17] has little consequence in the chemistry of mononuclear compounds derived from **6**, except that the fact must be remembered in interpreting the NMR spectra of complexes containing prochiral ligands, and may sometimes be used as an added NMR "handle" to aid interpretation. Binuclear compounds exist as diastereomeric pairs, often exhibiting surprisingly different stabilities and solubilities. In many instances these diastereoisomers may be readily separated by fractional crystallisation, although interconversion between the two forms makes lengthy chromatographic separations impractical.

One possibility for future work involves the resolution of the two enantiomers of the "Ru(η^3:η^3-$C_{10}H_{16}$)" fragment. Very recently we have shown that the anionic compound [PPh_4][Ru(η^3:η^3-$C_{10}H_{16}$)Cl_3] may be readily generated by reaction of **6** with [PPh_4]Cl. If [PPh_4]$^+$ were replaced by a chiral phosphonium salt then the resulting trichloride anion would exist as two diastereomers which may be separable. We have found that reaction of [PPh_4][Ru(η^3:η^3-$C_{10}H_{16}$)Cl_3] with H[BF_4] results in the re-formation of **6**. It would therefore be easy to test the efficiency of the resolution technique described above because a successful resolution would result in solely the C_2 form of **6** (**6b**) in an optically pure state, from the reaction of the resolved anionic complex with H[BF_4]. This is because the C_2 diastereoisomer of **6** consists solely of "Ru(η^3:η^3-$C_{10}H_{16}$)" fragments of the same

handedness (and hence **6b** exists as two enantiomers; either "RR" or "SS"). In contrast the *meso* C_i isomer (**6a**) contains one left and one right handed fragment (and hence exists in an optically pure state; "RS" = "SR"). Formation of **6** from optically resolved "Ru(η^3:η^3-$C_{10}H_{16}$)Cl_2" moieties could therefore only result in a C_2 isomer.

8.2.3 Properties of the Metal Ion

The metal centre in compounds derived from **6** and other organometallic ruthenium(IV) complexes such as [Ru(η^3:η^2:η^3-$C_{12}H_{18}$)Cl_2] **39**, might be expected to be both smaller and harder (*i.e.* less polarisable) than analogous compounds of ruthenium(II). This difference is highlighted by the chemistry of **6** with carboxylato ligands described in Chapter 3. The small size of the Ru(IV) ion results in ligands such as trifluoroacetate adopting a monodentate mode of coordination, whilst the hardness of the metal centre results in strong electrostatic attractions to non-polarisable bases such as water (*e.g.* [Ru(η^3:η^3-$C_{10}H_{16}$)(O_2CCF_3)$_2$(OH_2)] **73** and [Ru(η^3:η^2:η^3-$C_{12}H_{18}$)Cl(OH_2)][BF_4] **83**). The small size of the Ru(IV) ion is also evident from the crystal structure determinations of [Ru(η^3:η^3-$C_{10}H_{16}$)Cl(bipy)][BF_4] **64** and [Ru(η^3:η^3-$C_{10}H_{16}$)(terpy)][BF_4]$_2$ **66** (Chapter 2). In the former case the two pyridyl rings exhibit significant deviations from mutual coplanarity, in order to chelate the Ru(IV) centre, whilst in **66** the distortions observed in the coordinated terpyridyl ligand indicate that the metal centre is smaller than in related compounds of Ni(II), for example.

8.2.4 Future Work

In this thesis much of the basic coordination chemistry of **6** has been explored. Some attempts have also been made to capitalise on the novel geometry, oxidation state and chirality of the "Ru(η^3:η^3-$C_{10}H_{16}$)" fragment. Further investigations planned for the immediate future concern the synthesis of thiolato compounds derived from **6** which have demonstrable redox activity and may find application as DNA cleavage agents (DNA cleavage under anaerobic conditions has been achieved by transition metal oxidising agents such as [Ru(terpy)(bipy)O]$^{2+}$ and such reagents may be applicable in cancer chemotherapy as selective cytotoxins[172]). Many of the thiolate complexes which we have recently synthesised also exhibit interesting new geometries and a series of structural investigations

are in progress.

Some unsuccessful attempts have been made to examine the reactivity of the open chain organic ligand towards nucleophiles and strong bases. It is anticipated that a more thorough study may result in the observation of coupling reactions such as observed for compounds derived from $[Ru(\eta^3:\eta^2:\eta^3\text{-}C_{12}H_{18})Cl_2]$ **39** (Section 1.4.3).

Other future work may include careful studies on the applications of **6** in olefin polymerisation reactions[111] (*e.g.* Ziegler-Natta polymerisation of isoprene may be used to generate 1,4-*cis*-polyisoprene, an excellent substitute of natural rubber) or, if a catalytic system can be developed in which the *bis*(allyl) ligand remains bound to the metal centre, compounds derived from **6** may find application in asymmetric synthesis or polymerisations in which there is a need for high stereoregularity.

Attention may also be usefully directed towards the chemistry of $[Ru(\eta^3:\eta^2:\eta^3\text{-}C_{12}H_{18})Cl_2]$ **39**. Formation of simple derivatives of **39** is apparently hampered by the bulky nature of the organic ligand and the material has proved quite unreactive in our hands. Decomposition by elimination of the organic ligand seems to occur more readily than in the case of **6** and its derivatives. It is clear however that, with the right choice of ligands, derivitisation of **39** is possible (*e.g.* $[Ru(\eta^3:\eta^2:\eta^3\text{-}C_{12}H_{18})Cl(OH_2)][BF_4]$) and the compound may well exhibit further interesting chemistry.

References

1. T. A. Kaden, *Top. Curr. Chem.*, 1984, **121**, 157.
2. D. J. Cram, M. E. Tanner and R. Thomas, *Angew. Chem. Int. Ed. Engl.*, 1991, **30**, 1024.
3. J. E. Baldwin and P. Perlmutter, *Top. Curr. Chem.*, 1984, **121**, 157.
4. J. Okuda, *Top. Curr. Chem.*, 1991, **160**, 97.
5. J. W. Kang, K. Mosely and P. W. Maitlis, *J. Am. Chem. Soc.*, 1969, **91**, 5970.
6. J. C. W. Chien, W. -M. Tsai and M. D. Rausch, *J. Am. Chem. Soc.*, 1991, **113**, 8570; J. C. W. Chien, G. H. Llinas, M. D. Rausch, G. -Y. Lin, H. H. Winter, J. L. Atwood and S. G. Bott, *J. Am. Chem. Soc.*, 1991, **113**, 8569; D. T. Mallin, M. D. Rausch, G. -Y. Lin, S. Dong and J. C. W. Chien, *J. Am. Chem. Soc.*, 1990, **112**, 2030.
7. R. T. Swann, A. W. Hanson and V. Boekelheide, *J. Am. Chem. Soc.*, 1986, **108**, 3324.
8. C. C. Neto and D. A. Sweigart, *J. Chem. Soc., Chem. Commun.*, 1990, 1703.
9. D. Jones, L. Pratt and G. Wilkinson, *J. Chem. Soc.*, 1962, 4458.
10. M. I. Rybinskaya, V. S. Kaganovich and A. R. Kudinov, *J. Organomet. Chem.*, 1982, **235**, 215.
11. S. G. Davies, M. L. H. Green and D. M. P. Mingos, *Tetrahedron*, 1978, **34**, 3047.
12. L. Porri, M. C. Galazzi, A. Colombo and G. Allegra, *Tetrahedron Lett.*, 1965, 4187.
13. A. Colombo and G. Allegra, *Acta Crystallogr., Sect. B*, 1971, **27**, 1653.
14. M. A. Bennett and A. K. Smith, *J. Chem. Soc., Dalton Trans.*, 1974, 233.
15. P. B. Hitchcock, J. F. Nixon and J. Sinclair, *J. Organomet. Chem.*, 1975, **86**, C34.
16. R. A. Head, J. F. Nixon, R. Swain and C. M. Woodard, *J. Organomet. Chem.*, 1974, **76**, 393.
17. D. N. Cox and R. Roulet, *Inorg. Chem.*, 1990, **29**, 1360.
18. W. A. Hermann, *Angew. Chem., Int. Ed. Engl.*, 1988, **27**, 1297.
19. C. Che, W. Cheng and T. C. W. Mak, *J. Chem. Soc., Chem. Commun.*, 1987, 418.
20. B. R. Manzano, F. A. Jalon, F. J. Lahoz, B. Chaudret and D. de Montauzon, *J. Chem. Soc., Dalton Trans.*, 1992, 977.
21. S. K. Mandal and A. R. Chakravarty, *J. Organomet. Chem.*, 1991, **417**, C59.
22. P. Pertici, P. Salvadori, A. Biasci, G. Vitulli, M. A. Bennett and L. A. P. Kane-Maguire, *J. Chem. Soc., Dalton Trans.*, 1988, 315.

23. Ch. Elschenbroich and A. Salzer, *Organometallics*, VCH, Weinheim, FRG, 1989.
24. W. E. Silverthorn, *Adv. Organomet. Chem.*, 1975, **13**, 47.
25. D. Mandon and D. Astruc, *J. Organomet. Chem.*, 1989, **369**, 383.
26. E. O. Fischer, Ch. Elschenbroich and C. G. Kreiter, *J. Organomet. Chem.*, 1967, **7**, 481.
27. E. O. Fischer and Ch. Elschenbroich, *Chem. Ber.*, 1970, **103**, 162.
28. P. L. Timms, *Proc. R. Soc. Lond., Sect. A*, 1984, **396**, 1.
29. M. L. H. Green, *J. Organomet. Chem.*, 1980, **200**, 119.
30. R. Benn, N. E. Blank, M. W. Haenel, J. Klein, A. R. Koray, K. Weidenhammer and M. L. Ziegler, *Angew. Chem. Int. Ed. Engl.*, 1980, **19**, 44.
31. A. R. Koray, M. L. Ziegler, N. E. Blank and M. W. Haenel, *Tetrahedron Lett.*, 1979, **26**, 2465.
32. N. E. Blank, M. W. Haenel, A. R. Koray, K. Weidenhammer and M. L. Ziegler, *Acta Crystallogr. Sect. B*, 1980, **36**, 2054.
33. Ch. Elschenbroich, R. Möckel and U. Zenneck, *Angew. Chem. Int. Ed. Engl.*, 1978, **17**, 7.
34. Ch. Elschenbroich, J. Hurley, W. Massa and G. Baum, *Angew. Chem. Int. Ed. Engl.*, 1988, **27**, 684.
35. M. A. Bennett and T. W. Matheson, *J. Organomet. Chem.*, 1979, **175**, 87.
36. S. J. Thompson, P. M. Bailey, C. White and P. M. Maitlis, *Angew. Chem. Int. Ed. Engl.*, 1976, **15**, 490.
37. C. White, S. J. Thompson and P. M. Maitlis, *J. Organomet. Chem.*, 1977, **134**, 319.
38. M. I. Rybinskaya, A. R. Kudinov and V. S. Kaganovich, *J. Organomet. Chem.*, 1983, **246**, 279.
39. C. White and P. M. Maitlis, *J. Chem. Soc. (A)*, 1971, 3322.
40. C. White, S. J. Thompson and P. M. Maitlis, *J. Chem. Soc., Dalton Trans.*, 1977, 1654.
41. E. L. Muetteries, J. R. Bleeke, E. J. Wuchter and T. A. Albright, *Chem. Rev.*, 1982, **82**, 499.
42. M. A. Bennett in *Comprehensive Organometallic Chemistry*, Pergamon, Oxford, 1982, Vol. 4, Ch 32.

43. G. Consiglio and F. Morandini, *Chem. Rev.*, 1987, **87**, 761.
44. H. Le Bozec, D. Touchard and P. H. Dixneuf, *Adv. Organomet. Chem.*, 1989, **29**, 163.
45. G. Winkhaus and H. Singer, *J. Organomet. Chem.*, 1967, **7**, 487.
46. R. A. Zelonka and M. C. Baird, *J. Organomet. Chem.*, 1972, **35**, C43.
47. P. Pertici, P. Salvadori, A. Biasci, G. Vitulli, M. A. Benett and L. A. P. Kane-Maguire, *J. Chem. Soc., Dalton Trans.*, 1988, 315.
48. M. A. Bennett, T. N. Huang, T. W. Matheson and A. K. Smith, *Inorg. Synth.*, 1982, **21**, 74.
49. M. A. Bennett, T. W. Matheson, G. B. Robertson, A. K. Smith and P. A. Tucker, *Inorg. Chem.*, 1980, **19**, 1014.
50. R. A. Zelonka and M. C. Baird, *Can. J. Chem.*, 1972, **50**, 3063.
51. P. Pertici, G. Vitulli, R. Lazzaroni, P. Salvadori and L. Barili, *J. Chem. Soc., Dalton Trans.*, 1982, 1019.
52. R. T. Swann and V. Boekelheide, *Tetrahedron Lett.*, 1984, **25**, 899.
53. R. Dussel, D. Pilette, P. H. Dixneuf and W. P. Fehlhammer, *Organometallics*, 1991, **10**, 3287.
54. H. Werner and R. Werner, *J. Organomet. Chem.*, 1979, **174**, C67.
55. D. A. Tocher, R. O. Gould, T. A. Stephenson, M. A. Bennett, J. P. Ennett, T. W. Matheson, L. Sawyer and V. K. Shah, *J. Chem. Soc., Dalton Trans.*, 1983, 1571.
56. H. Werner and R. Werner, *Chem. Ber.*, 1982, **115**, 3766.
57. D. R. Robertson and T. A. Stephenson, *J. Organomet. Chem.*, 1977, **142**, C31.
58. D. R. Robertson, I. W. Robertson and T. A. Stephenson, *J. Organomet. Chem.*, 1980, **202**, 309.
59 R. H. Crabtree and A. J. Pearman, *J. Organomet. Chem.*, 1977, **141**, 325.
60. D. R. Robertson and T. A. Stephenson, *J. Chem. Soc., Dalton Trans.*, 1978, 486.
61. E. C. Morrison, C. A. Palmer and D. A. Tocher, *J. Organomet. Chem.*, 1988, **349**, 405.
62. P. Lahuerta, J. Latorre, M. Sanaú, F. A. Cotton and W. Schwotzer, *Polyhedron*, 1988, **7**, 1311.
63. J. R. Polam and L. C. Porter, *Inorg. Chim. Acta*, 1993, **205**, 119.

64. R. A. Zelonka and M. C. Baird, *J. Organomet. Chem.*, 1972, **44**, 383.
65. H. Werner and R. Werner, *Angew. Chem.*, 1978, **90**, 721.
66. H. Werner and R. Werner, *Chem. Ber.*, 1982, **115**, 3781.
67. D. R. Robertson and T. A. Stephenson, *J. Organomet. Chem.*, 1978, **162**, 121.
68. R. O. Gould, T. A. Stephenson and D. A. Tocher, *J. Organomet. Chem.*, 1984, **263**, 375.
69. R. O. Gould, C. L. Jones, T. A. Stephenson and D. A. Tocher, *J. Organomet. Chem.*, 1984, **264**, 365.
70. R. O. Gould, C. L. Jones, D. R. Robertson, T. A. Stephenson and D. A. Tocher, *J. Organomet. Chem.*, 1982, **226**, 199.
71. D. Astruc, *New. J. Chem.*, 1992, **16**, 305.
72. P. Michaud and D. Astruc, *J. Am. Chem. Soc.*, 1982, **104**, 3755.
73. J. F. Helling and G. G. Cash, *J. Organomet. Chem.*, 1974, **73**, C10.
74. G. Winkhaus, L. Pratt and G. Wilkinson, *J. Chem. Soc. (A)*, 1961, 3807 and references therein.
75. D. Jones, L. Pratt and G. Wilkinson, *J. Chem. Soc. (A)*, 1962, 4458.
76. P. H. Bird and M. R. Churchill, *J. Chem. Soc., Chem. Commun.*, 1967, 777.
77. M. R. Churchill and F. R. Scholer, *Inorg. Chem.*, 1969, **8**, 1950.
78. D. Astruc, *Top. Curr. Chem.*, 1991, **160**, 47.
79. T. S. Cameron, M. D. Clerk, A. Linden, K. C. Sturge and M. J. Zaworotko, *Organometallics*, 1988, **7**, 2571.
80. J. W. Hull, Jr., C. Mann and W. J. Gladfelter, *Organometallics*, 1992, **11**, 3117.
81. J. W. Hull, Jr. and W. J. Gladfelter, *Organometallics*, 1982, **1**, 1716.
82. J. W. Hull, Jr., K. J. Roesselet and W. J. Gladfelter, *Organometallics*, 1992, **11**, 3630.
83. M. A. Bennett, L. Y. Goh, I. J. McMahon, T. R. B. Mitchell, G. B. Robertson, T. W. Turney and W. A. Wickramasinghe, *Organometallics*, 1992, **11**, 3069.
84. Y. K. Chung, E. D. Honig and D. A. Sweigart, *J. Organomet. Chem.*, 1983, **256**, 277.
85. N. A. Vol'kenau, I. N. Bolesova, L. S. Shul'pina and A. N. Kitaigorodskii, *J. Organomet. Chem.*, 1984, **267**, 313.
86. R. Werner and H. Werner, *J. Organomet. Chem.*, 1981, **210**, C11.

87. D. Astruc, P. Michaud, A. M. Mardonik, J. -Y. Saillard and R. Hoffman, *Nouv. J. Chim.*, 1985, **9**, 41.

88. G. Wilke, B. Bogdanović, P. Hardt, P. Heimbach, W. Keim, M. Kröner, W. Oberkirch, K. Tanaka, E. Steinrucke, W. Walter and H. Zimmerman, *Angew. Chem. Int. Ed. Engl.*, 1966, **5**, 151.

89. F. A. Cotton and J. R. Pipal, *J. Am. Chem. Soc.*, 1971, **93**, 5441.

90. R. J. Blau, M. S. Goetz and R. -J. Tsay, *Polyhedron*, 1991, **10**, 605.

91. J. Powell and B. L. Shaw, *J. Chem. Soc. (A)*, 1968, 159.

92. J. Powell and B. L. Shaw, *J. Chem. Soc., Chem. Commun.*, 1966, 174.

93. J. Powell and B. L. Shaw, *J. Chem. Soc., Chem. Commun.*, 1966, 237.

94. J. Powell and B. L. Shaw, *J. Chem. Soc., Chem Commun.*, 1966, 323.

95. G. Sbrana, G. Braca, F. Piacenti and P. Pino, *J. Organomet. Chem.*, 1968, **13**, 240.

96. A. Vitagliano, B. Åkermark and S. Hansson, *Organometallics*, 1991, **10**, 2592.

97. J. G. Toerien, *J. Organomet. Chem.*, 1991, **405**, C43.

98. G. E. Herberich and T. P. Spaniol, *J. Chem. Soc., Chem. Commun.*, 1991, 1457.

99. P. Betz, P. W. Jolly and C. Krüger and U. Zakrzewski, *Organometallics*, 1991, **10**, 3520.

100. M. McPartlin and R. Mason, *J. Chem. Soc., Chem Commun.*, 1967, 16.

101. Steven A. King, D. van Engen, H. E. Fischer and J. Schwartz, *Organometallics*, 1991, **10**, 1195.

102. Y. Wakatsuki, H. Yamazaki, Y. Maruyama and I. Shimizu, *J. Organomet. Chem.*, 1992, **430**, C60.

103. G. Wilke, *Angew. Chem. Int. Ed. Engl.*, 1963, **2**, 105.

104. A. Doehring, P. W. Jolly, R. Mynott, K. P. Schick and G. Wilke, *Z. Naturforsch (B): Anorg. Chem., Org. Chem.*, 1981, **36**, 1198; *Chem. Abstr.*, 1982, **96**, no. 20249.

105. J. E. Lydon, J. K. Nicholson, B. L. Shaw and M. R. Truter, *Proc. Chem. Soc.*, 1964, 421.

106. J. K. Nicholson and B. L. Shaw, *J. Chem. Soc. (A)*, 1966, 807.

107. J. E. Lydon and M. R. Truter, *J. Chem. Soc. (A)*, 1968, 363.

108. L. Porri and A. Lionetti, *J. Organomet. Chem.*, 1966, **6**, 422.

109. L. Porri, A. Lionetti, G. Allegra and A. Immirzi, *J. Chem. Soc., Chem. Commun.*,

1965, 336.

110. J. Powell and B. L. Shaw, *J. Chem. Soc. (A)*, 1968, 597.
111. L. Porri, R. Rossi, P. Diversi and A. Lucherini, *Makromol. Chem.*, 1974, **175**, 3097.
112. F. P. Pruchnik, H. Pasternak, M. Zuber, G. Kluczewska, *Chem. Abstr.*, 1980, **92**, no. 93847; V. A. Gorshkov, S. Yu. Pavlov, S. G. Kuznetsov, V. N. Churkin, G. A. Stepanov, B. S. Krotkevich, V. A. Andreev, V. I. Bytina, N. V. Lemaev, *Chem. Abstr.*, 1980, **92**, no. 93875; K. Hiraki, S. Kaneko and H. Hirai, *Chem. Abstr.*, 1971, **75**, no. 21199; A. Misono, Y. Uchida, M. Hidai and I. Inomata, *J. Chem. Soc., Chem. Commun.*, 1968, 704.
113. K. Hiraki and H. Hirai, *Macromolecules*, 1970, **3**, 382; *Chem. Abstr.*, 1970, **73**, no. 77652.
114. D. N. Cox and R. Roulet, *J. Chem. Soc., Chem. Commun.*, 1988, 951.
115. U. Koelle, B. -S. Kang, T. P. Spaniol and U. Englert, *Organometallics*, 1992, **11**, 249.
116. H. Nagashima, T. Ohshima and K. Itoh, *Chem. Lett.*, 1984, 789.
117. H. Nagashima, T. Ohshima and K. Itoh, *Chem. Lett.*, 1984, 793.
118. M. A. Bennett and G. Wilkinson, *Chem. Ind.*, 1959, 1516.
119. R. R. Schrock, B. F. G. Johnson and J. Lewis, *J. Chem. Soc., Dalton Trans.*, 1974, 952.
120. B. F. G. Johnson, J. Lewis and I. E. Ryder, *J. Chem. Soc., Dalton Trans.*, 1977, 719.
121. J. Müller, C. G. Kreiter, B. Mertschenk and S. Schmitt, *Chem. Ber.*, 1975, **108**, 273.
122. T. -A. Mitsudo, Y. Hori and Y. Watanabe, *J. Organomet. Chem.*, 1987, **334**, 157.
123. F. Bouachir, B. Chaudret, D. Dahan, F. Agbossou and I. Tkatchenko, *Organometallics*, 1991, **10**, 455.
124. F. Bouachir, B. Chaudret and I. Tkatchenko, *J. Chem. Soc., Chem. Commun.*, 1986, 94.
125. J. Müller and S. Schmitt, *J. Organomet. Chem.*, 1975, **97**, 275.
126. R. H. Vogeli, H. C. Kang, R. G. Finke and V. Boekelheide, *J. Am. Chem. Soc.*, 1986, **108**, 7010.
127. H. C. Kang, K. -D. Plitzko, V. Boekelheide, H. Higuchi and S. Misumi, *J. Organomet. Chem.*, 1987, **321**, 79.

128. M. R. J. Elsegood and D. A. Tocher, *J. Organomet. Chem.*, 1990, **391**, 239.

129. B. Kovač, M. Mohraz, E. Heilbronner, V. Boekelheide and H. Hopf, *J. Am. Chem. Soc.*, 1980, **102**, 4314.

130. S. Canuto and M. C. Zerner, *J. Am. Chem. Soc.*, 1990, **112**, 2114.

131. K. -D. Plitzko, B. Rapko, B. Gollas, G. Wehrle, T. Weakly, D. T. Pierce, W. E. Geiger, Jr., R. C. Haddon and V. Boekelheide, *J. Am. Chem. Soc.*, 1990, **112**, 6545.

132. R. H. Voegli, H. C. Kang, R. G. Finke and V. Boekelheide, *J. Am. Chem. Soc.*, 1986, **108**, 7010.

133. K. -D. Plitzko and V. Boekelheide, *Organometallics*, 1988, **7**, 1573.

134. W. J. Bowyer, W. E. Geiger and V. Boekelheide, *Organometallics*, 1984, **3**, 1079.

135. H. Ohno, H. Horita, T. Otsubo, Y. Sakata and S. Misumi, *Tetrahedron Lett.*, 1977, **3**, 265.

136. P. J. Fagan, M. D. Ward and J. C. Calabrese, *J. Am. Chem. Soc.*, 1989, **111**, 1698.

137. P. J. Fagan, M. D. Ward and J. C. Calabrese and D. C. Johnson, *J. Am. Chem. Soc.*, 1989, **111**, 1719.

138. W. Siebert, *Adv. Organomet. Chem.*, 1980, **18**, 301.

139. R. N. Grimes, *Coord. Chem. Rev.*, 1979, **28**, 47.

140. N. M. Kostić and R. F. Fenske, *Organometallics*, 1983, **2**, 1319.

141. D. F. Dustin, G. B. Dunks and M. F. Hawthorne, *J. Am. Chem. Soc.*, 1973, **95**, 1109.

142. M. R. Churchill and B. G. DeBoer, *Inorg. Chem.*, 1974, **13**, 1411.

143. R. Khattar, C. B. Knobler, S. E. Johnson and M. F. Hawthorne, *Inorg. Chem.*, 1990, **30**, 1970.

144. Ch. Elschenbroich, J. Koch, J. Kroker, M. Wüensch, W. Massa, G. Baum and G. Stork, *Chem. Ber.*, 1988, **121**, 1983.

145. A. J. Ashe III and J. C. Colburn, *J. Am. Chem. Soc.*, 1977, **99**, 8099.

146. Z. -Y. Li, W. -Y. Yu, C. -M. Che, C. -K. Poon, R. -J. Wang, T. C. W. Mak, *J. Chem. Soc., Dalton Trans.*, 1992, 1657.

147. A. A. Danopoulos, G. Wilkinson, B. Hussain-Bates and M. B. Hursthouse, *Polyhedron*, 1992, 2961.

148. F. L. Joslin, M. P. Johnson, J. T. Mague and D. M. Roundhill, *Organometallics*, 1991, **10**, 2781.

149. U. Furholz, H. -B. Burgi, F. E. Wagner, A. Stebler, J. H. Ammeter, E. Krausz, R. J. H. Clark, M. J. Stead and A. Ludi, *J. Am. Chem. Soc.*, 1984, **106**, 121.

150. A. Anillo, R. Obeso-Rosete, M. A. Pellinghelli and A. Tiripicchio, *J. Chem. Soc., Dalton Trans.*, 1991, 2019.

151. C. Redshaw, G. Wilkinson, B. Hussain-Bates and M. B. Hursthouse, *J. Chem. Soc., Dalton Trans.*, 1992, 555.

152. A. Anillo, C. Barrio, S. Garcia-Granda and R. Obeso-Rosete, *J. Chem. Soc., Dalton Trans.*, 1993, 1125.

153. A. Anillo, J. A. Cabeza, R. Obeso-Rosete and V. Riera, *J. Organomet. Chem.*, 1990, **393**, 423; S. Garcia-Granda, R. Obeso-Rosete, J. M. Rubio and A. Anillo, *Acta Crystallogr., Sect. C*, 1990, **26**, 2043.

154. C. Redshaw, G. Wilkinson, B Hussain-Bates and M. B. Hursthouse, *J. Chem. Soc., Dalton Trans.*, 1992 1803.

155. L. F. Warren, *Inorg. Chem.*, 1977, **16**, 2814.

156. A. L. Balch and R. H. Holm, *J. Am. Chem. Soc.*, 1966, **88**, 5201.

157. E. C. Constable, *Adv. Inorg. Radiochem.*, 1986, **30**, 69.

158. J. G. Toerien and P. H. van Rooyen, *J. Chem. Soc., Dalton Trans.*, 1991, 2693.

159. J. G. Toerien and P. H. van Rooyen, *J. Chem. Soc., Dalton Trans.*, 1991, 1563.

160. S. O. Sommerer and G. J. Palenik, *Organometallics*, 1991, **10**, 1223.

161. D. N. Cox, R. W. H. Small and R. Roulet, *J. Chem. Soc., Dalton Trans.*, 1991, 2013.

162. D. J. Darensbourg, F. Joo, M. Kannisto, A. Katho and J. H. Reibenspies, *Organometallics*, 1992, **11**, 1990.

163. H. Nagao, M. Shibayama, Y. Kitanaka, F. S. Howell, K. Shimizu, M. Mukaida and H. Kakihana, *Inorg. Chim. Acta*, 1991, **185**, 75.

164. C. -K. LI, C. -M. Che, W. -F. Tong and T. -F. Lai, *J. Chem. Soc., Dalton Trans.*, 1992, 813.

165. W. P. Griffith, *Chem. Soc. Rev.*, 1992, 179.

166. C. -M. Che, C. Ho and T. -C. Lau, *J. Chem. Soc., Dalton Trans.*, 1991, 1901.

167. B. A. Moyer, M. S. Thompson and T. J. Meyer, *J. Am. Chem. Soc.*, 1980, **102**, 2310.

168. A. J. Bailey, W. P. Griffith, S. I. Mostafa and P. A. Sherwood, *Inorg. Chem.*, 1993, **32**, 268.

169. C. -M. Che, W. -T. Tang, K. -Y. Wong and C. -K. Li, *J. Chem. Soc., Dalton Trans.*, 1991, 3277.

170. C. Ho, W. -H. Leung and C. -M. Che, *J. Chem. Soc., Dalton Trans.*, 1991, 2933.

171. C. -M. Che, W. -T. Tang, W. -O. Lee, K. -Y. Wong and T. -C. Lau, *J. Chem. Soc., Dalton Trans.*, 1992, 1551.

172. N. Grover and H. H. Thorp, *J. Am. Chem. Soc.*, 1991, **113**, 7030.

173. N. Gupta, N. Grover, G. A. Neyhart, P. Singh and H. H. Thorp, *Inorg. Chem.*, 1993, **32**, 310 and references therein.

174. G. M. Sheldrick, *SHELXTL PLUS, an integrated system for refining and displaying crystal structures from diffraction data*, University of Göttingen, F. R. G., 1986.

175. G. Jia, A. L. Rheingold, B. S. Haggerty and D. W. Meek, *Inorg. Chem.*, 1992, **31**, 900.

176. J. Catterick and P. Thornton, *Adv. Inorg. Radiochem.*, 1977, **20**, 291.

177. A. Dobson, D. S. Moore, S. D. Robinson, M. B. Hursthouse, L. New, *Polyhedron*, 1985, **4**, 1119.

178. J. W. Kang and P. M. Maitlis, *J. Organomet. Chem.*, 1971, **30**, 127.

179. C. White, A. J. Oliver and P. M. Maitlis, *J. Chem. Soc., Dalton Trans.*, 1973, 1901.

180. G. B. Deacon and R. J. Phillips, *Coord. Chem. Rev.*, 1980, **33**, 227.

181. U. Kölle, G. Flunkert, R. Görissen, M. U. Schmidt and U. Englert, *Angew. Chem, Int. Ed. Engl.*, 1992, **31**, 440.

182. S. O. Sommerer, J. D. Baker, M. C. Zerner and G. J. Palenik, *Inorg. Chem.*, 1992, **31**, 563.

183. W. Frank and B. Bertsch-Frank, *Angew. Chem. Int. Ed. Engl.*, 1992, **31**, 436.

184. C. G. Swain and E. C. Lupton, *J. Am. Chem. Soc.*, 1968, **90**, 4328

185. T. H. Lowry and K. S. Richardson, *Mechanism and Theory in Organic Chemistry*, 2nd Ed., Harper and Row, New York, 1981 and references therein.

186. C. Hansch and A. J. Leo, *Substituent Constants for Correlation Analysis in Chemistry and Biology*, Wiley, New York, 1979.

187. E. P. Serjeant and B. Dempsey (Eds.), *Ionisation Constants of Organic Acids in Aqueous Solution*, IUPAC, London, 1979.

188. D. Grdenić, Z. Popović, M. Bruvo and B. Korpar-Čolig, *Inorg. Chim. Acta*, 1991,

190, 169,

189. G. S. Herrmann, H. G. Alt and U. Thewalt, *J. Organomet. Chem.*, 1990, **399**, 83.
190. A. R. Chakravarty, F. A. Cotton and D. A. Tocher, *Inorg. Chem.*, 1985, **24**, 2857.
191. D. Schreiber and D. A. Tocher, unpublished work.
192. C. J. Pouchert (ed.), *Aldrich Library of Infrared Spectra*, 3rd ed., 1981.
193. K. Nakamoto, *Infrared and Raman Spectra of Inorganic and Coordination Complexes*, 4th Ed., Wiley, New York, 1986.
194. C. C. Addison, N. Logan, S. C. Wallwork and C. D. Gardner, *Quart. Rev. Chem. Soc.*, 1971, **25**, 289.
195. H. Schöllhorn, U. Thewalt and B. Lippert, *Inorg. Chim. Acta.*, 1987, **135**, 155.
196. E. C. Alyea, G. Ferguson and R. J. Restivo, *Inorg. Chem.*, 1975, **14**, 2491.
197. P. B. Critchlow and S. D. Robinson, *Inorg. Chem.*, 1978, **17**, 1896.
198. A. C. Cope and E. R. Trumbull, in *Organic Reactions*, A. C. Cope (Ed.), Wiley, New York, 1960, vol. 11, ch. 5.
199. A. J. Deeming, M. N. Meah, P. A. Bates and M. B. Hursthouse, *Inorg. Chim. Acta*, 1988, **142**, 37.
200. E. Block, G. Ofori-Okai, H. Kang and J. A. Zubieta, *Inorg. Chim. Acta*, 1991, **187**, 59.
201. J. Renault, *Bull. Soc. Chim. Fr.*, 1953, 1001.
202. H. L. Yale, in *Pyridine and its Derivatives*, Part IV, E. Klingsberger (ed.), Interscience, New York, 1964.
203. T. Nimry and R. A. Walton, *Inorg. Chem.*, 1977, **16**, 2829.
204. U. A. Gregory, J. A. J. Jarvis, B. T. Kilbourn and P. G. Owston, *J. Chem. Soc. (A)*, 1970, 2771.
205. M. Taniguchi and A. Ouchi, *Bull. Chem. Soc. Jpn.*, 1986, **59**, 3277.
206. T. Rojo, R. Cortés, L. Lezama, M. I. Arriortua, K. Urtiaga and G. Villeneuve, *J. Chem. Soc. Dalton Trans.*, 1991, 1779.
207. J. Chatt and F. A. Hart, *J. Chem. Soc.*, 1953, 2363.
208. J. Chatt and F. A. Hart, *J. Chem. Soc.*, 1960, 2807.
209. M. H. Rowley, *Third Year Project Report*, University College London, 1993.
210. G. Belchem, *Third Year Project Report*, University College London, 1993.

211. T. Shibahara, H. Kuroya, K. Matsumo and S. Ooi, *Inorg. Chim. Acta*, 1981, **54**, L75.

212. K. Butler and M. Snow, *J. Chem. Soc., Dalton Trans.*, 1976, 251.

213. I. Castro, J. Faus, M. Julve and A. Gleizes, *J. Chem. Soc., Dalton Trans.*, 1991, 1937.

214. R. Deyrieux and A. Peneloux, *Bull. Soc. Chim. Fr.*, 1969, 2675.

215. M. H. Chou, C. Creutz and N. Sutin, *Inorg. Chem.*, 1992, **31**, 2318.

216. M. Uemura, H. Nishimura, T. Minami and Y. Hayashi, *J. Am. Chem. Soc.*, 1991, **113**, 5402.

217. M. I. Rybinskaya, A. R. Kurdinov and V. S. Kaganovich, *J. Organomet. Chem.*, 1987, **323**, 111.

218. D. N. Cox and R. Roulet, *Organometallics*, 1986, **5**, 1886.

219. R. P. Bauman, *Absorption Spectroscopy*, Wiley, New York, 1962. pp 289 & 338.

220. M. R. J. Elsegood, *PhD. Thesis*, University College London, 1991.

221. P. L. Pauson and J. A. Segal, *J. Chem. Soc., Dalton Trans.*, 1975, 1683.

222. X. Luo, G. A. Arteca, C. Zhang and P. G. Mezey, *J. Organomet. Chem.*, 1993, **444**, 131.

223. D. J. Cram and H. Steinberg, *J. Am. Chem. Soc.*, 1951, **73**, 5691.

224. C. J. Brown and A. C. Farthing, *Nature (London)*, 1949, **164**, 915.

225. E. D. Laganis, R. G. Finke and V. Boekelheide, *Tet. Lett.*, 1980, **21**, 4405.

226. M. A. Bennett, T. W. Matheson, G. B. Robertson, W. L. Steffen and T. W. Turney, *J. Chem. Soc., Chem. Commun.*, 1979, 32.

227. A. L. Burrows, B. F. G. Johnson, J. Lewis and D. G. Parker, *J. Organomet. Chem.*, 1980, **194**, C11.

228. R. D. Pike, W. J. Ryan, N. S. Lennhoff, J. Van Epp and D. A. Sweigart, *J. Am. Chem. Soc.*, 1990, **112**, 4798.

229. M. Brookhart, M. L. H. Green and L. -L. Wong, *Prog. Inorg. Chem.*, 1988, **36**, 1.

230. W. W. Paudler, "Nuclear Magnetic Resonance", Wiley, New York, 1987, p 147.

231. M. Brookhart, W. Lamanna and M. B. Humphrey, *J. Am. Chem. Soc.*, 1982, **104**, 2117.

232. M. A. Bennett and T. W. Matheson, *J. Organomet. Chem.*, 1978, **153**, C25.

233. M. L. H. Green, A. K. Hughes, N. A. Popham, A. H. H. Stephens and L. -L. Wong, *J. Chem. Soc., Dalton Trans.*, 1992, 3077.

234. J. K. M. Saunders and B. K. Hunter, *Modern NMR Spectroscopy. A Guide for Chemists*, Oxford, 1987, pp 299 - 302.

235. J. T. S. Andrews and E. F. Westrum, Jr., *J. Phys. Chem.*, 1970, **74**, 2170.

Appendices

Appendix I:

^{1}H NMR Spectroscopy of η^3:η^3-$C_{10}H_{16}$ and η^6-$C_{16}H_{16}$

A1.1 ^1H NMR Spectroscopy of η^3:η^3-$C_{10}H_{16}$

The fixed orientation of the *bis*(allyl) dimethyloctadienediyl ligand about the metal centre (Fig. A1.1) in complexes derived from $[\{Ru(\eta^3:\eta^3\text{-}C_{10}H_{16})Cl(\mu\text{-}Cl)\}_2]$ **6** and the chirality of the "$Ru(\eta^3:\eta^3\text{-}C_{10}H_{16})$" fragment result in a high degree of sensitivity of the ^1H NMR spectra of complexes containing this ligand, to the substitution of the remaining coordination sites about the metal centre, and the complexes' nuclearity.

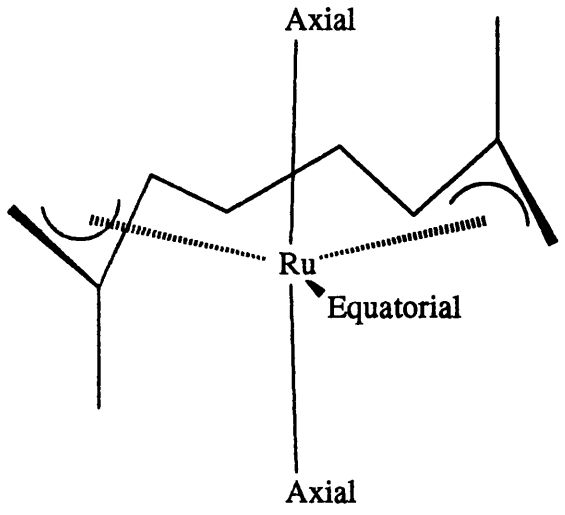

Fig. A1.1: Geometry of the "$Ru(\eta^3:\eta^3\text{-}C_{10}H_{16})$" fragment showing pseudo-eclipsing of each axial site with the plane of one of the allylic functionalities

The partial ^1H NMR spectrum of the symmetrical compound $[Ru(\eta^3:\eta^3\text{-}C_{10}H_{16})(NO_3)_2]$ **89** is shown in Fig. A1.2a. In this compound the two axial sites are equivalent (both occupied by nitrato ligands) and hence the two halves of the *bis*(allyl) ligand are magnetically degenerate, resulting in the observation of only two singlet resonances for the terminal allyl protons (H_a, H_b, $^2J_{H\text{-}H}$ not observed) and one methyl resonance. In the analogous 1 : 1 chelate compound $[Ru(\eta^3:\eta^3\text{-}C_{10}H_{16})Cl(NO_3)]$ **89** (^1H NMR spectrum Fig. A1.2b) one allyl fragment lies parallel to the nitrato ligand whilst the other is pseudo-eclipsed with the chloride substituent, hence both halves of the *bis*(allyl)

ligand become magnetically unique resulting in the observation of four terminal allyl signals and two methyl resonances. Four terminal allyl resonances are also observed for the pyrazene bridged binuclear complex $[\{Ru(\eta^3:\eta^3\text{-}C_{10}H_{16})Cl_2\}_2(\mu\text{-}N_2C_4H_4)]$ **106**. In this case the axial sites of each metal atom are equivalent but, because two chiral "$Ru(\eta^3:\eta^3\text{-}C_{10}H_{16})$" fragments are present in the molecule, two diastereoisomers are formed each of which exhibits two terminal allyl signals and a single methyl resonance, Fig. A1.2c. The separation between the signals for the respective diastereoisomers is not as great as the separation between the allyl signals in the oxalato compound **115** for example, because the chiral fragments are relatively far away from one another and the resulting changes in magnetic environment are not as great. In general, in binuclear complexes, the chemical shift difference between pairs of terminal allyl or pairs of methyl resonances due to different diastereoisomers decreases with increasing metal-metal separation. Thus, in the *p*-phenylenediamine bridged compound $[\{Ru(\eta^3:\eta^3\text{-}C_{10}H_{16})Cl_2\}_2\{\mu\text{-}(NH_2)_2C_4H_4\}]$ **56** the signals for the two diastereoisomers are not resolved. Also, unlike mononuclear compounds such as **72**, the terminal allyl signals in binuclear species need not be of the same intensity because each diastereoisomer need not be present in equal amounts, thus in the case of **106** the outer allyl signals belonging to the C_2 type isomer are of slightly greater intensity than the inner pair.

Binuclear complexes such as **6** and the thiocyanate bridged dimer **114** also exist as two diastereoisomers and in addition the axial sites are inequivalent, hence each diastereoisomer contributes four terminal allyl resonances and two methyl signals resulting in the spectrum of the mixture of diastereoisomers (Fig. A1.2d) exhibiting eight terminal allyl and four methyl resonances.

The complexity of the ^1H NMR spectra of higher nuclearity compounds such as $[\{Ru(\eta^3:\eta^3\text{-}C_{10}H_{16})Cl_2\}_3(\mu^3\text{-}N_3C_3H_3)]$ **110** rapidly increases as the formation of more stereoisomers becomes possible. Binding of chiral ligands will also result in doubling of the number of ^1H NMR resonances as a result of diastereoisomer formation.

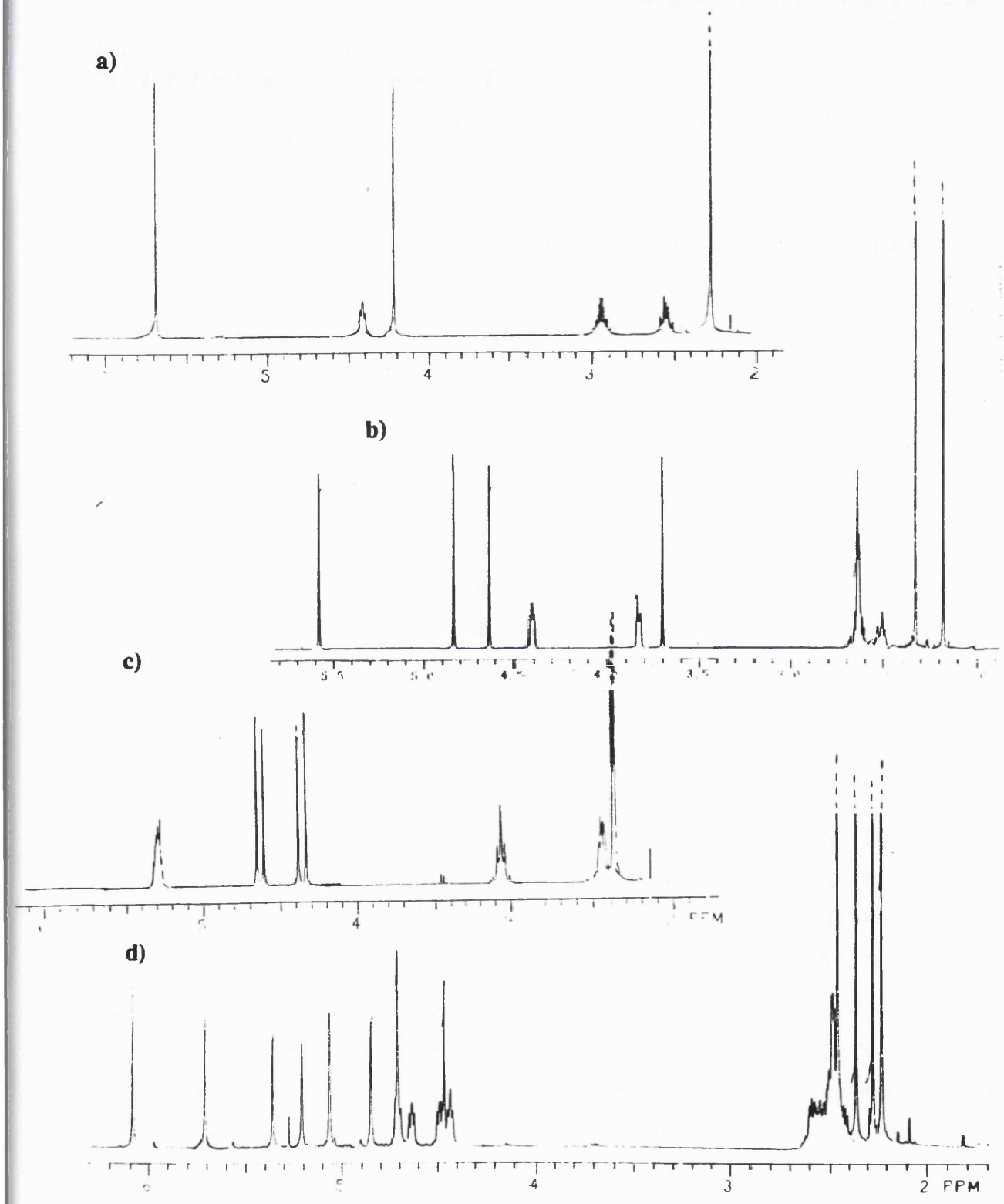

Fig. A1.2: Partial ^1H NMR spectra of a) $[Ru(\eta^3:\eta^3\text{-}C_{10}H_{16})(NO_3)_2]$ **89**; b) $[Ru(\eta^3:\eta^3\text{-}C_{10}H_{16})Cl(NO_3)]$ **88**; c) $[\{Ru(\eta^3:\eta^3\text{-}C_{10}H_{16})Cl_2\}_2(\mu\text{-}N_2C_4H_4)]$ **106** and d) $[\{Ru(\eta^3:\eta^3\text{-}C_{10}H_{16})Cl(\mu\text{-}Cl)\}_2]$ **6**

A1.2 ^1H NMR Spectroscopy of η^6-$C_{16}H_{16}$

A useful feature of the metal coordinated [2.2]paracyclophane ligand is that both the ring and bridge protons are diastereotopic and hence the ^1H NMR spectrum of the ligand is sensitive to chirality at the metal centre. This effect is readily observed in the mononuclear compounds $[Ru(\eta^6\text{-}C_{16}H_{16})Cl(phen)][PF_6]$ **148** and $[Ru(\eta^6\text{-}C_{16}H_{16})Cl(py)(PMe_2Ph)][PF_6]$ **149**.[220] The room temperature ^1H NMR spectrum of **148** exhibits a singlet resonance for the coordinated [2.2]paracyclophane ring and the usual AA'BB' pattern for the bridge protons (Fig. A1.3a). In contrast the metal centre in **149** is chiral and hence an AB (strictly AA'BB') pattern is observed for the protons of the coordinated cyclophane ring whilst the signals for the bridge protons is significantly more complex (Fig. A1.3b).[220]

Such effects of magnetic inequivalence are well documented[234] and occur even though molecular motions such as rotation about the Ru-cyclophane bond, and the twisting of one cyclophane ring with respect to the other, are rapid on the NMR timescale. In fact, inter-ring torsion in [2.2]paracyclophane is an extremely rapid motion and has been estimated from heat capacity measurements to be an active solid state vibrational mode above 50 K in the free molecule and hence may be neglected for the purposes of interpreting NMR spectra.[235] Rotation about M-arene bonds is also generally assumed to be a rapid process in the absence of extreme steric hinderance. At very low temperatures such as studied in Chapter 7 however, the signal due to the cyclophane coordinated ring occurs as a more complex pattern in the asymmetric compounds **142**, **144**, **146** and **147**. At -138°C compound **144**, for example, demonstrates four broad lines (δ 5.60, 4.94, 4.47 and 4.26 ppm) for the coordinated deck of the cyclophane ligand, Fig. A1.3c. At this temperature we were unable to resolve three bond couplings as a consequence of solvent broadening and it is therefore possible that these lines represent unique environments for all four coordinated ring protons, and hence that rotation about the Ru-cyclophane bond is slow. At -100°C these four signals coalesce into two broad resonances consistent with the expected AA'BB' pattern expected for fast rotation about the M-cyclophane bond in **144** and at -80°C and above the onset of other fluxional processes in **144** results in the observation of a singlet resonance.

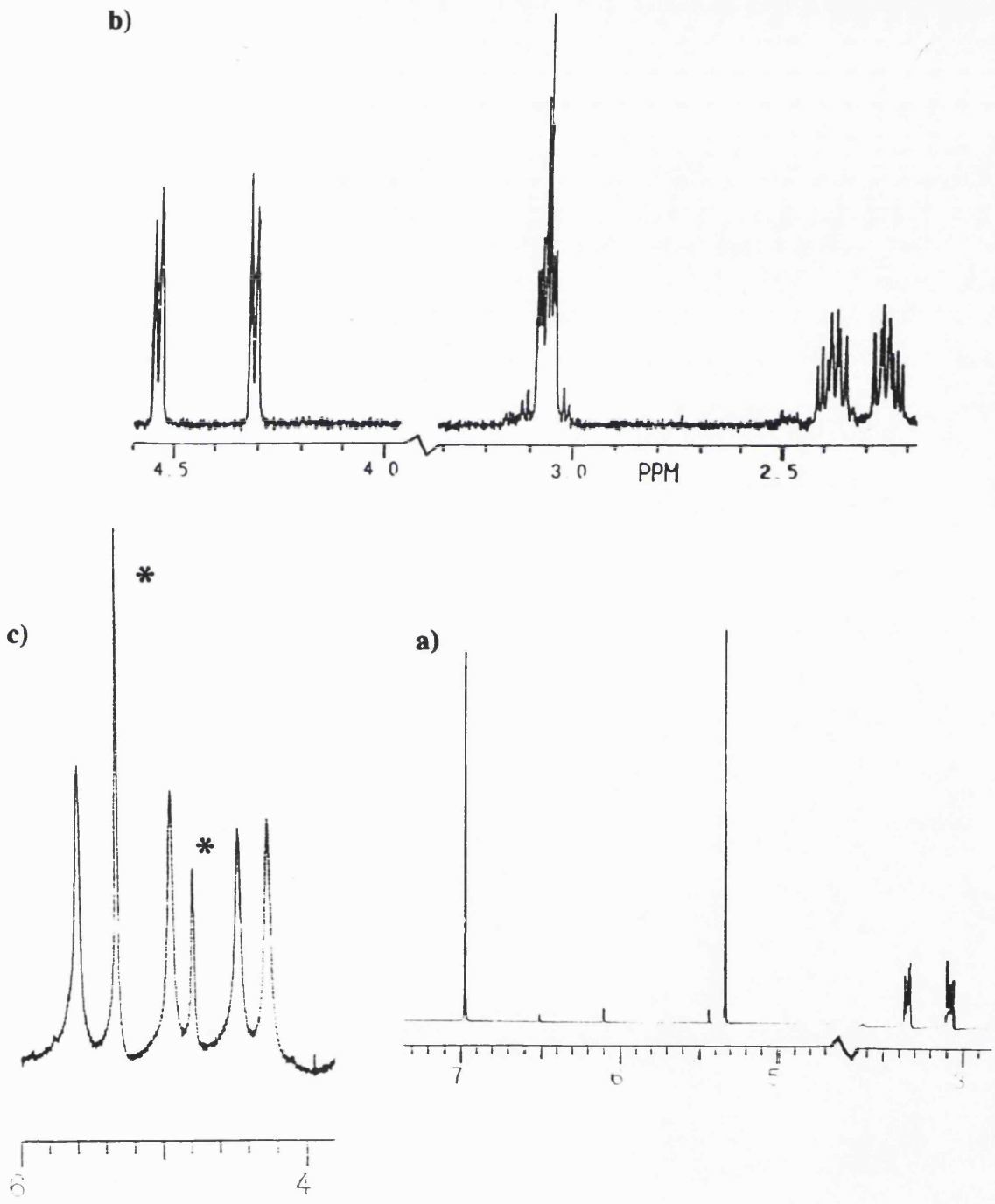

Fig. A1.3: Partial ^1H NMR spectra of a) $[Ru(\eta^6\text{-}C_{16}H_{16})Cl(phen)][PF_6]$ **148**; b) $[Ru(\eta^6\text{-}C_{16}H_{16})Cl(py)(PMe_2Ph)][PF_6]$ **149** (taken from ref. 220) and c) $[Ru(\eta^6\text{-}C_{16}H_{16})\{\eta^3\text{-}(HCH_2)(CH_2)C_6Me_4H_4\}]$ **144** (recorded at -138°C, peaks marked '*' are due to residual $CHDCl_2$ and an unidentified cyclophane-containing impurity).

Appendix II:

Compound Numbers

1 $C_{16}H_{16}$

2 $\eta^3{:}\eta^3\text{-}C_{10}H_{16}$

3a $[Ru(\eta^6\text{-}C_{16}H_{16})(\eta^6\text{-}C_6H_6)][BF_4]_2$

3b $[Ru(\eta^6\text{-}C_{16}H_{16})(\eta^6\text{-}C_6Me_6)][BF_4]_2$

3c $[Ru(\eta^6\text{-}C_{16}H_{16})(\eta^6\text{-}4\text{-}MeC_6H_4CHMe_2)][BF_4]_2$

3d $[Ru(\eta^6\text{-}C_{16}H_{16})(\eta^6\text{-}C_6Me_4H_2)][BF_4]_2$

3e $[Ru(\eta^6\text{-}C_{16}H_{16})(\eta^6\text{-}C_6Me_5H)][BF_4]_2$

3f $[Ru(\eta^6\text{-}C_{16}H_{16})_2][BF_4]_2$

4 $[Ru(\eta^6\text{-}C_{16}H_{16})(\eta^4\text{-}5,6\text{-}C_6H_8)]$

4' $[Ru(\eta^6\text{-}C_{16}H_{16})(\eta^4\text{-}\textit{exo,exo}\text{-}5,6\text{-}C_6H_6D_2)]$

5 $[Ru(\eta^6\text{-}C_{16}H_{16})(\eta^4\text{-}\textit{exo,exo}\text{-}3,6\text{-}C_6Me_6H_2)]$

5' $[Ru(\eta^6\text{-}C_{16}H_{16})(\eta^4\text{-}\textit{exo,exo}\text{-}3,6\text{-}C_6Me_6D_2)]$

6a *meso*-$[\{Ru(\eta^3{:}\eta^3\text{-}C_{10}H_{16})Cl(\mu\text{-}Cl)\}_2]$ C_i

6b *rac*-$[\{Ru(\eta^3{:}\eta^3\text{-}C_{10}H_{16})Cl(\mu\text{-}Cl)\}_2]$ C_2

7a $[\{Ru(\eta^6\text{-}C_6H_6)Cl(\mu\text{-}Cl)\}_2]$

7b $[\{Ru(\eta^6\text{-}C_6Me_6)Cl(\mu\text{-}Cl)\}_2]$

7c $[\{Ru(\eta^6\text{-}4\text{-}MeC_6H_4CHMe_2)Cl(\mu\text{-}Cl)\}_2]$

8a $[Ru(\eta^6\text{-}C_6H_6)(\eta^4\text{-}C_6H_8)Cl][BPh_4]$

8b $[Ru(\eta^6\text{-}C_6H_6)(\eta^4\text{-}C_6H_8)Cl]_2[Hg_3Cl_4]$

9 $[Ru(\eta^6\text{-arene})Cl_2L]$

10 $[Ru(\eta^6\text{-arene})ClL_2]^+$

11 $[Ru(\eta^6\text{-arene})(PR_3)L_2]^{2+}$

12 $[Ru(\eta^6\text{-arene})Cl(L\text{-}L)]$

13 $[Ru(\eta^6\text{-arene})(L\text{-}L)_2]$

14a $[(\eta^6\text{-}C_6H_6)Ru(\mu\text{-}OH)_3Ru(\eta^6\text{-}C_6H_6)]^+$

14b $[(\eta^6\text{-arene})Ru(\mu\text{-}OR)_3Ru(\eta^6\text{-arene})]^+$

15 $[(\eta^6\text{-arene})_2Ru_2(\mu^2\text{-}OH)_2(\mu^4\text{-}O)Ru_2(\mu^2\text{-}OH)_2(\eta^6\text{-arene})]^{2+}$

16 $[\{Ru(\eta^6\text{-arene})(\mu^3\text{-}OH)\}_4][SO_4]_2.12H_2O$

17 $[Fe(\eta^6\text{-}C_6Me_6)_2]^{2+}$

18 $[Fe(\eta^6\text{-}C_6R_6)(\eta^5\text{-}C_6R_6N)]^+$

19 $[Fe(\eta^6\text{-}C_6R_6)(\eta^4\text{-}C_6R_6NN')]$

20 $[Fe(\eta^5\text{-}C_5H_5)(\eta^6\text{-}C_6Me_6)]$

21 $[Fe(\eta^6\text{-}C_6Me_6)\{\eta^4\text{-}C_6Me_4(CH_2)_2\}]$

22 $[Ru(\eta^6\text{-}C_6Me_6)\{\eta^4\text{-}C_6Me_4(CH_2)_2\}]$

23 $[Ru(\eta^6\text{-}C_6Me_6)\{\eta^5\text{-}C_6Me_5(CH_2)\}]^+$

24 $[Ru\{\eta^4\text{-}C_6Me_4(CH_2)_2\}(PR_3)_3]$

25 $[Ru\{\eta^3\text{-}C_6Me_5(CH_2)\}(PR_3)_3]^+$

26 $[Ru(\eta^6\text{-}C_6R_6)(\eta^5\text{-}C_6R_6N)]^+$

27 $[Ru(\eta^5\text{-}C_6R_6N)L_3]^+$

28 $[Ni(\eta^3\text{-}C_3H_5)_2]$

29 $[Ru(\eta^4\text{-}C_8H_{12})(\eta^3\text{-allyl})_2]$

30 $[\{Rh(\eta^3\text{-allyl})_2(\mu\text{-Cl})\}_2]$

31 $[Ru(\eta^6\text{-}C_8H_{10})(\eta^3\text{-}C_5H_9)(CO)][BF_4]$

32 $[Ru(\eta^6\text{-}C_6Me_6)(\eta^3\text{-}C_3H_4Me)Cl]$

33 $[Cr(PR_3)_2(\eta^3\text{-}C_3H_4R')_2]$

34 $[RuCl(CO)(H)(PPh_3)_3]$

35 $[Ru\{\eta\text{-}(R^2)CH{=}CCH{=}CHR^1\}Cl(CO)(PPh_3)_2]$

36 $[Ni(\eta^2{:}\eta^2{:}\eta^2\text{-}C_{12}H_{18})]$

37 $[Ni(\eta^3{:}\eta^2{:}\eta^3\text{-}C_{12}H_{18})]$

38 $[Pd(\eta^1{:}\eta^3\text{-}C_8H_{12})(PMe_3)]$

39 $[Ru(\eta^3{:}\eta^2{:}\eta^3\text{-}C_{12}H_{18})Cl_2]$

40 $[RhCl(\eta^4\text{-}C_4H_6)_2]$

41 $[Rh_2(\eta^3\text{-}C_4H_7)_2Cl_2(\mu\text{-Cl})_2(\mu\text{-}C_4H_6)]$

42 $[Ru(\eta^3{:}\eta^3\text{-}C_{10}H_{16})Cl_2L]$

43 $[Ru(\eta^3{:}\eta^2{:}\eta^3\text{-}C_{12}H_{18})(Me)I]$

44 $[Ru\{\eta^3\text{-}C_3H_4(CH_2)_2CH{=}CH(CH_2)_2CH(Me)CH{=}CH_2\}(L)_3I]$

45 $[\{Ru(\eta^6\text{-}C_7H_8)Cl(\mu\text{-Cl})\}_2]$

46 $[\{Ru(\eta^6\text{-}C_8H_{10})Cl_2\}_n]$

47 $[\{Ru(diene)Cl_2\}_n]$

48a $[Ru(\eta^6\text{-}C_7H_8)(\eta^6\text{-diene})]$

48b $[Ru(\eta^6\text{-}C_8H_{10})(\eta^6\text{-diene})]$

49 $[Ru(\eta^7\text{-}C_7H_7)(\eta^4\text{-diene})]^+$

50 $[Mo(\eta^6\text{-}C_7H_8)(CO)_3]$

51 $[Ru(\eta^5\text{-}C_7H_8L)L(XPh_3)]$

52 $[\{Ru(\eta^6\text{-}C_6Me_6)\}_2(\eta^6{:}\eta^6\text{-}C_{16}H_{16})]^{4+}$

53 $[(\eta^6\text{-}C_6H_6)Os(\eta^6{:}\eta^6\text{-}C_{16}H_{16})Ru(\eta^6{:}\eta^6\text{-}C_{16}H_{16})Os(\eta^6\text{-}C_6H_6)]^{6+}$

54 $[Ru(\eta^3{:}\eta^3\text{-}C_{10}H_{16})Cl_2(NH_2Ph)]$

55 $[Ru(\eta^3{:}\eta^3\text{-}C_{10}H_{16})Cl_2(1,4\text{-}NH_2C_6H_4NH_2)]$

56 $[\{Ru(\eta^3{:}\eta^3\text{-}C_{10}H_{16})Cl_2\}_2\{\mu\text{-}1,4\text{-}(NH_2)_2C_6H_4\}]$

57 $[Ru(\eta^3{:}\eta^3\text{-}C_{10}H_{16})Cl_2(1,2\text{-}NH_2C_6H_4NH_2)]$

58 $[\{Ru(\eta^3{:}\eta^3\text{-}C_{10}H_{16})Cl_2\}_2\{\mu\text{-}1,2\text{-}(NH_2)_2C_6H_4\}]$

59 $[Ru(\eta^3{:}\eta^3\text{-}C_{10}H_{16})Cl\{1,2\text{-}(NH_2)_2C_6H_4\}]Cl$

60 $[Ru(\eta^3:\eta^3\text{-}C_{10}H_{16})Cl\{1,2\text{-}(NH_2)_2C_6H_4\}][PF_6]$

61 $[Ru(\eta^3:\eta^3\text{-}C_{10}H_{16})Cl\{(NH_2C_6H_4)_2\}]Cl$

62 $[Ru(\eta^3:\eta^3\text{-}C_{10}H_{16})Cl\{(NH_2C_6H_4)_2\}][BF_4]$

63 $[Ru(\eta^3:\eta^3\text{-}C_{10}H_{16})Cl_2(NC_3H_3NH)]$

64 $[Ru(\eta^3:\eta^3\text{-}C_{10}H_{16})Cl(N_2C_{10}H_8)][BF_4]$

65 $[Ru(\eta^3:\eta^3\text{-}C_{10}H_{16})Cl(N_2C_{12}H_8)][BF_4]$

66 $[Ru(\eta^3:\eta^3\text{-}C_{10}H_{16})(N_3C_{15}H_{11})][BF_4]_2$

67 $[Ru(\eta^3:\eta^3\text{-}C_{10}H_{16})Cl_2(PF_3)]$

68 $[Ru(\eta^3:\eta^3\text{-}C_{10}H_{16})Cl\{NC_7H_4S(S)\}]$

69 $[Ru(\eta^3:\eta^3\text{-}C_{10}H_{16})(NCMe)\{NC_7H_4S(S)\}]^+$

70 $[Ru(\eta^3:\eta^3\text{-}C_{10}H_{16})(N_2C_{10}H_8)(OH_2)][BF_4]_2$

71 $[Ru(\eta^3:\eta^3\text{-}C_{10}H_{16})(N_2C_{12}H_8)(OH_2)][BF_4]_2$

72 $[Ru(\eta^3:\eta^3\text{-}C_{10}H_{16})Cl(O_2CMe)]$

73 $[Ru(\eta^3:\eta^3\text{-}C_{10}H_{16})(O_2CCF_3)_2(OH_2)]$

74 $[Ru(\eta^3:\eta^3\text{-}C_{10}H_{16})(O_2CCF_3)_2(N_2C_4H_4)]$

75 $[Ru(\eta^3:\eta^3\text{-}C_{10}H_{16})(O_2CCCl_3)_2(OH_2)]$

76 $[Ru(\eta^3:\eta^3\text{-}C_{10}H_{16})(O_2CCHCl_2)_2(OH_2)]$

77 $[Ru(\eta^3:\eta^3\text{-}C_{10}H_{16})(O_2CCHF_2)_2(OH_2)]$

78a $[Ru(\eta^3:\eta^3\text{-}C_{10}H_{16})Cl(O_2CCH_2Cl)]$

78b $[Ru(\eta^3:\eta^3\text{-}C_{10}H_{16})(O_2CCH_2Cl)_2(OH_2)]$

78c $[Ru(\eta^3:\eta^3\text{-}C_{10}H_{16})Cl(\eta^1\text{-}O_2CCH_2Cl)(OH_2)]$

79a $[Ru(\eta^3:\eta^3\text{-}C_{10}H_{16})Cl(O_2CCH_2F)]$

79b $[Ru(\eta^3:\eta^3\text{-}C_{10}H_{16})(O_2CCH_2F)_2(OH_2)]$

79c $[Ru(\eta^3:\eta^3\text{-}C_{10}H_{16})Cl(\eta^1\text{-}O_2CCH_2F)(OH_2)]$

80 $[Ru(\eta^3:\eta^3\text{-}C_{10}H_{16})Cl\{F_3CC(O)CHC(O)CF_3\}]$

81 $[Ru(\eta^3:\eta^3\text{-}C_{10}H_{16})Cl\{F_3CC(O)CHC(O)Me\}]$

82 $[Ru(\eta^3:\eta^3\text{-}C_{10}H_{16})Cl\{MeCC(O)CHC(O)Me\}]$

83 $[Ru(\eta^3:\eta^2:\eta^3\text{-}C_{12}H_{18})Cl(H_2O)][BF_4]$

84 $[Ru(\eta^3:\eta^3\text{-}C_{10}H_{16})Cl_2\{HO(S)CMe\}]$

85 $[Ru(\eta^3:\eta^3\text{-}C_{10}H_{16})Cl(OSCMe)]$

86 $[Ru(\eta^3:\eta^3\text{-}C_{10}H_{16})Cl(OSC^tBu)]$

87 $[Ru(\eta^3:\eta^3\text{-}C_{10}H_{16})Cl(OSCPh)]$

88 $[Ru(\eta^3:\eta^3\text{-}C_{10}H_{16})Cl(NO_3)]$

89 $[Ru(\eta^3:\eta^3\text{-}C_{10}H_{16})(NO_3)_2]$

90 $[Ru(\eta^3:\eta^3\text{-}C_{10}H_{16})(ONO_2)_2(CO)]$

91 $[Ru(\eta^3:\eta^3\text{-}C_{10}H_{16})(ONO_2)_2(NC_5H_5)]$

92a $[Ru(\eta^3:\eta^3\text{-}C_{10}H_{16})Cl_2(mcbtH)]$

92b $[Ru(\eta^3:\eta^3\text{-}C_{10}H_{16})Cl_2(pyrSH)]$

93a $[Ru(\eta^3:\eta^3\text{-}C_{10}H_{16})Cl(mcbt)]$

93b $[Ru(\eta^3:\eta^3\text{-}C_{10}H_{16})Cl(pyrS)]$

94a $[Ru(\eta^6\text{-}C_6H_6)Cl(NC_5H_4O)]$

94b $[Ru(\eta^6\text{-}C_6H_6)Cl(NC_5H_3O\text{-}6\text{-}Cl)]$

94c $[Ru(\eta^6\text{-}C_6H_6)Cl(NC_5H_3O\text{-}6\text{-}Me)]$

94d $[Ru(\eta^6\text{-}p\text{-}MeC_6H_4CHMe_2)Cl(NC_5H_4O)]$

95 $[Ru(\eta^6\text{-}C_6H_6)Cl_2(OC_5H_4NH)]$

96 $[Ru(\eta^3:\eta^3\text{-}C_{10}H_{16})Cl(NC_5H_4O)]$

97 $[Ru(\eta^3:\eta^3\text{-}C_{10}H_{16})Cl(NC_5H_3O\text{-}6\text{-}Cl)]$

98 $[Ru(\eta^3:\eta^3\text{-}C_{10}H_{16})Cl(NC_9H_5O\text{-}4\text{-}Me)]$

99 $[Ru(\eta^3:\eta^3\text{-}C_{10}H_{16})Cl(NC_5H_3O\text{-}6\text{-}Me)]$

100 $[Ru(\eta^3:\eta^3\text{-}C_{10}H_{16})Cl(NC_9H_6O)]$

101 $[Ru(\eta^3:\eta^3\text{-}C_{10}H_{16})Cl(NC_4H_6O)]$

102 $[Ru(\eta^3:\eta^3\text{-}C_{10}H_{16})Cl_2(NC_9H_6SH)]$

103 $[Ru(\eta^3:\eta^3\text{-}C_{10}H_{16})Cl_2(NC_5H_3MeSH)]$

104 $[Ru(\eta^3:\eta^3\text{-}C_{10}H_{16})Cl(NC_9H_6S)]$

105 $[Ru(\eta^3:\eta^3\text{-}C_{10}H_{16})Cl(NC_5H_3S\text{-}6\text{-}Me)]$

106 $[\{Ru(\eta^3:\eta^3\text{-}C_{10}H_{16})Cl_2\}_2(\mu\text{-}N_2C_4H_4)]$

107 $[Ru(\eta^3:\eta^3\text{-}C_{10}H_{16})Cl_2(N_2C_4H_4)]$

108 $[Ru(\eta^3:\eta^3\text{-}C_{10}H_{16})Cl_2(N_3C_3H_3)]$

109 $[\{Ru(\eta^3:\eta^3\text{-}C_{10}H_{16})Cl_2\}_2(\mu^2\text{-}N_3C_3H_3)]$

110 $[\{Ru(\eta^3:\eta^3\text{-}C_{10}H_{16})Cl_2\}_3(\mu^3\text{-}N_3C_3H_3)]$

111 $[(\eta^3:\eta^3\text{-}C_{10}H_{16})Cl_2Ru(\mu\text{-}N_2C_4H_4)RuCl_2(\eta^6\text{-}p\text{-}MeC_6H_4CHMe_2)]$

112 $[\{Ru(\eta^6\text{-}p\text{-}MeC_6H_4CHMe_2)Cl_2\}_2(\mu\text{-}N_2C_4H_4)]$

113 $[Ru(p\text{-}MeC_6H_4CHMe_2)Cl_2(N_2C_4H_4)]$

114 $[\{Ru(\eta^3:\eta^3\text{-}C_{10}H_{16})Cl(\mu\text{-}SCN)\}_2]$

115 $[\{Ru(\eta^3:\eta^3\text{-}C_{10}H_{16})Cl\}_2(\mu\text{-}O_4C_2)]$

116 $[\{Ru(\eta^3:\eta^3\text{-}C_{10}H_{16})Cl\}_2(\mu\text{-}O_4C_3H_2)]$

117 $[Ru(\eta^3:\eta^3\text{-}C_{10}H_{16})Cl_2(p\text{-}NC_5H_4CO_2H)]$

118 $[Ru_2(\eta^3:\eta^3\text{-}C_{10}H_{16})_2Cl_3(\mu\text{-}m\text{-}NC_5H_4CO_2)]$

119 $[Ru_2(\eta^3:\eta^3\text{-}C_{10}H_{16})_2Cl_3(\mu\text{-}p\text{-}NC_5H_4CO_2)]$

120 $[(\eta^3:\eta^3\text{-}C_{10}H_{16})Cl_2Ru(\mu\text{-}NC_5H_4CO_2)RuCl(\eta^6\text{-}p\text{-}MeC_6H_4CHMe_2)$

121 $[Ru(\eta^6\text{-}C_{16}H_{16})(\eta^5\text{-}C_6H_7)][BF_4]$

121' $[Ru(\eta^6\text{-}C_{16}H_{16})(\eta^5\text{-}C_6H_6D)][BF_4]$

122 $[Ru(\eta^6\text{-}C_{16}H_{16})(\eta^5\text{-}C_6H_6CN)][BF_4]$

123 $[Ru(\eta^6\text{-}C_{16}H_{16})(\eta^5\text{-}C_6H_6OMe)][BF_4]$

124 $[Ru(\eta^6\text{-}C_{16}H_{16})(\eta^5\text{-}C_6H_6Me)][BF_4]$

125 $[Os(\eta^6\text{-}C_{16}H_{16})(\eta^5\text{-}C_6H_7)][BF_4]$

126a $[Ru(\eta^6\text{-}C_{16}H_{16})(\eta^5\text{-}4\text{-}MeC_6H_5\text{-}1\text{-}CHMe_2)][BF_4]$

126b $[Ru(\eta^6\text{-}C_{16}H_{16})(\eta^5\text{-}1\text{-}MeC_6H_5\text{-}4\text{-}CHMe_2)][BF_4]$

127a $[Ru(\eta^6\text{-}C_{16}H_{16})(\eta^5\text{-}4\text{-}MeC_6H_5\text{-}1\text{-}CHMe_2)][BPh_4]$

127b $[Ru(\eta^6\text{-}C_{16}H_{16})(\eta^5\text{-}1\text{-}MeC_6H_5\text{-}4\text{-}CHMe_2)][BPh_4]$

128a $[Ru(\eta^6\text{-}C_{16}H_{16})(\eta^5\text{-}4\text{-}MeC_6H_4\text{-}1\text{-}CHMe_2\text{-}6\text{-}CN)][BF_4]$

128b $[Ru(\eta^6\text{-}C_{16}H_{16})(\eta^5\text{-}1\text{-}MeC_6H_4\text{-}4\text{-}CHMe_2\text{-}6\text{-}CN)][BF_4]$

129 $[Ru(\eta^6\text{-}C_{16}H_{16})(\eta^5\text{-}1,4\text{-}(CHMe_2)_2C_6H_5)][BF_4]$

130 $[Ru(\eta^6\text{-}C_{16}H_{16})(\eta^5\text{-}C_6Me_6H)][BF_4]$

130' $[Ru(\eta^6\text{-}C_{16}H_{16})(\eta^5\text{-}C_6Me_6D)][BF_4]$

131 $[Ru(\eta^6\text{-}C_{16}H_{16})(\eta^5\text{-}C_6Me_6CN)][BF_4]$

132 $[Ru(\eta^6\text{-}C_{16}H_{16})(\eta^5\text{-}C_6Me_7)][BF_4]$

133 $[Ru(\eta^6\text{-}C_{16}H_{16})\{\eta^5\text{-}C_6Me_5(CH_2)\}][BF_4]$

134 $[Ru(\eta^6\text{-}C_{16}H_{16})(\eta^5\text{-}C_{16}H_{17})][BF_4]$

135 $[Ru(\eta^6\text{-}C_{16}H_{16})(\eta^4\text{-}\textit{exo,exo}\text{-}5,6\text{-}C_6Me_6H_2)]$

136 $[Ru(\eta^6\text{-}C_{16}H_{16})(1\text{-}\sigma\text{-}3\text{-}5\text{-}\eta\text{-}\textit{exo,exo}\text{-}2,6\text{-}C_6Me_6H_2)]$

137 $[Ru(\eta^6\text{-}C_{16}H_{16})(\eta^4\text{-}C_6Me_5H_3)]$

138 $[Ru(\eta^6\text{-}C_{16}H_{16})(\eta^4\text{-}C_6Me_4H_4)]$

139a $[Ru(\eta^6\text{-}C_{16}H_{16})\{\eta^4\text{-}1\text{-}Me\text{-}4\text{-}(CHMe_2)C_6H_6\}]$

139b $[Ru(\eta^6\text{-}C_{16}H_{16})\{\eta^4\text{-}2\text{-}(CHMe_2)\text{-}5\text{-}MeC_6H_6\}]$

140 $[Ru(\eta^6\text{-}C_{16}H_{16})\{\eta^4\text{-}C_6Me_6H(CN)\}]$

141 $[Ru(\eta^6\text{-}C_{16}H_{16})\{\eta^4\text{-}C_6Me_4(CH_2)_2\}]$

142 $[Ru(\eta^6\text{-}C_{16}H_{16})(\eta^3\text{-}C_6Me_6H_3)][BF_4]$

143 $[Ru(\eta^6\text{-}C_{16}H_{16})(\eta^3\text{-}H_2C_6Me_6D)][H(CF_3CO_2)_2]$

144 $[Ru(\eta^6\text{-}C_{16}H_{16})\{\eta^3\text{-}(HCH_2)(CH_2)C_6Me_4H_4\}][BF_4]$

145 $[Ru(\eta^6\text{-}C_{16}H_{16})\{\eta^4\text{-}(CH_2)_2C_6Me_4H_4\}]$

146 $[Ru(\eta^6\text{-}C_{16}H_{16})(\eta^3\text{-}C_6Me_5H_4)][BF_4]$

147 $[Ru(\eta^6\text{-}C_{16}H_{16})(\eta^3\text{-}C_6Me_4H_5)][BF_4]$

148 $[Ru(\eta^6\text{-}C_{16}H_{16})Cl(phen)][PF_6]$

149 $[Ru(\eta^6\text{-}C_{16}H_{16})Cl(py)(PMe_2Ph)][PF_6]$

Appendix III:

List of Figures, Schemes and Tables

Figures

Schemes

Tables

Appendix IV:

Publications Arising from this Work

i) *Bis*(allyl)Ruthenium(IV) Chemistry

1. "Synthesis and Characterisation of a Pyrazene Bridged Bis-allyl Ruthenium(IV) Complex. Crystal Structure of $[\{(\eta^3:\eta^3\text{-}C_{10}H_{16})RuCl_2\}_2(\mu\text{-}C_4H_4N_2)].2CHCl_3$"
   J. W. Steed and D. A. Tocher, *J. Organomet. Chem.*, 1991, **412**, C34.
2. "Characterisation of the Air and Water Stable Organometallic Ruthenium(IV) Complex $[(\eta^3:\eta^2:\eta^3\text{-}C_{12}H_{18})RuCl(H_2O)][BF_4]$"
   J. W. Steed and D. A. Tocher, *J. Chem. Soc., Chem. Commun.*, 1991, 1609.
3. "Organometallic Carboxylato Compounds of Ruthenium(IV)"
   J. W. Steed and D. A. Tocher, *Inorg. Chim. Acta*, 1991, **189**, 135.
4. "Synthesis of Cationic Ruthenium(IV) Allyl Compounds Containing Chelating N-Donor Ligands: X-ray Crystal Structure of $[(\eta^3:\eta^3\text{-}C_{10}H_{16})Ru(N_3C_{15}H_{11})]\text{-}[BF_4]_2.CH_3NO_2$"
   J. W. Steed and D. A. Tocher, *Inorg. Chim. Acta*, 1992, **191**, 29.
5. "A Novel Ruthenium(IV) Thiocyanato Bridged Dimer"
   J. W. Steed and D. A. Tocher, *J. Chem. Soc., Dalton Trans.*, 1992, 459.
6. "Binuclear Carboxylato Bridged Complexes of Ruthenium(IV)"
   J. W. Steed and D. A. Tocher, *Polyhedron*, 1992, **11**, 1849.
7. "Geometrical Isomerism in 2-Hydroxypyridinate and Pyridine-2-thiolate Complexes of Ruthenium(IV)"
   J. W. Steed and D. A. Tocher, *J. Chem. Soc., Dalton Trans.*, 1992, 2765.
8. "Bi- and Trinuclear Complexes of Ruthenium(IV) with N-Donor Ligands"
   J. W. Steed and D. A. Tocher, *Polyhedron*, 1992, **11**, 2729.
9. "Mono- and Bidentate Carboxylato Complexes of Ruthenium(IV)"
   B. Kavanagh, J. W. Steed and D. A. Tocher, *J. Chem. Soc., Dalton Trans.*, 1993, 327.

ii) ([2.2]Paracyclophane)Ruthenium Chemistry

1. "Some Reactions of $[(\eta^6\text{-}C_6Me_6)Ru(\eta^6\text{-}[2.2]paracyclophane)][BF_4]_2$ with Nucleophiles"
   J. W. Steed and D. A. Tocher, *J. Organomet. Chem.*, 1991, **412**, C37.

2. "Reactions of [(η^6-arene)Ru(η^6-[2.2]paracyclophane)][BF_4]$_2$ Complexes with Nucleophiles"
   M. R. J. Elsegood, J. W. Steed and D. A. Tocher, *J. Chem. Soc., Dalton Trans.*, 1992, 1797.
3. "Cyclohexenyl [2.2]Paracyclophane Complexes of Ruthenium(II): Highly Fluxional Agostics from the Sequential Reduction of Arenes"
   J. W. Steed and D. A. Tocher, *J. Organomet. Chem.*, 1993, **444**, C47.
4. "Sterically Controlled Double Nucleophilic Addition Reactions of ([2.2]Paracyclophane)(Arene)Ruthenium(II) Complexes and Reactions to Form Highly Fluxional Agostic Cyclohexenyls"
   J. W. Steed and D. A. Tocher, *J. Chem. Soc., Dalton Trans.*, in press.

Journal of Organometallic Chemistry, 412 (1991) C34–C36
Elsevier Sequoia S.A., Lausanne
JOM 22019PC

Preliminary communication

Synthesis and characterisation of a pyrazine bridged bis-allyl ruthenium(IV) complex. Crystal structure of $[\{(\eta^3:\eta^3\text{-}C_{10}H_{16})RuCl_2\}_2(\mu\text{-}C_4H_4N_2)]\cdot 2CHCl_3$

Jonathan W. Steed and Derek A. Tocher *

Department of Chemistry, University College London, 20 Gordon Street, London WC1H 0AJ (UK)

(Received April 8th, 1991)

Abstract

The reaction of pyrazine with the ruthenium(IV) bis-allyl dimer $[(\eta^3:\eta^3\text{-}C_{10}H_{16})RuCl(\mu\text{-}Cl)]_2$ gives the bridged binuclear complex $[\{(\eta^3:\eta^3\text{-}C_{10}H_{16})RuCl_2\}_2(\mu\text{-}C_4H_4N_2)]$ in high yield. The complex has been characterised by ^1H NMR spectroscopy and by a single-crystal X-ray diffraction study.

The organometallic chemistry of transition metals in high formal oxidation states is an area of growing interest [1,2]. An organometallic compound that has been known for many years yet has been little studied is the ruthenium(IV) dimer $[(\eta^3:\eta^3\text{-}C_{10}H_{16})RuCl(\mu\text{-}Cl)]_2$ [3], which is rather surprising given the profusion of studies on the related chloro-bridged ruthenium(II) dimers $[(\eta^6\text{-arene})RuCl(\mu\text{-}Cl)]_2$.

The crystal structure of $[(\eta^3:\eta^3\text{-}C_{10}H_{16})RuCl(\mu\text{-}Cl)]_2$ shows that the complex has C_i symmetry in the solid state, with the coordination about each metal atom best described as trigonal bipyramidal [4]. Nevertheless ^1H NMR studies clearly establish that in solution two diastereoisomers are present [5]. While one isomer is assumed to have the C_i symmetry observed in the solid state it is proposed that the second isomer has C_2 symmetry. In coordinating solvents the dimer is observed to be cleaved and exist as both equatorially and axially solvated monomers [5]. Reactions with neutral monodentate ligands also result in bridge cleavage and the formation of the simple adducts $[(\eta^3:\eta^3\text{-}C_{10}H_{16})RuCl_2L]$ (L = CO, PR_3, C_5H_5N, ^{t}BuNC) [6,7,8]. In this report we present our preliminary results on the synthesis of polynuclear compounds containing the "$[(\eta^3:\eta^3\text{-}C_{10}H_{16}Ru]^{2+}$" unit.

The reaction of $[(\eta^3:\eta^3\text{-}C_{10}H_{16})RuCl(\mu\text{-}Cl)]_2$ with between 1 and 10 molar equivalents of pyrazine in chloroform proceeds smoothly to give a compound with the stoichiometry $[\{(\eta^3:\eta^3\text{-}C_{10}H_{16})RuCl_2\}_2(\mu\text{-}C_4H_4N_2)]$ as the sole product (C,H,N,Cl analysis). The formation of appreciable quantities of the monomeric compound $[\{(\eta^3:\eta^3\text{-}C_{10}H_{16})RuCl_2(C_4H_4N_2)]$ was only observed when > 15 molar equivalents of the ligand were used. The ^1H NMR spectrum of the dinuclear compound recorded in $CDCl_3$ exhibited twice as many resonances as was expected

0022-328X/91/$03.50

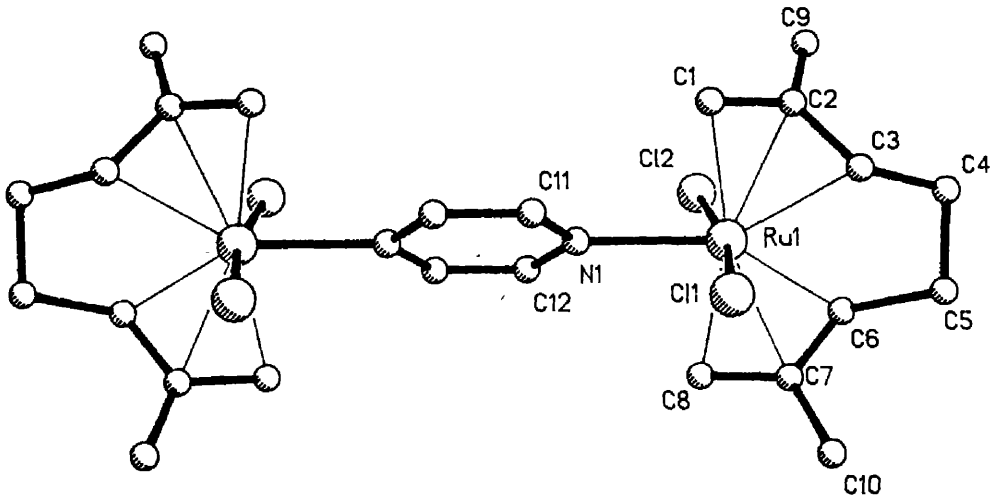

Fig. 1. Molecular structure of $[\{(\eta^3:\eta^3\text{-}C_{10}H_{16})RuCl_2\}_2(\mu\text{-}C_4H_4N_2)]$ showing the atom numbering scheme adopted. Selected bond lengths (Å): Ru(1)–N(1) 2.191(10), Ru(1)–Cl(1) 2.406(3), Ru(1)–Cl(2) 2.425(3), Ru(1)–C(1) 2.226(13), Ru(1)–C(2) 2.303(12), Ru(1)–C(3) 2.256(15), Ru(1)–C(6) 2.240(16), Ru(1)–C(7) 2.264(14), Ru(1)–C(8) 2.235 (12). Selected interbond angles (°): Cl(1)–Ru(1)–Cl(2) 170.2(1), Cl(1)–Ru(1)–N(1) 85.4(2), Cl(2)–Ru(1)–N(1) 84.8(2), Cl(1)–Ru(1)–C(2) 101.7(3), Cl(1)–Ru(1)–C(7) 83.3(4), Cl(2)–Ru(1)–C(2) 82.4(3), Cl(2)–Ru(1)–C(7) 100.8(4), C(2)–Ru(1)–C(7) 131.2(5), N(1)–Ru(1)–C(2) 114.7(4), N(1)–Ru(1)–C(7) 114.2(5).

for this formulation (e.g. four terminal allyl signals at δ 4.65, 4.62, 4.39, and 4.34 ppm). However, since both pyrazine resonances appeared as singlets (at δ 9.32 and 9.23 ppm) we were confident that the products were binuclear pyrazine-bridged species. It is likely that the doubling of the number of signals can be attributed to the presence of diastereoisomers similar to those observed in solutions of $[(\eta^3:\eta^3\text{-}C_{10}H_{16})RuCl(\mu\text{-}Cl)]_2$ [5]. To establish conclusively the structure of the product formed in this reaction we carried out a single crystal structural analysis *.

The X-ray study shows (Fig. 1) that in the crystalline material only one of the isomers is present. That isomer has overall C_i symmetry, while the organic ligands have local C_2 symmetry. This arrangement is similar to that observed for the parent chloro-bridged dimer in the solid state [3,4]. The geometry about the crystallographically unique metal ion is that of a distorted trigonal bipyramid with the chloride ligands occupying the axial positions, Cl(1)–Ru(1)–Cl(2) bond angle 170.2(1)°, and the organic moiety and neutral pyrazine ligand occupying the

* *Crystal data for* $C_{26}H_{38}N_2Cl_{10}Ru_2$: $M = 935.27$, a 7.297(2), b 9.889(2), c 13.411(4) Å, α 70.77, β 83.29, γ 89.70°, V 906.9 Å^3, $Z = 1$, d_{calc} 1.71 g/cm^3, $F(000)$ 466, μ(Mo-K_α) 15.8 cm^{-1}, triclinic space group $P\bar{1}$ (the asymmetric unit contains one half of the centrosymmetric molecule and one molecule of chloroform of crystallisation).

Structure determination: A crystal of dimensions 0.10×0.17×0.30 mm was used to collect 3122 unique data in the range $5° \leqslant 2\theta \leqslant 50°$ on a Nicolet R3m/V diffractometer equipped with graphite-monochromated Mo-K_α radiation. The data were corrected for Lorentz and polarisation effects, and for crystal decay (ca. 40%). The structure was solved by conventional Patterson and difference-Fourier techniques. Non-hydrogen atoms were refined anisotropically while hydrogens were placed in idealised positions (C–H 0.96 Å) and assigned a common isotropic thermal parameter ($U = 0.08$ Å^2). Full-matrix least-squares refinement gave $R = 0.064$ and $R_w = 0.066$ ($w^{-1} = \sigma^2(F) + 0.0008F^2$) for the 1864 unique data with $I \geqslant 3\sigma(I)$. All calculation were performed on a MicroVax II computer using SHELXTL PLUS software. A table of atom coordinates and a list of bond lengths and angles has been deposited at the Cambridge Crystallographic Data Centre.

equatorial sites. Equatorial coordination of a neutral ligand was also observed in the X-ray crystal structure of $[(\eta^3:\eta^3\text{-}C_{10}H_{16})RuCl_2(PF_3)]$ [8]. The $Ru-N_{(pyrazine)}$ distance is 2.19(1) Å, which is considerably greater than that observed in several well defined $[(NH_3)_5Ru(\mu\text{-pyz})Ru(NH_3)_5]^{n+}$ ($n = 4$, 3, 6) ions, 1.99–2.11 Å [9]. It is however similar to that observed in the organometallic ruthenium(II) cation $[(\eta^6\text{-}p\text{-}MeC_6H_4CHMe_2)Ru(pyz)_2Cl]^+$, 2.17 Å [10], although of course the pyrazine ligands in that complex are only coordinated to a single metal. The pyrazine ligand is inclined at an angle of 38.0° to the plane of the metal ion and halide ligands. The most likely structure for the second isomer, observed in solution, would have overall C_2 symmetry. Since the isomer ratio is independent of the precise conditions used in the synthesis we intend to study and report the kinetics of isomerism reaction at a later date.

Finally, using analogous synthetic procedures to those described above we examined the reaction of $[(\eta^3:\eta^3\text{-}C_{10}H_{16})RuCl(\mu\text{-}Cl)]_2$ with 1,3,5-triazine. In contrast to the results described above, these reaction lead to mixtures of products, viz. $[(\eta^3:\eta^3\text{-}C_{10}H_{16})RuCl_2(C_3H_3N_3)]$, $[\{(\eta^3:\eta^3\text{-}C_{10}H_{16})RuCl_2\}_2(\mu\text{-}C_3H_3N_3)]$, and $[\{(\eta^3:\eta^3\text{-}C_{10}H_{16})RuCl_2\}_3(\mu\text{-}C_3H_3N_3)]$.

Acknowledgements. We thank Johnson Matthey plc for generous loans of ruthenium trichloride and the SERC for financial support (J.W.S.) and for provision of the X-ray equipment.

References

1 C. Che, W. Cheng and T.C.W. Mak, J. Chem. Soc., Chem. Commun., (1987) 418.
2 W.A. Hermann, Angew. Chem., Int. Ed. Engl., 27 (1988) 1297.
3 L. Porri, M.C. Gallazzi, A. Colombo and G. Allegra, Tetrahedron Lett., (1965) 4187.
4 A. Colombo and G. Allegra, Acta Crystallogr., B27 (1971) 1653.
5 D.N. Cox and R. Roulet, Inorg. Chem., 29 (1990) 1360.
6 R.A. Head, J.F. Nixon, J.R. Swain and C.M. Woodard, J. Organomet. Chem., 76 (1974) 393.
7 D.N. Cox and R. Roulet, J. Chem. Soc., Chem. Commun., (1988) 951.
8 P.B. Hitchcock, J.F. Nixon and J. Sinclair, J. Organomet. Chem., 86 (1975) C34.
9 U. Furholz, H.-B. Burgi, F.E. Wagner, A. Stebler, J.H. Ammeter, E. Krausz, R.J.H. Clark, M.J. Stead and A. Ludi, J. Am. Chem. Soc., 106 (1984) 121.
10 D.A. Tocher, R.O. Gould, T.A. Stephenson, M.A. Bennett, J.P. Ennett, T.W. Matheson, L. Sawyer and V.K. Shah, J. Chem. Soc., Dalton Trans., (1983) 1571.

Characterisation of the Air- and Water-stable Organometallic Ruthenium(IV) Complex $[(\eta^3:\eta^2:\eta^3\text{-}C_{12}H_{18})RuCl(H_2O)][BF_4]$

Jonathan W. Steed and Derek A. Tocher*

Department of Chemistry, University College London, 20 Gordon Street, London WC1H 0AJ, UK

The reaction of $[(\eta^3:\eta^2:\eta^3\text{-}C_{12}H_{18})RuCl_2]$ with $Ag[BF_4]$ (1 : 1 mole ratio) in water–acetone gives an air-stable aqueous solution of $[(\eta^3:\eta^2:\eta^3\text{-}C_{12}H_{18})RuCl(H_2O)][BF_4]$; the isolated complex has been characterised by ^1H and ^{13}C NMR spectroscopy and X-ray crystallography.

At the present time there is considerable interest in water-soluble organometallic compounds for a variety of catalytic reactions[1] and in organometallic compounds with high formal oxidation states,[2] although the two features rarely appear concurrently. In many cases water-solubility is conferred on the metal complex by the use of ligands which are themselves water-soluble *e.g.* $(m\text{-}NaSO_3C_6H_4)_3P$,[3] although in other instances genuine aquo complexes must be the important intermediates in the catalytic cycle.

The ruthenium(IV) compound $[(\eta^3:\eta^2:\eta^3\text{-}C_{12}H_{18})RuCl_2]$ **1** was first prepared and characterised[4] by Shaw and Truter in the 1960s. The compound is diamagnetic and the geometry about the metal centre is best described as approximately pentagonal bipyramidal. There are several reports of catalytic applications[5] of **1** but only a single study of its chemistry.[6] We now report a new reaction of **1** giving rise to an air- and moisture-stable organometallic ruthenium(IV) compound which also contains a strongly bonded water ligand.

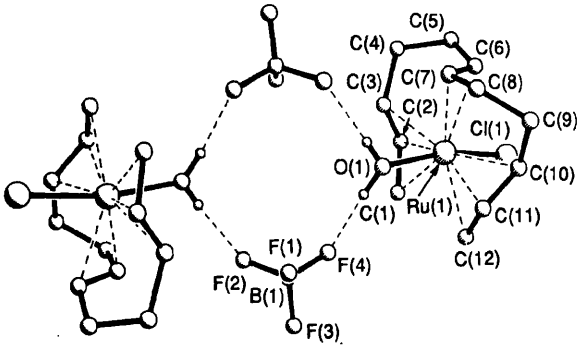

Fig. 1 The crystal and molecular structure of $[(\eta^3:\eta^2:\eta^3\text{-}C_{12}H_{18})\text{-}RuCl(H_2O)][BF_4]$ showing the atom numbering scheme adopted. Selected bond lengths (Å) and angles (°): Ru(1)–Cl(1) 2.396(2), Ru(1)–C(1) 2.196(6), Ru(1)–C(2) 2.207(6), Ru(1)–C(3) 2.282(6), Ru(1)–C(6) 2.314(5), Ru(1)–C(7) 2.291(5), Ru(1)–C(10) 2.320(5), Ru(1)–C(11) 2.210(6), Ru(1)–C(12) 2.214, Ru(1)–O(1) 2.165(5), O(1)···F(4) 2.74(3), O(1A)···F(2) 2.68(3); O(1)–Ru(1)–Cl(1) 169.0(1), C(2)–Ru(1)–C(11) 150.5(2).

The reaction of **1** with one molar equivalent of $Ag[BF_4]$ in acetone–water (1:1 v/v) gives a straw-brown solution from which brown crystals of $[(\eta^3:\eta^2:\eta^3\text{-}C_{12}H_{18})RuCl(H_2O)][BF_4]$ **2** are deposited.† The ^1H NMR spectrum‡ of diamagnetic compound **2** is substantially more complicated than that of **1** and is generally similar to that previously reported for $[(\eta^3:\eta^2:\eta^3\text{-}C_{12}H_{18})RuI(CH_3)]$[6] indicating that the two axial sites of the pentagonal bipyramidal complex are inequivalent. This is confirmed by the $^{13}C\{H\}$ NMR spectrum‡ which exhibits twelve resonances for the dodeca-2,6,10-triene-1,12-diyl ligand rather than the six observed for **1**. The presence of a water molecule is indicated by the appearance of a broad singlet in the ^1H NMR spectrum, at δ 2.21, integrating for two protons, and ν(OH) bands in the infrared spectrum at 3369 and 3169 cm^{-1}. The structure has been confirmed by X-ray crystallography.§

† Satisfactory elemental analysis (C, H, Cl) has been obtained.

‡ *^1H NMR data* (400 MHz, $CDCl_3$): $\eta^3:\eta^2:\eta^3\text{-}C_{12}H_{18}$; δ 2.45 (m, 2H), 2.63 (m, 2H), 2.82 (m, 1H), 3.16 (m, 1H), 3.19 (m, 2H), 3.39 (d, $^3J_{HH}$ 12 Hz, 1H), 3.87 (d, $^3J_{HH}$ 12 Hz, 1H), 4.40 (m, 1H), 5.15 (dd, $^2J_{HH}$ 2, $^3J_{HH}$ 8 Hz, 1H), 5.26 (m, 2H), 5.30 (m, 1H), 5.68 (m, 1H), 5.78 (d, $^3J_{HH}$ 13 Hz, 1H), 5.93 (dd, $^3J_{HH}$ 13 and 4.5 Hz, 1H); H_2O, δ 2.21 (s, 2H). $^{13}C\{^1H\}$ NMR data (100.6 MHz, CD_3CN): $\eta^3:\eta^2:\eta^3\text{-}C_{12}H_{18}$; δ 24.2, 24.6, 36.3, 37.0, 63.2, 66.4, 108.5, 109.0, 113.2, 118.0, 122.2, 128.6.

§ *Crystal data*: $C_{12}H_{20}BClF_4ORu$, brown needles, M = 403.65, monoclinic, space group $P2_1/n$, a = 7.366(1), b = 14.132(3), c = 14.510(3) Å, β = 101.22(2)°, U = 1482 Å^3, Z = 4, D_c = 1.81 g cm^{-3}, Mo-Kα radiation (λ = 0.71073 Å), μ(Mo-Kα) = 12.5 cm^{-1}. A total of 2915 reflections were measured in the range 5° ≤ 2θ ≤ 50° on a Nicolet R3mV diffractometer. Data corrected for Lorentz and polarisation effects and an empirical absorption correction applied. The 1803 unique data with $I \geq 3\sigma(I)$ were used to solve (Patterson method) and refine (full-matrix least-squares) the structure. All non-hydrogen atoms were refined anisotropically, the hydrogens on the water molecule were located and their coordinates refined, while the remaining hydrogens were placed in idealised positions (C–H 0.96 Å). The fluorines of the $[BF_4]^-$ ions were disordered over two positions (occupancy refined to 50%). At the conclusion of refinement R = 0.0323, R_w = 0.0372, and the largest shift/esd was 0.02. Calculations were performed on a Microvax II computer using the SHELXTL PLUS program package. Atomic coordinates, bond lengths and angles, and thermal parameters have been deposited at the Cambridge Crystallographic Data Centre. See Notice to Authors, Issue No. 1.

The crystal and molecular structure of **2**, together with the atom numbering scheme adopted, is shown in Fig. 1. For reasons which have been discussed in detail previously[4] the geometry about the ruthenium(IV) centre is best described as a distorted pentagonal bipyramid. A chloride ion and a water molecule occupy the two axial sites. The bonds to these ligands [Ru(1)–Cl(1) 2.396(2), Ru(1)–O(1) 2.165(5) Å] are not collinear but subtend an angle of 169.0(1)° at the metal ion. The six carbon atoms of the two η^3-allyl functionalities are not equidistant from the metal but form two distinct sets [av. Ru(1)–C(1), C(2), C(11), C(12) 2.206(6), av. Ru(1)–C(3), C(10) 2.301(5) Å] indicative of an imbalance between the steric requirements of the metal and that of the ligand. The distortions in the organic ligand which arise on coordination to this metal centre also result in long bonds to the alkenic functionality [Ru(1)–C(6) 2.314, Ru(1)–C(7) 2.291(5) Å]. This situation can be contrasted with that observed in related bis-allyl compounds of ruthenium(IV), containing the ligand $\eta^3:\eta^3\text{-}C_{10}H_{16}$, in which the six ruthenium carbon bond lengths are invariably statistically indistinguishable.[7] Examination of Fig. 1 clearly explains the reason behind the complexity of the NMR spectra. While the proton on C(2) is pseudo-eclipsed with the chloride ligand, that on C(11) has a similar orientation with respect to the coordinated water molecule, hence all the protons and carbon atoms of the organic ligand are unique. In the crystalline solid pairs of cations are hydrogen-bonded together *via* bridging tetrafluoroborate anions. Each tetrafluoroborate anion forms two relatively short hydrogen bonds [av. O···F 2.71(3) Å] to coordinated water molecules.

Compound **2** is readily redissolved in aqueous solution and these solutions are stable in air for periods of up to five days. This observation is virtually without precedent in π-allyl chemistry, only one other recently reported compound, $[(\eta^3:\eta^3\text{-}C_{10}H_{12})RuCl(CH_5N_3O)]Cl$,[8] having similar properties. The existence of **2** offers the potential for the development of water-based organometallic compounds with the metal in a non-traditional oxidation state. Indeed it is not at all unlikely that related species may exist in aqueous solutions of ruthenium trichloride containing unsaturated organic molecules. Studies on the reactions and possible catalytic activity of **2** are planned.

We thank the SERC for financial support (J. W. S.) and provision of the X-ray equipment and Johnson Matthey plc for generous loans of ruthenium trichloride.

Received, 22nd August 1991; Com. 1/04413C

References

1 T.-K. Chan and C.-J. Li, *Organometallics*, 1990, **9**, 2649.
2 W. A. Hermann, *Angew. Chem., Int. Ed. Engl.*, 1988, **27**, 1297.
3 E. Fache, F. Senocq, C. Santini and J.-M. Basset, *J. Chem. Soc., Chem. Commun.*, 1990, 1776.
4 J. E. Lydon, J. K. Nicholson, B. L. Shaw and M. R. Truter, *Proc. Chem. Soc.*, 1964, 421; J. K. Nicholson and B. L. Shaw, *J. Chem. Soc., (A)*, 1966, 807; J. E. Lydon and M. R. Truter, *J. Chem. Soc., (A)*, 1968, 362.
5 A. Misono, Y. Uchida, M. Hidai and I. Inomata, *J. Chem. Soc., Chem. Commun.*, 1968, 704; M. Hidai, K. Ishimi, M. Iwase, E. Tanaka and Y. Uchida, *Tetrahedron Lett.*, 1973, 1189.
6 H. Nagashima, T. Ohshima and K. Itoh, *Chem. Lett.*, 1984, 789.
7 A. Colombo and G. Allegra, *Acta Crystallogr., Sect. B*, 1971, **27**, 1653; J. G. Toerien and P. H. van Rooyen, *J. Chem. Soc., Dalton Trans.*, 1991, 1563; J. W. Steed and D. A. Tocher, *J. Organomet. Chem.*, 1991, **412**, C34.
8 S. O. Sommerer and G. J. Palenik, *Organometallics*, 1991, **10**, 1223.

Inorganica Chimica Acta

LETTER

Organometallic carboxylato compounds of ruthenium(IV)

Jonathan W. Steed and Derek A. Tocher*

Department of Chemistry, University College London, 20 Gordon Street, London WC1H 0AJ (UK)

(Received September 4, 1991)

Since the discovery of $[(\eta^3:\eta^3\text{-}C_{10}H_{16})RuCl(\mu\text{-}Cl)]_2$ (**1**) in 1965 [1, 2] its chemistry, in comparison to that of the related compounds $[(\eta^6\text{-arene})RuCl(\mu\text{-}Cl)]_2$ [3, 4], has been relatively neglected. Recent interest in the organometallic chemistry of metals in relatively high formal oxidation states [5, 6] has however revived interest in this compound.

Compound **1** exists as two diastereoisomers of C_i and C_2 symmetry [7] which arise as a consequence of the chirality of the '$(\eta^3:\eta^3\text{-}C_{10}H_{16})Ru^{2+}$' fragment. This feature is reflected in the ^1H NMR spectrum of **1** which shows twice the number of expected resonances [76]. The geometry about the metal atom is loosely described as trigonal bipyramidal [8] with the axial sites being occupied by one bridging and one terminal chloride ligand. The number of resonances in the ^1H NMR spectrum of **1** is further redoubled as a consequence of the inequivalence of these axial sites thus giving, for example, eight resonances for the terminal allyl protons and four resonances for the allylic methyl groups [7]. The sensitivity of the NMR spectra of the bis(allyl) ligand to the geometry about the metal centre makes this technique an excellent probe for studying ligand substitution reactions at the ruthenium(IV) centre.

Carboxylates, particularly trifluoroacetates, have been shown in (arene)ruthenium(II) chemistry [9, 10] to make particularly good leaving groups rendering (arene)ruthenium trifluoroacetate complexes useful precursors to a wide range of arene(ruthenium) complexes. We now report the synthesis and ^1H NMR characterisation of three bis(allyl)-ruthenium(IV) carboxylates and highlight the differences in reactivity compared with their ruthenium(II) analogues.

In common with the analogous $[(\eta^6\text{-arene})RuCl(\mu\text{-}Cl)]_2$ complexes (arene = benzene, *p*-cymene, hexamethylbenzene) [9], reaction of **1** with 2 molar equivalents of silver acetate at room temperature in acetone/water gives a chelate complex, $[(\eta^3:\eta^3\text{-}C_{10}H_{16})RuCl(O_2CCH_3)]$ (**3**) in 70% yield. The complex exhibits four terminal allyl singlets (δ 5.51, 4.65, 4.63, 3.56 ppm) and two methyl resonances (δ 2.29, 2.12 ppm) in its ^1H NMR spectrum, indicative of the inequivalent axial sites of the trigonal bipyramidal ruthenium centre. In contrast the analogous reaction with a 4:1 mole ratio of silver trifluoroacetate produces a complex displaying only half this number of ^1H NMR resonances, i.e. two terminal allyl singlets (δ 5.68, 4.23 ppm) and a single methyl resonance (δ 2.12 ppm). A sharp peak of integral 2H is also observed at 7.11 ppm. The IR spectrum of this material displays two broad bands at 3362 and 3196 cm^{-1} in addition to bands due to ν(CO) at 1703, 1670 and 1421 cm^{-1}, and ν(CF) at 1196 and 1143 cm^{-1}. From this data and in conjunction with microanalytical and mass spectroscopic measurements the complex is identified as the novel water solvate $[(\eta^3:\eta^3C_{10}H_{16})Ru(O_2CCF_3)_2(OH_2)]$ (**2**). Differences in reactivity of the two carboxylate ligands must be a consequence of the different electronic properties of the substituent groups.

Compound **2** decomposes above 140 °C but will sublime intact at *c.* 80 °C under reduced pressure with no trace of displacement of the water molecule. Refluxing **2** in dichloromethane containing anhydrous magnesium sulfate results in recovery of the starting material. Interestingly **2** is also obtained from refluxing **1** in trifluoroacetic acid. From these observations we infer the water ligand to be extremely tightly bound to the metal centre, an observation supported by its low substitutional lability. Preliminary results indicate displacement of the water ligand by pyrazene to be *c.* 50% complete after 24 h at room temperature.

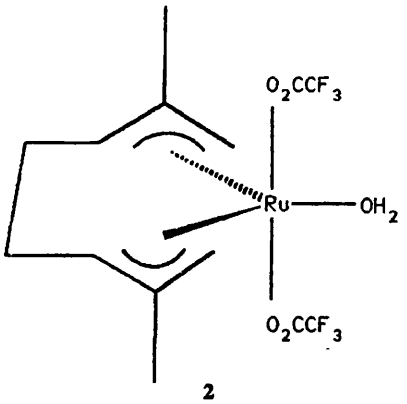

2

*Author to whom correspondence should be addressed.

0020-1693/91/$3.50

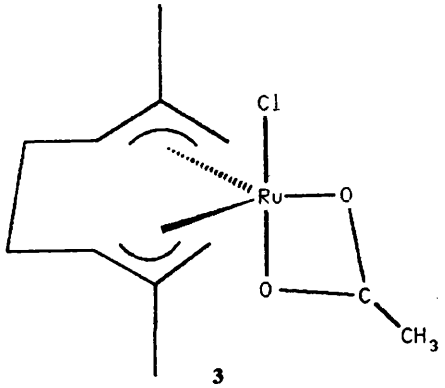

3

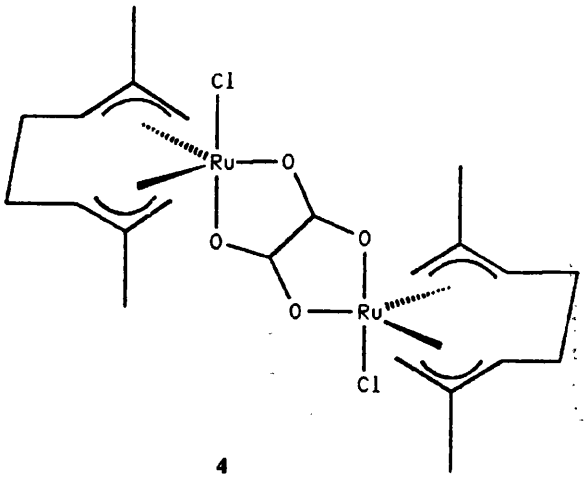

4

Reaction of **1** with a 1:2 mole ratio of silver trifluoroacetate, surprisingly, also gives **2**, along with a large quantity of unreacted starting material.

Reaction of **1** with silver oxalate in both 1:2 and 1:4 mole ratios produces, as the sole product, the binuclear bridged species $[\{(\eta^3:\eta^3\text{-}C_{10}H_{16})RuCl\}_2(\mu_2\text{-}O_2CCO_2)]$ (**4**) the ^1H NMR spectrum of which displays eight terminal allyl resonances (δ 5.32, 5.19, 4.52, 4.43, 4.33, 4.18, 3.36, 3.24 ppm) and four methyl resonances (δ 2.33, 2.30, 2.19, 2.15 ppm). This observation is consistent with the presence of two diastereoisomers, of C_1 and C_2 symmetry, similar to those observed for **1**. The oxalate ligand also raises the possibility of linkage isomerism since it may bind to a metal centre in either monodentate fashion or bidentately, through either a three or four atom linkage. Preliminary results of a single crystal X-ray diffraction study indicate a bidentate mode of coordination through a four atom linkage so forming two fused five membered rings. This is the normal mode of coordination for binuclear oxalato bridged systems [11, 12].

Compounds **2**, **3** and **4** exhibit three different modes of coordination for the carboxylate ligands. Compound **2** can be contrasted with the ruthenium(II) compound $[(\eta^6\text{-}C_6H_6)RuCl(O_2CCF_3)]$ which is formed by analogous synthetic routes [9] and in which the trifluoroacetate ligand exhibits bidentate coordination. Work is in progress with a number of chlorinated carboxylates to determine the 'crossover' point, in terms of the electronic effects of the substituent groups, between monodentate and bidentate coordination modes and investigations into the reactivity of the compounds described in this short report are being undertaken.

Acknowledgements

We thank Johnson Matthey PLC for generous loans of ruthenium trichloride and the SERC for a studentship (J.W.S.).

References

1 L. Porri. M.C. Gallazzi, A. Colombo and G. Allegra, *Tetrahedron Lett., 47* (1965) 4187.
2 A. Colombo and G. Allegra, *Acta Crystallogr., Sect. B, 27* (1971) 1653.
3 P. M. Maitlis, *Chem. Soc. Rev., 10* (1981) 1.
4 M. A. Bennett, *Comprehensive Organometallic Chemistry*, Vol. IV, Pergamon, Oxford, 1982, Ch. 32.
5 C. Che, W. Cheng and T. C. W. Mak, *J. Chem. Soc., Chem. Commun.*, (1987) 418.
6 W. A. Hermann, *Angew. Chem., Int. Ed. Engl., 27* (1988) 1297.
7 D. N. Cox and R. Roulet, *Inorg. Chem., 29* (1990) 1360.
8 J. G. Toerien and P. H. van Rooyen, *J. Chem. Soc., Dalton Trans.*, (1991) 1563.
9 D. A. Tocher, R. O. Gould, T. A. Stephenson, M. A. Bennett, J. P. Ennett, T. W. Matheson, L. Sawyer and V. K. Shah, *J. Chem. Soc., Dalton Trans.*, (1983) 1571.
10 E. C. Morrison, C. A. Palmer and D. A. Tocher, *J. Organomet. Chem., 349* (1988) 405.
11 H. D. Hausen, K. Mertz and J. Weidlein, *J. Organomet. Chem., 67* (1974) 7.
12 R. Deyrieux and A. Peneloux, *Bull. Soc. Chim. Fr.*, (1969) 2675.

Inorganica Chimica Acta

LETTER

Synthesis of cationic ruthenium(IV) allyl compounds containing chelating N-donor ligands: X-ray crystal structure of $[(\eta^3:\eta^3\text{-}C_{10}H_{16})Ru(N_3C_{15}H_{11})][BF_4]_2 \cdot CH_3NO_2$

Jonathan W. Steed and Derek A. Tocher*

Department of Chemistry, University College London, 20 Gordon Street, London WC1H 0AJ (UK)

(Received July 5, 1991; revised October 17, 1991)

The chemistry of the ruthenium(IV) chloro bridged dimer $[(\eta^3:\eta^3\text{-}C_{10}H_{16})RuCl(\mu\text{-}Cl)]_2$ (**1**) has been surprisingly neglected in spite of the fact that it has been known since 1965 [1, 2]. Recent interest, however, in the chemistry of organometallic compounds in high formal oxidation states [3, 4], especially those possessing the property of water solubility [5], has renewed interest into the reactions of **1** by virtue of its ready preparation and versatile chemistry.

Previous reports [6, 7] have described **1** as existing as two diastereoisomers of C_2 and C_i symmetry, the latter having been characterised by X-ray crystallography [2].

Compound **1** is known to react with neutral, monodentate ligands L (L=PF_3, PPh_3, pyridine, CO etc.) to form simple adducts $[(\eta^3:\eta^3\text{-}C_{10}H_{16})RuCl_2L]$. **1** will also react with bidentate chelating ligands such as benzothiazole-2-thiolate [7] and semicarbazide [5]. These complexes are diastereotopic (due to inequivalent axial sites) and characteristically exhibit two singlet resonances due to magnetically inequivalent methyl groups and four resonances due to the terminal allylic protons of the $\eta^3:\eta^3\text{-}C_{10}H_{16}$ ligand. In alcoholic solvents the reaction of **1** with $Ag[BF_4]$ has been shown to produce solvated Ru^{2+} cations [8]. We now report preliminary results on some reactions of **1** with the chelating ligands 2,2′:6,2″-terpyridine (terpy), 2,2′-bipyridyl (bipy) and 1,10-phenanthroline (phen) via pretreatment with silver tetrafluoroborate in the non-reducing solvent, acetone.

In common with the analogous ruthenium(II) arene complexes [9], we find that, in acetone, treatment of **1** with $Ag[BF_4]$ leads to monocationic and dicationic solvate species which readily react with Lewis bases. Treatment of **1** with four equivalents of $Ag[BF_4]$ in acetone proceeds smoothly to generate an orange solution of the tris solvate complex. Stirring the filtered solution with two equivalents of 2,2′:6′,2″-terpyridine over several hours gives a yellow precipitate of $[(\eta^3,\eta^3\text{-}C_{10}H_{16})Ru(terpy)][BF_4]_2$ (**3**) (C, H, N analysis). The ^1H NMR spectrum of this material shows a single set of resonances for the allyl moiety (i.e. two terminal allyl singlets at δ 3.94, 2.94 ppm and one methyl singlet resonance at δ 2.11 ppm) and a further six signals due to the terpyridine ligand. This spectrum is consistent with a mononuclear complex ion with the two axial pyridyl rings equivalent [6].

The X-ray crystal structure of **3** (Fig. 1) shows the allyl ligand to have the usual C_2 symmetry [2, 5, 7, 10]. The geometry about the metal ion is best described as a distorted trigonal bipyramid with the terminal pyridyl rings occupying the axial sites, r(Ru–N_{ax}) 2.16(1) Å. The two Ru–N_{ax} bonds are not collinear (N(1)–Ru(1)–N(3) 154.5(4)°). Although much of the distortion is due to the chelating nature of the polypyridine ligand (cf. a corresponding angle of 156.4°

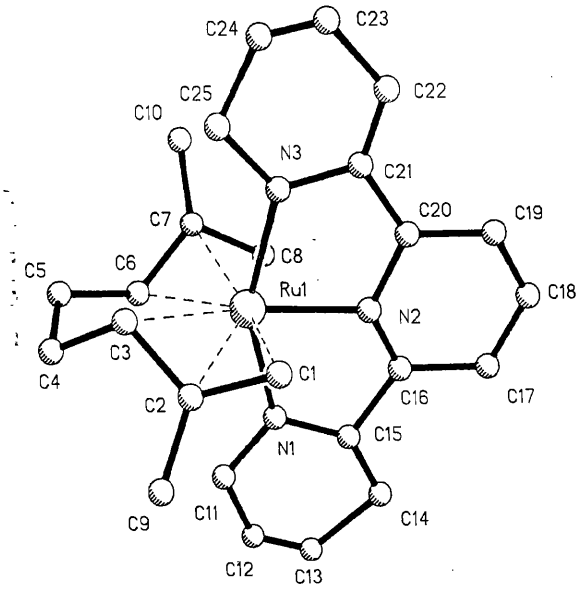

Fig. 1. View of the structure of one of the $[(\eta^3:\eta^3\text{-}C_{10}H_{16})Ru(N_3C_{15}H_{11})]$ cations (the other is essentially identical) showing the atom labelling adopted. Selected bond lengths (Å): Ru(1)–N(1) 2.172(10), Ru(1)–N(2) 2.018(10), Ru(1)–N(3) 2.147(9), Ru(1)–C(1) 2.283(18), Ru(1)–C(2) 2.241(15), Ru(1)–C(3) 2.423(18), Ru(1)–C(6) 2.281(15), Ru(1)–C(7) 2.294(12), Ru(1)–C(8) 2.203(15). Selected interbond angles (°): N(1)–Ru(1)–N(2) 77.1(4), N(1)–Ru(1)–N(3) 154.5(4), N(2)–Ru(1)–N(3) 77.5(4), N(1)–Ru(1)–C(2) 88.1(5), N(1)–Ru(1)–C(7) 103.4(4), N(3)–Ru(1)–C(2) 104.7(5), N(3)–Ru(1)–C(7) 84.7(4), C(2)–Ru(1)–C(7) 131.7(4), N(2)–Ru(1)–C(2) 114.5(5), N(2)–Ru(1)–C(7) 113.8(4).

*Author to whom correspondence should be addressed.

0020-1693/92/$5.00

in the benzothiazole-2-thiolate complex $[(\eta^3:\eta^3\text{-}C_{10}H_{16})RuCl(SNC_7H_4S\text{-}2)$ [7]) it should be noted that even in $[\{(\eta^3:\eta^3\text{-}C_{10}H_{16})RuCl_2\}_2(\mu\text{-}N_2C_4H_4)]$ the angle between the axial ligands is reduced to 170° [11]. The $Ru\text{–}N_{eq}$ distance is 2.02(1) Å, a value rather shorter than that observed in the equatorial adduct $[\{(\eta^3:\eta^3\text{-}C_{10}H_{16})RuCl_2\}_2(\mu\text{-}N_2C_4H_4)]$, 2.19 Å. This difference is attributed to the distortions of the terpyridine ligand which occur on coordination to a metal centre and are often observed in polypyridyl chemistry [12].

The single most remarkable feature of this compound is the combination of its stability and water solubility. As has been commented upon very recently [5] this observation has important implications for the nature of aqueous solutions of ruthenium trichloride with unsaturated organic molecules and indicates an area of water-based organometallic chemistry and catalysis which had previously gone unrecognised.

Using a 2:1:1 mole ratio of $Ag[BF_4]$:**1**:L_2 an analogous synthetic procedure gives the monocationic species $[(\eta^3:\eta^3\text{-}C_{10}H_{16})RuCl(L_2)][BF_4]$ (**2**) (L_2=2,2′-bipyridyl or 1,10-phenanthroline) which have been characterised by microanalysis and ^1H NMR spectroscopy. In contrast to the ^1H NMR spectrum of **3**, these compounds show twice as many resonances for the dimethyloctadienediyl ligands (e.g. terminal CH_2 δ 4.35, 4.02, 3.69, 2.49 ppm, CH_3 δ 2.45, 1.77 ppm, L_2=bipy; terminal CH_2 δ 4.36, 4.00, 3.47, 2.44 ppm, CH_3 δ 2.50, 1.76 ppm, L_2=phen) and eight resonances for the bipy and phen ligands. This type of pattern is consistent with inequivalent axial sites on the trigonal bipyramidal ruthenium(IV) ion, and closely mimics the pattern of resonances observed with other complexes containing chelating ligands [7].

Experimental

Crystal data for $C_{26}H_{30}N_4O_2F_8B_2Ru$

M=705.23, a=7.121(2), b=31.412(8), c=13.373(3) Å, β=101.13(2)°, monoclinic, space group *Pc*, V=2935 Å^3, Z=4, D_{calc}=1.60 g cm^{-1}, $F(000)$=1424, μ(Mo Kα)=6.03 cm^{-1}, the asymmetric unit contains two enantiomeric cations, four tetrafluoroborate anions and two molecules of nitromethane of crystallisation.

Structure determination

A yellow crystal of dimensions 0.4×0.4×0.6 mm was used to collect 5518 unique data in the range $5 \leqslant 2\theta \leqslant 50°$ on a Nicolet R3mV diffractometer equipped with graphite monochromated Mo Kα radiation. The data were corrected for Lorentz and polarisation effects and for crystal decay (*c.* 30%). An empirical absorption correction was applied. The space group was identified from the systematic absences as either *P2/c* or *Pc*. The 3689 reflections with $I \geqslant 3\sigma(I)$ were used to solve (direct methods) and refine (blocked least-squares) the structure in the space group *Pc*. We were very aware that problems are frequently encountered when the choice of space group is *Pc* or *P2/c*, however although the coordinates of the cations appear to be symmetry related the fact that only *one* of the four $[BF_4]^-$ anions, in the asymmetric unit in the *Pc* refinement, is disordered, is sufficient to lower the symmetry and establish *Pc* as the correct space group. Metal atoms were refined anisotropically but an isotropic model was used for the remaining light atoms due to the lack of data. Hydrogen atoms were placed in their predicted positions and allowed to ride on the atoms to which they were attached, r(CH) 0.96 Å, and were assigned a common isotropic temperature factor, U_{iso} 0.08 Å^2. One of the tetrafluoroborate anions was disordered and was fixed as an idealised tetrahedron. At the end of refinement (353 parameters) R=0.0640, R_w=0.0717 (w^{-1}=$\sigma^2(F)+0.000682F^2$). All calculations were carried out on a Micro Vax II computer using SHELXTL PLUS software [13].

Acknowledgements

We thank Johnson Matthey plc for generous loans of ruthenium trichloride and the SERC for financial support (J.W.S.) and for provision of the X-ray equipment. We also thank Professor M. R. Truter for helpful discussion of the crystallographic data.

References

1 L. Porri, M. C. Gallazzi, A. Colombo and G. Allegra, *Tetrahedron Lett.*, (1965) 4187.
2 A. Colombo and G. Allegra, *Acta Crystallogr. Sect. B, 27* (1971) 1658.
3 C. Che, W. Cheng and T. C. W. Mak, *J. Chem. Soc., Chem. Commun.*, (1987) 418.
4 W. A. Hermann, *Angew. Chem., Int. Ed. Engl., 27* (1988) 1297.
5 S. O. Sommerer and G. J. Palenik, *Organometallics, 10* (1991) 1223.
6 D. N. Cox and R. Roulet, *Inorg. Chem., 29* (1990) 1360.
7 J. G. Toerien and P. H. van Rooyen, *J. Chem. Soc., Dalton Trans.*, (1991) 1563.
8 D. N. Cox and R. Roulet, *J. Chem. Soc., Chem. Commun.*, (1988) 951.
9 M. A. Bennett and T. W. Matheson, *J. Organomet. Chem., 175* (1979) 87.
10 P. B. Hitchcock, J. F. Nixon and J. Sinclair, *J. Organomet. Chem., 86* (1975) C34.
11 J. W. Steed and D. A. Tocher, *J. Organomet. Chem., 412* (1991) C34.
12 E. C. Constable, *Adv. Inorg. Radiochem., 30* (1986) 69.
13 G. M. Sheldrick, *SHELXTL PLUS*, an integrated system for refining and displaying crystal structures from diffraction data, University of Gottingen, FRG, 1986.

A Novel Organometallic Ruthenium(IV) Thiocyanato-bridged Dimer†

Jonathan W. Steed and Derek A. Tocher*
Department of Chemistry, University College London, 20 Gordon St., London WC1H 0AJ, UK

Treatment of the ruthenium(IV) chloro-bridged dimer $[\{Ru(\eta^3:\eta^3\text{-}C_{10}H_{16})Cl(\mu\text{-}Cl)\}_2]$ **1** with silver thiocyanate in acetone–water gives the thiocyanato S,N-bridged dimer $[\{Ru(\eta^3:\eta^3\text{-}C_{10}H_{16})Cl(\mu\text{-}SCN)\}_2]$ **2** which exists as two diastereomeric forms respectively of C_i **2a** and C_2 **2b** symmetry. The X-ray crystal structure of **2b** shows the molecule to contain an unusually puckered eight-membered '$Ru_2(SCN)_2$' ring.

The relatively unexplored chemistry of the ruthenium(IV) chloro-bridged dimer $[\{Ru(\eta^3:\eta^3\text{-}C_{10}H_{16})Cl(\mu\text{-}Cl)\}_2]$ **1**[1,2] is an area of fast growing interest.[3–5] Compound **1** has been shown, by ^1H NMR spectroscopy, to exist as two diastereoisomers,[6] the *meso* and *rac* forms, of C_i and C_2 symmetry respectively. Although the latter is slightly more stable in solution[6] $\{[C_2]/[C_i]\ (298\ K) = 1.25\}$ it is the *meso* form which has been crystallographically characterised.[2] We have prepared a related pyrazine-bridged binuclear compound[7] $[\{Ru(\eta^3:\eta^3\text{-}C_{10}H_{16})Cl_2\}_2(\mu\text{-}N_2C_4H_4)]$ **3** which also exists as two diastereoisomers as a consequence of the chirality of the '$(\eta^3:\eta^3\text{-}C_{10}H_{16})Ru$' fragment. Once again it is the C_i form which has been crystallographically characterised. We now report the synthesis of the *meso* and *rac* forms of a second dimeric species derived from **1**, namely $[\{Ru(\eta^3:\eta^3\text{-}C_{10}H_{16})Cl(\mu\text{-}SCN)\}_2]$ **2a** and **2b** respectively, and describe for the first time the crystal structure of a C_2 isomer, **2b**.

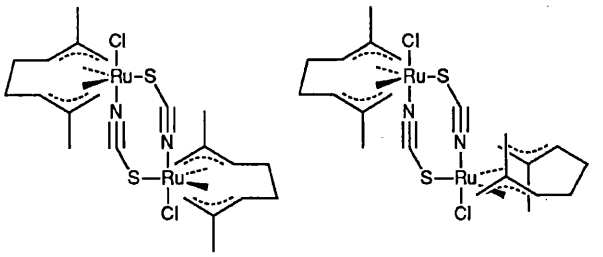

2a **2b**

Experimental

Infrared spectra were recorded on a Perkin-Elmer 983 grating spectrometer between 4000 and 200 cm^{-1} as KBr discs and Nujol mulls on CsI plates and NMR spectra on a Varian VXR400 spectrometer at University College London. Microanalyses were carried out by the departmental service. Mass spectra were run by the University of London Intercollegiate Research Service at the School of Pharmacy. All manipulations were carried out under nitrogen with degassed solvents using conventional Schlenk-line techniques.

The compound $[\{Ru(\eta^3:\eta^3\text{-}C_{10}H_{16})Cl(\mu\text{-}Cl)\}_2]$ was prepared by published methods.[1,3,6] Ruthenium trichloride hydrate was obtained on loan from Johnson Matthey plc and was purified before use by dissolution in water and boiling to dryness. All other reagents and materials were obtained from the usual commercial sources.

Preparation of $[\{Ru(\eta^3:\eta^3\text{-}C_{10}H_{16})Cl(\mu\text{-}SCN)\}_2]$ **2**.—The compound $[\{Ru(\eta^3:\eta^3\text{-}C_{10}H_{16})Cl(\mu\text{-}Cl)\}_2]$ (0.1107 g, 0.180 mmol) was suspended in degassed acetone (2.5 cm^3) and degassed water (2.5 cm^3). Silver(I) thiocyanate (0.0614 g, 0.370 mmol) was added and the mixture stirred for 1 h. The resulting yellow solution was filtered through Celite to remove the precipitate of AgCl and the volume was reduced to about one quarter, resulting in precipitation of the yellow product which was isolated by filtration, washed with acetone and diethyl ether and air dried. Yield: 0.0514 g, 0.078 mmol, 43% (Found: C, 40.0; H, 4.9; N, 3.9. Calc. for $C_{22}H_{32}Cl_2N_2Ru_2S_2$: C, 39.9; H, 4.9; N, 4.2%). ^1H NMR ($CDCl_3$): C_2 isomer: terminal allyl, δ 4.77 (s, 2 H), 4.70 (s, 2 H), 4.13 (s, 2 H), 3.56 (s, 2 H); internal allyl, δ 4.90 (m, 2 H), 4.68 (m, 2 H); CH_2, δ 3.14 (m, 4 H), 2.57 (m, 4 H); CH_3, δ 2.35 (s, 6 H), 2.26 (s, 6 H); C_i isomer: terminal allyl, δ 4.81 (s, 2 H), 4.65 (s, 2 H), 4.05 (s, 2 H), 3.68 (s, 2 H); internal allyl, δ 4.90 (m, 2 H), 4.68 (m, 2 H); CH_2, δ 3.14 (m, 4 H), 2.57 (m, 4 H); CH_3, δ 2.29 (s, 6 H), 2.26 (s, 6 H). Infrared spectrum: ν(CN) 2141, ν(CS) 723, ν(RuCl) 280 and ν(RuS) 251 cm^{-1}. Mass spectrum (based on ^{35}Cl and ^{102}Ru): *m/z* 662, $[Ru_2(\eta^3:\eta^3\text{-}C_{10}H_{16})_2Cl_2(SCN)_2]^+$; 627, $[Ru_2(\eta^3:\eta^3\text{-}C_{10}H_{16})_2Cl(SCN)_2]^+$; 273, $[Ru(\eta^3:\eta^3\text{-}C_{10}H_{16})Cl]^+$; and 238, $[Ru(\eta^3:\eta^3\text{-}C_{10}H_{16})]^+$.

Crystals of isomerically pure compound **2b** were obtained by fractional crystallisation from a nitromethane solution.

Crystallography.—Crystal data. $C_{22}H_{32}Cl_2N_2Ru_2S_2$ **2b**, $M = 661.67$, triclinic, space group $P\bar{1}$, $a = 7.831(3)$, $b = 12.882(3)$, $c = 14.109(6)$ Å, $\alpha = 112.48(3)$, $\beta = 100.52(3)$, $\gamma = 91.45(3)°$, $U = 1285(1)$ Å^3 (by least-squares refinement of diffractometer angles for 29 automatically centred reflections in the range $13 \leqslant 2\theta \leqslant 22°$, $\lambda = 0.710\,73$ Å), $Z = 2$, $F(000) = 664$, $D_c = 1.71$ g cm^{-3}, μ(Mo-Kα) = 15.3 cm^{-1}. Orange block $0.10 \times 0.20 \times 0.50$ mm.

Data collection and processing. The ω–2θ technique was used to collect 4448 unique reflections in the range $5 \leqslant 2\theta \leqslant 50°$ on a Nicolet R3mV diffractometer equipped with graphite-monochromated Mo-Kα radiation. Three standard reflections measured every 97 reflections showed no significant change in intensity throughout the data collection. The data were corrected for Lorentz and polarisation effects and for absorption, based on additional azimuthal scan data. Of the 4448 data measured $(+h, \pm k, \pm l)$, 2772 reflections were judged to be observed $[I \geqslant 3\sigma(I)]$ and were employed in the analysis.

Structure analysis and refinement. The structure was solved by conventional Patterson and Fourier-difference techniques, the asymmetric unit containing one complete molecule. All non-hydrogen atoms were refined anisotropically and hydrogen

† *Supplementary data available:* see Instructions for Authors, *J. Chem. Soc., Dalton Trans.*, 1992, Issue 1, pp. xx xxv.

Table 1 Atomic coordinates ($\times 10^4$) for *rac*-[{Ru(η^3:η^3-$C_{10}H_{16}$)Cl-(μ-SCN)}$_2$]

Atom	*x*	*y*	*z*
Ru(1)	1733(1)	1543(1)	2919(1)
Ru(2)	4561(1)	3529(1)	7276(1)
Cl(1)	783(5)	−335(3)	1610(3)
Cl(2)	5187(5)	5420(3)	8612(3)
S(1)	2941(5)	414(3)	3929(3)
S(2)	4456(4)	4606(3)	6138(3)
N(1)	3961(13)	2106(8)	5976(8)
N(2)	2713(13)	2990(8)	4193(9)
C(1)	−674(17)	1295(13)	3538(13)
C(2)	−836(16)	2233(12)	3240(13)
C(3)	−754(16)	2010(12)	2191(14)
C(4)	−583(25)	2903(15)	1716(15)
C(5)	884(24)	2652(14)	1208(14)
C(6)	2425(21)	2504(13)	1975(12)
C(7)	3414(22)	1628(14)	1783(13)
C(8)	4488(16)	1523(15)	2669(13)
C(9)	−983(21)	3398(13)	4008(14)
C(10)	3303(25)	755(15)	703(14)
C(11)	1766(16)	3868(11)	7176(11)
C(12)	1911(16)	2993(11)	7490(11)
C(13)	3165(17)	3171(11)	8401(10)
C(14)	3806(20)	2260(12)	8767(12)
C(15)	5792(20)	2380(12)	8924(11)
C(16)	6170(18)	2472(11)	7953(10)
C(17)	7323(18)	3314(12)	7965(11)
C(18)	7273(16)	3449(13)	7026(11)
C(19)	886(18)	1856(11)	6829(11)
C(20)	8452(19)	4128(13)	8938(11)
C(21)	3593(14)	1392(9)	5147(10)
C(22)	3431(16)	3661(10)	4970(10)

Table 2 Selected bond lengths (Å) and angles (°) for *rac*-[{Ru(η^3:η^3-$C_{10}H_{16}$)Cl(μ-SCN)}$_2$]

Ru(1)–Cl(1)	2.409(3)	Ru(1)–S(1)	2.490(4)
Ru(1)–N(2)	2.039(8)	Ru(1)–C(1)	2.280(16)
Ru(1)–C(2)	2.271(13)	Ru(1)–C(3)	2.239(15)
Ru(1)–C(6)	2.255(20)	Ru(1)–C(7)	2.283(20)
Ru(1)–C(8)	2.248(14)	Ru(2)–Cl(2)	2.412(3)
Ru(2)–S(2)	2.483(4)	Ru(2)–N(1)	2.004(8)
Ru(2)–C(11)	2.232(13)	Ru(2)–C(12)	2.278(14)
Ru(2)–C(13)	2.257(16)	Ru(2)–C(16)	2.236(16)
Ru(2)–C(17)	2.273(14)	Ru(2)–C(18)	2.214(13)
S(1)–C(21)	1.671(11)	S(2)–C(22)	1.666(11)
N(1)–C(21)	1.158(14)	N(2)–C(22)	1.136(14)
C(1)–C(2)	1.425(26)	C(2)–C(3)	1.410(27)
C(2)–C(9)	1.500(20)	C(3)–C(4)	1.551(30)
C(4)–C(5)	1.442(29)	C(5)–C(6)	1.535(25)
C(6)–C(7)	1.354(24)	C(7)–C(8)	1.429(26)
C(7)–C(10)	1.493(22)	C(11)–C(12)	1.360(24)
C(12)–C(13)	1.404(19)	C(12)–C(19)	1.511(17)
C(13)–C(14)	1.514(24)	C(14)–C(15)	1.525(22)
C(15)–C(16)	1.500(24)	C(16)–C(17)	1.386(22)
C(17)–C(18)	1.394(25)	C(17)–C(20)	1.475(16)
Cl(1)–Ru(1)–S(1)	80.3(1)	Cl(1)–Ru(1)–N(2)	169.9(4)
S(1)–Ru(1)–N(2)	89.6(4)	Cl(2)–Ru(2)–S(2)	80.7(1)
Cl(2)–Ru(2)–N(1)	169.1(4)	S(2)–Ru(2)–N(1)	88.5(4)
Ru(1)–S(1)–C(21)	102.9(5)	Ru(2)–S(2)–C(22)	102.8(6)
Ru(2)–N(1)–C(21)	169.7(12)	Ru(1)–N(2)–C(22)	167.0(12)
S(1)–C(21)–N(1)	175.7(11)	S(2)–C(22)–N(2)	177.2(15)

atoms were placed in their predicted positions and allowed to ride on the atoms to which they were attached (C–H 0.96 Å, U_{iso} 0.08 Å^2). The final full-matrix least-squares refinement included 271 parameters and gave $R = 0.0557$, $R' = 0.0596$ [weighting scheme $w^{-1} = \sigma^2(F) + 0.001\,216\,7F^2$], and did not shift any parameter by more than 0.002 times its standard deviation. The largest residual peak was 1.21 e Å^{-3} associated with one of the metal atoms. No short intermolecular contacts were observed.

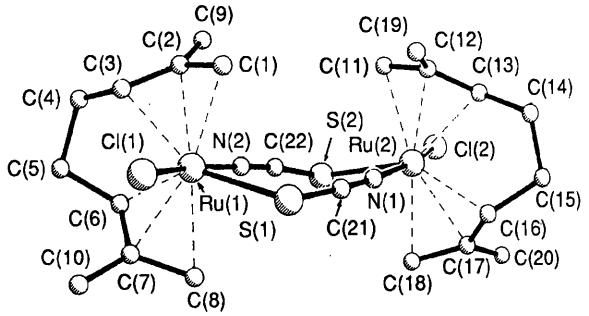

Fig. 1 Molecular structure of *rac*-[{Ru(η^3:η^3-$C_{10}H_{16}$)Cl(μ-SCN)}$_2$] showing the atom labelling scheme

All calculations were carried out using the SHELXTL PLUS program package[8] on a MicroVax II computer. Final fractional atomic coordinates are given in Table 1 and selected bond lengths and angles in Table 2.

Additional material available from the Cambridge Crystallographic Data Centre comprises H-atom coordinates, thermal parameters and remaining bond lengths and angles.

Results and Discussion

In alcoholic solvents the chloro-bridged dimer **1** is reduced to solvated Ru^{2+} ions by the action of Ag[BF_4].[9] However in less-reducing media the abstraction of chloride ions results in the formation of stable solutions containing the '(η^3:η^3-$C_{10}H_{16}$)$RuCl^{+}$' and '(η^3:η^3-$C_{10}H_{16}$)Ru^{2+}' moieties, which readily react with Lewis bases such as nitriles[4] and polypyridines.[10] Other silver salts will also abstract halide ions from **1**, and if the counter ion is a co-ordinating one it can be directly introduced onto the metal centres. In mixed acetone–water solvent, over short reaction times, Ag[SCN] reacts with **1** to give a yellow material, in *ca.* 50% yield, displaying a ν(CN) band at 2141 cm^{-1} in the solid-state infrared spectrum, indicative of an S,N-bridged complex.[11] The binuclear nature of the complex was confirmed by an electron-impact mass spectrum which showed a molecular ion peak at *m/z* 662 ([$C_{22}H_{32}Cl_2N_2Ru_2S_2$]$^+$) with an isotope distribution characteristic of two ruthenium atoms. The ^{1}H NMR spectrum of this material showed a typical eight-line pattern for the terminal allyl protons of the 2,7-dimethylocta-2,6-diene-1,8-diyl ligand (δ 4.81, 4.77, 4.70, 4.65, 4.13, 4.05, 3.68 and 3.56) and four-line pattern for the methyl groups (δ 2.35, 2.29, 2.26 and 2.26) similar to that observed[6] for the parent compound **1** and characteristic of a binuclear, diastereomeric material with an inequivalence of the axial sites on the distorted trigonal-bipyramidal ruthenium ions. Over reaction times of several hours the product displays progressively less of one subset of these signals until, after 24 h, the spectrum contains predominantly only four terminal allyl signals (δ 4.77, 4.70, 4.13 and 3.56) and two methyl resonances (δ 2.35 and 2.26) consistent with the survival of only one of the diastereoisomers. In order to characterise fully this material a single-crystal structure determination was undertaken.

Fractional crystallisation of a reaction mixture containing compound **2** gave a single isomer (NMR evidence) which was examined by X-ray diffraction. The results of that study, in contrast to those on two related binuclear compounds,[2,7] show the isomer to be of C_2 symmetry (Fig. 1). The molecule consists of two distorted trigonal-bipyramidal ruthenium ions with two of the equatorial co-ordination sites occupied by the bis(allyl) ligand which exhibit the usual local C_2 symmetry[2–4,7] and one axial site occupied by a chloride ligand [Ru–Cl 2.409(3) and 2.412(3) Å]. The two ruthenium ions are linked by two S,N-bound thiocyanate bridges [Ru–S 2.490(4) and 2.483(4), Ru–N 2.039(8) and 2.004(8) Å] with the more bulky sulfur atoms occupying the remaining less-hindered, equatorial co-ordination sites. In contrast to most if not all other structures containing

two thiocyanate ligands bridging a pair of metal ions [12–14] the two halves of the molecule are not related by a crystallographic inversion centre because the atoms of the thiocyanate bridge do not lie in the same plane. Instead, a puckered 'butterfly' type conformation is adopted by the eight-membered ring. This results in a torsion angle in the Cl–Ru–Ru–Cl linkage which deviates from the ideal value of 180° by 9.4°. It has been suggested [12,15] that π overlap renders a planar conformation for thiocyanate-bridged structures significantly more stable and it therefore seems likely that it is the large steric requirement of the 2,7-dimethylocta-2,6-diene-1,8-diyl ligand which, in this instance, causes the distortions from planarity. Steric interactions between the methyl substituents on the bis(allyl) ligand and the axial chloride ligands cause a significant reduction in the Cl–Ru–(equatorial ligand) angle in all compounds of this type [2–4,7] and the Cl–Ru–S angles in this case are significantly compressed [80.3(1)° and 80.7(1)°] in spite of the bulk of the sulfur atom. The corresponding angle (Cl–Ru–N) in $[\{Ru(\eta^3:\eta^3\text{-}C_{10}H_{16})Cl_2\}_2(\mu\text{-}N_2C_4H_4)]$ **3** is 85.4(2)°. The puckering of the ring system is thus due to the increased Cl • • • S interactions which, synergically, cause further chloride–methyl interactions.

From these observations it is easy to rationalise the thermodynamic preference for the C_2 isomer. The chloride ligands are constrained by the geometry of the 'Ru(SCN)$_2$Ru' unit to adopt a transoid configuration and, in the *rac* form, their out-of-plane distortion is angled away from the methyl groups of the bis(allyl) ligand. In the C_i isomer the opposite effect would be in evidence and so give rise to greater unfavourable chloride–methyl steric interactions which destabilise the *meso*, **2a**, form.

Low-temperature dissolution of crystalline compound **2b** allowed the unequivocal assignment of the resonances observed in the room-temperature ^{1}H NMR spectrum.

Investigations are in progress into the reactions of **2** and the kinetics of the isomerisation process.

Acknowledgements

We thank the SERC for provision of the diffractometer and for a studentship (to J. W. S.), and Johnson Matthey plc for generous loans of ruthenium trichloride.

References

1 L. Porri, M. C. Gallazzi, A. Colombo and G. Allegra, *Tetrahedron Lett.*, 1965, **47**, 4187.
2 A. Colombo and G. Allegra, *Acta Crystallogr., Sect. B*, 1971, **27**, 1653.
3 J. G. Toerien and P. H. van Rooyen, *J. Chem. Soc., Dalton Trans.*, 1991, 1563.
4 D. N. Cox, R. W. H. Small and R. Roulet, *J. Chem. Soc., Dalton Trans.*, 1991, 2013.
5 S. O. Sommerer and G. J. Palenik, *Organometallics*, 1991, **10**, 1223.
6 D. N. Cox and R. Roulet, *Inorg. Chem.*, 1990, **29**, 1360.
7 J. W. Steed and D. A. Tocher, *J. Organomet. Chem.*, 1991, **412**, C34.
8 G. M. Sheldrick, SHELXTL PLUS, University of Gottingen, 1986.
9 D. N. Cox and R. Roulet, *J. Chem. Soc., Chem. Commun.*, 1988, 951.
10 J. W. Steed and D. A. Tocher, *Inorg. Chim. Acta*, in the press.
11 K. Nakamoto, *Infrared and Raman Spectra of Inorganic and Coordination Complexes*, 4th edn., Wiley, New York, 1986, pp. 283–287.
12 U. A. Gregory, J. A. J. Jarvis, B. T. Kilbourn and P. G. Owston, *J. Chem. Soc. A*, 1970, 2771.
13 M. Taniguchi and A. Ouchi, *Bull. Chem. Soc. Jpn.*, 1986, **59**, 3277.
14 T. Rojo, R. Cortés, L. Lezama, M. I. Arriortua, K. Urtiaga and G. Villeneuve, *J. Chem. Soc., Dalton Trans.*, 1991, 1779.
15 J. Chatt and F. A. Hart, *J. Chem. Soc.*, 1953, 2363; 1960, 2807.

Received 10*th October* 1991; *Paper* 1/05146F

Polyhedron Vol. 11, No. 15, pp. 1849–1854, 1992
Printed in Great Britain

0277–5387/92 $5.00+.00

DINUCLEAR CARBOXYLATO-BRIDGED COMPLEXES OF RUTHENIUM(IV)

JONATHAN W. STEED and DEREK A. TOCHER†

Department of Chemistry, University College London, 20 Gordon Street, London WC1H 0AJ, U.K.

(*Received* 18 *March* 1992; *accepted* 14 *April* 1992)

Abstract—Treatment of the ruthenium(IV) chloro bridged dimer $[(\eta^3:\eta^3\text{-}C_{10}H_{16})RuCl(\mu\text{-}Cl)]_2$ (**1**) with silver oxalate in acetone/water gives the oxalato bridged dimer $[\{(\eta^3:\eta^3\text{-}C_{10}H_{16})RuCl\}_2(\mu\text{-}O_4C_2)]$ (**2**), which exists in two diastereomeric forms of C_i and C_2 symmetry, **2a** and **2b**, respectively. Similar treatment of **1** with potassium malonate gives the bridged complex $[\{(\eta^3:\eta^3\text{-}C_{10}H_{16})RuCl\}_2(\mu\text{-}O_4C_3H_2)]$ (**3**). The X-ray crystal structure of **2a** is reported.

The ruthenium(IV) bis(allyl) complex $[(\eta^3:\eta^3\text{-}C_{10}H_{16})RuCl(\mu\text{-}Cl)]_2$[1,2] (**1**) was first synthesized in 1965 from the reaction of ethanolic ruthenium trichloride and isoprene. In contrast, the reaction of $RuCl_3 \cdot nH_2O$ with 1,3- and 1,4-cyclohexadienes gives the ruthenium(II) arene compounds $[(\eta^6\text{-arene})RuCl(\mu\text{-}Cl)]_2$ (arene = benzene, mesitylene, *p*-cymene, etc.).[3] While numerous studies on the chemistry of the arene complexes have been made the chemistry of **1** has not yet been extensively investigated,[4,5] despite the fact that **1** is known to be an effective catalyst for the ring opening polymerization of norbornene.[6] The use of **1** as a facile gateway into the higher oxidation state organometallic chemistry of ruthenium has been recognized recently, and this has brought about a significant resurgence of interest in its reactivity.[7–14]

The X-ray crystal structure of **1** shows the molecule to possess overall C_i symmetry.[2] Cox and Roulet,[11] however, established that in solution a second more stable isomer possessing (as a consequence of the chirality of the "$C_{10}H_{16}Ru$" unit) overall C_2 symmetry exists ($[C_2]/[C_i] = 1.25$ at 298 K), see Fig. 1.

The mixture of isomers is readily observed in the ^1H NMR spectrum of **1** which exhibits a characteristic "doubling" of the number of resonances expected for a single diastereoisomer. Such diastereoisomerism has also been observed in the related binuclear compounds $[\{(\eta^3:\eta^3\text{-}C_{10}H_{16})RuCl_2\}_2(\mu\text{-pyz})]$, $[\{(\eta^3:\eta^3\text{-}C_{10}H_{16})RuCl_2\}_2(\mu\text{-dppm})]$ and $[(\eta^3:\eta^3\text{-}C_{10}H_{16})RuCl(\mu\text{-SCN})]_2$ (pyz = pyrazene, dppm = diphenylphosphinomethane).[12–14] We now report the use of dicarboxylate ligands to form further examples of binuclear species derived from **1**.

RESULTS AND DISCUSSION

Reaction of **1** in mixed acetone/water solvent with both 1 or 2 mol equivalents of silver oxalate gives the oxalato bridged complex $[\{(\eta^3:\eta^3\text{-}$

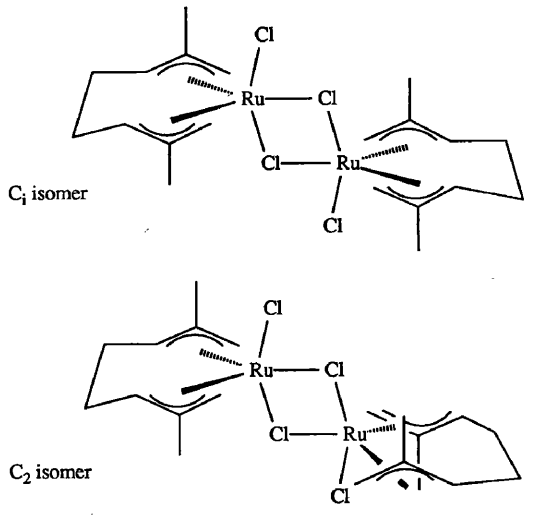

1

Fig. 1. The two diastereomeric forms of $[(\eta^3:\eta^3\text{-}C_{10}H_{16})RuCl(\mu\text{-}Cl)]_2$.

† Author to whom correspondence should be addressed.

$C_{10}H_{16})RuCl\}_2(\mu\text{-}O_4C_2)]$ (**2**) in near quantitative yield. The presence of the oxalato ligand is confirmed by strong bands assignable[15,16] to $\nu(OCO)_{asym}$, at 1627 cm^{-1}, and $\nu(OCO)_{sym}$, at 1384 and 1333 cm^{-1}, in the IR spectrum. Compound **2** might be expected to exist as up to four different isomers distinguishable by NMR spectroscopy, viz. two pairs of diastereoisomers with, respectively, *cisoid* (**2c**, **2d**) and *transoid* (**2a**, **2b**) bridge configurations, as shown in Fig. 2.

In practice the ^1H NMR spectrum of **2** is qualitatively similar to that of **1**, i.e. eight singlet resonances attributable to the terminal allyl protons of the 2,7-dimethylocta-2,6-diene-1,8-diyl ligand (δ 5.32, 5.19, 4.53, 4.44, 4.34, 4.19, 3.37 and 3.24 ppm) and four assigned to the methyl groups (δ 2.33, 2.30, 2.20 and 2.15 ppm). This observation is consistent with the formation of only two isomers. A pure sample of a single isomer was obtained by fractional crystallization from chloroform/diethylether and was dissolved in chloroform-d at 210 K. The ^1H NMR spectrum of this solution displayed only half the number of resonances of the bulk sample: δ 5.32, 4.44, 4.19, 3.37 (terminal allyl), 2.33 and 2.15 ppm (methyl). A single crystal X-ray structure determination (*vide infra*) showed these resonances to be due to isomer **2a** possessing a *transoid* bridge configuration and overall C_i molecular symmetry. Raising the temperature in the NMR probe from 210 to 323 K produced little immediate change in the spectrum indicating that, in contrast to the parent compound **1**, and to $[\{(\eta^3\text{:}\eta^3\text{-}C_{10}H_{16})RuCl_2\}_2(\mu\text{-}pyz)]$,[12] interconversion of isomers by bridge rupture is slow even at higher temperatures. The NMR tube containing **2a** was sealed and allowed to stand at room temperature for several weeks. Spectra were recorded periodically during this time and showed the gradual partial conversion of **2a** into **2b**. Close examination of the spectra revealed that there were also additional weak resonances: eight singlet resonances due to terminal allylic protons (δ 5.38, 5.32, 4.66, 4.56, 4.38, 4.27, 3.43 and 3.19 ppm), four methyl resonances (δ 2.33, 2.32, 2.15 and 2.02 ppm), as well as additional multiplets (δ 4.56, 3.95 and 2.64 ppm). The appearance of these signals is completely consistent with the accumulation of small amounts of the *cisoid* isomers **2c** and **2d**. After *ca* 1 month, nearly equimolar quantities of **2a** and **2b** were present in the sample together with small quantities of the *cisoid* isomers, which never constituted more than 20% of any of the samples which we studied. It is unclear whether this ratio represents the true equilibrium concentrations of the four isomers.

The observation of two metal centres linked by a potentially delocalized bridging ligand, as is the case here, raises the question of whether the metal centres can communicate with one another. The cyclic voltammogram of **2** recorded in CH_2Cl_2 with tetrabutylammonium tetrafluoroborate as a supporting electrolyte is unencouraging, however, displaying a single, irreversible reduction at -0.92 V, along with a partial oxidation wave on the return scan at $+1.04$ V ($v = 200$ mV s^{-1}), possibly indica-

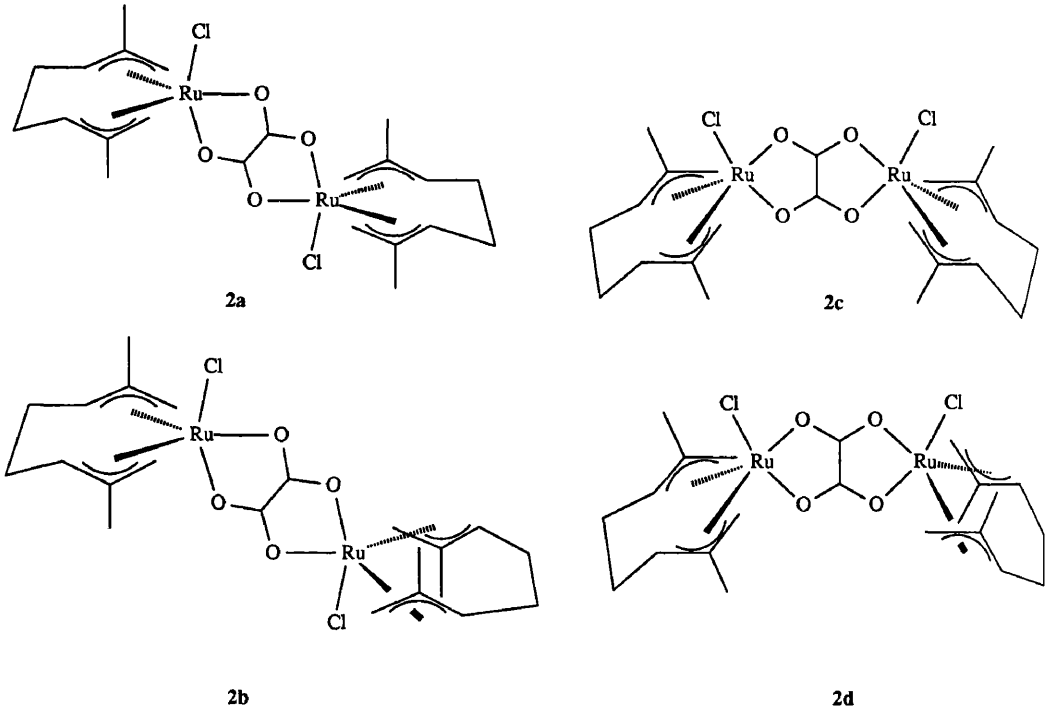

Fig. 2. Four possible isomers of $[\{(\eta^3\text{:}\eta^3\text{-}C_{10}H_{16})RuCl\}_2(\mu\text{-}O_4C_2)]$.

tive of an ECE process. Irreversible reduction is consistent with the observation of Cox *et al.*[17] that the parent compound **1** is chemically reduced by $Ag[BF_4]$ in alcoholic solvents with the irreversible loss of the bis(allyl) ligand.

The reaction of **1** with potassium malonate was also examined. The orange product was found to decompose slowly in chlorinated solvents to reform **1**, presumably as a consequence of the presence of trace quantities of HCl in the solvent. The complex was sufficiently stable, however, to permit an examination of its ^1H NMR spectrum in $CDCl_3$. The spectrum is a surprising one in that it displays only six resonances for the terminal allyl protons (δ 5.54, 5.53, 4.83, 4.82, 4.64 and 3.74 ppm) and three resonances for the methyl hydrogen atoms (δ 2.29, 2.15 and 2.10 ppm), as opposed to the eight and four, respectively, which might have been expected for a binuclear compound. The IR spectrum of the material displays a band at 1516 cm^{-1} assigned to $\nu(OCO)_{asym}$ (cf. 1516 cm^{-1} for $[(\eta^3:\eta^3\text{-}C_{10}H_{16})RuCl(O_2CCH_3)]$[7] (**4**) and 1510 cm^{-1} for the ruthenium(II) arene compound $[(\eta^6\text{-}C_6H_6)RuCl(O_2CCH_3)]$[18]) and ν(RuO) at 457 cm^{-1}. Analytical data are fully consistent with the binuclear compound $[\{(\eta^3:\eta^3\text{-}C_{10}H_{16})RuCl\}_2(\mu\text{-}O_2C_3H_2)]$ (**3**). In fact, the reduced number of ^1H NMR signals is due to the accidental degeneracy of some of the resonances, thus two terminal allyl and one methyl resonance have twice the integral of their counterparts where the separate peaks are resolved. This deduction is further supported by the observation of only a single second-order multiplet resonance, arising from the two protons of the malonate ligand (cf. the case of $[\{(\eta^3:\eta^3\text{-}C_{10}H_{16})RuCl_2\}_2(\mu\text{-pyz})]$[12] where the two singlet resonances for the protons of the pyrazene ligand are observed at similar, but nevertheless resolved, chemical shifts). Such degeneracy indicates that there is little difference from an NMR standpoint between the two diastereoisomers of **3** and is consistent with the fact that the two chiral fragments are linked by a ligand containing a long continuous chain of five atoms, as opposed to only four atoms in the case of the pyrazene bridged dimer.[12] Although it is possible that the linkage between the two metal ions consists of two fused six-membered heterocyclic rings this seems unlikely from our examination of models which show that such a mode of coordination would result in severe steric congestion. Certainly the similarities in the frequencies of $\nu(OCO)_{asym}$ for **3** and **4** (both 1516 cm^{-1}), compared with the much greater value for **2** (1627 cm^{-1}), suggest that **3** contains four-membered heterocyclic rings. When malonate ligands form six-membered rings with metal ions the separations between symmetric and asymmetric stretching frequencies is expected to be large.[19,20] Assuming the bridging malonate to act as two essentially independent chelating carboxylate ligands and assuming free rotation about the two interconnecting carbon–carbon bonds implies that the possibility of *cisoid* and *transoid* geometries for the chloride ligands does not need to be considered. Hence, the experimental evidence is consistent with **3** having the diastereomeric structures shown in Fig. 3.

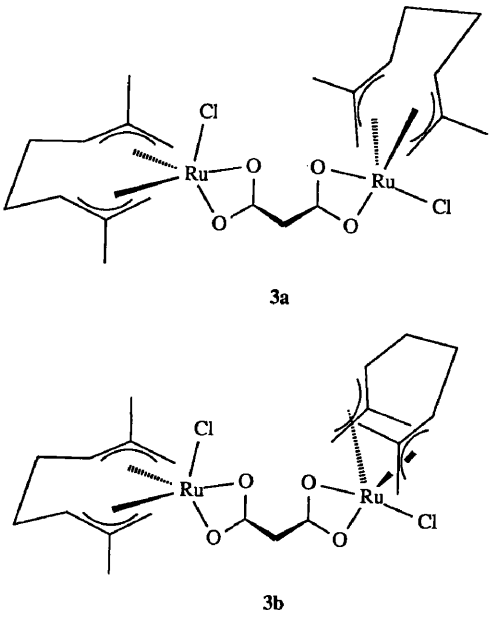

Fig. 3. Two diastereomeric forms of $[\{(\eta^3:\eta^3\text{-}C_{10}H_{16})RuCl\}_2(\mu\text{-}O_2C_3H_2)]$.

X-ray crystal structure determination

The crystallographically determined structure of **2a** is shown in Fig. 4. Selected bond lengths and angles are summarized in Table 1, while technical considerations are outlined in the Experimental. The asymmetric unit contains half the centrosymmetric binuclear molecule. Due to the presence of a significant disorder of the bis(allyl) ligand, taking the form of two alternative positions for the carbon atoms C(2) through C(7), it was not possible to determine crystallographically whether the sample consisted uniquely of C_i or C_2 diastereoisomers or a mixture of the two. Given that the disordered molecule was symmetric about an inversion centre, however, it seemed likely that the former diastereoisomer was predominant. This was confirmed by low temperature dissolution of the crystalline sample which possessed a ^1H NMR spectrum consistent with only a single diastereoisomer.

Each ligand shows the usual local C_2 symmetry and the metal adopts an approximately trigonal

Table 1. Selected bond lengths (Å) and angles (°) for $[\{(\eta^3:\eta^3\text{-}C_{10}H_{16})RuCl\}_2(\mu\text{-}O_4C_2)]$

Bond lengths			
Ru(1)—Cl(1)	2.368(2)	Ru(1)—O(1)	2.144(5)
Ru(1)—O(2)	2.182(6)	Ru(1)—C(1)	2.219(10)
Ru(1)—C(2)	2.219(16)	Ru(1)—C(3)	2.194(17)
Ru(1)—C(6)	2.240(18)	Ru(1)—C(7)	2.189(18)
Ru(1)—C(8)	2.209(10)	O(1)—C(11)	1.245(9)
O(2)—C(11)*[a]	1.245(9)	C(11)—C(11)*[a]	1.532(15)
Bond angles			
Cl(1)—Ru(1)—O(1)	161.8(2)	Cl(1)—Ru(1)—O(2)	84.8(2)
O(1)—Ru(1)—O(2)	77.0(2)	Ru(1)—O(1)—C(11)	114.5(5)
Ru(1)—O(2)—C(11)*[a]	112.9(5)		

[a] C(11)* is generated by the inversion centre at the origin.

bipyramidal geometry as previously observed in related compounds.[2,8–10,12,13] The central portion of the molecule consists of two fused five-membered heterocyclic rings (a geometry typical of the oxalato ligand coordinated in the bridging mode[15,21]) consisting of one bridging oxalato ligand and two metal centres, $r(Ru—O_{ax})$ 2.144(5) Å, $r(Ru—O_{eq})$ 2.182(6) Å (cf. 2.120(5) Å for Ru—O_{eq} in $[(\eta^6\text{-}C_6H_6)RuCl(NC_6H_6O)]$[22]), ∠O(1)—Ru(1)—O(2) 77.0(2)°. The ruthenium to chloride distance is 2.368(2) Å, which is at the lower end of the range of Ru—Cl distances in related compounds, 2.38–2.42 Å.[2,8–10,12,13] The angle between the apical ligands, Cl(1)—Ru(1)—O(1), is 161.8(2), somewhat less than that observed for unconstrained systems such as $[\{(\eta^3:\eta^3\text{-}C_{10}H_{16})RuCl_2\}_2(\mu\text{-pyz})]$[12] [170.2(1)°] but typical of that observed in other related systems containing chelate rings.[10,23] The angle is notably larger than the corresponding Cl—Ru—S angle in the benzothiazole-2-thiolate complex $[(\eta^3:\eta^3\text{-}C_{10}H_{16})RuCl(mcbt)]$[8] [156.4(1)°], which contains a four-membered heterocyclic ring, but is roughly similar to the Cl—Ru—N angle in the bipyridine complex $[(\eta^3:\eta^3\text{-}C_{10}H_{16})RuCl(bipy)][BF_4]$[24] [166.9(2)°]. The metal–carbon distances are all approximately equal and fall into the range 2.19–2.25 Å, while the two metal centres are 5.59 Å apart.

Work is currently in progress on a range of mononuclear carboxylate derivatives of **1** and we are carrying out further investigations into the oligomerization of "$C_{10}H_{16}Ru$" units with a variety of multidentate ligands.

EXPERIMENTAL

Instrumental

IR spectra were recorded on a PE983 grating spectrometer between 4000 and 200 cm^{-1} as Nujol

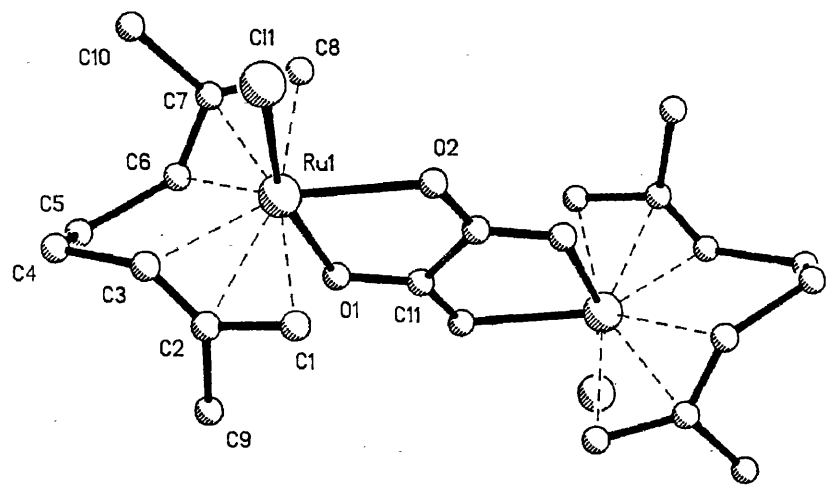

Fig. 4. Molecular structure of *meso*-$[\{(\eta^3:\eta^3\text{-}C_{10}H_{16})RuCl\}_2(\mu\text{-}O_4C_2)]$ showing the atom numbering scheme adopted.

mulls on CsI plates and as KBr discs. NMR spectra were recorded on a Varian VXR400 spectrometer at UCL and microanalyses were carried out by the departmental service. Cyclic voltammetric measurements were performed using a Metrohm E506 potentiostat interfaced with a Metrohm E612 scanner and a Hewlett–Packard 7035B *X–Y* recorder. Electrolyte solutions were 0.2 M in tetra-n-butyl ammonium tetrafluoroborate. Deaeration of the solution was performed before the experiment and a stream of nitrogen passed throughout. The working electrode was a platinum wire (Metrohm EA285). A non-aqueous $Ag/AgCl/Cl^-$, CH_2Cl_2 electrode was used as a reference electrode and a platinum wire as the auxiliary. All potentials are reported with respect to the Ag/AgCl electrode against which ferrocene is oxidized at a potential of +0.60 V. All manipulations were carried out under nitrogen with degassed solvents using conventional Schlenk line techniques, although no significant air or moisture sensitivity of the products was noted.

Materials

$[(\eta^3:\eta^3\text{-}C_{10}H_{16})RuCl(\mu\text{-}Cl)]_2$ was prepared by published literature methods.[1,8,11] Ruthenium trichloride hydrate was obtained on loan from Johnson Matthey plc and was purified before use by dissolution in water and boiling to dryness. Silver salts were prepared by reaction of silver(I) oxide with the appropriate carboxylic acid. All other reagents and materials were obtained from the usual commercial sources.

$[\{(\eta^3:\eta^3\text{-}C_{10}H_{16})RuCl\}_2(\mu\text{-}O_4C_2)]$ (2)

$[(\eta^3:\eta^3\text{-}C_{10}H_{16})RuCl]_2$ (0.99 g, 0.16 mmol) was suspended in degassed acetone (2.5 cm^3) and degassed water (2.5 cm^3). $Ag_2[O_4C_2]$ (0.98 g, 0.32 mmol) was added and the mixture stirred for 1 h. The resulting orange solution was filtered over celite to remove the precipitate of AgCl which formed and the volume of the filtrate reduced to *ca* $\frac{1}{4}$ resulting in the deposition of the yellow product, which was isolated by filtration, washed with acetone and diethyl ether and air dried. Yield: 0.08 g, 0.13 mmol, 83%. Found: C, 42.3; H, 5.3. Calc. for $C_{22}H_{32}Cl_2O_4Ru_2$: C, 41.7; H, 5.1%. ^1H NMR ($CDCl_3$): C_i (**2a**): 5.32 (s, 1H); 4.44 (s, 1H); 4.19 (s, 1H); 3.37 (s, 1H) (terminal allyl); 4.49 (m, 2H); 4.13 (virtual t, 2H) (internal allyl); 2.65 (m, 4H) (—CH_2—); 2.33 (s, 3H); 2.15 (s, 3H) (methyl). C_2 (**2b**): 5.19 (s, 1H); 4.53 (s, 1H); 4.34 (s, 1H); 3.24 (s, 1H) (terminal allyl); 4.49 (m, 2H); 4.08 (virtual t, 2H) (internal allyl); 2.65 (m, 4H) (—CH_2—); 2.30 (s, 3H); 2.20 (s, 3H) (methyl). IR: ν(OCO) 1627 cm^{-1}, ν(RuO) 437 cm^{-1}, ν(RuCl) 280 cm^{-1}.

$[\{(\eta^3:\eta^3\text{-}C_{10}H_{16})RuCl\}_2(\mu\text{-}O_4C_3H_2)]$ (3)

$[(\eta^3:\eta^3\text{-}C_{10}H_{16})RuCl]_2$ (0.064 g, 0.10 mmol) was suspended in degassed acetone (5 cm^3). $K_2[O_4C_3H_2]$ (0.021 g, 0.12 mmol) was added and the mixture stirred for 24 h. The resulting orange solution was filtered through celite to remove the precipitate of KCl and any unreacted starting materials and the solvent removed *in vacuo* resulting in a pinkish residue which was recrystallized from diethyl ether. Yield: 0.046 g, 0.064 mmol, 62%. Found: C, 42.8; H, 5.2. Calc. for $C_{23}H_{34}Cl_2O_4Ru_2$: C, 42.7; H, 5.3%. ^1H NMR ($CDCl_3$), 2 unresolved diastereoisomers: 5.54 (s, 1H); 5.53 (s, 1H); 4.83 (s, 1H); 4.82 (s, 1H); 4.64 (s, 2H); 3.74 (s, 2H) (terminal allyl); 4.26 (m, 2H); 3.60 (m, 2H) (internal allyl); 2.55 (m, 8H) (—CH_2—); 2.29 (s, 6H); 2.15 (s, 3H); 2.10 (s, 3H) (methyl); 2.94 (virtual s, 2H) ($O_2CCH_2CO_2$). IR: ν(OCO) 1516 cm^{-1}, ν(RuO) 457 cm^{-1}, ν(RuCl) 278 cm^{-1}.

X-ray crystal structure determination

Crystal data. $C_{22}H_{32}Cl_2O_4Ru_2$, *fw* 633.58 g mol^{-1}, monoclinic space group $P2_1/n$, $a = 7.636(2)$, $b = 20.168(5)$, $c = 7.902(2)$ Å, $\beta = 90.74(2)°$, $U = 1216.9$, $z = 2$, $D_c = 1.73$ g cm^{-1}, $F(000) = 636$, $\mu = 14.64$ cm^{-1}.

A deep red crystal of approximate dimensions $0.4 \times 0.3 \times 0.2$ mm was prepared, by diffusion of diethyl ether into a chloroform solution of the compound, and was mounted on a glass fibre using a fast setting epoxy resin. A Nicolet R3mV four-circle diffractometer was used to irradiate the crystal with graphite-monochromated Mo-K_α radiation ($\lambda = 0.71073$ Å) and to collect geometric and intensity data. Initial lattice vectors were determined by the automatic indexing routines of the diffractometer from 30 accurately located reflections in the range $12° \leqslant 2\theta \leqslant 25°$, measured from a rotation photograph. Unit cell dimensions were verified by axial photography. A primitive data set consisting of 2134 unique reflections was collected using the ω–2θ technique. Three standard reflections monitored throughout the data collection showed no appreciable change in intensity. The data were corrected for Lorentz and polarization effects and for absorption based on additional azimuthal scan data. The 1669 reflections with $I \geqslant 3\sigma(I)$ were used in structure solution and refinement. The space group was identified as $P2_1/n$ from the systematically absent data.

The asymmetric unit contains one half of the

binuclear molecule. The structure was solved by conventional Patterson and difference Fourier techniques. Heavy atoms were refined anisotropically but an isotropic model was adopted for the light atoms due to the presence of a significant disorder in the crystal, which took the form of two alternative positions for the carbon atoms of the allyl ligand with the exception of the terminal carbon atoms C(1) and C(8) which were common to both orientations. The disorder was modelled satisfactorily by two ligand positions of fractional occupancy (refined to a value of 0.6 for the major position). Hydrogen atoms were not included in the model. Full-matrix least-squares refinement gave $R = 0.0541$ and $R_w = 0.0648$ in the final cycle from 104 parameters. A weighting scheme of $w^{-1} = \sigma^2(F) + 0.005368F^2$ was applied and the maximum shift to error ratio in the final cycle was 0.006. The largest residual peak was 1.0 e $Å^{-3}$ close to the metal atom. No short intermolecular contacts were observed. All calculations were carried out using the SHELXTL PLUS program package.[25]

Acknowledgements—We thank the SERC for provision of the diffractometer and for a studentship (J.W.S.) and Johnson Matthey plc for generous loans of ruthenium trichloride.

REFERENCES

1. L. Porri, M. C. Gallazzi, A. Colombo and G. Allegra, *Tetrahedron Lett.* 1965, **47**, 4187.
2. A. Colombo and G. Allegra, *Acta Cryst., Sect. B* 1971, **27**, 1653.
3. M. A. Bennett and A. K. Smith, *J. Chem. Soc., Dalton Trans.* 1974, 233.
4. R. A. Head, J. F. Nixon, J. R. Swain and C. M. Woodard, *J. Organomet. Chem.* 1974, **76**, 393.
5. P. B. Hitchcock, J. F.Nixon and J. Sinclair, *J. Organomet. Chem.* 1975, **86**, C34.
6. L. Porri, R. Rossi, P. Diversi and A. Licherini, *Makromolec. Chem.* 1974, **175**, 3097.
7. J. W. Steed and D. A. Tocher, *Inorg. Chim. Acta* 1991, **189**, 135.
8. J. G. Toerien and P. H. van Rooyen, *J. Chem. Soc., Dalton Trans.* 1991, 1563.
9. D. N. Cox, R. W. H. Small and R. Roulet, *J. Chem. Soc., Dalton Trans.* 1991, 2013.
10. S. O. Sommerer and G. J. Palenick, *Organometallics* 1991, **10**, 1223.
11. D. N. Cox and R. Roulet, *Inorg. Chem.* 1990, **29**, 1360.
12. J. W. Steed and D. A. Tocher, *J. Organomet. Chem.* 1991, **412**, C34.
13. J. G. Toerien and P. H. van Rooyen, *J. Chem. Soc., Dalton Trans.* 1991, 2693.
14. J. W. Steed and D. A. Tocher, *J. Chem. Soc., Dalton Trans.* 1992, 459.
15. I. Castro, J. Faus, M. Julve and A. Gleizes, *J. Chem. Soc., Dalton Trans.* 1991, 1937.
16. M. Bianchi, P. Frediani, U. Matteoli, G. Menchi, F. Piacenti and G. Petrucci, *J. Organomet. Chem.* 1983, **259**, 207.
17. D. N. Cox and R. Roulet, *J. Chem. Soc., Chem. Commun.* 1988, 951.
18. D. A. Tocher, R. O. Gould, T. A. Stephenson, M. A. Bennett, J. P. Ennett, T. W. Matheson, L. Sawyer and V. K. Shah, *J. Chem. Soc., Dalton Trans.* 1983, 1571.
19. T. Shibahara, H. Kuroya, K. Matsumo and S. Ooi, *Inorg. Chim. Acta* 1981, **54**, L75.
20. K. Butler and M. Snow, *J. Chem. Soc., Dalton Trans.* 1976, 251.
21. R. Deyrieux and A. Peneloux, *Bull. Soc. Chim. Fr.* 1969, 2675.
22. E. C. Morrison, C. A. Palmer and D. A. Tocher, *J. Organomet. Chem.* 1988, **349**, 405.
23. J. W. Steed and D. A. Tocher, *Inorg. Chim. Acta* 1992, **191**, 29.
24. J. W. Steed and D. A. Tocher, unpublished work.
25. G. M. Sheldrick, SHELXTL PLUS, An Integrated System for Refining and Displaying Crystal Structures from Diffraction Data. University of Göttingen, F.R.G. (1986).

Geometrical Isomerism in 2-Hydroxypyridinate and Pyridine-2-thiolate Complexes derived from the Ruthenium(IV) Bis(allyl) Dimer $[\{Ru(\eta^3:\eta^3\text{-}C_{10}H_{16})Cl(\mu\text{-}Cl)\}_2]$†

Jonathan W. Steed and Derek A. Tocher*
Department of Chemistry, University College London, 20 Gordon St., London WC1H 0AJ, UK

Reaction of the ruthenium(IV) chloro-bridged dimer $[\{Ru(\eta^3:\eta^3\text{-}C_{10}H_{16})Cl(\mu\text{-}Cl)\}_2]$ with a range of 2-hydroxypyridinate and pyridine-2-thiolate ligands (HL = 2-hydroxypyridine, 6-chloro-2-hydroxypyridine, 2-hydroxy-6-methylpyridine, 2-hydroxy-4-methylquinoline, 8-hydroxyquinoline, pyrrolidin-2-one, quinoline-2-thiol and 6-methylpyridine-2-thiol) gives the neutral, chelate compounds $[Ru(\eta^3:\eta^3\text{-}C_{10}H_{16})Cl(L)]$ each of which exists as both axial and equatorial geometric isomers. These isomers occur in varying ratios and may be distinguished by their characteristic ^1H NMR spectra. The X-ray crystal structures of eq-$[Ru(\eta^3:\eta^3\text{-}C_{10}H_{16})Cl\{NC_6H_3(O)Cl\text{-}6\}]$ and of eq-$[Ru(\eta^3:\eta^3\text{-}C_{10}H_{16})Cl(NC_9H_6S)]$ are reported.

Recent interest[1–6] has focused strongly on the chemistry of the hitherto neglected ruthenium(IV) bis(allyl) chloro-bridged dimer $[\{Ru(\eta^3:\eta^3\text{-}C_{10}H_{16})Cl(\mu\text{-}Cl)\}_2]$ **1**[7,8] especially in connection with ligands related to pyridine-2-thiol,[5] which are of considerable interest in their own right.[9,10] Previously we have investigated the reactions of the closely related ruthenium(II) arene complexes $[\{Ru(\eta^6\text{-arene})Cl(\mu\text{-}Cl)\}_2]$[11] with a range of ligands related to 2-hydroxypyridine[12] and with a wide range of carboxylates (arene = C_6H_6, *p*-$MeC_6H_4CHMe_2$, $C_6H_3Me_3$-1,3,5, $C_6H_2Me_4$-1,2,4,5 or C_6Me_6).[13] Cotton and co-workers[14] have also characterised the complex $[Ru(p\text{-}MeC_6H_4CHMe_2)Cl(NC_5H_4O)]$. Toerien and van Rooyen[5] recently demonstrated that the reaction of **1** with benzothiazole-2-thiol ($N_2C_7H_5SH$) and pyridine-2-thiol (NC_5H_4SH) proceeds *via* a two-step process initially involving bridge cleavage to give a neutral complex exhibiting equatorial co-ordination of the pyridyl nitrogen atom. Subsequent refluxing of these complexes in solutions containing $Na_2[CO_3]$ brings about the intramolecular loss of HCl and gives complexes containing $N_2C_7H_5S$ and NC_5H_4S as anionic chelates.

2-Hydroxypyridine has been shown[12] to co-ordinate initially through the pyridone oxygen atom in ruthenium(II) arene systems, at room temperature, to give complexes such as $[Ru(\eta^6\text{-}C_6H_6)Cl_2(OC_5H_4NH)]$ **2**. Subsequent deprotonation on refluxing forms the chelate complex $[Ru(\eta^6\text{-}C_6H_6)Cl(NC_5H_4O)]$ **3**, which is related to those described by Toerien and van Rooyen[5] for the ruthenium(IV) system. These workers[5] also attempted the reaction of **1** with 2-hydroxypyridine but were unable to identify the products formed. As an extension to our previous work we now report the reactions of **1** with a range of ligands related to 2-hydroxypyridine and pyridine-2-thiol.

The geometry about the ruthenium ion in complex **1** is loosely described as trigonal bipyramidal[5] with chloride ligands occupying the axial sites and one equatorial position, while the bis(allyl) ligand is in the remaining two equatorial sites. Complex **1** has been shown to exist as two diastereoisomers, of C_i and C_2 symmetry,[3] which arise as a consequence of the chirality of the '$C_{10}H_{16}Ru$' unit. This phenomenon is readily observed in the ^1H NMR spectrum which displays eight lines corresponding to the terminal allyl protons and four resonances attributable to the methyl substituents. Mononuclear species derived from **1**, while existing as two enantiomers, display

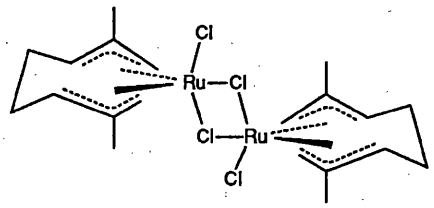

C_i isomer

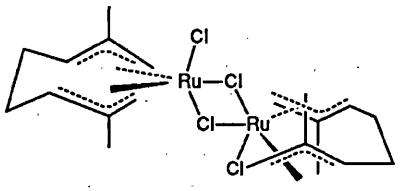

C_2 isomer

1

signals corresponding to only a single diastereoisomer (four terminal allyl and two methyl resonances) if the two halves of the bis(allyl) ligand are inequivalent (*e.g.* as a consequence of inequivalent axial sites of the trigonal bipyramid[3,5,15]) or, in the more symmetrical equatorially substituted compounds $[Ru(\eta^3:\eta^3\text{-}C_{10}H_{16})Cl_2L]$ (L = pyridine, PPh_3, PF_3, CO, Bu^{t}CN, *etc.*),[16] two terminal allyl and a single methyl resonance.

Results and Discussion

In our previous study we showed that the chelate complex $[Ru(\eta^6\text{-}C_6H_6)Cl(O_2CCF_3)]$ was a useful synthetic precursor to **3** and related products. This synthetic route is not available in the case of the bis(allyl)ruthenium(IV) system, however, since the reaction of **1** with trifluoroacetic acid or silver trifluoroacetate gives the relatively inert aqua complex $[Ru(\eta^3:\eta^3\text{-}C_{10}H_{16})(O_2CCF_3)_2(OH_2)]$.[17] Fortunately, we find that direct interaction of **1** with 2-hydroxypyridine in CH_2Cl_2 at room temperature gives a good yield (*ca.* 70%) of an orange-red complex **4**. The infrared spectrum showed no bands attributable to ν(OH) or to ν(NH) but did display a band at 1596 cm^{-1} (*cf.* 1585 cm^{-1} for Tl$[NC_5H_4O]$ and 1635 cm^{-1} for the free ligand[18]) which is tentatively attributed to ν_{asym}(OCN) of the co-ordinated hydroxypyridinate anion. The assignment

† *Supplementary data available:* see Instructions for Authors, *J. Chem. Soc., Dalton Trans.*, 1992, Issue 1, pp. xx–xxv.

of ν_{sym}(OCN) at lower wavenumber is ambiguous due to the presence of bands arising from the pyridyl ring. A weak band is also observed at 317 cm^{-1} corresponding to ν(RuCl). The ^1H NMR spectrum shows the characteristic four-line pattern (Table 1) for the terminal allyl protons of the 2,7-dimethylocta-2,6-diene-1,8-diyl ligand (δ 5.05, 4.24, 4.07 and 3.00) and two relatively widely separated signals for the methyl substituents (δ 2.38 and 2.24) indicative of inequivalent axial sites on the trigonal-bipyramidal ruthenium atom. A fast atom bombardment (FAB) mass spectrum displayed a strong molecular ion peak at m/z = 367 (based on ^{102}Ru and ^{35}Cl) with the expected isotope distribution pattern. Fragmentation peaks associated with loss of a single chloride ligand and loss of both chloride and hydroxypyridinate ligands were also observed, and a peak at m/z = 136 is due to the 2,7-dimethylocta-2,6-diene-1,8-diyl ligand. These observations, in conjunction with microanalytical data, lead us to formulate **4** as a chelate complex [Ru(η³:η³-$C_{10}H_{16}$)Cl(NC_5H_4O)], which is structurally related to **3** and to the complexes prepared by Toerien and van Rooyen.[5] It was also noted that the ^1H NMR spectrum of crude **4** produced in this way showed small traces of a second compound with only two terminal allyl resonances (δ 4.90 and 4.04) and a broad peak at δ 10.40. We were unable to isolate this second product but tentatively suggest it to be an analogue of the ruthenium(II) monodentate pyridone adduct [Ru(η⁶-C_6H_6)Cl_2(OC_5H_4NH)], for which the amine proton is observed at δ 11.56. The ready formation of chelate complexes such as **4** markedly contrasts with studies on the pyridine-2-thiolate analogues,[5] and is attributed to the greater acidity of the hydroxyl proton.

Unlike its ruthenium(II) arene analogues, **4** might be expected to exist as two geometrical isomers (**4a**, **4b**) distinguishable by ^1H NMR spectroscopy, as a consequence of the stereochemical inequivalence of the axial and equatorial sites of the trigonal-bipyramidal ruthenium atom. However, both [Ru(η³:η³-$C_{10}H_{16}$)Cl($N_2C_7H_5S$)] and [Ru(η³:η³-$C_{10}H_{16}$)Cl(NC_5H_4S)][5] are reported to exist solely as equatorial isomers (type **a**), with the pyridyl nitrogen atom occupying the equatorial site of the trigonal-bipyramidal ruthenium atom. The ^1H NMR spectrum of **4** (obtained from a sample synthesised by direct interaction of **1** with the non-deprotonated 2-hydroxypyridine ligand) is interpreted in terms of a single isomer, possessing a set of resonances qualitatively similar, in the allyl region, to those exhibited by [Ru(η³:η³-$C_{10}H_{16}$)Cl($N_2C_7H_5S$)] and [Ru(η³:η³-$C_{10}H_{16}$)Cl(NC_5H_4S)].[5]

It might be supposed that, analogously to the ruthenium(II) arene system,[12] 2-hydroxypyridine would react with compound **1** in a two-step process, co-ordinating initially *via* the pyridone oxygen atom at the equatorial site of the '$C_{10}H_{16}RuCl_2$' unit (as observed in all previous cases of monodentate co-ordination to the $C_{10}H_{16}RuCl_2$ unit[3,4,6,16] and suggested by the ^1H NMR spectrum of the trace product described above). Subsequent deprotonation of such an adduct would then be expected to give a complex possessing a pyridyl ring occupying an axial site, a geometry at variance with that observed crystallographically for [Ru(η³:η³-$C_{10}H_{16}$)Cl($N_2C_7H_5S$)].[5] However, at some stage in the reaction a rearrangement must take place such that the relatively unhindered pyridone oxygen atom of the 2-hydroxypyridinate ligand preferentially occupies the more hindered axial site. This proposal is consistent with the isomerisation of **1** in MeCN solution,[3] where the predominant species is observed to be a monomeric, bridge-cleaved complex with a chloride ligand in the equatorial position and the acetonitrile axially located.

Indirect evidence for an intramolecular rearrangement of a pyridone intermediate in the formation of compound **4** comes from reaction of sodium 2-hydroxypyridinate with **1**. Again the major product (95%, evaluated by integration of the ^1H NMR spectrum) consists of the isomer **4a**, however smaller quantities of a geometric isomer **4b** are also observed. The ^1H NMR data of **4b** are in Table 1. This reaction, which uses the performed anionic ligand, presumably increases the rate of the chelation step such that there is insufficient time for the equatorial–axial rearrangement to occur and hence a significant quantity of the less-stable axial isomer is observed.

In an attempt to confirm the formulation of **4a** and **4b** and synthesise further compounds displaying both axial and equatorial pyridyl fragments, we investigated the reaction of **1** with 6-chloro-2-hydroxypyridine, 2-hydroxy-4-methylquinoline and 2-hydroxy-6-methylpyridine. These ligands contain bulky *ortho* substituents which might be expected to interact unfavourably with the remaining axial chloride ligand in complexes of type **a** and thus may display less preference for the equatorial form. Reaction with the neutral pyridinols was found to be slow at room temperature and significantly more efficient conversions were obtained through use of the sodium salts of the ligands or addition of anhydrous sodium carbonate to the reaction mixtures. In this way compounds of formula [Ru(η³:η³-$C_{10}H_{16}$)Cl{NC_5H_3(O)Cl-6}] **5**, [Ru(η³:η³-$C_{10}H_{16}$)Cl{NC_9H_5(O)Me-4}] **6** and [Ru(η³:η³-$C_{10}H_{16}$)Cl{NC_5H_3(O)Me-6}] **7** were obtained (C,H,N analysis) in good yields. Like **4**, complexes **5**–**7** display no bands attributable to ν(OH) or ν(NH) in their infrared spectra but possess peaks at 1589 (**5**), 1550 (**6**) and 1558 cm^{-1} (**7**) tentatively assigned to ν_{asym}(OCN) as well as peaks arising as a consequence of pyridyl C=C modes[17] (see Experimental section) and bands due to ν(RuCl). The ^1H NMR spectra of these materials proved complex, each possessing two sets of signals, present in a ratio of approximately 3:1 in the case of **5**, 6:1 for **6** and 3:2 for **7**. The spectrum of **5**, for example, displays four singlets for the major product due to terminal allyl protons (δ 5.25, 4.36, 4.27 and 4.96) and two methyl resonances (δ 2.32 and 2.16) and similarly the minor product **5b** displays resonances at δ 4.95, 4.66, 4.56 and 3.73 (terminal allyl) and 2.49 and 2.37 (methyl). These spectra could conceivably be attributed to pairs of diastereoisomers of **5**–**7** if the compounds were dimeric, since binuclear compounds containing two 'η³:η³-$C_{10}H_{16}$Ru' units have been shown to display a total of eight terminal allyl resonances and four methyl signals.[3,18-20] However, electron-impact mass spectra exhibit strong molecular ion peaks at m/z 401 (**5**), 431 (**6**) and 381 (**7**) with isotope distribution patterns consistent with the presence of a single ruthenium atom in each case, implying the formation of mononuclear complexes. The mononuclear nature of **5** was confirmed by a single-crystal X-ray structure determination (see below). Fractional crystallisation of **5** from an acetone solution gave red-brown crystals of a single isomer which was shown to be the major isomer **5a**, by low-temperature dissolution of the crystalline material and simultaneous recording of its ^1H NMR spectrum (193 K). The structure determination (Fig. 1) showed **5a** to be a mononuclear chelate compound, with the nitrogen atom equatorial, closely related to the equatorial structure assigned to **4a**, and observed crystallographically in the case of [Ru(η³:η³-$C_{10}H_{16}$)Cl($N_2C_7H_5S$)].[5] Complex **5b** is therefore assigned a similar structure with the pyridyl nitrogen atom axial. By analogy, similar isomeric structures are assigned to **6a**, **6b** and **7a**, **7b**. The major products are assigned the structures with the nitrogen atoms equatorially co-ordinated, allowing the bulky pyridyl fragments to avoid the axial sites which are sterically crowded by the methyl groups of the bis(allyl), 2,7-dimethylocta-2,6-diene-1,8-diyl ligand.

Good evidence for the equatorial nature of compounds **4a**–**7a** comes from their ^1H NMR spectra which, in common with those of [Ru(η³:η³-$C_{10}H_{16}$)Cl($N_2C_7H_5S$)] and [Ru(η³:η³-$C_{10}H_{16}$)Cl(NC_5H_4S)],[5] have the two central resonances, due to the terminal allyl protons, occurring at very similar chemical shifts. The pattern differs markedly from that observed for **4b**–**7b** and [Ru(η³:η³-$C_{10}H_{16}$)Cl(L–L)][BF_4][15] (L–L = 2,2′-bipyridyl or 1,10-phenanthroline) where one of these resonances is shifted significantly upfield relative to the other three, possibly as a consequence of ring-current effects of the aromatic moiety. Another observation which may serve to distinguish between the two possible isomers is the differences in the resonances assigned to the internal allyl protons. In the case of **4a**–**7a** these

Table 1 Proton NMR data for new complexes[a]

Compound	δ				
	Terminal allyl	Internal allyl	Ethylenic	Me	Ligand
4a $[Ru(\eta^3:\eta^3\text{-}C_{10}H_{16})Cl(NC_5H_4O)]$ (N equatorial)	5.05 (s, 1 H) 4.24 (s, 1 H) 4.07 (s, 1 H) 3.00 (s, 1 H)	4.19 (m, 1 H) 3.46 (m, 1 H)	2.78 (m, 4 H)	2.38 (s, 3 H) 2.24 (s, 3 H)	8.30 (d, 1 H, ^3J = 5.4) 7.48 (t, 1 H, ^3J = 8.6) 6.66 (t, 1 H, ^3J = 6.0) 5.94 (d, 1 H, ^3J = 8.6)
4b $[Ru(\eta^3:\eta^3\text{-}C_{10}H_{16})Cl(NC_5H_4O)]$ (O equatorial)	5.24 (s, 1 H) 4.69 (s, 1 H) 4.36 (s, 1 H) 3.24 (s, 1 H)	4.40 (m, 1 H) 3.31 (m, 1 H)	2.78 (m, 4 H)	2.42 (s, 3 H) 2.12 (s, 3 H)	7.43 (t, 1 H)[b] 7.08 (d, 1 H, ^3J = 5.9) 6.32 (t, 1 H, ^3J = 6.1) 6.16 (d, 1 H, ^3J = 8.7)
5a $[Ru(\eta^3:\eta^3\text{-}C_{10}H_{16})Cl\{NC_5H_3(O)Cl\text{-}6\}]$ (N equatorial)	5.25 (s, 1 H) 4.36 (s, 1 H) 4.27 (s, 1 H) 2.96 (s, 1 H)	4.32 (m, 1 H) 3.59 (m, 1 H)	2.69 (m, 4 H)	2.32 (s, 3 H) 2.16 (s, 3 H)	7.48 (dd, 1 H, ^3J = 8.4, 7.6) 6.62 (d, 1 H, ^3J = 7.6) 5.92 (d, 1 H, ^3J = 8.4)
5b $[Ru(\eta^3:\eta^3\text{-}C_{10}H_{16})Cl\{NC_5H_3(O)Cl\text{-}6\}]$ (O equatorial)	4.95 (s, 1 H) 4.66 (s, 1 H) 4.56 (s, 1 H) 3.73 (s, 1 H)	4.81 (m, 1 H) 4.56 (t, 1 H, ^3J = 5.4)	2.69 (m, 4 H)	2.49 (s, 3 H) 2.37 (s, 3 H)	7.45 (dd, 1 H, ^3J = 7.6, 8.6) 6.35 (d, ^3J = 7.6) 6.08 (d, ^3J = 8.6)
6a $[Ru(\eta^3:\eta^3\text{-}C_{10}H_{16})Cl\{NC_9H_5(O)Me\text{-}4\}]$ (N equatorial)	5.31 (s, 1 H) 4.43 (s, 1 H) 4.36 (s, 1 H) 2.97 (s, 1 H)	4.43 (m, 1 H) 3.64 (m, 1 H)	2.76 (m, 4 H)	2.39 (s, 3 H) 2.21 (s, 3 H)	8.49 (d, 1 H, ^3J = 8.4) 7.76 (d, 1 H, ^3J = 8.2) 7.54 (t, 1 H, ^3J = 7.0) 7.28 (t, 1 H, ^3J = 7.0) 6.01 (s, 1 H) 2.54 (s, 3 H, CH_3)
6b $[Ru(\eta^3:\eta^3\text{-}C_{10}H_{16})Cl\{NC_9H_5(O)Me\text{-}4\}]$ (O equatorial)	5.15 (s, 1 H) 4.80 (s, 1 H) 4.56 (s, 1 H) 3.53 (s, 1 H)	4.62 (t, 1 H, ^3J = 5.6) 4.39 (m, 1 H)	2.65 (m, 4 H)	2.45 (s, 3 H) 2.30 (s, 3 H)	7.73 (d, 1 H, ^3J = 8.2) 7.39 (t, 1 H, ^3J = 7.0) 7.18 (t, 1 H, ^3J = 7.6) 6.88 (d, 1 H, ^3J = 8.4) 6.32 (s, 1 H) 2.52 (s, 3 H, CH_3)
7a $[Ru(\eta^3:\eta^3\text{-}C_{10}H_{16})Cl\{NC_5H_3(O)Me\text{-}6\}]$ (N equatorial)	5.21 (s, 1 H) 4.31 (s, 1 H) 4.30 (s, 1 H) 2.91 (s, 1 H)	4.37 (m, 1 H) 3.56 (m, 1 H)	2.73 (m, 4 H)	2.36 (s, 3 H) 2.17 (s, 3 H)	7.28 (dd, 1 H, ^3J = 8.4, 7.6) 6.33 (d, 1 H, ^3J = 7.6) 5.71 (d, 1 H, ^3J = 8.4)
7b $[Ru(\eta^3:\eta^3\text{-}C_{10}H_{16})Cl\{NC_5H_3(O)Me\text{-}6\}]$ (O equatorial)	5.10 (s, 1 H) 4.77 (s, 1 H) 4.51 (s, 1 H) 3.70 (s, 1 H)	4.61 (t, 1 H, ^3J = 6.2) 4.14 (m, 1 H)	2.59 (m, 4 H)	2.33 (s, 3 H) 2.11 (s, 3 H)	7.28 (m, 1 H) 6.07 (virtual t, 2 H)
8a $[Ru(\eta^3:\eta^3\text{-}C_{10}H_{16})Cl(NC_9H_6O)]$ (N equatorial)	4.34 (s, 1 H) 3.98 (s, 1 H) 3.87 (s, 1 H) 2.70 (s, 1 H)	4.95 (AXX′, 1 H, ^3J = 6.2) 4.37 (AXX′, 1 H, ^3J = 5.6)	3.22 (m, 2 H) 2.72 (m, 1 H) 2.64 (m, 1 H)	2.41 (s, 3 H) 2.08 (s, 3 H)	9.28 (dd, 1 H, ^3J = 4.9, ^4J = 1.3) 8.13 (dd, 1 H, ^3J = 8.4, ^4J = 1.2) 7.39 (dd, 1 H, ^3J = 5.0, 5.0) 7.24 (t, 1 H, ^3J = 7.9) 6.85 (d, 1 H, ^3J = 7.9) 6.67 (d, 1 H, ^3J = 8.0)

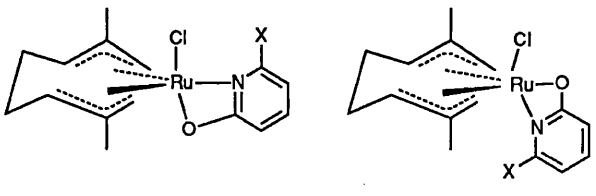

X = H(4), Cl(5), Me(7)

Equatorial isomer (type a) Axial isomer (type b)

4a **4b**
5a **5b**
7a **7b**

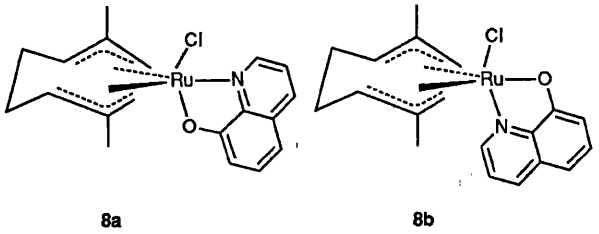

8a **8b**

occur as two broad, poorly resolved, singlet-like resonances at δ *ca.* 4.3 and 3.5. Conversely, the spectra of **4b**–**7b** display the corresponding resonances as much sharper signals at δ *ca.* 4.7 and 4.2–4.5, one occurring as a virtual triplet and the other as a well resolved five-line multiplet.

To confirm these observations the reaction of compound **1** with 8-hydroxyquinoline (NC_9H_6OH) was examined, Both isomers resulting from this reaction might be expected to possess an aromatic ring in the axial site and so display ^1H NMR spectra typical of type **b** compounds. Two products were indeed obtained, $[Ru(\eta^3:\eta^3\text{-}C_{10}H_{16})Cl(NC_9H_6O)]$ **8a**, **8b** although, presumably due to the relatively unhindered nature of the ligand, the isomer ratio was in excess of 20:1 (in retrospect an unsurprising result given the observation of only a single isomer of **4** arising from reaction with the neutral ligand). The mononuclear nature of these materials was confirmed by a FAB mass spectrum. The ^1H NMR spectra of both materials displayed the expected four-line patterns for the terminal allyl protons [δ 4.34, 3.98, 3.87 and 2.70 (major isomer **8a**); 4.87, 4.58, 4.02 and 3.09 (minor isomer **8b**)] which are qualitatively similar to those of type **b** complexes. The signals attributed to the internal allyl protons occurred as sharp resonances strongly resembling those observed for the cationic bipyridine and phenanthroline complexes.[15] Logically, and by analogy with **4a**, **4b**, the major product will be of the N-equatorial, O-axial type. Evidence for this comes from the consistent upfield shift of the signals due to the allyl protons of the major isomer relative to the minor one, presumably as a consequence of the closer proximity of the aromatic ring to the bis(allyl) ligand when the pyridyl fragment occupies the axial site.

Reaction of compound **1** with α-pyrrolidinone, HNC_4H_6O, also gives rise to an axial and an equatorial isomer, related to **5**–**7**, namely $[Ru(\eta^3:\eta^3\text{-}C_{10}H_{16})Cl(NC_4H_6O)]$ **9a**, **9b**. The solid-state infrared spectrum of **9** displays strong, broad peaks at 1540 and 1407 cm^{-1} (signals due to individual isomers not resolved) corresponding to the antisymmetric and symmetric ν(OCN) modes [in this particular case the assignment may be made with confidence due to the absence of pyridyl ν(C=C) bands]. The ^1H NMR data are in Table 1. The major product (present in a ratio of approximately 5:2) displays a pattern of four terminal allyl proton resonances characteristic of an equatorial isomer. The relatively abundant minor isomer exhibits a spectrum similar to those of complexes of type **b**, although in the absence of an aromatic ring the distinction is less obvious. Clearly isomerism in **9** is unlikely to be a consequence of unfavourable steric interactions between the chloride ligand and bulky *ortho* ring substituents which are absent in this case. The formation of substantial quantities of the axial isomer is rather attributed to the stereochemical non-rigidity of the saturated five-membered ring of the hydroxypyrrolidinate ligand which allows the relief of otherwise unfavourable steric interactions between the co-ordinated ligands.

Reactions with Pyridine-2-thiols.—Sterically hindered ligands such as 6-chloro-2-hydroxypyridine, 2-hydroxy-4-methylquinoline and 2-hydroxy-6-methylpyridine are often observed to bridge across two metal centres[21] rather than form strained four-membered chelate rings. Nevertheless we have described above how the reaction of compound **1** with these ligands leads to the formation of mononuclear complexes **5**–**7**. We reasoned though that reaction of **1** with ligands containing larger donor atoms such as sulfur, as well as a sterically hindering *ortho* substituent, might lead to the formation of bridged, binuclear complexes. It should be noted however that pyridine-2-thiol has already been observed to form a mononuclear compound on reaction with **1**,[5] this mode of co-ordination being attributed to the slowness of the deprotonation step relative to the rate of co-ordination of the ligand in a monodentate fashion *via* the pyridyl nitrogen atom.[5]

We have now investigated the reaction of the more hindered pyridinethiols, quinoline-2-thiol and 6-methylpyridine-2-thiol and of their sodium salts with compound **1** in an attempt to prepare binuclear species. The reactions involving the free ligands gave only mononuclear bridge-cleaved species $[Ru(\eta^3:\eta^3\text{-}C_{10}H_{16})Cl_2(NC_9H_6SH)]$ **10** and $[Ru(\eta^3:\eta^3\text{-}C_{10}H_{16})Cl_2(NC_5H_3MeSH)]$ **11** in which the ligands are probably co-ordinated in a monodentate fashion *via* the pyridyl nitrogen atom, by analogy with $[Ru(\eta^3:\eta^3\text{-}C_{10}H_{16})Cl(N_2C_7H_5S)]$ and $[Ru(\eta^3:\eta^3\text{-}C_{10}H_{16})Cl(NC_5H_4S)]$.[5] The infrared spectra (Nujol) of both of these complexes display several strong bands in the region 1600–1400 cm^{-1} corresponding to ν(C=C) and ν(C=N) ring modes, and ν(RuCl) bands are observed at 316, 289 and 317, 297 cm^{-1} for **10** and **11** respectively. No bands unambiguously assignable to ν(SH) or ν(NH) were seen, as was the case in Toerien and van Rooyen's study.[5] Reaction of **1** with the preformed sodium salt of quinoline-2-thiol led to a species displaying a ^1H NMR spectrum containing a four-line pattern for the terminal allyl protons (δ 5.00, 4.57, 4.19 and 3.14), which was difficult unambiguously to assign to either axial or equatorial co-ordination but consistent with the chelate complex $[Ru(\eta^3:\eta^3\text{-}C_{10}H_{16})Cl(NC_9H_6S)]$ **12a**. The internal allyl resonances, which consist of two narrow multiplets, occurring at δ 4.88 and 4.06, imply equatorial co-ordination. The solid-state infrared spectrum of **12a** (KBr disc) displays similar bands to **10** at 1608, 1589, 1498 and 1421 cm^{-1}. In addition, two bands of medium intensity are observed at 1545 and 1448 cm^{-1} and are tentatively assigned to ν(S–C=N). The Nujol spectrum displays ν(RuCl) 303 cm^{-1} and the FAB mass spectrum exhibits a strong molecular ion peak at *m*/*z* 433 along with fragmentation peaks consistent with the proposed structure. A quantity of a second isomer **12b** was also observed (**12a**:**12b** 5:1). A single-crystal X-ray structure determination (Fig. 2) revealed a complex possessing an equatorial structure, very similar to that of **5a** and $[Ru(\eta^3:\eta^3\text{-}C_{10}H_{16})Cl(N_2C_7H_5S)]$.[5] Low-temperature dissolution of the crystalline sample and simultaneous recording of its ^1H NMR spectrum showed this structure to represent **12a**, the form strongly predominant in solution.

The relationship between the mode of ligand co-ordination and the ^1H NMR spectral pattern is less well defined for the pyridinethiolate complexes than it was for hydroxypyridinates, especially in terms of the positions of the terminal allyl resonances {the anomaly is, to some extent, shared by the pyridine-2-thiolate complex $[Ru(\eta^3:\eta^3\text{-}C_{10}H_{16})Cl(NC_5H_4S)]$[5]} to the extent that it is not possible unambiguously to assign structure for a given isomer in isolation.

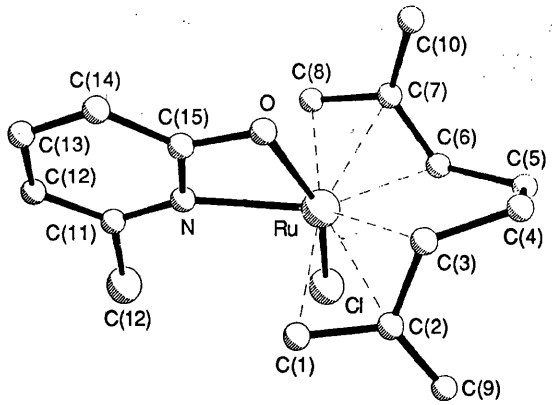

Fig. 1 Molecular structure of $[Ru(\eta^3:\eta^3\text{-}C_{10}H_{16})Cl\{NC_5H_3(O)Cl\text{-}6\}]$ **5a** showing the atom numbering scheme adopted

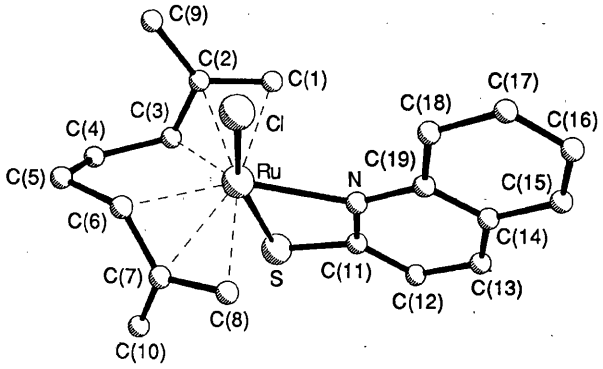

Fig. 2 Molecular structure of $[Ru(\eta^3:\eta^3\text{-}C_{10}H_{16})Cl(NC_9H_6S)]$ **12a** showing the atom numbering scheme adopted

Table 2 Fractional atomic coordinates ($\times 10^4$) for $[Ru(\eta^3:\eta^3\text{-}C_{10}H_{16})Cl\{NC_5H_3(O)Cl\text{-}6\}]$ **5a**

Atom	*x*	*y*	*z*
Ru	1896(1)	3798	5763(1)
Cl(1)	2024(3)	5845(2)	5592(2)
Cl(2)	−1071(6)	5917(4)	7002(2)
N	88(6)	3826(12)	6687(4)
O	1224(11)	2211(7)	6259(4)
C(1)	−608(10)	3783(15)	5139(4)
C(2)	800(10)	3695(12)	4615(4)
C(3)	1904(12)	2728(8)	4757(6)
C(4)	3572(15)	2528(12)	4347(5)
C(5)	4938(12)	3403(10)	4566(6)
C(6)	4596(10)	3930(12)	5312(5)
C(7)	4638(13)	3283(10)	5981(6)
C(8)	3977(10)	3926(14)	6596(4)
C(9)	1113(14)	4573(11)	4045(6)
C(10)	5103(19)	2038(12)	6050(7)
C(11)	−924(13)	4446(12)	7145(6)
C(12)	−1843(13)	3941(25)	7705(6)
C(13)	−1728(18)	2740(19)	7782(7)
C(14)	−710(18)	2108(13)	7319(6)
C(15)	202(17)	2650(11)	6744(6)

A comparison of the spectra of two isomers of the same compound may however provide a worthwhile indication as to the likely geometry.

Reaction of compound **1** with the sodium salt of 6-methylpyridine-2-thiol also led to mononuclear species (FAB mass spectrum, molecular ion *m/z* 397), $[Ru(\eta^3:\eta^3\text{-}C_{10}H_{16})Cl\{NC_5H_3(S)Me\text{-}6\}]$ (**13a**, **13b**; ratio 1:3), directly analogous to **7a**, **7b**.

Isomer Ratios.—If a model invoking two sets of competing steric interactions (*i*) between axial ligand fragments and

Table 3 Fractional atomic coordinates ($\times 10^4$) for $[Ru(\eta^3:\eta^3\text{-}C_{10}H_{16})Cl(NC_9H_6S)]$ **12a**

Atom	*x*	*y*	*z*
Ru	2539(1)	842(1)	2926(1)
S	1601(2)	1212(2)	4190(1)
Cl	3717(2)	−113(2)	1950(1)
N	2364(5)	−601(4)	3765(4)
C(1)	619(7)	211(6)	1946(5)
C(2)	936(7)	1167(6)	1551(5)
C(3)	1014(6)	2061(6)	2170(5)
C(4)	1517(8)	3168(6)	2016(6)
C(5)	2973(8)	3144(6)	2016(5)
C(6)	3727(7)	2185(5)	2593(5)
C(7)	4069(6)	2102(6)	3618(5)
C(8)	4567(7)	1101(6)	4000(6)
C(9)	1208(9)	1233(7)	580(5)
C(10)	3841(8)	2997(6)	4239(6)
C(11)	1892(6)	−144(6)	4435(4)
C(12)	1653(8)	−696(6)	5195(5)
C(13)	1894(8)	−1765(7)	5265(5)
C(14)	2342(7)	−2304(6)	4565(6)
C(15)	2555(9)	−3421(7)	4580(7)
C(16)	2954(10)	−3910(7)	3892(8)
C(17)	3155(8)	−3325(7)	3136(7)
C(18)	2959(8)	−2217(6)	3092(6)
C(19)	2561(7)	−1715(5)	3801(5)

Table 4 Selected bond lengths (Å) and angles (°) for compound **5a**

Ru–Cl(1)	2.381(3)	Ru–C(1)	2.219(8)
Ru–O	2.099(8)	Ru–C(2)	2.239(8)
Ru–N	2.166(6)	Ru–C(3)	2.195(10)
O–C(15)	1.278(14)	Ru–C(6)	2.222(8)
N–C(15)	1.361(18)	Ru–C(7)	2.211(10)
Cl(2)–C(11)	1.718(15)	Ru–C(8)	2.193(8)
Cl(1)–Ru–N	96.4(4)	Ru–O–C(15)	95.6(7)
Cl(1)–Ru–O	158.1(2)	Ru–N–C(15)	90.2(7)
N–Ru–O	61.9(4)	N–C(15)–O	112.4(10)

Table 5 Selected bond lengths (Å) and angles (°) for compound **12a**

Ru–Cl	2.461(2)	Ru–C(1)	2.209(6)
Ru–S	2.386(2)	Ru–C(2)	2.206(6)
Ru–N	2.221(5)	Ru–C(3)	2.229(6)
S–C(11)	1.741(7)	Ru–C(6)	2.231(7)
N–C(11)	1.351(9)	Ru–C(7)	2.245(6)
		Ru–C(8)	2.225(7)
Cl–Ru–N	93.7(2)	Ru–S–C(11)	83.2(3)
Cl–Ru–S	160.0(1)	Ru–N–C(11)	99.5(4)
N–Ru–S	67.0(2)	N–C(11)–S	110.2(5)

dimethyloctadienediyl methyl substituents and (*ii*) between *ortho*-pyridyl substituents and axial chloride ligands is assumed it becomes possible to rationalise the preferences in isomer ratio. The unsubstituted 2-hydroxypyridinate and pyridine-2-thiolate[5] ligands display uniquely equatorial pyridyl co-ordination (type **a**). When bulky ring substituents are introduced *ortho* to the pyridyl nitrogen atom (*e.g.* complexes **5**–**7**) the interactions of these substituents with the axial chloride ligands destabilise the type **a** form relative to **b** and thus two isomers are observed. The axial (type **b**) form would thus be expected to become more predominant as the size of the ring substituent increases. This argument is qualitatively compatible with the observed isomer ratios for complexes **4**–**7**.

In the case of **13a**, **13b** the isomer ratio was observed to be 1:3, *i.e.* for **13** it is the N_{axial} (type **b**) form which predominates. Evidence for this comes from the allyl region of the ^1H NMR spectra of **7** and **13**. The terminal allyl signals for the *major* isomer in the spectrum of **13** display a grouping characteristic of

an axial isomer with three signals between δ 4.5 and 5 and the other one shifted upfield to δ 3.88 (*cf.* **7b**, δ 5.10, 4.77, 4.51 and 3.70). The signals for the minor isomer are much more evenly distributed (δ 4.91, 4.45, 4.15 and 3.10; *cf.* **7a**, 5.21, 4.31, 4.30 and 2.91). Turning to the internal allyl proton resonances, **4a**, **5a** and **7a** (equatorial isomers) display poorly resolved, singlet-like multiplets (δ 4.19 and 3.46, **4**: 4.32 and 3.59 ppm, **5a**; 4.37 and 3.56, **7a**) as does the *minor* product in the case of **13** (δ 4.79 and 3.96), although the actual values are shifted downfield by 0.5 ppm (an observation consistent with most of the other signals on moving to the sulfur donor atom of the pyridinethiolate ligand). In contrast the corresponding signals for **5b** and **7b** occur as a sharp triplet and sharp, five-line multiplet pair (δ 4.81 and 4.56, **5b**; 4.61 and 4.14, **7b**) as do the corresponding resonances for the major isomer in the case of **13**, again with an overall downfield chemical shift (δ 5.02 and 4.66).

Complete proof of these deductions on the identity of **13a**, **13b** must await a single-crystal X-ray structure determination and concomitant low-temperature NMR experiment, but the evidence would seem to point towards a consistent relationship between equatorial:axial isomer ratio and the relative magnitudes of the various steric interactions.

X-Ray Structure Determinations.—The crystal structures of compounds **5a** and **12a** are shown in Figs. 1 and 2, and fractional atomic coordinates and selected bond lengths and angles are given in Tables 2 and 3, and, 4 and 5. The details of the structure solutions and refinement are in the Experimental section. As observed in previous structures containing the '(η^3:η^3-$C_{10}H_{16}$)Ru' unit[2,4–6,8,19] the geometry about the ruthenium ions in both **5a** and **12a** is conveniently described as a distorted trigonal bipyramid, although a pentagonal-bipyramidal description can also be justified in this type of bis(allyl)-ruthenium(IV) system.[22] The 2,7-dimethylocta-2,6-diene-1,8-diyl ligand shows the usual local C_2 symmetry and there is no significant variation in the Ru–C distances. The ruthenium chloride distances in **5a** and **12a** are 2.381(3) and 2.461(2) Å respectively. The former is similar to that observed for $Ru-Cl_{terminal}$ (2.386 Å) in the parent chloro-bridged dimer[8] but rather shorter than the norm for other (η^3:η^3-$C_{10}H_{16}$)Ru systems (2.40–2.42 Å).[4–6] It is similar to that observed in [Ru(η^6-C_6H_6)Cl{NC_5H_3(O)Me-6}][12] [2.392(2) Å]. The longer Ru–Cl bond in **12a** may be attributed to the *trans* effect of the sulfur donor atom. The ruthenium–oxygen distance is rather short in **5a** [2.099(8) when compared to 2.120(5)[12] and 2.153(6) Å[14] in related ruthenium(II) arene systems] whereas the ruthenium–nitrogen distance is somewhat longer [2.166(6) as against 2.091(5)[12] and 2.084(7) Å].[14] In general the structure of **5a** is closely related to that of [Ru(η^6-C_6H_6)Cl{NC_5H_3(O)Me-6}][12] with one important difference. In the latter structure the *ortho*-methyl group possesses apparently little stereochemical consequence and resides on the opposite side of the molecule to the chloride ligand. The more sterically demanding nature of the bis(allyl) ligand in **5a** causes the chloride ligand and the *o*-chloride ring substituent to lie virtually eclipsed with one another (the pyridyl ring is inclined at 6.2° to the plane containing the chlorine, nitrogen and oxygen atoms), the chlorine–chlorine non-bonded distance being 3.48(1) Å. As a result the Ru–N–C(11) angle is opened up to 149(1)°, compared to 143.4(5)° in the case of **3**[12] and 124(1)° when the 2-hydroxy-6-methylpyridinate ion is in the less sterically demanding bridging mode,[21] and is indicative of significant strain in the complex. Steric strain in the complex is also apparent in the very large Cl(1)–Ru–N angle 96.4(4)°. In undistorted structures this angle averages *ca.* 85°[1,4] and indeed the Cl–Ru–S angle in [{Ru(η^3:η^3-$C_{10}H_{16}$)Cl(μ-SCN)}$_2$][20] is only 80.3(1)°. Values of 88.6(3)° in [Ru(η^3:η^3-$C_{10}H_{16}$)Cl($N_2C_7H_5S$)][5] and 90.3(1)° in [{Ru(η^3:η^3-$C_{10}H_{16}$)Cl_2}$_2$(μ-dppm)] [dppm = bis-(diphenylphosphino)methane][6] have been found.

The steric strain in this complex is a significant contributory factor in the observation of appreciable quantities of the axial isomer **5b**, where no strong chlorine–chlorine interactions would be apparent. However, resulting steric interactions between the bis(allyl) ligand and the chloride substituent in **5b** mean that **5a** is still the predominant isomer observed.

For compound **12a** the Ru–S distance [2.386(2) Å] is significantly shorter than the equivalent distances in [Ru(η^3:η^3-$C_{10}H_{16}$)Cl($N_2C_7H_5S$)][5] [2.425(4) Å] and in [{Ru(η^3:η^3-$C_{10}H_{16}$)Cl(μ-SCN)}$_2$][19] [2.490(4) Å] (where the sulfur atom occupies the equatorial site). In the former case a geometrical factor may be involved since the sulfur atom in **12a** is attached to a six-membered ring, as opposed to a five-membered one in the $N_2C_7H_5S$ complex. This is also reflected in the angle Cl–Ru–S which is opened out to 160.0(1)° compared to 156.4(1)° in [Ru(η^3:η^3-$C_{10}H_{16}$)Cl($N_2C_7H_5S$)].[5] The ruthenium–nitrogen distance, 2.221(5) Å, is remarkably long when compared to the bond lengths noted above (2.09–2.16 Å) and probably, like the long Ru–Cl distance, is a reflection of the better donor properties of the sulfur atom and also perhaps its greater bulk.

Conclusion

In spite of the use of preformed salts of ligands expected to bring about bridged, binuclear complexation, only mononuclear species have been observed. It has been shown that ligands related to 2-hydroxypyridine show two distinct chelate co-ordination geometries when bound to the 'η^3:η^3-$C_{10}H_{16}Ru^{IV}$' moiety. These isomers may be distinguished from one another by analysis of the allyl regions of their ^{1}H NMR spectra. By variation of the substitution of the *ortho* site of the ligand and the donor atoms it is possible selectively to synthesise a predominance of either co-ordination geometry.

Experimental

Instrumental.—The IR spectra were recorded on a PE983 grating spectrometer between 4000 and 200 cm^{-1} as either KBr disks or Nujol mulls on CsI plates, NMR spectra on a Varian VXR400 spectrometer. Microanalyses were carried out by the departmental service at University College London. Mass spectra were run by the University of London Intercollegiate Research Service (ULIRS) at the School of Pharmacy. All manipulations were carried out under nitrogen with degassed solvents using conventional Schlenk-line techniques, although no significant air sensitivity of the products was noted.

Starting Materials.—The compound [{Ru(η^3:η^3-$C_{10}H_{16}$)-Cl(μ-Cl)}$_2$] was prepared by published literature methods[3,5,7] by prolonged heating of ruthenium trichloride in ethanol in the presence of a large excess of isoprene. Ruthenium trichloride hydrate was obtained on loan from Johnson Matthey plc and was purified before use by dissolution in water and boiling to dryness. Sodium salts were prepared from reaction of sodium metal with the relevant ligand in dry tetrahydrofuran (thf), or in the neat ligand. All other reagents and materials were obtained from the usual commercial sources, with the exception of 6-methylpyridine-2-thiol which was synthesised by the literature method.[23,24]

Preparations.—[Ru(η^3:η^3-$C_{10}H_{16}$)Cl(NC_5H_4O)] **4**. The compound [{Ru(η^3:η^3-$C_{10}H_{16}$)Cl(μ-Cl)}$_2$] (0.0970 g, 0.157 mmol) was dissolved in dichloromethane (5 cm^3) and 2-hydroxypyridine (0.1018 g, 1.070 mmol) added. After stirring for 5 h the reaction mixture was evaporated to *ca.* ¼ volume and the solution diluted with hexane (5 cm^3). The product separated on standing at *ca.* 250 K for 1 h and was filtered off and washed with hexane. Yield: 0.0844 g, 0.230 mmol, 73% (Found: C, 49.70; H, 5.70; Cl, 10.80; N, 4.50. Calc. for $C_{15}H_{20}ClNORu$: C, 49.10; H, 5.50; Cl, 9.70; N, 3.80%). Infrared: ν_{asym}(OCN) 1596, ν(RuCl) 317 cm^{-1}. The product may also be prepared more cleanly, in comparable yield, by suspension of **1** in acetone (5 cm^3) and

addition of sodium 2-hydroxypyridinate. The reaction mixture was stirred for 5 h during which time it changed from pink to orange and the starting material was taken up into solution. The mixture was filtered over Celite and evaporated to an oil. This oil was dissolved in diethyl ether (1 cm^3) and layered with hexane (1 cm^3) from which the product separated as orange crystals after 12 h.

$[Ru(\eta^3:\eta^3\text{-}C_{10}H_{16})Cl\{NC_5H_3(O)Cl\text{-}6\}]$ **5**. The compound $[\{Ru(\eta^3:\eta^3\text{-}C_{10}H_{16})Cl(\mu\text{-}Cl)\}_2]$ (0.0728 g, 0.118 mmol) was suspended in acetone (5 cm^3) and sodium 6-chloro-2-hydroxypyridinate (0.0366 g, 0.242 mmol) added. The reaction mixture was stirred for 36 h during which time it changed from pink to orange and the starting material was taken up into solution. The mixture was filtered over Celite and evaporated to an oil. This oil was dissolved in diethyl ether (1 cm^3) and layered with hexane (1 cm^3) from which the product separated as deep red crystals after 12 h. Yield: 0.0452 g, 0.113 mmol, 48% (Found: C, 44.85; H, 4.50; N, 3.35. Calc. for $C_{15}H_{19}Cl_2NORu$: C, 44.90; H, 4.75; N, 3.50%). Infrared: 1589, 1437; ν(RuCl) 312 cm^{-1}.

$[Ru(\eta^3:\eta^3\text{-}C_{10}H_{16})Cl\{NC_9H_5(O)Me\text{-}4\}]$ **6**. Following a procedure analogous to that described for **5** using sodium 2-hydroxy-4-methylquinolinate an orange-yellow powder was isolated. Yield: 0.104 g, 0.241 mmol, 67% (Found: C, 56.15; H, 6.15; N, 2.85. Calc. for $C_{20}H_{24}ClNORu$: C, 55.75; H, 5.60; N, 3.25%). Infrared: 1657, 1600, 1550, 1507, 1465, 1446, 1416, 1403; ν(RuCl) 310 cm^{-1}.

$[Ru(\eta^3:\eta^3\text{-}C_{10}H_{16})Cl\{NC_5H_3(O)Me\text{-}6\}]$ **7**. The compound $\{Ru(\eta^3:\eta^3\text{-}C_{10}H_{16})Cl(\mu\text{-}Cl)\}_2]$ (0.0920 g, 0.149 mmol) was dissolved in dichloromethane (5 cm^3) and 2-hydroxy-6-methylpyridine (0.0325 g, 0.298 mmol) added. The mixture was stirred with $Na_2[CO_3]$ (0.05 g, excess) for 24 h during which time an orange colouration was observed to form. The reaction mixture was filtered over Celite and the filtrate evaporated to an orange oil. The product was obtained as orange crystals by recrystallisation from diethyl ether. Yield: 0.0831 g, 0.218 mmol, 73% (Found: C, 50.30; H, 5.80; N, 3.55. Calc. for $C_{14}H_{22}ClNORu$: C, 50.45; H, 5.80; N, 3.70%). Infrared: 1558, 1464; ν(RuCl) 322 cm^{-1}. The complex was also synthesised in similar yield by use of the sodium salt of the ligand in a similar way to that outlined for **4**.

$[Ru(\eta^3:\eta^3\text{-}C_{10}H_{16})Cl(NC_9H_6O)]$ **8**. The compound $[\{Ru(\eta^3:\eta^3\text{-}C_{10}H_{16})Cl(\mu\text{-}Cl)\}_2]$ (0.0744 g, 0.121 mmol) was suspended in acetone (5 cm^3) and 8-hydroxyquinoline (0.0361 g, 0.249 mmol) added. The reaction mixture was stirred for 2 h in the presence of $Na_2[CO_3]$ (0.05 g, excess) during which time it changed from pink to orange and the starting material was taken up into solution. The mixture was filtered over Celite and evaporated to an oil which was recrystallised from diethyl ether to give an orange product. Yield: 0.0750 g, 0.180 mmol, 74% (Found: C, 54.40; H, 5.65; N, 3.40. Calc. for $C_{19}H_{22}ClNORu$: C, 54.75; H, 5.30; N, 3.35%). Infrared: 1591, 1562, 1493; ν(RuCl) 318 cm^{-1}.

$[Ru(\eta^3:\eta^3\text{-}C_{10}H_{16})Cl(NC_4H_6O)]$ **9**. The compound $[\{Ru(\eta^3:\eta^3\text{-}C_{10}H_{16})Cl(\mu\text{-}Cl)\}_2]$ (0.1185 g, 0.192 mmol) was dissolved in dichloromethane (5 cm^3) and α-pyrrolidinone (0.05 cm^3, 0.6 mmol) added. The mixture was stirred with $Na_2[CO_3]$ (0.05 g, excess) for 24 h during which time a dark colouration was observed. The reaction mixture was filtered over Celite and the filtrate evaporated to an oil. The product was obtained as yellow crystals by recrystallisation from diethyl ether. Yield: 0.0280 g, 0.078 mmol, 20% (Found: C, 45.85; H, 6.50; N, 4.00. Calc. for $C_{14}H_{22}ClNORu$: C, 47.10; H, 6.20; N, 3.95%). Infrared: ν(OCN) 1540, 1407; ν(RuCl) 313 cm^{-1}.

$[Ru(\eta^3:\eta^3\text{-}C_{10}H_{16})Cl_2(NC_9H_6SH)]$ **10**. The compound $[\{Ru(\eta^3:\eta^3\text{-}C_{10}H_{16})Cl(\mu\text{-}Cl)\}_2]$ (0.1064 g, 0.173 mmol) was suspended in acetone (5 cm^3) and quinoline-2-thiol (0.0557 g, 0.345 mmol) added. The reaction mixture was stirred for 3 h during which time it changed from pink to orange and the starting material was taken up into solution. The mixture was filtered and evaporated to *ca.* $\frac{1}{4}$ volume. Diethyl ether (4 cm^3) was added and the product obtained as an orange precipitate. Yield: 0.0870 g, 0.185 mmol, 53% (Found: C, 48.60; H, 4.75; N, 2.90. Calc. for $C_{19}H_{23}Cl_2NRuS$: C, 48.60; H, 4.95; N, 3.00%). Infrared: 1617, 1585; ν(RuCl) 289, 316 cm^{-1}.

$[Ru(\eta^3:\eta^3\text{-}C_{10}H_{16})Cl_2\{NC_5H_3(SH)Me\text{-}6\}]$ **11**. Following a procedure analogous to that outlined for compound **10** above using 6-methylpyridine-2-thiol over a period of 24 h an orange-brown product was obtained. Yield: 0.0817 g, 0.205 mmol, 88% (Found: C, 43.35; H, 5.05; N, 2.60. Calc. for $C_{16}H_{23}Cl_2NRuS$: C, 44.30; H, 5.35; N, 3.25%). Infrared: 1612, 1589; ν(RuCl) 297, 317 cm^{-1}.

$[Ru(\eta^3:\eta^3\text{-}C_{10}H_{16})Cl(NC_9H_6S)]$ **12**. Following a procedure analogous to that described for compound **5** using sodium quinoline-2-thiolate an orange-brown powder was isolated. Yield: 0.050 g, 0.115 mmol, 46% (Found: C, 52.10; H, 5.15; N, 3.20. Calc. for $C_{19}H_{22}ClNRuS$: C, 52.70; H, 5.10; N, 3.25%). Infrared: ν(C=C) 1608, 1589, 1498, 1421; ν(S–C=N) 1545, 1448; ν(RuCl) 303 cm^{-1}.

$[Ru(\eta^3:\eta^3\text{-}C_{10}H_{16})Cl\{NC_5H_3(S)Me\text{-}6\}]$ **13**. Following a procedure analogous to that described for compound **5** using sodium 6-methylpyridine-2-thiolate an orange-brown powder was isolated. Yield: 0.045 g, 0.124 mmol, 66% (Found: C, 48.50; H, 6.10; N, 2.95. Calc. for $C_{16}H_{22}ClNRuS$: C, 48.40; H, 5.60; N, 3.50%). Infrared: 1597, 1583, 1545; ν(RuCl) 303 cm^{-1}.

X-Ray Crystal Structure Determinations.—(*i*) $[Ru(\eta^3:\eta^3\text{-}C_{10}H_{16})Cl\{NC_5H_3(O)Cl\text{-}6\}]$ **5a**. *Crystal data.* $C_{15}H_{19}Cl_2NORu$, $M = 401.32$, orthorhombic, space group $Pc2_1n$, $a = 7.636(3)$, $b = 11.519(3)$, $c = 18.054(8)$ Å, $U = 1588$ Å^3 (by least-squares refinement of diffractometer angles for 32 automatically centred reflections in the range $14 \leqslant 2\theta \leqslant 24°$, $\lambda = 0.710\,73$ Å), $F(000) = 808$, $D_c = 1.68$ g cm^{-3}, μ(Mo-Kα) = 13.0 cm^{-1}, $Z = 4$. Orange block, 0.35 × 0.20 × 0.20 mm.

Data collection and processing. Nicolet R3mV diffractometer equipped with graphite-monochromated Mo-Kα radiation. The ω–2θ technique was used to collect a data set $(+h,+k,+l)$ consisting of 1715 reflections in the range $5 \leqslant 2\theta \leqslant 50°$. Of the 1455 unique data 1302 were observed to have $I \geqslant 1.5\sigma(I)$ and used in structure solution and refinement. Three standard reflections monitored throughout the data collection showed no appreciable change in intensity. The data were corrected for Lorentz and polarisation effects and for absorption, from additional azimuthal scan data (maximum, minimum transmission 0.903, 0.818).

Structure solution and refinement. The structure was solved by conventional direct methods and Fourier difference techniques. Refinement was attempted in the orthorhombic space groups *Pcmn* and $Pc2_1n$ and proceeded most smoothly in the latter, the asymmetric unit being observed to contain one complete molecule. All non-hydrogen atoms were refined anisotropically. Hydrogen atoms were placed in idealised positions with a common isotropic thermal parameter [*r*(CH) 0.96 Å, U_{iso} 0.08 Å^2]. Full-matrix least-squares refinement gave $R = 0.0386$, $R' = 0.0439$ in the final cycle from 180 parameters. A weighting scheme $w^{-1} = \sigma^2(F) + 0.003\,058F^2$ was applied and the maximum shift/e.s.d. in the final cycle was 0.03. The largest residual peak was 0.51 e Å^{-3}. No short intermolecular contacts were observed.

(*ii*) $[Ru(\eta^3:\eta^3\text{-}C_{10}H_{16})Cl(NC_9H_6S)]$ **12a**. *Crystal data.* $C_{19}H_{22}ClNRuS$, $M = 433.0$, monoclinic, space group $P2_1/c$, $a = 10.434(3)$, $b = 12.518(2)$, $c = 14.561(4)$ Å, $\beta = 108.30(2)°$, $U = 1805.6$ Å^3 (by least-squares refinement of diffractometer angles for 29 reflections in the range $13 \leqslant 2\theta \leqslant 28°$, $\lambda = 0.710\,73$ Å), $F(000) = 880$, $D_c = 1.59$ g cm^{-3}, μ(Mo-Kα) = 11.1 cm^{-1}, $Z = 4$. Orange block, 0.50 × 0.40 × 0.25 mm.

Data collection and refinement. As described above. A total of 3491 reflections were collected $(+h,+k,\pm l)$. Of the 3148 unique data 2314 were observed $[I \geqslant 3\sigma(I)]$ and employed in structure solution and refinement. An absorption correction was applied (maximum, minimum transmission 0.955, 0.725).

Structure analysis and refinement. Direct methods followed by alternating cycles of least-squares refinement and Fourier-

difference analysis. Non-hydrogen atoms anisotropic. Hydrogen atoms were placed in idealised positions, r(CH) 0.96 Å, and a common isotropic thermal parameter, U_{iso}, refined to 0.090(6) Å^2. Full-matrix least-squares refinement gave $R = 0.0435$, $R' = 0.0503$ in the final cycle from 209 parameters. A weighting scheme of $w^{-1} = \sigma^2(F) + 0.003\,564F^2$ was applied and the maximum shift/e.s.d. in the final cycle was 0.06. The largest residual peak was 0.90 e Å^{-3} associated with the ruthenium atom.

All calculations were carried out using the SHELXTL PLUS[25] program package on a MicroVax II computer.

Additional material for both structures available from the Cambridge Crystallographic Data Centre comprises H-atom coordinates, thermal parameters and remaining bond lengths and angles.

Acknowledgements

We thank Johnson Matthey plc for generous loans of ruthenium trichloride and the SERC for a studentship (to J. W. S.) and for provision of the X-ray diffractometer. Grateful acknowledgement is also given to the ULIRS mass spectrometry service at the School of Pharmacy.

References

1 D. N. Cox, R. W. H. Small and R. Roulet, *J. Chem. Soc., Dalton Trans.*, 1991, 2013.
2 S. O. Sommerer and G. J. Palenik, *Organometallics*, 1991, **10**, 1203.
3 D. N. Cox and R. Roulet, *Inorg. Chem.*, 1990, **29**, 1360.
4 J. W. Steed and D. A. Tocher, *J. Organomet. Chem.*, 1991, **412**, C34.
5 J. G. Toerien and P. H. van Rooyen, *J. Chem. Soc., Dalton Trans.*, 1991, 1563.
6 J. G. Toerien and P. H. van Rooyen, *J. Chem. Soc., Dalton Trans.*, 1991, 2693.
7 L. Porri, M. C. Gallazzi, A. Colombo and G. Allegra, *Tetrahedron Lett.*, 1965, **47**, 4187.
8 A. Colombo and G. Allegra, *Acta Crystallogr., Sect. B*, 1971, **27**, 1653.
9 A. J. Deeming, M. N. Meah, P. A. Bates and M. B. Hursthouse, *Inorg. Chim. Acta*, 1988, **142**, 37.
10 E. Block, G. Ofori-Okai, H. Kang and J. A. Zubieta, *Inorg. Chim. Acta*, 1991, **187**, 59.
11 M. A. Bennett and A. K. Smith, *J. Chem. Soc., Dalton Trans.*, 1974, 233.
12 E. C. Morrison, C. A. Palmer and D. A. Tocher, *J. Organomet. Chem.*, 1988, **349**, 405.
13 D. A. Tocher, R. O. Gould, T. A. Stephenson, M. A. Bennett, J. P. Ennett, T. W. Matheson, L. Sawyer and V. K. Shah, *J. Chem. Soc., Dalton Trans.*, 1983, 1571.
14 P. Lahuerta, J. Latorre, M. Sanaú, F. A. Cotton and W. Schwotzer, *Polyhedron*, 1988, **7**, 1311.
15 J. W. Steed and D. A. Tocher, *Inorg. Chim. Acta*, 1991, **191**, 29.
16 R. A. Head, J. F. Nixon, J. R. Swain and C. M. Woodard, *J. Organomet. Chem.*, 1974, **76**, 393.
17 C. J. Pouchert (Editor), *Aldrich Library of Infrared Spectra*, 3rd edn., 1981.
18 J. W. Steed and D. A. Tocher, *Inorg. Chim. Acta*, 1991, **189**, 135.
19 J. W. Steed and D. A. Tocher, *J. Chem. Soc., Dalton Trans.*, 1992, 459.
20 J. W. Steed and D. A. Tocher, unpublished work.
21 A. R. Chakravarty, F. A. Cotton and D. A. Tocher, *Inorg. Chem.*, 1985, **24**, 2857.
22 J. E. Lydon, J. K. Nicholson, B. L. Shaw and M. R. Truter, *Proc. Chem. Soc.*, 1964, 421; J. E. Lydon and M. R. Truter, *J. Chem. Soc. A*, 1968, 362.
23 J. Renault, *Bull. Soc. Chim. Fr.*, 1953, 1001.
24 H. L. Yale, in *Pyridine and its Derivatives*, ed. E. Klingsberger, Interscience, New York, 1964, part 4.
25 G. M. Sheldrick, SHELXTL PLUS, an integrated system for refining and displaying crystal structures from diffraction data, University of Göttingen, 1986.

Received 14*th May* 1992; *Paper* 2/02505A

Polyhedron Vol. 11, No. 21, pp. 2729–2737, 1992
Printed in Great Britain

0277–5387/92 $5.00+.00

MONO-, BI- AND TRINUCLEAR BIS(ALLYL) COMPLEXES OF RUTHENIUM(IV) CONTAINING N-DONOR LIGANDS

JONATHAN W. STEED and DEREK A. TOCHER*

Department of Chemistry, University College London, 20 Gordon St, London WC1H OAJ, U.K.

(*Received* 30 *June* 1992; *accepted* 3 *August* 1992)

Abstract—The ruthenium(IV) bis(allyl) complex $[\{Ru(\eta^3:\eta^3\text{-}C_{10}H_{16})Cl(\mu\text{-}Cl)\}_2]$ (**1**) reacts with pyrazene to give a binuclear complex, $[\{Ru(\eta^3:\eta^3\text{-}C_{10}H_{16})Cl_2\}_2(\mu\text{-}N_2C_4H_4)]$ (**2**), which exists in two diastereomeric forms of C_i (*meso*) and C_2 (*rac*) symmetries. The analogous reaction with 1,3,5-triazine yields a mixture of mono-, bi- and trinuclear complexes, $[\{Ru(\eta^3:\eta^3\text{-}C_{10}H_{16})Cl_2\}_n(N_3C_3H_3)]$ [$n = 1$ (**4**), $n = 2$ (**5**), $n = 3$ (**6**)], which interconvert with one another in chloroform solution at room temperature. Complexes **5** and **6** have been isolated and, like **2**, **5** exists as two diastereoisomers. Complex **6**, however, possesses four isomeric forms. The class I mixed-valence Ru^{IV}–Ru^{II} pyrazene-bridged complex $[Ru(\eta^3:\eta^3\text{-}C_{10}H_{16})Cl_2(\mu\text{-}N_2C_4H_4)RuCl_2(\eta^6\text{-}p\text{-}MeC_6H_4CHMe_2)]$ (**7b**) is also reported. Pretreatment of **1** with $Ag[BF_4]$ in acetone generates mono- and dicationic solvate species which readily react with polypyridyl and related ligands to generate the chelate species $[Ru(\eta^3:\eta^3\text{-}C_{10}H_{16})Cl(L\text{-}L)][BF_4]$ [L-L = 2,2′-bipyridyl (**11**), L-L = 1,10-phenanthroline (**12**)] and $[Ru(\eta^3:\eta^3\text{-}C_{10}H_{16})(terpy)][BF_4]_2$ (**13**) (terpy = 2,2′:6′,2″-terpyridine). Complex **11** has been characterized by X-ray crystallography.

Current interest[1–7] in the literature has focused strongly on the unusual bis(allyl) ruthenium(IV) chloro-bridged dimer $[\{Ru(\eta^3:\eta^3\text{-}C_{10}H_{16})Cl(\mu\text{-}Cl)\}_2]$ (**1**)[8,9] which contains the chiral organometallic fragment "$(\eta^3:\eta^3\text{-}C_{10}H_{16})Ru$". Recent results obtained by ourselves and others indicate that the chemistry of **1** is both surprising and versatile and it has been noted that complexes derived from **1** possess a number of features which make them particularly appealing to study. These include: (1) The high formal oxidation state (+4) of the metal centre, which offers the prospect of a facile entry into high oxidation state organometallics; an area of considerable current interest.[10–12] (2) The chirality of the metal coordinated 2,7-dimethylocta-2,6-diene-1,8-diyl ligand, which might be of interest[13,14] in areas such as a symmetric synthesis. (3) The unusual geometry about the metal centre, loosely described as trigonal bipyramidal, giving three "free" *mer*-coordination sites available on the "$(\eta^3:\eta^3\text{-}C_{10}H_{16})Ru$" fragment, in contrast to the *fac*-geometry usually observed in related (arene)ruthenium(II) chemistry. (4) The high reactivity offered by the chloro-bridged structure of **1**. Bridge cleavage reactions form the starting point for a wide range of chemistry in related systems.[15,16]

In solution, complex **1** has been shown[3] to exist in two diastereomeric forms (*meso*, C_i, and *rac*, C_2), arising as a consequence of the three ways of joining together the two chiral "$(\eta^3:\eta^3\text{-}C_{10}H_{16})Ru$" fragments. The diastereoisomers are readily distinguished from one another by ^1H NMR spectroscopy, giving rise to the characteristic "doubling" of the number of resonances expected for a single complex. This is most usefully observed in the number of singlet resonances arising from the terminal allyl and methyl protons of the dimethylocta dienediyl ligand (eight and four, respectively). Mononuclear complexes derived from **1**, whilst still chiral, exist in a single diastereomeric form.

The inequivalence of the axial sites on the trigonal bipyramidal ruthenium ion (e.g. in the acetate complex $[Ru(\eta^3:\eta^3\text{-}C_{10}H_{16})Cl(O_2CCH_3)]$[7]) is sufficient to render the two halves of the (bis)allyl ligand unique, giving rise to four terminal allyl and two methyl resonances in the ^1H NMR spectrum. Simple, symmetric adducts such as $[Ru(\eta^3:\eta^3\text{-}$

* Author to whom correspondence should be addressed.

$C_{10}H_{16})Cl_2(CO)]$[17] give rise to only two terminal allyl and a single methyl resonances.

In previous studies we have examined the reactivity of **1** towards carboxylate ligands[7,18,19] and α-hydroxypyridinates.[20] We now report the full results of our investigations into the reactions of **1** with polypyridyls and related aromatic N-donor ligands.* Preliminary reports of parts of this work have been published.[21,22]

EXPERIMENTAL

IR spectra were recorded on a PE983 grating spectrometer between 4000 and 180 cm^{-1}, as either KBr discs or Nujol mulls on CsI plates. NMR spectra were recorded either on Varian XL200 or VXR400 spectrometers at UCL, and the data are reported in Table 2. Microanalyses were carried out by the departmental service. Cyclic voltammetric measurements were performed using a Metrohm E506 potentiostat interfaced with a Metrohm 5612 scanner and a Hewlett–Packard 7035B *X–Y* recorder. Electrolyte solutions were 0.2 M in tetra-n-butyl ammonium tetrafluoroborate. Deaeration of the solution was performed before the experiment and a stream of nitrogen passed throughout. The working electrode was a platinum wire (Metrohm EA285). A non-aqueous Ag/AgCl/Cl^-, CH_2Cl_2 electrode was used as a reference electrode and a platinum wire as the auxiliary. All potentials are reported with respect to the Ag/AgCl electrode against which ferrocene is oxidized at a potential of +0.60 V. All manipulations were carried out under nitrogen with degassed solvents using conventional Schlenk-line techniques, although no significant air-sensitivity of the products was noted.

$[\{Ru(\eta^3:\eta^3\text{-}C_{10}H_{16})Cl(\mu\text{-}Cl)\}_2]$ and $[\{Ru(4\text{-}MeC_6H_4CHMe_2)Cl(\mu\text{-}Cl)\}_2]$ were prepared by published literature methods.[3,4,8,15] Ruthenium trichloride hydrate was obtained on loan from Johnson Matthey plc and was purified before use by dissolution in water and boiling to dryness. All other reagents and materials were obtained from the usual commercial sources.

Preparations

$[\{Ru(\eta^3:\eta^3\text{-}C_{10}H_{16})Cl_2\}_2(\mu\text{-}N_2C_4H_4)]$ (**2**). The complex $[\{Ru(\eta^3:\eta^3\text{-}C_{10}H_{16})RuCl(\mu\text{-}Cl)\}_2]$ (0.082 g, 0.13 mmol) was stirred in CH_2Cl_2 (5 cm^3) with pyrazene (0.011 g, 0.13 mmol) for 1 h, during which time a colour change from pink to orange was observed. Evaporation to *ca* ¼ volume and slow addition of n-hexane (10 cm^3) gave the product as an orange powder, which was isolated by filtration, washed with diethyl ether and air-dried. Yield 0.077 g, 0.11 mmol, 83%. Found: C, 41.1; H, 5.0; N, 3.5. Calc. for $C_{24}H_{36}Cl_4N_2Ru_2$: C, 41.4; H, 5.2; N, 4.0%.

$[\{Ru(\eta^3:\eta^3\text{-}C_{10}H_{16})Cl_2\}_2(\mu^2\text{-}N_3C_3H_3)]$ (**5**). $[\{Ru(\eta^3:\eta^3\text{-}C_{10}H_{16})Cl(\mu\text{-}Cl)\}_2]$ (0.102 g, 0.16 mmol) was treated with 1,3,5-triazine (0.014 g, 0.17 mmol) following a procedure analogous to that outlined for **2**. Reaction time: 15 min. Yield 0.091 g, 0.13 mmol, 79%. Found: C, 39.8; H, 5.0; N, 6.0. Calc. for $C_{23}H_{35}Cl_4N_5Ru_2$: C, 39.6; H, 5.0; N, 6.0%.

$[\{Ru(\eta^3:\eta^3\text{-}C_{10}H_{16})Cl_2\}_3(\mu^3\text{-}N_3C_3H_3)]$ (**6**). $[\{Ru(\eta^3:\eta^3\text{-}C_{10}H_{16})Cl(\mu\text{-}Cl)\}_2]$ (0.153 g, 0.25 mmol) was treated with 1,3,5-triazine (0.030 g, 0.37 mmol) following a procedure analogous to that outlined for **2**. The resulting orange solution was concentrated under reduced pressure to *ca* 2 cm^3 and diethyl ether vapour was allowed to diffuse slowly into it within a closed system. After 24 h small, well-formed crystals were formed and were filtered off and dried *in vacuo*. Microanalysis and ^1H NMR spectroscopy showed the product to consist solely of **6**. Yield 0.056 g, 0.06 mmol, 20%. Found: C, 38.9; H, 5.4; N, 4.1. Calc. for $C_{33}H_{51}Cl_6N_3Ru_3$: C, 39.4; H, 5.1; N, 4.2%.

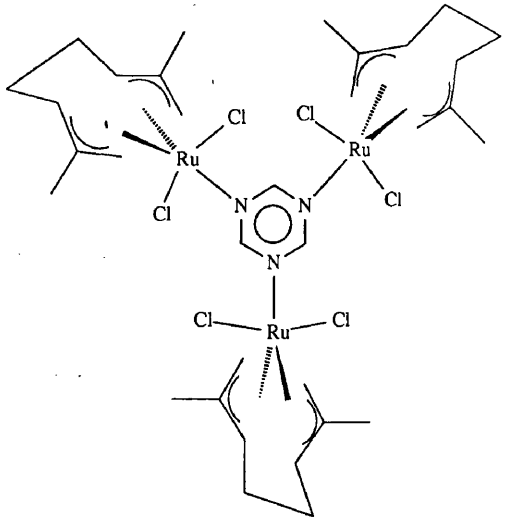

6

$[\{Ru(\eta^3:\eta^3\text{-}C_{10}H_{16})Cl_2\}_2(\mu\text{-}N_2C_4H_4)RuCl_2(\eta^6\text{-}MeC_6H_4CHMe_2)]$ (**7b**). (1) $[\{Ru(\eta^6\text{-}p\text{-}MeC_6H_4CHMe_2)Cl(\mu\text{-}Cl)\}_2]$ (0.098 g, 0.16 mmol) was stirred in acetone (5 cm^3) with pyrazene (0.272 g, 3.39 mmol) for 5 h to give a brown precipitate of the known ruthenium(II) complex $[\{Ru(p\text{-cymene})Cl_2\}_2(\mu\text{-pyz})]$ (**8**), and a red solution. The filtered solution was concentrated to *ca* half volume and diethyl ether added to give a red precipitate [shown

* During the course of this work complex **2** was also reported independently by Toerien and van Rooyen.[5]

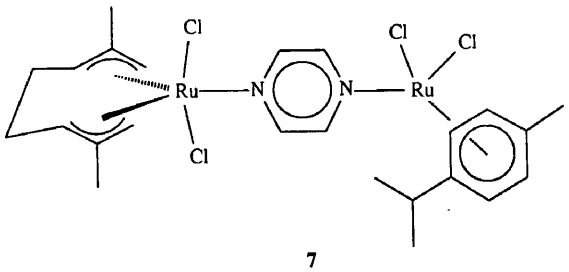

7

by ^{1}H NMR spectroscopy to be an approximately 2:1 mixture of **8** and [Ru(*p*-cymene)Cl_2(pyz)] (**9**)], which was used without further purification.

(2) To the product from (1) (0.055 g) in toluene (5 cm^3) was added [{Ru(η^3:η^3-$C_{10}H_{16}$)Cl(μ-Cl)}$_2$] (0.043 g, 0.07 mmol) and the mixture stirred for 30 min to give a brown precipitate. The filtered solid was dissolved in toluene/acetone (1:10 v/v) and filtered over Celite to remove excess **1**. Diethyl ether (5 cm^3) was added to precipitate unreacted **8** as a brown solid. After filtration, the remaining orange–red solution was evaporated to *ca* $\frac{1}{4}$ volume and n-hexane slowly added to give the product as red microcrystals. (^{1}H NMR spectroscopy showed this material to consist of pure **7b** with one molecule of toluene of crystallization.) Yield 0.029 g, 0.04 mmol, 13% based on [{Ru(η^6-*p*-$MeC_6H_4CHMe_2$)Cl(μ-Cl)}$_2$]. Found: C, 48.0; H, 5.5; N, 3.6. Calc. for $C_{31}H_{42}Cl_4N_2Ru_2$: C, 47.3; H, 5.4; N, 3.5%.

[Ru(η^3:η^3-$C_{10}H_{16}$)Cl_2(NC_3H_3NH)] (**10**). [{Ru(η^3:η^3-$C_{10}H_{16}$)Cl(μ-Cl)}$_2$] (0.092 g, 0.15 mmol) was treated with pyrazole (0.018 g, 0.27 mmol) in toluene, following a procedure analogous to that outlined for **2**. Yield 0.076 g, 0.20 mmol, 68%. Found: C, 41.7; H, 5.1; N, 7.2. Calc. for $C_{13}H_{20}Cl_2N_2Ru$: C, 41.5; H, 5.3; N, 7.4%.

[Ru(η^3:η^3-$C_{10}H_{16}$)Cl($N_2C_{10}H_8$)][BF_4] (**11**). [{Ru(η^3:η^3-$C_{10}H_{16}$)Cl(μ-Cl)}$_2$] (0.098 g, 0.16 mmol) was suspended in acetone (5 cm^3) and stirred with Ag[BF_4] (0.062 g, 0.32 mmol) for 1 h. The resulting orange solution was filtered over Celite and treated with 2 mol equivalents (relative to **1**) of 2,2′-bipyridyl (0.051 g, 0.33 mmol) and the mixture stirred for a further 2 h. The resulting red solution was evaporated to dryness *in vacuo* and the residue recrystallized from acetone/hexane (1:1 v/v) to give yellow crystals, which were isolated by filtration, washed with diethyl ether and air-dried. Yield 0.076 g, 0.15 mmol, 46%. Found: C, 46.1; H, 4.5; N, 5.5. Calc. for $C_{20}H_{24}BClF_4N_2Ru$: C, 46.6; H, 4.7; N, 5.4%.

[Ru(η^3:η^3-$C_{10}H_{16}$)RuCl($N_2C_{12}H_8$)][BF_4] (**12**). [{Ru(η^3:η^3-$C_{10}H_{16}$)RuCl(μ-Cl)}$_2$] (0.158 g, 0.26 mmol) was suspended in acetone (5 cm^3) and treated with Ag[BF_4] (0.101 g, 0.52 mmol) in a similar way as described for **11**. The resulting orange solution was treated with 1,10-phenanthroline (0.092 g, 0.52 mmol) and the product isolated as described above. Yield 0.169 g, 0.31 mmol, 61%. Found: C, 48.2; H, 4.5; N, 5.4. Calc. for $C_{22}H_{24}BClF_4N_2Ru$: C, 48.9; H, 4.5; N, 5.2%.

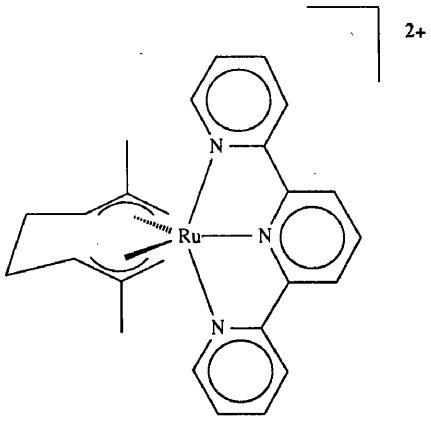

13

[Ru(η^3:η^3-$C_{10}H_{16}$)($N_3C_{15}H_{11}$)][BF_4]$_2$ (**13**). [{Ru(η^3:η^3-$C_{10}H_{16}$)RuCl(μ-Cl)}$_2$] (0.076 g, 0.12 mmol) was suspended in acetone (5 cm^3) and treated with Ag[BF_4] (0.098 g, 0.50 mmol). The resulting orange solution was filtered over Celite and treated with 2 mol equivalents (relative to **1**) of 2,2′:6′,2″-terpyridine (0.047 g, 0.20 mmol) and the mixture stirred for a further 2 h, during which time a colour change to deep red and the formation of a yellow precipitate were observed. The yellow precipitate was collected by filtration and washed with acetone and diethyl ether, and then air-dried. The red solution was concentrated to *ca* 1 cm^3 to give a further crop of the product. Combined yield 0.106 g, 0.16 mmol, 67%. Found: C, 46.6; H, 4.5; N, 6.0. Calc. for $C_{25}H_{27}B_2F_8N_3Ru$: C, 46.6; H, 4.2; N, 6.5%.

Crystallography

Crystal data. $C_{20}H_{24}BClF_4N_2Ru$ (**11**), M = 515.79 g mol^{-1}, triclinic, space group $P\bar{1}$, a = 9.464(2), b = 10.493(3), c = 12.070(3) Å, U = 1047 $Å^3$ (by least-squares refinement of diffractometer angles for 31 automatically centred reflections in the range $13 \leqslant 2\theta \leqslant 25°$, λ = 0.71073 Å), Z = 2, $F(000)$ = 520, D_c = 1.64 g cm^{-3}, μ(Mo-K_α) = 9.04 cm^{-1}. Yellow plate, 0.4 × 0.3 × 0.05 mm.

Data collection and processing

The ω–2θ technique was used to collect 3927 (3685 unique) data in the range $5 \leqslant 2\theta \leqslant 50°$ on a Nicolet R3mV diffractometer equipped with graphite monochromated Mo-K_α radiation. Three standard reflections monitored every 97 reflections showed no appreciable change in intensity through-

out the data collection. Data were corrected for Lorentz and polarization effects and for absorption based on additional azimuthal scan data. Omission of intensities with $I \leqslant 3\sigma(I)$ gave 2878 observed data which were employed in the analysis.

Structure analysis and refinement

The structure was solved by a combination of conventional Patterson and difference-Fourier techniques. The asymmetric unit contained one complex cation and one tetrafluoroborate anion. All non-hydrogen atoms were refined anisotropically, while hydrogen atoms were placed in idealized positions and allowed to ride on the atoms to which they were attached (C—H 0.96 Å, $U_{iso} = 0.08$ Å^2). The fluorine atoms of the tetrafluoroborate anion were found to be disordered and were modelled as two interpenetrating tetrahedra (occupancies refined to 0.67 and 0.33). The final cycle of full-matrix least-squares refinement included 298 parameters [weighting scheme applied: $w^{-1} = \sigma^2(F) + 0.001368F^2$] and the largest shift-to-error ratio was 0.327, associated with a temperature factor of one of the disordered fluorine atoms. The final R values were $R = 0.0433$ and $R_w = 0.0461$. The largest peak in the final electron density difference map was 0.95 e Å^{-3}, close to the metal atom.

All calculations were carried out using the SHELXTL PLUS program package[23] on a MicroVax II computer. Selected bond lengths and angles are presented in Table 1.

Additional material is available from the Cambridge Crystallographic Data Centre and comprises hydrogen-atom coordinates, thermal parameters and remaining bond lengths and angles.

RESULTS AND DISCUSSION

Bridge cleavage reactions

Reaction of **1** with a single mole equivalent of pyrazene (pyz) in CH_2Cl_2 at room temperature results in the formation of a bright orange solution from which the pyrazene bridged binuclear complex $[\{Ru(\eta^3:\eta^3\text{-}C_{10}H_{16})Cl_2\}_2(\mu\text{-pyz})]$ (**2**) may be isolated. The ^1H and $^{13}C\{^1H\}$ NMR spectra of **2** clearly demonstrate that, in solution, the material exists in two diastereomeric forms analogous to the C_i (*meso*) and C_2 (*rac*) isomers of **1**,[3] although the linear bridge geometry results in the analogous forms of **2** possessing approximate C_{2h} and D_2 symmetries (*meso* and *rac*, respectively). For the sake of convenience these materials will be referred to as "C_i" and "C_2" isomers. The ^1H NMR spectrum of **2** thus displays two singlet resonances (δ 9.32 and 9.24 ppm, each 4H) corresponding to the pyrazene protons of the two diastereoisomers. Similarly, each isomer displays two singlet resonances due to the terminal allyl protons (δ 4.66, 4.34 and 4.61, 4.39 ppm). In the $^{13}C\{^1H\}$ NMR spectrum the resonances assigned to the pyrazene carbon atoms, in the two isomers, occur at δ 149.43 and 149.20 ppm. Likewise, twice as many signals as would have been expected are observed for the carbon atoms of the bis(allyl) ligand.

Table 1. Selected bond lengths (Å) and angles (°) for $[Ru(\eta^3:\eta^3\text{-}C_{10}H_{16})Cl(N_2C_{10}H_8)][BF_4]$ (**11**)

Ru(1)—Cl(1)	2.433(2)	Ru(1)—N(1)	2.140(5)
Ru(1)—N(2)	2.115(4)	Ru(1)—C(1)	2.219(5)
Ru(1)—C(2)	2.294(7)	Ru(1)—C(3)	2.270(7)
Ru(1)—C(6)	2.259(5)	Ru(1)—C(7)	2.303(5)
Ru(1)—C(8)	2.246(6)	N(1)—C(16)	1.344(8)
N(1)—C(20)	1.346(9)	N(2)—C(11)	1.340(9)
N(2)—C(15)	1.369(8)	C(1)—C(2)	1.410(11)
C(2)—C(3)	1.420(10)	C(2)—C(9)	1.491(13)
C(3)—C(4)	1.515(10)	C(4)—C(5)	1.519(11)
C(5)—C(6)	1.503(10)	C(6)—C(7)	1.415(11)
C(7)—C(8)	1.405(10)	C(7)—C(10)	1.507(11)
C(11)—C(12)	1.397(10)	C(12)—C(13)	1.359(14)
C(13)—C(14)	1.378(13)	C(14)—C(15)	1.378(9)
C(15)—C(16)	1.476(10)	C(16)—C(17)	1.401(10)
C(17)—C(18)	1.381(12)	C(18)—C(19)	1.352(11)
C(19)—C(20)	1.382(11)		
Cl(1)—Ru(1)—N(1)	89.5(1)	Cl(1)—Ru(1)—N(2)	166.9(2)
N(1)—Ru(1)—N(2)	77.7(2)		

We have shown[21] that in the solid state, crystals grown from a chloroform/diethyl ether solution of **2** possess a geometry analogous to the C_i isomer of **1**, i.e. the *meso* form. Low-temperature dissolution of crystalline **2** and immediate recording of its ^{1}H NMR spectrum (240 K) revealed the presence of only a single set of resonances and allowed unequivocal assignment of the signals observed in the room-temperature spectrum to their respective diastereoisomers, Table 2. At room temperature the ^{1}H NMR spectrum of the crystalline sample displayed resonances corresponding to two diastereoisomers as before, $K = [rac]/[meso] = 1.14$ (cf. 1.25 in the case of **1**[3]). This is interpreted in terms of an intermolecular exchange between the *meso* and *rac* forms of **2**. We would suggest, therefore, that the coalescence of these two sets of resonances at temperatures above *ca* 323 K[5] is due to rapid Ru—N bond fission and interchange of chiral "$(\eta^3:\eta^3\text{-}C_{10}H_{16})Ru$" units between isomers as opposed to an increase in the rate of rotation about the Ru—N single bond,[5] which is presumably rapid over all the temperature ranges studied. This suggestion is further supported by the fluxionality observed in the triazine complexes **4**, **5** and **6** (*vide infra*).

In contrast to the straightforward isolation of **2**, the mononuclear adduct $[Ru(\eta^3:\eta^3\text{-}C_{10}H_{16})Cl_2(pyz)]$ (**3**) has only been observed by us in solution, by ^{1}H NMR spectroscopy, in the presence of 15 mol equivalents of free pyrazene. In **3** the two singlet resonances of the pyrazene ligand in **2** are replaced by an AA′BB′ pattern, δ 9.29 and 8.63 ppm, ^3J(H—H) = 3.25, ^5J(H—H) = 1.0 Hz (cf. the multiplet resonance centred on 8.72 ppm observed for the terminal bis(pyrazene) complex $[Ru(\eta^6\text{-}C_6H_6)Cl(pyz)_2][PF_6]$[24]). The relative instability of **3** with respect to disproportionation into free pyrazene and **2** has also been noted by Toerien and van Rooyen who estimate[5] the equilibrium constant for the process to be *ca* 6.8 at ambient temperatures.

The observation of two metal centres linked by a delocalized π-electron ligand raises the possibility of electronic interactions between the two metal ions and consequently the cyclic voltammetry of **2** was examined ($CH_2Cl_2/[Bu^n_4N][BF_4]$). A single, irreversible reduction was observed (*ca* −1.12 V vs Ag/AgCl) over a variety of scan speeds (50–500 mV s^{-1}). On the return scan a coupled irreversible oxidation was apparent (+0.53 V). Such behaviour is suggestive of an ECE process, but implies that there is no reversible electron transfer between the two metal centres. Similar observations have been made by us on the oxalato-bridged complex $[\{Ru(\eta^3:\eta^3\text{-}C_{10}H_{16})Cl\}_2(\mu\text{-}O_4C_2)]$.[18] Hence, the behaviour of **2** differs markedly from the rich electrochemistry of the class of mixed-valence complexes $[(NH_3)_5Ru(\mu\text{-pyz})Ru(NH_3)_5]^{n+}$ (n = 4, 5 or 6).[25] We have established that the parent complex **1** exhibits two irreversible reductions at −0.63 and −0.87 V (v = 200 mV s^{-1}) and an irreversible oxidation on the return scan (+0.88 V). Such behaviour is consistent with the observed irreversible chemical reduction of **1** to solvated ruthenium(II) ions by the action of $Ag[BF_4]$ in alcoholic solvents, reported by Cox and Roulet.[26]

In contrast to the ready formation of **2**, interaction of **1** with 1,3,5-triazine (tra) leads to a mixture of products, viz $[Ru(\eta^3:\eta^3\text{-}C_{10}H_{16})Cl_2(tra)]$ (**4**), $[\{Ru(\eta^3:\eta^3\text{-}C_{10}H_{16})Cl_2\}_2(\mu^2\text{-tra})]$ (**5**) and $[\{Ru(\eta^3:\eta^3\text{-}C_{10}H_{16})Cl_2\}_3(\mu^3\text{-tra})]$ (**6**). Fractional crystallization of this mixture by slow diffusion of diethyl ether into a chloroform solution led to the isolation of a pure sample of the trinuclear complex **6**. At room temperature the ^{1}H NMR spectrum ($CDCl_3$) of **6** displays a single broad resonance (10.70 ppm) due to the protons of the triazine ligand and two broad terminal allyl signals (δ 4.91 and 4.46 ppm), consistent with the presence of only one diastereoisomer. Lowering the temperature of the NMR probe causes the resonances to split until, at 248 K, four sharp singlet resonances of approximately equal intensity are observed in the triazine region of the spectrum (δ 10.53, 10.52, 10.47 and 10.40 ppm), consistent with the appearance of the expected four isomeric forms of **6**.

The binuclear complex **5** is more readily isolated than **6** (short reaction time and 1:1 mole ratio of **1** to triazine). Like **6**, the ^{1}H NMR spectrum of complex **5** displays broad lines at room temperature, ostensibly consistent with the presence of a single diastereoisomer [e.g. δ 10.64 (s, 1H) and 9.85 (s, 2H)]. At 248 K, however, the peaks are resolved and reveal the presence of two diastereoisomers (δ 10.52, 10.39 and 9.81, 9.75 ppm), analogous to those of **2**.

Treatment of **1** with excess triazine over several hours gives a mixture of **5**, **6** and a third complex, which displays two new peaks in the triazine region of its ^{1}H NMR spectrum (δ 9.87 and 9.21 ppm, 2H and 1H, respectively) which do not split at low temperature. These signals are ascribed to the mononuclear adduct $[Ru(\eta^3:\eta^3\text{-}C_{10}H_{16})Cl_2(tra)]$ (**4**).

On warming an NMR sample containing a mixture of **4**, **5** and **6** to 55°C, the triazine signals broaden further and eventually merge. The upfield region of the spectrum is more informative, however, with coalescence clearly occurring between all three sets of allyl resonances to give an averaged spectrum exhibiting only two terminal

Table 2. ^{1}H NMR data for new compounds[a]

Compound	Terminal allyl	Internal allyl	—CH_2—	Me	δ(ppm), J(H—H) (Hz), $CDCl_3$ Other
[{Ru(η^3:η^3-$C_{10}H_{16}$)Cl_2}$_2$(μ-pyz)] (**2**)	4.61 (s, 4H)	5.29 (m, 4H)	3.07 (m, 4H)	2.37 (s, 12H)	9.32 (s, 4H)
C_i diastereoisomer	4.39 (s, 4H)		2.44 (m, 4H)		
[{Ru(η^3:η^3-$C_{10}H_{16}$)Cl_2}$_2$(μ-pyz)] (**2**)	4.66 (s, 4H)	5.29 (m, 4H)	3.07 (m, 4H)	2.38 (s, 12H)	9.24 (s, 4H)
C_2 diastereoisomer	4.34 (s, 4H)		2.44 (m, 4H)		
[Ru(η^3:η^3-$C_{10}H_{16}$)Cl_2(pyz)] (**3**)	4.59 (s, 2H)	5.29 (m, 2H)	3.06 (m, 2H)	2.38 (s, 6H)	9.29, 8.63 (AA′BB′, 4H, ^3J = 3.25, ^5J = 1.0)
	4.40 (s, 2H)		2.43 (m, 2H)		
[{Ru(η^3:η^3-$C_{10}H_{16}$)Cl_2}$_2$(μ^2-tra)] (**5**)[b]	4.76 (s, 4H)	5.20 (m, 4H)	2.97 (m, 4H)	2.41 (s, 12H)	9.85 (s, 2H)
	4.42 (s, 4H)				10.63 (s, 1H)
[{Ru(η^3:η^3-$C_{10}H_{16}$)Cl_2}$_3$(μ^3-tra)] (**6**)[b]	4.91 (s, 6H)	5.20 (m, 6H)	2.97 (m, 6H)	2.41 (s, 18H)	10.70 (s, 3H)
	4.46 (s, 6H)		2.50 (m, 6H)		
[Ru(η^3:η^3-$C_{10}H_{16}$)Cl_2(μ-pyz)]	4.59 (s, 2H)	5.26 (m, 2H)	3.04 (m, 2H)	2.38 (s, 6H)	8.99, 8.83 (AA′BB′, 4H, ^3J = 5.3, ^5J = 1.5, $N_2C_4H_4$)
[$RuCl_2$(η^6-*p*-$MeC_6H_4CHMe_2$)] (**7b**)	4.44 (s, 2H)		2.39 (m, 2H)		5.40, 5.18 (AB, 4H, ^3J = 6.1, $MeC_6H_4CHMe_2$)
					2.97 (se, 1H, ^3J = 7.0, $MeC_6H_4CHMe_2$)
					2.08 (s, 3H, $MeC_6H_4CHMe_2$)
					1.28 (d, 6H, ^3J = 7.0, $MeC_6H_4CHMe_2$)
[Ru(η^3:η^3-$C_{10}H_{16}$)Cl_2(pyrazole)] (**10**)	4.45 (s, 2H)	5.18 (m, 2H)	3.07 (m, 2H)	2.33 (s, 6H)	12.10 (d, 1H, ^3J = 0.9, N*H*), 8.30 (d, 1H, ^3J = 4.8)
	4.35 (s, 2H)		2.43 (m, 2H)		7.69 (dd, 1H, ^3J = 2.4 and 0.9), 6.48 (dd, 1H, ^3J = 4.8 and 2.4)
[Ru(η^3:η^3-$C_{10}H_{16}$)Cl(bipy)][BF_4] (**11**)	4.35 (s, 1H)	5.53 (dd, 1H, ^3J = 12.1 and 4.0)	3.70 (m, 1H)	2.45 (s, 3H)	9.70 (d, 1H, ^3J = 5.7), 8.60 (d, 1H, ^3J = 7.6)
	4.02 (s, 1H)	4.79 (dd, 1H, ^3J = 11.5 and 4.2)	3.42 (m, 1H)	1.77 (s, 3H)	8.58 (d, 1H, ^3J = 5.3), 8.48 (d, 1H, ^3J = 8.1)
	3.69 (s, 1H)		2.93 (m, 1H)		8.25 (t, 1H, ^3J = 7.7), 8.06 (t, 1H, ^3J = 7.2)
	2.49 (s, 1H)		2.67 (m, 1H)		7.81 (t, 1H, ^3J = 6.1), 7.69 (t, 1H, ^3J = 6.1)
[Ru(η^3:η^3-$C_{10}H_{16}$)Cl(phen)][BF_4] (**12**)	4.36 (s, 1H)	5.63 (dd, 1H, ^3J = 11.9 and 4.0)	3.89 (m, 1H)	2.50 (s, 3H)	10.06 (d, 1H, ^3J = 5.4), 9.15 (d, 1H, ^3J = 5.4)
	4.00 (s, 1H)	5.11 (dd, 1H, ^3J = 11.3 and 4.3)	3.48 (m, 1H)	1.76 (s, 3H)	8.71 (d, 1H, ^3J = 8.2), 8.58 (d, 1H, ^3J = 8.2)
	3.47 (s, 1H)		3.06 (m, 1H)		8.26 (t, 1H, ^3J = 6.6), 8.15 (s, 2H)
	2.44 (s, 1H)		2.74 (m, 1H)		8.05 (t, 1H, ^3J = 8.2)
[Ru(η^3:η^3-$C_{10}H_{16}$)(terpy)][BF_4]$_2$ (**13**)[c]	3.94 (s, 2H)	5.08 (m, 2H)	3.91 (m, 2H)	2.11 (s, 6H)	8.69 (d, 2H, ^3J = 8.1), 8.61 (t, 1H, ^3J = 8.1)
	2.94 (s, 2H)		3.18 (m, 2H)		8.55 (d, 2H, ^3J = 8.1), 8.48 (d, 2H, ^3J = 5.1)
					8.32 (t, 2H, ^3J = 8.1), 7.82 (t, 2H, ^3J = 6.8)

[a] s = singlet, d = doublet, dd = doublet of doublets, t = triplet, se = septet, m = multiplet, br = broad.
[b] Room-temperature (292 K) spectrum, all signals broad due to exchange between diastereoisomers.
[c] Solvent is nitromethane-d_3.

allyl signals (δ 4.81 and 4.29 ppm), one internal allyl resonance (δ 5.19 ppm), two ethylenic multiplets (δ 2.98 and 2.47 ppm) and a single methyl resonance (δ 2.40 ppm).

The coalescence of the signals of all three complexes present is due to intermolecular exchange of "($\eta^3:\eta^3$-$C_{10}H_{16}$)Ru" units, such that not only are the diastereomeric forms of one complex averaged but the mono-, bi- and trinuclear species themselves are in dynamic equilibrium with each other. The observed temperature dependence is analogous to that observed for **2**[5] and lends strong support to the suggestion that such an intermolecular exchange is also occurring for that complex, albeit at a slightly slower rate, presumably as a consequence of the better donor abilities of the pyrazene ligand or reduced steric crowding.

In view of the limited electrochemical activity displayed by **2** we attempted the synthesis of the mixed-valence pyrazene-bridged ruthenium complexes such as the Ru^{IV}–Ru^{II} complexes [($\eta^3:\eta^3$-$C_{10}H_{16}$)$RuCl_2$(μ-pyz)Cl_2Ru(η^6-arene)] [arene = benzene (**7a**), arene = *p*-cymene (**7b**)], in the hope that they might display a more versatile electrochemistry. The preparation of **7a** and **7b** proved tedious because of the limited availability of monodentate pyrazene precursors to such compounds. Also it is known that the complexes [Ru(η^6-arene)Cl(pyz)$_2$][PF_6] display a very limited reactivity of the non-complexed pyrazene nitrogen atoms.[24]

In attempting to prepare a complex of type **7** efforts were made to optimize the conditions necessary for the formation of the mixed-valence species, as opposed to **2** and the known[24] Ru^{II}–Ru^{II} pyrazene-bridged complexes [{Ru(arene)Cl_2}$_2$(μ-pyz)] (**8**). To this end the ruthenium(II) *p*-cymene complex [Ru(*p*-cymene)Cl_2(μ-pyz)] (**9**) was chosen as the precursor because of the greater solubility conferred by the alkylated arene (more comparable with that of complex **1**). A crude sample of **9** was treated with a small excess of **1** in toluene and the mixture stirred at room temperature for half an hour to give a brown precipitate, which was found to be an approximately equimolar mixture of **7b** and **8**. A pure sample of **7b** was obtained by fractional crystallization (see Experimental).

In contrast to **2** and **8**, the pyrazene resonances in the ^{1}H NMR spectrum of **7b** do not appear as singlets, but rather as an AA′BB′ pattern [δ 8.99, 8.83 ppm, ^3J(H—H) = 5.3, ^5J(H—H) = 1.5] similar to that observed for the adduct **3** and indicative of the inequivalence of the two termini of the complex.

Disappointingly, the cyclic voltammogram of **7b** proved to be similar to that of **2** with a single irreversible reduction at *ca* −1.44 V (v = 400–100 mV s^{-1}) and irreversible oxidations observed at +1.08 and +1.35 V. This observation would seem to indicate that the complex is a class I mixed-valence species with each metal ion in a discrete oxidation state (+2 or +4) with no interaction between them on the cyclic voltammetric time-scale, in spite of the delocalized bonding in the bridging ligand. Complex **7b** is thus electronically analogous to the diphenylphosphinomethane-bridged (dppm) mixed-valence complex prepared by Toerien and van Rooyen.[5]

Reaction of **1** with pyrazole (NC_3H_3NH) in toluene, acetone and methanol results in the isolation of the adduct [Ru($\eta^3:\eta^3$-$C_{10}H_{16}$)Cl_2(NC_3H_3NH)] (**10**) in good yield. From ^{1}H NMR (δ N*H* 12.10 ppm) and IR [ν(NH) 3246 cm^{-1}] data we infer the ligand to be bound in a monodentate fashion through the unsaturated nitrogen atom. Reaction of **1** with sodium pyrazolate in acetone at room temperature resulted in decomposition.

Polypyridyl complexes

Complex **1** is known to form neutral chelate complexes with ligands such as carboxylates,[7,19] hydroxy- and mercaptopyridines,[4,20] and semicarbazide[2], etc.; cationic complexes with nitrile ligands have also been reported.[1,26]

We find that reaction of **1** with 2,2′-bipyridyl (bipy) in CH_2Cl_2 at room temperature proceeds poorly to give low yields and mixtures of products. In general, however, pre-treatment of dichloride dimer species such as **1** with silver salts of non-coordinating anions such as $[BF_4]^-$ affords mono- and dicationic solvate species which are excellent precursors to cationic ruthenium complexes. Some problems are encountered using this procedure with compound **1**, as a consequence of its decomposition in alcoholic solvents in the presence of Ag[BF_4] to form solvato Ru^{2+} ions.[26] However, air- and moisture-stable solvates may readily be generated in acetone solution.

In this way we have synthesized the monocationic species [Ru($\eta^3:\eta^3$-$C_{10}H_{16}$)Cl(L-L)][BF_4] [L-L = 2,2′-bipyridyl (**11**), L-L = 1,10-phenanthroline (**12**)] and the dicationic species [Ru($\eta^3:\eta^3$-$C_{10}H_{16}$)(terpy)][BF_4]$_2$ (**13**) (terpy = 2,2′:6′,2″-terpyridine). The ^{1}H NMR spectra of complexes **11** and **12** display four resonances for the terminal allyl protons (e.g. δ 4.35, 4.02, 3.69 and 2.49 ppm in complex **11**) characteristic of inequivalent axial sites on the trigonal bipyramidal ruthenium atom. In each case one resonance occurs at an uncharacteristically low chemical shift, possibly as a consequence of ring current effects in the aromatic moiety.[20] Complex **13** on the other hand displays

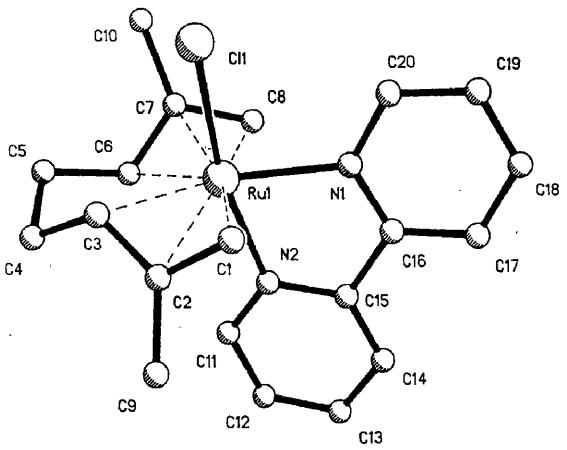

Fig. 1. Molecular structure of the cation $[Ru(\eta^3:\eta^3\text{-}C_{10}H_{16})Cl(N_2C_{10}H_8)]^+$, showing the atom numbering scheme adopted.

only two terminal allyl resonances (δ 3.94 and 2.94 ppm) and a single methyl resonance (δ 2.11 ppm) characteristic of equivalent axial sites, and as expected for the proposed tridentate, chelating geometry.

One of the more striking features of complex **13** is its high solubility in water although, with hindsight, this is not a surprising observation given the dicationic nature of the compound. Water-soluble organometallic complexes are of considerable current interest[2,27] and the discovery of several water-soluble bis(allyl) ruthenium(IV) complexes suggests an area of aqueous chemistry and catalysis which merits further investigation.

Complex **11** has been characterized by X-ray crystallography, Fig. 1 and Table 1. In general the structure is related to those observed for the 6-chloro-2-hydroxypyridinate complex $[Ru(\eta^3:\eta^3\text{-}C_{10}H_{16})Cl(NC_5H_4O\text{-}6\text{-}Cl)]$ (**14**) and the quinoline-2-thiolate complex $[Ru(\eta^3:\eta^3\text{-}C_{10}H_{16})Cl(NC_9H_6S)]$ (**15**)[20] with the bis(allyl) ligand adopting the usual local C_2 symmetry and each Ru—C distance being approximately equal within experimental error. The ruthenium chloride distance of 2.433(2) Å is similar to the corresponding distances observed in the structure of **2**[21] [2.406(3) and 2.425(3) Å] and **15** [2.461(2) Å], although notably longer than the distance of 2.381(3) Å in complex **14**. The ruthenium–nitrogen distances, 2.140(5) and 2.115(4) Å, are similar to Ru—N(pyrazene) in complex **2** [2.191(10) Å][21] and to Ru—N(axial) in complex **13**[22] [2.172(10) Å]. The shorter Ru—N (equatorial) distance in **13** [2.018(10) Å] is due to distortions in the terpyridine ligand on chelation. The angle Cl—Ru—N(1) of 89.5(1)° is large compared to the average "unconstrained" value[1,9,21] of *ca* 85°, but unexceptional in comparison to the value of 96.4(4)° observed by us for **14**.

The most striking feature of the structure of **11** is the distortion of the two aromatic rings of the bipy ligand. While each is planar within experimental error, they are inclined at an angle of 8.2° to one another and the equatorial ring [N(1)—C(16)—C(17)—C(18)—C(19)—C(20)] is inclined to an angle of 13.9° to the plane containing Cl(1), Ru(1) and N(2). This may be compared to a deviation of only 6.2° in complex **14**,[20] and presumably arises as a consequence of an imbalance in the steric requirements of the ligand and the metal centre.

Acknowledgements—We thank Johnson Matthey plc for generous loans of ruthenium trichloride and the SERC for a studentship (to J.W.S.) and for provision of the X-ray diffractometer.

REFERENCES

1. D. N. Cox, R. W. H. Small and R. Roulet, *J. Chem. Soc., Dalton Trans.* 1991, 2013.
2. S. O. Sommerer and G. J. Palenik, *Organometallics* 1991, **10**, 12203.
3. D. N. Cox and R. Roulet, *Inorg. Chem.* 1990, **29**, 1360.
4. J. G. Toerien and P. H. van Rooyen, *J. Chem. Soc., Dalton Trans.* 1991, 1563.
5. J. G. Toerien and P. H. van Rooyen, *J. Chem. Soc., Dalton Trans.* 1991, 2693.
6. J. W. Steed and D. A. Tocher, *J. Chem. Soc., Dalton Trans.* 1992, 459.
7. J. W. Steed and D. A. Tocher, *Inorg. Chim. Acta* 1991, **189**, 135.
8. L. Porri, M. C. Gallazzi, A. Colombo and G. Allegra, *Tetrahedron Lett.* 1965, **47**, 4187.
9. A. Colombo and G. Allegra, *Acta Cryst., Sect. B* 1971, **27**, 1653.
10. W. A. Hermann, *Angew. Chem., Int. Edn Engl.* 1988, **27**, 1297.
11. C. Che, W. Cheng and T. C. W. Mak, *J. Chem. Soc., Chem. Commun.* 1987, 418.
12. B. R. Manzano, F. A. Jalon, F. J. Lahoz, B. Chaudret and D. de Montauzon, *J. Chem. Soc., Dalton Trans.* 1992, 977.
13. S. K. Mandal and A. R. Chakravarty, *J. Organomet. Chem.* 1991, **417**, C59.
14. P. Pertici, P. Salvadori, A. Biasci, G. Vitulli, M. A. Bennett and L. A. P. Kane-Maguire, *J. Chem. Soc., Dalton Trans.* 1988, 315.
15. M. A. Bennett and A. K. Smith, *J. Chem. Soc., Dalton Trans.* 1974, 233.
16. C. H. Elschenbroich and A. Salzer, *Organometallics. A Concise Introduction.* VCH, Weinheim (1989).
17. R. A. Head, J. F. Nixon, J. R. Swain and C. M. Woodard, *J. Organomet. Chem.* 1974, **76**, 393.
18. J. W. Steed and D. A. Tocher, *Polyhedron* 1992, **11**, 1849.
19. B. A. Kavanagh, J. W. Steed and D. A. Tocher, unpublished results.

20. J. W. Steed and D. A. Tocher, *J. Chem. Soc., Dalton Trans.*, in press.
21. J. W. Steed and D. A. Tocher, *J. Organomet. Chem.* 1991, **412**, C34.
22. J. W. Steed and D. A. Tocher, *Inorg. Chim. Acta* 1992, **191**, 29.
23. G. M. Sheldrick, SHELXTL PLUS, An Integrated System for Refining and Displaying Crystal Structures from Diffraction Data. University of Göttingen, F.R.G. (1986).
24. D. A. Tocher, R. O. Gould, T. A. Stephenson, M. A. Bennett, J. P. Ennett, T. W. Matheson, L. Sawyer and V. K. Shah, *J. Chem. Soc., Dalton Trans.* 1983, 1571.
25. U. Fouholz, H.-B. Burgi, F. E. Wagner, A. Stebler, J. H. Ammeter, E. Krausz, R. J. H. Clark, M. J. Stead and A. Ludi, *J. Am. Chem. Soc.* 1984, **106**, 121.
26. D. N. Cox and R. Roulet, *J. Chem. Soc., Chem. Commun.* 1988, 951.
27. J. W. Steed and D. A. Tocher, *J. Chem. Soc., Chem. Commun.* 1991, 1609.

Mono- and Bi-dentate Carboxylato Complexes of Ruthenium(IV)†

Brian Kavanagh, Jonathan W. Steed and Derek A. Tocher*
Department of Chemistry, University College London, 20 Gordon St., London WC1H 0AJ, UK

Treatment of the ruthenium(IV) chloro-bridged dimer $[\{Ru(\eta^3:\eta^3\text{-}C_{10}H_{16})Cl(\mu\text{-}Cl)\}_2]$ **1** with sodium acetate or silver acetate at room temperature in acetone gives the chelate complex $[Ru(\eta^3:\eta^3\text{-}C_{10}H_{16})Cl(O_2CMe)]$ **2**. Refluxing **1** in trifluoroacetic acid, or reaction of **1** at room temperature with $Ag[CF_3CO_2]$ gives the monodentate, dicarboxylate species $[Ru(\eta^3:\eta^3\text{-}C_{10}H_{16})(O_2CCF_3)_2(OH_2)]$ **3**, which contains a tightly bound water ligand. A range of chloro and fluoro substituted carboxylato complexes has been prepared (**5**–**9**) and the 'cross-over' point between mono- and bi-dentate co-ordination determined. The hexafluoro β-diketonate complex $[Ru(\eta^3:\eta^3\text{-}C_{10}H_{16})Cl\{F_3CC(O)CHC(O)CF_3\}]$ **10**, exhibits the expected bidentate mode of co-ordination. Reaction of **1** with thioacetic acid over short reaction times yields the adduct $[Ru(\eta^3:\eta^3\text{-}C_{10}H_{16})Cl_2\{SC(OH)Me\}]$ **11**. The corresponding chelate species $[Ru(\eta^3:\eta^3\text{-}C_{10}H_{16})Cl(SOCMe)]$ **12**, is formed over longer reaction times. Analogous reactions with thiopivalic and thiobenzoic acids result only in the isolation of the chelate products $[Ru(\eta^3:\eta^3\text{-}C_{10}H_{16})Cl(SOCR)]$ (R = Bu^t **13** or Ph **14**). The structures of complexes **2** and **3** have been verified by X-ray crystallography.

The bis(allyl) ruthenium(IV) complex $[\{Ru(\eta^3:\eta^3\text{-}C_{10}H_{16})Cl(\mu\text{-}Cl)\}_2]$ **1**[1,2] is clearly related to the well known family of ruthenium(II) chloro-bridged dimer compounds $[\{Ru(\eta^6\text{-arene})Cl(\mu\text{-}Cl)\}_2]$ (arene = C_6H_6, 1,3,5-$C_6H_3Me_3$, C_6Me_6 *etc.*).[3,4] In contrast to the intensely studied[5–10] arene analogues however, the chemistry of **1** has remained relatively neglected. Compound **1** offers a facile gateway into the higher oxidation state organometallic chemistry of ruthenium, and that fact, coupled with the unusual steric requirements of the bis(allyl) 2,7-dimethylocta-2,6-diene-1,8-diyl ligand have recently brought about a strong surge of interest in its reactivity.[11–18]

Compound **1** has been shown[13] to exist as two diastereoisomers, referred to as the C_i (*meso*) and C_2 (*rac*) forms, arising as a consequence of the chirality of the $(\eta^3:\eta^3\text{-}C_{10}H_{16})Ru$ unit. These isomers are readily distinguished by ^1H NMR spectroscopy, giving rise to a characteristic 'doubling' of the number of resonances expected for a single compound. Thus in **1** there are eight singlet resonances arising from the terminal allyl protons of the bis(allyl) ligand and four from the methyl groups. Non-diastereomeric (though still chiral), mononuclear complexes derived from **1** display half this number of resonances if the axial sites of the approximately trigonal-bipyramidal ruthenium ion are different from one another. More symmetric equatorial, adducts such as $[Ru(\eta^3:\eta^3\text{-}C_{10}H_{16})Cl_2(CO)]$,[19] give rise to only two terminal allyl and a single methyl signal.

In previous reports[20,21] we have examined the reactions of areneruthenium(II) complexes with a wide range of carboxylate and α-hydroxypyridinate ligands while, more recently, we have investigated the formation of binuclear, carboxylato-bridged complexes, such as the oxalato derivative $[\{Ru(\eta^3:\eta^3\text{-}C_{10}H_{16})Cl\}_2(\mu\text{-}C_2O_4)]$.[22] We now describe our investigations into the reactions of **1** with a range of carboxylato ligands to form mononuclear complexes containing mono- and bi-dentate carboxylates. Our studies on the reactions of **1** with α-hydroxypyridinate ligands are reported elsewhere.[23] A preliminary report of part of this work has already been published.[24]

† *Supplementary data available*: see Instructions for Authors, *J. Chem. Soc., Dalton Trans.*, 1993, Issue 1, pp. xxiii–xxviii.

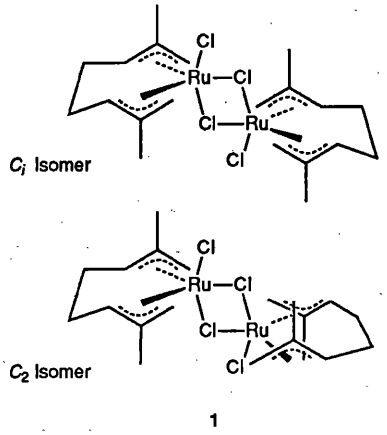

1

Experimental

Infrared spectra were recorded on a PE983 grating spectrometer between 4000 and 180 cm^{-1} as either KBr discs or Nujol mulls on CsI plates, NMR spectra on Varian XL200 and VXR400 spectrometers. Microanalyses were carried out by the departmental service at University College London. Mass spectra were run by the University of London Intercollegiate Research Service at the School of Pharmacy. All manipulations were carried out under nitrogen with degassed solvents using conventional Schlenk-line techniques, although no significant air sensitivity of the products was noted.

The compound $[\{Ru(\eta^3:\eta^3\text{-}C_{10}H_{16})Cl(\mu\text{-}Cl)\}_2]$ was prepared by published literature methods.[1,13,15] Ruthenium trichloride hydrate was obtained on loan from Johnson Matthey plc and was purified before use by dissolution in water and boiling to dryness. Sodium carboxylates were prepared by reaction of sodium metal with solutions of the acids in dry tetrahydrofuran (thf), or alternatively with the neat acid, for those that are liquids. Silver salts were prepared by the reaction of the aqueous acid with Ag_2O.[25] All other reagents and materials were obtained from the usual commercial sources.

Preparations.—$[Ru(\eta^3:\eta^3\text{-}C_{10}H_{16})Cl(O_2CMe)]$ **2**. (*a*) The

compound $[\{Ru(\eta^3:\eta^3\text{-}C_{10}H_{16})Cl(\mu\text{-}Cl)\}_2]$ (0.040 g, 0.065 mmol) was suspended in acetone (5 cm^3), $Ag[MeCO_2]$ (0.022 g, 0.133 mmol) was added and the mixture stirred for 1 h. The resulting orange-red solution was filtered through Celite to remove the precipitate of AgCl and the solvent removed *in vacuo* to give an orange oil which was recrystallised from diethyl ether. Yield: 0.026 g, 0.078 mmol, 60% (Found: C, 43.65; H, 5.85. Calc. for $C_{12}H_{19}ClO_2Ru$: C, 43.45; H, 5.75%).

(*b*) The compound $[\{Ru(\eta^3:\eta^3\text{-}C_{10}H_{16})Cl(\mu\text{-}Cl)\}_2]$ (0.200 g, 0.324 mmol) was suspended in acetone (5 cm^3), $Na[MeCO_2]$ (0.05 g, excess) was added and the mixture stirred for 24 h. The resulting product was recovered in a similar manner to (*a*). Yield: 0.185 g, 0.559 mmol, 86%.

(*c*) Attempts to prepare **2** by refluxing **1** in acetic acid resulted in the formation of a dark brown colouration over a period of *ca.* 4 h. However no product could be isolated probably due to high solubility in this reaction mixture.

$[Ru(\eta^3:\eta^3\text{-}C_{10}H_{16})(O_2CCF_3)_2(OH)_2]$ **3**. (*a*) The compound $[\{Ru(\eta^3:\eta^3\text{-}C_{10}H_{16})Cl(\mu\text{-}Cl)\}_2]$ (0.096 g, 0.156 mmol) was suspended in 'wet' acetone (5 cm^3). Silver trifluoroacetate (0.127 g, 0.574 mmol) was added and the mixture stirred for 1 h. The resulting orange solution was filtered through Celite to remove the precipitate of AgCl and the volume reduced to *ca.* one quarter resulting in the precipitation of the orange product which was isolated by filtration, washed with acetone and diethyl ether and air dried. Yield: 0.096 g, 0.200 mmol, 64% (Found: C, 35.10; H, 3.75. Calc. for $C_{14}H_{18}F_6O_5Ru$: C, 34.95; H, 3.75%).

(*b*) The compound $[\{Ru(\eta^3:\eta^3\text{-}C_{10}H_{16})Cl(\mu\text{-}Cl)\}_2]$ (0.195 g, 0.316 mmol) was refluxed in trifluoroacetic acid (15 cm^3) in the presence of trifluoroacetic anhydride (3 cm^3) for 4 h. The resulting red-brown solution was filtered through Celite to remove particulate matter, evaporated to *ca.* half volume and layered with hexane. The product separated out as large, orange crystals after standing for 48 h at 250 K. Yield: 0.215 g, 0.446 mmol, 71%.

(*c*) The product may also be prepared in near-quantitative yield by refluxing of the acetate complex $[Ru(\eta^3:\eta^3\text{-}C_{10}H_{16})Cl(O_2CMe)]$ **2** in neat CF_3CO_2H, followed by work-up in a similar manner as described in (*b*).

$[Ru(\eta^3:\eta^3\text{-}C_{10}H_{16})(O_2CCF_3)_2(N_2C_4H_4)]$ **4**. To $[Ru(\eta^3:\eta^3\text{-}C_{10}H_{16})(O_2CCF_3)_2(OH_2)]$ (0.079 g, 0.165 mmol) was added pyrazine (0.017 g, 0.212 mmol) and the mixture stirred in CH_2Cl_2 (5 cm^3) for 72 h. The resulting orange solution was evaporated to *ca.* one quarter volume and hexane added to precipitate the product as an orange, microcrystalline solid which was isolated by filtration, washed with diethyl ether and air dried. Yield: 0.068 g, 0.126 mmol, 76% (Found: C, 39.55; H, 3.60; N, 5.15. Calc. for $C_{18}H_{20}F_6N_2O_4Ru$: C, 39.80; H, 3.70; N, 5.15%).

$[Ru(\eta^3:\eta^3\text{-}C_{10}H_{16})(O_2CCCl_3)_2(OH_2)]$ **5**. To a solution of $[\{Ru(\eta^3:\eta^3\text{-}C_{10}H_{16})Cl(\mu\text{-}Cl)\}_2]$ (0.120 g, 0.195 mmol) in CH_2Cl_2 (4 cm^3) was added an acetone (4 cm^3) suspension of $Na[CCl_3CO_2]$ (0.181 g, 0.979 mmol). The mixture was stirred for 12 h at room temperature. The resulting brown-orange solution was filtered through Celite to remove the precipitate of NaCl and the solvents removed *in vacuo* to give a dark solid. Recrystallisation from chloroform–diethyl ether (1:1 v/v) yielded bright yellow crystals which were isolated by filtration and air dried. Yield: 0.102 g, 0.176 mmol, 45% (Found: C, 28.75; H, 3.25; Cl, 37.45. Calc. for $C_{14}H_{18}Cl_6O_5Ru$: C, 29.00; H, 3.15; Cl, 36.65%).

$[Ru(\eta^3:\eta^3\text{-}C_{10}H_{16})(O_2CCHCl_2)_2(OH_2)]$ **6**. A similar procedure to that employed for **5** was followed using $[\{Ru(\eta^3:\eta^3\text{-}C_{10}H_{16})Cl(\mu\text{-}Cl)\}_2]$ (0.120 g, 0.195 mmol) and $Na[CHCl_2CO_2]$ (0.146 g, 0.967 mmol). Yield: 0.100 g, 0.196 mmol, 50% (Found: C, 32.80; H, 4.00; Cl, 27.75. Calc. for $C_{14}H_{20}Cl_4O_5Ru$: C, 32.90; H, 3.90; Cl, 28.50%).

$[Ru(\eta^3:\eta^3\text{-}C_{10}H_{16})(O_2CCHF_2)_2(OH_2)]$ **7**. A similar procedure to that employed for **5** was followed using $[\{Ru(\eta^3:\eta^3\text{-}C_{10}H_{16})Cl(\mu\text{-}Cl)\}_2]$ (0.060 g, 0.097 mmol) and $Na[CHF_2CO_2]$ (0.058 g, 0.492 mmol). The product was purified by dry flash column chromatography and recrystallised from CH_2Cl_2–diethyl ether (1:1 v/v). Yield: 0.020 g, 0.045 mmol, 23% (Found: C, 37.80; H, 4.75. Calc. for $C_{14}H_{20}F_4O_5Ru$: C, 37.75; H, 4.55%).

$[Ru(\eta^3:\eta^3\text{-}C_{10}H_{16})Cl(O_2CCH_2Cl)]$ **8a** *and* $[Ru(\eta^3:\eta^3\text{-}C_{10}H_{16})(O_2CCH_2Cl)_2(OH_2)]$ **8b**. To a solution of $[\{Ru(\eta^3:\eta^3\text{-}C_{10}H_{16})Cl(\mu\text{-}Cl)\}_2]$ (0.120 g, 0.195 mmol) in CH_2Cl_2 (4 cm^3) was added $Na[CH_2ClCO_2]$ (0.116 g, 0.996 mmol) in acetone (4 cm^3). The mixture was stirred at room temperature for 12 h. Removal of the solvents *in vacuo* gave a yellow oily product which was recrystallised from diethyl ether–hexane (1:4 v/v) to give 0.055 g of orange-yellow crystals which were shown by ^1H NMR spectroscopy to be a mixture of **8a**, **8b** and unreacted starting material. Pure samples of **8a** and **8b** were isolated by dry flash column chromatography (Found: C, 39.75; H, 5.25. Calc. for $C_{12}H_{18}Cl_2O_2Ru$, **8a**: C, 39.35; H, 4.95%. Found: C, 36.80; H, 5.20. Calc. for $C_{14}H_{22}Cl_2O_5Ru$, **8b**: C, 38.00; H, 5.00%).

$[Ru(\eta^3:\eta^3\text{-}C_{10}H_{16})Cl(O_2CCH_2F)]$ **9a** *and* $[Ru(\eta^3:\eta^3\text{-}C_{10}H_{16})(O_2CCH_2F)_2(OH_2)]$ **9b**. A similar procedure to that adopted for **8a** and **8b** was employed using $[\{Ru(\eta^3:\eta^3\text{-}C_{10}H_{16})Cl(\mu\text{-}Cl)\}_2]$ (0.120 g, 0.195 mmol) and $Na[CH_2FCO_2]$ (0.100 g, 0.998 mmol) to give 0.017 g of a yellow material shown by ^1H NMR to be a mixture of **9a** and **9b**. The products were separated by dry flash column chromatography (Found: C, 40.40; H, 5.55. Calc. for $C_{12}H_{18}ClF_2O_2Ru$, **9a**: C, 41.20; H, 5.20%. Found: C, 39.85; H, 5.70. Calc. for $C_{14}H_{22}F_2O_5Ru$, **9b**: C, 41.05; H, 5.40%).

$[Ru(\eta^3:\eta^3\text{-}C_{10}H_{16})Cl\{F_3CC(O)CHC(O)CF_3\}]$ **10**. (*a*) The compound $[\{Ru(\eta^3:\eta^3\text{-}C_{10}H_{16})Cl(\mu\text{-}Cl)\}_2]$ (0.043 g, 0.070 mmol) was suspended in acetone (5 cm^3), $Ag[CF_3C(O)CHC(O)CF_3]$ (0.1 g, excess) was added and the mixture stirred for 24 h. The resulting pale orange solution was filtered through Celite to remove the precipitate of AgCl and unreacted starting material and the solvent removed *in vacuo* to give an orange oil which was recrystallised from diethyl ether. Yield: 0.015 g, 0.031 mmol, 22% (Found: C, 36.90; H, 3.50. Calc. for $C_{15}H_{17}ClF_6O_2Ru$: C, 37.55; H, 3.55%). Some difficulty was noted in the separation of the product from the excess of silver hexafluoroacetylacetonate.

(*b*) The compound $[\{Ru(\eta^3:\eta^3\text{-}C_{10}H_{16})Cl(\mu\text{-}Cl)\}_2]$ (0.053 g, 0.086 mmol) was suspended in acetone (5 cm^3), $Na[CF_3C(O)CHC(O)CF_3]$ (0.040 g, 0.194 mmol) was added and the mixture stirred at room temperature for 2 weeks. The product was isolated as in (*a*). Yield: 0.028 g, 0.059 mmol, 34%.

$[Ru(\eta^3:\eta^3\text{-}C_{10}H_{16})Cl_2\{SC(OH)CH_3\})]$ **11**. The compound $[\{Ru(\eta^3:\eta^3\text{-}C_{10}H_{16})Cl(\mu\text{-}Cl)\}_2]$ (0.072 g, 0.117 mmol) was stirred in acetone (5 cm^3) containing a small excess of thioacetic acid (0.2 cm^3) for 15 min during which time the solution became bright orange. The solvent was removed *in vacuo* to give an orange oil from which the product was deposited as orange crystals. These were filtered off and washed with *n*-hexane, then air dried. Yield: 0.074 g, 0.193 mmol, 82% (Found: C, 37.60; H, 5.50. Calc. for $C_{12}H_{20}Cl_2ORuS$: C, 37.50; H, 5.25%).

$[Ru(\eta^3:\eta^3\text{-}C_{10}H_{16})Cl(SOCMe)]$ **12a**, **12b**. The compound $[\{Ru(\eta^3:\eta^3\text{-}C_{10}H_{16})Cl(\mu\text{-}Cl)\}_2]$ (0.111 g, 0.180 mmol) was stirred in CH_2Cl_2 (5 cm^3) with a small excess of thioacetic acid (0.2 cm^3) for 24 h during which time the bright orange colouration initially formed darkened to a deep brown. The reaction mixture was evaporated to *ca.* one quarter volume and diethyl ether added to precipitate the product as a red-brown solid which was isolated by filtration and air dried. Yield: 0.08 g, 0.196 mmol, 54% (Found: C, 42.40; H, 5.55. Calc. for $C_{12}H_{19}ClORuS$: C, 41.45; H, 5.50%).

$[Ru(\eta^3:\eta^3\text{-}C_{10}H_{16})Cl(SOCBu^t)]$ **13a**, **13b**. The compound $[\{Ru(\eta^3:\eta^3\text{-}C_{10}H_{16})Cl(\mu\text{-}Cl)\}_2]$ (0.057 g, 0.093 mmol) was stirred in acetone (5 cm^3) with a small excess of thiopivalic acid (0.2 cm^3) for 1 h during which time a deep orange solution formed. The reaction mixture was evaporated to an orange oil which yielded an orange precipitate on trituration with methanol–hexane (1:2 v/v). The product was isolated by filtration and air dried. Yield: 0.064 g, 0.164 mmol, 88% (Found: C, 47.15; H, 6.90. Calc. for $C_{15}H_{25}ClORuS$: C, 46.20; H, 6.45%).

Table 1 Atomic coordinates ($\times 10^4$) for [Ru(η^3:η^3-$C_{10}H_{16}$)Cl(O_2CMe)] **2**

Atom	x	y	z
Ru	872(1)	1555(1)	1185(1)
Cl	−870(2)	1787(2)	630(2)
O(1)	1494(5)	1150(5)	−168(4)
O(2)	2468(5)	1226(4)	1051(4)
C(1)	563(7)	−1(6)	1231(6)
C(2)	278(7)	389(6)	2076(6)
C(3)	1106(7)	884(6)	2506(6)
C(4)	962(8)	1473(7)	3374(6)
C(5)	315(9)	2375(8)	3184(7)
C(6)	411(7)	2646(6)	2175(6)
C(7)	1358(8)	2936(6)	1752(7)
C(8)	1283(8)	3016(7)	798(7)
C(9)	−832(8)	383(7)	2417(7)
C(10)	2392(8)	3025(8)	2240(7)
C(11)	2376(8)	1045(6)	192(6)
C(12)	3283(7)	682(8)	−350(8)

Table 2 Atomic coordinates ($\times 10^4$) for [Ru(η^3:η^3-$C_{10}H_{16}$)(O_2CCF_3)$_2$(OH_2)] **3**

Atom	x	y	z
Ru	5000	6634(1)	2500
O(1)	5000	5394(2)	2500
O(2)	6282(3)	6578(2)	1373(3)
O(3)	5630(4)	5654(3)	−281(5)
C(1)	6375(4)	6081(3)	448(6)
C(2)	7505(5)	6075(4)	70(8)
C(3)	3488(4)	6436(3)	560(5)
C(4)	3918(3)	7167(3)	388(4)
C(5)	3996(3)	7676(2)	1587(4)
C(6)	4586(5)	8456(3)	1728(6)
C(7)	4383(4)	7351(3)	−924(5)
F(1)	7778(17)	6749(7)	−321(32)
F(2)	8283(15)	5875(20)	1143(22)
F(3)	7538(15)	5640(15)	−1008(27)
F(1A)	7424(17)	6353(22)	−1238(24)
F(2A)	8337(13)	6396(16)	1007(25)
F(3A)	7893(15)	5360(9)	−25(41)

[Ru(η^3:η^3-$C_{10}H_{16}$)Cl(SOCPh)] **14a,14b**. The compound [{Ru(η^3:η^3-$C_{10}H_{16}$)Cl(μ-Cl)}$_2$] (0.01 g, 0.116 mmol) was stirred in acetone (5 cm^3) with a small excess of thiobenzoic acid (0.1 cm^3) for 1 h resulting in the formation of a bright orange solution. The solvent was removed *in vacuo* and the residue dissolved in diethyl ether (1 cm^3) and layered with hexane resulting in the formation of a deep red crystalline product over a period of *ca.* 12 h. This product was collected by filtration and air dried. Yield: 0.057 g, 0.139 mmol, 60% (Found: C, 49.65; H, 5.00. Calc. for $C_{17}H_{21}ClORuS$: C, 49.80; H, 5.15%).

Crystallography.—Crystal data. $C_{12}H_{19}ClO_2Ru$ **2**, M = 331.80, orthorhombic, space group *Pbca*, a = 12.742(6), b = 14.082(6), c = 14.614(6) Å, U = 2622 $Å^3$ (by least-squares refinement of diffractometer angles for 30 automatically centred reflections in the range $10 \leqslant 2\theta \leqslant 23°$, λ = 0.710 73 Å), Z = 8, $F(000)$ = 1344, D_c = 1.68 g cm^{-3}, μ(Mo-Kα) = 13.63 cm^{-1}. Pink plate, 0.4 × 0.3 × 0.05 mm.

$C_{14}H_{18}O_5F_6Ru$ **3**, M = 481.39, monoclinic, space group $C2/c$, a = 12.191(3), b = 17.318(5), c = 9.314(2) Å, β = 105.14(2)°, U = 1898 $Å^3$ (by least-squares refinement diffractometer angles for 46 automatically centred reflections in the range $15 \leqslant 2\theta \leqslant 30°$, λ = 0.710 73 Å), Z = 4, $F(000)$ = 960, D_c = 1.68 g cm^{-3}, μ(Mo-Kα) = 8.80 cm^{-1}. Orange wedge, 0.6 × 0.25 × 0.2 mm.

Data collection and processing. The ω–2θ technique was used to collect 2576 (compound **2**, 2270 unique) and 2116 (compound **3**, 1675 unique) data in the range $5 \leqslant 2\theta \leqslant 50°$ on a Nicolet R3mV diffractometer equipped with graphite-monochromated Mo-Kα radiation. Three standards monitored every 97 reflections showed no appreciable change in intensity throughout either data collection. Data were corrected for Lorentz and polarisation effects and for absorption based on additional azimuthal scan data. Omission of intensities of $I \leqslant 3\sigma(I)$ gave 1381 (**3**) and 1568 (**3**) observed data which were employed in the analysis.

Table 3 Selected bond lengths (Å) and angles (°) for [Ru(η^3:η^3-$C_{10}H_{16}$)Cl(O_2CMe)] **2**

Ru–Cl	2.385(3)	Ru–O(1)	2.205(6)
Ru–O(2)	2.095(6)	Ru–C(1)	2.227(8)
Ru–C(2)	2.227(9)	Ru–C(3)	2.169(9)
Ru–C(6)	2.191(9)	Ru–C(7)	2.203(9)
Ru–C(8)	2.197(10)	O(1)–C(11)	1.249(11)
O(2)–C(11)	1.287(10)	C(11)–C(12)	1.491(14)
Cl–Ru–O(1)	93.7(2)	Cl–Ru–O(2)	154.4(2)
O(1)–Ru–O(2)	60.7(2)	O(1)–C(11)–O(2)	118.0(8)

Table 4 Selected bond lengths (Å) and angles (°) for [Ru(η^3:η^3-$C_{10}H_{16}$)(O_2CCF_3)$_2$(OH_2)] **3**

Ru–O(1)	2.146(4)	Ru–O(2)	2.100(3)
Ru–C(3)	2.245(4)	Ru–C(4)	2.260(4)
Ru–C(5)	2.221(4)	O(2)–C(1)	1.244(6)
O(3)–C(1)	1.229(6)	C(1)–C(2)	1.509(9)
O(1)–Ru–O(2)	87.4(1)	O(2)–Ru–O(2A)	174.8(1)
Ru–O(2)–C(1)	126.3(3)	O(2)–C(1)–O(3)	127.7(5)

Atoms labelled A generated by two-fold rotation about $\frac{1}{2}$, y, $\frac{1}{4}$.

Structure analysis and refinement. The structures were solved by a combination of conventional direct methods (**2**), Patterson methods (**3**) and Fourier difference synthesis. The asymmetric unit for **2** contained one complete molecule, while for **3** it was one half of the molecule, which sits on a crystallographic two-fold axis. In both cases all non-hydrogen atoms were refined anisotropically while hydrogen atoms were placed in idealised positions and allowed to ride on the atoms to which they were attached (C–H 0.96 Å, U_{iso} 0.08 $Å^2$). For compound **2** the final cycle of least-squares refinement included 145 parameters [weighting scheme $w^{-1} = \sigma^2(F) + 0.000\,338F^2$] and did not shift any parameter by more than 0.002 times its standard deviation (R = 0.0447, R' = 0.0458). The largest residual peak was 0.523 e $Å^{-3}$.

In the case of compound **3** the final cycle included 146 parameters [weighting scheme $w^{-1} = \sigma^2(F) + 0.000\,350F^2$] and gave R = 0.0384, R' = 0.0395. The fluorine atoms of the CF_3 groups were found to be disordered and were each modelled as having two positions, each of 50% occupancy. The largest shift to error ratio was 0.116 (associated with a thermal parameter for one of the disordered fluorine atoms) and the largest residual peak was 0.81 e $Å^{-3}$. Intermolecular short contacts of 2.70 Å were observed between oxygen atoms of the co-ordinated water molecules and the unco-ordinated oxygen atoms of trifluoroacetate ligands in adjacent molecules (see Discussion). Attempts to refine the structure of **3** in the non-centrosymmetric space group *Cc* (in which disorder need not be present) were unsuccessful.

All calculations were carried out using the SHELXTL PLUS program package [26] on a MicroVax II computer. Final fractional atomic coordinates are given in Tables 1 and 2 and selected bond lengths and angles in Tables 3 and 4 for compounds **2** and **3** respectively.

Additional material available from the Cambridge Crystallographic Data Centre comprises H-atom coordinates, thermal parameters and remaining bond lengths and angles.

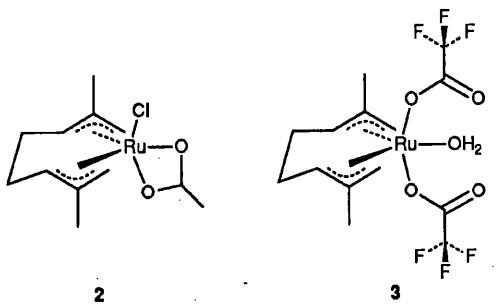

2 3

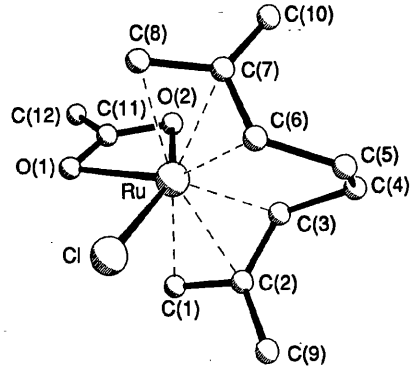

Fig. 1 Crystal structure of $[Ru(\eta^3:\eta^3\text{-}C_{10}H_{16})Cl(O_2CMe)]$ **2** showing the atom numbering scheme adopted

Results and Discussion

In our previous work[20] we demonstrated that areneruthenium(II) carboxylato complexes may be synthesised by one or more of three general methods: (*i*) reflux of the appropriate areneruthenium(II) chloro-bridged dimer in a mixture of the neat acid and the acid anhydride; (*ii*) treatment of $[\{Ru(arene)Cl(\mu\text{-}Cl)\}_2]$ with two mole equivalents of silver carboxylate in acetone or benzene; or (*iii*) reaction of $[\{Ru(arene)Cl(\mu\text{-}Cl)\}_2]$ with an excess of sodium carboxylate in acetone.

The greater solubility of complexes derived from **1**, in comparison to their areneruthenium(II) analogues, makes method (*i*) unsuitable for all but the most insoluble products and it is found that, in general, reaction of **1** with silver- or sodium-carboxylates is most likely to lead to the formation and isolation of the desired products.

The reaction of **1** with $Ag[MeCO_2]$ proceeds rapidly at room temperature in acetone to give a red solution from which the chelate complex $[Ru(\eta^3:\eta^3\text{-}C_{10}H_{16})Cl(O_2CMe)]$ **2**, analogous to the areneruthenium(II) complexes previously synthesised,[20] may be isolated in good yield. The reaction also proceeds, albeit more slowly, with sodium acetate but we were unable to recover any complexes from the direct interaction of **1** with refluxing acetic acid because of the high solubility of the products in this medium. The solid-state infrared spectrum of **2** (Table 5) displays two strong bands at 1517 and 1461 cm^{-1}, assignable respectively to $\nu_{asym}(OCO)$ and $\nu_{sym}(OCO)$[27] {*cf.* 1510, 1470 cm^{-1} for $[Ru(\eta^6\text{-}C_6H_6)Cl(O_2CMe)]$[20]}. A $\Delta\nu$ ($=\nu_{asym} - \nu_{sym}$) value of 56 cm^{-1} clearly indicates a chelate mode of co-ordination for the carboxylate ligand.[27] Medium intensity bands at 345 and 273 cm^{-1} are assigned to ν(RuO) and ν(RuCl) respectively. An electron impact mass spectrum (^{102}Ru, ^{35}Cl) of this material displayed peaks centred on *m/z* 317 $\{[Ru(\eta^3:\eta^3\text{-}C_{10}H_{16})Cl(O_2C)]^+\}$, 297 $\{[Ru(\eta^3:\eta^3\text{-}C_{10}H_{16})(O_2CMe)]^+\}$ and 235 $\{[Ru(\eta^3:\eta^3\text{-}C_{10}H_{16})]^+\}$ with isotope distribution patterns consistent with the presence of one ruthenium atom. The ^1H NMR spectrum of **2** (Table 6) displays a pattern of $\eta^3:\eta^3\text{-}C_{10}H_{16}$ resonances closely analogous to those already reported for the chelate benzothiazole-2-thiolate complex $[Ru(\eta^3:\eta^3\text{-}C_{10}H_{16})Cl(SNC_7H_4SH\text{-}2)]$[15] and the 2,2′-bipyridine (bipy) complex $[Ru(\eta^3:\eta^3\text{-}C_{10}H_{16})Cl(bipy)][BF_4]$.[18] The terminal allylic protons of the 2,7-dimethylocta-2,6-diene-1,8-diyl ligand give rise to four singlet signals (δ 5.51, 4.65, 4.63 and 3.56, $^2J_{syn-anti}$ not observed) while the methyl substituents resonate at δ 2.29 and 2.12, a spectrum consistent with inequivalent axial sites on the trigonal-bipyramidal ruthenium ion. A further singlet resonance, observed at δ 1.85, is due to the acetate methyl group. The formulation and structure of **2** was unequivocally confirmed by a single-crystal X-ray structure determination, Fig. 1.

The formation of **2** contrasts sharply with the much more insoluble deep orange trifluoroacetate product $[Ru(\eta^3:\eta^3\text{-}C_{10}H_{16})(O_2CCF_3)_2(OH_2)]$ **3**,* readily obtained by methods (*i*) and (*ii*) above. We have however, been unable to isolate the corresponding 1:1 chelate complex $[Ru(\eta^3:\eta^3\text{-}C_{10}H_{16})Cl(O_2CCF_3)]$ since the interaction of **1** with only two mole equivalents of $Ag[CF_3CO_2]$ gives a low yield of **3** along with a large quantity of unreacted starting material. This observation contrasts with that made in the area of areneruthenium(II) chemistry where the compounds $[Ru(\eta^6\text{-arene})Cl(O_2CCF_3)]$ (arene = C_6H_6 or C_6Me_6) can be readily synthesised by methods (*i*) and (*ii*).[20] Interestingly the reaction of the bis(acetato) complexes $[Ru(\eta^6\text{-arene})(O_2CMe)_2]$ with trifluoroacetic acid gives bis(trifluoroacetato) complexes, tentatively formulated as $[Ru(\eta^6\text{-arene})(O_2CCF_3)_2]\cdot H_2O$, which crystallise as monohydrates.[20] The water of crystallisation in these complexes occurs as a broad resonance at δ *ca.* 6 in the ^1H NMR spectrum and is thought to be only loosely associated with the metal atom.

The ^1H NMR spectrum of **3**, in $CDCl_3$, displays only half the number of $\eta^3:\eta^3\text{-}C_{10}H_{16}$ resonances of **2**, *viz* two terminal allyl singlets (δ 5.68 and 4.23) and a single methyl resonance (δ 2.12) indicative of equivalent axial sites on the trigonal-bipyramidal ruthenium atom and inconsistent with a compound containing both mono- and bi-dentate carboxylate ligands. The water ligand occurs as a sharp singlet resonance at δ 7.11, broadening somewhat in $[^2H_3]$nitromethane solution. The ^{19}F NMR spectrum displays a single singlet resonance at δ −76.50 (relative to $CFCl_3$), close to the value observed for the free acid (δ −76.41) but somewhat upfield of the corresponding resonance in the fluxional arene complex $[Ru(\eta^6\text{-}C_6H_6)(O_2CCF_3)_2]\cdot H_2O$ (δ −74.71).[20] This latter signal represents an average between mono- and bi-dentate co-ordination. In the infrared spectrum, **3** displays a strong, broad band at 3362 cm^{-1} assignable to ν(OH) and indicative of hydrogen bonding in the solid state. The trifluoroacetate ligands give ν(CF) bands at 1196 and 1143 cm^{-1}, $\nu_{asym}(OCO)$ at 1703 and 1670 cm^{-1} and $\nu_{sym}(OCO)$ at 1421 cm^{-1}. The much larger value of Δν (249–282 cm^{-1}) is suggestive of a monodentate mode of co-ordination.

Compound **3** will sublime intact at *ca.* 100 °C under reduced pressure with no trace of displacement of the water molecule and similarly refluxing **3** in dry dichloromethane containing anhydrous magnesium sulfate results in the recovery of the unchanged material. These observations suggest that the water molecule in **3** is strongly bound and actually forms part of the co-ordination sphere of the metal ion with the two trifluoroacetate ligands bonding in a monodentate mode at the axial sites, consistent with the ^1H NMR data. This contention is further supported by the low substitutional lability of the water ligand which is slowly displaced by pyrazine over a period of days at room temperature, to give the adduct $[Ru(\eta^3:\eta^3\text{-}C_{10}H_{16})(O_2CCF_3)_2(N_2C_4H_4)]$ **4** along with a quantity of residual **3**.

The formulation of **3** was confirmed by a single-crystal X-ray structure determination. Fig. 2 shows the water molecule to occupy one of the equatorial co-ordination sites of the trigonal-bipyramidal ruthenium ion while the two trifluoroacetato

* A trifluoroacetato bridged complex $[\{Ru(\eta^3:\eta^3\text{-}C_{10}H_{16})(O_2CCF_3)_2\}_2]$ has been reported[28] to be formed from the reaction of thallium trifluoroacetate with **1** although no spectroscopic data were quoted and we find no evidence for the existence of this material.

Table 5 Selected infrared data for new complexes[a]

Compound	Infrared absorption/cm^{-1} ν_{asym}(OCO)	ν_{sym}(OCO)	$\Delta\nu$	ν(OH$_2$)	ν(RuCl)	Other
2 [Ru(η^3:η^3-$C_{10}H_{16}$)Cl(O_2CMe)]	1517s	1461s	56	—	273m	345m ν(RuO)
3 [Ru(η^3:η^3-$C_{10}H_{16}$)(O_2CCF_3)$_2$(OH_2)]	1703vs, 1670vs	1421m	249–282	3362s (br)	—	1196s, 1143s ν(CF)
5 [Ru(η^3:η^3-$C_{10}H_{16}$)(O_2CCCl_3)$_2$(OH_2)]	1702vs, 1680vs	1323s	379–357	3390s (br)	—	844s, 831s ν(CCl)
6 [Ru(η^3:η^3-$C_{10}H_{16}$)(O_2CCHCl_2)$_2$(OH_2)]	1671s, 1629s	1359s, 1341s	270–330	3372s	—	814s, 787s ν(CCl)
7 [Ru(η^3:η^3-$C_{10}H_{16}$)(O_2CCHF_2)$_2$(OH_2)]	1660s, 1625s	1436	189–224	3317s	—	1117s, 1064s ν(CF)
8a [Ru(η^3:η^3-$C_{10}H_{16}$)Cl(O_2CCH_2Cl)]	1526s, 1519s	1452s, 1441s	67–85	—	*b*	790m ν(CCl)
8b [Ru(η^3:η^3-$C_{10}H_{16}$)(O_2CCH_2Cl)$_2$(OH_2)]	1612s	1374s	238	3326s	—	784m ν(CCl)
9a [Ru(η^3:η^3-$C_{10}H_{16}$)Cl(O_2CCH_2F)]	1556s, 1536s	1466s, 1454s	70–102	—	*b*	1076s, 1066s ν(CF)
9b [Ru(η^3:η^3-$C_{10}H_{16}$)(O_2CCH_2F)$_2$(OH_2)]	1617s	1419s	198	3328s	—	1085s ν(CF)
10 [Ru(η^3:η^3-$C_{10}H_{16}$)Cl{$F_3CC(O)CHC(O)CF_3$}]	1655m, 1623s[c]	—	—	—	317s	1258s (br), 1205s (br), 1143s (br) ν(CF)

[a] Spectra run in Nujol mulls or as KBr disc. Abbreviations: s = strong, m = medium, w = weak, v = very, br = broad. [b] Impossible to assign unambiguously. [c] ν(CO).

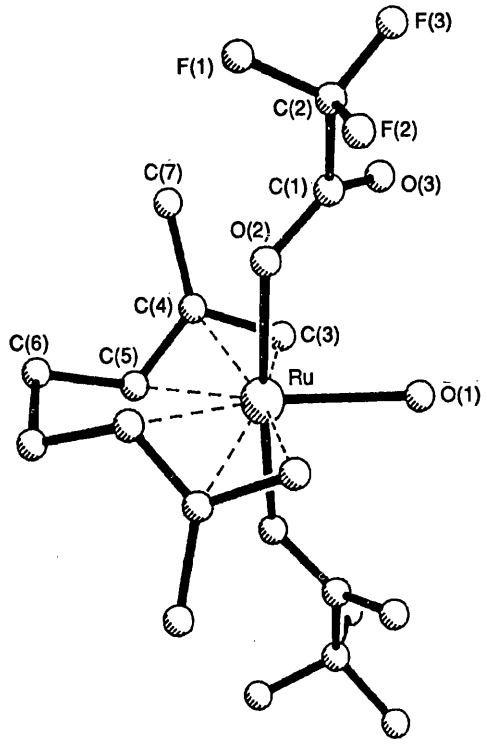

Fig. 2 Crystal structure of [Ru(η^3:η^3-$C_{10}H_{16}$)(O_2CCF_3)$_2$(OH_2)] **3** showing the atom numbering scheme adopted

ligands are bound in a monodentate fashion in the axial positions. The Ru–OH_2 distance, 2.146(4) Å, is only slightly longer than the Ru–O bond lengths to the axial trifluoroacetate ligands, 2.100(3) Å, and is very similar to other Ru–L_{eq} distances (L = acetate, pyrazine[14] or 2,2′:6′,2″-terpyridine[18]) and suggests clearly that the water molecule is relatively strongly bound to the metal centre. A similar Ru^{IV}–OH_2 distance [2.165(5) Å] has been observed by us in the related complex [Ru(η^3:η^2:η^3-$C_{12}H_{18}$)Cl(OH_2)][BF_4].[29] Similarly, the cyclo-octa-1,5-diene (cod) complex [Ru(cod)(OH_2)$_4$][$O_3SC_6H_4$-Me-4]$_2$[30] exhibits Ru–OH_2 distances of 2.158(1) Å *trans* to cod and 2.095(2) Å *trans* to water, while the Fe^{II}–OH_2 distance in the 2,6-diacetylpyridine bis(semicarbazone) (L) complex [FeL(H_2O)$_2$]$^{2+}$ is 2.214 Å.[31]

In solution the aqua ligand is presumably intramolecularly hydrogen bonded to the trifluoroacetato ligands. In the solid state however, an infinite intermolecular hydrogen bonded lattice exists (Fig. 3) with short contacts O(1)···O(3′) of 2.70 Å, implying relatively strong[32] interactions.

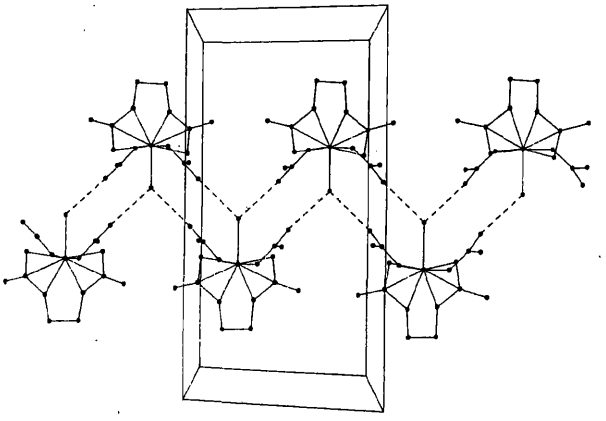

Fig. 3 Crystal packing diagram of [Ru(η^3:η^3-$C_{10}H_{16}$)(O_2CCF_3)$_2$(OH_2)] **3**, viewed down the *a* axis (fluorine atoms omitted for clarity)

'Cross-over' between Mono- and Bi-dentate Co-ordination.— The differences in the reactivity of **1** towards acetate and trifluoroacetate ligands is presumably a consequence of the differing electronic properties of the $-CH_3$ and $-CF_3$ substituents. These electronic properties may be quantified, either (*i*) simply by consideration of the pK_a of the neutral acid (a parameter which contains both inductive and resonance components), or (*ii*) by examination of substituent polarity parameters such as the $\mathcal{F}$ parameter of Swain and Lupton[33] (a wide variety of $\mathcal{F}$ values are available, derived from the Hammett constants σ_m and σ_p[34]) which deals solely with the field (*i.e.* inductive as opposed to resonance) effects of substituent groups [$\mathcal{F}(CF_3) = 0.38$, $\mathcal{F}(CH_3) = -0.052$[35]]. Logically there must be a certain value of $\mathcal{F}$ (or pK_a) where the cross-over from mono- to bi-dentate co-ordination occurs. With this in mind, a range of simple chloro- and fluoro-carboxylates has been examined in the hope determining that point and perhaps of finding a ligand exhibiting both types of co-ordination.

We find that interaction of **1** with an excess of the sodium salts of trichloro-, dichloro- and difluoro-acetic acids ($\mathcal{F}_{\text{acid substituent}} = 0.31, 0.17, 0.27$;[35] acid p$K_a$ = 0.52, 1.35 and 1.34[36]) gives the complexes [Ru(η^3:η^3-$C_{10}H_{16}$)($O_2CCH_{3-n}X_n$)$_2$(OH_2)] (X = Cl, *n* = 3 **5**; X = Cl, *n* = 2 **6**; X = F, *n* = 2 **7**) which are structurally related to **3**. The ^{1}H NMR spectra of these complexes are all consistent with a geometry incorporating equivalent axial sites. In addition complex **6** displays a single, singlet resonance at δ 5.45 assigned to the $CHCl_2$– group, while the corresponding CHF_2– resonance in **7** appears as a triplet (δ 5.34, $^2J_{H-F}$ = 54.8 Hz).

In analogous reactions involving the sodium salts of chloro- and fluoro-acetic acids mixtures of two complexes are formed, namely [Ru(η^3:η^3-$C_{10}H_{16}$)Cl(O_2CCH_2X)] (X = Cl **8a** or F **9a**)

Table 6 Proton NMR data for new complexes[a]

Compound	δ (J_{H-H}/Hz) Terminal allyl	Internal allyl	Ethylinic	Me	Ligand
2 $[Ru(\eta^3:\eta^3\text{-}C_{10}H_{16})Cl(O_2CMe)]$	5.51 (s,1 H), 4.65 (s, 1 H) 4.63 (s, 1 H), 3.56 (s, 1 H)	4.20 (m, 1 H) 3.49 (m, 1 H)	2.53 (m, 4 H)	2.29 (s, 3 H) 2.12 (s, 3 H)	1.85 (s, 3 H, CH_3)
3 $[Ru(\eta^3:\eta^3\text{-}C_{10}H_{16})(O_2CCF_3)_2(OH_2)]$	5.68 (s, 2 H), 4.23 (s, 2 H)	4.42 (m, 2 H)	3.07 (m, 2 H) 2.47 (m, 2 H)	2.12 (s, 6 H)	7.11 (s, 2 H, OH_2)
4 $[Ru(\eta^3:\eta^3\text{-}C_{10}H_{16})(O_2CCF_3)_2(N_2C_4H_4)]$	5.22 (s, 2 H), 4.16 (s, 2 H)	6.17 (m, 2 H)	3.47 (m, 2 H) 2.71 (m, 2 H)	2.15 (s, 6 H)	8.72, 8.44 (AB, 4 H, ^3J = 3.2, $N_2C_4H_4$)
5 $[Ru(\eta^3:\eta^3\text{-}C_{10}H_{16})(O_2CCCl_3)_2(OH_2)]$	5.77 (s, 2 H), 4.29 (s, 2 H)	4.56 (m, 2 H)	3.11 (m, 2 H) 2.50 (m, 2 H)	2.23 (s, 6 H)	7.13 (s, 2 H, OH_2)
6 $[Ru(\eta^3:\eta^3\text{-}C_{10}H_{16})(O_2CCHCl_2)_2(OH_2)]$	5.67 (s, 2 H), 4.29 (s, 2 H)	4.52 (m, 2 H)	3.09 (m, 2 H) 2.48 (m, 2 H)	2.17 (s, 6 H)	7.52 (s, 2 H, OH_2) 5.45 (s, 2 H, $CHCl_2$)
7 $[Ru(\eta^3:\eta^3\text{-}C_{10}H_{16})(O_2CCHF_2)_2(OH_2)]$	5.65 (s, 2 H), 4.22 (s, 2 H)	4.38 (m, 2 H)	3.08 (m, 2 H) 2.48 (m, 2 H)	2.15 (s, 6 H)	7.68 (s, br, 2 H, OH_2) 5.34 (t, 2 H, $^2J_{H-F}$ = 54.8, CHF_2)
8a $[Ru(\eta^3:\eta^3\text{-}C_{10}H_{16})Cl(O_2CCH_2Cl)]$ (*i*) 20 °C (average between **8a** and **8c**) (*ii*) −50 °C	5.59 (s, 1 H), 4.74 (s, br, 1 H) 4.70 (s, 1 H), 3.69 (s, br, 1 H) 5.61 (s, 1 H), 4.75 (s, 1 H) 4.66 (s, 1 H), 3.71 (s, 1 H)	4.31 (m, br, 1 H) 3.71 (m, br, 1 H) 4.29 (m, 1 H) 3.73 (m, 1 H)	2.58 (m, 4 H) 2.58 (m, 4 H)	2.30 (s, 3 H) 2.15 (s, 3 H) 2.30 (s, 3 H) 2.17 (s, 3 H)	3.80, 3.74 (AB, 2 H, ^2J = 14.3, CH_2Cl) 3.80, 3.74 (AB, 2 H, ^2J = 14.3, CH_2Cl)
8b $[Ru(\eta^3:\eta^3\text{-}C_{10}H_{16})(O_2CCH_2Cl)_2(OH_2)]$	5.56 (s, 2 H), 4.16 (s, 2 H)	4.28 (m, br, 2 H)	3.02 (m, br, 2 H) 2.48 (m, br, 2 H)	2.12 (s, 6 H)	8.10 (s, br, 2 H, OH_2) 3.64 (s, br, 2 H, CH_2Cl)
8c $[Ru(\eta^3:\eta^3\text{-}C_{10}H_{16})Cl(O_2CCH_2Cl)(OH_2)]$[b]	5.46 (s, 1 H), 5.34 (s, 1 H) 4.87 (s, 1 H), 4.10 (s, 1 H)	4.98 (m, 1 H) 4.32 (m, 1 H)	2.92 (m, 4 H)	2.39 (s, 3 H) 2.06 (s, 3 H)	6.39 (s, br, 2 H, OH_2) 3.78 (s, 2 H, CH_2Cl)
9a $[Ru(\eta^3:\eta^3\text{-}C_{10}H_{16})Cl(O_2CCH_2F)]$ (*i*) 20 °C (average between **9a** and **9c**) (*ii*) −50 °C	5.56 (s, br, 1 H), 4.89 (s, br, 1 H) 4.75 (s, 1 H), 3.86 (s, br, 1 H) 5.63 (s, 1 H), 4.83 (s, 1 H) 4.69 (s, 1 H), 3.80 (s, 1 H)	4.46 (m, br, 1 H) 3.86 (m, br, 1 H) 4.42 (m, 1 H) 3.79 (m, 1 H)	2.50 (m, br, 4 H) 2.50 (m, 4 H)	2.32 (s, 3 H) 2.13 (s, 3 H) 2.30 (s, 3 H) 2.17 (s, 3 H)	4.58 (d, br, $^2J_{H-F}$ = 47.1, CH_2F) 4.61, 4.55 (dAB, $^2J_{H-H}$ = 8.2, $^2J_{H-F}$ = 47.1, CH_2F)
9b $[Ru(\eta^3:\eta^3\text{-}C_{10}H_{16})(O_2CCH_2F)_2(OH_2)]$	5.58 (s, 2 H), 4.21 (s, 2 H)	4.37 (m, 2 H)	3.01 (m, 2 H) 2.50 (m, 2 H)	2.10 (s, 6 H)	8.18 (s, br, 2 H, OH_2) 4.32 (d, 2 H, $^2J_{H-F}$ = 48.3, CH_2F)
9c $[Ru(\eta^3:\eta^3\text{-}C_{10}H_{16})Cl(O_2CCH_2F)(OH_2)]$[b]	5.47 (s, 1 H), 5.37 (s, 1 H) 4.79 (s, 1 H), 4.13 (s, 1 H)	5.00 (m, 1 H) 4.59 (m, 1 H)	2.90 (m, 4 H)	2.41 (s, 3 H) 2.05 (s, 3 H)	6.52 (s, br, 2 H, OH_2) 4.30 (m, br, 2 H, CH_2F)
10 $[Ru(\eta^3:\eta^3\text{-}C_{10}H_{16})Cl\{F_3CC(O)CHC(O)CF_3\}]$	6.08 (s, 1 H), 4.92 (s, 1 H) 4.89 (s, 1 H), 3.50 (s, 1 H)	5.19 (m, 1 H) 4.44 (m, 1 H)	3.04 (m, 2 H) 2.43 (m, 2 H)	2.45 (s, 3 H) 1.99 (s, 3 H)	4.96 (s, 1 H, $CF_3COCHCOCF_3$)[c]
11 $[Ru(\eta^3:\eta^3\text{-}C_{10}H_{16})Cl_2\{SC(OH)CH_3\}]$	4.76 (s, 2 H), 4.00 (s, 2 H)[d]	5.08 (m, 2 H)	3.26 (m, 2 H) 2.57 (m, 2 H)	2.30 (s, 6 H)	13.99 (s, 1 H, OH) 2.69 (s, 3 H, CH_3)
12a $[Ru(\eta^3:\eta^3\text{-}C_{10}H_{16})Cl(SOCMe)]$ (*S equatorial*)	5.28 (s, 1 H), 4.24 (s, 1 H) 4.06 (s, 1 H), 2.61 (s, 1 H)	4.31 (m, 1 H) 3.30 (m, 1 H)	2.83 (m, 4 H)	2.32 (s, 3 H) 2.07 (s, 3 H)	1.66 (s, 3 H, CH_3)
12b $[Ru(\eta^3:\eta^3\text{-}C_{10}H_{16})Cl(SOCMe)]$ (*S axial*)	5.28 (s, 1 H), 4.68 (s, 1 H) 4.36 (s, 1 H), 3.52 (s, 1 H)	4.41 (m, 1 H) 3.67 (m, 1 H)	2.65 (m, 4 H)	2.21 (s, 3 H) 2.13 (s, 3 H)	1.68 (s, 3 H, CH_3)
13a $[Ru(\eta^3:\eta^3\text{-}C_{10}H_{16})Cl(SOBu^t)]$ (*S equatorial*)	5.27 (s, 1 H), 4.05 (s, 1 H) 4.04 (s, 1 H), 2.36 (s, 1 H)	4.32 (m, 1 H) 3.27 (m, 1 H)	2.88 (m, 4 H)	2.36 (s, 3 H) 2.09 (s, 3 H)	1.05 [s, 9 H, $C(CH_3)_3$]
13b $[Ru(\eta^3:\eta^3\text{-}C_{10}H_{16})Cl(SOBu^t)]$ (*S axial*)	5.21 (s, 1 H), 4.66 (s, 1 H) 4.18 (s, 1 H), 3.20 (s, 1 H)	4.43 (m, 1 H) 3.63 (m, 1 H)	2.69 (m, 4 H)	2.44 (s, 3 H) 2.19 (s, 3 H)	1.14 [s, 9 H, $C(CH_3)_3$]
14a $[Ru(\eta^3:\eta^3\text{-}C_{10}H_{16})Cl(SOCPh)]$ (*S equatorial*)	5.33 (s, 1 H), 4.28 (s, 1 H) 4.11 (s, 1 H), 2.69 (s, 1 H)	4.30 (m, 1 H) 3.50 (m, 1 H)	2.93 (m, 4 H)	2.39 (s, 3 H) 2.17 (s, 3 H)	7.84 (dd, 2 H, ^3J = 8.4, ^4J = 1.2, *o*-C_6H_5) 7.54 (dt, 1 H, ^3J = 7.5, ^4J = 1.2, *p*-C_6H_5) 7.37 (t, 2 H, ^3J = 7.9, *m*-C_6H_5)
14b $[Ru(\eta^3:\eta^3\text{-}C_{10}H_{16})Cl(SOCPh)]$ (*S axial*)	5.33 (s, 1 H), 4.69 (s, 1 H) 4.38 (s, 1 H), 3.45 (s, 1 H)	4.51 (m, 1 H) 3.79 (m, 1 H)	2.44 (m, 4 H)	2.48 (s, 3 H) 2.26 (s, 3 H)	7.96 (dd, 2 H, ^3J = 7.8, ^4J = 0.6, *o*-C_6H_5) 7.55 (dt, 1 H, ^3J = 7.6, ^4J = 1.3, *p*-C_6H_5) 7.42 (t, 2 H, ^3J = 7.5, *m*-C_6H_5)

[a] Recorded at 298 K unless otherwise stated. s = singlet, d = doublet, dd = doublet of doublets, t = triplet, dt = doublet of triplets, AB = AB pattern, dAB = doublet of AB patterns, m = multiplet and br = broad. [b] At −50 °C. [c] Unambiguous assignment of this resonance is not possible since it occurs at a very similar chemical shift to two other 1 H singlet signals arising from the bis(allyl) ligand. [d] Signals noticeably broader than the corresponding resonances for the other half of the bis(allyl) ligand.

and $[Ru(\eta^3:\eta^3\text{-}C_{10}H_{16})(O_2CCH_2X)_2(OH_2)]$ **8b**, **9b**. In both cases the complex with chelating ligands (**8a**, **9a**) forms the bulk of the isolated yields [product ratios: 7:1 (**8a**:**8b**), 6:1 (**9a**:**9b**)]. The ^{1}H NMR spectra of **8a** and **9a** exhibit the expected four singlet resonances for the terminal allylic protons of the dimethyloctadienyl ligand and two signals for the methyl groups, indicative of inequivalent axial sites. At 20 °C two of the terminal allyl resonances in each spectrum are broad whilst the other two are much sharper, implying a fluxional process may be occurring in which the major changes take place on only one side of the molecule. This process is slightly slower in the case of **9a** than **8a** as indicated by an increased peak width. In both cases raising the temperature to 50 °C results in sharp, four-line patterns for the terminal allyl protons, consistent with inequivalent axial sites, even in a rapid-exchange regime. Lowering the temperature results in a gradual broadening of all the lines in the spectrum until, at −20 °C, they are significantly flattened into the baseline. At −50 °C eight sharp singlet resonances are observed in the allylic region of the spectrum, half of them four times the intensity of the other four. Similarly, four methyl signals can now be observed. In addition broad peaks are also observed at δ 6.39 and 6.52 respectively [close to the value of δ *ca.* 6 for the exchanging water of crystallisation in the areneruthenium(II) carboxylato compounds[20]]. Other new resonances corresponding to the carboxylates and the remainder of the bis(allyl) ligands are also apparent. Complete NMR data for these processes are given in Table 6.

These temperature-dependent NMR spectra are interpreted in terms of an equilibrium involving mono- and bi-dentate co-ordination of the $[CH_2XCO_2]^-$ ligands analogous to that observed in the trisphosphine complex *fac*-$[RuCl(O_2CMe)\{PPh[C_3H_6P(C_6H_{11})_2]_2\}]$,[37] and activated by means of residual water in the deuteriated chloroform solvent. Thus we believe complexes **8a** and **9a** are each in equilibrium with further aqua complexes, $[Ru(\eta^3:\eta^3\text{-}C_{10}H_{16})Cl(O_2CCH_2X)(OH_2)]$ **8c**, **9c** each of which also possesses inequivalent axial sites, Scheme 1. The equilibrium constant at −50 °C for this process (K = [*N*a]/[*N*c]) is *ca.* 5 in both cases.

The NMR spectra of the bis(carboxylato) aqua complexes **8b** and **9b** also display evidence of fluxionality. Raising the temperature to 50 °C results in a gradual broadening of all the resonances in the spectra, most notably those corresponding to the water ligands. At 0 °C however, all the resonances are sharp, as in the case of **3**. Further lowering of the temperature produces no further changes in the spectra. These observations are consistent with a simple exchange of co-ordinated water with that in the bulk solvent.

The ^{1}H NMR spectrum of **8a** at room temperature displays a closely spaced AB pattern (δ 3.80 and 3.74, $^2J_{H-H}$ = 14.3 Hz) assigned to the protons of the chloroacetate ligand. These protons are diastereotopic and the presence of the chiral metal centre results in the splitting of the expected singlet into the observed AB pattern. The analogous protons in **9a** give rise to an eight-line pattern because of additional coupling to fluorine ($^2J_{H-F}$ = 47.1 Hz). The effect is analogous to that observed in the ^{19}F NMR spectrum of the adduct $[Ru(\eta^3:\eta^3\text{-}C_{10}H_{16})Cl_2(Me_2NPF_2)]$ where the diastereotopic fluorine atoms* give rise to an eight-line pattern due to coupling to phosphorus.

In summary, the more electron withdrawing carboxylates favour the formation of complexes with monodentate ligands and equatorially co-ordinated water molecules. Increasing the electron releasing properties of the substituent group on the carboxylate leads to fluxional behaviour involving mono- and bi-dentate co-ordinated ligands. In the limiting case (R = Me **2**) the second carboxylate oxygen atom is a sufficiently good donor to bind more rigidly to the metal centre resulting in the formation of the 1:1 chelate complex. It would thus appear that the 'cross-over' between these two bonding modes occurs gradually over acid pK_a values of *ca.* 1.3–2.9; $\underset{\sim}{F}$ of *ca.* 0.1–0.27.

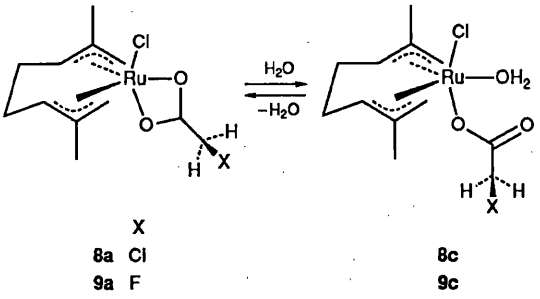

X
8a Cl — **8c**
9a F — **9c**

Scheme 1 Fluxional behaviour of the halogenoacetato complexes $[Ru(\eta^3:\eta^3\text{-}C_{10}H_{16})Cl(O_2CCH_2X)]$ (X = F or Cl)

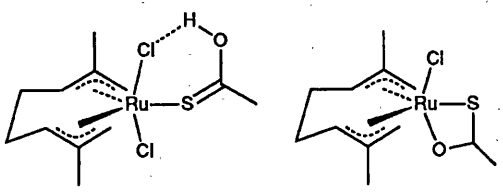

11 **12a**

In a further attempt to observe aqua complexes we have also investigated the reaction of **1** with other electron-withdrawing ligands such as the hexafluoroacetylacetonate anion, $[CF_3C(O)CHC(O)CF_3]^-$. We find that in this case a chelate complex $[Ru(\eta^3:\eta^3\text{-}C_{10}H_{16})Cl\{F_3CC(O)CHC(O)CF_3\}]$ **10** is formed, analogous to the ruthenium(II) complex $[Ru(\eta^6\text{-}C_6H_6)Cl(acac)]$[38] (Hacac = acetylacetone). The less strained nature of the six-membered heterocyclic ring no doubt stabilises the bidentate co-ordination mode.

Reactions with Thiocarboxylic Acids.—Reaction of **1** with a small excess of thioacetic acid in acetone rapidly produces a bright orange solution from which may be isolated a complex of formula $[Ru(\eta^3:\eta^3\text{-}C_{10}H_{16})Cl_2\{SC(OH)Me\}]$ **11**, containing a neutral co-ordinated thioacetic acid molecule. The infrared spectrum of this molecule shows two broad bands of medium intensity at surprisingly low wavenumber (2606, 2458 cm^{-1}) which fall in the region expected for ν(SH) or for hydrogen-bonded carboxylic acid dimers.[39] No bands assignable to co-ordinated C=O in the region[21] of 1600 cm^{-1} were observed however, instead the complex exhibits two strong bands at 1437 and 1347 cm^{-1} assignable to ν(O–C=S) in addition to the usual weaker bands arising from the bis(allyl) ligand. The far infrared spectrum contains two strong ν(RuCl) absorptions at 310 and 239 cm^{-1}. The ^{1}H NMR spectrum of **11** displays two resonances arising from the terminal allyl protons of the dimethyloctadienediyl ligand, δ 4.76 and 4.00, the latter signal being noticeably broader than the former at room temperature, perhaps indicating a hydrogen-bonding interaction involving one of the axial chloride ligands. In addition, an extremely sharp singlet resonance is observed at δ 13.99 assignable to a strongly hydrogen bonded acidic proton. This evidence leads us to suggest that the thioacetic acid molecule is S-bound with the hydroxyl proton involved in a strong hydrogen-bonding interaction with one of the axial chloride ligands both in the solid state and in solution, giving rise to ν(O · · · H · · · Cl) at an anomalously low wavenumber.

Reaction of **1** with thioacetic acid over longer reaction times, up to 24 h, gives the chelate complex $[Ru(\eta^3:\eta^3\text{-}C_{10}H_{16})Cl(OSCMe)]$ **12**, analogous to **2**. Because of the asymmetry of the thioacetate ligand the existence of axial and/or equatorial isomers arises. In this case **12** is found to exist as both

* At the time this inequivalence was thought to be a consequence of restricted rotation about the Ru–P bond. The phenomenon has since been reinterpreted by Cox and Roulet[13] however.

geometrical isomers **12a** and **12b** (distinguished by their ^1H NMR spectra) in a ratio of approximately 4:1. It is unclear whether the major isomer has the sulfur atom equatorially or axially bound but it seems likely that the more bulky donor atom occupies an equatorial position in order to minimise unfavourable axial ligand–methyl substituent steric interactions. A number of examples of the related 2-hydroxypyridinate complexes $[Ru(\eta^3:\eta^3\text{-}C_{10}H_{16})Cl(NC_5H_4O)]$ exhibit analogous isomerism, and have been studied by us in some detail.[23]

The two-step mechanism of co-ordination of thioacids, initially proceeding *via* adducts such as **11**, is analogous to the reaction of **1** with pyridine-2-thiol[15] which proceeds initially *via* the monoadduct $[Ru(\eta^3:\eta^3\text{-}C_{10}H_{16})Cl_2(NC_5H_4SH)]$ before base-induced deprotonation occurs to form the chelate compound $[Ru(\eta^3:\eta^3\text{-}C_{10}H_{16})Cl(NC_5H_4S)]$. In contrast, in the reaction of **1** with 2-hydroxypyridine only the complexes $[Ru(\eta^3:\eta^3\text{-}C_{10}H_{16})Cl(NC_5H_4O)]$ are isolated.[23]

Reaction of **1** with thiopivalic and thiobenzoic acids also gives chelate species $[Ru(\eta^3:\eta^3\text{-}C_{10}H_{16})Cl(OSCR)]$ (R = Bu^t **13** or Ph **14**), although in these cases we have been unable to observe the formation of simple adduct intermediates related to **11**. We infer that the chelation step in these instances is more rapid than in the former case. Also the high solubility of the complexes makes it difficult to isolate them quickly and chelation may well occur during the recrystallisation procedure. As with **12**, complexes **13** and **14** exist as *axial* and *equatorial* isomers, each possessing similar, but distinct, ^1H NMR spectra (Table 6). Isolated isomer ratios were 25:1 and 6:1 for **13** and **14** respectively. In the absence of competing interactions the major isomers are again assigned S-equatorial structures for reasons outlined above.

X-Ray Crystal Structure Determinations.—The X-ray crystal structures of complexes **2** and **3** are shown in Figs. 1 and 2 respectively. Fractional atomic coordinates are listed in Tables 1 and 2 and selected bond lengths and angles in Tables 3 and 4. In both compounds the geometry about the ruthenium atom may be loosely described as approximately trigonal bipyramidal with the bis(allyl) ligands occupying two of the equatorial co-ordination sites and possessing the usual local C_2 symmetry.[2,11,12,14–18] No significant variation is observed in the Ru–C bond lengths. The bonds to the two axial oxygen atoms [O(2)] are virtually identical in length in the two complexes (2.10 Å) and are somewhat shorter than the corresponding distances in the fluxional ruthenium(II) complex *fac*-$[RuCl(O_2CMe)\{PPh[C_3H_6P(C_6H_{11})_2]_2\}]$ (2.21–2.23 Å).[37] In complex **3**, the equatorial Ru–OH_2 bond, 2.146(4) Å, is actually somewhat shorter than the Ru–O(1) distance in **2**, 2.205(6) Å. This arises as a consequence of the strained nature of the four-membered heterocyclic ring which is evinced in the characteristically small bite angle, O(1)–Ru–O(2) 60.7(2)°, comparable to the value observed in *fac*-$[RuCl(O_2CMe)\{PPh[C_3H_6P(C_6H_{11})_2]_2\}]$,[37] 58.9(1)°, and in the 6-chloro-2-hydroxypyridinate compound $[Ru(\eta^3:\eta^3\text{-}C_{10}H_{16})Cl\{NC_5H_3(O)Cl\text{-}6\}]$,[23] 61.9(4)°. The large Cl–Ru–O(1) angle in complex **2**, 93.7(2)°, is also indicative of the strained nature of the chelate ring. The angles between axial and equatorial ligands normally fall in the region of *ca.* 85°[2,14–16] although a value of only 80.3(1)° has been observed by us for the thiocyanato-bridged complex $[\{Ru(\eta^3:\eta^3\text{-}C_{10}H_{16})Cl(\mu\text{-}SCN)\}_2]$.[17] The analogous unstrained angle in complex **3** is 87.4(1)°. Similarly, the endocyclic, O(1)–C(11)–O(2), angle is 118.0(8)° whereas the corresponding parameter in complex **3** is 127.7(5)°, again indicative of the fact that the acetate ligand is distorting significantly in order to chelate the small ruthenium(IV) centre.

This lengthening of the equatorial Ru–O bond in the chelate complex as a result of strain in the heterocyclic ring is almost certainly a contributory factor in the formation of aqua complexes as the donor ability of the carboxylato ligand decreases. The small size of the ruthenium(IV) centre exacerbates the effect, thus resulting in the observed differences in reactivity, compared to the analogous carboxylates of ruthenium(II).[20]

Conclusion

It has been demonstrated that the small size of the ruthenium(IV) centre, coupled with the inherently strained nature of four-membered heterocyclic rings acts to destabilise the formation of bidentate carboxylates containing the '$(\eta^3:\eta^3\text{-}C_{10}H_{16})Ru$' moiety, resulting in fluxionality and, ultimately, the formation of aqua species beyond a threshold in the electron withdrawing properties of the carboxylate substituent group. Notwithstanding this however the electron withdrawing ligand hexafluoroacetylacetonate forms a more stable six-membered chelate ring and shows no propensity for a monodentate mode of co-ordination, or fluxional behaviour in solution. The apparent strength and stability of the Ru^{IV}–OH_2 bond augers well for the potential synthesis of oxo species derived from aqua complexes[40–43] of ruthenium(IV) which may, given the unusual stereochemical requirements of the dimethyloctadienyl ligand, exhibit interesting selectivity in organic oxidations, and in the oxidative cleavage of DNA.[29]

Acknowledgements

We thank Johnson Matthey plc for generous loans of ruthenium trichloride and the SERC for a studentship (to J. W. S.) and for provision of the X-ray diffractometer.

References

1 L. Porri, M. C. Gallazzi, A. Colombo and G. Allegra, *Tetrahedron Lett.*, 1965, **47**, 4187.
2 A. Colombo and G. Allegra, *Acta Crystallogr., Sect. B*, 1971, **27**, 1653.
3 G. Winkhaus and H. Singer, *J. Organomet. Chem.*, 1967, **7**, 487.
4 M. A. Bennett and A. K. Smith, *J. Chem. Soc., Dalton Trans.*, 1974, 233.
5 H. LeBozec, D. Touchard and P. H. Dixneuf, *Adv. Organomet. Chem.*, 1989, **29**, 163.
6 R. A. Zelonka and M. C. Baird, *J. Organomet. Chem.*, 1972, **44**, 383.
7 M. A. Bennett, G. B. Robertson and A. K. Smith, *J. Organomet. Chem.*, 1972, **43**, C41.
8 R. O. Gould, T. A. Stephenson and D. A. Tocher, *J. Organomet. Chem.*, 1984, **263**, 375.
9 R. Aronson, M. R. J. Elsegood, J. W. Steed and D. A. Tocher, *Polyhedron*, 1991, **10**, 1727.
10 S. K. Mandal, A. R. Chakravarty, *J. Organomet. Chem.*, 1991, **417**, C59.
11 D. N. Cox, R. W. H. Small and R. Roulet, *J. Chem. Soc., Dalton Trans.*, 1991, 2013.
12 S. O. Sommerer and G. J. Palenik, *Organometallics*, 1991, **10**, 12203.
13 D. N. Cox and R. Roulet, *Inorg. Chem.*, 1990, **29**, 1360.
14 J. W. Steed and D. A. Tocher, *J. Organomet. Chem.*, 1991, **412**, C34.
15 J. G. Toerien and P. H. van Rooyen, *J. Chem. Soc., Dalton Trans.*, 1991, 1563.
16 J. G. Toerien and P. H. van Rooyen, *J. Chem. Soc., Dalton Trans.*, 1991, 2693.
17 J. W. Steed and D. A. Tocher, *J. Chem. Soc., Dalton Trans.*, 1992, 459.
18 J. W. Steed and D. A. Tocher, *Inorg. Chim. Acta*, 1992, **191**, 29.
19 R. A. Head, J. F. Nixon, J. R. Swain and C. M. Woodard, *J. Organomet. Chem.*, 1974, **76**, 393.
20 D. A. Tocher, R. O. Gould, T. A. Stephenson, M. A. Bennett, J. P. Ennett, T. W. Matheson, L. Sawyer and V. K. Shah, *J. Chem. Soc., Dalton Trans.*, 1983, 1571.
21 E. C. Morrison, C. A. Palmer and D. A. Tocher, *J. Organomet. Chem.*, 1988, **349**, 405.
22 J. W. Steed and D. A. Tocher, *Polyhedron*, 1992, **11**, 1849.
23 J. W. Steed and D. A. Tocher, *J. Chem. Soc., Dalton Trans.*, 1992, 2765.
24 J. W. Steed and D. A. Tocher, *Inorg. Chim. Acta*, 1991, **189**, 135.
25 A. C. Cope and E. R. Trumbull, in *Organic Reactions*, ed. A. C. Cope, Wiley, New York, 1960, vol. 11, ch. 5.
26 G. M. Sheldrick, SHELXTL PLUS, an integrated system for refining and displaying crystal structures from diffraction data, University of Göttingen, 1986.
27 G. B. Deacon and R. J. Phillips, *Coord. Chem. Rev.*, 1980, **33**, 227.

28 L. Porri, R. Rossi, P. Diversi and A. Lucherini, *Makromol. Chem.*, 1974, **175**, 3097.
29 J. W. Steed and D. A. Tocher, *J. Chem. Soc., Chem. Commun.*, 1991, 1609.
30 U. Kölle, G. Flunkert, R. Görissen, M. U. Schmidt and U. Englert, *Angew. Chem., Int. Ed. Engl.*, 1992, **31**, 440.
31 S. O. Sommerer, J. D. Baker, M. C. Zerner and G. J. Palenik, *Inorg. Chem.*, 1992, **31**, 563.
32 W. Frank and B. Bertsch-Frank, *Angew. Chem., Int. Ed. Engl.*, 1992, **31**, 436.
33 C. G. Swain and E. C. Lupton, *J. Am. Chem. Soc.*, 1968, **90**, 4328.
34 T. H. Lowry and K. S. Richardson, *Mechanism and Theory in Organic Chemistry*, 2nd edn., Harper and Row, New York, 1981 and refs. therein.
35 C. Hansch and A. J. Leo, *Substituent Constants for Correlation Analysis in Chemistry and Biology*, Wiley, New York, 1979.
36 E. P. Serjeant and B. Dempsey (Editors), *Ionisation Constants of Organic Acids in Aqueous Solution*, IUPAC, London, 1979.
37 G. Jia, A. L. Rheingold, B. S. Haggerty and D. W. Meek, *Inorg. Chem.*, 1992, **31**, 900.
38 M. R. Stevens, PhD Thesis, Australian National University, 1981.
39 C. J. Pouchert (Editor), *Aldrich Library of Infrared Spectra*, 3rd edn., 1981.
40 W. P. Griffith, *Transition Met. Chem.*, 1990, **15**, 251.
41 C.-K. Li, C.-M. Che, W.-F. Tong and T.-F. Lai, *J. Chem. Soc., Dalton Trans.*, 1992, 813.
42 C.-M. Che, W.-T. Tang, K.-Y. Wong and C.-K. Li, *J. Chem. Soc., Dalton Trans.*, 1991, 3277.
43 H. Nagao, M. Shibayama, Y. Kitanaka, F. S. Howell, K. Shimizu, M. Mukaida and H. Kakihana, *Inorg. Chim. Acta*, 1991, **185**, 75.

Received 29*th September* 1992; *Paper* 2/05246F

Journal of Organometallic Chemistry, 412 (1991) C37–C39
Elsevier Sequoia S.A., Lausanne
JOM 22018PC

Preliminary communication

Some reactions of $[(\eta^6\text{-}C_6Me_6)Ru(\eta^6\text{-}[2.2]paracyclophane)][BF_4]_2$ with nucleophiles

Jonathan W. Steed and Derek A. Tocher *

Department of Chemistry, University College London, 20 Gordon St., London WC1H 0AJ (UK)

(Received April 12th, 1991)

Abstract

Single addition of the nucleophiles X^- (X = H, CN, OH) to the less sterically hindered ring in $[(\eta^6\text{-}C_6Me_6)Ru(\eta^6\text{-}C_{16}H_{16})][BF_4]_2$ (**1**) proceeds smoothly to produce, as the sole product, $[(exo\text{-}\eta^5\text{-}C_6Me_6X)Ru(\eta^6\text{-}C_{16}H_{16})][BF_4]$. Use of $Na[BD_4]$ in place of $Na[BH_4]$ gives the expected shift in $\nu(C\text{–}H_{exo})$ in the infrared spectrum.

Nucleophilic addition to coordinated arenes is of significant interest as a synthetic route to arene functionalisation [1]. While bis(arene)ruthenium complexes are expected [2] to be around thirty times less electrophilic than their iron analogues they display a number of advantages which make them the more attractive alternative in this type of work. These advantages include, (a) the ready availability, via the Bennett [3] and Rybinskaya [4,5] syntheses, of unsymmetrical bis(arene)Ru complexes, and (b) the absence of interfering electron transfer reactions [6,7,8] which can occur on the addition of carbon donor nucleophiles and result in the formation and rapid decomposition of unstable nineteen and twenty electron species. Use of the highly sterically hindered [2.2]paracyclophane ligand has recently been shown to direct nucleophilic attack onto less hindered arenes coordinated to the same metal centre [9], to produce η^4-diene complexes such as $[(\eta^4\text{-}C_6Me_6H_2)Ru(\eta^6\text{-}C_{16}H_{16})]$. In addition, protonation of an η^4-[2.2]paracyclophane compound, $[(\eta^6\text{-}C_6Me_6)Ru(\eta^4\text{-}C_{16}H_{16})]$, gives a coordinated η^5-cyclophane, in $[(\eta^6\text{-}C_6Me_6)Ru(\eta^5\text{-}C_{16}H_{17})]^+$, with the added hydrogen atom in the *endo* position [9]. The reaction is believed to involve the initial formation of a metal hydride followed by proton transfer to the carbocyclic ring. We now report preliminary results of a study involving the use of the paracyclophane ligand to direct *single* nucleophilic attack onto a number of η^6-arenes. The question of *exo* or *endo* addition has been examined by a study of the effects of deuterium isotopic substitution on the solid state infrared spectra of the products.

The starting material $[(\eta^6\text{-}C_6Me_6)Ru(\eta^6\text{-}C_{16}H_{16})][BF_4]_2$ (**1**) was prepared by a published procedure [3,10–12]. Reaction of **1** with sodium borohydride in methanol at room temperature caused an immediate colour change to dark greenish brown.

0022-328X/91/$03.50

Subsequent extraction with dichloromethane and precipitation gave an air-stable, bright yellow product [(*exo*-η^5-C_6Me_6H)Ru(η^6-$C_{16}H_{16}$)][BF_4] (**2**) in ca. 50% yield. This compound is isomeric with that reported by Boekelheide et al. [9]. The ^1H NMR spectrum * of **2** clearly shows the expected quartet due to the incoming hydrogen at 2.00 ppm and a corresponding doublet for the adjacent methyl group (1.01 ppm, ^3J(H–H) 7.0 Hz). The infrared spectrum displays a band at 2813 cm^{-1} corresponding to ν(C–H_{exo}) and microanalytical data supports the proposed formulation. Interestingly **2** is not the product predicted by the rules proposed by Davies et al. [13], which suggest that a charge controlled attack at the less alkylated, i.e. paracyclophane, coordinated ring should occur. This result indicates that for this particular type of compound the nucleophilic addition reactions are sterically rather than electronically controlled. When OH^- and CN^- were used as nucleophiles analogous products were obtained, attack occurring solely at the hexamethylbenzene ring. As expected for a ruthenium compound no problems arising from competing electron transfer decomposition pathways were encountered when the carbon donor CN^- was used [6,7,8].

When sodium borodeuteride, $Na[BD_4]$, was used compounds with a deuteron added to the arene ring were obtained *. Studies of infrared isomer shifts can reveal whether attack has been *exo* or *endo*. The compound [(*exo*-η^5-C_6Me_6D)Ru(η^6-$C_{16}H_{16}$)][BF_4] (**3**) exhibits the expected differences in its infrared spectrum [14] compared with that of **2**. The absence of the band at 2813 cm^{-1} and appearance of a band at 2107 cm^{-1} indicate that nucleophilic addition is *exo*, an observation which is consistent with virtually all previous work on this type of system [13].

Although it might seem surprising that the $Na[BH_4]$ reduction of a dication gives a monocation rather than a neutral compound, there is a well established precedent for such a reaction in areneruthenium(II) chemistry [15], the reaction of $Na[BH_4]$ with [(η^6-$C_6H_3Me_3$)Ru(PMe_2Ph)(1,10-phen)][PF_6]$_2$ being known to give [(η^5-$C_6H_4Me_3$)Ru(PMe_2Ph)(1,10-phen)][PF_6]. In earlier studies [16] of the reduction of various [(η^6-arene)$_2$Ru]$^{2+}$ ions by $Na[BH_4]$ in anhydrous THF indicated that neutral arene-cyclohexadiene complexes were formed exclusively in high yield, but it was noted that the use of H_2O as a solvent led to the formation of small amounts of monocationic arene-cyclohexadienyl-ruthenium products [16]. In the light of this observation it seems likely that the choice of methanol as the solvent for these studies is responsible for the observation of single hydride attack, leading to the formation of the monocationic product.

We are carrying out further studies of nucleophilic addition to the compounds [(η^6-arene)M(η^6-[2.2]paracyclophane)]$^{2+}$, with a view to investigating further the factors governing the site of attack within the arene ring. Attempts are also in progress to observe attack by nucleophiles on the [2.2]paracyclophane ligands of [(η^6-$C_{16}H_{16}$)$_2$Ru]$^{2+}$.

* ^1H NMR data for [(*exo*-η^5-C_6Me_6H)Ru(η^6-$C_{16}H_{16}$)][BF_4] (400 MHz, $CDCl_3$, 298 K): δ 5.04 (s, 4H), 6.81 (s, 4H), 2.86 (m, 4H), 3.23 (m, 4H) ppm, η^6-$C_{16}H_{16}$; δ 1.01 (d, ^3J(H–H) 7.0 Hz, 3H), 1.34 (s, 6H), 1.87 (s, 6H), 2.28 (s, 3H), 2.00 (q, ^3J(H–H) 7.0 Hz, 1H) ppm, η^5-C_6Me_6H.
^1H NMR data for [(*exo*-η^5-C_6Me_6D)Ru(η^6-$C_{16}H_{16}$)][BF_4] (400 MHz, $CDCl_3$, 298 K): δ 5.10 (s, 4H), 6.83 (s, 4H), 2.88 (m, 4H), 3.26 (m, 4H) ppm, η^6-$C_{16}H_{16}$; δ 1.02 (s, 3H), 1.36 (s, 6H), 1.89 (s, 6H), 2.30 (s, 3H) ppm, η^5-C_6Me_6D.

Acknowledgement. We thank the SERC for financial support (J.W.S.) and Johnson Matthey PLC for generous loans of ruthenium trichloride.

References

1 C. Camaioni Neto and D.A. Sweigart, J. Chem. Soc., Chem. Commun., (1990) 1703 and references therein.
2 Y.K. Chung, E.D. Honig and D.A. Sweigart, J. Organomet. Chem., 256 (1983) 277.
3 M.A. Bennett and T.W. Matheson, J. Organomet. Chem., 175 (1979) 87.
4 M.I. Rybinskaya, A.R. Kudinov and V.S. Kaganovich, J. Organomet. Chem., 246 (1983) 279.
5 M.I. Rybinskaya, A.R. Kurdinov and V.S. Kaganovich, J. Organomet. Chem., 323 (1987) 111.
6 D. Astruc and P. Michaud, J. Am. Chem. Soc., 104 (1982) 3755.
7 T.S. Cameron, M.D. Clerk, A. Linden, K.C. Sturge and M.J. Zaworotko, Organometallics, 7 (1988) 2571.
8 D. Astruc and D. Mandon, J. Organomet. Chem., 369 (1989) 383.
9 R.T. Swann, A.W. Hanson, and V. Boekelheide, J. Am. Chem. Soc., 108 (1986) 3324.
10 E.D. Laganis, R.G. Finke and V. Boekelheide, Tetrahedron Lett., 21 (1980) 4405.
11 M.A. Bennett and A.K. Smith, J. Chem. Soc., Dalton Trans., (1974) 233.
12 M.A. Bennett, T.W. Matheson, G.B. Robertson, W.L. Steffen and T.W. Turney, J. Chem. Soc., Chem. Commun., (1979) 32.
13 S.G. Davies, M.L.H. Green and D.M.P. Mingos, Tetrahedron, 34 (1978) 3047.
14 R.P. Bauman, Absorption Spectroscopy, Wiley, New York, 1962, pp. 289 and 338.
15 D.R. Robertson, I.W. Robertson and T.A. Stephenson, J. Organomet. Chem., 202 (1980) 309.
16 M.I. Rybinskaya, V.S. Kaganovich and A.R. Kudinov, J. Organomet. Chem., 235 (1982) 215.

Reactions of (η^6-arene)(η^6-[2.2]paracyclophane)ruthenium(II) Complexes with Nucleophiles

Mark R. J. Elsegood, Jonathan W. Steed and Derek A. Tocher*
Department of Chemistry, University College London, 20 Gordon St., London WC1H 0AJ, UK

Single addition of the nucleophiles $X^- = H^-$, CN^- or OH^- to (η^6-arene)(η^6-[2.2]paracyclophane)-ruthenium(II) tetrafluoroborate (arene = benzene, *p*-cymene, 1,4-diisopropylbenzene or hexamethylbenzene) and the osmium(II) η^6-C_6H_6 analogue produces the (η^5-cyclohexadienyl)(η^6-[2.2]paracyclophane)metal(II) complexes as the sole products. These compounds have been identified by ^{1}H NMR and by infrared spectroscopy. The expected isotope shift is observed when $Na[BD_4]$ is used in place of $Na[BH_4]$. The steric factors influencing the site of nucleophilic attack are discussed and nucleophilic addition to $[Ru(\eta^6\text{-}C_{16}H_{16})_2][BF_4]_2$ is also examined.

Both single and double nucleophilic addition to co-ordinated arenes is of significant interest as a synthetic route to arene functionalisation[1] and a single nucleophilic attack is a key initial step in the recently reported synthesis of (±)-dihydroxyserrulatic acid.[2] While bis(arene)ruthenium complexes are expected[3] to be around thirty times less electrophilic than their iron analogues they display a number of advantages which make them the more attractive alternative in this type of work. These advantages include (*a*) the ready availability, *via* the Bennett[4] and Rybinskaya[5,6] syntheses, of unsymmetrical complexes and (*b*) the elimination of interfering electron-transfer reactions[7–9] which can occur on the addition of carbon-donor nucleophiles and result in the formation and often rapid decomposition of unstable nineteen- and twenty-electron species. Use of the highly sterically hindered [2.2]paracyclophane ligand has recently been shown to direct nucleophilic attack onto less-hindered arenes co-ordinated to the same metal centre[10] to produce η^4-diene complexes such as $[Ru(\eta^6\text{-}C_{16}H_{16})(\eta^4\text{-}C_6Me_6H_2)]$($C_6Me_6H_2$ = 1,2,3,4,5,6-hexamethylcyclohexa-1,4-diene). In addition, protonation of an η^4-[2.2]paracyclophane compound gives a co-ordinated η^5-cyclophane with the added hydrogen atom in the *endo* position.[10] That reaction is believed to involve the initial formation of a metal hydride followed by proton transfer to the carbocyclic ring. We now report the use of the [2.2]paracyclophane ligand to direct *single* nucleophilic attack onto a number of η^6-arenes and examine the question of *exo* or *endo* addition by a study of the effects of deuterium isotopic substitution on solid-state infrared and solution ^{1}H NMR spectra.

A preliminary report of part of this work has been published.[11]

Results and Discussion

Treatment of an almost colourless methanolic suspension of $[Ru(\eta^6\text{-}C_{16}H_{16})(\eta^6\text{-}C_6H_6)][BF_4]_2$ **1** with $Na[BH_4]$ gives a rapid darkening to deep green, possibly indicative of the formation of an intermediate charge-transfer complex.[7,9] Extraction of the reaction mixture with dichloromethane and precipitation gives the stable bright yellow cyclohexadienyl complex $[Ru(\eta^6\text{-}C_{16}H_{16})(\eta^5\text{-}C_6H_7)][BF_4]$ **2** in *ca.* 40% yield as the sole product (Scheme 1). A similar synthetic procedure utilising KCN gives the mildly air-sensitive complex $[Ru(\eta^6\text{-}C_{16}H_{16})(\eta^5\text{-}C_6H_6CN)][BF_4]$ **3**. Proton NMR data for these complexes are summarised in Table 1. The singlet resonance for the benzene ligand in the parent compound is replaced with one multiplet and three triplet resonances covering a wide chemical shift range (*e.g.* δ 6.20, 4.86, 3.33 and 2.32 for compound **2**)

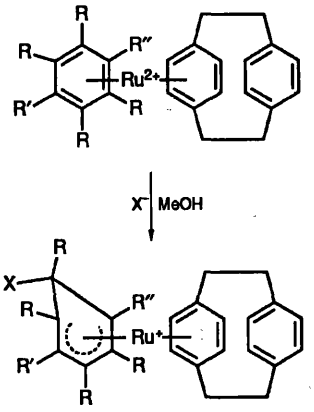

Scheme 1 Nucleophilic addition to (arene)([2.2]paracyclophane)-ruthenium(II) dications. R = H or Me; R′, R″ = H, Me or Pr^i; X = H, CN or OH

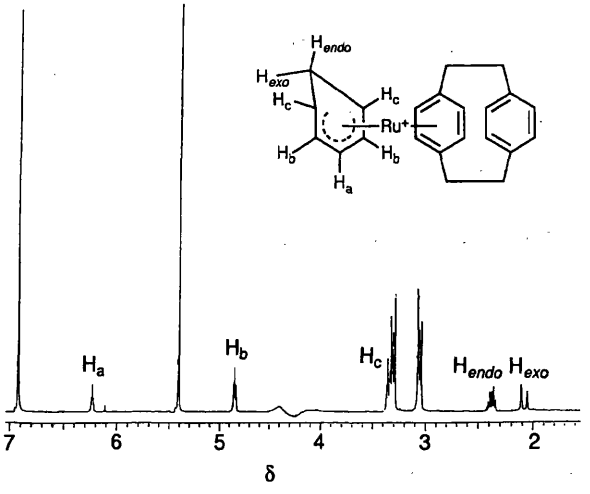

Fig. 1 Proton NMR spectrum of $[Ru(\eta^6\text{-}C_{16}H_{16})(\eta^5\text{-}C_6H_7)]^+$

consistent with previous observations[12] and indicative of the formation of a cyclohexadienyl complex. In addition a widely spaced doublet resonance ($^2J_{HH}$ = 13.5 Hz) is observed at δ 2.06 and is assigned to H_{exo} (Fig. 1). Vicinal coupling to H_c is not observed since the dihedral angle between the two protons H_c and H_{exo} is close to 90°. In the infrared spectrum **2** exhibits

Table 1 Proton NMR data for new compounds[a]

Compound	δ, J_{HH}/Hz		
	Cyclophane		
	Aromatic decks	Bridge	Cyclohexadienyl
2 $[Ru(\eta^6\text{-}C_{16}H_{16})(\eta^5\text{-}C_6H_7)][BF_4]$	6.84 (s, 4, H), 5.36 (s, 4 H)	3.26, 3.02 (AA'XX', 8 H)	6.20 (t, 1 H, ^3J = 5.1), 4.86 (t, 2 H, ^3J = 5.6), 3.33 (t, 2 H, ^3J = 6.6), 2.32 (m, 1 H), 2.06 (d, 1 H, ^2J = 13.5)
2' $[Ru(\eta^6\text{-}C_{16}H_{16})(\eta^5\text{-}C_6H_6D)][BF_4]$	6.84 (s, 4 H), 5.31 (s, 4 H)	3.29, 3.00 (AA'XX', 8 H)	6.21 (t, 1 H, ^3J = 5.2), 4.87 (t, 2 H, ^3J = 5.5), 3.35 (t, 2 H[b]), 2.29 (t, 1 H, ^3J = 5.4)
3 $[Ru(\eta^6\text{-}C_{16}H_{16})(\eta^5\text{-}C_6H_6CN)][BF_4]$[c]	6.84 (s, 4 H), 5.42 (s, 4 H)	3.23, 2.92 (AA'XX', 8 H)	6.30 (t, 1 H, ^3J = 4.9), 4.94 (t, 2 H, ^3J = 5.7), 3.47 (t, 2 H, ^3J = 6.3), 3.43 (q, 1 H, ^3J = 6.0)
4 $[Os(\eta^6\text{-}C_{16}H_{16})(\eta^5\text{-}C_6H_7)][BF_4]$	6.95 (s, 4 H), 5.57 (s, 4 H)	3.34, 2.97 (AA'XX', 8 H)	6.58 (t, 1 H, ^3J = 5.1), 5.19 (t, 2 H, ^3J = 5.4), 3.63 (t, 2 H, ^3J = 5.9), 3.58 (d, 1 H, ^2J = 12.4), 2.33 (m, 1 H)
6a $[Ru(\eta^6\text{-}C_{16}H_{16})(\eta^5\text{-}4\text{-}MeC_6H_5CHMe_2)][BF_4]$ Minor isomer	6.83 (s, 4 H), 5.54, 5.04 (AB, 4 H, ^3J = 6.7)	3.23 (m, 4 H), 2.94 (m, 2 H), 2.82 (m, 2 H)	6.05 (d, 1 H, ^3J = 4.6), 4.70 (d, 1 H[b]), 3.44 (d, 1 H[b]), 2.32 (dd, 1 H[b]), 2.08 (d, 1 H, ^2J = 13.2), 1.71 (s, 3 H), 1.65 (spt, 1 H, ^3J = 6.7), 0.90 (d, 3 H, ^3J = 6.8), 0.78 (d, 3 H, ^3J = 6.9)
6b $[Ru(\eta^6\text{-}C_{16}H_{16})(\eta^5\text{-}4\text{-}MeC_6H_5CHMe_2)][BF_4]$ Major isomer	6.84 (s, 4 H), 5.61, 5.02 (AB, 4 H, ^3J = 6.1)	3.23 (m, 4 H), 2.94 (m, 2 H), 2.82 (m, 2 H)	5.95 (d, 1 H, ^3J = 4.4), 4.71 (d, 1 H, ^3J = 4.8), 3.44 (d, 1 H, ^3J = 6.2), 2.34 (dd, 1 H, ^3J = 6.2, ^2J = 13.2), 2.24 (d, 1 H, ^2J = 13.2), 1.36 (s, 3 H), 1.88 (spt, 1 H, ^3J = 6.8), 0.97 (d, 3 H, ^3J = 7.1), 0.95 (d, 3 H, ^3J = 7.7)
$[Ru(\eta^6\text{-}C_{16}H_{16})(\eta^5\text{-}4\text{-}MeC_6H_5CHMe_2)][BPh_4]$[d] Minor isomer	6.67, 6.63 (AB, 4 H, ^3J = 7.1), 4.86, 4.28 (AB, 4 H, ^3J = 6.0)	3.13 (m, 4 H), 2.68 (m, 2 H), 2.55 (m, 2 H)	5.58 (d, 1 H, ^3J = 5.0), 4.28 (d, 1H[d]), 3.19 (br s, 1 H), 2.17 (m, 1 H), 2.02 (d, 1 H, ^2J = 13.1), 1.52 (s, 3 H), 1.46 (spt, 1 H, ^3J = 5.3), 0.85 (d, 3 H, ^3J = 7.0), 0.74 (d, 3 H, ^3J = 6.9)
$[Ru(\eta^6\text{-}C_{16}H_{16})(\eta^5\text{-}4\text{-}MeC_6H_5CHMe_2)][BPh_4]$[d] Major isomer	6.67, 6.63, (AB, 4 H, ^3J = 7.1), 4.90, 4.25 (AB, 4 H, ^3J = 5.7)	3.13 (m, 4 H), 2.68 (m, 2 H), 2.55 (m, 2 H)	5.64 (d, 1 H, ^3J = 5.4), 4.20 (d, 1 H, ^3J = 5.3), 3.19 (br s, 1 H), 2.17 (m, 1 H), 2.17 (d, 1 H, ^2J = 12.4), 1.71 (spt, 1 H, ^3J = 6.8), 1.19 (s, 3 H), 0.92 (dd, 3 H, ^3J = 3.7), 0.86 (m, 3 H)
6a' $[Ru(\eta^6\text{-}C_{16}H_{16})(\eta^5\text{-}4\text{-}MeC_6H_4DCHMe_2)][BF_4]$ Minor isomer	6.87 (s, 4 H), 5.63, 5.09 (AB, 4 H, ^3J = 5.8)	3.28 (m, 4 H), 2.90 (m, 2 H), 2.86 (m, 2 H)	6.13 (d, 1 H, ^3J = 5.0), 4.77 (d, 1 H, ^3J = 4.7), 3.36 (d, 1 H, ^3J = 6.7), 2.30 (d, 1 H, ^3J = 6.0), 1.76 (s, 3 H), 1.66 (spt, 1 H, ^3J = 6.5), 0.93 (d, 3 H, ^3J = 7.0), 0.81 (d, 3 H, ^3J = 6.9)
6b' $[Ru(\eta^6\text{-}C_{16}H_{16})(\eta^5\text{-}4\text{-}MeC_6H_4DCHMe_2)][BF_4]$ Major isomer	6.88 (s, 4 H), 5.70, 5.09 (AB, 4 H, ^3J = 5.8)	3.28 (m, 4 H), 2.90 (m, 2 H), 2.86 (m, 2 H),	6.01 (d, 1 H, ^3J = 4.7), 4.83 (d, 1 H, ^3J = 4.4), 3.36 (d, 1 H, ^3J = 8.9), 2.34 (d, 1 H, ^3J = 6.0), 1.91 (spt, 1 H, ^3J = 6.7), 1.41 (s, 3 H), 1.01 (d, 3 H, ^3J = 6.7), 0.98 (d, 3 H, ^3J = 6.6)
7a $[Ru(\eta^6\text{-}C_{16}H_{16})\{\eta^5\text{-}4\text{-}MeC_6H_4CHMe_2\text{-}(CN)\}][BF_4]$ Minor isomer	6.86 (s, 4 H), 5.82, 5.22 (AB, 4H[d])	3.26 (m, 4 H), 2.98 (m, 2 H), 2.84 (m, 2 H)	6.28 (d, 1 H, ^3J = 5.6), 5.01 (d, 1 H, ^3J = 5.4), 3.74 (d, 1 H[d]), 3.48 (d, 1 H, ^3J = 6.0), 1.85 (s, 3 H), 1.80 (m, 1 H), 1.01 (m, 6 H)
7b $[Ru(\eta^6\text{-}C_{16}H_{16})\{\eta^5\text{-}4\text{-}MeC_6H_4CHMe_2\text{-}(CN)\}][BF_4]$ Major isomer	6.86 (s, 4 H), 5.83, 5.22 (AB, 4 H, ^3J = 6.4)	3.26 (m, 4 H), 2.98 (m, 2 H), 2.84 (m, 2 H)	6.13 (d, 1 H, ^3J = 5.5), 4.91 (d, 1 H, ^3J = 5.4), 3.70 (d, 1 H, ^3J = 6.2), 3.54 (d, 1 H, ^3J = 6.2), 2.01 (spt, 1 H, ^3J = 6.8), 1.52 (s, 3 H), 1.05 (d, 3 H, ^3J = 6.9), 1.04 (d, 3 H, ^3J = 6.9)
8 $[Ru(\eta^6\text{-}C_{16}H_{16})\{\eta^5\text{-}1,4\text{-}(Me_2CH)_2C_6H_5\}][BF_4]$	6.82 (s, 4 H), 5.59, 5.04 (AB, 4 H, ^3J = 6.3)	3.24 (m, 4 H), 2.96 (m, 2 H), 2.82 (m, 2 H)	6.05 (d, 1 H, ^3J = 5.1), 4.78 (d, 1 H, ^3J = 5.1), 3.38 (d, 1 H, ^3J = 6.5), 2.36 (dd, 1 H, ^3J = 6.5, ^2J = 13.4), 2.10 (d, 1 H, ^2J = 13.4), 1.92 (spt, 1 H, ^3J = 6.7), 1.68 (spt, 1 H, ^3J = 6.7), 1.04 (d, 3 H, ^3J = 6.8), 0.94 (d, 3 H, ^3J = 6.7), 0.92 (d, 3 H, ^3J = 6.7), 0.80 (d, 3 H, ^3J = 6.7)
10 $[Ru(\eta^6\text{-}C_{16}H_{16})(\eta^5\text{-}C_6Me_6H)][BF_4]$	6.81 (s, 4 H), 5.04 (s, 4 H)	3.23, 2.86 (AA'XX', 8 H)	2.28 (s, 3 H), 2.00 (q, 1 H, ^3J = 6.7), 1.87 (s, 6 H), 1.34 (s, 6 H), 1.01 (d, 3 H, ^3J = 7.0)
10' $[Ru(\eta^6\text{-}C_{16}H_{16})(\eta^5\text{-}C_6Me_6D)][BF_4]$	6.83 (s, 4 H), 5.10 (s, 4 H)	3.26, 2.88 (AA'XX', 8 H)	2.30 (s, 3 H), 1.89 (s, 6 H), 1.36 (s, 6 H), 1.02 (s, 3 H)
11 $[Ru(\eta^6\text{-}C_{16}H_{16})(\eta^5\text{-}C_6Me_6CN)][BF_4]$	6.87 (s, 4 H), 5.30 (s, 4 H)	3.30, 2.90 (AA'XX', 8 H)	2.37 (s, 3 H), 2.01 (s, 6 H), 1.50 (s, 6 H), 1.46 (s, 3 H)
12 $[Ru(\eta^6\text{-}C_{16}H_{16})(\eta^5\text{-}C_6Me_6OH)][BF_4]$	6.84 (s, 4 H), 5.10 (s, 4 H)	3.24, 2.88 (AA'XX', 8 H)	3.72 (s, 3 H), 2.23 (s, 3 H), 1.99 (s, 6 H), 1.76 (s, 6 H)

Table 1 (*Continued*)

Compound	δ, J_{HH}/Hz		
	Cyclophane		
	Aromatic decks	Bridge	Cyclohexadienyl
14 $[Ru(\eta^6\text{-}C_{16}H_{16})(\eta^5\text{-}C_{16}H_{17})][BF_4]$	6.80 (s, 4 H), 5.14 (s, 4 H)	3.28, 2.92 (AA'XX', 8 H)	(Unco-ordinated ring H) 7.17, 6.95 (AB, 4 H, ^3J = 8.1) (Co-ordinated ring H) 4.33 (d, 2 H, ^3J = 7.3), 3.10 (t, 2 H, ^3J = 7.8) (Bridge) 3.22 (m, 2 H), 2.53 (t, 2 H, ^3J = 6.4), 2.45 (t, 2 H, ^3J = 7.4), 1.78 (t, 2 H, ^3J = 6.7) (Nucleophile) 3.28 (m, 1 H)

[a] In $CDCl_3$. s = Singlet, d = doublet, t = triplet, q = quartet, spt = septet and br = broad. [b] Coupling masked by overlapping signals from major isomer. [c] Solvent CD_3CN. [d] $[BPh_4]$: δ 6.99 (t, ^3J = 7.1, 4 H), 7.13 (t, ^3J = 7.6 Hz, 8 H) and 7.49 (br s, 8 H).

Table 2 Carbon-13 NMR data for selected compounds in $CDCl_3$

Compound	δ				
	Aryl C	Bridgehead	CH_2	Cyclohexadienyl	CN
3 $[Ru(\eta^6\text{-}C_{16}H_{16})(\eta^5\text{-}C_6H_6CN)][BF_4]$	133.9 87.7	139.8 127.5	34.0 32.1	89.5, 84.6, 32.8, 26.4	119.3
10 $[Ru(\eta^6\text{-}C_{16}H_{16})(\eta^5\text{-}C_6Me_6H)][BF_4]$	133.6 88.0	139.2 124.5	34.2 31.8	101.7, 100.5, 52.7, 38.4, 29.7, 18.1, 16.5, 16.0	
11* $[Ru(\eta^6\text{-}C_{16}H_{16})(\eta^5\text{-}C_6Me_6CN)][BF_4]$	133.8 89.3	139.1 126.6	34.1 31.7	99.9, 49.9, 21.1, 21.0, 17.0, 16.9	120.6

* Solvent CD_3CN.

Table 3 Deuterium isotope shifts of $\nu(CH_{exo})$

Compound	$\nu(C\text{–}H_{exo})$/cm^{-1}	
	X = H	X = D
$[Ru(\eta^6\text{-}C_{16}H_{16})(\eta^5\text{-}C_6H_6X)][BF_4]$	2813	2113
$[Ru(\eta^6\text{-}C_{16}H_{16})(\eta^5\text{-}C_6Me_6X)][BF_4]$	2813	2107
$[Ru(\eta^6\text{-}C_{16}H_{16})(\eta^5\text{-}4\text{-}MeC_6H_4XCHMe_2)][BF_4]$*	2804	2129

* Signals for individual isomers unresolved.

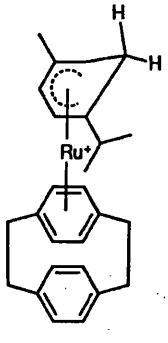

6a

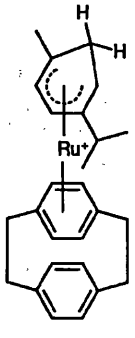

6b

strong bands at 2926 and 2813 cm^{-1} which may be assigned as $\nu(CH_{endo})$ and $\nu(CH_{exo})$ respectively.[10,13] A similar band is observed in the infrared spectrum of **3** at 2923 cm^{-1} but there are no bands in the ν(CH) region below 2850 cm^{-1}. The ^{13}C NMR spectrum of **3** (Table 2) displays a peak at δ 119.3 which is assigned as the resonance corresponding to the CN carbon atom. Treatment of **1** with $Na[BD_4]$ gives a product with a very similar ^1H NMR spectrum to **2** except for the absence of the doublet resonance at δ *ca.* 2. The infrared spectrum of this material displays $\nu(CH_{endo})$ at 2925 cm^{-1} but the band observed at 2813 cm^{-1} for **2** occurs at 2113 cm^{-1}, a typical deuterium isotope shift.[13,14] The reaction of $Na[BH_4]$ with $[Os(\eta^6\text{-}C_{16}H_{16})(\eta^6\text{-}C_6H_6)][BF_4]_2$[15] proceeds cleanly to give the analogous product $[Os(\eta^6\text{-}C_{16}H_{16})(\eta^5\text{-}C_6H_7)][BF_4]$ **4**, with no obvious decrease in rate in spite of the presumed lower electrophilicity of the osmium complex.[2] These results clearly indicate a single nucleophilic attack on the less-alkylated ring, to give a monocationic product with the added nucleophile in the *exo* position, an observation consistent with the rules of Davies *et al.*[16]

The action of $Na[BH_4]$ on the *p*-cymene complex $[Ru(\eta^6\text{-}C_{16}H_{16})(\eta^6\text{-}4\text{-}MeC_6H_4CHMe_2)][BF_4]_2$ **5**, however, gives two products, of the same empirical formula, in an approximate ratio of 5:2, which may be distinguished by their ^1H NMR spectra (Table 1). The infrared spectrum of these materials shows $\nu(CH_{endo})$ 2928 cm^{-1} and $\nu(CH_{exo})$ 2804 cm^{-1}. The two complexes were not separated but extensive decoupling experiments on the ^1H NMR spectrum of the mixture leads us to formulate these compounds as the two isomeric structures **6a** and **6b**. The major isomer, from the relative intensities in the ^1H NMR spectrum of the resonances due to the substituents on the cyclohexadienyl ring, is assigned the structure **6b**, with nucleophilic attack occurring at the site *ortho* to the methyl (as opposed to isopropyl) substituent.

An interesting feature of the ^1H NMR spectra of compounds **6a** and **6b** is that in each case the resonances corresponding to the four co-ordinated ring protons of the [2.2]paracyclophane ligand are not singlets as has been previously observed for metal–[2.2]paracyclophane complexes[10,15] but form a widely spaced AB pattern (δ 5.02 and 5.61 for the major isomer). The reason for this would appear to be the sensitivity of the [2.2]paracyclophane ligand to chirality at the metal centre[17] caused, for example, by the presence of three different ligands in addition to the cyclophane, co-ordinated to the ruthenium.

Recently it has been noted[18] that the presence of two different *ortho*-related substituents on a six-membered co-ordinated ring causes the formation of a chiral centre and is thus capable of rendering the cyclophane aromatic protons magnetically inequivalent in spite of the rapid rotation of the ligand. In these particular cases, **6a** and **6b**, either the isopropyl or methyl group is *ortho* to the attack site. In effect the alkyl substituent and the tetrahedral CH_2 group may be regarded as two very different ring sites and hence, due to the chirality when co-ordinated to a metal centre, cause a large splitting of the cyclophane resonances, as has been observed in other [2.2]-paracyclophane systems.[15]

The tetraphenylborate salts of these compounds were also prepared and their ^1H NMR spectra recorded. Surprisingly, while the general form of the spectrum remained the same, the coupling patterns were significantly more complex than those observed for the corresponding tetrafluoroborate salts. This is probably due to specific cation–anion interactions but the precise nature of the effects is unknown. The changes are consistent with those which occur on changing to a $[BPh_4]^-$ counter ion[15] in related chiral systems.

The reaction of compound **5** with KCN was also investigated and analogous products $[Ru(\eta^6\text{-}C_{16}H_{16})\{\eta^5\text{-}4\text{-}MeC_6H_4\text{-}CHMe_2(CN)\}][BF_4]$, **7a** and **7b**, obtained in a similar isomer ratio, the most favourable site of attack again being the one *ortho* to the smaller (methyl) substituent. A steric dependence in the formation of isomers of this kind has also been observed in nucleophilic addition to cations of the type $[Mn(\eta^6\text{-}4\text{-}Me\text{-}C_6H_4X)(CO)_3]^+$. The larger the substituent, X, the more nucleophilic attack is favoured *ortho* to the methyl group.[19] Parallel studies employing $Na[BD_4]$ gave the expected isotope shift, with $\nu(CD_{exo})$ appearing at 2129 cm^{-1}, confirming *exo* addition. The results of the deuteriation studies are summarised in Table 3.

The proposed structures for compounds **6a** and **6b** were further confirmed by an examination of the action of $Na[BH_4]$ on the 1,4-diisopropylbenzene derivative $[Ru(\eta^6\text{-}C_{16}H_{16})\{\eta^6\text{-}1,4\text{-}(Me_2CH)_2C_6H_4\}][BF_4]_2$ which was synthesised from 1,4-diisopropylbenzene and $[Ru(\eta^6\text{-}C_{16}H_{16})(OCMe_2)_3][BF_4]_2$ using the general method reported by Boekelheide and co-workers.[10] The product of this reaction, $[Ru(\eta^6\text{-}C_{16}H_{16})\{\eta^5\text{-}1,4\text{-}(Me_2CH)_2C_6H_5\}][BF_4]$ **8**, took the form of a single isomer and exhibited a ^1H NMR spectrum consistent with the expected single addition of hydride to the diisopropylbenzene ring. As in the case of **6a**,**6b** and **7a**,**7b** the proton resonances for the co-ordinated cyclophane deck took the form of an AB pattern (δ 5.04 and 5.59, ^3J = 6.3 Hz) indicating the presence of two different *ortho*-related substituents on the cyclohexadienyl ring, and the four methyl groups of the isopropyl substituents occurred as four separate doublet resonances (δ 1.04, 0.94, 0.92 and 0.80) indicating a unique environment for each substituent.

The reaction of $[Ru(\eta^6\text{-}C_{16}H_{16})(\eta^6\text{-}C_6Me_6)][BF_4]_2$ **9** with H^-, CN^- or OH^- under the conditions described above results in isolation of compounds of formulation $[Ru(\eta^6\text{-}C_{16}H_{16})(\eta^5\text{-}C_6Me_6X)][BF_4]$ (X = H **10**, CN **11** or OH **12**). Compound **10** displays a band in the infrared spectrum at $\nu(CH_{exo})$ 2813 cm^{-1}, which appears at 2107 cm^{-1} for the deuteriated analogue. This band is absent in the spectra of both **11** and **12**. The ^1H NMR spectrum of **10** (Table 1) clearly shows a quartet resonance (^3J = 6.7 Hz) for the added hydride (δ 2.00) and a corresponding methyl doublet at δ 1.01. The ^{13}C NMR spectrum of **11** displays a resonance at δ 120.6 corresponding to the CN carbon atom. For kinetically controlled reactions the rules of Davies *et al.*[16] predict attack at the less-alkylated ring (*i.e.* [2.2]paracyclophane), yet this is clearly not the case in this instance. This may be readily rationalised in terms of (*i*) the steric bulk of the [2.2]paracyclophane ligand, the unco-ordinated aromatic deck shielding the *exo* attack sites on the co-ordinated ring, and (*ii*) the deactivation of the co-ordinated deck of the cyclophane *via* π overlap with the unco-ordinated ring; interannular interactions within [2$_n$]cyclophanes are a well known phenomenon.[20–22]

Reduction of compound **9** with aluminium metal followed by protonation with HCl has been observed[10] to produce an isomer of **10** containing an η^5-cyclophane with the added proton in the *endo* position. In an attempt to examine the relative importance of the potential attack sites within the [2.2]paracyclophane ligand itself the action of $Na[BH_4]$ on $[Ru(\eta^6\text{-}C_{16}H_{16})_2][BF_4]_2$ **13** was examined. The reaction is not a clean one and proceeds with much decomposition and we were unable to isolate any pure product. However crude samples showed ^1H NMR spectra (Table 1) related to those observed by Boekelheide and co-workers,[10] consistent with a single *endo* addition of hydride to the more-alkylated bridgehead site of one of the co-ordinated aromatic decks to give a product $[Ru(\eta^6\text{-}C_{16}H_{16})(\eta^5\text{-}C_{16}H_{17})][BF_4]$ **14**. We would expect an *exo* attack at a non-bridgehead site, by the rules of Davies *et al.*[16] The reason for this surprising reactivity might well lie in the geometry of the co-ordinated cyclophane ligand which, in contrast to conventional η^6-arenes, is bent into a shallow boat conformation, the distortion being some 13° in the free ligand,[23] although this is reduced somewhat on co-ordination.[14] This results in the relevant molecular orbitals on the bridgehead atoms pointing outwards away from the metal ion and so an *endo* attack pathway could be less sterically unfavourable than in planar systems, especially since *exo* attack pathways are all blocked by the unco-ordinated deck of the [2.2]paracyclophane ligand.

Although it may seem surprising that reaction of $Na[BH_4]$ with these dications give monocationic, rather than a neutral, species, there is a well established precedent for such a reaction in (arene)ruthenium(II) chemistry,[24] where treatment of the mesitylene complex $[Ru(\eta^6\text{-}C_6H_3Me_3\text{-}1,3,5)(PMe_2Ph)(phen)][PF_6]_2$ (phen = 1,10-phenanthroline) with $Na[BH_4]$ in methanol gives $[Ru(\eta^5\text{-}C_6H_4Me_3)(PMe_2Ph)(phen)][PF_6]$. Similarly $[Fe(\eta^6\text{-}C_6H_3Me_3\text{-}1,3,5)_2]^{2+}$ reacts with KCN in acetone to form $[Fe(\eta^6\text{-}C_6H_3Me_3\text{-}1,3,5)\{\eta^5\text{-}C_6H_3Me_3\text{-}(CN)\}]^+$.[25] Conversely, reactions of various $[Ru(\eta^6\text{-arene})_2]^{2+}$ ions with $Na[BH_4]$ in anhydrous tetrahydrofuran (thf) are consistent with the exclusive formation of neutral arene–cyclohexadiene complexes in high yield although it was noted that in water low yields of monocationic arene–cyclohexadienyl complexes were obtained.[26] It has also been noted that reaction of $[Fe(\eta^6\text{-}C_6Me_6)_2]^{2+}$ with LiMe will give both η^5 and η^4 products, depending upon the precise reaction conditions employed.[27] Hence it seems likely that the choice of methanol as a solvent for this study is responsible for the observation of only single hydride attack, leading to the formation of monocationic products.

We intend to carry out further studies into nucleophilic attack on co-ordinated [2,2]paracyclophane and related ligands as well as on the more highly charged bi- and tri-nuclear 'cylinder complexes' in which both decks of the cyclophane ligands are complexed.[10,28]

Experimental

Instrumental.—The IR spectra were recorded on a PE983 grating spectrometer between 4000 and 200 cm^{-1} as either KBr disks or Nujol mulls on CsI plates, NMR spectra on either Varian XL200 or VXR400 spectrometers. Microanalyses were carried out by the departmental service at University College London. All manipulations were carried out under nitrogen with degassed solvents using conventional Schlenk-line techniques.

Starting Materials.—The compounds $[M(\eta^6\text{-}C_{16}H_{16})(\eta^6\text{-arene})][BF_4]_2$ (M = Ru or Os) were prepared by published literature methods[4,28–30] or simple modifications thereof. Ruthenium trichloride hydrate and sodium hexachloroosmate were obtained on loan from Johnson Matthey plc and all other

reagents and materials were obtained from the usual commercial sources.

Preparations.—$[Ru(\eta^6\text{-}C_{16}H_{16})(\eta^5\text{-}C_6H_7)][BF_4]$ **2**. The compound $[Ru(\eta^6\text{-}C_{16}H_{16})(\eta^6\text{-}C_6H_6)][BF_4]_2$ (0.107 g, 0.191 mmol) was suspended in methanol (5 cm^3) and to the stirred mixture excess of $Na[BH_4]$ (0.05 g) was gradually added over 15 min during which time a rapid colour change from yellow to deep green was observed. Water (5 cm^3) was added to destroy any remaining $Na[BH_4]$ and the mixture was extracted with one aliquot of dichloromethane (20 cm^3). The separated organic layer was dried over magnesium sulfate, filtered and evaporated to dryness. The residue was recrystallised from acetone, isolated by filtration and washed with a few drops of acetone and diethyl ether to give a pale yellow product. Yield 0.037 g, 41% (Found: C, 55.10; H, 4.35. Calc. for $C_{22}H_{23}BF_4Ru$: C, 55.60; H, 4.90%).

$[Ru(\eta^6\text{-}C_{16}H_{16})(\eta^5\text{-}C_6H_6CN)][BF_4]$ **3**. The compound $[Ru(\eta^6\text{-}C_{16}H_{16})(\eta^6\text{-}C_6H_6)][BF_4]_2$ (0.098 g, 0.175 mmol) was suspended in methanol (5 cm^3) and KCN (0.012 g, 0.184 mmol) added. The mixture was stirred for 15 min until a bright yellow solution was obtained. The mixture was filtered and diethyl ether added to give a pale yellow precipitate. This was filtered off and the residue dissolved in dichloromethane (5 cm^3). After further filtration the solution was evaporated to dryness to give a bright yellow product. Yield 0.054 g, 65% (Found: C, 54.85; H, 4.70; N, 2.40. Calc. for $C_{23}H_{22}BF_4NRu$: C, 55.20; H, 4.45; N, 2.80%).

$[Os(\eta^6\text{-}C_{16}H_{16})(\eta^6\text{-}C_6H_7)][BF_4]$ **4**. Using an analogous method to that for compound **2**, $[Os(\eta^6\text{-}C_{16}H_{16})(\eta^6\text{-}C_6H_6)][BF_4]_2$ (0.068 g, 0.105 mmol) was treated with $Na[BH_4]$ to give an off-white solid. Yield 0.028 g, 48% (Found: C, 46.85; H, 3.85. Calc. for $C_{22}H_{23}BF_4Os$: C, 46.80; H, 4.10%).

$[Ru(\eta^6\text{-}C_{16}H_{16})(\eta^5\text{-}C_6Me_6H)][BF_4]$ **10**. Using an analogous method to that for compound **2**, $[Ru(\eta^6\text{-}C_{16}H_{16})(\eta^6\text{-}C_6Me_6)][BF_4]_2$ (0.102 g, 0.159 mmol) was treated with $Na[BH_4]$ to give a yellow solid. Yield 0.036 g, 41% (Found: C, 59.95; H, 6.10. Calc. for $C_{28}H_{35}BF_4Ru$: C, 60.10; H, 6.30%).

$[Ru(\eta^6\text{-}C_{16}H_{16})(\eta^5\text{-}4\text{-}MeC_6H_5CHMe_2)][BF_4]$ **6a** *and* **6b**. Using an analogous method to that for compound **2**, $[Ru(\eta^6\text{-}C_{16}H_{16})(\eta^6\text{-}4\text{-}MeC_6H_4CHMe_2)][BF_4]_2$ (0.137 g, 0.223 mmol) was treated with $Na[BH_4]$ to give a yellow solid containing two isomers, **6a**:**6b** 2:5 (NMR evidence). Yield 0.069 g, 59% (Found: C, 58.95; H, 5.80. Calc. for $C_{26}H_{31}BF_4Ru$: C, 58.80; H, 5.90%).

$[Ru(\eta^6\text{-}C_{16}H_{16})(\eta^5\text{-}4\text{-}MeC_6H_5CHMe_2)][BPh_4]$. To a solution of compound **6** (0.074 g, 0.139 mmol) in methanol (3 cm^3) was added a solution containing an excess of sodium tetraphenylborate (0.1 g) in methanol (3 cm^3). The yellow product was filtered off, washed with methanol and diethyl ether, and air dried. Yield 0.100 g, 94% (Found: C, 78.40; H, 6.75. Calc. for $C_{50}H_{51}BRu$: C, 78.60; H, 6.70%).

$[Ru(\eta^6\text{-}C_{16}H_{16})(\eta^5\text{-}C_6Me_6CN)][BF_4]$ **11**. The compound $[Ru(\eta^6\text{-}C_{16}H_{16})(\eta^6\text{-}C_6Me_6)][BF_4]_2$ (0.099 g, 0.154 mmol) was suspended in methanol (5 cm^3) and KCN (0.0133 g, 0.204 mmol) added. The mixture was stirred for 15 min until a bright yellow solution was obtained. It was filtered and diethyl ether added to precipitate a pale yellow solid. The solid was filtered off and then extracted with dichloromethane (5 cm^3). Filtration of this solution followed by evaporation gave a bright yellow product. Yield 0.030 g, 34% (Found: C, 59.65; H, 6.05; N, 2.70. Calc. for $C_{29}H_{34}BF_4Ru$: C, 59.60; H, 5.85; N, 2.40%).

$[Ru(\eta^6\text{-}C_{16}H_{16})(\eta^5\text{-}4\text{-}MeC_6H_4CHMe_2CN)][BF_4]$ **7a** *and* **7b**. Using the method described for compound **11**, $[Ru(\eta^6\text{-}C_{16}H_{16})(\eta^6\text{-}4\text{-}MeC_6H_4CHMe_2)][BF_4]_2$ (0.136 g, 0.221 mmol) was treated with KCN to give an off-white product consisting of two isomers **7a**:**7b** 2:5 (NMR evidence). Yield 0.067 g, 54% (Found: C, 57.75; H, 5.30; N, 2.50. Calc. for $C_{27}H_{30}BF_4NRu$: C, 58.30; H, 5.45; N, 2.50%).

$[Ru(\eta^6\text{-}C_{16}H_{16})\{\eta^5\text{-}1,4\text{-}(Me_2CH)_2C_6H_5\}][BF_4]$ **8**. Using a similar method to that described for compound **2**, $[Ru(\eta^6\text{-}C_{16}H_{16})\{\eta^6\text{-}1,4\text{-}(Me_2CH)_2C_6H_4\}][BF_4]_2$ (0.345 g, 0.0535 mmol) was treated with $Na[BH_4]$ to give a yellow solid. Yield 0.072 g, 24% (Found: C, 60.30; H, 6.25. Calc. for $C_{28}H_{35}BF_4Ru$: C, 60.10; H, 6.30%).

$[Ru(\eta^6\text{-}C_{16}H_{16})(\eta^5\text{-}C_6Me_6OH)][BF_4]$ **12**. Using a similar method to that described for compound **11**, $[Ru(\eta^6\text{-}C_{16}H_{16})(\eta^6\text{-}C_6Me_6)][BF_4]_2$ (0.053 g, 0.0821 mmol) was treated with sodium hydroxide (0.001 g, 0.125 mmol) to give an orange product. Yield 0.022 g, 47% (Found: C, 59.15; H, 6.00. Calc. for $C_{28}H_{35}BF_4ORu$: C, 58.45; H, 6.15%).

The deuterides of compounds **2**, **6** and **10** were prepared in an identical fashion to their undeuteriated counterparts substituting $Na[BD_4]$ for $Na[BH_4]$ (Found: C, 55.50; H, 5.00. Calc. for $C_{22}H_{22}BDF_4Ru$ **2'**: C, 55.50; H, 5.10. Found: C, 59.70; H, 6.00. Calc. for $C_{26}H_{30}BDF_4Ru$ **6'**: C, 60.00; H, 6.50. Found: C, 58.60; H, 5.85. Calc. for $C_{28}H_{34}BDF_4Ru$ **10'**: C, 58.65; H, 6.05%).

Acknowledgements

We thank the SERC for financial support (to M. R. J. E. and J. W. S.) and Johnson Matthey plc for generous loans of ruthenium trichloride.

References

1 C. Camaioni Neto and D. A. Sweigart, *J. Chem. Soc., Chem. Commun.*, 1990, 1703 and refs. therein.
2 M. Uemura, H. Nishimura, T. Minami and Y. Hayashi, *J. Am. Chem. Soc.*, 1991, **113**, 5402.
3 Y. K. Chung, E. D. Honig and D. A. Sweigart, *J. Organomet. Chem.*, 1983, **256**, 277.
4 M. A. Bennett and T. W. Matheson, *J. Organomet. Chem.*, 1979, **175**, 87.
5 M. I. Rybinskaya, A. R. Kurdinov and V. S. Kaganovich, *J. Organomet. Chem.*, 1983, **246**, 279.
6 M. I. Rybinskaya, A. R. Kurdinov and V. S. Kaganovich, *J. Organomet. Chem.*, 1987, **323**, 111.
7 D. Astruc and P. Michaud, *J. Am. Chem. Soc.*, 1982, **104**, 3755.
8 T. S. Cameron, M. D. Clerk, A. Linden, K. C. Sturge and M. J. Zaworotko, *Organometallics*, 1988, **7**, 2571.
9 D. Astruc and D. Mandon, *J. Organomet. Chem.*, 1989, **369**, 383.
10 R. T. Swann, A. W. Hanson and V. Boekelheide, *J. Am. Chem. Soc.*, 1986, **108**, 3324.
11 J. W. Steed and D. A. Tocher, *J. Organomet. Chem.*, 1991, **412**, C37.
12 N. A. Vol'kenau, I. N. Bolesova, L. S. Shul'pina and A. N. Kitaigorodskii, *J. Organomet. Chem.*, 1984, **267**, 313.
13 G. Winkaus, L. Pratt and G. Wilkinson, *J. Chem. Soc.*, 1961, 3807.
14 R. P. Bauman, *Absorption Spectroscopy*, Wiley, New York, 1962, pp. 289 and 338.
15 M. R. J. Elsegood and D. A. Tocher, *J. Organomet. Chem.*, 1990, **391**, 239.
16 S. G. Davies, M. L. H. Green and D. M. P. Mingos, *Tetrahedron*, 1978, **34**, 3047.
17 M. R. J. Elsegood, Ph.D. Thesis, University College London, 1991.
18 P. Pertici, P. Salvadori, A. Biasci, G. Vitulli, M. A. Bennett and L. A. P. Kane-Maguire, *J. Chem. Soc., Dalton Trans.*, 1988, 315.
19 P. L. Pauson and J. A. Segal, *J. Chem. Soc., Dalton Trans.*, 1975, 1683.
20 D. J. Cram and H. Steinberg, *J. Am. Chem. Soc.*, 1951, **73**, 5691.
21 B. Kovač, M. Mohraz, E. Heilbronner, V. Boekelheide and H. Hopf, *J. Am. Chem. Soc.*, 1980, **102**, 4314.
22 S. Canuto and M. C. Zerner, *J. Am. Chem. Soc.*, 1990, **112**, 2114.
23 C. J. Brown and A. C. Farthing, *Nature (London)*, 1949, **164**, 915.
24 D. R. Robertson, I. W. Robertson and T. A. Stephenson, *J. Organomet. Chem.*, 1980, **202**, 309.
25 J. F. Helling and G. G. Cash, *J. Organomet. Chem.*, 1974, **73**, C10.
26 M. I. Rybinskaya, V. S. Kaganovitch and A. R. Kurdinov, *J. Organomet. Chem.*, 1982, **235**, 215.
27 D. Mandon and D. Astruc, *J. Organomet. Chem.*, 1989, **369**, 383.
28 E. D. Laganis, R. G. Finke and V. Boekelheide, *Tetrahedron Lett.*, 1980, **21**, 4405.
29 M. A. Bennett and A. K. Smith, *J. Chem. Soc., Dalton Trans.*, 1974, 233.
30 M. A. Bennett, T. W. Matheson, G. B. Robertson, W. L. Steffen and T. W. Turney, *J. Chem. Soc., Chem. Commun.*, 1979, 32.

Received 14*th January* 1992; *Paper* 2/00201I

Journal of Organometallic Chemistry, 444 (1993) C47–C50

JOM 23291PC

Preliminary Communication

Cyclohexenyl [2.2]paracyclophane complexes of ruthenium(II): highly fluxional agostics from the sequential reduction of arenes

Jonathan W. Steed and Derek A. Tocher

Department of Chemistry, University College London, 20 Gordon Street, London WC1H 0AJ (UK)

(Received September 3, 1992)

Abstract

Reduction of the (arene)(paracyclophane)ruthenium(II) complex $[Ru(\eta^6\text{-}C_6Me_6)(\eta^6\text{-}C_{16}H_{16})][BF_4]_2$ (**1b**) with $Na[BH_4]$ gives in contrast to the analogous Red–Al reduction a mixture of ruthenium(0) diene products, chiefly the 1,3-diene complex $[Ru(\eta^4\text{-}1,3\text{-}C_6Me_6H_2)(\eta^6\text{-}C_{16}H_{16})]$ (**2c**). Complex **2c** reacts with aqueous $H[BF_4]$ to generate the agostic species $[Ru(\eta^3\text{-}C_6Me_6H_3)(\eta^6\text{-}C_{16}H_{16})][BF_4]$ (**3**). The complex is highly fluxional with the single *endo* agostic hydrogen atom exchanging rapidly between the two terminal olefinic carbon atoms of the cyclohexadiene unit. The formulation of the complex has been confirmed by the preparation of the di-deutero analogue.

It is well established that the coordination of unsaturated organic fragments to a transition metal centre results in activation of the olefin to nucleophilic attack, and it has been both suggested and experimentally realised that such reactions can form the basis for a viable synthetic method for arene and diene functionalisation [1–4].

Recently we have shown that the polyaromatic arene [2,2]paracyclophane displays only a very limited reactivity towards nucleophiles when coordinated to a metal centre [5,6]. The reactivity and size of paracyclophane make it an effective "blocking agent", exerting steric, as opposed to kinetic [7], control over reaction products. Indeed, even poorly electrophilic arenes such as hexamethylbenzene display a significant reactivity towards nucleophiles when complexed with metal-paracyclophane fragments [5,6]. We have established that single nucleophilic additions may readily occur to the arene ligands in a range of (arene)(paracyclophane) ruthenium(II) complexes under wet aerobic conditions, and have briefly examined the regioselectivities of such reactions.

Paracyclophane also directs double nucleophilic additions of hydride on to other arenes coordinated to the same metal centre; the action of the reducing agent Red–Al on the cations $[Ru(arene)([2.2]paracyclophane)]^{2+}$ (arene = benzene, **1a**; and hexamethylbenzene, **1b**) results in the formation of the ruthenium(0) 1,3-diene compound $[Ru(\eta^4\text{-}C_6H_8)(\eta^6\text{-}C_{16}H_{16})]$ (**2a**) and the 1,4-diene compound $[Ru(\eta^4\text{-}C_6Me_6H_2)(\eta^6\text{-}C_{16}H_{16})]$ (**2b**) [8], respectively. These reactions contrast with those in which double nucleophilic addition to $[Ru(\eta^6\text{-arene})_2]^{2+}$ cations gives bis(cyclohexadienyl)ruthenium(II) species [4,9,10].

Electron-rich ruthenium(0) complexes such as **2a** and **2b** display little further reactivity towards nucleophiles but the metal centre is reactive towards electrophiles. Protonation of the η^4-cyclophane compound $[Ru(\eta^6\text{-}C_6Me_6)(\eta^4\text{-}C_{16}H_{16})]$ with HCl gives a cyclohexadienyl ruthenium(II) complex $[Ru(\eta^6\text{-}C_6Me_6)(\eta^5\text{-}C_{16}H_{17})][HCl_2]$, probably *via* a ruthenium(II) hydride intermediate [8]. Action of HCl on **2a**, however, brings about loss of the diene ligand to form the dichloride dimer $[\{Ru(\eta^6\text{-}C_{16}H_{16})Cl(\mu\text{-}Cl)\}_2]$ [8]. We now report the preliminary results of our investigations into the regioselectivity of double hydride additions to complexes of type **1** and the subsequent reactivities of the resulting diene species towards protonation.

It has previously been shown by Boekelheide *et al.* [8] that reduction of $[Ru(\eta^6\text{-}C_6Me_6)(\eta^6\text{-}C_{16}H_{16})][BF_4]_2$

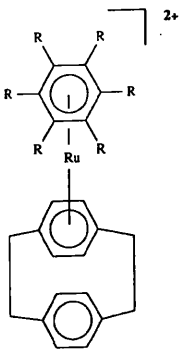

1a R=H
1b R=Me

Correspondence to: Dr. D.A. Tocher.

0022-328X/93/$6.00

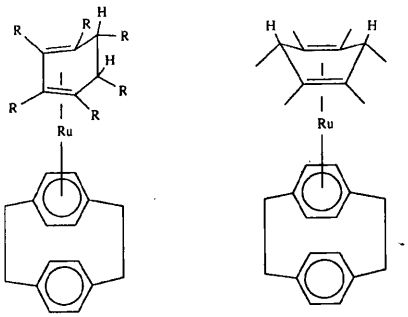

2a R=H
2c R=Me

2b

(**1b**) with Red–Al proceeds smoothly to give a high yield of the 1,4-diene complex, **2b**, which has been characterised by X-ray diffraction. We find that using the reducing agent $Na[BH_4]$, over reaction times of *ca.* 24 h a mixture of **2b** and a second product, **2c**, is obtained. Complex **2c** displays an ^1H NMR spectrum ($CDCl_3$) similar in the low field region to that of **2b**, with the singlet resonance for the protons of the coordinated deck of the [2.2]paracyclophane ligand appearing at δ 4.09 ppm, a chemical shift characteristic of a ruthenium(0) complex (*cf.* **2b** 3.95 ppm) [8]. In contrast to **2b**, which displays only two methyl resonances, **2c** exhibits three methyl signals (δ 1.74 (s), 1.10 (s) and 0.56 (d) ppm, all integrating for six protons) as well as the expected quartet resonance (δ 1.18 ppm) for the two *exo* hydrogen atoms. The spectrum of **2c** is consistent with the formation of a 1,3-diene complex, isomeric with **2b**, and generated either by two hydride additions to the hexamethylbenzene ring *ortho* to one another, or by a rearrangement of **2b**. It has been proposed that the 1,3-diene complex **2a**, derived from **1a**, is initially formed as a 1,4-diene but rearranges *via* metal hydride intermediates to give the more thermodynamically stable 1,3-diene product. Such a process requires the availability of *endo* hydrogen atoms on the cyclohexadiene ring, which are clearly absent in the hexamethylbenzene case. Longer reaction times, up to 7 days, do not lead to the formation of **2b**; instead the product consists of **2c** along with small amounts of a third species possibly arising from two nucleophilic additions at *meta* carbon atoms, or alternatively from subsequent slow rearrangements.

Diene complexes of type **2** display little further reactivity towards nucleophiles but the electron rich ruthenium(0) centre is susceptible to attack by electrophiles and we have investigated the reaction of **2c** with $H[BF_4]$. In view of the apparent propensity for isomerisation in this system, reaction conditions were chosen to allow isolation of products as rapidly as possible. To this end aqueous $H[BF_4]$ (40%) was added dropwise with vigorous stirring to a hexane solution of **2c**. Under these conditions a bright yellow precipitate forms at the interface between the aqueous acid and the hexane solution, and after *ca.* 1 h the organic layer is colourless. The yellow precipitate of $[Ru(C_6Me_6H_3)(\eta^6\text{-}C_{16}H_{16})][BF_4]$ (**3**), was isolated by filtration, washed with diethyl ether to remove residual $H[BF_4]$, and subsequently examined by ^1H, $^{13}C\{^1H\}$ and ^{13}C NMR spectroscopy. The presence of the tetrafluoroborate anion was confirmed by infrared spectroscopy.

The ^1H NMR spectrum of **3** * exhibits typical paracyclophane resonances, confirming the retention of that ligand in an unmodified form [11]. The $C_6Me_6H_3$ ligand gives rise to three methyl signals, δ 1.95 (s), 1.38 (d) and 0.72 (d) ppm, each of integral 6H, a doublet of quartets resonance (δ 1.22 ppm) assigned to the two *exo* protons of the C_6 ring, and a high field "hydridic" multiplet, δ −10.80 ppm. Selective homonuclear decoupling experiments demonstrated that this hydridic resonance exhibits significant coupling (i) to the *exo* ring protons and (ii) the methyl resonance at 1.38 ppm. The higher field methyl signal (δ 0.72 ppm) was coupled solely to the *exo* ring protons. This relatively simple spectrum would be consistent with the formulation of **3** as possessing a hydride ground state and a η^4-cyclohexadiene ligand.

In general, however, protonolysis products such as **3** fall somewhere between the two limiting cases of 18 valence electron metal hydrides [such as the cyclopentadienyl iridium complex $[IrH(\eta^5\text{-}C_5H_5)(\eta^4\text{-}C_4H_4Me_2)]^+$ (**4**)] and 16 electron η^3-allylic species. The cobalt and rhodium analogues of **4** display an intermediate, agostic mode of coordination [12]. The existence of significant coupling in **3** between the resonance at δ −10.80 ppm and the methyl and *exo* ring protons of the new ligand ($C_6Me_6H_3$) is not consistent with the formulation of the product as a full hydride, but rather as an agostic species, the agostic interaction taking place at one of the two terminal carbon atoms of the 1,3-diene unit. The relatively simple nature of the room temperature ^1H and ^{13}C (*vide infra*) NMR spectra may be explained in terms of a rapid fluxional

* ^1H NMR data for complex **3** (400 MHz, $CDCl_3$, 293 K): δ 6.85 (s, 4H), 4.80 (s, 4H), 3.25 and 2.98 (AA'XX', 8H), $\eta^6\text{-}C_{16}H_{16}$; 1.95 (s, 6H), 1.38 (d, 6H, J_{obs} (av.) 2.5 Hz), 1.22 (d of q, 2H, J_{obs} (av.) 6.6 and 4.1 Hz), 0.72 (d, J_{obs} (av.) = 6.6 Hz), −10.80 (t of sp, 1H, J_{obs} (av.) 2.5 and 4.1 Hz) ppm, $\eta^3\text{-}C_6Me_6H_3$. ^{13}C NMR (100.6 MHz): δ 139.08 (s), 133.43 (d, J_{obs} (av.) 160.8 Hz), 125.07 (s), 82.18 (d, J_{obs} (av.) 174.6 Hz), 34.22 (t, J_{obs} (av.) 131.2 Hz), 31.35 (t, J_{obs} (av.) 129.9 Hz), $\eta^6\text{-}C_{16}H_{16}$; 91.51 (s, C_c), 59.25 (d, J_{obs} (av.) 36.0 (*ca.* (72+0)/2) Hz, C_b), 38.45 (d, J_{obs} (av.) 129.8 Hz, C_a), 20.43 (q, J_{obs} (av.) 127.6 Hz), 15.47 (q, J_{obs} (av.) 128.0 Hz), 13.20 (q, J_{obs} (av.) 126.8 Hz) ppm, $\eta^3\text{-}C_6Me_6H_3$.

process involving a metal hydride mediated exchange between two equivalent agostic modes shown in Scheme 1. This was partly confirmed by a low temperature ^1H NMR experiment, although a limiting spectrum could not be reached within the accessible temperature range (as observed in related systems [15,16]).

Strong supporting evidence for the agostic nature of **3** comes from its proton-coupled ^{13}C NMR spectrum *, which at room temperature displays three resonances for the ring carbon atoms of the hexamethylbenzene derived ligand (δ 91.51, 59.25 and 38.45 ppm). The former resonance is a singlet while the latter two are doublets. The coupling constant of the doublet resonance at δ 38.45 ppm is 129.8 Hz, consistent with the non-agostic, saturated carbon atoms, C_a (Scheme 1) [13]. The resonance at δ 59.25 ppm displays a smaller separation of only 36.0 Hz, strongly indicative of a reduced C–H bond order, while its chemical shift indicates a partial olefinic character. This smaller separation arises from the dynamic averaging of two carbon environments (^1J(C–H) *ca.* 72 Hz – agostic coupling, and *ca.* 0 Hz – uncoupled). Related unsubstituted cyclohexenyl systems [14,17] containing agostic CH bonds exhibit coupling constants in the range 70–100 Hz.

The assignment of the resonance due to C_b was confirmed by a selective heteronuclear decoupling experiment. Continuous irradiation of the proton resonance at δ −10.80 ppm resulted in the observation of a singlet ^{13}C resonance at δ 59.25 ppm, displaying a strong NOE enhancement relative to the remaining resonances in the ^{13}C spectrum. Hence, we deduce that the terminal olefinic carbon atoms are both coupled-to, and relaxing *via*, the agostic proton.

The absence of *exo/endo* hydrogen atom exchange in these complexes was confirmed by the preparation of the di-deutero analogue of **2c**, *viz.* [Ru(η^4-C_6Me_6

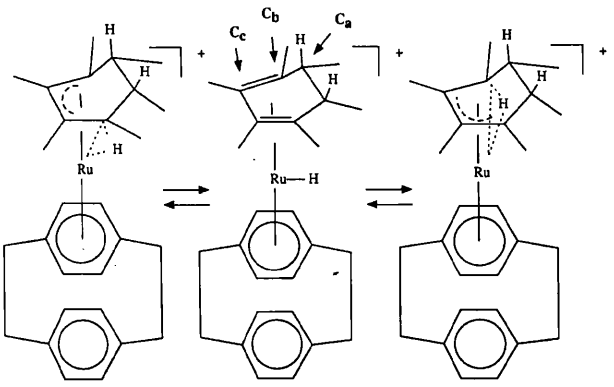

3

Scheme 1. Fluxionality in the agostic complex [Ru(η^3-$C_6Me_6H_3$)(η^6-$C_{16}H_{16}$)][BF_4] (3).

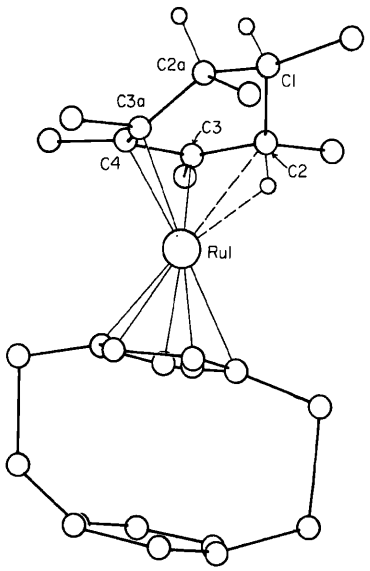

Fig. 1. Structure of the cation [Ru(η^3-$C_6Me_6H_3$)(η^6-$C_{16}H_{16}$)]$^+$ of complex **3** as determined by X-ray diffraction.

D_2)(η^6-$C_{10}H_{16}$)] (**2c′**) (from the action of sodium borodeuteride upon **1b**) and its subsequent protonation to form the agostic complex [Ru(η^3-$C_6Me_6D_2H$)(η^6-$C_{16}H_{16}$)][BF_4] (**3′**). In the ^1H NMR spectra of **2c′** and **3′** the doublet resonances occurring at δ 0.56 and 0.72 ppm respectively in their undeuteriated counterparts, collapsed into broad singlets (^3J(H–D) not resolved) while the multiplet resonance due to the *exo* protons (1.22 ppm) in **3** was absent in **3′**. The $^{13}C\{^1H\}$ spectrum of **3′** showed a 1:1:1 triplet resonance at 37.85 ppm, ^1J(C–D) 20.2 Hz.

The formulation of **3** as being derived from a 1,3- rather than a 1,4-diene was also qualitatively confirmed by a single crystal X-ray structure determination, Fig. 1. Unfortunately the structure is of very limited precision owing to severe disorder of the cyclophane ligand and tetrafluoroborate anion and so quantitative data are not presented. Attempts are in progress to obtain diffraction quality crystals of a sample containing the tetraphenylborate anion.

Detailed work is currently in progress on understanding the regioselectivity of double nucleophilic addition reactions and the isomerism of the resulting ruthenium(0) species. We are also attempting the synthesis of functionalised diene complexes by nucleophilic addition, and the preparation of benzene, *p*-cymene and pentamethylbenzene derived analogues of **3**.

Acknowledgements

We thank the SERC for a studentship (to J.W.S.) and Johnson Matthey plc for generous loans of ruthenium trichloride.

References

1 D. Astruc, *New J. Chem., 16* (1992) 305.
2 M. Uemura, T. Minami, Y. Shinoda, H. Nishimura, M. Shiro and Y. Hayashi, *J. Organomet. Chem., 406* (1991) 371.
3 M. Uemura, H. Nishimura, T. Minami and Y. Hayashi, *J. Am. Chem. Soc., 113* (1991) 5402.
4 C. C. Neto and D. A. Sweigart, *J. Chem. Soc., Chem. Commun.*, (1990) 1703.
5 J. W. Steed and D. A. Tocher, *J. Organomet. Chem., 412* (1991) C37.
6 M. R. J. Elsegood, J. W. Steed and D. A. Tocher, *J. Chem. Soc., Dalton Trans.*, (1992) 1797.
7 S. G. Davies, M. L. H. Green and D. M. P. Mingos, *Tetrahedron, 34* (1978) 3047.
8 R. T. Swann, A. W. Hanson and V. Boekelheide, *J. Am. Chem. Soc., 108* (1986) 3324.
9 D. Jones, L. Pratt and G. Wilkinson, *J. Chem. Soc.*, (1962) 4458.
10 M. I. Rybinskaya, V. S. Kaganovitch and A. R. Kudinov, *J. Organomet. Chem., 235* (1982) 215.
11 M. R. J. Elsegood, *PhD Thesis*, University College London, 1991.
12 Ch. Elschenbroich and A. Salzer, *Organometallics - A Concise Introduction*, VCH, 1989.
13 W. W. Paudler, *Nuclear Magnetic Resonance - General Concepts and Applications*, Wiley, New York, 1987.
14 M. Brookhart, W. Lamanna and M. Beth Humphrey, *J. Am. Chem. Soc., 104* (1982) 2117.
15 M. A. Bennett and T. W. Matheson, *J. Organomet. Chem., 153* (1978) C25.
16 M. Brookhart, M. L. H. Green and R. B. A. Pardy, *J. Chem. Soc., Chem. Commun.*, (1983) 691.
17 M. Brookhart, M. L. H. Green and L.-L. Wong, *Prog. Inorg. Chem., 36* (1988) 1.